ISSN: 2456-1878

International Journal of Environment Agriculture and Biotechnology

(IJEAB)

An open access Peer-Reviewed InternationalJournal

DOI: 10.22161/ijeab.113

Vol.- 11 | Issue - 3 | May-Jun 2026

editor.ijeab@gmail.com | editor@ijeab.com | https://www.ijeab.com/

International Journal of Environment, Agriculture and Biotechnology

(ISSN: 2456-1878)

DOI: 10.22161/ijeab

Vol-11, Issue-3

May - June, 2026

Editor in Chief

Dr. Pietro Paolo Falciglia

Publisher

Infogain Publication

Email: editor.ijeab@gmail.com ; editor@ijeab.com

Web: www.ijeab.com

FOREWORD

I am honoured to introduce this latest issue to the International Journal of Environment, Agriculture and Biotechnology (IJEAB). Our journal is dedicated to disseminating high-quality research and innovative findings that contribute to advancing knowledge in these critical fields.

In this issue, we present a collection of papers that exemplify the diversity and depth of contemporary environmental, agriculture, and biotechnology research. The articles include various topics, from sustainable agricultural practices and environmental conservation strategies to cutting-edge biotechnological innovations. Each contribution has undergone a rigorous peer-review process, ensuring the publication of only the most significant and original research.

Our commitment at IJEAB is to provide a robust platform for researchers, academicians, and practitioners to share their work and engage with a global audience. By fostering an interdisciplinary approach, we aim to bridge the gaps between different areas of study and promote holistic understanding and solutions to the challenges we face in these domains.

We are grateful to our dedicated authors, whose hard work and intellectual rigour are the backbone of our journal. We also extend our appreciation to our reviewers and editorial board members, whose expertise and diligence ensure the high standards of our publication. Finally, we thank our readers for their continued support and engagement.

We hope you find the articles insightful and inspiring as you explore this issue. We encourage you to contribute your research to future issues and join us in our mission to advance knowledge and drive positive change in the environment, agriculture, and biotechnology fields.

Sincerely,
Editor-in-Chief
International Journal of Environment, Agriculture and Biotechnology (IJEAB)
NAAS Score Journal
www.ijeab.com

International Editorial Board/ Reviewer Board

Vol-11, Issue-3, May - June, 2026
(DOI: 10.22161/ijeab.113)

International Journal of Environment, Agriculture and Biotechnology
Vol-11, Issue-3; May-Jun, 2026
Peer-Reviewed International Journal
Journal Home Page Available: https://ijeab.com/
Journal DOI: 10.22161/ijeab

Effect of Activity-Led Instructional Program in Enhancing Environmental Responsibility among Secondary Students

Vidushi Mishra[1], Dr. Sangeeta Chauhan[2]

[1]M.Ed. Student, Department of Education, Babasaheb Bhimrao Ambedkar University (A Central University), Vidya Vihar, Raebareli Road, Uttar Pradesh Lucknow- 226025, India
[2]Assistant Professor, Department of Education, Babasaheb Bhimrao Ambedkar University (A Central University), Vidya Vihar, Raebareli Road, Uttar Pradesh Lucknow- 226025, India

Received: 25 Mar 2026; Received in revised form: 24 Apr 2026; Accepted: 28 Apr 2026; Available online: 06 May 2026

***Abstract*— *Traditional, lecture-based pedagogical models often fail to translate environmental knowledge into real-world sustainable habits, creating a persistent "knowledge-action gap" among young learners. While students may memorize theoretical facts, they frequently lack the practical social consciousness required to drive meaningful green campus transformations. This study evaluated the efficacy of an activity-led instructional intervention in enhancing environmental responsibility and sustainability literacy among secondary school students. The research focused on critical dimensions that are sustainable lifestyles and eco-conscious practices, energy usage patterns and their broader environmental footprints and resource conservation and energy efficiency. A quasi-experimental research design was employed with 11th 70 grade students from a CBSE-Board school in Lucknow city. The experimental group (N=35) received a 45-day structured instructional program using cooperative learning strategies, while the control group (N=35) followed the traditional teaching learning. Data were analysed using non-parametric Wilcoxon Signed Ranks and Mann-Whitney U tests via SPSS to measure internal growth and comparative significance. The findings revealed that the activity-led program caused a highly significant improvement in the experimental group across all dimensions. Notably, the energy usage dimension showed a near-universal internal improvement rate. Comparative analysis proved the experimental group achieved significantly higher mean ranks than the control group in resource conservation and energy efficiency, demonstrating the superior impact of structured interventions. The study demonstrates that specialized, activity-based interventions are superior to conventional methods in fostering ecological stewardship. It recommends integrating hands-on modules into mainstream curricula to bridge the gap between environmental awareness and active conservation.*

Keywords*— Activity-Led Learning, Energy Footprints, Environmental Responsibility, Green Campus Transformation, Sustainable Practices.

I. INTRODUCTION

"Education is the most powerful weapon which you can use to change the world".

- Nelson Mandela

These words of Nelson Mandela establish the foundation for this research that the escalating global environmental crisis requires a profound internal transformation of human behavior. By 2024, the global average surface temperature reached roughly 0.55 ° C above pre-industrial levels, with atmospheric CO_2 concentrations hitting 420 ppm (IPCC,2024). The decade of 2024–2025 officially ranks as the warmest on record, creating a "Red Alert" for biodiversity and human civilization. Despite these critical figures, a persistent "knowledge-action gap" prevents younger generations from translating theoretical awareness into responsible ecological stewardship. UNESCO emphasizes that education for sustainable development is the essential bridge to empower learners to make informed decisions for environmental integrity (UNESCO, 2020). In

India, the National Education Policy (NEP) 2020 explicitly recognizes this urgency, advocating for holistic, multidisciplinary, and experiential learning to address sustainability challenges (NEP, 2020). UNESCO aligns with the "Green School" movement and the UNESCO Greening Education Partnership, which officially began its core mission on June 5, 2024, to get "Every Learner Climate-Ready" (UNESCO, 2024). The present research is designed as a structured instructional intervention aimed at bridging the gap between theoretical knowledge and practical action. Utilizing a quasi-experimental design with 11th grade 70 students in Lucknow city, this study evaluates the efficacy of a specialized instructional program against traditional pedagogical methods. By focusing on active, participatory modules, the study supports national visions like Viksit Bharat @2047 and the "Ek Ped Maa Ke Naam" campaign launched in 2024, which aims to plant 40 crore trees by March 2025 (MoEFCC, 2024). Ultimately, this intervention seeks to transform students from passive observers into active agents of a green campus transformation.

II. REVIEW OF RELATED LITERATURE

The reviewed studies are highly relevant to this research as they provide strong evidence for the effectiveness of structured interventions in improving Sustainable Practices and Energy Usage patterns, while highlighting the need for active learning to bridge the knowledge-action gap in these specific areas. Ablak and Yeşiltaş (2020) empirically demonstrated that secondary school students generally possess a favorable level of baseline awareness regarding basic, highly visible ecological concepts. This baseline is often built through everyday observation rather than just formal instruction. Aldawsari et al. (2025) concluded that teaching comprehensive green education successfully bridges the gap between fragmented theoretical knowledge and deep, practical environmental responsibility. Ayerbe López and Perales Palacios (2024) noted that traditional teaching methods are frequently insufficient for conveying complex ecological topics effectively. They argued that innovative methodologies are required to connect students emotionally to the natural world. Barman (2023) observed that dedicated, school-based environmental initiatives exert a massive positive influence on young learners. The study proved that targeted curriculums are essential for helping students successfully comprehend complex ecological problems that are often ignored in traditional settings. Fernandes et al. (2024) conducted a document analysis revealing that environmental education in standard high school curricula is often treated too generically. Their work highlights that traditional frameworks lack the deep practical application required for genuine behavior change. Firmanshah et al. (2023) found a very strong positive connection between environmental knowledge, attitudes, and awareness. Their results prove that high environmental knowledge consistently leads to better ecological attitudes in students. Khofi (2024) found that green school concepts significantly improve students' environmental awareness and influence their pro-environmental behavior. Lace-Jeruma and Birzina (2009) demonstrated how standard biology lessons frequently integrate practical sustainability goals. However, the research noted that without specialized modules, students often miss the deeper connection to global environmental systems. Lozano et al. (2022) found that utilizing active teaching methodologies greatly improves students' knowledge about climate change. The study also highlighted that such programs successfully trigger strong positive emotions toward scientific learning. Mahinay et al. (2023) explored the relationship between environmental literacy levels and pollution, finding that higher ecological knowledge directly shapes student behaviors. Specifically, students with higher literacy displayed a much stronger willingness to take responsible actions against pollution. Marcelino et al. (2024) established that integrating ecology into the formal curriculum is fundamental for developing conscious citizens. Their theoretical investigation supports the role of basic curricular science in delivering the structural framework of ecological knowledge. Mavhungu (2023) investigated students' perceptions and found a favorable correlation between human capital aspiration and individual approach to new environmental initiatives. Mebane et al. (2023) emphasized that promoting climate change awareness requires specialized socio-affective education and empowerment training. Their research confirmed that instructional programs provide students with the intellectual clarity needed to transform anxiety into structured, scientific awareness. Reutotar (2023) found that students build their baseline awareness through physical encounters with issues like improper waste segregation in their immediate environments. This experiential, real-world learning acts as a vital supplement to traditional classroom instruction. Sass et al. (2024) developed a framework to advance action competence in sustainability education. Their research emphasizes shifting pedagogical focus from passive learning to "climate-ready" competencies.

Suarez Solis (2024) established that structured intervention programs are essential for cultivating ecological consciousness. The research proved that dedicated environmental initiatives produce highly measurable benefits compared to control groups. Suarlin (2023) established that integrating environmental education into formal schooling is absolutely necessary to form "environmental care characters". The research highlighted that structured, active interventions result in massive improvements in environmental knowledge and positive behavioral shifts. Zogaj et al. (2024) pointed out that regions facing severe pollution problems urgently need effective environmental education systems. Their data confirmed that higher ecological education directly correlates with better awareness and more responsible daily practices. Despite existing awareness, current educational models often treat environmental topics too generically, failing to bridge the knowledge-action gap. This research addresses the lack of structured, activity-led interventions specifically designed to transform theoretical knowledge into practical sustainable practices and energy-saving behaviours among students.

III. SIGNIFICANCE OF THE STUDY

The importance of this research lies in its strategic response to the ecological and social needs of 2026. While it directly addresses the "knowledge-action gap," with a primary reason to combat the urgent need of "Environmental Apathy". In today's digital world, many people feel disconnected from the physical damage happening to our planet. This study provides a practical way to fix that broken connection between human choices and the health of nature. Additionally, this research is vital because it moves past the limits of traditional classroom teaching, which often leaves students informed but uninspired to make a difference. By using a structured instructional program, this study gives learners the tools to take real, measurable action. This work is highly relevant to today's society as it aligns with India's National Education Policy (NEP) 2020 and the Viksit Bharat @2047 vision. Instead of just memorizing facts, it focuses on building the skills and values needed for a sustainable future. Ultimately, this study offers a tested model for schools to turn passive awareness into active care, protecting the natural systems that keep our world alive.

RESEARCH QUESTIONS

Question 1: What is the effect of an activity-led instructional intervention on the post-test scores of 11th grade students in the domain of long-term sustainable lifestyles and eco-conscious practices?

Question 2: How does the implementation of an activity-led instructional intervention change a student's capacity to analyze and manage their daily energy usage patterns and environmental footprints?

Question 3: Is there any significant difference exist between Post-test scores of students receiving activity-led instruction and those receiving conventional instruction on the dimension of resource conservation and energy efficiency?

RESEARCH OBJECTIVES

Objective 1: To compare the effect of a structured activity-led instructional program on the Pre-test and Post-Test scores of experimental group on sustainable lifestyles and eco-conscious practices.

Objective 2: To compare the effect of a structured activity-led instructional program on the Pre-test and Post-Test scores of experimental group on personal energy usage patterns and their broader environmental footprints.

Objective 3: To compare between the Post-test scores of the Experimental Group and Control Group on the dimension of resource conservation and energy efficiency.

RESEARCH HYPOTHESIS

H_1: There is a significant difference between the Pre-test and Post-test scores of sustainable lifestyles and eco-conscious practices of the Experimental Group.

H_2: There is a significant difference between the Pre-test and Post-test scores of personal energy usage patterns and their broader environmental footprints of the Experimental Group.

H_3: There is a significant difference between the Post-test scores of the Experimental Group and Control Group on the dimension of resource conservation and energy efficiency.

IV. METHODOLOGY

Research Method

The study adopts a quantitative research approach, for exploring the insights of environmental responsibility.

Research Design

The researcher employed a Quasi-Experimental Research, specifically the Pre-test Post-test Non-Equivalent Control Group design.

Variables of the Study

Independent Variable: Activity-Led Instructional Program, defined as a structured, participatory instructional intervention delivered via cooperative learning strategies.

Dependent Variable: Environmental Responsibility, which serves as the metric of the students' cognitive and affective growth across critical environmental dimensions.

Population of the study: Students of 11th class of CBSE Board of secondary schools of Uttar Pradesh as population of the study.

Target Population: Students of 11th class of CBSE Board in Lucknow City as target population.

Sample Size: A total sample of 70 students was utilized for the study.

Sampling Technique: Purposive Sampling was employed for the research.

Group Distribution: The sample was divided into an Experimental Group (N=35) and a Control Group (N=35).

Tool for data collection

The primary tool for data collection was a self-developed Environmental Awareness Test. It was administered as a Pre-test to establish a statistical baseline and as a Post-test to evaluate the change following the intervention period.

Experimental Procedure and Intervention

The study was conducted over an intensive 45-day duration.

Phase I (Pre-test): Both groups were assessed to determine their initial environmental awareness scores.

Phase II (Treatment): The Experimental Group received the activity-led instructional program, utilizing mechanics such as the Jigsaw II strategy and Problem-Based Learning (PBL). The Control Group was exposed exclusively to the traditional academic curriculum.

Phase III (Post-test): After the intervention, both groups were reassessed to measure cognitive and behavioral shifts.

V. ANALYSIS AND DISCUSSION

Statistical analysis was performed using SPSS at a 0.05 level of significance. Due to the non-parametric nature of the data, the following tests were utilized.

- **Wilcoxon Signed Ranks Test:** To analyze the significance of internal growth within each group (Pre-test vs. Post-test).
- **Mann-Whitney U Test:** To determine the comparative superiority of the instructional intervention by analysing the difference in post-test scores between the independent groups.

Analysis 1:

Objective 1: To compare the effect of a structured activity-led instructional program on the Pre-test and Post-Test scores of experimental group on sustainable lifestyles and eco-conscious practices.

H_{01}: There is no significant difference between the Pre-test and Post-test scores of sustainable lifestyles and eco-conscious practices of the Experimental Group.

Table 1. (A): Wilcoxon Signed Ranks Test for Experimental Group (Sustainable Lifestyles and Eco-Conscious Practices).

Ranks	N	Mean Rank	Sum of Ranks
Negative Ranks	0	0.00	0.00
Positive Ranks	34	7.50	595.00
Ties	1		
Total	35		

Table 1. (B): Test Statistics for Sustainable Lifestyles and Eco-Conscious Practices (Experimental Group)

Test Statistic	Value
Z-value	-5.487
Asymp. Sig. (2-tailed)	0.001

Tables 1. (A) and 1. (B) present the comparison between the pre-test and post-test scores of the experimental group on the dimension of sustainable lifestyles and eco-conscious practices. The Wilcoxon Signed Ranks Test was applied to determine whether a significant difference existed between the two sets of scores. The results indicate that 34 students obtained higher scores in the post-test, while no student showed a decline in performance. One case remained unchanged. The calculated Z value is -5.487 and the p-value is .001, which is lower than the 0.05 level of significance. Therefore, the difference is statistically significant, proving that the instructional program significantly improved students' understanding of sustainable practices. Consequently, the null hypothesis is not accepted.

Analysis for Objective 2:

Objective 2: To compare the effect of a structured activity-led instructional program on the Pre-test and Post-Test scores of experimental group on personal energy usage patterns and their broader environmental footprints.

H_{02}: There is no significant difference between the Pre-test and Post-test scores of personal energy usage patterns and their broader environmental footprints of the Experimental Group.

Table 2.1 (A): Wilcoxon Signed Ranks Test for Experimental Group (Energy Usage Patterns and their broader environmental footprints)

Ranks	N	Mean Rank	Sum of Ranks
Negative Ranks	0	0.00	0.00
Positive Ranks	35	8.00	630.00

Ties			
Total	35		

Table 2.2 (B): Test Statistics for Energy Usage Patterns and their broader environmental footprints (Experimental Group)

Test Statistic	Value
Z-value	-5.593
Asymp. Sig. (2-tailed)	0.001

Tables 2.1(A) and 2.2(B) detail the comparison of pre-test and post-test scores for the experimental group regarding energy footprints and their broader environmental footprints. The data indicates that all 35 students achieved positive ranks, representing a 01% rate of internal improvement without negative ranks or ties. The obtained Z value is -5.593 and the p-value is .001, which is less than the 0.05 significance level. It is concluded that the instructional program significantly enhanced students' understanding of energy footprints and their environmental impacts. This mastery demonstrates that structured modules can effectively dismantle the complexity of abstract technical concepts. Thus, the null hypothesis is not accepted.

Analysis for Objective 3

Objective 3: To compare between the Post-test scores of the Experimental Group and Control Group on the dimension of resource conservation and energy efficiency.

H_{03}: There is no significant difference between the Post-test scores of the Experimental Group and Control Group on the dimension of resource conservation and energy efficiency.

Table 3.1. Ranks for Post-test Scores of Control and Experimental Groups (N=70)

Group	N	Mean Rank	Sum of Ranks
Control Group	35	23.50	822.50
Experimental Group	35	47.50	1662.50
Total	**70**		

Table 3.2. Mann-Whitney U Test Statistics for Post-test Scores on Resource Conservation and Energy Efficiency

Test Statistic	Value
Mann-Whitney U	92.500
Wilcoxon W	822.500
Z-value	-5.545
Asymp. Sig. (2-tailed)	.000

Table 3.3. Summary of Mann-Whitney U Test Results for Resource Conservation and Energy Efficiency

Dimension	Group	N	Mean Rank	U	Z	p
Resource Conservation & Energy Efficiency	**Control**	35	23.50	92.500	-5.545	<.001
	Experimental	35	47.50			

Table 3.1 displays the rank distribution for the post-test scores of 70 students across two independent cohorts. The Experimental Group (N=35) achieved a Mean Rank of 47.50, which is substantially higher than the Mean Rank of 23.50 recorded for the Control Group (N=35). This descriptive gap in mean ranks suggests that the students who underwent the activity-led instructional program demonstrated a higher level of mastery in resource conservation and energy efficiency than those taught via traditional pedagogy. The Mann-Whitney U test was utilized to determine if the observed difference between the groups was statistically significant. As per the test statistics in Table 3.2, the calculated Mann-Whitney U value is 92.500 with a Z-value of -5.545. The associated Asymptotic Significance (p-value) is .001. The significance is tested at the 0.05 level. Since the obtained *p*-value (.001) is less than the alpha level of 0.05, the result is statistically significant. Table 3.3 provides a comprehensive summary of the comparative analysis between the specialized instructional program and traditional methods. The statistical divergence (U = 92.500, Z = -5.545, p < .001) necessitates the non-acceptance of the null hypothesis (H_{03}), which stated there would be no significant difference between the groups.

VI. OVERALL DISCUSSION

The overall discussion of this research is grounded in a critical interpretation of the data obtained through the comparative analysis of post-test scores across the experimental and control cohorts. It serves as the analytical heart of the dissertation by transforming raw scores into meaningful scientific findings that prove the efficacy of the instructional intervention. While internal growth was observed in both groups over the academic term, this comparative analysis serves as the definitive analytical crucible by isolating the true impact of the activity-led variable. By directly contrasting the final performance of 70 eleventh-grade students (35 per group), the study provided empirical evidence that the specialized instructional program was superior to standard pedagogy in fostering environmental responsibility. In the dimension of Sustainable Practices, the experimental group achieved a significantly higher mean rank compared to the control group, yielding a p-value of .001. This statistical divergence highlights that traditional "chalk-and-talk" methods are often insufficient for teaching complex sustainability frameworks, which demand active and targeted learning environments to bridge the gap between theoretical knowledge and practical application.

The superiority of the activity-led approach was further evidenced in the dimension of Energy Usage Patterns, where the experimental group demonstrated a statistically significant advantage. The analysis revealed that students who underwent the specialized modules were better able to internalize technical concepts, such as energy footprints, which are often perceived as abstract or distant by adolescent learners. By utilizing participatory strategies and real-life examples, the experimental program successfully demystified these concepts, whereas standard textbooks in the control group failed to connect global energy depletion to personal daily habits. The statistically significant difference between the two groups clearly indicates that traditional teaching methods are less effective in promoting sustainability-oriented thinking and energy conservation awareness.

The final evaluation of Overall Environmental Responsibility demonstrated a massive victory for the specialized program, with the experimental group achieving a considerably higher mean rank compared to the control group. This holistic improvement proves that the instructional program did not merely impart isolated facts but successfully developed a comprehensive, interconnected environmental mind-set. In conclusion, while standard schooling imparts basic vocabulary and theoretical awareness, it often fails to alter deep-rooted habits or foster an active conservation consciousness. The consistent improvement observed in the experimental group across the major dimensions underscores the necessity of integrating specialized green pedagogies into the modern educational framework to equip students with the skills and attitudes necessary to address future environmental challenges.

VII. FINDING

The findings of this study provide empirical evidence that a structured, activity-led instructional program is significantly more effective than traditional pedagogical methods in fostering environmental responsibility among secondary students. Through a quasi-experimental analysis of 70 eleventh-grade students, the research revealed that the experimental group achieved a highly significant improvement across all assessed environmental dimensions, including sustainable practices and energy usage patterns. Notably, the dimension of energy footprints saw a near-universal internal growth rate within the experimental cohort, suggesting that participatory strategies like Problem-Based Learning (PBL) successfully demystify complex technical concepts that standard textbooks often fail to address. Comparative data using the Mann-Whitney U test confirmed the superior impact of the intervention, as the experimental group secured substantially higher mean ranks in sustainable practices ($Z = -5.545$, $p < .001$) and energy management compared to the control group. While traditional "Chalk-And-Talk" schooling was found to establish a basic theoretical vocabulary, it reached a "Theoretical Ceiling" that failed to bridge the persistent "Knowledge-Action Gap" or alter deep-rooted habits. Ultimately, the study concludes that transforming learners from passive observers into active participants through specialized green pedagogy is essential for developing a comprehensive, interconnected ecological mind-set and preparing a "Climate-Ready" generation.

VIII. CONCLUSION

The conclusion of this study provides a definitive synthesis of the research findings, confirming the transformative power of activity-led instructional programs in fostering environmental stewardship. Based on the rigorous statistical analysis of the experimental group, it is concluded that a structured, activity-based intervention is significantly more effective than traditional lecture-based methods in enhancing ecological literacy and bridging the persistent "Knowledge-Action Gap". While traditional schooling establishes a basic theoretical vocabulary, the specialized modules utilized in this research allowed students to master abstract and technical dimensions, such as energy usage patterns and sustainable practices, which are often lost in conventional pedagogical setups. The near-universal improvement observed among the participants suggests that when learners are transformed from passive observers into active participants through cooperative learning and problem-solving, they develop a deeper, internalized connection to environmental issues. Furthermore, the study establishes that the instructional intervention successfully cultivated a comprehensive and interconnected environmental mind-set, effectively sensitizing students to the long-term consequences of human activities. By rejecting the null hypotheses across the major dimensions of sustainable responsibility, the research provides undeniable empirical evidence that moving beyond the "Theoretical Ceiling" of standard pedagogy is essential for preparing a "Climate-Ready" generation. Ultimately, these findings underscore the urgent need for curricular reform that prioritizes experiential and learner-centred strategies, as advocated by national educational frameworks. In summary, this research validates that specialized green pedagogy is not merely a beneficial supplement but a necessary requirement to equip modern students with the robust, measurable knowledge needed to protect the planet's future.

REFERENCES

[1] Aldawsari, A., et al. (2025). Bridging the gap: The impact of green education on practical responsibility. Sustainability. https://doi.org/0.3390/su70024

[2] Ayerbe López, P., & Perales Palacios, F. J. (2024). Traditional vs. innovative teaching in biodiversity conservation. Sustainability. https://doi.org/0.3390/su603245

[3] Barman, P. (2023). The influence of school-based environmental programs on young learners. The Journal of Environmental Education. https://doi.org/0.080/00958964.2023.220454

[4] Creswell, J. W., & Guetterman, T. C. (209). Educational research: Planning, conducting, and evaluating quantitative and qualitative research (6th ed.). Pearson.

[5] Fernandes, R., et al. (2024). A document analysis of high school environmental curricula. Sustainability. https://doi.org/0.3390/su6052024

[6] Firmanshah, A., et al. (2023). Knowledge and attitudes as predictors of ecological awareness. Eurasia Journal of Mathematics, Science and Technology Education. https://doi.org/0.29333/ejmste/30

[7] Khofi, L. (2024). Green school concepts and environmental awareness. Sustainability. https://doi.org/0.3390/su604524

[8] Lozano, R., et al. (2022). Active teaching methodologies and climate change knowledge. Sustainability. https://doi.org/0.3390/su40350

[9] Mahinay, J., et al. (2023). Environmental literacy and pollution: A statistical analysis. Education Journal. https://doi.org/0.648/j.edu.2023204.2

[10] Marcelino, V., et al. (2024). Integrating ecology into formal curricula for conscious citizenship. Sustainability. https://doi.org/0.3390/su6062548

[11] Mavhungu, M. (2023). Impact of extrinsic factors on students' attitudes. Asian Journal of Management, Entrepreneurship and Social Science. https://doi.org/0.55227/ajmess.2023.v3i3.694

[12] Mebane, M., et al. (2023). Socio-affective education and climate change awareness. Frontiers in Psychology. https://doi.org/0.3389/fpsyg.2023.4562

[13] Ministry of Education. (2020). *National Education Policy 2020*. Government of India. https://www.education.gov.in/sites/upload_files/mhrd/files/NEP_Final_English_0.pdf

[14] Sansanwal, D. N. (2020). Research Methodology and Applied Statistics. Shipra Publications.

[15] Sass, W., et al. (2024). A quality education for sustainability teaching (QUEST) framework. The Journal of Environmental Education. https://doi.org/0.080/00958964.2023.229567

[16] Suarez Solis, L. (202). Leaving green footprints: Measuring ecological consciousness in schools. International Journal of Environmental Education.

[17] Suarlin, S. (2023). Forming environmental care characters through formal schooling. International Journal of Instruction. https://doi.org/0.29333/iji.2023.63a

[18] UNESCO. (2020). Education for sustainable development: A roadmap. United Nations Educational, Scientific and Cultural Organization.

[19] World Health Organization. (2023, December 19). Ambient (outdoor) air pollution. https://www.who.int/news-room/fact-sheets/detail/ambient-(outdoor)-air-quality-and-health

[20] World Meteorological Organization. (2024). State of the global climate 2023 (WMO-No. 1347). https://library.wmo.int/idurl/4/68835

[21] Zogaj, A., et al. (2024). Ecological education and responsible practices in polluted regions. Sustainability. https://doi.org/0.3390/su602042

International Journal of Environment, Agriculture and Biotechnology
Vol-11, Issue-3; May-Jun, 2026
Peer-Reviewed International Journal
Journal Home Page Available: https://ijeab.com/
Journal DOI: 10.22161/ijeab

Assessment of Landscape Elements Effectiveness on Users' Wellbeing in selected Tertiary Institutions in Lagos State

Tashok Yusuf H.[1], Babamboni Adekunle S.[2], Onwuamaegbu Will[3], Oderinde Oluwanifemi[4], Oginni Princess[5]

[1]Department of Architecture, Ambrose Alli University, Ekpoma, Edo
[2]Department of Architecture, Lagos State University of Science and Technology, Lagos
[3,4,5]Department of Architecture, Caleb University, Lagos
Corresponding Author: oderinde.oluwanifemi@calebuniversity.edu.ng

Received: 02 Apr 2026; Received in revised form: 30 Apr 2026; Accepted: 04 May 2026; Available online: 13 May 2026

***Abstract*— *Landscape elements within tertiary institutions play a significant role in enhancing users' physical, psychological, and social well-being by providing spaces for relaxation, interaction, and environmental comfort. In rapidly urbanizing environments such as Lagos State, public tertiary institutions often experience high population density and infrastructural pressure, making the quality and effectiveness of outdoor landscapes critical to users' daily experiences. However, many institutional landscapes face challenges such as poor maintenance, inadequate design, limited vegetation, and insufficient seating or shading, which may reduce their potential benefits. While previous studies have examined green spaces in urban contexts, limited research has focused on how specific landscape elements within tertiary institutions influence users' well-being. This study therefore assesses the effectiveness of landscape elements on users' well-being in selected public tertiary institutions in Lagos State. The objectives are to identify key landscape elements, examine users' perceptions, and evaluate their impact on physical, psychological, and social well-being. A quantitative research approach will be adopted using structured questionnaires and site observations. Data will be analyzed using descriptive and inferential statistics. The study aims to provide evidence-based recommendations for improving landscape design and management in tertiary institutions to enhance user well-being and overall campus experience.*

***Keywords*— Landscape elements, User well-being, Tertiary institutions, Campus environment, Green infrastructure, Lagos State.**

I. INTRODUCTION

Landscape elements are essential components of campus environments, contributing significantly to environmental quality, user comfort, and overall well-being (Sadeq, Ismail, & Manaf, 2026). In tertiary institutions, outdoor spaces such as courtyards, gardens, walkways, and green areas provide opportunities for relaxation, social interaction, and informal learning.

In densely populated cities like Lagos, where academic environments are often characterized by intense schedules and high stress levels, access to well-designed landscapes becomes increasingly important (Akindejoye, Ezedinma, & Ike, 2021). Landscape elements such as trees, lawns, water features, and shaded seating areas help reduce environmental stressors, improve microclimate conditions, and promote mental and physical well-being (Tongyun, Wei & Fei, 2024).

Natural environments have been widely recognized for their restorative effects. The Attention Restoration Theory suggests that exposure to natural settings helps improve concentration and reduce mental fatigue, while the Stress Reduction Theory highlights the calming effects of green environments (Berto, 2014).

Problem Statement

However, despite the importance of landscape elements in tertiary institutions, there are challenges such as poor landscaping maintenance and a lack of vegetation and green cover. Lack of usable outdoor furniture, Insufficient shading and thermal comfort, poor spatial planning of outdoor spaces.

These factors limit the potential of landscape spaces in promoting the well-being of users.

Moreover, there is a lack of empirical research that establishes the connection between certain landscape elements (vegetation, outdoor furniture, shading, walkways, among others) and the physical, psychological, and social well-being of users in Nigerian tertiary institutions.

Aim of the study

This study aims to assess the effectiveness of landscape elements on users" well-being in selected public tertiary institutions in Lagos State

Objectives of the study

The study aims to:

- Identify key landscape elements within selected tertiary institutions
- Examine users' perceptions and usage patterns of these landscape spaces
- Evaluate the relationship between landscape elements and users' well-being
- Provide recommendations for improving campus landscape design and management

II. LITERATURE REVIEW

Landscape architecture is an essential tool for the promotion of health benefits. Various studies have shown that the presence of well-designed outdoor spaces is beneficial for physical health, reduces stress levels, and promotes social interaction.

Vegetation is one of the most important landscape elements, contributing to microclimate regulation, air quality improvement, and psychological restoration (Murugadoss, Singh & Thakur, 2024). Trees and green areas provide shade, reduce heat, and create calming environments that improve mood and reduce anxiety (Gungormus, & Pérez-Mármol,2025).

Accessibility and usability of outdoor spaces also influence their effectiveness (Yin, Wang, Xu, & Heng,2025). Well-connected walkways, seating areas, and open spaces encourage frequent use and social engagement (Alnaim, Dano & AlQahtany,2025).

Maintenance of the built environment is an essential determinant of user satisfaction. Poorly maintained built environments are not beneficial for the creation of user satisfaction.

2.1. Key Concepts

Landscape Elements

Landscape elements are the physical features of the outdoor environment. It includes the presence of vegetation, walkways, seating areas, water features, lighting, and space.

User Well-Being

User well-being is the physical comfort, psychological restoration, and social interaction experienced by the user of the environment.

Campus Landscape

Campus landscape is the outdoor spatial environment of an educational institution, encompassing all open spaces, natural elements, and built features that exist outside the enclosed structures. It includes a wide range of components such as green areas (lawns, gardens, and tree canopies), circulation networks (pedestrian walkways, roads, and bicycle paths), recreational and social spaces (courtyards, plazas, and sports fields), as well as hardscape elements like pavements, seating, lighting, and water features.

2.2. Conceptual Model

In this study, landscape elements are conceptualized as an independent variable impacting users' well-being in some public tertiary institutions in Lagos State. In more specific terms, landscape elements are defined by some critical physical and environmental attributes, including density of vegetation, provision of shades, provision of sitting areas, walkability, aesthetic qualities, and maintenance of landscape spaces. Together, they capture the quality and performance of outdoor spaces in campus environments.

Users' well-being is conceptualized as a multi-dimensional construct encompassing physical comfort, psychological restoration, and social interaction. Physical comfort pertains to users' thermal satisfaction and usability of outdoor spaces, while psychological restoration pertains to users' stress reduction and mental relaxation through landscape spaces, and finally, social interaction pertains to users' experience of communication and group activities through landscape spaces.

In essence, the conceptual model posits that better landscape qualities would positively impact each dimension of users' well-being, thereby enhancing overall users' satisfaction and experience in campus environments. Moreover, the model posits that landscape elements would not only positively impact users' well-being but also their conditions, designs, and maintenance would influence their effectiveness in impacting users' well-being.

2.3. Theoretical Framework

Attention Restoration Theory

Attention Restoration Theory (Kaplan & Kaplan, 1989) suggests that natural environments help individuals recover from mental fatigue caused by prolonged concentration and cognitive effort. Natural settings such as parks provide restorative experiences that improve mental focus and emotional balance.

Stress Reduction Theory

Stress Reduction Theory (Ulrich, 1984) proposes that exposure to natural environments reduces psychological stress and promotes relaxation. Green landscapes, water features, and open spaces create calming environments that enhance emotional well-being.

Biophilia Hypothesis

The Biophilia Hypothesis, introduced by Wilson (1984), suggests that humans have an innate connection with nature. Interaction with natural environments therefore satisfies psychological needs and contributes to improved well-being.

These theories explain why urban parks can significantly influence physical, psychological, and social well-being when properly designed and maintained.

III. METHODOLOGY

This study adopts a quantitative approach to examine the relationship between landscape elements and users' well-being in selected public tertiary institutions in Lagos State. The methodology is designed to capture users' perceptions, behavioral patterns, and well-being outcomes associated with campus landscape usage, while also incorporating physical observations of landscape conditions. The approach integrates survey-based data with environmental assessment to provide a comprehensive understanding of how landscape attributes influence user experience. The methodological framework is structured to ensure representativeness, statistical reliability, and analytical depth suitable for empirical research in campus environmental studies.

3.1. Research Design

A quantitative research approach was adopted to assess the relationship between landscape elements and user well-being. This approach is widely used in environmental and public health studies to measure user perceptions and behavioral patterns Rhee, Ma, Seo, & Cha, 2022).

A cross-sectional research design was employed to collect data from park users at a single point in time. This design is appropriate for identifying relationships between environmental variables and human responses.

3.2. Study Area and Campus Selection

The study will be conducted in selected public tertiary institutions in Lagos State chosen based on Student population, Availability of landscape features and Accessibility

- Caleb University, Imota Lagos State
- Lagos State University of Science and Technology, Ikorodu Lagos State
- Lagos State University Teaching Hospital, Department of Medicine, Idi-araba, Surulere, Lagos State

Sample Size and Sampling Technique

A total sample size of 300 **respondents** was adopted to ensure statistical robustness. The sample was evenly distributed across the 3 universities (100 respondents per park).

A systematic random sampling method was adopted for collecting data. Every third user encountered during the study period in the chosen landscapes of the tertiary institution was chosen for the study, provided they were using the outdoor spaces of the institution and were willing to respond to the queries. This sampling method has reduced the chances of selection bias and has provided a wide coverage of various categories of users at different times of the academic session.

3.3. Data Collection Methods

Questionnaire Survey

A structured questionnaire was administered to respondents. The instrument was divided into

four major sections:

i. Demographic characteristics
ii. landscape accessibility and functionality
iii. aesthetic and ecological quality
iv. impact on physical health.

Site Observation

The campuses were assessed based on:

i. Vegetation quality
ii. Cleanliness
iii. Shading
iv. Seating availability
v. Accessibility

IV. DATA ANALYSIS AND RESULTS

Data were analyzed using SPSS through:

i. Descriptive statistics (mean, frequency, percentage)

ii. Correlation analysis

iii. Multiple regression analysis

DEMOGRAPHIC DISTRIBUTION

Table 4.1: Demographic Distribution

Demographic Variable	Category	Number	Percentage (%)
Gender	Female	136	45%
	Male	137	45%
	Prefer not to say	27	9.1%
Age	15–20 years	245	80%
	21–25 years	54	17%
	26–30 years	2	0.3%
	31 years and above	0	0%
Academic Level	Undergraduate	192	64%
	Postgraduate (MSc)	96	32%
	Postgraduate (PhD)	12	4%
Average Hours Spent on Campus	Less than 4 hrs	63	21%
	4–8 hrs	192	64%
	More than 8 hrs	45	15%
Years Spent on Campus	1 year	60	20%
	2 years	120	40%
	3 years	30	10%
	4 years and above	60	20%

LANDSCAPE ACCESSIBILITY AND FUNCTIONALITY

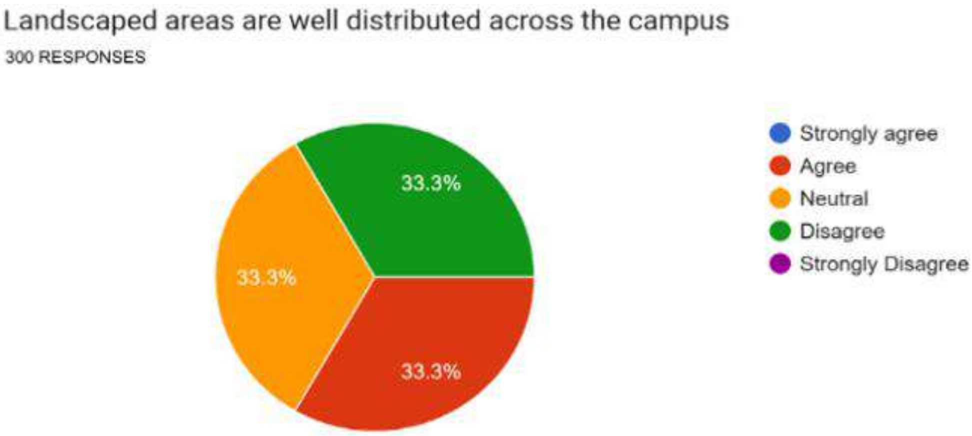

Fig.1: Pie chart showing students access to landscape areas

ANALYSIS

The results indicate a **mixed perception of landscape distribution across the campus**. While 36.4% of respondents agree that landscaped areas are well distributed, an equal proportion (36.4%) disagree, suggesting inconsistency in spatial planning. Additionally, 27.3% remain neutral, indicating uncertainty or variability in user experience.

Overall, this implies that **landscape distribution is not uniformly effective**, and improvements are needed to ensure balanced accessibility across the campus destinations. Weekly usage dominance reflects structured recreational patterns, while daily users are more associated with physical exercise and routine relaxation activities.

LANDSCAPE ELEMENTS CHARACTERISTICS

Table 4.2: Perception of landscape elements

Variable	Mean	Std. Dev
Vegetation Quality	4.18	0.68
Accessibility	3.95	0.72
Walkability	3.88	0.75
Maintenance Condition	3.62	0.83
Shading Provision	3.79	0.77
Seating Availability	3.34	0.91

Analysis

Vegetation quality recorded the highest mean score, (4.18), which implies that students are highly satisfied with greenery and natural elements in the campus environment. Accessibility and walkability also recorded high mean scores, implying that most students can easily access landscaped environments.

However, seating availability recorded a lower mean score, (3.34), implying that students are concerned about insufficient outdoor furniture in the campus landscape. In addition, maintenance condition recorded a lower mean score, (3.62), implying that students are concerned about the poor maintenance of the campus landscape. Shading provision recorded a moderate mean score, implying that although some areas are comfortable, more improvement is needed.

USER WELL-BEING INDICATOR

Table 4.3: Well-Being Indicators

Indicator	Mean	Std. Dev
Psychological Restoration	4.26	0.63
Mood Improvement	4.08	0.69
Physical Comfort	3.87	0.74
Social Interaction	3.76	0.80

Analysis

Psychological restoration showed the highest mean value for psychological restoration, at 4.26. This showed that campus elements play a significant role in alleviating stress and promoting mental relaxation. Improvement of mood showed a high mean value, showing the positive effects of a green environment on mood.

For physical comfort, a moderate mean value of 3.87 was noted. This showed that physical comfort is generally satisfactory. For social interaction, a slightly low mean value of 3.76 was noted.

Site Observation Analysis

Observations in different tertiary institutions showed that:

- Areas with high vegetation density, such as tree canopies, showed higher concentrations of users, especially on hot days
- Inadequate seating arrangements resulted in a lower time spent in outdoor areas
- Shaded areas showed higher usage compared to open areas
- Maintenance levels directly affected users' perceptions of cleanliness and usage
- Walkways with good connectivity showed higher pedestrian activity

4.1. DESCRIPTIVE STATISTICS

Descriptive analysis based on 300 respondents revealed that:

- Most of the users belonged to the 18-30 age group, thus campus landscapes were used by young adults
- Frequent users of landscaped areas had higher well-being
- Landscapes with better vegetation, accessibility, and shading had higher satisfaction levels
- Landscapes with poor maintenance and insufficient seating had a negative effect on the comfort of users and increased usage

4.2. CORRELATION BETWEEN LANDSCAPE ELEMENTS AND USER WELL-BEING

Correlation Analysis (Pearson's r)

Variables	Correlation (r)	Significance
Vegetation vs Psychological Restoration	0.71	$p < 0.01$
Shading vs Physical Comfort	0.64	$p < 0.01$
Seating vs Social Interaction	0.58	$p < 0.05$
Maintenance vs Overall Satisfaction	0.66	$p < 0.01$
Accessibility vs Usage Frequency	0.60	$p < 0.01$

Interpretation

A strong positive correlation exists between vegetation and psychological restoration, implying that the greener the campus environment, the better the mental well-being. There is also a strong positive correlation between shading and physical comfort, which implies the significance of the feature in the environment. The seating availability moderately correlates with social interaction, implying that the provision of seating areas can enhance the interaction of the environment's users. Maintenance condition has a strong impact on satisfaction, while accessibility has a significant impact on the use of the environment.

4.3. MULTIPLE REGRESSION ANALYSIS

A regression model was developed to predict overall well-being:

Model Summary:

- $R^2 = 0.66$
- Adjusted $R^2 = 0.64$
- $F (6, 293) = 142.5$, $p < 0.001$

INFLUENCE OF PARK CHARACTERISTICS ON WELL-BEING

Regression Coefficients

Variable	Beta (β)	Significance
Vegetation	0.45	$p < 0.001$
Shading	0.33	$p < 0.01$
Maintenance	0.29	$p < 0.01$
Accessibility	0.21	$p < 0.05$
Walkability	0.18	$p < 0.05$
Seating	0.15	$p < 0.05$

Interpretation

Vegetation was found to be the most important predictor of users' well-being, reinforcing the significance of green spaces in campus design. Shading and maintenance were also found to be important, suggesting that users' comfort with the environment, as well as maintenance, are vital. The model accounts for 66% of the variance in users' well-being, indicating a strong relationship between users' outcomes and landscape elements.

SUMMARY OF FINDINGS

This analysis has shown that:

1. Campus landscape elements contribute to psychological restoration and satisfaction
2. Vegetation and greenery have the greatest impact on user experiences
3. Shading and maintenance have a critical impact on physical satisfaction and comfort
4. Accessibility and walkability have an impact on the frequency of use
5. V Lack of seating provision impacts social interaction and stay duration

V. DISCUSSION

The findings of this study confirm that landscape elements within public tertiary institutions significantly influence users' well-being in Lagos State. The strong relationship between vegetation and psychological well-being supports recent studies which show that exposure to green spaces is positively associated with improved mental health, reduced loneliness, and enhanced overall well-being (Zhang, Mavoa, Zhao, Raphael, & Smith, 2020).

The high impact of vegetation also aligns with contemporary research emphasizing the restorative capacity of natural environments, where interaction with greenery enhances cognitive functioning, emotional stability, and mental recovery (Wang, Lin, & Lin,2025). Within the campus context, this suggests that students exposed to well-designed green landscapes experience reduced academic stress and improved concentration levels.

Shading, accessibility, and overall spatial quality were found to significantly influence landscape usage, which is consistent with recent studies identifying accessibility, comfort, and safety as fundamental determinants of effective public space utilization and user engagement (Huang, Ye, & Chen, 2025). Similarly, maintenance conditions influenced user satisfaction, supporting recent findings that emphasize the importance of landscape quality and upkeep in enhancing user experience and perceived environmental value.

The findings also support recent research indicating that well-designed and frequently used green spaces contribute to improved life satisfaction, physical activity, and overall health outcomes. The high levels of psychological restoration, mood improvement, and physical comfort observed in this study further confirm the critical role of landscape elements in promoting users' well-being within tertiary institutions

5.1. Conclusion

This study, therefore, sought to investigate the significance of landscape elements in enhancing the well-being of users in tertiary institutions in Lagos State. From the study, the significance of vegetation, shading, maintenance, accessibility, walkability, and seating in enhancing the well-being of users in tertiary institutions was confirmed. In particular, this study showed that vegetation is a very significant factor in enhancing the well-being of users in tertiary institutions in Lagos State. Shading and maintenance are also very significant factors in enhancing the well-being of users in tertiary institutions in Lagos State.

From this study, it is also evident that the campus landscape is highly used by young adults, particularly students in tertiary institutions in Lagos State. It is also evident that the campus landscape is a regular space used by users in tertiary institutions in Lagos State. However, the moderate levels of social interaction and physical comfort in the campus landscape suggest that more inclusive, functional, and user-centered design strategies are needed to cater to the diverse needs of users in tertiary institutions in Lagos State.

5.2. Recommendations

According to the findings, the study recommends that:

- Campus planners and administrators should strive for the incorporation of GI in tertiary institutions for psychological restoration and student well-being
- The management of institutions should strive for improved security and safety in the campus landscape for increased usage and user comfort
- Maintenance and management of the landscape should be enforced for sustainability of environmental quality and user satisfaction
- The landscape should be designed with adequate seats, shaded areas, and interactive spaces for increased social interaction and usage
- The campus landscape should be made inclusive, accommodating users of different ages, physical, and academic needs in the institution

REFERENCES

[1] Sadeq, A. Z., Ismail, W. N. W., & Manaf, A. A. (2026). Green spaces design in university campus: A review of landscape practice of sustainability and students' well-being. *Malaysian Journal of Sustainable Environment, 13*(1), 165–190. https://doi.org/10.24191/myse.v13i1

[2] Akindejoye, F., Ezedinma, U., & Ike, N. (2021). A case study of urban design for wellbeing and mental health in Lagos, Nigeria. *Journal of Urban Design and Mental Health, 7*, 10. https://www.urbandesignmentalhealth.com/journal-7-case-study-lagos

[3] Tongyun, W., Wei, Z., & Fei, X. (2024). The role of landscape design in enhancing environmental sustainability and human well-being. https://doi.org/10.1016/j.landurbplan.2024

[4] Hartig, T., Mang, M., & Evans, G. W. (1991). Restorative effects of natural environment experiences. *Environment and Behavior, 23*(1), 3–26. https://doi.org/10.1177/0013916591231001

[5] Berto, R. (2014). The role of nature in coping with psycho-physiological stress: A literature review on restorativeness. *Behavioral Sciences, 4*(4), 394–409. https://doi.org/10.3390/bs4040394

[6] Murugadoss, D., Singh, H., & Thakur, P. (2024). Urban forests and microclimate regulation. In *Urban forests, climate change and environmental pollution*. Springer. https://doi.org/10.1007/978-3-031

[7] Gungormus, D. B., & Pérez-Mármol, J. M. (2025). Participating in tree planting improves mood, reduces stress, and alleviates anxiety. *Ecopsychology, 17*(2), 94–107. https://doi.org/10.1089/eco.2024

[8] Yin, B., Wang, L., Xu, Y., & Heng, K. C. (2025). A study on spatial perception and inclusive characteristics of outdoor activity spaces. *Buildings, 15*(6), 895. https://doi.org/10.3390/buil+dings15060895

[9] Alnaim, A. A., Dano, U. L., & AlQahtany, A. (2025). Factors influencing social interaction among neighborhood residents in public open spaces. *Future Cities and Environment, 11*. https://doi.org/10.5334/fce

[10] Rhee, J. H., Ma, J. H., Seo, J., & Cha, S. H. (2022). Review of applications and user perceptions of smart home technology. *Journal of Computational Design and Engineering, 9*(3), 857–889. https://doi.org/10.1093/jcde/qwac032

[11] Zhang, Y., Mavoa, S., Zhao, J., Raphael, D., & Smith, M. (2020). The association between green space and adolescents' mental well-being: A systematic review. *International Journal of Environmental Research and Public Health, 17*(18), 6640. https://doi.org/10.3390/ijerph17186640

[12] Wang, P., Lin, J., & Lin, W. (2025). Effects of restorative environments on mental health and its cognitive neural mechanisms. *Frontiers in Forests and Global Change, 8*, 1651800. https://doi.org/10.3389/ffgc.2025.1651800

International Journal of Environment, Agriculture and Biotechnology
Vol-11, Issue-3; May-Jun, 2026
Peer-Reviewed International Journal
Journal Home Page Available: https://ijeab.com/
Journal DOI: 10.22161/ijeab

Analysis of Spatiotemporal Variations and Driving Mechanisms of Ecological Environment Quality in Yantai City Based on the XGBoost-SHAP Model

Jinli Zhou, Ruei-Yuan Wang*

School of Sciences, Guangdong University of Petrochem Technology (GDUPT), Maoming 525000, China

Received: 30 Mar 2026; Received in revised form: 27 Apr 2026; Accepted: 03 May 2026; Available online: 13 May 2026

Abstract— *Conducting long-term spatiotemporal monitoring of ecological environment quality and identifying its driving mechanisms are of great significance for coordinating ecological protection with high-quality regional economic development. Based on Landsat remote sensing data from 2005 to 2025 on the Google Earth Engine (GEE) platform, this study employed Principal Component Analysis (PCA) to construct the Remote Sensing Ecological Index (RSEI), analyzing the spatiotemporal evolution patterns of RSEI in Yantai City. The study further utilized the explainable extreme gradient boosting model (XGBoost-SHAP) to reveal key natural and anthropogenic drivers of ecological environment quality, along with their nonlinear and interactive effects. The results indicate that: (1) On a temporal scale, the RSEI of Yantai City exhibited a fluctuating trend of initial decline followed by an increase, then another decline and subsequent rise, with a multi-year average of 0.438, indicating an overall moderate level of ecological environment quality; (2) Spatially, the RSEI in the study area showed significant heterogeneity, with high-value areas concentrated in central Yantai and low-value areas distributed near the coast; (3) Ecological quality was primarily driven by land use type and precipitation, with anthropogenic factors also playing a significant role. This research provides methodological references and scientific foundations for ecological monitoring, risk assessment, and territorial spatial optimization in coastal cities.*

Keywords— ***Remote Sensing Ecological Index (RSEI), XGBoost-SHAP Model, Google Earth Engine (GEE), Principal Component Analysis (PCA), Ecological Environment Quality (EEQ), Yantai City***

I. INTRODUCTION

Environmental degradation caused by human activities, along with intensive urbanization, has posed severe crises and challenges to global ecosystems (Yang et al., 2024). The ecological environment serves as a critical foundation for the sustainable development of human society, directly influencing regional economic growth potential and residents' well-being (Liu et al., 2024). In the face of these pressing ecological challenges, effectively monitoring environmental changes has become a key priority in current conservation efforts. Remote sensing technology, with its advantages of large-scale, rapid, comprehensive, and continuous observation, enables holistic monitoring of ecological changes (Geng et al., 2022). Building on this, Xu Hanqiu (2013) proposed the Remote Sensing Ecological Index (RSEI) (Xu, 2013), which integrates multiple indicator factors based on remote sensing data. It identifies greenness, wetness, heat, and dryness as four crucial indicators linked to human survival, development, and subjective perception of ecological conditions. By synthesizing various ecological factors, RSEI provides a quantitative method for assessing ecosystem health and environmental quality, now widely applied for rapid and objective evaluation of regional ecological conditions (Huang et al., 2024).

Moreover, long-term ecological environment quality (EEQ) monitoring is essential for a comprehensive understanding of environmental changes and for providing substantial data to support decision-making. However, this approach heavily relies on large-scale, high-frequency remote sensing data, and traditional assessment methods are often constrained by bottlenecks in acquiring and preprocessing massive remote sensing datasets. Google Earth Engine (GEE), with its integrated multi-source data resources and powerful cloud computing capabilities, effectively addresses the time-consuming and labor-intensive challenges of conventional methods. The platform eliminates the need for local downloads and complex preprocessing steps such as radiometric calibration and atmospheric correction, enabling efficient large-scale time-series analysis. It has been widely applied in regional long-term ecological environment quality research (Wang et al., 2025; Zhang et al., 2025).

Accurately identifying the key drivers of ecological environment quality changes is fundamental to scientifically formulating conservation and restoration strategies and implementing targeted measures. Current studies commonly employ methods such as multiple regression analysis (Wei et al., 2021), structural equation modeling (Xu et al., 2025), geographically weighted regression (Sun et al., 2024), and geographical detectors (Zhang et al., 2024). In contrast, machine learning approaches, with their strong nonlinear fitting and high-dimensional data processing capabilities, offer a new research pathway for identifying and attributing RSEI driving factors. Among these, the extreme gradient boosting (XGBoost) algorithm combined with Shapley additive explanations (SHAP) models establishes an analytical paradigm that balances predictive performance and interpretability, significantly outperforming traditional methods (Bao et al., 2025). This approach has been widely adopted across numerous fields.

Currently, there is limited research on ecological environment monitoring in coastal cities. Therefore, this study takes the coastal city of Yantai as an example, using the RSEI index to conduct ecological monitoring and analysis of the area. It constructs and calculates the remote sensing ecological index of Yantai City to promptly and objectively assess the quality of the ecological environment and its spatiotemporal distribution characteristics. The aim is to provide a scientific basis for urban construction and ecological environmental protection under the context of rapid urbanization (Yuan et al., 2022).

II. STUDY AREA AND DATA SOURCES

2.1 Study Area

Yantai City is located in the eastern part of the Shandong Peninsula (between E121°57′~E119°34′ and N38°23′~N36°16′), situated between the two major economic zones of Beijing-Tianjin-Hebei and the Yangtze River Delta, serving as a crucial port city in the Bohai Rim region (Figure 1). The city administers five municipal districts—Zhifu, Fushan, Muping, Laishan, and Penglai—as well as six county-level cities: Longkou, Laiyang, Laizhou, Zhaoyuan, Qixia, and Haiyang, boasting significant geographical advantages. The region is predominantly characterized by low mountains and hills, featuring a composite landform of mountains, hills, and plains, with distinct spatial variations in hydrothermal conditions and underlying surface types.

As a typical area of land-sea interaction and rapid urbanization, its ecosystem is driven by both natural evolution and human activities, resulting in prominent spatiotemporal heterogeneity in environmental quality. This study employs the RSEI and XGBoost models to dynamically assess ecological environment quality, providing an interpretative method for identifying the evolution of ecological quality and its driving mechanisms in the region.

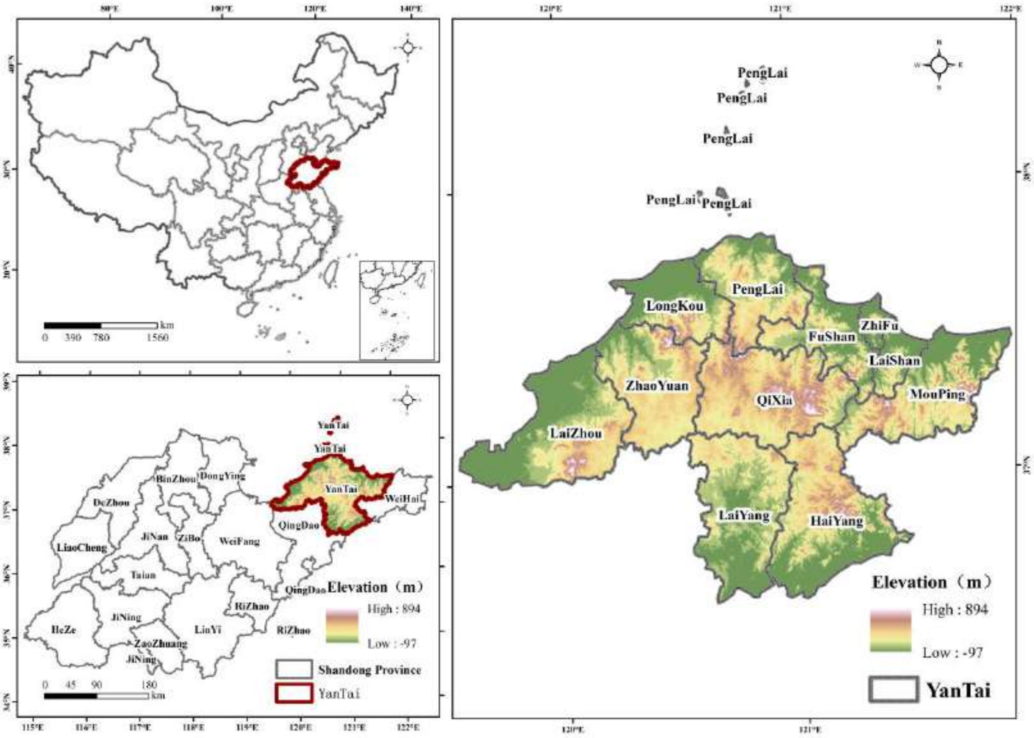

Fig.1 Topographic Overview Map of Yantai City

2.2 Data Sources

The data used in this study can be broadly categorized into two types: (1) RSEI data generated from remote sensing imagery and (2) various data sources for driving factor analysis, as detailed below.

(1) RSEI Data Generated from Remote Sensing Imagery

The Landsat remote sensing imagery data from the Google Earth Engine (GEE) platform consists of Tier 1 (T1) Surface Reflectance (SR) products (Wang et al., 2023). The remote sensing data involved include surface reflectance data from Landsat 5 (TM) and Landsat 8 (OLI), with a spatial resolution of 30 meters. These datasets have undergone preprocessing steps such as radiometric correction, atmospheric correction, and geometric correction.

GEE provides a robust cloud-based platform capable of processing and analyzing large-scale remote sensing datasets, making RSEI computation faster and more convenient. Additionally, GEE's parallel cloud computing capabilities significantly enhance image processing efficiency, addressing issues of data gaps caused by cloud cover. This platform also holds potential for expanding the application of RSEI in large-scale, long-term ecological monitoring.

Based on the aforementioned Landsat SR data, the four core component indicators for calculating RSEI were extracted and computed in GEE: Normalized Difference Vegetation Index (NDVI), Normalized Difference Bare Soil and Built-up Index (NDBSI), Wetness Component (WET), and Land Surface Temperature (LST). Subsequently, principal component analysis (PCA) was applied to integrate these four indicators, constructing the comprehensive EEQ index RSEI. To ensure the scientific validity and reliability of the inversion results, the selection and correction of image data adhered to strict standards. Considering the impact of vegetation phenological differences on image data, this study exclusively utilized images from the peak vegetation growth season (June to October) (Li et al., 2025), with water bodies masked (threshold value of 0.05).

(2) Various Data Sources for Driving Factor Analysis

The formation of regional ecological environments is the result of interactions between natural factors and human activities. Drawing on previous research and considering the actual conditions of the study area, ten indicators were selected from two dimensions—natural and human activities. These include:

X1: Slope (SLO), X2: Elevation (DEM), X3: Population distribution (POP), X4: Annual precipitation (PRE), X5: GDP, X6: Annual mean air temperature (AT), X7: Nighttime light intensity (NTL), Under the Land use type (China Land Cover Dataset, CLCD): X8: Built-up land (BL), X9: Grassland (GL), X10: Forest land (FL).

These indicators are used to explore the influencing mechanisms of RSEI in the study area for each year, as detailed in Table 1. Among them,

A. NDVI, NDBSI, WET, and LST were derived from calculations on the GEE platform.

B. AT data was sourced from the China Meteorological Data Network, with a spatial resolution of 1000m; used to explore the driving factors of RSEI.

C. PRE data was obtained from the National Tibetan Plateau Data Center, with a spatial resolution of 1000m; used to explore the driving factors of RSEI.

D. DEM data was sourced from the Geospatial Data Cloud, with a spatial resolution of 30m; used to explore the driving factors of RSEI.

E. Slope data was calculated from DEM, with a spatial resolution of 30m; used to explore the driving factors of RSEI.

F. Land use data was derived from Wuhan University's China 30m Annual Land Cover Dataset (CLCD), with a spatial resolution of 30m; used to explore the driving factors of RSEI.

G. NTL data was sourced from the National Oceanic and Atmospheric Administration (NOAA), with a spatial resolution of 1000m; used to explore the driving factors of RSEI.

H. POP data was obtained from the Oak Ridge National Laboratory's LandScan Global Population Dataset, with a spatial resolution of 1000m; used to explore the driving factors of RSEI.

For data preprocessing, the fishnet tool in ArcGIS 10.8 was used to create a 1km × 1km grid, followed by processing natural factor data (including AT, PRE, DEM, SLO, and CLCD) and human activity factor data (including NTL, GDP, and POP) using the "Extract Multi Values to Points" tool for subsequent RSEI influencing factor analysis. All geographic data in this study were uniformly projected in the WGS_1984_UTM_Zone_50N coordinate system.

Name	Source	Purpose
NDVI	Generated from running on the GEE platform (https://developers.google.cn/earth-engine?hl=zh-cn)	For subsequent RSEI calculations
NDBSI		
WET		
LST		
Temperature(AT)	China Meteorological Data Network（http://data.cma.cn/）	To explore the driving factors of RSEI
Average annual precipitation(PRE)	Qinghai-Tibet Plateau Scientific Data Center (https://data.tpdc.ac.cn/)	
Elevation(DEM)	Geospatial Data Cloud（https://www.gscloud.cn/）	
Slope (SLO)	Calculated from DEM	
Land use(CLCD)	Wuhan University's CLCD China 30m Annual Land Cover Dataset（https://doi.org/10.5281/zenodo.18180184）	
Population(POP)	Oak Ridge National Laboratory, USA, LandScan Global Population Dataset（https://landscan.ornl.gov/）	

GDP	China GDP Spatial Distribution Dataset (https://github.com/thestarlab/ChinaGDP)
Nighttime light data (NTL)	Earth Observation Group under the National Oceanic and Atmospheric Administration (NOAA) of the United States (Earth Observation Group, EOG) (https://payneinstitute.mines.edu/eog/)

Table 1: Required Data and Sources

III. METHODOLOGY

3.1 Method

This study utilized the GEE platform to acquire remote sensing ecological indicator data, including NDVI, WET, NDBSI, and LST metrics. These indicators were synthesized into an ecological index (RSEI) through PCA to interpret the spatiotemporal distribution patterns after grading. The XGBoost model was employed to establish nonlinear response relationships between ecological quality and driving factors. Key driving mechanisms were then analyzed using SHAP importance analysis and PDP (Partial Dependence Plot). Finally, a coupled analysis of the results was conducted to derive scientific evidence for the study area (Figure 2).

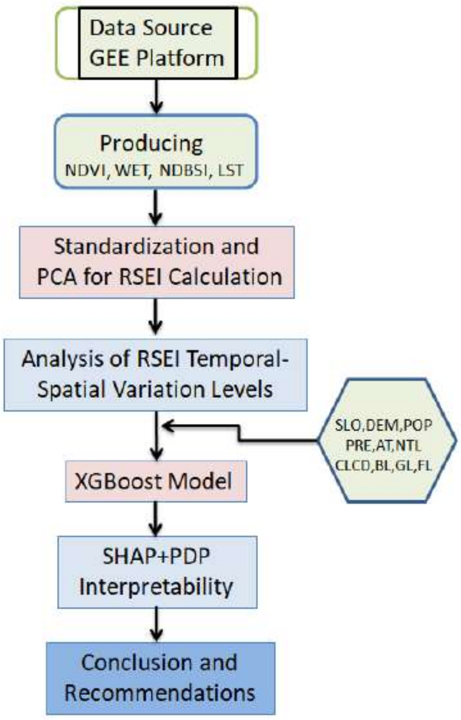

Fig.2 The Technical Roadmap of the Study

3.2 Construction Principle of RSEI

RSEI is a comprehensive model for quantitatively assessing regional ecological environment quality based on multi-source remote sensing data. This model integrates four key ecological parameters: greenness (NDVI), wetness (WET), dryness (NDBSI), and heat (LST). It converts the values of these factors into dimensionless index values ranging from [0,1], where higher values indicate better regional ecological environment quality (Zhang et al., 2026).

Referencing the five-level classification concept from the "Technical Criterion for Eco-Environmental Assessment" (HJ/T192-2006) and following the RSEI grading convention established by Xu Hanqiu et al. (2013), the normalized RSEI values (0-1) are divided into five levels at intervals of 0.2: 0.8-1.0 (Excellent), 0.6-0.8 (Good), 0.4-0.6 (Moderate), 0.2-0.4 (Fair), and 0-0.2 (Poor) (Zhou et al., 2023).

The Normalized Difference Vegetation Index (NDVI) is one of the core indicators of RSEI, calculated as shown in Equation (1).

$$NDVI = \frac{\rho_{NIR} - \rho_{RED}}{\rho_{NIR} + \rho_{RED}} \quad (1)$$

Here, NIR represents the near-infrared band reflectance, and R is the red band reflectance. NDVI utilizes the strong absorption of the red band and the high reflectance of the near-infrared band by vegetation to measure vegetation coverage and growth vitality. A higher NDVI indicates denser vegetation, reflecting stronger ecosystem functions such as photosynthetic production and soil-water conservation. Conversely, a lower NDVI suggests sparser vegetation, which may indicate issues like bare land expansion, urban development, or ecological degradation.

The Wetness Index (WET) is constructed based on the Tasseled Cap Wetness (TCW) transformation, with tailored algorithms for different sensors (e.g., the Landsat series). Taking Landsat 8 as an example, WET is derived from a linear combination of reflectance values in the blue, green, red, near-infrared, shortwave infrared 1, and shortwave infrared 2 bands. The formula is (2):

$$WET = 0.1511\rho_{Blue} + 0.1973\rho_{Green} + 0.3283\rho_{Red} + 0.3407\rho_{NIR} - 0$$

(2)

The Wetness Index (WET) simulates the moisture content of an ecosystem. High values correspond to wet surface conditions (such as water bodies, wetlands, and areas with high vegetation coverage), indicating good water retention and regulation in wetland systems. Low values correspond to dry conditions (such as arid regions and built-up areas), representing water stress in ecosystems or disruption of the hydrological cycle due to human interference.

The Dryness Index employs the Normalized Difference Built-up and Barren Index (NDBSI) to focus on surface desiccation and human construction disturbances, calculated using formulas (3), (4), and (5).

$$NDBSI = \frac{(SI+BI)}{2} \quad (3)$$

$$SI = \frac{\rho_{SWIR1}+\rho_{RED}-\rho_{NIR}-\rho_{Blue}}{\rho_{SWIR1}+\rho_{RED}+\rho_{NIR}+\rho_{Blue}} \quad (4)$$

$$SI = \frac{\rho_{SWIR1}-\rho_{NIR}}{\rho_{SWIR1}+\rho_{NIR}} \quad (5)$$

The NDBSI integrates bare soil and construction information, with high values corresponding to built-up areas and bare land, reflecting the compression of ecological space and surface desiccation caused by human development, which are typical indicators of ecological degradation. Low values are associated with ecological land such as vegetation and water bodies, representing the natural baseline of the ecosystem.

The Heat Index is derived from Land Surface Temperature (LST) retrieved through remote sensing. Taking Landsat 8 as an example, the thermal infrared band (TIRS) is first used to calculate radiance via the radiative transfer equation, which is then converted to land surface temperature, as shown in Formula (6).

$$LST = \frac{K_2}{Ln\left(\frac{K_1}{L_\lambda}+1\right)} \quad (6)$$

Among them, K1 and K2 are sensor calibration parameters, L_λ represents radiance, and LST reflects the energy balance and thermal environmental stress of the ecosystem. The following conclusions can be drawn: the LST in urban heat island (UHI) areas and industrial agglomeration zones is significantly higher than in other regions, indicating that human activities continuously intensify surface thermal stress and disrupt the spatial structure of biological habitats and material cycles in ecosystems. In contrast, the LST in natural vegetation areas and water bodies is lower than average, demonstrating their stronger thermal regulation capacity within the ecosystem.

3.3 Calculation and Standardization of RSEI

Due to the significant differences in dimensions and value ranges among NDVI, WET, NDBSI, and LST, normalization is required to compress their values into the [0,1] interval, calculated as Equation (7):

$$X_{norm} = \frac{X - X_{min}}{X_{max} - X_{min}} \quad (7)$$

Among them, X is the original indicator value, and Xmin and Xmax are the minimum and maximum values of the indicator in the study area, respectively. To ensure that all indicators are positively correlated (i.e., the higher the indicator value, the better the ecological quality), it is necessary to normalize and then reverse-process indicators such as NDBSI and LST. The normalized NDVI, WET, NDBSI (after reversal), and LST (after reversal) are incorporated into PCA to extract the first principal component (PC1). PC1 contains the maximum variance information of the original indicators and can comprehensively reflect the main differences in ecological quality. The RSEI is constructed using PC1 and calculated as shown in Equation (8).

$$RSEI = \frac{PC1 - PC1_{min}}{PC1_{max} - PC1_{min}} \quad (8)$$

The final RSEI value ranges between [0,1]. A value closer to 1 indicates better ecological quality, while a value closer to 0 signifies poorer ecological quality. By integrating multiple indicators through PCA, the RSEI achieves a comprehensive quantification of the "greenness-wetness-dryness-heat" interactions within ecosystems and provides regionalized results for remote sensing quality assessment (Xu and Deng, 2022).

3.4 XGBoost Model

This study employs the XGBoost algorithm to investigate the independent and interactive effects of natural and anthropogenic factors on the dependent variable RSEI. The XGBoost algorithm, proposed by Chen et al. (2016), is an efficient gradient boosting technique (Chen and Guestrin, 2016). As a forward additive model, it sequentially constructs multiple decision trees and combines them into a strong classifier. The final prediction for each sample is obtained by aggregating the results from all individual decision trees (Meng et al., 2016). Using the selected RSEI influencing factors mentioned above, the model is trained to generate an optimal objective function (Obj) for the decision trees, calculated as Equation (9).

$$\mathrm{Ob}_j = -\frac{1}{2}\sum_{j=1}^{T}\frac{G_j^2}{H_j + \lambda} + \gamma^T \quad (9)$$

In the equation, $G_j = \sum_{i \in I_j} g_i$ represents the sum of the gradients for all samples gi belonging to the j-th leaf node, where gi is the first-order derivative of the function; $H_j = \sum_{i \in I_j} h_i + \lambda$, denotes the sum of all samples hi belonging to the j-th leaf node, where hi is the second-order derivative of the loss function; Tis the number of leaf nodes; λ and γ are hyperparameters. The above formula is used to measure the quality of the tree structure, where a smaller value indicates a better tree structure. The mean absolute error (MAE), root mean square error (RMSE), and coefficient of determination (R^2) are selected as metrics to evaluate the accuracy of model simulation (Niazkar et al., 2024). The calculation formulas are given by (10), (11), and (12).

$$R^2 = \frac{\sum_{i=1}^{n}(y_i - y_i')^2}{\sum_{i=1}^{n}(y_i - y)^2} \quad (10)$$

$$\mathrm{MAE} = \frac{1}{n}\sum_{i=1}^{n}|y_i - y_i'| \quad (11)$$

$$\mathrm{RMSE} = \sqrt{\frac{1}{n}\sum_{i=1}^{n}(y_i - y_i')^2} \quad (12)$$

In the equation, yi represents the actual value, and yi' represents the predicted value. The coefficient of determination R^2 ranges from (−∞, 1], and the closer it is to 1, the better the model's performance, indicating that the predicted results are closer to the true values. MAE and RMSE measure the difference between the model's predicted values and the true values, with smaller values indicating more accurate model results. The training and validation of the model were implemented using Python's XGBoost package.

3.5 SHAP Interpretability Analysis

Although machine learning models excel in predictive performance, their "black box" nature often limits interpretability, making it difficult to uncover the underlying mechanisms between independent and dependent variables. To address this issue and further reveal the intrinsic mechanisms and contribution levels of various natural and human activity factors on RSEI, this study applies SHAP (Shapley Additive Explanations) value analysis. SHAP analysis, proposed by Lundberg et al. (2017), is an interpretable artificial intelligence method based on game theory (Lundberg and Lee, 2017). Its core idea is to provide consistent and reliable local and global explanations for model predictions by calculating the average marginal contribution of each independent variable across all possible feature combinations (i.e., Shapley values).

SHAP values quantify the independent contribution of each variable to the final RSEI prediction for a specific sample (positive values indicate an increase in RSEI, while negative values indicate a decrease). Through aggregated analysis, they can reveal the global importance ranking of variables and their nonlinear relationship patterns with RSEI. Additionally, SHAP interaction values further quantify the strength and direction of the interaction effects between any two independent variables on RSEI, enabling an in-depth exploration of the complex interplay between natural and human activity factors. For detailed SHAP calculation methods, refer to Lundberg and Lee (2017). In this study, SHAP values and their interactions were computed and visualized using the Python shapviz package (Yao et al., 2026).

3.6 PDP Model

The Partial Dependence Plot (PDP) is a model-agnostic global interpretability analysis method that characterizes the marginal effect of one or two features on the model's prediction results, intuitively revealing linear, monotonic, or nonlinear relationships between features and target variables (Friedman, 2001). Its core principle is to calculate the average of the model's prediction results when the target feature takes different values while keeping the distribution of other features unchanged, as mathematically defined in Equation (13).

$$\hat{f}_{x_S}(x_S) = \mathbb{E}_{x_C}\left[\hat{f}(x_S, x_C)\right] = \int \hat{f}(x_S, x_C)d\mathbb{P}(x_C)$$

(13)

In practical calculations, the Monte Carlo method is usually adopted for approximate estimation, as shown in Formula (14).

$$\hat{f}_{x_S}(x_S) = \frac{1}{n}\sum_{i=1}^{n}\hat{f}(x_S, x_C^{(i)})$$ **(14)**

This study combines the results of SHAP feature importance ranking, selects key driving factors to plot PDP curves, analyzes the nonlinear response relationship of each factor to the ecological environmental quality (RSEI) of Yantai City, breaks the "black box" dilemma of the XGBoost model, and provides a more targeted explanatory basis for the driving mechanism of ecological environmental quality (Friedman, 2001).

IV. ANALYSIS AND RESULTS

4.1 Rationality Analysis of RSEI

The analysis shows that the contribution rate of PC1 ranges from 81.40% to 86.34%, indicating that the first principal component effectively explains the major variations in the ecological environmental quality of Yantai City (Table 2). In terms of load coefficients, NDBSI (-0.68) and NDVI (+0.58) have the largest absolute values, which suggests that the expansion of built-up land and vegetation coverage are the two core factors driving the changes in ecological quality of Yantai. Moreover, this dominant mechanism remained highly stable from 2009 to 2025 (Figure 3).

Additional implications are as follows:

1. The contribution rate of PC1 reaches as high as 80%-86%, proving that RSEI is indeed an efficient ecological evaluation tool.

2. Driving mechanism: NDBSI and NDVI play a dominant role, indicating that the ecological environmental quality of Yantai mainly depends on the interplay between "urbanization construction (negative effect)" and "vegetation restoration (positive effect)".

Table 2 PC1 of RSEI in Yantai City during 2005—2025

Index/Year	2005	2009	2016	2021	2025
NDVI	0.59256	0.5774	0.57534	0.58728	0.59135
WET	0.36562	0.3965	0.39452	0.35905	0.35947
NDBSI	-0.69304	-0.68623	-0.68779	-0.69899	-0.68904
LST	-0.18659	-0.19616	-0.20072	-0.19388	-0.21521
Eigenvalue	0.02327	0.2791	0.03699	0.03939	0.04263
Contribution Rate/(%)	81.4091	84.8255	86.3346	86.1506	85.7708

Fig.3 Loading Coefficients of the PC1 of RSEI in Yantai City, 2005—2025

4.2 Spatiotemporal Characteristics of EEQ

4.2.1 Annual Variation of RSEI

In terms of temporal variation, the multi-year average of the RSEI from 2005 to 2025 is 0.438, and the overall EEQ is at the average level (Figure 4), showing a fluctuating trend of initial decline, subsequent rise, another decline and then a further rise. The above periodic fluctuations are closely related to policy orientation in different periods.

From 2005 to 2009, affected by the rapid advancement of urbanization, investment in ecological governance was relatively insufficient, leading to a slight decline in ecological quality. During 2009 to 2016, driven by ecological construction policies such as "Forest City" and "Water Ecological Civilization City", the ecological quality continued to improve and reached its peak. From 2016 to 2021, with the development of new urban areas and the expansion of industrial land, ecological space was squeezed, resulting in a marked drop in ecological quality. From 2021 to 2025, with the implementation of the "Three Lines and One List" zoning control, ecological restoration projects and green low-carbon development policies, the ecological quality has shown a steady improvement trend. Essentially, the periodic fluctuations of ecological quality in Yantai City stem from the interactive effect of development policies and ecological policies in different stages.

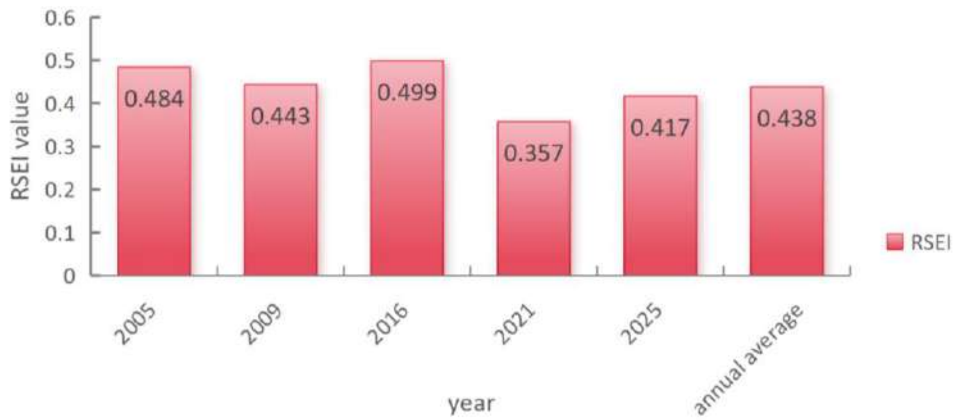

Fig.4 Annual RSEI and Multi-year Mean Value

4.2.2 Spatiotemporal Variation Analysis of RSEI

From 2005 to 2025, the spatial pattern of RSEI in Yantai City exhibited significant phased evolution (Figure 5). In 2005, the overall ecological quality was predominantly moderate, with high-value areas concentrated in the mountainous and hilly regions of Penglai, Zhaoyuan, Laizhou, and Haiyang. The mountainous areas of Qixia were mainly at a moderate level, with localized low-value patches (Figure 6a). By 2009, ecological quality declined across the entire region, with a significant shrinkage of high-value areas in Qixia, forming contiguous low-value zones in the eastern and western plains and urban areas (Figure 6b). In 2016, ecological quality improved slightly, with the core high-value area in Qixia strengthening and forming a contiguous high-value zone with surrounding regions (Figure 6c). After 2021, ecological quality declined again, with Qixia becoming the core low-value area of the entire region, forming an east-west contiguous low-value belt with Laizhou and Zhaoyuan (Figure 6d). By 2025, the overall pattern showed a "central collapse and coastal isolation" scenario, with only fragmented high-value patches remaining in the coastal areas of Penglai, Longkou, Laizhou, and Haiyang. Ecological quality returned to a below-moderate level, highlighting the intensifying pressure of human activities on ecological spaces (Figure 6e).

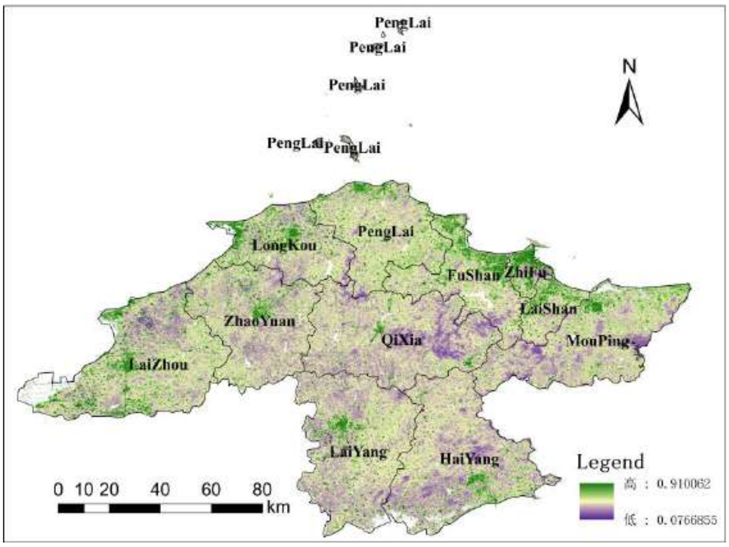

Fig.5 Mean RSEI from 2005 to 2025

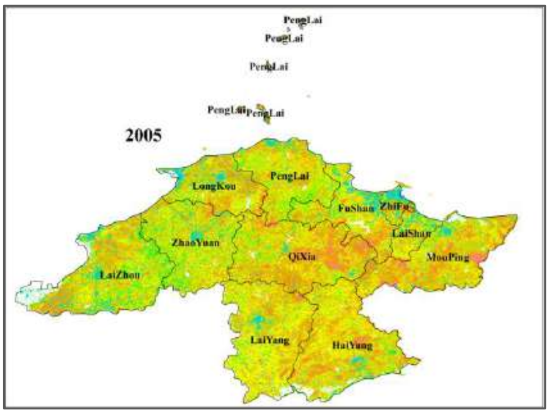

(a)2005 RSEI

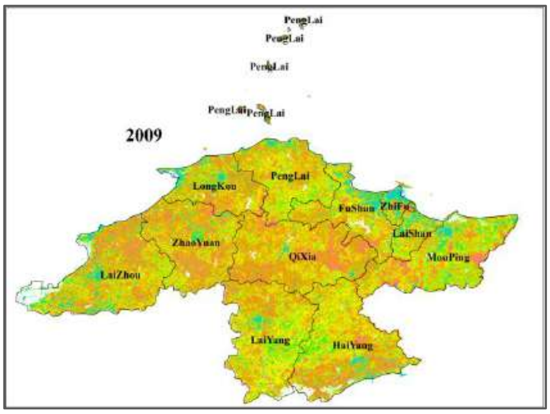

(b)2009 RSEI

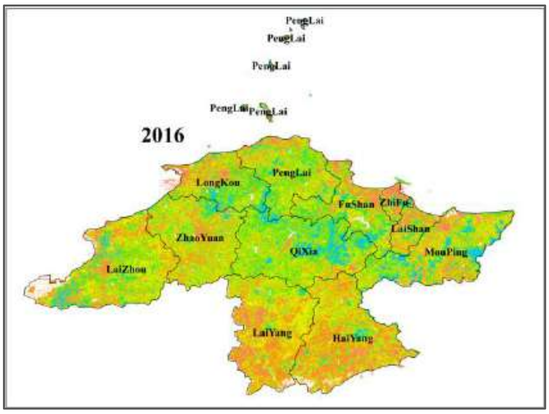

(c)2016 RSEI

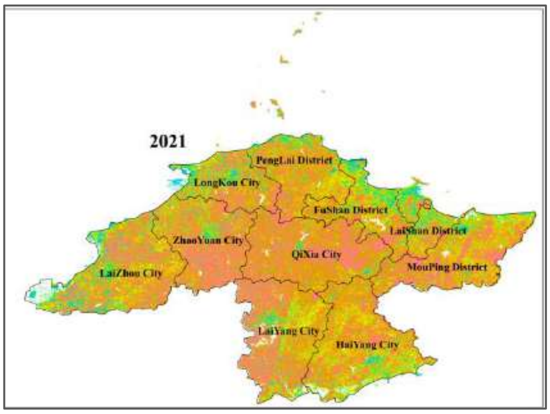

(d)2021 RSEI

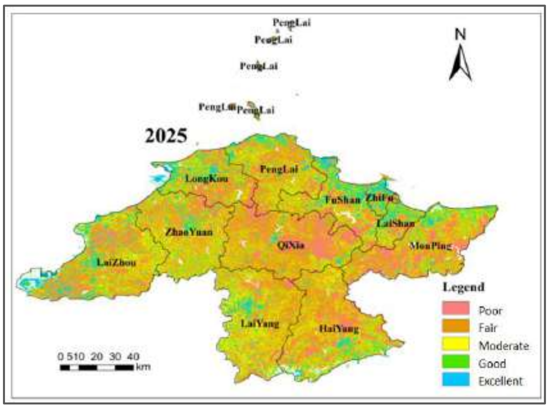

(e)2025 RSEI

Fig.6 Grading Results of Ecological Environment Quality in Yantai City

From 2005 to 2025, the EEQ of Yantai City underwent a significant phased transformation, characterized by initial deterioration followed by restoration, with an overall positive trend (Figures 7 and 8). In 2005, the ecological quality of Yantai was predominantly at moderate and relatively poor levels, with poor-grade areas accounting for only 3%, relatively poor-grade areas reaching 30%, and moderate-grade areas constituting the highest proportion at 44%. Good and excellent-grade areas accounted for merely 17% and 6%, respectively, indicating that the ecological foundation was primarily moderate, with a relatively low proportion of high-quality ecological space.

With rapid urbanization from 2005 to 2021, the ecological environment faced sustained pressure: both the area and proportion of poor and relatively poor grades increased sharply. By 2021, poor-grade areas rose to 26%, and relatively poor-grade areas reached 42%, together accounting for nearly 70% of the total. The proportion of moderate-grade areas significantly shrank to 17%, while good-grade areas declined to 10%, and excellent-grade areas remained low. During this period, urban expansion and the encroachment of construction land on ecological spaces, coupled with declining vegetation coverage, led to continuous degradation of ecological quality in central urban areas and northern coastal plains.

From 2021 to 2025, ecological restoration efforts yielded remarkable results, with quality grades showing a comprehensive rebound: the proportion of poor-grade areas decreased from 26% to 17%, and relatively poor-grade areas dropped from 42% to 37%, with both categories experiencing simultaneous reductions in area. The proportion of moderate-grade areas rebounded to 27%, good-grade areas increased to 12%, and excellent-grade areas recovered to 8%, reflecting a continued expansion of high-quality and moderate ecological spaces.

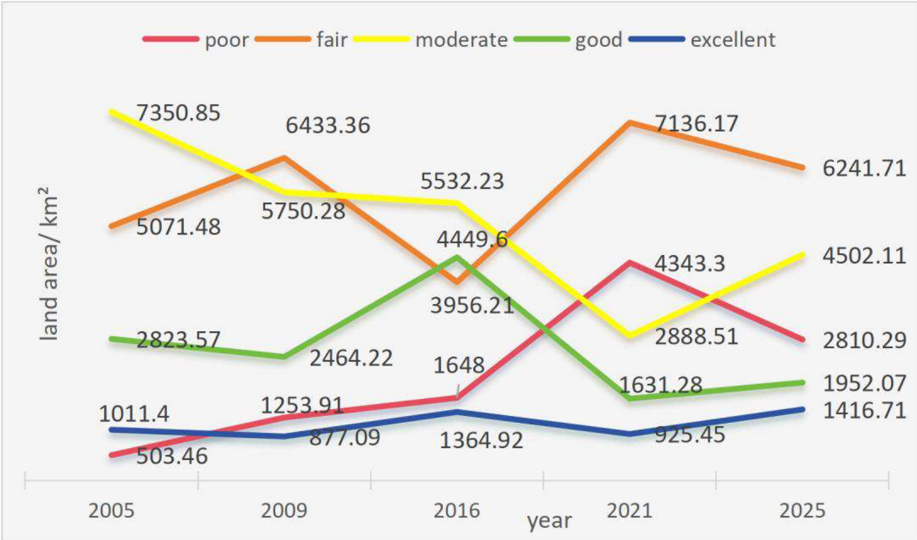

Fig.7 Statistics on Land Area of Each Ecological Environment Quality Grade, 2005–2025

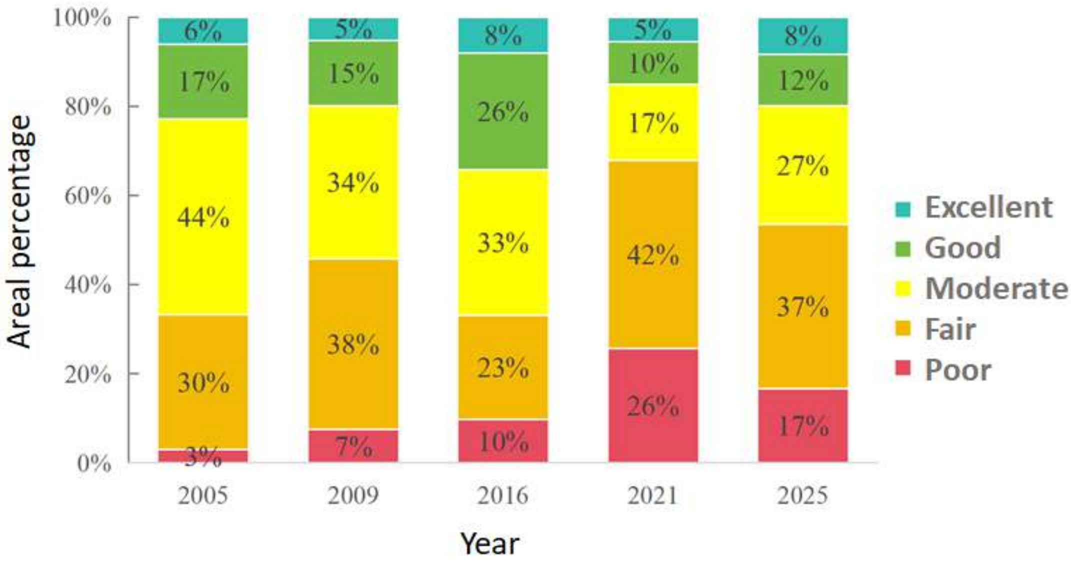

Fig.8 Proportions of Graded Areas of Ecological Environment Quality in Yantai City, 2005–2025

4.3 Analysis of Driving Factors for EEQ

4.3.1 Analysis Based on the XGBoost-SHAP Model

2016 was the peak year for RSEI, exhibiting the most typical spatial differentiation of ecological conditions (Figure 4). Therefore, this year was selected for driving mechanism analysis. The 2016 dataset and influencing indicators were fitted using the XGBoost model in Python, with a random 70%/30% split between the training and testing sets. The model evaluation results showed an R^2 of 0.6485, RMSE of 0.1513, and MAE of 0.151. This R^2 value indicates that the selected factors explain approximately 65% of the RSEI variation, while the remaining portion may be influenced by factors such as soil type, human policies, local micro-topography, etc.

Figure 9 displays the ranking of the importance of various environmental features in predicting RSEI using the XGBoost model. The results show that built-up land (BL) contributes the most to RSEI prediction, followed by precipitation (PRE), forest land (FL), annual average temperature (AT), and grassland (GL), indicating a strong nonlinear relationship between urbanization intensity and ecological quality in the model. Additionally, elevation (DEM), slope (SLO), population (POP), GDP, and nighttime light data (NTL) also exhibit significant importance, exerting notable effects on RSEI distribution.

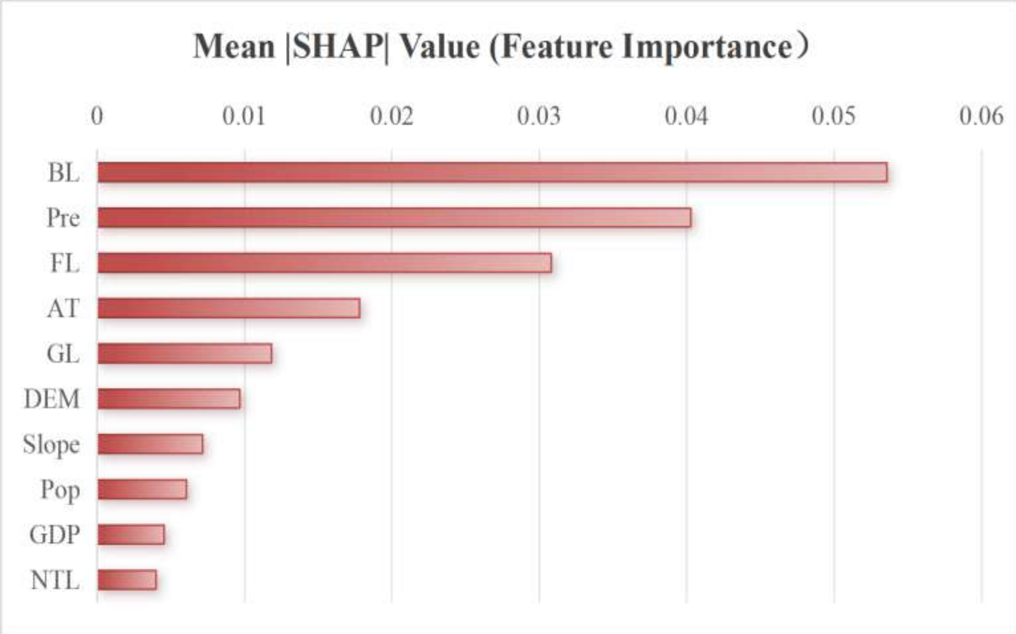

Fig.9 SHAP-based Feature Importance Ranking

Figure 10 further reveals the nonlinear response characteristics of various environmental variables to RSEI predictions. Regions with higher annual precipitation generally correspond to higher RSEI predictions, indicating that sufficient moisture is conducive to improving regional ecological quality. Areas with higher forest coverage also promote RSEI enhancement, which aligns with the regulatory role of water in vegetation growth and surface ecological processes. Construction land has a significant negative impact on RSEI, meaning that regions with a higher proportion of construction land tend to exhibit a declining trend in RSEI, while grassland also shows a negative inhibitory effect on RSEI.

Areas with a higher proportion of construction land tend to have lower RSEI levels, which may be related to ecological degradation processes such as the expansion of impervious surfaces, reduced vegetation cover, and deterioration of surface thermal environments. Indicators reflecting high-quality vegetation conditions, such as forest cover, generally exhibit a positive influence on RSEI in the SHAP scatter plot, suggesting that vegetation growth status is one of the key controlling factors for the spatial distribution of RSEI. The influence patterns of annual average temperature and elevation on RSEI are more complex, indicating that their relationship with RSEI may be jointly regulated by the interaction of multiple climatic and topographic factors.

The interpretative analysis based on SHAP reveals that land use type, precipitation conditions, and human activity intensity are the dominant environmental drivers influencing the spatial distribution of RSEI in the study area, providing a scientific basis for formulating regional ecological protection and land-use optimization strategies.

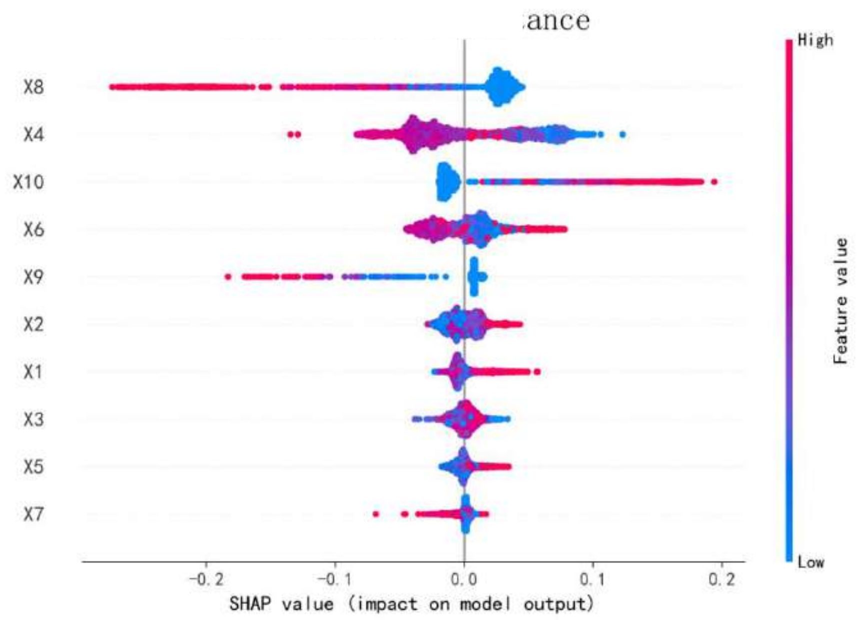

Notes：X1：SLO X2：DEM X3：POP X4：PRE X5：GDP X6：AT X7：NTL X8：BL X9：GL X10: FL

Fig.10 SHAP Feature Dependence Distributions

4.3.2 Interpretability Analysis Based on the PDP Model

According to the analysis results of the PDP (Figure 11), the ecological environment quality (RSEI) of Yantai City exhibits significant nonlinear response characteristics to various driving factors. Combined with the ranking results of feature importance, core driving factors with high contribution rates, including built-up land (BL), annual average precipitation (PRE), forest land (FL), and annual average temperature (AT), are selected to further analyze their nonlinear response patterns.

The PDP curve of annual average precipitation (X4) indicates that within the range of 440~480 mm, the RSEI remains at a high level above 0.56 and stays relatively stable. When the precipitation exceeds 480 mm, the RSEI drop rapidly, reaches a trough around 540 mm, and then rebounds slightly but remains significantly lower than the initial level. The results reveal that moderate precipitation can maintain the stability of regional ecosystems, while excessive precipitation is prone to triggering ecological problems such as soil erosion and runoff scouring, thereby leading to the deterioration of ecological environment quality.

The PDP curve of annual average temperature (X6) shows that in the range of 12.6~12.8℃, the predicted RSEI value rises rapidly and peaks near 12.8℃. Within 12.8~13.4℃, the RSEI decreases continuously with the rise of temperature and falls to the minimum value around 13.4℃. After the temperature exceeds 13.4℃, the RSEI presents a rising trend again. This characteristic suggests that appropriate temperature conditions can optimize the regional hydrothermal matching status and promote vegetation growth and the virtuous cycle of ecosystems. Excessively high temperature will intensify evaporative dissipation, induce drought stress, and exert a negative impact on ecological environment quality. In the high-temperature range, as thermal conditions further increase, ecosystems gradually adapt to the high-temperature environment, resulting in a certain rebound of the RSEI.

The PDP curve of built-up land (X8) demonstrates that when the proportion of built-up land is lower than 0.2, the predicted RSEI value stays at a relatively high level above 0.49. With the continuous increase in the proportion of built-up land, the RSEI shows a sustained downward trend; the decline slows down and remains at a low level within the range of 0.6~0.8, and the RSEI plummets sharply when the proportion approaches 1.0. This feature indicates that the expansion of built-up land has a significant negative stress effect on ecological environment quality, and the higher the intensity of urban development, the more prominent the risk of regional ecological quality degradation.

The PDP curve of forest land (X10) shows that the RSEI is at a low level when the proportion of forest land approaches 0. As the proportion of forest land increases, the RSEI rises rapidly and continuously, with the most obvious growth in the range of 0~0.2, followed by a steady increase and maintenance at a high level in the high-value interval. This characteristic proves that forest land coverage has a significant positive promoting effect on ecological environment quality, serving as a core positive driving factor for the improvement of regional ecological quality. The higher the proportion of forest land, the stronger the stability of the ecosystem.

The short vertical lines at the bottom of Figure 11 mark the distribution density of sample data. The response curves of all factors are mainly concentrated in the sample-dense interval, which verifies the reliability of the analysis conclusions. Overall, PDP analysis reveals the nonlinear response mechanism of ecological environment quality in Yantai City to key driving factors including built-up land, precipitation, forest land and temperature. Among them, low proportion of built-up land, moderate precipitation, high forest land coverage and suitable temperature jointly form the optimal environmental interval for maintaining and improving regional ecological quality.

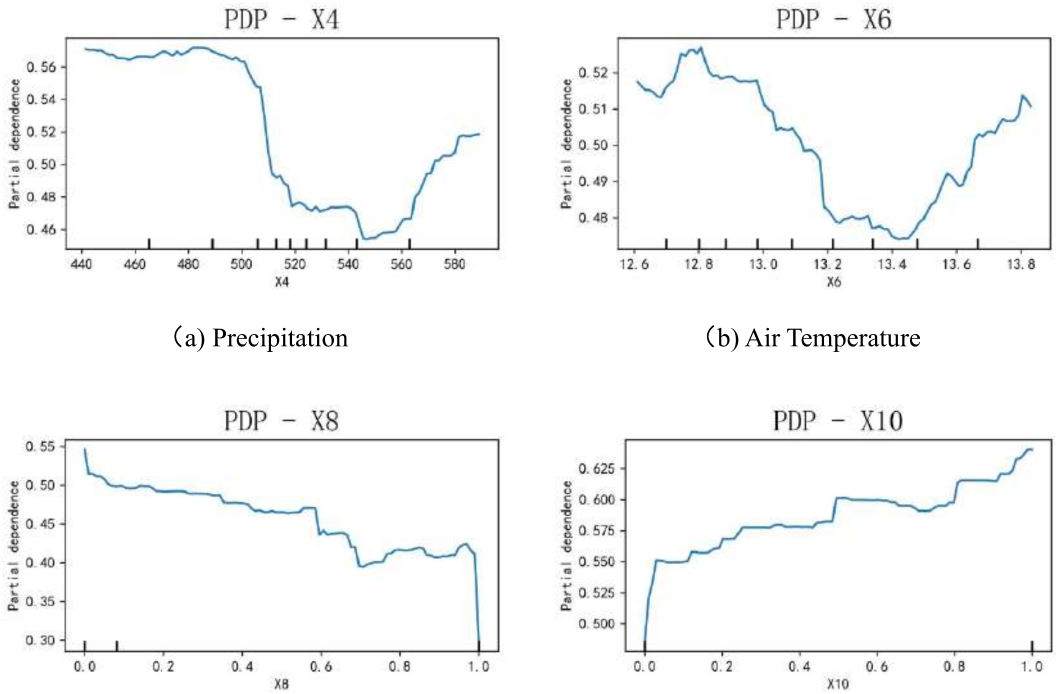

(a) Precipitation (b) Air Temperature

(c)Built-up Land (d) Forest Land

Fig.11 PDP Analysis of Key Environmental Factors

V. CONCLUSION

This study constructs the RSEI of Yantai City from 2005 to 2025 based on GEE platform data, adopts the XGBoost-SHAP model to analyze its influencing factors, and systematically explores the spatiotemporal characteristics of ecological quality in Yantai City during 2005–2025. The main conclusions are as follows:

(1) From 2005 to 2025, the temporal variation of EQQ showed a fluctuating upward trend with an overall moderate grade, experiencing phased changes of "deterioration—improvement—degradation—restoration", and the multi-year average value was 0.438. The phased fluctuation of ecological quality in Yantai City resulted

from the interactive effect of development policies and ecological policies in different periods.

(2) The ecological quality of Yantai City underwent phased changes from 2005 to 2025, eventually forming a spatial pattern of "central depression and coastal isolated high-value zones", with the overall ecological quality declining and the interference effect of human activities intensifying. In terms of spatial differentiation, high-value areas were periodically concentrated in the Qixia mountainous area in the central part, while low-value areas were contiguously distributed in plains and urban built-up areas.

(3) RSEI analysis indicates that NDBSI and NDVI are the core characteristic indicators affecting the ecological quality of Yantai City, corresponding respectively to the negative stress of construction land expansion and the positive promotion effect of vegetation coverage. The XGBoost model further reveals that land use type and annual precipitation are the key factors driving the spatiotemporal evolution of ecological quality. Construction land and forestland serve as the anthropogenic and natural foundations for ecological quality changes by directly altering the surface cover pattern; annual precipitation indirectly regulates the contribution of NDVI to ecological quality by affecting vegetation growth status. The three factors jointly form a complete driving chain of "climate-vegetation cover-anthropogenic disturbance".

Based on GEE and the XGBoost-SHAP model, this study realizes long-time series ecological quality monitoring and interpretable attribution analysis, which can provide scientific support for ecological protection and restoration as well as territorial spatial optimization of coastal cities. The limitations of this study lie in the failure to incorporate variables such as soil type and policy intervention, and the model coefficient of determination R^2 is 0.65. Subsequent research can introduce more feature variables or adopt deep learning models to further improve the model interpretability and explanatory power.

REFERENCES

[1] Bao, S. W., Yu, C. Z., Wan, Z. Y. Spatial mismatch and attribution analysis of flood risk and resilience in megacities: Insights from a “Risk-Resilience-Effect” framework and an interpretable XGBoost-SHAP model. Sustainable Cities and Society, 2025, 131. DOI:10.1016/j.scs.2025.106758.

[2] Chen, T., and Guestrin, C. XGBoost: A scalable tree boosting system. Proceedings of the 22nd ACM SIGKDD International Conference on Knowledge Discovery and Data Mining, 2016: 785-794.

[3] Friedman, J. H. (2001). Greedy function approximation: A gradient boosting machine. Annals of Statistics, 29(5): 1189-1232.

[4] Geng, J. Y., Yu, K., Xie, Z., et al. Analysis of spatiotemporal variation and drivers of ecological quality in Fuzhou based on RSEI. Remote Sensing, 2022, 14(19): 4900.

[5] Huang, Y. T., Yu, H. J., Xu, Y. P., et al. Evaluation and analysis of ecological environment quality in Linhai City based on GEE and remote sensing ecological index. Environmental Science & Technology, 2024, 47(11): 217-228.

[6] Li, J. S., Tu, W. Q., and Lu, X. Z. Long-term variation analysis of ecological environment quality in Ningbo City based on remote sensing ecological index. Urban Geotechnical Investigation & Surveying, 2025(3): 35-39.

[7] Liu, Q., Qiao, J. J., Li, M. J., et al. Spatiotemporal evolution of ecological environmental quality and its dynamic relationships with landscape pattern in the Zhengzhou Metropolitan Area: A perspective based on nonlinear effects and spatiotemporal heterogeneity. Journal of Cleaner Production, 2024, 480. DOI:10.1016/j.jclepro.2024.144102.

[8] Lundberg, S. M., and Lee, S. I. A unified approach to interpreting model predictions. Proceedings of the 31st International Conference on Neural Information Processing Systems, 2017: 4768-4777.

[9] Meng, X. R., Bradley, J., Yavuz, B., et al. MLlib: Machine learning in apache spark. The Journal of Machine Learning Research, 2016, 17(1): 1235-1241.

[10] Niazkar, M., Menapace, A., Brentan, B., et al. Applications of XGBoost in water resources engineering: A systematic literature review (Dec 2018–May 2023). Environmental Modelling & Software, 2024, 174. DOI:10.1016/j.envsoft.2024.105971.

[11] Sun, Q., Qiao, R. T., Jiao, Q. J., et al. Response of ecological quality to land use/cover change during rapid urbanization of Xiong’an New Area. Land, 2024, 13. DOI:10.3390/land13122167

[12] Wang, J. Y., Yang, L. P., Wang, M., et al. Spatiotemporal

change monitoring and driving force analysis of ecological environment quality in the Loess Plateau of northern Shaanxi. Environmental Science, 2025, 46(7): 4522-4533. DOI:10.13227/j.hjkx.202406111.

[13] Wang, Y. X., Xu, Y. Y., Yang, J. J., et al. Dynamic monitoring and spatiotemporal pattern evolution of ecological environment quality in Chongqing City based on Landsat. Acta Ecologica Sinica, 2023, 43(15): 6278-6292.

[14] Wei, Y. H., Qian, J. P., Fan, W. W., et al. Dynamic monitoring of ecological environment quality in Lijiang River Basin based on RSEI. Science of Soil and Water Conservation, 2021, 19(1): 122-131.

[15] Xu, H. Q. Development and application of remote sensing ecological index in urban areas. Acta Ecologica Sinica, 2013, 33(24): 7853-7862

[16] Xu, H. Q., and Deng, W. H. Rationality analysis of MRSEI index and its difference from RSEI index. Remote Sensing Technology and Application, 2022, 37(1): 1-7.

[17] Xu, Y. H., Zhang, T. B., Yi, G. H., et al. Spatiotemporal characteristics and influencing factors of ecological environment quality in the Taihang Mountain Area. Environmental Science, 2025, 46(4): 2428-2438.

[18] Yang, L. Y., Chen, W. X., Zeng, J., et al. Gradient differences of urbanization impact on habitat quality in the Yangtze River Basin. Acta Ecologica Sinica, 2024, 44(10): 4038-4050. DOI:10.20103/j.stxb.202301280140.

[19] Yao, X., Chen, X., Wang, X. W. Spatiotemporal evolution and driving factors of ecological environment quality in Minnan Delta urban agglomeration based on XGBoost-SHAP model. Environmental Science, 2026. DOI:10.13227/j.hjkx.202508029.

[20] Yuan, B. X., Wu, N., Cheng, P. Spatiotemporal variation characteristics and driving forces of ecosystem types in Chaohu Basin from 2010 to 2020. Journal of Anhui Agricultural Sciences, 2022, 50(7): 59-64+77.

[21] Zhang, Q., Cao, G. C., Zhang, L. L., et al. Dynamic evaluation atlas and driving force analysis of ecological environment quality on the southern slope of Qilian Mountain based on GEE. Environmental Science, 2025, 46(7): 4534-4544. DOI:10.13227/j.hjkx.202406195.

[22] Zhang, X. M., Fan, H. B., Sun, L., et al. Identifying regional eco-environment quality and its influencing factors: A case study of an ecological civilization pilot zone in China. Journal of Cleaner Production, 2024, 435. DOI:10.1016/j.jclepro.2023.140308.

[23] Zhang, Y. F., Yang, Z. H., Zhou, Z. Y., et al. Dynamic assessment and prediction of ecological environment quality in Shantou City based on RSEI and XGBoost model. China Environmental Science, 2026. DOI:10.19674/j.cnki.issn1000-6923.20260104.001.

[24] Zhou, Z., Hu, X. S., Liu, C. Y., et al. Dynamic monitoring and evaluation of ecological environment quality in the upper Yellow River based on GEE: A case study from Longyangxia to Jishixia. Chinese Journal of Ecology, 2023, 42(10): 2545-2554. DOI:10.13292/j.1000-4890.202310.034.

International Journal of Environment, Agriculture and Biotechnology
Vol-11, Issue-3; May-Jun, 2026
Peer-Reviewed International Journal
Journal Home Page Available: https://ijeab.com/
Journal DOI: 10.22161/ijeab

Influence of Selected Soil Properties on Early Growth of *Tectona Grandis* Seedlings in Benue State, Nigeria

A.O Adaikwu[1], J.O Ihuma[2], K. O Ekpenyong[3] and F. Ibrahim[1]

[1&3]Department of Soil Science, Joseph Sarwuan Tarka University P.M.B 2373, Makurdi, Benue. State, Nigeria.
adaikwu.austin@uam.edu.ng
[2]Department of Biological Sciences, Bingham University, P.M.B. 005, Karu, Nasarawa State, Nigeria.
eromey2k@yahoo.com

Received: 05 Apr 2026; Received in revised form: 02 May 2026; Accepted: 07 May 2026; Available online: 15 May 2026

***Abstract*— *This study evaluated the effects of soil properties from five locations in Benue State, Nigeria, on the early growth of Tectona grandis (teak) seedlings. Bulk composite soil samples (0–30 cm depth) were collected 500 m from teak plantations in Amilogodo (Oju), Aghan (Makurdi), Mbagba (Ushongo), Ihugh (Vandekiya), and Ijami (Ohimini). Soils were analyzed for physico-chemical properties, and treated seeds were germinated then transplanted into polypots for six months. Growth parameters included seedling height (cm), leaf number, leaf area index (LAI; cm²), and dry biomass (g). Data were analyzed using one-way ANOVA and LSD tests ($p< 0.05$). Soil E (Ohimini; pH 6.10, CEC 7.52 cmol kg^{-1}, organic C 2.28%, total N 0.09%, available P 6.75 mg kg^{-1}) yielded superior performance (height 11.74 cm, LAI 11.30 cm², dry biomass 4.44 g). Well drained loamy soil with high nitrogen content, high CEC, organic matter content and available phosphorus is most suitable for the establishment of Tectona grandis plantation. Therefore, soils with characteristics similar to that of sample E (Ohimini) is recommended for the establishment of Teak (Tectona grandis) plantation Benue State.*

***Keywords*— Growth performance, Teak, Seedling, Soil samples and Leaf Area Index**

I. INTRODUCTION

Naturally, plant species perform according to the productive capacity of the soil under good management, this explains the intrinsic relationship between plant growth and soil fertility. Where nutrients necessary for plant to perform optimally are not available or inadequate, the need to supplement the soil nutrient is a key factor in agriculture, forestry, horticulture (Lal, 2015). Teak (*Tectona grandis*): Family Verbenaceae is a plantation species that was probably introduced to Nigeria from Burma. The first recorded planting of teak in Nigeria was made in 1889, when it was introduced to the Botanical Gardens at Ebute-metta Unwin (1920), and the oldest teak plantation in Nigeria was raised from Burma teak seeds and established at Olekemeji in Abeokuta province. Teak (*Tectona grandis*) is one of the most important hardwoods of the world trade. In Nigeria, teak is used as a subsidiary species to most indigenous species in plantation centers. It is a favoured species in Nigeria because it supports agroforestry and commercial plantations, also, its fast growth, site tolerance, and good stem form, straight and durable boles which can produce valuable immediate and final yield of wood makes if a highly value wood crop (Akor, 1981). Teak is one of the exotics, which its main uses relay on its aesthetic and decorative quality and its excellent working properties.

Recent studies highlight teak's sensitivity to soil pH (5.5–7.5), organic matter, N, P, and CEC, with optimal growth in loamy, moderately acidic soils (Behera *et al*., 2019; Onyekwelu *et al.,* 2021). In Nigeria, low N and P often limit seedling vigor (Adebayo *et al*., 2023; Eze *et al.*, 2024). This study assesses soil properties from Benue State teak sites on seedling performance, building on foundational work (Harpstead, 1973) with contemporary data to guide plantation establishment.

II. MATERIALS AND METHODS

2.1 Description of the Study Area

The experiment was conducted at the Teaching and the Research Farm of the Joseph Sarwuan Tarka University Makurdi, (JOSTUM) in Benue state, Nigeria between the months of December 2024 and May 2025. JOSTUM is located at latitude 7.41^{O}N and longitude 8.35^{O}E at an elevation of about 97 meters above the sea level. This location falls within the Southern Guinea Savanna Agro-ecological zone of Nigeria.

2.2 Experimental Design and soil sampling

The experimental design was a completely randomized design (CRD) with five treatments (soil samples A–E) and five replicates (n=25). The purpose for this type of design is to subject all samples to equal distribution of treatment regimes. Composite and undisturbed soil samples in replicates were obtained from the five locations. The samples were collected randomly at about 500 m from the edges of teak plantations at the depth of 0-30 cm. This was to minimize the influence of litter deposit on the soil around the perimeter of the plantations. The various bulk soil samples were then taken to the advance soil testing Laboratory, Joseph Sarwaun Tarka University, Makurdi, for analysis.

2.3 Soil Analysis

The soil samples were analyzed for selected physical and chemical properties. Physical properties such as Particle Size Distribution (PSD) were determined by hydrometer method, Bouyoucos (1951), while the soil textures were determined by the USDA textural triangle. Soil Bulk Density (BD) was determined using the core method. The chemical properties of the soil such as, the soil pH in KCl (1:1), Organic Carbon content of the soil were determined by electrometric method and wet oxidation method by Walkley and Black (1934) respectively. Macro-Kjeldahl digestion method was used in determining the total Nitrogen. Cation Exchange Capacity (CEC) was determined by neutral, 1N Ammonium acetate method while Bray-1 method of molybdate blue colorimetry was used to determine the extractable phosphorus.

2.4 Seed Source and Pre-treatments

Teak seeds were sourced locally from stands in the University Staff quarters of JOSTUM. The seeds were subjected to pre-treatments, where, 80 fruits soaked in running water (2 or 3 days, with alternate drying for cracking). Seeds germinated in boxes for 2 weeks, then transplanted to polypots and watered uniformly for the period of the experiment.

Seedling height (cm), leaf number, LAI (Watson, 1947), and dry biomass (g; oven-dried at 70°C) were measured at 6 months. Analysis of variance test (ANOVA) and least significant difference (LSD) ($P< 0.05$) were performed in R (v4.4).

III. RESULTS

3.1 Soil Analysis

The result of the particle size distribution presented in Table 1 indicated different textural composition of the soils. While sample E is a loamy soil, sample A belongs to the textural class of loamysand, soil samples B, C, and D are sandyloam. Also in Table 1, bulk density (BD) of the samples ranged from 1.51gcm^{-3} at A to 1.64gcm^{-3} at E.

The result in Table 1 shows that soil samples A, B, C, D and E have pH values that range from 6.10 to 6.55 (Average 6.36) which is slightly acidic. These are typical characteristics of savanna soils. Harpstead (1973) reported that Guinea Savanna soils are less leached and are of moderate to near neutral acid condition. The CEC varied from 5.35 cmol/kg. to 7.52 Cmol/kg. The organic carbon varied from 1.91% to 2.29% (Average 2.26%) while the total nitrogen and phosphorus varied from 0.03% to 0.09% averaging 0.06% and 5.70 mg kg^{-1} and 6.04 mg kg^{-1} respectively. From the result, a soil of pH 6.3, CEC 6.48 mol/kg, organic carbon 1.91% and total nitrogen and phosphorus 0.06% and 6.04 mg/kg.

3.2 Measures of performance:

Evaluation of early growth performance of Teak are presented in Table 2. Treatment E recorded the highest mean height (11.74cm) followed by A (10.5cm) with treatment C coming last (7.99cm). Though difference in height measurements were observed in the different soil samples (treatments). ANOVA, however, showed no significant difference in height among the treatments (Table 3). Number of leaves per plant showed a similar trend with plant height, the highest leave numbers were recorded in treatment E (13.60) while the least was recorded in treatment C (12.00) Table 2.

Table 1: Physico-Chemical Properties of the Soil samples

Sampled sites	Samples	Bulk Density (gcm^{-3})	Sand (%)	Silt (%)	Clay (%)	Textural Class	pH	CEC CMol/Kg	Organic. Carbon (%)	Total Nitrogen (%)	Avail.P (mg/kg)
Oju (Amilogodo)	A	1.51	85	12	3	Loamysand	6.18	5.50	2.29	0.09	6.40
Makurdi (Aghan)	B	1.49	78	15	7	Sandyloam	6.62	5.91	1.91	0.03	5.70
Ushongo (Mbagba)	C	1.54	76	13	11	Sandyloam	6.55	6.45	2.51	0.04	6.20
Vandekyi a (Ihugh)	D	1.56	78	14	8	Sandyloam	6.50	5.10	2.33	0.06	6.10
Ohimini (Ijami)	E	1.64	65	16	19	Loam	6.10	7.52	2.28	0.09	6.75

Table 2: Effect of soil properties on early growth parameters of Teak

Parameters	A	B	C	D	E	LSD (p>0.05)
Height (cm)	10.5	9.28	7.99	9.40	11.74	2.87
Leaf number	12.8	12.4	12.0	12.4	13.6	2.93
LAI (cm^2)	9.8	7.3	7.5	8.6	11.3	2.55
Dry biomass (g)	3.84	1.94	2.07	2.81	4.44	2.58

Table 2 further showed average leaf area index for each treatment at the end of the experiment. Treatment E recorded the highest mean leaf area index (11.30cm) followed by A (9.80cm) with treatment B coming last (7.30). ANOVA Table 3 showed significant difference between the treatments. A follow-up test was carried out using LSD and significant differences were observed between treatment E and B, and C as shown in Table 4.

The average biomass for each treatment at the end of the experiment are also presented in Table 2. Treatment E recorded the highest mean dry weight (4.44 g), followed by A (3.84g), with the treatment B coming last (1.94 g). The variation in the dry matter was tested with ANOVA, which showed significant difference between the treatments (Table 3). A follow up test was carried out using least significant difference (LSD >0.05) and significant differences were observed between treatments E and B, and C, E and D,A and B, A and C and finally between A and D as shown in Table 4.

Table 3: The ANOVA for plant height, number of leaves, leaf area index and dry matter biomass

SV	df	Ss	Ms	F.cal	F. Tab 5%	F. Tab 1%
Plant height						
Treatment	4	39.68	9.92	2.49	2.87	4.43
Error	20	79.64	3.98			
Total	24	119.32				
Leaf area index						
Treatment	4	55.90	13.975	5.12	2.87	4.43
Error	20	54.60	2.73			
Total	24	110.50				
Dry matter biomass						
Treatment	4	23.90	5.975	5.10	2.87	4.43
Error	20	23.41	1.1705			
Total	24	47.31				

Table 4: Follow up test LSD (t= 0.05,df = 20) for leaf area index and dry matter biomass

	*	E	A	D	C	B
Leaf area index (3.352)						
B	7.30	11.30	9.80	8.64	7.54	7.30
C	7.50	4.00*	2.50	1.30	-	
D	8.60	3.80*	2.30	-		
A	9.80	2.70	-			
E	11.30	-				
Dry matter biomass (0.984)						
B	1.94	4.44	3.84	2.81	2.07	1.94
C	2.07	2.50*	1.90*	0.87	-	-
D	2.81	2.37*	1.77*	-		
A	3.84	1.63*	-			
E	4.44	-				

*Significantly difference

3.3 Effect of soil properties on the early growth performance of Teak

The data in Table 5 summarizes the relationship between soil properties and early growth performance of Teak (Tectona grandis) across five soil treatments (A–E). Teak seedlings in Treatment E (Ohimini) grew tallest, suggesting more favorable soil conditions, possibly linked to higher nutrient availability or improved soil structure. A higher leaf count here, also indicates better vegetative growth and photosynthetic capacity in Treatment E. Leaf area correlates with nutrient uptake efficiency; Treatment E equally promotes greater canopy development. The biomass accumulation trend aligns with height and leaf index, confirming more robust growth in Treatment E.

Treatment E consistently produced superior growth outcomes, while B and C lagged (Table 5), implying differences in soil fertility, nutrient balance, and possibly moisture-holding capacity. The pH range of 6.10 – 6.52 across all the treatment (Table 5) are indicative of slightly acidic to neutral state of the soils, this are optimal for teak growth. Cation exchange capacity CEC were highest (7.52 cmol kg^{-1}) in treatment E and lowest in D (5.10 cmol kg^{-1}) (Table 5). High CEC in E is an indication of greater nutrient retention, supporting better growth. Organic carbon (%) was relatively stable (Table 5). Although B had the highest OC (2.91%), its poor growth suggests that OC alone wasn't the dominant factor possibly due to low nitrogen or imbalance in other nutrients. Total nitrogen (%) was highest in A and E (0.09%), Table 5. Nitrogen is essential for foliage and shoot growth, which aligns with taller plants and more leaves in these treatments. Available phosphorus (mg kg^{-1}) was highest in E (6.75). Adequate P enhances root formation and early vigor directly explaining higher dry matter and height.

Table 5. Summary of effect of soil properties on the early growth performance of Teak

Parameters	Treatments				
	A	B	C	D	E
Average height (cm)	10.5	9.28	7.99	9.40	11.74
Average no of leaves	12.80	12.40	12.00	12.40	13.60
Leaf index(g)	9.8	7.30	7.50	8.60	11.30
Dry matter(g)	3.84	1.94	2.07	2.81	4.44
pH	6.18	6.62	6.55	6.50	6.10
CEC cmol/kg	5.50	5.90	6.45	5.10	7.52
Organic carbon (%)	2.29	2.91	2.51	1.91	2.28
Total nitrogen (%)	0.09	0.03	0.03	0.06	0.09
Available phosphorus(p) (mg kg^{-1})	6.40	5.70	6.20	6.10	6.75

IV. DISCUSSION

Treatment E (the soils from Ohimini) offers the most fertile combination moderate pH (6.10), highest CEC (7.52), balanced OC (2.28%), and high N and P availability. These factors together enhance nutrient absorption, root proliferation, and photosynthetic efficiency, leading to superior height, leaf area, and biomass. By contrast, Treatments B and C, though slightly higher in pH and OC, show reduced nitrogen and phosphorus, resulting in stunted growth. That aligns with the nutrient limitation patterns noted by Abankwa et al. (2017), where teak plantations with nutrient deficiencies (especially N and P) demonstrated significantly reduced growth.

Soil E's superior performance correlates with higher CEC, N, P, and loam texture, facilitating nutrient retention and root development consistent with teak's preferences (Behera et al., 2019). Low N in B/C mirrors poor biomass in Nigerian savanna soils (Adebayo et al., 2023). Leaf area index (LAI) and biomass sensitivity underscores their utility for early vigor assessment (Onyekwelu et al., 2021; Eze et al., 2024), linking to photosynthesis and biomass allocation. Unlike height, these reflect fertility gradients, aligning with Williams & Richardson (1987) that nitrogen is the most important in tree nutrition and it accounts for about 1-3% dry weight of tree composition. And that high acidic condition of the soil inhibits activities of many common bacteria, algae and actinomycetes. Also phosphorus is vital to life and portion of all green plants. High organic carbon indicates high nutrient deposition.

Although, significant differences were not noted in the parameters like leaf count and height, dry matter and Leaf Area Index (LAI) showed significant differences. It is important to monitor the distribution and changes of LAI so that growth and vigour of vegetation on planet can be assessed. Important parameters for climate models and land-surface processes are obtained from LAI. Various processes such as photosynthesis, respiration, transpiration and rain interception which controls the links between biosphere and atmosphere are determined in the variables representing the amount of leaf material in ecosystems. The characteristics of all the parameters observed were more outstanding in sample E followed by A, this is an indication that, the nutrients available especially nitrogen supported the growth of the trees. High dry weights of treatment E and A could be attributed to high nitrogen composition, phosphorus, organic carbon and all other requisite for the growth of tree.

V. CONCLUSION AND RECOMMENDATION

A study was undertaken to evaluate the influence of soil nutrients on the early growth performance of Teak (*Tectona grandis*) in Benue state. The physical properties of the soil such as the Bulk density (BD), Particle size distributions (PSD) and the chemical properties such as the soil pH, total nitrogen, phosphorus, organic carbon and Cation Exchange Capacity (CEC) were analyzed. Also, data on plant parameters such the plant height, number of leave per plant, dry matter as well as leave area index were assessed to check their response to the soil nutrient elements studied.

Early growth performance of Tectona grandis is strongly influenced by nitrogen level, CEC, and available phosphorus. Treatments with higher nutrient-holding capacity and balanced soil chemistry (especially E) produced superior results. The study showed that the soil sample E from Ohimini, a deep and well drained loamy soil gave the highest response in terms of growth performance with respect to the soil nutrient elements studied.

Based on the findings of this investigation, the following recommendations have been advanced with respect to establishment of teak plantation.

1. Well drained loamy soil with high nitrogen content, high CEC, organic matter content and available phosphorus is most suitable for the establishment of *Tectona grandis* plantation. Therefore, soils with characteristics similar to that of sample E (Ohimini) is recommended for the establishment of Teak (T*ectona grandis)* plantation Benue State.
2. It is also recommended that similar research be carried out for a longer duration to cover the growth period beyond nursery to maturity, so as to assess its response to different soil conditions.
3. Furthermore, government should encourage the establishment of teak plantation because of its economic importance through subsidies on inputs so as to encourage prospective farmers to venture in the production.

REFERENCES

[1] Abankwa, M., Owusu-Ansah, F., & Osei-Bonsu, K. (2017). *Changes in soil nutrient levels under four teak plantations and their corresponding natural vegetations in Ghana.* Research Journal of Recent Sciences, 6(6), 5–12.isca+1

[2] Adebayo, O.A., et al. (2023). Soil nutrient effects on teak seedlings in Nigerian savannas. Agroforestry systems 97, 455–467.

[3] Akor, T (1981) The effect of seed treatment on the germination rate of teak seed. Forest Research Institute of Nigeria.

[4] Behera, M. D., Behera, P. R., Roy, P. S., & Kushwaha, S. P. S. (2019). Soil-site suitability for teak in tropics. *Forest Ecology and Management*, 435, 45–56.fao+1

[5] Bouyoucos, G.H. (1951) A Recalibration of the Hydrometer Method for making mechanical analysis of the soil. *Agron J.* **43**: 434-438

[6] Bray R.H and Kurtz L.T.(1945) Determination of total organic and available forms of phosphorus in soil. *Soil Science* **59**:39-45.

[7] Eze, P.C., et al. (2024). Teak growth in Guinea Savanna soils. Journal of Tropical forestry, 40, 112–125. Harpstead, M.T. (1973). The classification of some Nigerian Soils. *Soil Science.* **116**:437 – 442.

[8] Kowero, G., Liberador, F., Mbwilo, J., Mapinduzi, J., Megevand, C., & Ngwenya, M. (2018). Teak plantations in Africa. *International Forestry Review*, 20(2), 150–165.

[9] Lal, R. (2015). Carbon sequestration in soil. *Carbon Management*, 6(1), 1–11.sciencedirect

[10] Lal, R. (2015). Soil and plant growth. Soil science, 200, 1–12.

[11] Onyekwelu, J. C., Musa, J. J., Nkonya, E. M. L., & Ogunbameru, O. O. (2021). *Soil organic carbon stocks and nutrient dynamics under different land-use systems in southwestern Nigeria.* Journal of Environmental Management, 281, 111811.isca+1

[12] Unwin, H (1920) West African Forests and Forestry. Oxford University Press, London

[13] USDA–SCS (1974). Definitions and abbreviations for soil description. West technical service centre. Portland, Oregon

[14] Walkely, J.T and C. A. Black (1934) An examination of the Degtjarefft method of determining the organic matter and a proposed modification of the chromic acid titration method. *Soil Science* **37**: 29-38.

[15] Watson, D.J. (1947). Leaf area in crop growth. Annals of Botany, 11, 41–76.

[16] William L. and Richard F.F (1987). Properties and management of Forest Soils 2nd edition. John Wiley and Sons. New York

International Journal of Environment, Agriculture and Biotechnology
Vol-11, Issue-3; May-Jun, 2026
Peer-Reviewed International Journal
Journal Home Page Available: https://ijeab.com/
Journal DOI: 10.22161/ijeab

Characteristics of Soil Erosion in Guangdong Province Based on the USLE and InVEST Models

Qiaoyang Wen, Zhiming Huang, Boyang Han, Ruei-Yuan Wang, Chao Yuan*

School of Environmental Science and Engineering, Guangdong University of Petrochem Technology (GDUPT), Maoming 525000, China
*Corresponding author

Received: 10 Apr 2026; Received in revised form: 04 May 2026; Accepted: 08 May 2026; Available online: 16 May 2026

Abstract— *Taking Guangdong Province as the study area, this research integrates multi-source geospatial data—including DEM, precipitation, soil, and land cover—and couples the USLE and InVEST models. The study calculates five core factors: rainfall erosivity (R), soil erodibility (K), slope length and steepness (LS), vegetation cover (C), and conservation practice (P), to reveal the spatial heterogeneity and formation mechanisms of both potential and actual soil erosion. The results indicate that rainfall erosivity exhibits a spatial pattern that is generally higher in the south and west, and lower in the north and east. High values of soil erodibility are concentrated in the core Pearl River Delta (PRD) region and the coastal areas of western Guangdong (Zhanjiang), while low values are distributed in the mountainous and hilly regions of northern and eastern Guangdong. Land use is dominated by forestland, whereas construction land is clustered within the PRD urban agglomeration. High-risk zones for potential soil erosion are primarily located in the Nanling Mountains of northern Guangdong and the hilly areas of western Guangdong, largely controlled by natural background conditions such as topography and soil properties. Although vegetation cover and conservation measures significantly mitigate regional soil erosion intensity, moderate to severe erosion risks persist in the Leizhou Peninsula and the low-hilly agricultural areas of northern Guangdong. This study clarifies the spatial distribution patterns of soil erosion, providing a scientific basis for precise soil and water loss prevention, ecological restoration, and territorial spatial planning.*
Keywords— ***Guangdong Province, USLE model, InVEST model, Soil Erosion***

I. INTRODUCTION

Soil erosion is a natural process in which the Earth's surface soil is detached, transported, and deposited under the action of wind and water. This process leads to the thinning of soil layers, the decline of soil fertility, and the reduction of water retention capacity, ultimately resulting in land degradation, climatic deterioration, ecological degradation, and an increase in natural disasters [1]. Currently, soil erosion has become one of the major environmental issues on a global scale [2], posing severe threats to regional ecological security and the sustainable development of agriculture. Scientifically assessing regional soil erosion and revealing its spatial heterogeneity are fundamental to implementing precise prevention and control of soil and water loss, as well as optimizing ecosystem services.

The Universal Soil Loss Equation (USLE) is a classic method for the quantitative assessment of soil erosion. In conducting regional soil erosion assessments and predictions, some researchers have developed their own slope soil erosion prediction models by using the USLE as a reference framework and integrating local actual conditions [3-10]. Although the USLE can efficiently estimate slope soil erosion, it has certain limitations, as it tends to overlook sediment retention capacity at the plot scale and watershed hydrological processes during calculations [11]. The InVEST (Integrated Valuation of Ecosystem Services and Tradeoffs) model, jointly developed by Stanford University, the World Wide Fund for Nature (WWF), and other institutions, can integrate multi-source data such as topography, climate, soil, and land use. By accounting for both upslope sediment interception and the impact of watershed reservoirs, the InVEST model achieves precise quantification and spatial visualization of soil conservation services, thereby overcoming the shortcomings of the traditional USLE model [12-13].

Regarding the application of the InVEST model in soil conservation, foreign scholars have already conducted relevant studies. For instance, Marques et al. (2021) modeled sediment retention services and soil erosion changes in Portugal using a spatiotemporal analysis method [14], and Ureta et al. (2021) quantified the ecological benefits of landscapes through an analysis of the impacts of land cover change on ecosystem services in the United States [15]. Domestically, scholars have also successively applied the InVEST model to soil erosion research. For example, Zhou et al. (2010) simulated soil erosion in the mountainous areas of Beijing [2]; Wang et al. (2014) studied the soil conservation function of the ecosystem in Ningde, Fujian [16]; Chen et al. (2020) investigated the current status and function of soil conservation in the Qilian Mountain National Nature Reserve [17]; He et al. (2019) researched the characteristics of soil erosion in the Qihe River Basin of the Taihang Mountains [18]; and Wang et al.(2019) examined the soil erosion intensity in Yan'an City before and after the Grain for Green Program [19].

Located on the southern coast of China, Guangdong Province features a subtropical monsoon climate with abundant rainfall and concentrated rainstorms. The terrain is dominated by mountains and hills with complex geological conditions. Coupled with rapid urbanization and intensive land development, the risk of soil erosion in the region is prominent. Currently, existing studies on soil erosion in Guangdong mostly adopt a single model (either USLE or InVEST) or are limited to specific watersheds. At the provincial scale, there is a scarcity of research that systematically couples USLE (for calculating erosion potential) with InVEST (for ecosystem service assessment) to analyze the entire erosion-retention process. Meanwhile, relevant studies have largely focused on specific watersheds or local areas, and systematic analyses of erosion characteristics based on the coupling of USLE and InVEST models at the provincial scale remain relatively lacking. Therefore, this paper takes Guangdong Province as the study area and couples the USLE and InVEST models to quantitatively assess actual and potential soil erosion. It aims to clarify the spatial distribution patterns and driving factors of erosion, providing a scientific basis for soil and water loss prevention, ecological protection and restoration, and the optimization of territorial space.

II. DATA AND METHODS

2.1. Overview of the Study Area

Guangdong Province is located between 20°13′N–25°31′N and 109°39′E–117°19′E at the southernmost tip of mainland China. It borders Fujian Province to the east, Guangxi to the west, Hunan and Jiangxi provinces to the north, and faces the South China Sea to the south, with a total land area of approximately 179,800 km². The province administers 21 prefecture-level cities and features a prominent land-sea location, characterized by a vast sea area and a mainland coastline stretching 4,114.3 km (Fig. 1).

The overall terrain is high in the north and low in the south. The geomorphology is dominated by mountains and hills, which together account for nearly 60% of the province's area, while terraces and plains make up the remaining 40%. The northern Nanling Mountains and the eastern Lianhua Mountains have relatively high elevations, with Shikengkong (1,902 m) being the highest peak in the province. The central region features an alternating distribution of hills and basins, while the south and coastal areas are mainly composed of the Pearl River Delta, Chaoshan Plain, and Leizhou Terrace. Granite is the most widely distributed bedrock in the region, followed by sandstone and metamorphic rocks. Large areas of limestone are distributed in northwestern Guangdong. The complex lithology easily induces natural soil erosion.

Climatically, the province belongs to the East Asian monsoon region, spanning the central subtropical, southern subtropical, and tropical zones from north to south. The annual average temperature ranges from 19 to 24℃, and the annual average precipitation reaches 1,771 mm. Rainfall is concentrated from April to September, with frequent rainstorms and typhoons. The high intensity and concentrated duration of rainfall provide sufficient hydrodynamic conditions for soil erosion. The dominant soil types include red soil, latosolic red soil, laterite, and paddy soil. These soils are generally heavy in texture, with poorly developed aggregate structure and relatively weak anti-erodibility and anti-scourability.

Land use is primarily composed of forestland, cultivated land, and construction land. Forestland is concentrated in the northern and eastern mountainous and hilly regions, while cultivated land is mostly distributed in coastal and river valley areas. The expansion of construction land is particularly significant in the Pearl River Delta and the central urban areas of various cities. Influenced by the combined effects of complex topography, a rainy climate, fragile soil texture, and high-intensity human activities, the risk of soil erosion in mountainous and hilly areas is prominent. Therefore, conducting research on soil erosion characteristics in this region holds significant practical implications.

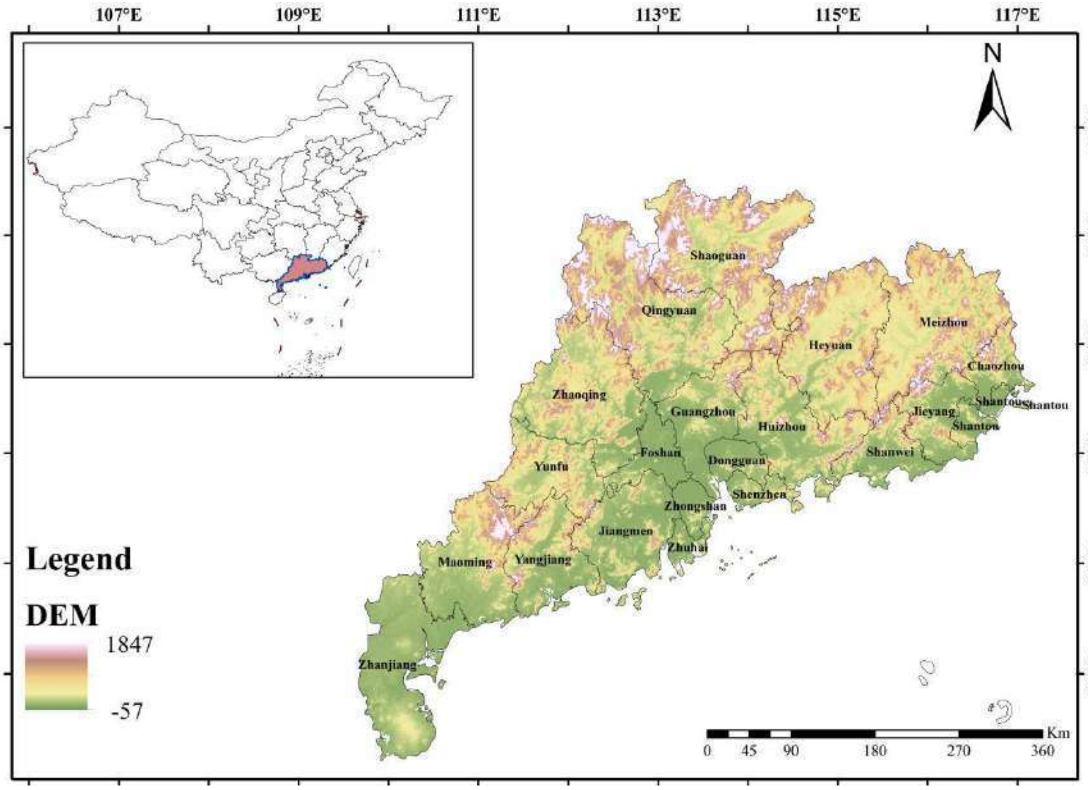

Fig. 1 Topographic overview of Guangdong Province

2.2. Data Sources

The operation of the InVEST model requires raster layers and parameter tables with consistent resolution and projected coordinate systems. In this study, all raster data were uniformly processed to a 90 m × 90 m resolution under the WGS_1984_EASE_Grid_Global projected coordinate system. The data required for the model and their sources are listed in Table 1. Specifically:

(1) The Rainfall Erosivity (R) layer was derived from the monthly precipitation data for the year 2020, which were downloaded from the Geographical Resources Sub-center of the National Earth System Science Data Center (National Science and Technology Infrastructure of China), and subsequently calculated using ArcGIS raster calculator.

(2) The Soil Erodibility (K) layer was calculated

using the Erosion-Productivity Impact Calculator (EPIC) model, based on the China soil dataset from the Harmonized World Soil Database (HWSD) downloaded from the National Tibetan Plateau Data Center.

(3) The Slope Length and Steepness factors (L, S) were derived from the 90 m SRTM DEM data downloaded from the Geospatial Data Cloud, and calculated using the topographic relief tools in ArcGIS.

(4) The watershed data for the study area were extracted from the 90 m SRTM DEM data (sourced from the Geospatial Data Cloud) using the hydrological analysis tools in ArcGIS.

(5) The land cover raster data were obtained from the annual 30 m resolution land cover dataset for China released by Professors Jie Yang and Xin Huang of Wuhan University, available on the Zenodo platform, and subsequently processed through reclassification in ArcGIS.

(6) The Biophysical Table consists of the land use code (lucode), the cover-management factor (usle_c), and the support practice factor (usle_p).

Table 1 Research data and their sources

Data Requirements	Data Sources	Purpose
Annual precipitation data	(https://gre.geodata.cn)	Generate R factor layer
Soil texture data	（https://data.tpdc.ac.cn/home）	Generate K factor layer
90m DEM data	（https://www.gscloud.cn/home#page1/1）	Generate K factor layer
Land cover raster data	（https://zenodo.org/records/18180184）	Generate land use layer

2.3. Research Methods

2.3.1. Technical Route

This study is based on data including 90m DEM, precipitation in 2020, HWSD, and land cover raster data of Guangdong Province. The main analysis steps (as shown in Fig. 2) are as follows:

(1) Preparation of parameters required for the InVEST model operation: The 90m DEM data were mosaicked and extracted by mask to obtain the topographic relief of the study area using the Focal Statistics tool in ArcGIS. Subsequently, the mosaicked 90m DEM data were processed using the Hydrological Analysis tools in ArcGIS to extract the watershed data of the study area.

(2) The monthly precipitation data for 2020 were extracted by mask. The annual precipitation was first calculated using the Raster Calculator in ArcGIS, and then the R factor was computed based on the R factor formula.

(3) The HWSD data were extracted by mask, and the K factor was calculated using the Raster Calculator in ArcGIS based on the EPIC model.

(4) The land cover raster data were reclassified according to the *Current Land Use Classification (GB/T 21010—2017)* standard to obtain the land use data meeting the model requirements.

(5) The values for the C and P factors were assigned based on existing literature.

(6) The above parameters were input into the InVEST model to obtain the actual and potential soil erosion moduli.

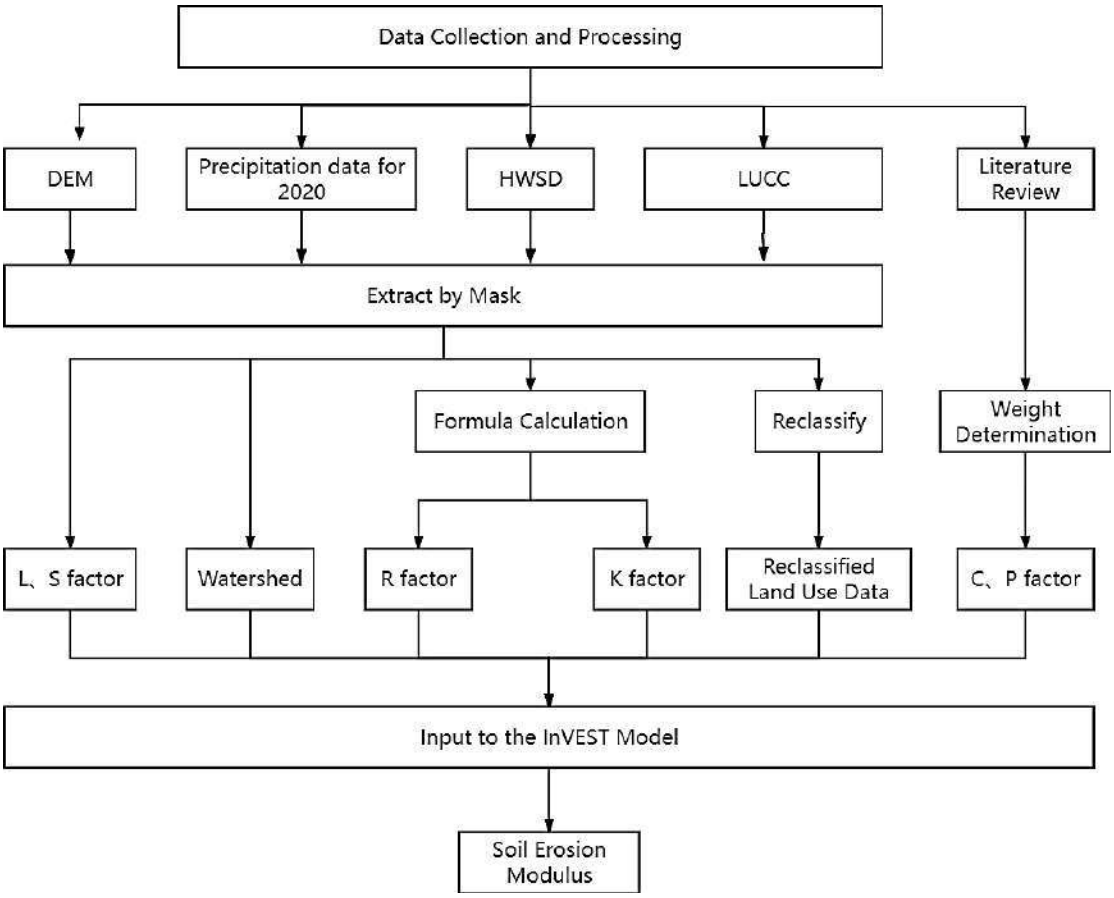

Fig. 2 Flowchart of the technical route

2.3.2 USLE and InVEST Models

The InVEST model is a comprehensive assessment tool for ecosystem services and tradeoffs. Supported by the Natural Capital Project, it was successfully developed in 2007 through the collaboration of Stanford University, the World Wildlife Fund (WWF), and The Nature Conservancy (TNC). Currently, it has been widely applied both domestically and internationally. The model not only achieves quantitative assessment of ecosystem service functions but also realizes their spatial expression with the support of 3S technology. The assessment results are presented in the form of maps, which can reflect the spatial heterogeneity of ecosystem service functions, enabling decision-makers to better grasp the actual situation and make further plans and countermeasures [20].

According to module service types, InVEST can be divided into three groups: supporting services, ultimate services, and enhancement tools (Table 2) [21]. Among them, supporting services serve as the foundation for other types of ecosystem services, from which humans cannot directly benefit. Ultimate services are divided into two parts: biophysical provision and services, from which humans can directly benefit [22].

Table 2 InVEST Model Framework

Supporting Services	Ultimate Services		Enhancement Tools
	Provision: Services	Undifferentiated Provision and Services	
Habitat Quality	Forest Carbon Edge Effect	Timber Production and Management	Scenario Generator: Proximity Based
Habitat Risk Assessment	Coastal Blue Carbon	Wave Energy Production	Coastal Vulnerability

Crop Pollination	Carbon Storage and Sequestration	Visitation: Recreation and Tourism	DelineateIt
Water Quality	Water Yield	Coastal Protection	Scenario Generator
	Nutrient Delivery Ratio	Wind Energy Production	Script and API
	Viewshed: Scenic Quality	Marine Fisheries Production	Route DEM
	Sediment Delivery Ratio（SDR）	Marine Aquacultur	GLOBIO
	Nutrient Delivery Ratio	Crop Production	

This study employs the Sediment Delivery Ratio (SDR) module within the soil conservation component. This module represents various integrated measures capable of preventing soil erosion, conserving soil resources, and maintaining or enhancing land productivity. The soil conservation service function refers to the ability of surface cover, such as vegetation, to reduce soil erosion on a given plot while simultaneously intercepting sediment originating from upstream areas [23].

The Universal Soil Loss Equation (USLE) is currently the most widely used method for calculating soil conservation. Its principle involves calculating the potential soil erosion (RKLS) and the actual soil erosion (USLE) for each raster cell, respectively. The soil conservation for each cell is then obtained by subtracting the actual erosion from the potential erosion. The relevant formulas are as follows (1) and (2):

$$RKLS=R\times K\times LS \quad \dots\dots\dots\dots\dots (1)$$

$$ULSE=R\times K\times LS\times C\times P \quad \dots\dots (2)$$

where R is the rainfall erosivity factor, K is the soil erodibility factor, LS is the topographic factor, C is the cover-management factor, and P is the support practice factor.

However, in the actual soil erosion process, not all actual soil erosion reaches the watershed outlet. There exists a Sediment Delivery Ratio (SDR) in this process, because downstream plots cause deposition of the sediment load coming from upstream plots. The amount deposited during the entire flow process towards the watershed outlet is defined as the sediment deposition amount [24].

The InVEST model calculates regional soil conservation based on an improvement of the Universal Soil Loss Equation. Specifically, the InVEST model fully accounts for sediment deposition, thereby enabling a more accurate estimation of regional soil conservation services. The relevant formulas are as follows (3), (4), and (5):

$$SM_i=RKLS_i-USLE_i+SR_i \quad \dots\dots\dots (3)$$

$$SR_i=SE_{i-1}\times(1-SDR_i) \quad \dots\dots\dots\dots (4)$$

$$SE_i=USLE_i+SE_{i-1}\times SDR_i \quad \dots\dots\dots (5)$$

where SM is the soil conservation amount, SR is the sediment deposition amount, SE is the sediment transport amount, and i－1 represents the upstream pixel of pixel i.

2.4 Model Parameter Construction

2.4.1 Rainfall Erosivity Factor (R)

Rainfall erosivity is the primary foundational factor of the USLE model. It is a dynamic indicator used to evaluate rainfall-induced soil detachment and transport, reflecting the potential impact of rainfall conditions on soil erosion [18]. In this study, following the Guidelines for Calculating Soil Loss in Production and Construction Projects (SL773-2018), the rainfall erosivity factor R was assigned the value of Rd after obtaining the average precipitation data for 2020. The annual average precipitation erosivity factor was calculated using Formula (6):

$$R_d=0.067\,P_d^{\,1.627} \quad \dots\dots\dots (6)$$

In Formula (6): Rd is the annual precipitation erosivity factor, with units of MJ·mm/(hm²·h); Pd is the annual average precipitation, with units of mm.

2.4.2 Soil Erodibility Factor (K)

Soil erodibility is a crucial indicator for evaluating the sensitivity of soil to erosion and is also a vital parameter for soil erosion prediction [25]. The most commonly used methods for determining the K value include the median particle size method, direct measurement, and the EPIC model. Most of these methods require numerous soil property parameters, such as soil texture, structure, organic matter, and permeability. However, acquiring data on soil structure and permeability is often challenging. Therefore, this study adopts the K value calculation method from the Erosion-Productivity Impact Calculator (EPIC) model proposed by Williams et al. [26-27] as a surrogate model. This method is primarily related to the contents of sand, silt, clay, and organic matter. Focusing more on soil properties, this model can scientifically reflect soil erodibility. Thus, it was calculated using soil particle composition and organic carbon content data. The result was multiplied by 0.1317 to convert it to international units. The calculation method is shown in Formula (7):

$$K=\{0.2+0.3\exp[-0.0256\,SAN(1-SIL/100)]\}\,[SIL/(CLA+SIL)]^{0.2}\,\{1-0.25C/[C+\exp(3.72-2.95C)]\}\,\{1-0.7SN_1/[SN_1+\exp(-5.51+22.9SN_1)]\} \quad \text{………………(7)}$$

In Formula (7): K is the soil erodibility [$t\cdot hm^2\cdot/(MJ\cdot mm\cdot hm^2)$]; SAN is the sand content (%); SIL is the silt content (%); CLA is the clay content (%); $SN_1=1-SAN/100$; C is the organic carbon content (%) [28].

2.4.3 Slope Length and Steepness Factors (L, S)

The L and S factors are among the most critical parameters in the USLE equation. They reflect the relationship between slope gradient and the land surface, and their essence lies in the distance a raindrop or sediment travels until its energy is exhausted. Slope height characterizes ground flatness; generally, slope length refers to the specific projection length of the water flow trajectory on the slope surface onto the horizontal plane. The steeper the slope, the more severe the soil erosion; conversely, the longer the slope, the more the runoff formation tends to decrease. The InVEST model automatically completes the calculation of the L and S factors based on user-inputted slope thresholds and generates the corresponding L and S layers [18]. It is worth noting that the model automatically selects different formulas for calculations in low-slope and high-slope areas [12].

2.4.4 Land Cover Raster Data

Land cover raster data can reflect the different land use types within the study area. Since different land use types have varying erosion intensities and soil and water conservation measures, they must be analyzed and understood. In this study, we downloaded the annual land cover raster data of China with a 30-meter resolution, released by Professors Yang Jie and Huang Xin from Wuhan University, via the Zenodo platform. According to the *Current Land Use Classification (GB/T 21010—2017)* standard, the remote sensing image data were reclassified into six land use types: cultivated land, forest land, grassland, water bodies, unused land, and construction land.

2.4.5 Cover-Management Factor (C)

The cover-management factor C is defined as the ratio of soil erosion under a specific vegetation cover and management condition to the soil erosion on a continuously fallow, clean-tilled plot. It reflects the impact of vegetation or crops and management practices on soil loss, with values ranging between 0 and 1 [29].

2.4.6 Support Practice Factor (P)

In the InVEST or USLE model, the P factor is typically not determined by a formula but is assigned empirically based on land use types and soil and water conservation engineering. The support practice factor P refers to the ratio of soil loss after adopting conservation measures to the soil loss when planting along the slope (up and down the slope). Its value ranges from 0 to 1; an extreme value of 0 represents an area with no erosion, while an extreme value of 1 indicates an area where no conservation measures have been taken [13]. According to previous studies [30], after years of soil and water loss control in the local area, soil erosion in some regions has been effectively controlled.

III. RESULTS AND ANALYSIS

3.1. Spatial Distribution of the R Factor

The rainfall erosivity factor is the core driver of soil erosion. The data results (Fig. 3) show that the rainfall erosivity (R factor) in Guangdong Province generally exhibits a spatial pattern of "higher in the south and lower in the north, and higher in the west and lower in the east." The northern Guangdong mountainous areas (Shaoguan, Qingyuan, Meizhou) and the eastern coastal regions (Chaozhou, Shantou, Jieyang, Shanwei) are low-value zones, with the R factor dropping to as low as 6428.13 $MJ\cdot mm/(hm^2\cdot h)$. In contrast, the southern part of Jiangmen

City and the southeastern part of Yangjiang City are high-value zones, with the R factor peaking at 16793.8 MJ·mm/(hm²·h). Although the eastern Guangdong region is coastal, it contains many mountainous areas. Influenced by the leeward slope effect or the seasonal distribution of precipitation, the rainfall erosivity index in this area is relatively low. In the core area of the Pearl River Delta (such as Guangzhou and Foshan), high urbanization and the urban heat island effect have altered the local microclimate. Additionally, station interpolation is affected by impervious surfaces, resulting in relatively low R factor values in this region compared to the rest of the province.

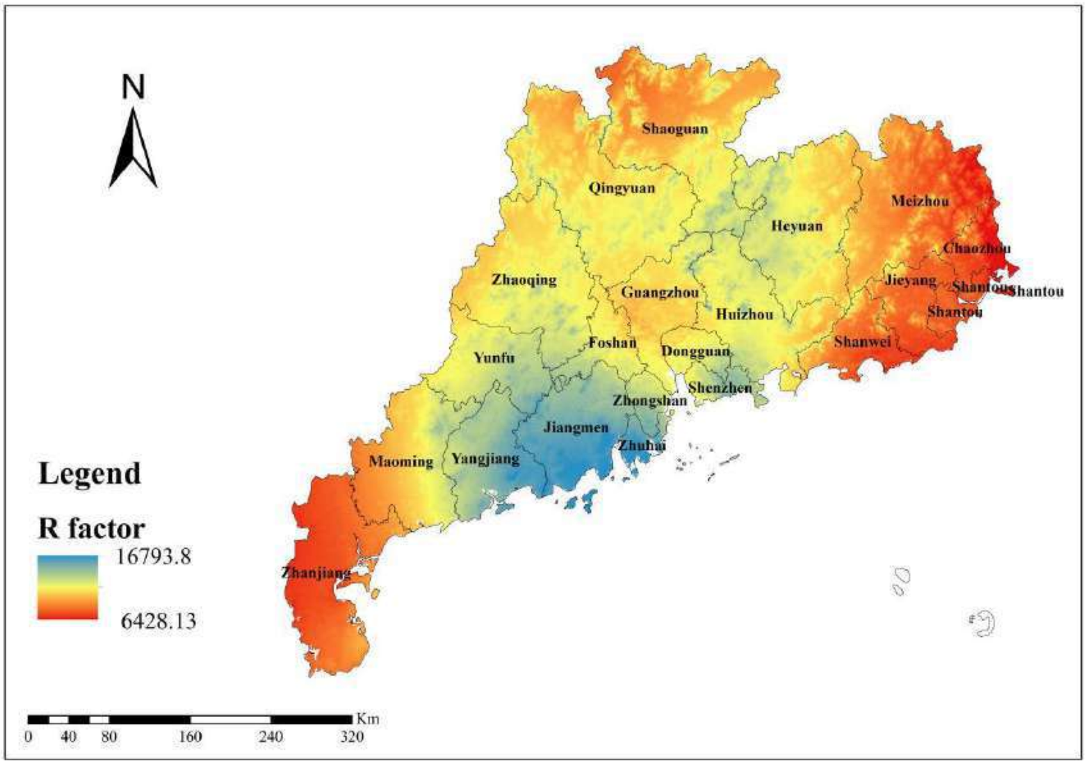

Fig. 3 Spatial distribution of the R factor

3.2. Spatial Distribution of the K Factor

Soil erodibility reflects the sensitivity of soil to erosion. Data analysis results indicate significant spatial differences in the soil erodibility factor (K factor) across Guangdong Province (Fig. 4). High-value zones are concentrated in the core area of the Pearl River Delta and the coastal zones of Zhanjiang in western Guangdong. These areas are dominated by latosolic red soil and laterite, characterized by heavy soil texture and loose structure, resulting in weak resistance to erosion. Low-value zones are mainly distributed in the mountainous and hilly regions of northern and eastern Guangdong, where red soil and yellow soil prevail. These soils have relatively high organic matter content and well-developed aggregate structure, leading to lower erodibility. Overall, the intrinsic soil conditions in the Pearl River Delta and coastal plain areas are more susceptible to erosion, making them key regions for soil conservation efforts.

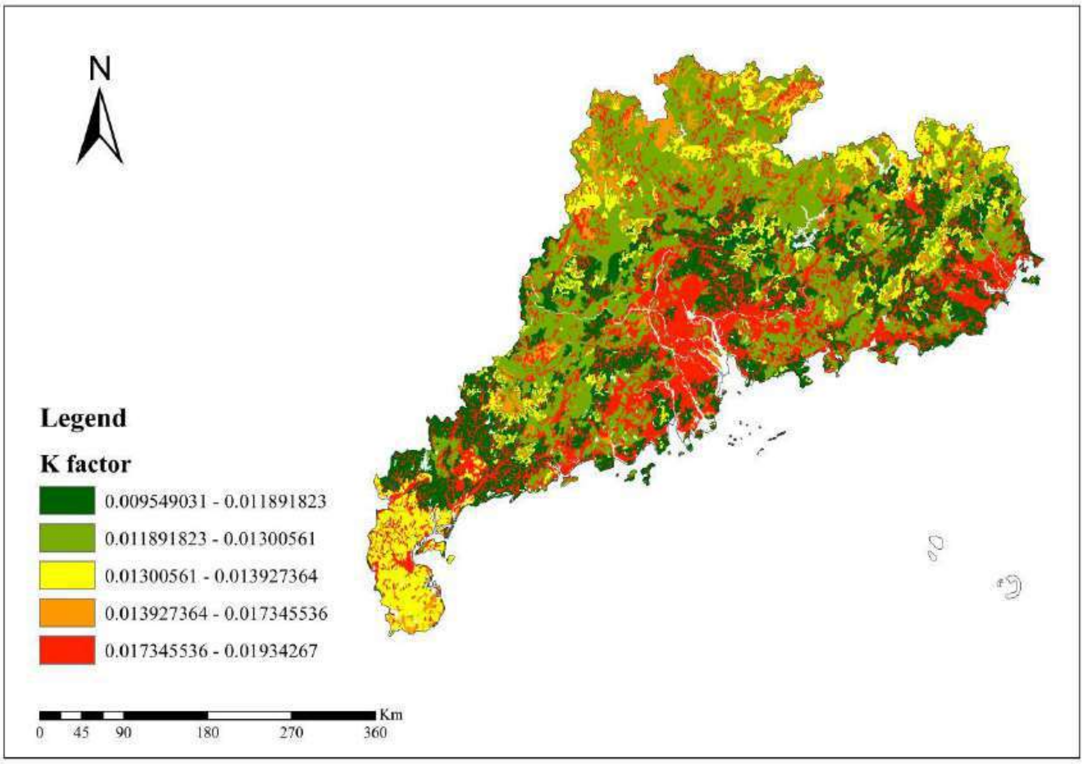

Fig. 4 Spatial distribution of the K factor

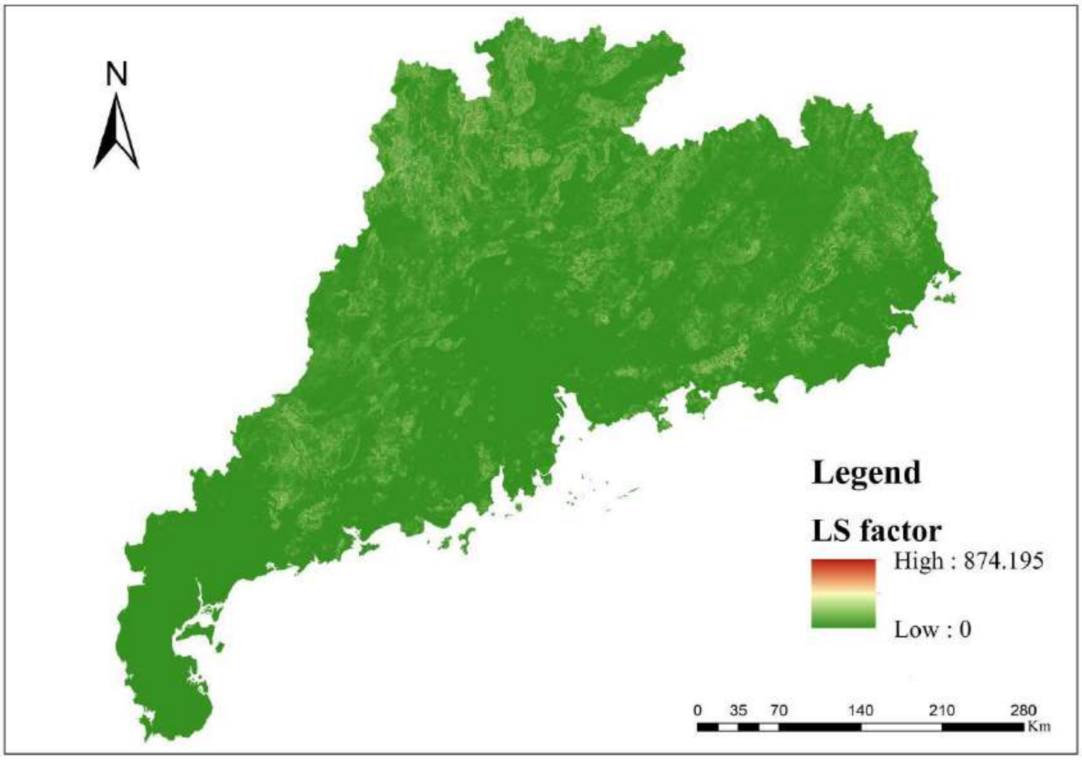

Fig. 5 Spatial distribution of the L and S factors

3.3. Spatial Distribution of the L and S Factors

The spatial distribution maps of the slope length (L) and steepness (S) factors, extracted based on a 90 m × 90 m resolution DEM, reveal that the topographic relief in

Guangdong Province exhibits a distinct gradient feature of "higher in the north and lower in the south, and higher in the west and lower in the east" (Fig. 5). This pattern aligns closely with the distribution of geomorphological units in the province.

The high-value zones of the L and S factors are mainly concentrated in the Nanling Mountains of northern Guangdong (Shaoguan, northern Qingyuan), the Yunwu Mountain system of western Guangdong (Yunfu, northern Maoming), and the Lianhua Mountains of eastern Guangdong (Meizhou, eastern Heyuan). These areas are characterized by high elevation, intense terrain dissection, and extended slope lengths, constituting the peak zones for the L and S factors. In the absence of vegetation cover and human intervention, these regions serve as the strongest natural driving sources of potential soil erosion. The low-value zones of the LS factors are widely distributed across the Pearl River Delta alluvial plain (Guangzhou, Foshan, Dongguan, southern Huizhou) and coastal zones (Zhanjiang, southern Maoming, and the Chaoshan Plain in Shantou). These areas feature flat terrain, minimal slopes, and short slope lengths. The slow velocity of water flow convergence results in a weak topographic driving force for soil erosion.

3.4. Spatial Distribution of Land Use

Land use directly influences surface cover and the intensity of human activities. The land use pattern in Guangdong Province is dominated by forest land (Fig. 6), which accounts for over 60% of the total area. It is mainly concentrated in the mountainous and hilly regions of northern and eastern Guangdong, playing a significant positive role in soil conservation. Cultivated land is primarily distributed in Zhanjiang (western Guangdong), the periphery of the Pearl River Delta, and the plains of eastern Guangdong, serving as the main area of disturbance from agricultural activities. Construction land is concentrated in the urban agglomerations of the Pearl River Delta (such as Guangzhou, Shenzhen, and Dongguan) and the central urban areas of various prefecture-level cities, exhibiting a distribution pattern that radiates from the center outward. High-intensity development in these areas tends to destroy surface vegetation and exacerbate local erosion risks. Water bodies, grassland, and unused land account for a relatively low proportion, being sporadically distributed along rivers, coastal zones, and the edges of mountainous areas.

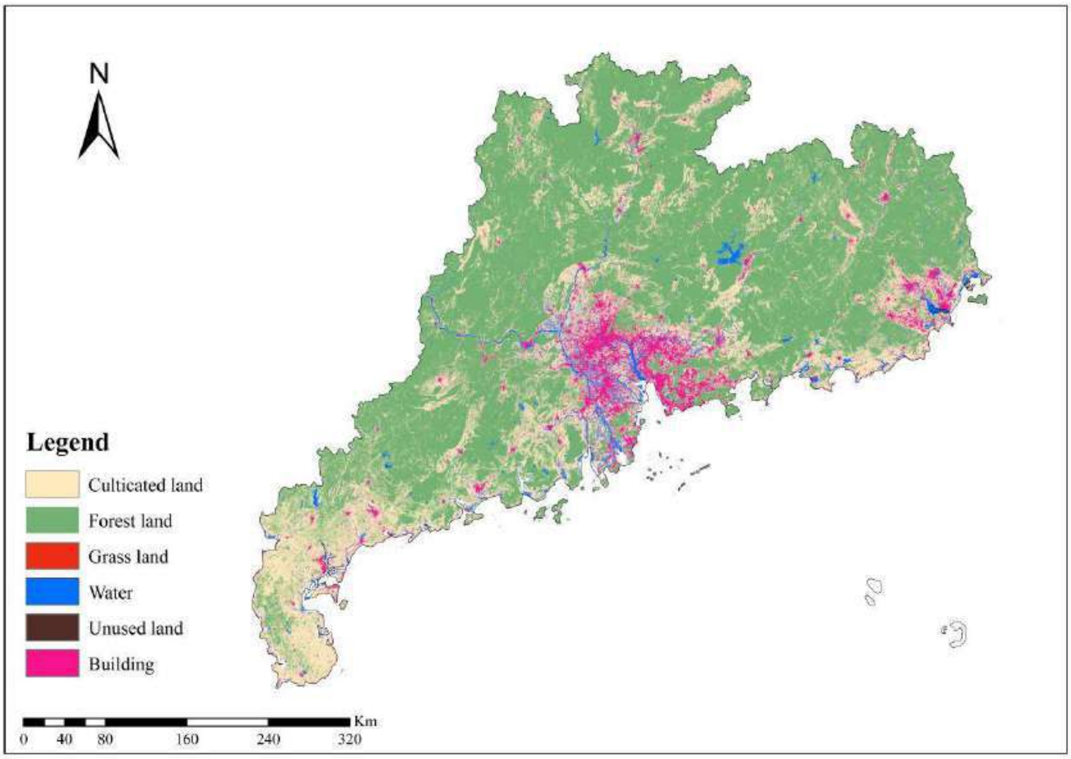

Fig. 6 Spatial distribution of land use types

3.5. Assignment of C and P Factors

The values of the C factor were referenced from the studies of Ma Guofu and Pan Meihui et al. [31-32]. The value was assigned as 0.05 for cultivated land, 0.03 for forest land, 0.04 for grassland, 0 for water bodies and construction land, and 1 for unused land, as shown in Table 3.

Table 3 C factor assignment table

lucode	USLE_C
1（Cultivated land）	0.05
2（Forest land）	0.04
3（Grass land）	0.03
4（Water）	0
5（Unused land）	1
6（Building）	0

The values of the P factor were referenced from the study of Li Ting et al. [13]. The P value for cultivated land was assigned as 0.35. Except for water bodies and construction land, which were assigned a value of 0 as no erosion occurs, the remaining land use types were assigned a value of 1, as no soil and water conservation measures were adopted. The specific assignments are shown in Table 4.

Table 4 P factor assignment table

lucode	USLE_P
1（Cultivated land）	0.35
2（Forest land）	1
3（Grass land）	1
4（Water）	0
5（Unused land）	1
6（Building）	0

3.6. Soil Erosion Characteristics

The distribution of potential soil erosion (RKLS) in Guangdong Province exhibits distinct spatial differentiation between mountainous areas and plains (Fig. 7). Data analysis results show that areas with intense and extremely intense erosion are concentrated in the Nanling Mountains of northern Guangdong (such as Shaoguan and Qingyuan) and the hilly regions of western Guangdong (such as Yunfu and Maoming). These areas are characterized by drastic topographic relief. Influenced by natural topography (L and S factors) and soil properties (K factor), they constitute the natural high-risk background for soil erosion across the province.

In contrast, the Pearl River Delta region (surrounding Guangzhou and Shenzhen) and coastal plains (such as Zhanjiang and Chaoshan) are predominantly shown in dark green and light green, indicating slight and mild erosion. This indicates that under ideal conditions excluding the interference of vegetation and human activities, the flat terrain greatly weakens the erosive power of surface runoff, keeping the potential erosion risk in plain areas at an extremely low level.

With the introduction of vegetation cover (C factor) and soil and water conservation measures (P factor), the spatial pattern of actual soil erosion (USLE) undergoes significant changes, and the overall erosion intensity is substantially mitigated compared to potential erosion (Fig. 8). The most prominent feature is that the color of the mountainous areas in northern Guangdong (Shaoguan and Qingyuan) has noticeably faded from the orange-yellow in the RKLS map to predominantly light green, indicating a decline in erosion intensity from intense to mild or moderate levels. This shift intuitively reflects the remarkable effectiveness of large-scale afforestation projects in this region, where forest land effectively intercepts storm runoff and reduces the actual erosion modulus.

However, in western Guangdong and some low mountainous and hilly gentle slope areas of northern Guangdong, the actual erosion map still retains a considerable number of yellow and partially light orange patches, indicating the presence of moderate erosion and some intense erosion. These areas are often associated with a lack or simplification of vegetation cover caused by agricultural reclamation (such as dryland farming and orchards). This suggests that human agricultural activities have, to a certain extent, offset the improvement of natural geographical conditions, leading to relatively obvious risks of soil and water loss in local areas.

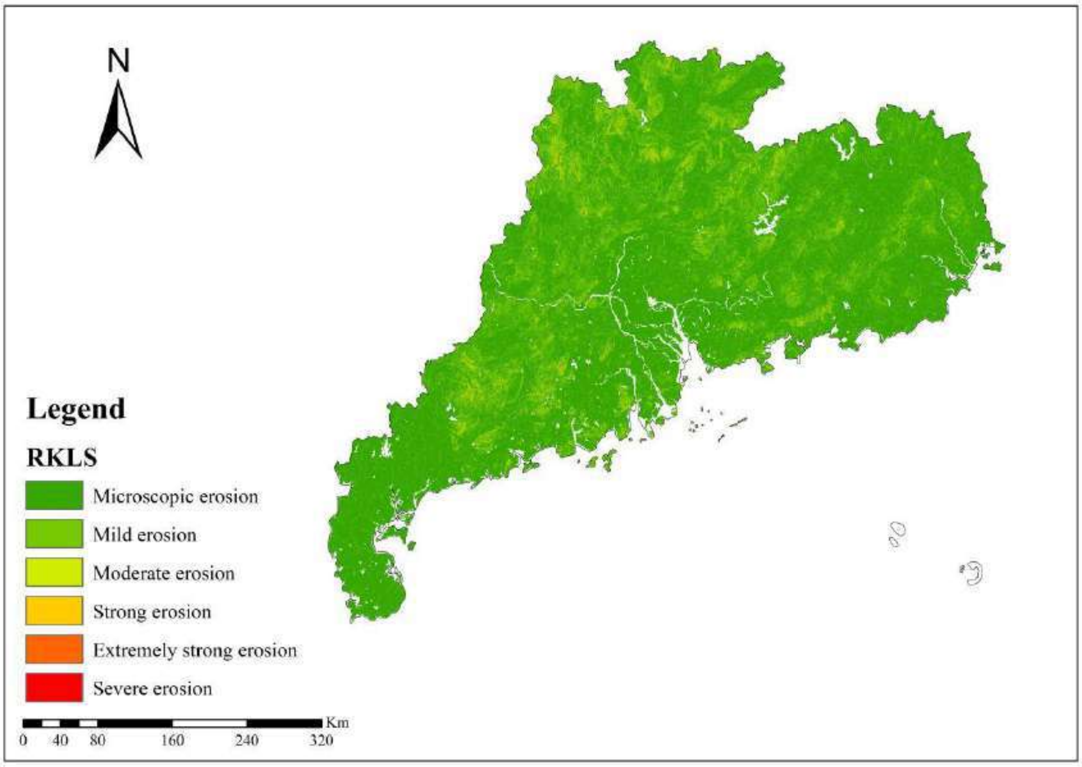

Fig. 7 Spatial distribution of potential soil erosion

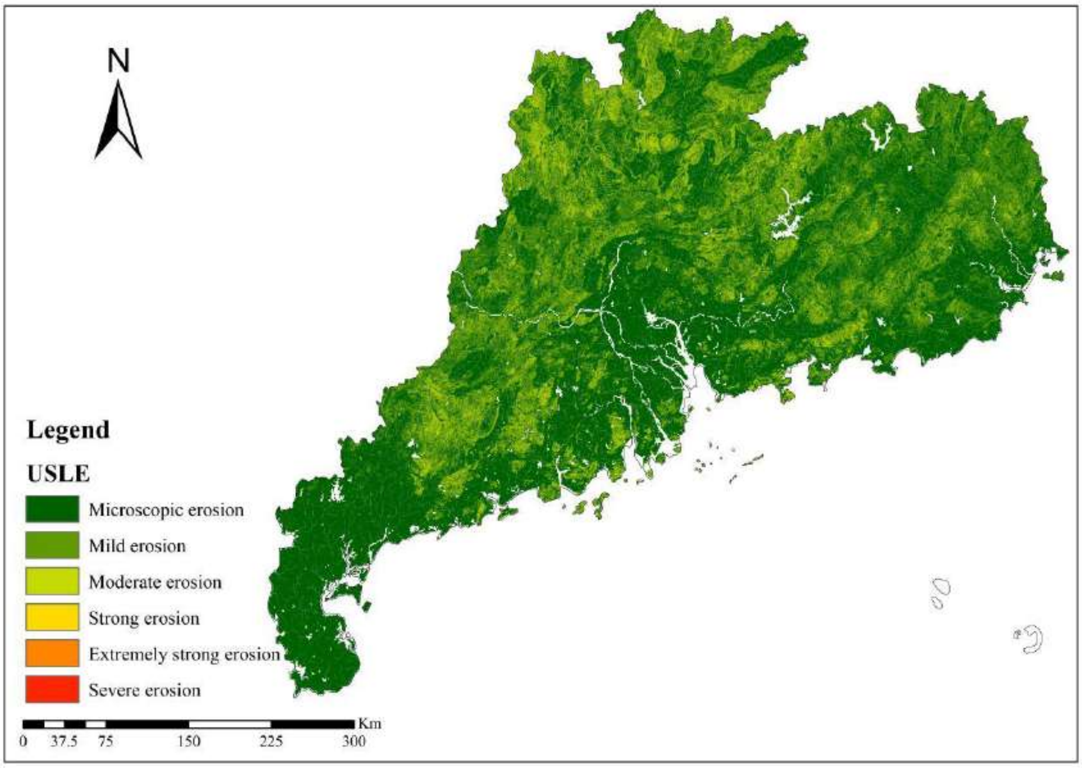

Fig. 8 Spatial distribution of actual soil erosion

IV. CONCLUSIONS AND PROSPECTS

4.1. Conclusions

Based on the USLE and InVEST models, combined with multi-source geospatial data from Guangdong Province, this study calculated the rainfall erosivity factor (R), soil erodibility factor (K), slope length factor (L), slope steepness factor (S), vegetation cover factor (C), and support practice factor (P). Consequently, the spatial distribution map of soil erosion in the study area was generated to analyze the regional soil erosion characteristics.

Rainfall Erosivity (R factor): Exhibits a spatial pattern of "higher in the south and lower in the north, and higher in the west and lower in the east." High-value zones are concentrated in the southern parts of Jiangmen and the southeastern parts of Yangjiang. Low-value zones are distributed in the mountainous areas of northern Guangdong (Shaoguan, Qingyuan, Meizhou) and the eastern coastal regions (Chaozhou, Shantou, etc.). The rainfall erosivity in eastern Guangdong is relatively low due to the leeward slope effect, while the R factor in the Pearl River Delta remains at a low level due to localized microclimate changes caused by urbanization and interpolation deviations.

Soil Erodibility (K factor): High-value zones are concentrated in the core area of the Pearl River Delta and the coastal areas of Zhanjiang (dominated by latosolic red soil and laterite, characterized by heavy texture and weak erosion resistance). Low-value zones are distributed in the mountainous and hilly regions of northern and eastern Guangdong (dominated by red soil and yellow soil, with high organic matter content and good aggregate structure). This indicates that the intrinsic soil conditions in plain and coastal areas are more susceptible to erosion.

Land Use: The province is dominated by forest land (accounting for over 60%, concentrated in northern and eastern Guangdong). Cultivated land is mainly distributed in Zhanjiang, the Pearl River Delta, and the plains of eastern Guangdong, while construction land is concentrated in the urban agglomerations of the Pearl River Delta.

Potential Erosion (RKLS): Dominated by natural factors (topography LS, soil K, and rainfall R), high-value zones (intense/extremely intense erosion) are concentrated in the Nanling Mountains of northern Guangdong (Shaoguan, Qingyuan) and the hilly regions of western Guangdong (Yunfu, Maoming), constituting the natural high-risk background for the entire province. In contrast, potential erosion in the Pearl River Delta and coastal plains is predominantly slight/mild due to the flat terrain.

Actual Erosion (USLE): Significantly modulated by anthropogenic factors (vegetation C and measures P). In the mountainous areas of northern Guangdong, large-scale afforestation projects have reduced the erosion intensity from a potentially high level to mild/moderate. However, in the gentle slope areas of western Guangdong and the low mountains and hills of northern Guangdong, moderate/intense erosion patches persist due to the lack of vegetation cover caused by agricultural reclamation (dryland farming, orchards). This reflects the mutual offsetting effect between human agricultural activities and natural erosion resistance.

In summary, natural factors (R, K, LS) determine the potential high-risk areas for soil erosion, while anthropogenic factors (land use, vegetation cover, and soil and water conservation measures) are the key modulating variables for actual erosion intensity. Ecological engineering can effectively reduce erosion levels in natural high-risk areas such as northern Guangdong, whereas unreasonable agricultural activities exacerbate erosion risks in regions like western and northern Guangdong.

4.2. Limitations and Prospects

This study still has certain limitations, and future research can be deepened in the following directions:

(1) Data Precision and Parameter Optimization

The current study employs data with a 90 m resolution, which has limited accuracy in depicting small-scale erosion (such as on sloping farmland and construction sites). Furthermore, the C and P factors were assigned based on empirical values without calibration using local measured data from Guangdong Province. Future research can utilize long-term positioning monitoring and high-resolution satellite remote sensing (such as Sentinel-2) to retrieve dynamic C factors, thereby improving the localization level of the parameters.

(2) Quantitative Disentanglement of Driving Factors

This study primarily focuses on the qualitative description of the spatial correlation of factors. Future studies could introduce methods such as the Geodetector and Structural Equation Modeling (SEM) to quantify the contribution rates of factors like R, K, LS, C, and P to soil erosion. This would help reveal the coupling mechanisms between soil erosion and climate change (e.g., frequency of extreme rainfall) as well as the intensity of human activities (e.g., GDP, population density).

(3) Spatiotemporal Dynamics and Scenario Simulation

The existing analysis is based solely on data from the year 2020. Future research could incorporate long-term time-series data (e.g., 2000–2020) to analyze the spatiotemporal evolution trends of erosion. Meanwhile, scenarios involving different land use changes (such as urban expansion and cultivated land protection) and climate changes (such as RCP scenarios) can be established to simulate future erosion risks. This would provide more precise decision-making support for soil and water conservation planning and the construction of the Nanling ecological barrier in Guangdong Province.

ACKNOWLEDGEMENTS

Guangdong Provincial Key Laboratory for Green Agricultural Production and Intelligent Equipment, School of Environmental Science and Engineering, Guangdong University of Petrochemical Technology, Maoming 525000, China

National Natural Science Foundation of China (22276041), the Guangdong Basic and Applied Basic Research Foundation (2023A1515030008), the Projects of Talents Recruitment of GDUPT (2022rcyj2002).

REFERENCES

[1] Zhao, Z. H. Remote sensing investigation of soil erosion in the northern area of Miyun Reservoir, Beijing. Journal of Geological Hazards and Environment Preservation, 2005, (04): 387-390.

[2] Zhou, B., Yu, X. X., and Chen, L. H., et al. Simulation of soil erosion in Beijing mountainous area based on InVEST model. Research of Soil and Water Conservation, 2010, 17(06): 9-13+19.

[3] Huang, Y. H., Lu, C. L., Fu, Q., et al. Study on soil loss prediction in southeast Fujian. Journal of Soil and Water Conservation, 1993, (04): 13-18.

[4] Lin, S. L., Huang, Y., Nie, Z. G., et al. Establishment of soil loss equation for sloping farmland in low hilly region of northern Liaoning. Chinese Journal of Soil Science, 1997, (06): 12-14.

[5] Cai, Q. G., Lu, Z. X., and Wang, G. P. Process model of erosion and sediment yield in a typical small watershed of the Loess Hilly and Gully Region. Acta Geographica Sinica, 1996, (02): 108-117.

[6] Li, B., and Zhang, J. T. Study on soil erosion in different vegetation regions of the Loess Plateau based on GIS. Journal of Agro-Environment Science, 2010, 29(01): 134-138.

[7] Zhang, X. K., Xu, J. H., Lu, X. Q., et al. Study on soil loss equation in Heilongjiang Province. Bulletin of Soil and Water Conservation, 1992, (04): 1-9+18.

[8] Qin, W., Zhu, Q. K., and Zhang, Y. Assessment of soil erosion in small watershed of the Loess Plateau based on GIS and RUSLE. Transactions of the Chinese Society of Agricultural Engineering, 2009, 25(08): 157-163+4.

[9] Mou, J. Z., and Meng, Q. M. Preliminary study on rainfall erosion and soil loss prediction equation. Science of Soil and Water Conservation in China, 1983, (06): 25-29.

[10] Yang, Z. S. Study on soil loss equation of sloping farmland in mountainous areas of northeastern Yunnan. Bulletin of Soil and Water Conservation, 1999, (01): 4-12.

[11] Cai, C. F., Ding, S. W., Shi, Z. H., et al. Study on predicting soil erosion amount in small watershed using USLE model and GIS IDRISI. Journal of Soil and Water Conservation, 2000, (02): 19-24.

[12] Hu, S., Cao, M. M., Liu, Q., et al. Comparison of soil conservation function of InVEST model from different perspectives. Geographical Research, 2014, 33(12): 2393-2406.

[13] Li, T., Liu, K., Hu, S., et al. Evaluation of ecological benefits of soil loss and soil conservation in Qinling Mountains based on InVEST model. Resources and Environment in the Yangtze Basin, 2014, 23(09): 1242-1250.

[14] Marques, S. M., Campos, F. S., David, J., and Cabral, P. Modelling Sediment Retention Services and Soil Erosion Changes in Portugal: A Spatio-Temporal Approach. ISPRS International Journal of Geo-Information, 2021, 10(4): 262.

[15] Ureta, J. C., Clay, L., Motallebi, M., and Ureta, J. Quantifying the Landscape's Ecological Benefits—An Analysis of the Effect of Land Cover Change on Ecosystem Services. Land, 2021, 10(1): 21.

[16] Wang, M., Ruan, J. J., Yao, J., et al. Study on ecosystem soil conservation function based on InVEST model—a case study of Ningde, Fujian. Research of Soil and Water Conservation, 2014, 21(04): 184-189.

[17] Chen, T. Y., Jia, Y. F., Wang, J. N., et al. Soil conservation status and function of Qilian Mountain National Nature Reserve based on InVEST model. Arid Zone Research, 2020, 37(01): 150-159.

[18] He, S. S., Zhu, W. B., Cui, Y. P., He, C. L., Ye, L. P., Feng, X. Y., and Zhu, L. Q. Study on soil erosion characteristics in Qihe River Basin of Taihang Mountains based on InVEST model. Resources and Environment in the Yangtze Basin, 2019, 28(02): 426-439.

[19] Wang, S., Wang, H. Y., Xie, Y. S., and Luo, H. Evaluation of soil conservation ecological service function before and after Grain for Green in Yan'an City. Research of Soil and Water Conservation, 2019, 26(01): 280-286.

[20] Sun, X. Q. Assessment of ecosystem service function in Shangri-La City based on InVEST model. Yunnan Normal University, 2017.

[21] Wang, Z. L. Gap analysis of wetland nature reserves in Nenjiang River Basin. Northeast Institute of Geography and Agroecology, Chinese Academy of Sciences, 2016.

[22] Wang, Y., Meng, J. J., Qi, Y., et al. Review of ecosystem management based on InVEST model. Chinese Journal of Ecology, 2015, 34(12): 3526-3532.

[23] Zhou, P. Issues related to the benefits of soil and water conservation in reducing sediment in the Yellow River by Mr. Zhou Peihua, an expert in soil erosion and soil and water conservation. Bulletin of Soil and Water Conservation, 2002, (01): 2.

[24] Jing, K., Jiao, J. Y., and Li, L. Y. Study on soil erosion and sediment delivery ratio in purple hilly area of the upper Yangtze River—A case study of Fujiang River Basin. Science of Soil and Water Conservation, 2010, 8(05): 1-7.

[25] Zhang, K. L., Peng, W. Y., and Yang, H. L. Soil erodibility value in China and its estimation. Acta Pedologica Sinica, 2007, (01): 7-13.

[26] Williams, J. R., Jones, C. A., Kiniry, J. R., and Spanel, D. A. The EPIC Crop Growth Model. Transactions of the ASAE, 1989, 32(2): 0497-0511.

[27] Williams, J. R. The erosion-productivity impact calculator (EPIC) model: a case history. Philosophical Transactions of the Royal Society of London. Series B: Biological Sciences, 1990, 329(1255): 421–428.

[28] Han, J., Cui, J. F., Yang, W., et al. Analysis of soil erosion change and driving factors in low hilly area based on InVEST model. Research of Soil and Water Conservation, 2022, 29(05): 32-39.

[29] Dang, H., Ge, L. J., Zhao, C. Y., et al. Study on soil conservation function in Chengou River Basin based on InVEST model. Journal of Lanzhou University (Natural Sciences), 2018, 54(05): 633-639.

[30] Liang, R. T. Reflections on the construction and development of Xiaoliang Soil and Water Conservation Science and Technology Demonstration Park in Maoming City. Primary Agricultural Technology Extension, 2019, 7(11): 115-118.

[31] Ma, G. B. Quantitative evaluation of soil erosion in small watershed of the Loess Plateau based on GIS. Nanjing Normal University, 2003.

[32] Pan, M. H., Wu, Y. Q., Ren, F. P., et al. Estimation of soil erosion in Dongjiang River Basin based on USLE. Journal of Natural Resources, 2010, 25(12): 2154-2164.

International Journal of Environment, Agriculture and Biotechnology
Vol-11, Issue-3; May-Jun, 2026
Peer-Reviewed International Journal
Journal Home Page Available: https://ijeab.com/
Journal DOI: 10.22161/ijeab

Adaptability and stability of nine onion (*Allium cepa* L.) varieties for bulb yield in off-season cultivation at the Guinean high savannah zone of Cameroon

Yaya Haman[1]*, Katoukam Maygon[1], Dolinassou Souina[2], Mamoudou Malalha[1], Noubissie Tchiagam J.B.[1]

[1]Laboratory of Plant Biology and Applications (LR-BVA), Department of Biological Science, Faculty of Science, University of Ngaoundéré, P.O. Box 454, Ngaoundéré, Cameroon
[2]Department of Plant Biology, Faculty of Science, University of Maroua, P.O. Box 814 Maroua, Cameroon
* Corresponding author: *hamanyaya019@gmail.com*

Received: 06 Apr 2026; Received in revised form: 05 May 2026; Accepted: 10 May 2026; Available online: 16 May 2026

Abstract— *The sensitivity of onions (Allium cepa L.) genotypes to environmental changes significantly influences yield and quality, necessitating adaptability studies across diverse locations. In Cameroon, onions are produced mainly in the sudano-sahelian regions. They are grown worldwide at different latitudes between 10°S and 65°N and are a very important source of food and income for rural populations. The current study investigates how the genotype by environment interaction (GEI) affects the bulb yield of nine onions varieties grown in diverse conditions at the Guinean high savannah zone of Cameroon, in order to contribute to food security and local development.The analysis of variance through Statgraphics Plus 5.0 program was used to study the variability of yield of the nine onions varieties grown on four environmental conditions in two locations, Marza and Bini, during dry season 2024 and 2025. Employing a split-split plot design with three replications, with genotypes as the main factor and environments as sub-factor, we assessed GEI effects on onion yield using GEST 98 software and identified adaptable and stable varieties. The results showed that bulb yield varied significantly with genotypes and environments and ranged from 23.82 to 87.23 t.ha. Three varieties namely Safari, El Kara and Violet de Galmi exhibited the highest bulb yield while lowest yields were noted on Ares and Red Creole.The combination of organic chiken manure and mineral NPK fertilize (CM+NPK) appeared as the best environement. The site of Marza and the growing season 2024 offered best conditions for onions cultivation comparing to the site of Bini and growing season 2025. Stability indices and AMMI analyses showed that varieties Ares, Red Creole and Prema were the most stable but with poor yield performance, while the other genotypes were with specific adaptability. The sudy concluded that varieties Safari, El kara and Violet Galmi could be selected as potential candidates for developing onion cultivation in the Guinean high savanna zone of Cameroon.*

Keywords— ***Allium cepa L., adaptability, stability, Guinean high savannas, off-season, Cameroon.***

I. INTRODUCTION

Onion (*Allium cepa* L.) is among the oldest cultivated crops and one of the most economically important vegetables worldwide. The onion is a bulbous crop consumed on daily basis in fresh as well as dried form, throughout the world. It belongs to the family Alliaceae and genus *Allium*. It shows more variation in eastern Mediterranean countries like Tajikistan, Turkmenistan to Pakistan and India. Central Asia is considered its center of origin (Jokanovic *et al.*, 2016). In India, it is an integral part of daily cuisine and is often referred to as the 'Queen of the Kitchen' (Biswas *et al.*,2020). Onions are one of the most widely traded raw vegetables in the world due to their relatively long shelf life (Cattivelli *et al.*, 2021). They have dietary, nutritional, and therapeutic benefits (Bianchini and Vainio, 2001). On average, a person consumes roughly 10 kilograms of onions per year and can be eaten raw, cooked, pickled, or powdered (Cattivelli *et al*., 2021). The growing demand for onion is driven due to its nutritional value and health-promoting constituents, including essential minerals and vitamins (Gupta *et al.,*2025a). Historically, onions have also played an important role in traditional medicine, being recognized for their therapeutic properties in treating fever, bronchitis, and cardiovascular ailments, as well as for their diuretic, digestive, and lipid-lowering effects (Gupta *et al.,*2025a). Therapeutically, various studies have shown that regular consumption of raw onions plays a role in blood clotting and the prevention of various diseases as certain cardiovascular diseases, and cancers (Bianchini and Vainio, 20012; Graf *et al*., 2005).

Onion marketable yield can be greatly impacted by climate and environmental conditions (Gupta *et al.,* 2024). Varieties that thrive in one environment may not necessarily flourish in other environments or in a range of climates (Brdar-Jakanovic *et al*., 2012). The genotype-by-environment interaction (GEI) is an important phenomenon in plant breeding which defines the differential response of genotypes to various environments as multiple environment trials (Brancourt-Hulmel *et al*., 1997; Annichiarico, 2002; Gupta *et al*., 2024). The cultivation of onions is widespread throughout Africa, with farmers producing the crop across diverse agroecological zones and climatic conditions (Atnafu, 2023). The total onion production in Africa was 14.9 million tons (FAOSTAT, 2023). The main onion-producing countries in Africa are Egypt, Algeria, Sudan, Nigeria, Niger, and Morocco (FAOSTAT, 2023). In the Central African sub-region in particular, annual onion production was about 90000 tons with an average yield of 10 t.ha (FAOSTAT, 2023). In Cameroon, onions are produced mainly in the sudano-sahelian regions, and unfortunately their expansion at the national level is statistically low (Cathala *et al*., 2023). Production in the North and Far North regions of Cameroon accounts for 85% of national production. The diversity of agroecological zones in Cameroon poses an adaptability problem for certain crops, notably onions in the Guinean high savannah zone. In Cameroon, the onion sector is an agricultural sector that brings together the various actors and accounts for most of the national production, with a production of 390.000 tons (Cathala *et al*., 2023). The onion sector is an economic powerhouse that brings together various stakeholders and accounts for most of the national production (Cathala *et al*., 2003). The predominance of market gardening in Adamawa, is focused on tomatoes, potatoes, sweet potatoes, peppers, and eggplants. The abundance of rainfall and low temperatures make this environment a complex area for onion cultivation (Yonkeu, 1993; Kamga *et al*., 2016). The low productivity of this important vegetable crop is often attributable to the poor application of appropriate farming techniques and poor access to agricultural inputs (Ayalew *et al*., 2015). Furthermore, important genetic diversity has been reported in onions (Tignegre *et al*., 2022; Gupta *et al*., 2025b). Onion crop is known to require substantial amounts of nutrients to be applied before planting (Kazimierczak *et al*., 2021). Given these conditions, studying the adaptability and stability of nine onion varieties based on their genetic performance would be beneficial for food security and local development. Crop trait stability is known to be influenced by factors including the environment, genotype and the genotype-environment interaction. The objective of the present study was to identify adapted onion genotypes for sustainable production in the Guinean high savannah zone of Cameroon. The aim of the study was to evaluate bulb yield performance and stability in nine onion cultivars grown in two locations of the high Guinean savannah zone under conventional (mineral fertilization) and organic (chiken manure, unfertilized control) production systems during two-year trials (2024 and 2025).

II. MATERIALS AND METHODS

Testing environments

The field experiment was carried out in two consecutive dry seasons (october to march 2024 and 2025) at Bini (7°13' N; 13°34' E) and Marza (7°27' N; 13°61' E) in the Adamawa region of Cameroon. The Adamawa region belongs to the Guinean high savannah zone, characterized by a tropical Sudano-Guinean climate with a long rainy season from April to October and a dry season from November to March (Yonkeu, 1993). The annual rainfall is approximately 1440 mm and the temperatures are cool, averaging 22°C with a maximum of 34.6°C in May and a minimum of 9.9°C in January. Relative humidity is around 70% and the soils are predominantly red ferralitic soils developed on granite or old basalt, and hydromorphic (gleysoils) soils found near rivers (Yonkeu, 1993).

Genotypes

The experimental material (Table 1) comprised nine onion varieties including four cultivars (Goudami, Kada Goudami, El kara and Chagari) produced locally by onion farmers in the Far North region, and five improved varieties (Ares, Prema, Red Créole, Safari and Violet de Galmi) obtained from SEMAGRI compagny. Onion seedlings were produced for forty days in nurseries before transplantation into the experimental plots.

Table 1: Onion seed varieties and their characteristics

Genotype	Origin	Cycle (Days)	Suitable season
Ares	SEMAGRI	90-110	Rainy season
Chagari	Local, Mayo-Tsanaga	100-135	Rainy season
El-Kara	Local, Far North	100-130	Dry/rainy season
Goudami	Local, Far North & North	105-110	Dry season
Kada Goudami	Local, Far North	120-130	Dry season
Prema	Agricultural Seed Shop	110-120	Dry/rainy season
Red Creole	SEMAGRI	135 - 145	Dry season
Safari	SEMAGRI	110-120	Dry season
Violet de Galmi	SEMAGRI	120-143	Dry season

Field experimental trials

The study took place from October to March in 2024 and 2025, from nursery planting to harvest. In each location, the experimental design used is a split plot with three replications, the main factor being the genotypes and the sub-factor is the environments (negative control, chicken manure, NPK fertilizer, and combination of chicken manure and NPK 20-10-10 fertilizer). The experimental unit consists of a 1m² plot and a 30cm irrigation channel, as well as a 20cm earth embankment between the plots or experimental units on the same line. The experimental plot is 12 m long and 10.8 m wide, giving a total area of 129.6 m². On the experimental units, the plants are transplanted at equidistant intervals of 10 cm and 15 cm between rows.

The nursery was established on October 1 on a 1m² plot with 30g of seeds for each variety. The maximum time for plants in the nursery is 45 days. Transplanting consists of removing the plants from the nursery and returning them to the field. The plants are transplanted superficially. Transplanting is carried out on previously watered beds. On a 1m² experimental unit, the plants are transplanted at 10cm intervals and 15cm spacing, giving a density of 60 plants per 1m² unit.

The organic fertilizer was applied before transplanting at a rate of 1 kg per tray, then lightly watered for two weeks. The mineral NPK fertilizer was spreaded two weeks after transplanting and six weeks after transplanting. Weeding was carried out regularly at different stages of the plant's development.

The only variable measured concerned the bulb yield at maturity. The weight of ten selected bulbs was measured using an SF-400 digital scale with a capacity of 1000g×1g/353oz×0.1oz. The yield was extrapolated to t. ha as Tignegre *et al*. (2022)

$$\text{Bulb yield} = (\text{PmB x } (\text{NP/m}^2) \text{ x } 600000) / 10000$$

Where PmB is the average bulb weight and NP/m^2 is the number of plants per square meter.

Characterization of soils

Soil sampling was carried out according to the method described by Pauwels *et al*. (1992) at a depth of 30 cm. Once collected, the soils samples were mixed several times to ensure homogeneity, and analyzed at the laboratory of soil analysis and environmental chemistry of the the University of Dschang. The pH of the soil was determined in a 1:2.5 (w/v) soil: water suspension, according to the method described by Pauwels *et al*. (1992). The soil total nitrogen was determined after mineralization of substrate samples using the AFNOR method (1984) and the calorimetric technique described by Devani *et al*. (1984). The phosphorus content was determined by absorption spectrophotometry (Rodier, 1978). The organic matter was measured as described by Pauwels *et al*. (1992).

The determination of exchangeable bases in the soil was carried out using the Metson method for soils (Pauwels *et al*., 1992) with a pH below 7, and extraction was carried out with ammonium acetate at pH 7. The potassium in the extract was measured by flame spectrophotometry (Pauwels *et al*., 1992).

III. DATA ANALYSIS

Separate analysis of variance was performed for each location, environments and season to acess the variabiliy of the onions yield using STAGRAPHICS PLUS 5.0 software. The means were separated using the Least Significant Difference (LSD) at the 5% level of probability. The combined analysis of variance was done using Hardwick and Wood (1972) model with the nine genotypes being considered as fixed effects and replications within the 16 environments being random mode. GEI was quantified used pooled analysis of variance, which partitioned the total variance into its component parts (genotype, environment, interaction and error).

Different stability models were performed to support decision-making for varietal selection: Finlay and Wilkinson's (1963) joint regression analysis (bi), Wricke's (1962) ecovalence (Wi), Shukla's (1972) procedure of stability (σ^2i) and the AMMI analysis described by Yan and Tinker (2006).

The joint regression model of Finlay and Wilkinson (1963) assesses the stability and adaptability based on the regression coefficient (bi) of the mean of each variety in all environments on the environmental index.

The concept of ecovalence (Wi), introduced by Wricke (1962), quantifies genotypic contributions to the sum of squares of the GEI. The Wi value for the ith genotype is determined by squaring and summing its interactions across different environments. Genotypes characterized by lower Wi values exhibit minor deviations from the mean across environments, indicating heightened stability. The ecovalence stability coefficient, W_i, is a measure of genotype stability over locations and is computed as:

$$Wi=\sum(Y_{ij}-Yi-Yj+\mu)^2$$

where Y_{ij} is the mean performance of genotype i in the j^{th} environment; Y_i is means of i^{th} genotype across environments, Y_j is means of j^{th} environment across all genotypes and μ is the grand mean (Wricke, 1962)

Shukla (1972) stability variance σ_i^2, is a stability index given by the following formula:

$$\sigma^2 i= (p/ (p-2) (q-1)) \Sigma i (Y_{ij} - Y_i - Y_j + \mu)^2 - \Sigma i \Sigma j (Y_{ij} - Y_i - Y_j + \mu)^2/p/ (p-2)(q-1),$$

where Y_{ij} is the mean performance of genotype i in the j^{th} environment; Y_i is means of i^{th} genotype across environments, Y_j is means of j^{th} environment across all genotypes and μ is the grand mean, p is the number of genotypes and q is the number of environments (Shukla, 1972).

The stability analyses, the AMMI and biplot models were evaluated using the program GEST 98 (Ukai, 2000).

IV. RESULTS AND DISCUSSION

Physico-chemical characterization of the soil

The characterization of the experimental soil at the two locations, Marza and Bini (Table 2), revealed a sandy-clay texture at Marza with sand (57%) and clay (23.5%) and at Bini with sand (48.5%) and clay (36.5%). The water pH was slightly basic at Marza (7.5) and Bini (7.7). Similarly, the KCl pH was acidic (6.8) at Marza and neutral (7) at Bini. These results showed that the pH levels at Marza and Bini were within the favorable range (6 and 7) for onion cultivation (Gelahun and Getaneh, 2019). The locality of Bini had more macroelements (nitrogen nitrate, phosphorus, and potassium) available in the soil than Marza. The composition of organic matter, the sum of exchangeable bases, and the cation exchange capacity offered the locality of Marza the possibility of great water retention and accessible microelements for gardening crops. With a view to improving the exchangeable base capacity and cation exchange capacity in order to enhance the availability of macro- and microelements in different soils, it was necessary to apply undecomposed chicken manure as a base fertilizer, with or without the addition of synthetic NPK compound fertilizer (20-10-10).

Table 2: Physicochemical characteristics of the study soils

Characteristic	Marza	Bini
Clay (%)	23.5	36.5
Silt (%)	19.5	15
Sand (%)	57	48.5
pH water	7.5	7,7
pH KCl	6.8	7
Organic matter (%)	7.7	6.5
Nitrogen nitrate, N-NO3	2078.95	3518.53
Phosphorus (mg/Kg)	25.31	26.05
Potassium (méq/100g)	0.173	0.298
Exchange bases (méq/100)	11.11	3.25
Cation Exchange Capacity	21.45	11.74

Variability of bulb yield of nine onion varieties over environments

The yield values of the nine selected varieties at the locations of Marza and Bini during dry seasons 2024 and 2025, undrer four fertilizations regimes: control, chicken manure, NPK fertilizer and combination of NPK and chicken manure were presented on Tables 3, 4, 5 and 6. In the first year of the experiment in Marza in 2024 (Table 3), the most favorable environment for onion cultivation was the combination of chicken manure and mineral fertilizer CM+NPK (87.23 t ha^{-1}) and the least favorable was control (23.82 t ha^{-1}). The genotypes best suited to all environments were variety Safari (77.56 t ha^{-1}), Violet Galmi (70.07 t ha^{-1}), Prema (69.42 t ha^{-1}), Kada Goudami (64.24 t ha^{-1}) and El Kara (63.11 t ha^{-1}). The lowest yield values were noted on Ares (35.25 t ha^{-1}) and Red Creole (48.58 t ha^{-1}).

At Bini during 2024 growing period (Table 4), the most suitable growing environment is CM+NPK (57.33 t ha^{-1}) and the least suitable is control (21.64 t ha^{-1}). The most suitable genotypes were Chagari (51.09 t ha^{-1}), El Kara (46.12 t ha^{-1}), Safari (45.66 t ha^{-1}) and Prema (44.66 t ha^{-1}). The lowest yield values were recorded on Ares (18.67 t ha^{-1}) and Red Creole (30.23 t ha^{-1}). Globally, during the 2024, growing season, the tested genotypes significantly had poor performance at Bini (mean yield = 39.0 t ha^{-1}), comparing to Marza (mean yield = 60.85 t ha^{-1}).

During the second experimental campaign (2025), the study revealed that at Marza site highly significant difference were noted among genotype ($p<0.01$) (Table 5). Five varieties showed good yield performance: El Kara (89.34 t ha^{-1}), Goudami (76.32 t ha^{-1}), Galmi Violet (72.19 t ha^{-1}), Safari (68.05 t ha^{-1}), and Prema (63.03 t ha^{-1}). Genotype Ares, Chagari and Kada Goudami were the least suitable with yield values of 27.8 t ha^{-1}, 33.4 t ha^{-1} and 42.9 t ha^{-1}respectively. The most suitable environment for cultivation was CM+NPK (76.75 t ha^{-1}) and the poorest environment was the control (19.9 t ha^{-1}). At Marza, the growing season 2024 (mean yield = 60.85 t ha^{-1}) offered best conditions for onions cultivation comparing to growing season 2025 (mean yield = 57.89 t ha^{-1}).

At the Bini site during 2025 campaign, the analysis of variance showed highly significant difference ($p<0.01$) for genotypes (Table 6). The most suitable varieties in the different environments are: El Kara (51.26 t ha^{-1}), Safari (48.33 t ha^{-1}), Prema (44.05 t ha^{-1}) and Violet Galmi (42.71 t ha^{-1}) while the poorest varieties were Ares (21.20 t ha^{-1}) and Chagari ((23.33 t ha^{-1}). The best environment was the combination CM+NPK (50.8 t ha^{-1}). The growing season 2024 at Bini (mean yield = 39.00 t ha^{-1}) offered best conditions for onions cultivation comparing to growing season 2025 (mean yield = 37.98 t ha^{-1}).

Overall, for both the 2024 and 2025 campaigns, the study showed significant variability within varieties, environments, and locations. The variations observed between the different varieties are due to genotypic factors and environmental factors. Horn et al. (2018), Tignegre et al. (2022), Gupta et al. (2024), Gupta et al. (2025b) mentioned that, the highly significant differences in locations, years, and genotypes for onions bulb yields may be due to variable climatic and edaphic conditions between locations and the diversity of the genetic makeup of genotypes that may respond differently to locations. Ayalew *et al*. (2015); Gethaun and Getaneh (2019), also observed significant variations in the performance of garlic cultivars from different locations in Gonder, northern Ethiopia. As expected, the highest yields have been measured for onion grown on plots treated with mineral fertilizer and chicken manure. In Serbia, Brdar-Jakanovic *et al.* (2012) noted that highest yields were obtained from NPK fertilized plots and out of three organic production systems, onion grown under bacterial fertilization had the highest yield, whereas no significant yield differences have been observed between unfertilized and farmyard manure fertilized plots. Kazimierczak *et al.* (2021) clearly demonstrated that organic fertilizer products can deliver the same and possibly slightly higher yields when compared to the recommended mineral fertilization regimes in onions. The performance of the varieties fluctuated sightly during the two years of trials. In sudano-sahelian zone of Northern Cameroon, Moutsavara *et al.* (2025) noted high repeatability values (0.61 to 0.77) for bulb yield of seven varieties grown in three locations during two-year trials.

Table 3: Bulb yield (t ha^{-1}) of nine onion varieties in four environments at the Marza in 2024

Varieties	Control	CM	CM+NPK	NPK	Gen. Mean
Ares	14.9±3.63^{d}	40.52±2.59^{f}	56.62±5.52^{d}	28.94±5.87^{e}	35.25±4.40 (9)
Chagari	27.36±7.61^{a}	72.66±5.59^{d}	94.96±5.53^{b}	54.34±4.74^{c}	62.33±5.86 (6)
El Kara	18.24±3.5^{c}	93.4±3.64^{a}	101.4±8.42^{a}	38.4±6.21^{d}	62.86±5.44 (5)
Goudami	27.82±4.75^{a}	80.4±3.03^{c}	56.76±7.31^{d}	56.76±7.31^{c}	55.44±5.6 (7)
Kada Goudami	23.74±4.12^{b}	83.68±6.22^{bc}	87.66±6.45^{b}	61.88±5.76^{b}	64.24±5.63 (4)
Prema	27.9±6.32^{a}	87.74±5.14^{b}	101.9±18.79^{a}	60.14±8.79^{b}	69.42±9.76 (3)
Red Creole	13.74±3.85^{d}	62.16±5.22^{e}	76.91±7.76^{c}	41.5±7.29^{b}	48.58±6.03 (8)
Safari	29.76±1.63^{a}	95.58±4.09^{a}	108.24±5.64^{a}	76.66±6.66^{a}	77.56±4.51 (1)
Violet Galmi	20.9±3.25^{bc}	94.58±5.04^{a}	102.98±7.09d^{a}	61.8±9.03^{b}	70.07±6.10 (2)
Env. Mean	**23.82±4.4^{D}**	**78.97±7.08^{B}**	**87.23±9.54^{A}**	**53.38±8.15^{C}**	**60.85±9.16**
Probability	0.0001	0.0001	0.0001	0.0001	

CM: Chicken manure, CM+NPK: Chicken manure and synthetic NPK fertilizer (20-10-10) environment, Gen.: Genotypic, Env.: Environmental. In a column, numbers followed by the same small letter do not differ significantly at the 5% level. Number between parenthesis denote ranking order of genotypes. Environmental means followed by the same subscript in capital letter dot not differ significantly at 5% level.

Table 4: Bulb yield (t ha^{-1}) of nine onion varieties in four environments at the Bini site in 2024

Varieties	Control	CM	CM+NPK	NPK	Gen. Mean
Ares	10.56±0.78^{f}	25.68±3.30^{f}	28.78±5.80^{g}	9.66±1.59^{f}	18.67±2.86 (9)
Chagari	33.26±3.76^{a}	82.12±5.72^{a}	62.12±8.36^{c}	26.84±2.98^{bc}	51.09±5.20 (1)
El Kara	26.74±3.79^{b}	56.44±3.80^{cd}	74.48±14.89^{a}	26.8±9.42^{bc}	46.12±7.97 (2)
Goudami	25.94±3.89^{bc}	54.44±2.80^{d}	58.04±9.24^{de}	19.34±4.05^{de}	39.44±4.99 (6)
Kada Goudami	22.96±2.19^{cd}	61.52±4.59^{c}	56.92±6.90^{e}	17.2±8.48^{e}	39.65±5.54 (5)
Prema	24.02±2.91^{cd}	53.5±3.50^{d}	60.54±9.76^{cd}	38.54±3.81^{a}	44.15±4.99 (4)
Red Creole	13.1±1.49^{ef}	41.32±2.19^{e}	49.66±8.82^{f}	16.84±5.53^{e}	30.23±4.50 (8)
Safari	16.62±4.14^{e}	70.02±5.49^{b}	68±8.44^{b}	28.01±6.99^{b}	45.66±6.26 (3)
Violet Galmi	21.56±2.60^{d}	43.52±2.17^{e}	57.44±2.82^{de}	23.06±4.35^{cd}	36.4±2.98 (7)
Env. Mean	**21.64±5.31^{B}**	**54.28±9.20^{A}**	**57.33±11.37^{A}**	**22.74±5.27^{B}**	**39.00±11.78**
Probability	0.0001	0.0001	0.0006	0.0007	

CM: Chicken manure, CM+NPK: Chicken manure and synthetic NPK fertilizer (20-10-10) environment, Gen.: Genotypic, Env.: Environmental. In a column, numbers followed by the same small letter do not differ significantly at the 5% level. Number between parenthesis denote ranking order of genotypes. Environmental means followed by the same subscript in capital letter dot not differ significantly at 5% level.

Table 5: Bulb yield (t ha^{-1}) of nine onion varieties in four environments at the Marza site in 2025

Varieties	Control	CM	CM+NPK	NPK	Gen. Mean
Ares	11.88±2.02^{e}	38.78±7.79^{g}	36.10±4.92^{f}	24.42±4.73^{f}	27.8±4.86 (9)
Chagari	14.60±4.16^{d}	50.98±3.03^{ef}	39.84±6.22^{f}	28.22±7.37^{f}	33.41±5.19 (8)
El Kara	32.26±6.78^{a}	104.74±12.87^{a}	124.44±12.90^{a}	95.92±27.06^{a}	89.34±14.90 (1)
Goudami	21.36±3.86^{c}	87.10±7.86^{b}	101.76±7.05^{b}	95.04±4.94^{a}	76.32±5.92 (3)
Kada Goudami	15.60±4.78^{ab}	46.78±3.24^{f}	48.62±7.98^{e}	60.6±11.12^{d}	42.9±6.78 (7)
Prema	31.16±6.18^{a}	66.76±5.11^{d}	78.66±13.64^{cd}	75.52±2.81^{c}	63.03±6.93 (5)
Red Creole	11.06±2.95^{e}	52.68±5.30^{e}	73.58±7.83^{d}	54.44±13.55^{e}	47.94±7.40 (6)
Safari	25.64±4.59^{b}	73.00±3.37^{c}	86.2±15.10^{c}	87.34±4.31^{b}	68.05±6.84 (4)
Violet Galmi	15.50±4.64^{d}	86.94±5.02^{b}	101.52±9.0^{b}	84.8±12.53^{b}	72.19±6.79 (2)
Env. Mean	**19.89±8.67^{C}**	**67.53±12.04^{B}**	**76.75±20.15^{A}**	**67.37±12.72^{B}**	**57.89±11.89**
Probability	0.0001	0.0001	0.0001	0.0001	

CM: Chicken manure, CM+NPK: Chicken manure and synthetic NPK fertilizer (20-10-10) environment, Gen.: Genotypic, Env.: Environmental. In a column, numbers followed by the same small letter do not differ significantly at the 5% level. Number between parenthesis denote ranking order of genotypes. Environmental means followed by the same subscript in capital letter dot not differ significantly at 5% level.

Table 6: Bulb yield (t ha^{-1}) of nine onion varieties in four environments at the Bini site in 2025

Varieties	Control	CM	CM+NPK	NPK	Gen. Mean
Ares	14.73±3.37^{d}	26.94±4.62^{e}	26.84±5.64^{e}	16.30±2.39^{g}	21.20±4.00 (9)
Chagari	24.56±2.31^{b}	23.16±7.30^{f}	27.00±4.26^{e}	18.60±3.99^{g}	23.33±4.46 (8)
El Kara	24.23±2.58^{b}	49.34±6.49^{a}	68.50±8.58^{a}	57.98±7.38^{a}	50.01±6.25 (1)
Goudami	21.26±3.10^{c}	49.73±6.17^{a}	54.24±7.68^{c}	37.14±4.86^{e}	40.59±5.45 (5)
Kada Goudami	21.68±2.27^{c}	42.44±6.75^{b}	48.58±6.28^{d}	43.07±4.67^{d}	38.94±4.99 (6)
Prema	28.12±2.08^{a}	33.82±7.99^{d}	63.52±8.68^{b}	52.82±6.36^{b}	44.57±6.27 (3)
Red Creole	11.55±1.55^{e}	36.74±7.28^{cd}	48.58±6.90^{d}	30.26±9.68^{f}	31.73±6.35 (7)
Safari	30.80±2.60^{a}	42.58±9.63^{b}	66.54±3.75^{ab}	53.38±8.17^{b}	48.32±6.03 (2)
Violet Galmi	24.20±2.68^{b}	38.64±3.30^{c}	53.42±6.47^{c}	48.16±9.45^{c}	41.10±5.47 (4)
Env. Mean	**22.34±6.19^{C}**	**38.52±10.46^{B}**	**50.95±5.82^{A}**	**40.11±10.07^{B}**	**37.98±9.13**
Probability	0.0001	0.007	0.001	0.009	

CM: Chicken manure, CM+NPK: Chicken manure and synthetic NPK fertilizer (20-10-10) environment, Gen.: Genotypic, Env.: Environmental. In a column, numbers followed by the same small letter do not differ significantly at the 5% level. Number between parenthesis denote ranking order of genotypes. Environmental means followed by the same subscript in capital letter dot not differ significantly at 5% level.

Combined analysis of variance for bulb yield of nine genotypes over 16 environments

Hardwick and Wood (1972) analysis of variance for onion bulb yield (Table 7) showed that the mean square of environmental factors (66.51%) significantly affects yield compared to genotype-environment interaction (16.88%) and genotype (16.61%). These results showed a non-linear and insignificant interaction with genotype rank reversal (E>GEI>G). Yield variations are due mainly to environmental effects and genotype x environment effects. Although variety performance varied significantly depending on the environment, the GEI had great impacts on bulb yield. Tignegre *et al*. (2022) noted a similar result with environmental and GEI effects explaining most of the variation however, the magnitude of GEI was lower in the present study. Our result is consistent with many previous studies that reported significant GEI effects not only in onions. Environmental diversification could be a source of variability in onion bulb yield. Similarly, Bezu *et al*. (2014) noted an impact of environmental factors on the performance of garlic genotypes. This larger proportion of environmental variation can be attributed to significant disparities in soil types, annual precipitation, average temperatures, and other weather conditions (Gupta *et al.*, 2024).

Table 7: Combined analysis of variance for bulb yield

Source of variation	**Df**	**SS**	**MS**	**% SS**	**F-value**
Genotype (G)	8	17425.44	2178.18	16.61	182.18*
Environment (E)	15	69765.80	4651.05	66.51	390.51**
Interaction (GEI)	120	17709.94	147.58	16.88	12.39*
Residual	112	13342.18	11.91		
Total	143	10490118			

dl: Degree of freedom, GEI: Genotype x environment interaction, SS: Sum of squares, MS: Mean square, % SS: percentage of the sum of squares; **: significant at the 1% probability; *: significant at the 5% probability.

Stability and adaptability of genotypes

The values of different stability procedures and adaptability measure for bulb yield of each onion variety are presented in Table 8. The values of regression coefficient bi of Finlay and Wilkinson (1963) ranged from 0.526 (Ares) to 1.300 (Violet Galmi) (Figure 1). It can be seen that varieties 3 (El Kara), 8 (Safari), 9 (Violet de Galmi), and 4 (Goudami) had bi values larger than one (bi >1), and was therefore unstable. These varieties are specifically adapted to the favorable environments. Varieties that showed instability in different environments display a better performance for the breeder, but with a high risk of selecting varieties with weak genetic makeup. Varieties 1 (Ares), 2 (Chagari), 5 (Kada Goudami), 7 (Red Créole), and 6 (Prema) had regression coefficient smaller than one (bi < 1), which indicated highest stability. These varieties are considered to be generally adapted in the study area. Brancourt-Hulmel *et al.* (1997) indicated that the stability of a genotype depends on its resistance to fluctuations caused by variations in environmental conditions. According to Brdar-Jokanović *et al.* (2016), stability referred to the maintenance of a genotype's yield performance in various environments, and an assessment of a genotype's average performance and stability is necessary before selection. Gupta *et al.* (2022, 2024) stipulated that the identification of genotypes with both high mean performance and stability is therefore crucial for the development of cultivars suited to variable agro-climatic regions. An ideal genotype should not only demonstrate superior performance but also maintain stability within and across diverse environments.

International Journal of Environment, Agriculture and Biotechnology
Vol-11, Issue-3; May-Jun, 2026
Peer-Reviewed International Journal
Journal Home Page Available: https://ijeab.com/
Journal DOI: 10.22161/ijeab

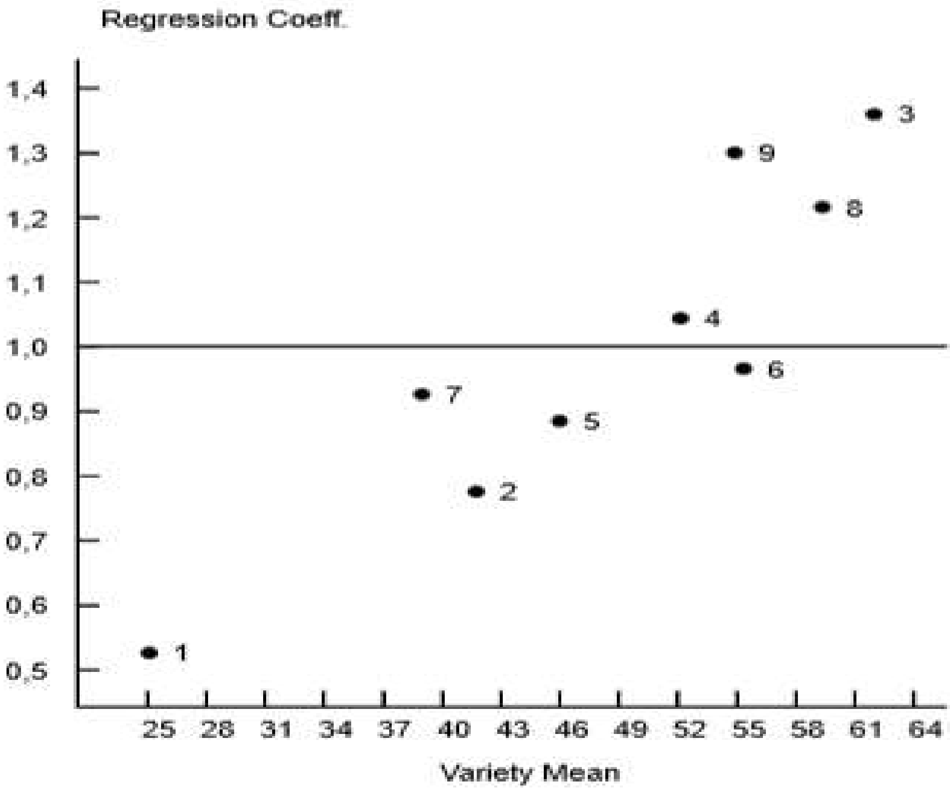

Fig.1: Adaptability and stability of nine onion varieties at the Marza and Bini sites in 2024 and 2025 according to the Finlay-Wilkinson (1963) regression

1 : Ares ; 2 : Chagari ; 3 : El Kara ; 4 : Goudami ; 5 : Kada Goudami ; 6 : Prema ; 7 : Red Creole ; 8 : Safari ; 9 : Violet de Galmi.

The Wricke (1962) ecovalence (Wi) values ranged from 211.34 (Ares) to 4770.94 (Chagari). The most stable genotypes with the lowest Wi values were Ares, Red Creole and Prema while those with highest values (Chagari, El Kara and Goudami) were the most unstable. The Wi values indicated the level of stability of the genotypes in multi-environments trials (Brancourt-Hulmel *et al.*, 1994; Annichiarico, 2002). When Wi = 0, stability is at its maximum, and when Wi is high, the genotypes are unstable.

Shukla (1972) stability variance σi^2 showed an index of stability varying from 167.57 (Ares) to 6020.96 (Chagari). Ares, Red Creole (461.40), Kada Goudami (491.58) and Prema (520.99) were the most stable, and genotypes Chagari and El Kara (1125.21) with the highest values were unstable.

In general, data obtained on stability showed that none of the tested varieties could be considered as completely stable. Similar observation has been previously reported in onion by Tignegre *et al.* (2022) in Ghana and Mali, Atnafu (2023) in Nigeria, Gupta *et al.* (2025a) in India, Moutsavara *et al.* (2015) in Northern Cameroon. The ideal genotype should have good yield performance and be absolutely stable with zero GEI. Among top yielding genotypes, Safari, El Kara and Violet Galmi could be exploited as specifically germplasm in favorable environment.

Table 8: Stability and adaptability of genotypes for bulb yield

Genotype	Code	*bi*	W_i	σ_i^2
Ares	1	0.526 (1)	211.34 (1)	167.57 (1)
Chagari	2	0.776 (2)	4770.94 (9)	6020.96 (9)
El Kara	3	1.360 (9)	3544.19 (8)	1125.21 (8)
Goudami	4	1.044 (6)	2646.97 (7)	738.93 (5)
Kada Goudami	5	0.885 (3)	1404.49 (5)	491.58 (3)
Prema	6	0.966 (5)	589.46 (3)	520.99 (4)
Red Creole	7	0.926 (4)	309.38 (2)	461.40 (2)
Safari	8	1.216 (7)	855.23 (4)	797.21 (6)
Violet Galmi	9	1.300 (8)	1477.95 (6)	925.88 (7)

bi: Finlay and Wilkinson regression coefficient; Wi: Wricke's ecovalence; σi2: Shukla's stability variance; A: Ares variety; C: Chagari variety; EK: El Kara variety; G: Goudami variety; KG: Kada Goudami; P: Prema variety; RC: Red Creole variety; S: Safari variety; and VG: Violet de Galmi.

AMMI biplot analysis

The AMMI (additive main effects and multiplicative interaction) analysis also showed the genotype x environment interaction for better selection of suitable genotypes and environments (Figure 2). This figure helps guide choices based on the distance of genotypes and environments from the center of the IPCA1 and IPCA2 axes (Yan and Tinker, 2006. The best environments were the combination of chiken manure and NPK fertilizer in 2024 and 2025 (BFP+NPK25, BFP+NPK24). These environments with shorter vectors and closer proximity to the origin are considered more reliable for selecting widely adaptable genotypes (Gauch, 2006). The top genotypes namely Safari, El Kara and Violet Galmi were in corner with a maximum distance from the origin of the biplot and were sensitive.

V. CONCLUSION

This study on adaptability and stability of the yield parameters of nine onion varieties showed that three genotypes, namely El Kara, Safari and Violet de Galmi exhibited good performance. The most suitable environments were CM+NPK at both study sites. This study showed the significant influence of genotype, environment, and their interaction on yield of onion cultivated in the high Guinean zone of Cameroon. The combined variance analysis revealed that environmental factors are more important than genotype and genotype x environment interaction. The stability analysis showed that not a single onion cultivar included in the trial exhibited both high yield and stability across conventional and organic environments. Therefore, breeding onion cultivars highly adapted to the organic production systems is required in order to obtain satisfactory high and stable yields. Top yielding varieties namely El Kara, Safari, Violet de Galmi and Goudami had specific adaptability. These lines are therefore potential candidates for release to contribute, in this way, to sustainably intensifying onion production in the region. One of the aspects that could be investigated is the assessment of genotype response to biotic constraints, which are often key to the long-term success of newly released varieties. Additionally, it would be very informative to have other quality parameters to support these results.

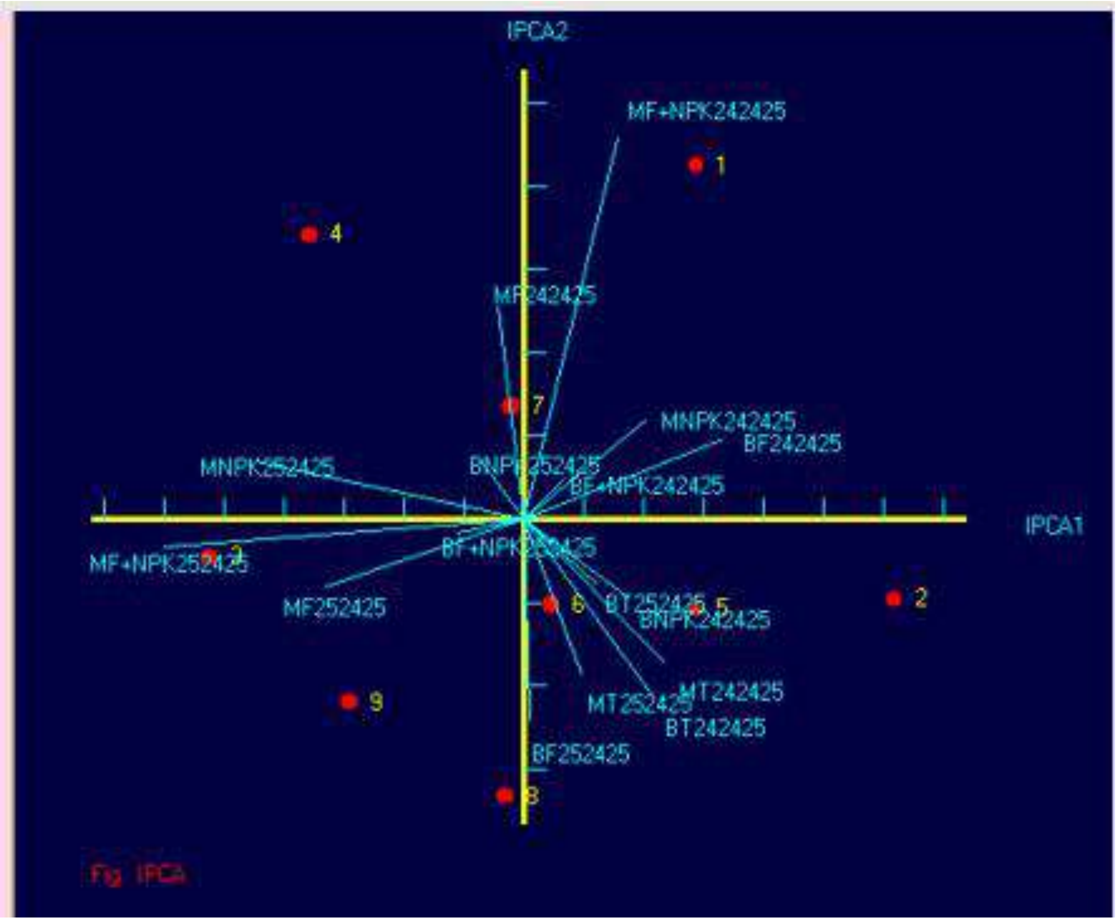

Fig.2: additive analysis of the main and multiplicative effects of interactions (AMMI) in a biplot

MT24: Marza Control 2024; MFP24: Marza Chicken Manure 2024; MFP+NPK24: Marza Chicken Manure + NPK Fertilizer 2024; MNPK24: Marza NPK Fertilizer 2024; BT24: Bini Control 2024. BFP24: Bini Chicken Manure 2024; BFP+NPK24: Bini Chicken Manure + NPK Fertilizer 2024; BNPK24: Bini NPK Fertilizer 2024; MT25: Marza Control 2025; MFP25: Marza Chicken Manure 2025; MFP+NPK25: Marza Chicken Manure + NPK Fertilizer 2025; MNPK25: Marza NPK Fertilizer 2025; BT25: Bini Control 2025. BFP25: Bini chicken manure 2025; BFP+NPK25: Bini chicken manure + NPK fertilizer 2025; BNPK25: Bini NPK 2025 fertilizer; 1: ARES variety; 2: Chagari variety; 3: El Kara variety; 4: Goudami; 5: Kada Goudami; 6: Prema; 7: Red Creole; 8: Safari; 9: Violet de Galmi

REFERENCES

[1] AFNOR (Association Française de Normalisation), 1984. Recueil de normes françaises. Produits agricoles alimentaires : directives générales pour le dosage de l'azote avec minéralisation selon la méthode de kjedahl. AFNOR, Paris, France, 26p.

[2] Annicchiarico P., 2002. Genotype × environment interactions. Challenges and opportunities for plant breeding and cultivar recommendations. Plant production and protection paper 174. FAO, Roma, Italy, 187p.

[3] Atnafu Y., 2023. Evaluating the adaptability of different released onion (*Allium cepa* L.) varieties in West Shewa, Ambo. *Plant,* 1 (2): 113-119.

[4] Ayalew A., Tadesse D., GebreMedhin Z. & Fantaw S., 2015. Evaluation of garlic (*Allium sativum* L.) varieties for bulb yield and growth at Dabat, Northwest ern Ethiopia. *Open Access Library Journal*, 2: 12-16.

[5] Bezu S., Kassie T. G., Shiferaw B. & Ricker-Gilbert J., 2014. Impact of improved maize adoption on welfare of farm households in Malawi: a panel data analysis. *World Development*, 59: 120-131

[6] Bianchini F. & Vainio H. 2001. Allium vegetables and organosulfur compounds: do they help prevent cancer? *Environ. Health Perspectives*, 109(9): 893-902.

[7] Biswas P., Das S., Bar A., Maity T. K. & Mandal A. R., 2020. Effect of micronutrient application on vegetative growth and bulb yield attributes of rabi onion (*Allium cepa* L.). *Int. J. Curr. Microbiol. Appl. Sci.* 9, 556-565. https://doi.org/10.20546/ijcmas.2020.903.065

[8] Brancourt-Hulmel M., Biarnès-Dumoulin V. & Denis J.B., 1997. Points de repère dans l'analyse de la stabilité et de

l'interaction génotype-milieu en amélioration des plantes. *Agronomie*, 17: 219 -246.

[9] Brdar-Jokanović M., Pavlović S., Ugrinović M., Zdravković J., Cvikić D., Zdravković M. & Zorić M. 2012. Genetic variation and environmental stability of onion yield under organic and mineral fertilization. *Acta Hortic*., 960: 111-116. https://doi.org/10.17660/ActaHortic.2012.960.14

[10] Cathala M., Woin N. & Essang T., 2003. L'oignon, une production en plein essor au Nord-Cameroun. *Cahiers Agricultures*, 12 : 261-266.

[11] Cattivelli A., Conte A., Martini S. & Tagliazucchi D., 2021. Influence of cooking methods on onion phenolic compounds bioaccessibility. *Foods*, 10(5): 1-19.

[12] Devani M., Shishoo C. J., Bhadtis V. S., Ananthan & Ullas G. V., 1984. Heterocyclization

[13] of functionalized ketene acetals: Synthesis of pyrimidines via vinylamidine intermediates. *Ttrahedron Letters*, 25(12) : 1291-1292.

[14] Emmanuel K. P., Sulaiman A. & Abu I. A., 2024. factors influencing adoption of recommended onion production technologies among farmers in western agricultural zone of Bauchi state, Nigeria. *Nigerian Journal of Agriculture and Agricultural Technology*, 4(2): 90-104.

[15] FAOSTAT. 2023. Onion production, area and productivity. FAO Statistics 2023. Available at: http://faostat3.fao.org/browse/Q/QC/E.

[16] Finlay K.W. & Wilkinson G.N., 1963. The analysis of adaptation in a plant breeding program. *Aust. J. Agri. Res*., 14: 742-754.

[17] Gauch H. G., 2006. Statistical analysis of yield trials by AMMI and GGE. *Crop Sci*. 46, 1488–1500. doi: 10.2135/cropsci2005.07-0193.

[18] Getahun D. & Getaneh M., 2019. Performance of garlic cultivars under rain-fed cultivation practice at South Gondar zone, Ethiopia. *African Journal of Agricultural Research* 14: 272–278.

[19] Graf B.A., Milbury P.E. & Blumberg J.B. 2005., Flavonols, flavones, flavanones and human health: epidemiological evidence. *J. Med. Food*, 8(3): 281-290. DOI: 10.1089/jmf.2005.8.281.

[20] Gupta A.J., Khade Y.P., Benke A.P., Mainkar P., Gedam P.A.& Mahajan V., 2024. Assessing onion genotypes stability and potential in diverse Indian environments. *Cogent Food and Agriculture*, 10(1): 154-166.

[21] Gupta A.J., Khar A., Aribenchi K.V., Kaldate S., Bhandari H.R., Gedam P.A, Khade Y.P., Kale R.B. & Mahajan V., 2025a. Assessment of stability and yield performance of onion (*Allium cepa* L.) genotypes across diverse Indian environments. *Scientific Reports*, 25: 1-15. https://doi.org/10.1038/s41598-025-30152-9.

[22] Gupta A. J., Anandhan S., Manjunathagowda D. C., Benke A. P., Mahajan V. & Kad S. K., 2022. Complement test for distinctiveness, uniformity and stability testing of kharif onion (*Allium cepa* L.) varieties. *Genet. Resour. Crop Evol*. 69, 2217–2229. doi: 10.1007/s10722-022-01372-z.

[23] Gupta A. J., Kaldate S., Volaguthala S. & Mahajan V., 2025b. Onion nutritional and nutraceutical composition and therapeutic potential of its phytochemicals assessed through preclinical and clinical studies. *J. Funct. Foods* 129: 106889. https://doi.org/10.1016/j.jff.2025.106889.

[24] Gupta A. J., Gorrepati K., Bibwe B., Kaldate S., Volaguthala S. & Mahajan V., 2025c. Studies on biochemical and nutraceutical profiling of 43 Indian onion (*Allium cepa* L.) genotypes. *J. Food Meas. Charact*. 111. https://doi.org/10.1007/s11694-02 5-03425-0

[25] Hardwick R.C. & Wood J.T., 1972. Regression methods for studying genotype - environment interactions. *Heredity*, 28: 209-222.

[26] Horn L., Shimelis H., Sarsu F., Mwadzingeni L. & Laing M.D., 2018.Genotype-by-environment interaction for grain yield among novel cowpea (*Vigna unguiculata* L.) selections derived by gamma irradiation. *Crop J*, 6, 306–313.

[27] Jokanovic, B.M., Z. Girek, M. Ugrinovic, V. Sikora, I. Đalović and J. & Zdravković., 2016. AMMI model in the analysis of genotype by environment interaction of conventionally and organically grown onion. *Genetika*, 48: 534-542.

[28] Kamga R.T., Tchouamo I. R., Chendjou R., Bidogeza J. C. & Afari-Sefa V., 2016. Gender inequality in small holder onion (*Allium cepa* L.) production in the far north region of Cameroon. *Journal of Gender, Agriculture and Food Security*, 1(3): 85-103.

[29] Kazimierczak R., Srednicka-Tober D., Baranski M., Góralska-Walczak R., Kopczynska K., Hallmann E., Rembiałkowska E., Górski J., Leifert C., Rempelos L. & StanisławKaniszewski S., 2021. The Effect of different fertilization regimes on yield, selected nutrients, and bioactive compounds profiles of onion. *Agronomy*, 11(883): 1-13, https://doi.org/10.3390/agronomy11050883

[30] Khalifa G.E., Eljack A.E., Mohammed M.I., Elamin O.N. & Mohamed E.S., 2013. Yield stability in common bean yield genotypes (*Phaseolus vulgaris* L.) in Sudan. *Global Journal of Plant Breeding and Genetics*, 1(1): 58-63.

[31] Khan M.M.H., Rafii M.Y., Ramlee S.I. & Jusoh M., Al Mamun, M., 2021. AMMI and GGE biplot analysis for yield performance and stability assessment of selected Bambara groundnut (*Vigna subterranea* L. Verdc.) genotypes under the multi-environmental trails (mets). *Sci. Rep*., 11, 22791.

[32] Moutsavara G., Yaya Haman, Philippe Kosma & Noubissié T.J.B., 2025. Repeatability and stability of agromorphological characteristics of onion cultivars (*Allium cepa* L.) in the Sudano-Sahelian zone of Cameroon. *Asian Research Journal of Agriculture* 18(4): 233-41. https://doi.org/10.9734/arja/2025/v18i4783.

[33] Nana W.L., 2016. Evaluation agro-morphologique d'une collection d'accessions d'oignon (*Allium cepa* L.) du Burkina Faso. Mémoire d'ingénieur, Université Polytechnique de Bobo-Dioulasso, Burkina Faso, 63p.

[34] Pauwels J. M., Van Ranst E., Mvondo Ze A., 1992. Manuel de laboratoire de pédologie. Méthodes d'analyses de sols et de plantes. Équipement et gestion des stocks de verrerie et de produits chimiques. Publications Agricoles no 28, Bruxelles, 265p

[35] Rodier J., 1978. L'analyse de l'eau : chimie, physico–chimie, bactériologie, biologie. *6ème* éd., Dunod Technique, Paris, France, 1336. 82p.

[36] Shukla. G.K., 1972. Some statistical aspects of partitioning genotype-environmental components of variability. *Heredity*, 29:237-245

[37] Tignegre J.B.S., Traore A.S., Konate M., Zaato P.A., Diarra B.G., Hanson P., Kizito F., Birhanu B.Z. & Afari-Sefa V., 2022. Bulb yield stability study of onion lines over locations and seasons in Ghana and Mali. *Agronomy*, 12(3037): 1-10. https://doi.org/10.3390/ agronomy12123037.

[38] Ukai Y., 2000., GEST. Programs for the analysis of genotype × environment interaction. *Migimomi, Tsuchiura, Ibaraki* 300-837, Japan.

[39] Wricke G., 1962. Ueber eine Methode zur Erfassung der oekologischen Streubreite in Feldversuchen. *Z. Pflanzenzucht*, 47: 92-96.

[40] Yan W. & Tinker N.A., 2006. biplot analysis of multienvironment trial data: principles and applications. *Canadian J. Plant Sci*. 86 :623-645.

[41] Yonkeu S., 1993. Végétation des pâturages de l'Adamaoua (Cameroun) : Ecologie et potentialités. Thèse de Doctorat, Université de Rennes I, France, 207p.

International Journal of Environment, Agriculture and Biotechnology
Vol-11, Issue-3; May-Jun, 2026
Peer-Reviewed International Journal
Journal Home Page Available: https://ijeab.com/
Journal DOI: 10.22161/ijeab

Geo-spatial mapping of soil fertility status of Akure South Local Government Area, Ondo state, Southwestern Nigeria

Johnson Toyin Fasinmirin[1*], Moses Oluwadamilare Adeoye[2], Bamidele Olajiga[3], Funke Florence Akinola[4], Oluwatoyin Esther Onibaba[5], Rotimi Joshua Fasinmirin[6], Akinola Olusegun Akinro[7]

[1,2,3,4,6]Department of Agricultural and Environmental Engineering, Federal University of Technology, P.M.B. 704, Akure, Ondo State, Nigeria
[5]Unversity of Rio Grande Valley, 1201 W University, Dr, Edinburg, TX 78539
[6]Department of Civil Engineering, Elizade University, Ilara-Mokin, Ondo State, Nigeria
[*]Corresponding author email: jtfasinmrin@futa.edu.ng

Received: 08 Apr 2026; Received in revised form: 08 May 2026; Accepted: 13 May 2026; Available online: 22 May 2026

Abstract*— Soil fertility assessment is important for sustainable agricultural productivity and land management, especially in rapidly urbanizing tropical regions. This study evaluated the spatial distribution of soil fertility in Akure South Local Government Area of Ondo State, Nigeria, with a view to assess the influence of land uses on fertility status of soil in the study area. Field-based analysis were conducted on soil samples of the study location, while Geographic Information Systems (GIS) and remote sensing tools were used to map the fertility of soil under the varying land uses. Soil samples at 0-15 cm depth were collected across four land use classes: Built-up, Vegetation, Bare ground, and Outcrop, and analyzed for Nitrogen (N), Phosphorus (P), Potassium (K), Organic Carbon (OC), Organic Matter (OM), and pH. The data were geo-referenced and processed in ArcGIS Pro using the Inverse Distance Weighting (IDW) method to produce spatial distribution maps and a composite Soil Fertility Index (SFI). Results revealed significant spatial heterogeneity in soil fertility. Vegetation areas recorded the highest nutrients, N 10.08 (±9.63 mg/kg), P 12.38 (±10.34 mg/kg), K 30.92 (±28.03 mg/kg), OC 1.27 (±0.82%), OM 2.19 (±1.41%), with pH value of 5.92 (±0.42), while built-up areas were the most depleted. The composite soil fertility index (SFI) map classified the study area into five fertility zones: Very Low (0.048-0.188), Low (0.189-0.271), Moderate (0.271-0.407), High (0.408-0.600), and Very High (0.601-0.994). The study demonstrates that GIS-based soil fertility mapping provides valuable spatial insights for precision agriculture and sustainable land management.

***Keywords*— Soil Fertility Index; Geographical Information System; Organic Matter; Vegetation Area; Built-up Area; Akure.**

I. INTRODUCTION

Soil is a fundamental component of ecosystems, playing a crucial role in agriculture, environmental stability, and human activities. It is a complex mixture of minerals, organic matter, water, air, and microorganisms that interact to support plant growth (Hillel, 2008). Soil fertility, a key attribute of soil quality, refers to the ability of soil to provide essential nutrients in adequate amounts for optimal plant growth.

Soil fertility is a major determinant of agricultural productivity and ecosystem sustainability (Brady and Weil, 2016). Physically, factors such as soil texture, structure, and water-holding capacity influence root penetration and nutrient availability. Chemically, pH levels, nutrient composition, and cation exchange capacity (CEC) affect plant growth. Biologically, organic matter and microbial activity contribute to nutrient cycling and overall soil health (Lal, 2015). However, soil fertility is not static; it can be enhanced or degraded by natural processes and human activities. Practices such as crop rotation, organic farming, and the application of appropriate fertilizers can improve soil fertility, while continuous monocropping, deforestation, and poor land management can lead to soil degradation (Ande *et al.,* 2017). The increasing global demand for food, driven by population growth, makes agricultural expansion essential (Singh *et al.,* 2023). Achieving food security and maximizing agricultural productivity require cultivating crops in optimal environments, which depends on the assessment and management of soil fertility. In agriculture, nutrient-rich soils promote high crop yields and better-quality produce, while nutrient-deficient soils lead to poor plant growth and reduced productivity. Beyond agriculture, soil fertility influences forestry, urban planning, and environmental management by affecting carbon sequestration, biodiversity conservation, and water filtration.

In Nigeria, continuous crop cultivation, inadequate fertilizer use, deforestation, and urbanization have contributed to soil degradation, leading to nutrient depletion and reduced agricultural productivity (Adejuwon and Ekanade, 2018). Studies have shown that soil fertility in some southwestern regions in Nigeria, is depleting due to poor soil management practices, overuse of chemical fertilizers without soil testing, and loss of topsoil through erosion (Ande *et al.,* 2023). Rapid urbanization has further worsened the situation by reducing available arable land for farming (Owoeye, 2019). These challenges pose significant threats to food security and sustainable land use in the region. Climate change and erratic rainfall patterns further compound soil degradation, as highlighted by global assessments (FAO, 2017).

In response to the need for detailed soil fertility assessments, advanced digital tools have become essential. Geographic Information Systems (GIS) have emerged as a powerful tool for accessing, analyzing, and visualizing soil properties and fertility levels (Singh *et al.,* 2023). GIS serves as a comprehensive platform for capturing, storing, and processing geographical data. When integrated with intensive field data collection, it enables the creation of detailed soil fertility maps that illustrate nutrient distribution and land suitability for agriculture (Mulder *et al.,* 2011).

Although satellite imagery has been used in some studies, its moderate spatial and spectral resolution in regions like Nigeria often limits the detection of fine-scale variability in soil properties (Mulla, 2013; Zhang *et al.,* 2019). As a result, many researchers advocate relying on ground-collected data analyzed through GIS to achieve more precise soil fertility mapping.

Geographic Information Systems (GIS) enables the integration and analysis of spatial and non-spatial data, facilitating the creation of detailed soil maps that reflect the variability of soil properties across large areas. By incorporating data from various sources, including field surveys and laboratory analyses, GIS can model spatial patterns of soil nutrients, pH levels, organic matter content, and other critical parameters. Akure, a southwestern city of Nigeria faces significant challenges related to soil fertility. Continuous cultivation without adequate replenishment of soil nutrients has led to nutrient depletion, adversely affecting crop yields and food security. These issues collectively threaten the sustainability of agriculture in Akure, necessitating immediate and informed intervention.

Given these limitations, this research focuses solely on leveraging detailed field data integrated with GIS to map soil fertility across Akure. GIS provides a robust framework for analyzing and visually representing ground-based measurements, thereby producing digital soil maps that accurately reflect nutrient distribution and overall soil quality (Nkwunonwo and Okeke, 2013). Studies by Fabiyi *et al.* (2011) have demonstrated the effectiveness of GIS in soil mapping, supporting better decision-making in agricultural practices and land-use planning. Similarly, Olorunfemi *et al.* (2020) and Adejuwon and Ekanade (2018) emphasize the need for sustainable soil management practices in Nigerian regions impacted by rapid urbanization and land-use changes. Despite these attempts, research outputs on GIS mapping of soil fertility remain limited especially in the sub-Saharan Africa. Therefore, this research was aimed at mapping the fertility status of soil in Akure South Local Government Area, in the humid rainforest climate of Nigeria using GIS techniques and comprehensive field data.

II. METHODOLOGY

2.1 Description of Study Location

The study location is Akure, the capital city of Ondo State, Southwestern Nigeria (Adeoye *et al.*, 2025). Akure is situated within the humid tropical rainforest zone, characterized by a bimodal rainfall pattern with an annual average of about 1,500 – 2,500 mm and a mean temperature range of 22°C to 32°C (Olanipon *et al.,* 2025). The climate supports luxuriant vegetation, dominated by tall trees, shrubs, and secondary forest growth, though much of this has been replaced by farmlands, residential areas, and infrastructure due to urbanization (Olujide *et al.,* 2018). Topographically, Akure South is generally undulating with gently rolling hills, while the geology is underlain predominantly by Precambrian basement complex rocks, which influence soil formation and nutrient composition (Olorunfemi *et al.,* 2018). The soils are typically ferruginous tropical soils, known for their weathering, moderate to low fertility, and susceptibility to leaching under intense rainfall (Akande and Adedamola, 2020). The socio-economic activities in the area include farming, trading, government services, and small-scale industries. Agriculture is mainly subsistence-based, with crops such as yam, cassava, maize, and vegetables cultivated in surrounding rural and peri-urban areas (Akinbode *et al.,* 2024). However, increasing urban expansion has reduced the extent of arable land, intensifying pressure on soil resources (Seto and Ramankutty, 2016). These natural and human-induced dynamics make Akure South LGA a strategic location for evaluating soil fertility patterns using GIS techniques, particularly in the context of rapid urbanization and changing land use (Fabiyi *et al.,* 2013; Singh *et al.,* 2023).

2.2 Land Use and Land Cover

Land use and land cover (LULC) analysis was conducted to characterize the spatial distribution of surface features across Akure South LGA and to guide soil sampling. The classification was based on four major land cover classes identified within the study area: vegetation, developed areas, barren land, and outcrops. These categories represent the dominant land cover patterns and provide a basis for examining soil fertility across varying land uses (Adeoye *et al.*, 2025). Satellite data were sourced from Landsat 9 Operational Land Imager (OLI-2) imagery for the year 2025, obtained through the Google Earth Engine (GEE) platform. Preprocessing steps included atmospheric and radiometric corrections using surface reflectance products to ensure spectral fidelity. The imagery was clipped to the boundary of Akure South Local Government Area using a shape-file of the study area.

Classification was performed in ArcGIS Pro 3.5.2 using the Support Vector Machine (SVM) supervised classification algorithm, which is widely recognized for its high accuracy in remote sensing applications. The resulting LULC map provided the spatial framework for soil sampling. Soil samples were collected across the four identified land cover classes, ensuring adequate representation of each category for fertility analysis. This stratified sampling approach was designed to capture variations in soil properties attributable to different land uses and surface conditions (Adeoye *et al.*, 2025).

2.3 Soil Sampling and Analysis

Soil samples were collected from the topsoil layer (0–15 cm depth). The selection of this depth reflects its importance as the most biologically active portion of the soil profile, where root activity, nutrient cycling, and organic matter accumulation are highest (Hao *et al.,* 2021). Sampling was conducted over a period from August 2025 to September 2025 to coincide with the post-rainy season when soil moisture conditions are stable yet not saturated. A total of 40 sampling points were selected across the study area, stratified by the four major land use / land cover classes (vegetation, developed area, barren land, and outcrops) to ensure representation. At each sample location, the GPS coordinates were recorded using a handheld GPS device and the soil was placed into clean nylon bags. This geo-referencing ensures spatial traceability of the samples for integration with GIS analyses. In the field, coarse debris such as stones, fresh roots, and plant residues were removed. The collected soil was air-dried in the laboratory to preserve microbial activity and the chemical integrity of the sample (i.e., to limit further decomposition or nutrient transformations). After air-drying, the samples were passed through a 2 mm sieve to standardize particle size and remove remaining coarse fragments. The sieved soil serves as the standard “fine earth” fraction for most fertility analyses (Carter, 2007).

The collected soil samples were analyzed for site specific chemical parameters commonly used to assess soil fertility: nitrogen (N), phosphorus (P), potassium (K), pH, organic carbon (OC), and organic matter (OM). The N, P, K of soil were measured directly using soil fertility speed sensor. The handheld soil sensor, based on Frequency Domain Reflectometry (FDR) technology, was employed to determine soil nitrogen (N), phosphorus (P), and potassium (K) concentrations from prepared soil samples. The instrument features a high-sensitivity stainless-steel probe, LCD digital display, and built-in lithium battery (DC 3.7V) for field portability and autonomous operation. It measures multiple soil components in real time, with a detection range of 1–1999 mg/kg and measurement accuracy of ± 2% sensitivity. The sensor operates using the FDR measurement principle, where an electromagnetic wave is transmitted into the soil medium and the reflected frequency signal is analyzed by a micro-control unit (MCU) to estimate the dielectric properties. These dielectric properties correlate with soil moisture, electrical conductivity, and ionic nutrient concentrations (Yao *et al.,* 2025). The FDR method provides rapid and non-destructive assessment of soil nutrient status by translating changes in the electromagnetic response into nutrient estimates (Chen *et al.,* 2019).

During measurement, the probe was vertically inserted into the soil to a depth exceeding 10 cm, ensuring full contact with the medium. To enhance data reliability, multiple points were measured, and the mean value was recorded for each sampling site. After each use, the probe was cleaned and dried to prevent oxidation and maintain accuracy, in line with the manufacturer's guidelines. FDR-based soil sensors such as the Jingxun model are increasingly used in precision agriculture and soil fertility monitoring due to their fast response, low power consumption, and good repeatability compared to conventional laboratory methods (Gao *et al.,* 2021). Their integration of real-time digital display and multi-parameter detection supports efficient field assessment and nutrient management.

2.3.1 Analytical Methods

pH measurement.

Soil pH was determined using a standard pH meter with soil–water suspension (e.g. 1:2.5 soil to water by weight). This is a widely used technique to measure the acidity or alkalinity of soils, which influences nutrient availability (Brady & Weil, 2017).

***Organic Carbon and Organic Matter Determination* (Walkley–Black Method)**

The organic carbon content of the soil samples was determined using the Walkley–Black wet oxidation method (Nelson and Sommers, 2018). This method quantifies the oxidizable portion of organic carbon in the soil, which serves as a key indicator of soil fertility and organic matter content. Approximately 1 g of each air-dried and sieved soil sample (<2 mm) was weighed into a 250 ml Erlenmeyer flask. To each sample, 10 ml of 0.167 M potassium dichromate ($K_2Cr_2O_7$) was added using a pipette, followed by 20 ml of concentrated sulphuric acid (H_2SO_4). The mixture was swirled gently to ensure complete dispersion and allowed to stand for 30 minutes to allow oxidation of the organic matter. After oxidation, 100 ml of distilled water was added to dilute the solution. Subsequently, 3 drops of phenanthroline indicator were added, and the mixture was titrated with 0.5 M iron (II) ammonium sulphate solution until the color changed sharply from dark green to brownish-red (maroon), indicating the endpoint. A blank titration (without soil) was also performed using the same reagents and conditions.

The percentage of organic carbon (% OC) and organic matter in each soil sample was calculated using the equations 1 and 2:

$$\%\, Organic\ Carbon = \frac{(B-T)\times M \times 1.33}{W} \quad (1)$$

where:

B = Titre value for blank (ml)

T = Titre value for soil sample (ml)

M = Molarity of $Fe(NH_4)_2(SO_4)_2{\cdot}6H_2O$

W = Weight of soil sample (g)

1.33 = Correction factor for incomplete oxidation of organic matter

The organic matter (OM) content was subsequently estimated by multiplying the % organic carbon by 1.724.

$$\%\, Organic\ Matter\ (OM) = \%\, Organic\ C \quad (2)$$

This method provides a reliable measure of soil organic carbon, which is an important indicator of soil fertility, nutrient retention capacity, and overall soil health.

2.3.2 Evaluation of Soil Fertility Index (SFI)

The Soil Fertility Index (SFI) was calculated using the Expert Opinion (EO) method to integrate multiple soil parameters into a single quantitative index representing the overall fertility status of each sampling location. This approach combines established agronomic principles with empirical soil data to provide a comprehensive assessment of soil fertility across Akure South LGA.

The Expert Opinion Method was adopted to assign relative weights to the selected soil fertility indicators, reflecting their importance in determining overall soil productivity, particularly in tropical environments. This approach draws from established agronomic principles and findings reported in literatures (Chaudhry *et al.,* 2024; Lenka *et al.,* 2022; Vasu *et al.,* 2016; Zhao *et al.,* 2023). Based on a comprehensive review of studies focused on tropical and sub-Saharan African soils, the following weights were assigned: Nitrogen (0.25) and Organic Carbon (0.25) received the highest weights, as they are recognized as the most critical factors influencing soil fertility. Nitrogen is often the most limiting macronutrient in tropical soils and is essential for vegetative growth (Zhang *et al.,*2015), while organic carbon serves as the foundation of soil fertility, acting as the main nutrient reservoir and enhancing microbial activity (Lal, 2020). Phosphorus was assigned a weight of 0.20, reflecting its frequent deficiency in acidic tropical soils due to fixation processes (Shen *et al.,* 2011). Potassium, also weighted at 0.20, plays a vital role in crop quality, stress tolerance, and overall plant metabolism (Römheld and Kirkby, 2010). Finally, pH was given a weight of 0.10, acknowledging its role in modulating nutrient availability and influencing the chemical environment of the soil (Brady & Weil, 2017).

Selection of Soil Fertility Indicators

Five key soil parameters were selected as fertility indicators based on their recognized importance in tropical soil systems and their routine use in soil fertility assessment (Chaudhry *et al.,* 2024; Isong *et al.,* 2022; Vasu *et al.,*2016):

i. Nitrogen (N, mg/kg): A primary macronutrient essential for vegetative growth, chlorophyll synthesis, and protein formation
ii. Phosphorus (P, mg/kg): Critical for energy transfer (ATP), root development, flowering, and seed formation
iii. Potassium (K, mg/kg): Essential for enzyme activation, water regulation, osmotic balance, and disease resistance
iv. Organic Carbon (OC, %): A fundamental indicator of soil organic matter content, nutrient retention capacity, soil structure, and biological activity
v. Soil pH: Controls nutrient availability, microbial activity, and chemical reactions in the soil

Organic matter (OM) was excluded from the SFI calculation to avoid multicollinearity, as it is directly derived from organic carbon through the conversion factor 1.724 (Shamrikova *et al.,* 2022), resulting in perfect correlation (r = 1.00) between these two parameters. The inclusion of both would artificially inflate the weight of organic matter in the final index.

Indicator Transformation and Scoring Functions

To integrate soil parameters measured in different units (mg/kg, %, unitless) onto a common dimensionless scale, transformation functions were applied. These scoring functions normalize each parameter to a 0-1 scale, where higher scores indicate more favorable conditions for plant growth (Yu *et al.,*2018).

i. Linear "More is Better" Scoring Function (N, P, K, OC): For nutrients and organic carbon, a linear scoring function was applied based on the principle that higher values indicate better fertility status:

$$S_i = \frac{x_i - x_{min}}{x_{max} - x_{min}} \qquad 3$$

where S_i =normalized score (0-1), $x_i = measured\ value,$ $x_{min}\ and\ x_{max}$ = minimum and maximum observed values

ii. Optimum Range Function (pH): In contrast, for soil pH, fertility is not simply proportional to its value; rather, it follows an optimum range, where extreme acidity or alkalinity can reduce nutrient availability. Therefore, an Optimum Range Function was used to normalize pH scores based on established fertility ranges (Brady & Weil, 2017):

$$S_{pH} = \begin{cases} 1.0 & if\ 6.0 \le pH \le 7.0 \\ \frac{pH-4.5}{1.5} & if\ pH < 6.0 \\ \frac{8.5-pH}{1.5} & if\ pH > 7.0 \end{cases} \qquad 4$$

This function assigns the maximum score (1.0) to soils within the optimal pH range (6.0–7.0), where nutrient availability and microbial activity are highest. Scores decrease linearly for values outside this range, reflecting the detrimental effects of both acidity (< 6.0) and alkalinity (> 7.0) on soil fertility.

SFI Calculation

The Soil Fertility Index (SFI) was computed using the equation 5:

$$SFI = (0.25 \times S_N) + (0.20 \times S_P) + (0.20 \times S_K) + (0.25 \times S_{OC}) + (0.10 \times S_{pH}) \quad \ldots 5$$

where:

S_N is Normalized score for Nitrogen, S_P is Normalized score for Phosphorus, S_K is Normalized score for Potassium, S_{OC} is Normalized score for Organic Carbon, and S_{pH} is Normalized score for soil pH

This weighted additive approach assumes that soil fertility is a composite property determined by the combined effects of multiple parameters, with each contributing proportionally to its assigned weight (Vasu *et al.,* 2016). The index theoretically ranges from 0 (all parameters at minimum values) to 1 (all parameters at maximum values), though actual values typically fall within a narrower range depending on the degree of parameter co-variation.

Interpolation of Soil Fertility Parameters

Spatial interpolation was carried out using the Inverse Distance Weighted (IDW) method available in ArcGIS Pro under the Spatial Analyst Tools (Mirzaei and Sakizadeh, 2022; Childs, 2022). The IDW technique was chosen for its simplicity and effectiveness in estimating values at unsampled locations based on the proximity and influence of nearby sampled points (Burrough *et al*, 2015). The method assumes that points closer to each other are more similar than those farther apart, assigning greater weight to nearer observations. The process involved importing the point data containing soil sample locations and their corresponding laboratory results into ArcGIS Pro. For each soil fertility parameter, namely nitrogen (N), phosphorus (P), potassium (K), pH, organic carbon (OC), and organic matter (OM), the respective attribute was selected as the Z-value to generate continuous raster surfaces representing their spatial distribution across the study area. This interpolation was performed separately for each parameter, producing individual spatial distribution maps that visualize variations in soil fertility across the region.

2.3.3 Soil Fertility Index Mapping

The Soil Fertility Index (SFI) was calculated by combining the normalized raster layers of nitrogen, phosphorus, potassium, organic carbon, and pH using the Raster Calculator tool (Spatial Analyst Tools) in ArcGIS Pro (Abdellatif *et al.,* 2021; Belayneh *et al.,* 2019). The weighted additive formula applied was the Soil Fertility Index formula as stated in equation 3.6, where each S represents the normalized score (0-1 scale) for the respective parameter. The resulting SFI raster, with values ranging from 0 to 1, was classified into five fertility classes (Very Low, Low, Moderate, High, and Very High) using manual classification breaks.

2.4 Statistical Analysis

Following laboratory analysis, descriptive statistics were computed for all soil fertility parameters to characterize their central tendency, dispersion, and variability across the study area. The statistical measures calculated included mean, median, mode, standard deviation, minimum, and maximum values for nitrogen (N), phosphorus (P), potassium (K), organic carbon (OC), organic matter (OM), and soil pH.

To quantify the degree of spatial heterogeneity in soil fertility, the coefficient of variation (CV) was calculated for each parameter using the formula:

$$Coefficient\ of\ Variation\ CV\ (\%) = \frac{Standard\ Deviation}{Mean} \times 100 \qquad 6$$

The CV provides a standardized measure of variability that facilitates comparison across parameters with different units and magnitudes. Variability classes are interpreted as follows: low variability (CV < 15%), moderate variability (15% ≤ CV ≤ 35%), and high variability (CV > 35%) (Tesfahunegn *et al.,* 2011). CV values exceeding 35% typically indicate strong spatial heterogeneity requiring site-specific management interventions, a classification widely applied in soil fertility studies across tropical and subtropical regions (Behera & Shukla, 2015).

Pearson's correlation coefficient (r) was employed. This statistical measure quantifies the strength and direction of linear relationships between pairs of variables and is expressed as:

$$r = \frac{\sum(x_i - \bar{x})(y_i - \bar{y})}{\sqrt{\sum(x_i - \bar{x})^2 (y_i - \bar{y})^2}} \qquad 7$$

where:

$x_{i,}y_i$ is observed value of two soil parameters (e.g., OC and N)

$\bar{x}, \bar{y}$ is mean value of each parameter

r ranges from -1 to +1

Positive r values indicate direct relationships, negative values indicate inverse relationships, and values near zero suggest no linear correlation. Correlation coefficients were tested for statistical significance at $p < 0.05$ and $p < 0.01$ levels. The correlation matrix was constructed to examine interactions among N, P, K, OC, OM, and pH, providing insights into nutrient dynamics and interdependencies within the soil system.

III. RESULTS AND DISCUSSION

3.1 Soil fertility parameters

The descriptive statistics of soil fertility parameters is presented in Table 1. The mean nitrogen concentration across the samples was 7.50 mg/kg, with a wide range of 1.00 - 38.00 mg/kg. Available phosphorus averaged 9.48 mg/kg, but similarly exhibited large variations (1.00 - 41.00 mg/kg). Potassium also showed high variability, with mean value of 23.45 mg/kg and values ranging from 2.00 to 108.00 mg/kg. Organic carbon content averaged 1.01%, with a minimum of 0.40% and a maximum of 3.34%. Organic matter followed a similar pattern (mean 1.74%), reflecting the expected conversion between OC and OM. Soil pH values were relatively stable, ranging from 5.00 to 6.60, with an overall mean of 5.87, indicating that soils of Akure South are slightly acidic.

Table 1: Descriptive statistics of soil fertility parameters in Akure South LGA

Parameter	Mean	Median	Mode	Std. Dev.	Min	Max	CV(%)	Variability
Nitrogen (N)	7.50	5.00	2.00	7.30	1.00	38.00	97.30	Very High
Phosphorus (P)	9.48	7.00	2.00	8.98	1.00	41.00	94.70	Very High
Potassium (K)	23.45	17.00	13.00	22.99	2.00	108.00	98.00	Very High
Organic Carbon (OC)	1.01	0.83	0.40	0.66	0.40	3.34	65.60	High
Organic Matter (OM)	1.74	1.43	1.34	1.14	0.69	5.76	65.50	High
pH	5.87	6.00	6.00	0.47	5.00	6.60	8.00	High

The results highlight clear differences in soil fertility status across the study area. Nitrogen, phosphorus, and potassium exhibited high ranges and standard deviations, which suggests significant spatial heterogeneity in nutrient distribution. This variability is typical of tropical soils where continuous cropping, nutrient mining, and fertilizer application patterns differ widely (Chandrakala *et al.,*2018; López-Granados *et al.,*2002). In contrast, soil pH was relatively uniform, with a standard deviation of 0.47, indicating that the soils are consistently acidic. This acidity has important implications for nutrient availability, particularly phosphorus, which tends to be immobilized in acidic conditions (Agegnehu *et al.,* 2021).

The coefficient of variation results indicate heterogeneity in the soil fertility parameters of Akure South. Nitrogen, phosphorus, and potassium all recorded CV values above 90%, reflecting extreme spatial variability. This suggests that fertility management in the area cannot rely on uniform recommendations, but rather requires site-specific nutrient management strategies. Soil pH showed very low variability (8%), confirming that soil acidity is relatively uniform across the study area.

High CV values (>35%) are generally interpreted as strong heterogeneity, typical of tropical soils that are subject to intensive cultivation, erosion, and uneven fertilizer application (Chandrakala *et al.,*2018; López-Granados *et al.,*2002). The relatively stable soil pH suggests that acidity is a consistent fertility constraint for Akure South, aligning with reports from other tropical humid regions where weathering and leaching processes dominate (Agegnehu *et al.,* 2021).

3.2 Soil Fertility Variation across Land Use Types

The mean values and standard deviations of soil fertility parameters across different land use types are presented in Table 2. The results reveal distinct fertility gradients linked to land use and management practices. Vegetation areas recorded the highest average nutrient levels with N 10.08 (±9.63 mg/kg), P 12.38 (±10.34 mg/kg), K 30.92 (±28.03 mg/kg), OC 1.27 (±0.82%), and OM 2.19 (±1.41%) reflecting continuous organic inputs from litter and minimal disturbance. Similarly, bare ground soils showed moderately high nutrient concentrations with N 11.50 (±12.66), P 12.50 (±12.66), K 26.17 (±32.14), likely due to natural accumulation and limited cultivation.

Table 2: Mean and standard deviation of soil fertility parameters across different land use types in Akure South LGA.

Land use	N(mg/kg) Mean(Std.)	P(mg/kg) Mean(Std.)	K(mg/kg) Mean(Std.)	OC(%) Mean(Std.)	OM(%) Mean(Std.)
Vegetation	10.08 (±9.63)	12.38 (±10.34)	30.92 (±28.03)	1.27 (±0.82)	2.19 (±1.41)
Built-up	5.44 (±4.27)	7.19 (± 5.97)	15.69 (±12.84)	0.78 (±0.45)	1.35 (±0.78)
Outcrop	7.40 (±7.47)	10.80 (±11.36)	28.60 (±32.93)	0.51 (±0.14)	0.88 (±0.24)
Bare Ground	11.50 (±12.66)	12.50 (±12.66)	26.17 (±32.14)	1.13 (±0.95)	1.95 (±1.64)

In contrast, built-up areas exhibited the lowest fertility, with markedly reduced nutrient contents, N 5.44 (±4.27), P 7.19 (±5.97), K 15.69 (±12.84), OC 0.78 (±0.45%), OM 1.35 (±0.78%), attributed to soil compaction, surface sealing, and low organic input. Outcrop soils were similarly poor in organics, OC 0.51 (±0.14%), OM 0.88 (±0.24%) but retained moderate nutrient levels due to residual mineral weathering.

Overall, these results confirm that land use strongly influences soil fertility in Akure South. Vegetated and fallow lands maintain higher nutrient reserves through organic recycling, while built-up and rocky areas show significant degradation. The large standard deviations across all parameters further indicate high spatial variability within each land use, consistent with findings from Chandrakala *et al.* (2018) and López-Granados *et al.,* (2002), and underscore the need for site-specific fertility management.

3.3 Correlation Matrix of Soil Parameters

The correlation analysis carried out among nitrogen (N), phosphorus (P), potassium (K), organic carbon (OC), organic matter (OM), and soil pH is presented in Table 3. The strongest positive correlation was observed between organic carbon (OC) and organic matter (OM) (r = 1.00), which is expected since OM is derived directly from OC through a conversion factor. This close relationship validates the consistency of the laboratory results and reinforces the importance of organic matter as a key fertility indicator (Chandrakala *et al.,* 2018). Nitrogen (N) also exhibited strong positive correlations with both OC (r = 0.84) and OM (r = 0.85), reflecting the role of organic matter as the primary reservoir of nitrogen in tropical soils. Similar findings have been reported in India and Spain, where higher organic matter content was associated with increased nitrogen availability (López-Granados *et al.,* 2002). Furthermore, phosphorus (P) and potassium (K) were strongly correlated with N (r = 0.94 and 0.94, respectively) and with each other (r = 0.96), suggesting that areas with higher fertility tend to have simultaneous enrichment of these macronutrients. These patterns are consistent with the synergistic accumulation of nutrients in soils under favorable land-use and organic matter conditions (Agegnehu *et al.,* 2017).

Table 3: Correlation matrix of soil fertility parameters in Akure South LGA (Pearson's r)

	N	P	K	OC	OM	pH
N	1.000					
P	0.942	1.000				
K	0.939	0.964	1.000			
OC	0.841	0.831	0.774	1.000		
OM	0.845	0.836	0.780	1.000	1.000	
pH	0.144	0.130	0.133	0.222	0.222	1.000

Note: All correlations among N, P, K, and OC/OM are strong and statistically significant ($p < 0.01$). Correlations involving pH are weak and not statistically significant ($p > 0.05$).

The correlation analysis revealed important interactions among soil fertility parameters in Akure South. By contrast, soil pH exhibited only weak positive correlations with N, P, K, and OC ($r \approx 0.13$–0.22), and these were not statistically significant ($p > 0.05$). This indicates that in the study area, soil acidity does not co-vary strongly with nutrient concentrations. However, studies in other tropical environments have shown that under more strongly acidic conditions, nutrient availability, particularly phosphorus can be reduced through fixation processes, while leaching may worsen nutrient losses (Jia *et al.,* 2023). Overall, the results highlight the central role of organic matter management in improving soil fertility in the area. Enhancing soil OC through organic amendments, residue incorporation, or biochar application would support nitrogen availability and general nutrient retention. The strong co-variation among N, P, and K suggests that fertility enrichment practices could yield broad improvements in nutrient status. Nevertheless, the weak relationship between pH and soil nutrients underscores the need to monitor soil acidity independently, as it remains a potential limiting factor for nutrient availability even if not strongly expressed in this dataset.

3.4 Fertility Classification

The soil fertility distribution classes is presented in Table 4. About 60% of the sampling points (24 out of 40) exhibited low or very low fertility (SFI < 0.45), while only 12.5% (5 sampling points) demonstrated high or very high fertility (SFI ≥ 0.60). The dominant fertility class across the study area was "Low," accounting for 47.5% of all sites. The mean SFI value of 0.379 indicates widespread fertility constraints across Akure South LGA, reflecting significant soil degradation. This pattern aligns with previous findings in southwestern Nigeria, where declining soil fertility has been linked to intensive cultivation, inadequate organic matter inputs, and rapid urbanization (Dhayanan *et al.,* 2016; Olorunfemi *et al.,*2018). Spatially, high-fertility zones (SFI ≥ 0.60) were concentrated in the northwestern and northeastern sectors, predominantly in vegetated and agricultural areas. These zones benefit from continuous organic inputs through litter decomposition, reduced erosion, and stable nutrient cycling, resulting in higher organic carbon content (2.2–3.3%) and elevated levels of nitrogen, phosphorus, and potassium. In contrast, low-fertility zones (SFI < 0.45) were dominant in the central and southern parts, corresponding largely to built-up and barren lands. These areas experience soil sealing, topsoil removal, and minimal organic matter additions, leading to low organic carbon (<0.7%) and depleted nutrient levels (Chang *et al.,* 2022; Weng, 2012). The pronounced spatial variability (CV = 41.2% for SFI and >90% for individual nutrients) highlights the need for site-specific nutrient management rather than uniform fertilizer recommendations. Tailored interventions guided by SFI classifications are essential to enhance input efficiency and restore soil productivity in degraded zones (Chandrakala *et al.,* 2018).

Table 4: Soil fertility distribution classes

Fertility Class	Number of Sites	Percentage
Very Low	5	12.5%
Low	19	47.5%
Moderate	11	27.5%
High	3	7.5%
Very High	2	5.0%

3.5 Spatial Distribution of Soil Nutrients

The spatial distribution of soil nutrients provides critical insights into the fertility status of Akure South LGA. The spatial analysis reveals how these nutrients vary across the landscape under different land use and land cover (LULC) conditions. This approach makes it possible to identify nutrient-rich hotspots, areas of deficiency, and the underlying drivers of spatial variability, including farming practices, vegetation cover, topography, and human activities. The use of GIS-based Inverse Distance Weighted (IDW) interpolation method shows the spatial variability of key fertility indicators: Nitrogen (N), Phosphorus (P), Potassium (K), Organic Carbon (OC), Organic Matter (OM), and Soil pH.

3.5.1 Spatial Distribution of Organic Carbon (OC)

The spatial distribution of organic carbon (OC) in the study area is presented in Figure 1. The maps reveal considerable heterogeneity, with higher concentrations predominantly occurring in the northern and northwestern zones. These areas are largely associated with vegetation-dominated land uses, including forest cover and farmlands, where litter deposition, root turnover, and incorporation of organic residues enhance carbon accumulation in the soil. In contrast, the central and southeastern sectors, particularly those under built-up and barren land uses, exhibit lower OC concentrations. This depletion is likely due to soil sealing, reduced organic inputs, and intensive disturbances associated with construction activities and surface exposure.

The spatial clustering of high OC zones aligns closely with natural vegetative cover, supporting the findings of Lima *et al.* (2025), who reported that forested and agricultural soils sustain higher carbon content due to continuous biomass input. Conversely, the low OC levels observed in urbanized and barren areas mirror patterns of nutrient depletion driven by topsoil erosion and organic matter oxidation (Chang *et al.,* 2022). Collectively, these results underscore the strong dependence of organic carbon enrichment on land use.

3.5.2 Spatial Distribution of Organic Matter (OM)

The spatial distribution of organic matter (OM) in the study area is presented in Figure 2. The maps indicate a pattern that closely mirrors the distribution of organic carbon, as expected due to their direct proportional relationship. High OM concentrations are observed in the northern and western parts of Akure South, coinciding with vegetation-dominated and cultivated lands. These areas benefit from the incorporation of organic residues, manure application, and natural litter accumulation, all of which contribute to humus formation and sustained soil fertility. In contrast, lower OM concentrations are dominant in the southern and central sectors, particularly within developed and barren land covers. These areas are characterized by minimal organic inputs, erosion, and soil sealing, which collectively reduce organic matter content.

This spatial pattern highlights the critical role of land cover in regulating organic matter dynamics. Vegetated lands act as sinks of organic matter, whereas urbanized and exposed lands serve as zones of degradation. Similar associations between OM and vegetation cover have been reported in tropical soils, where land management practices strongly influence soil organic matter content (Li *et al.,* 2022).

3.5.3 Spatial Distribution of Soil pH

The spatial distribution of soil pH in the study area is presented in Figure 3. The maps indicate a relatively uniform distribution, with most locations exhibiting slightly acidic conditions (pH 5.5–6.5). Marginal variations, however, are observable: slightly higher pH values occur in the central and western portions of the LGA, which coincide with vegetation and agricultural land uses, whereas lower pH values (<5.5) are concentrated in the southern and built-up zones. These areas of reduced pH are likely attributable to soil compaction, limited organic matter inputs, and acidifying anthropogenic activities such as surface runoff and waste deposition.

The predominance of acidic conditions across Akure South aligns with the characteristics of humid tropical environments, where high rainfall and intense leaching processes contribute to base cation loss and soil acidification (Bationo *et al.* 2007). Although the overall variability in pH is limited, localized acidity may significantly affect nutrient availability, particularly by promoting phosphorus immobilization and disrupting cation exchange balance. As such, periodic liming or other pH correction measures may be necessary in more acidic zones to optimize nutrient uptake and improve overall soil fertility.

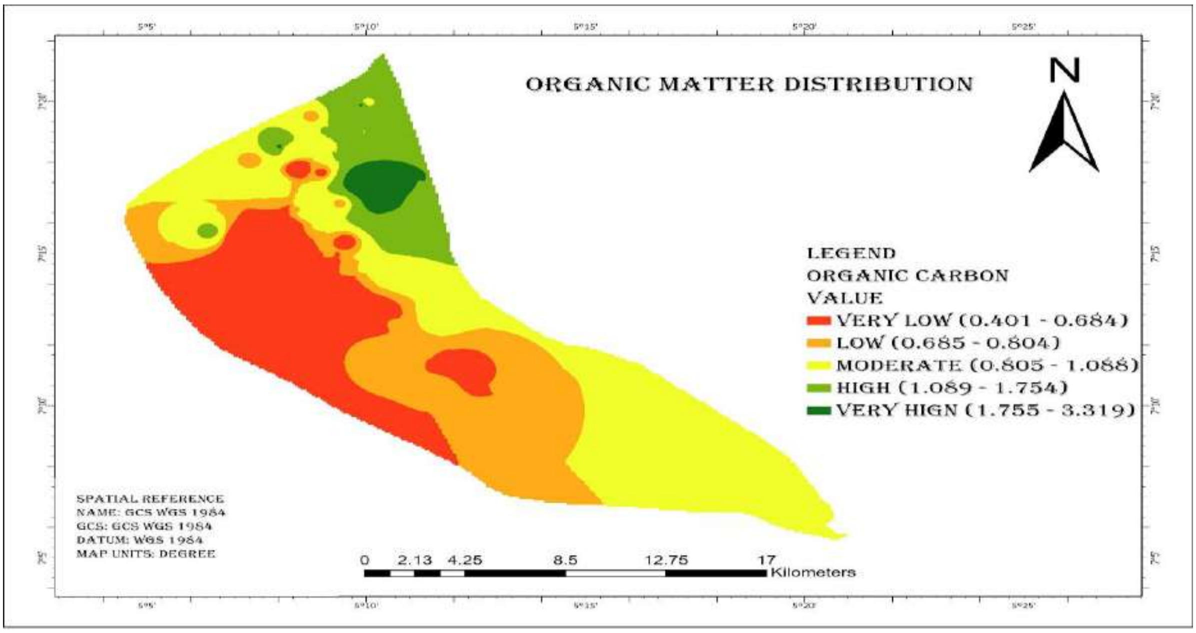

Fig.1: Organic carbon distribution in Akure South LGA

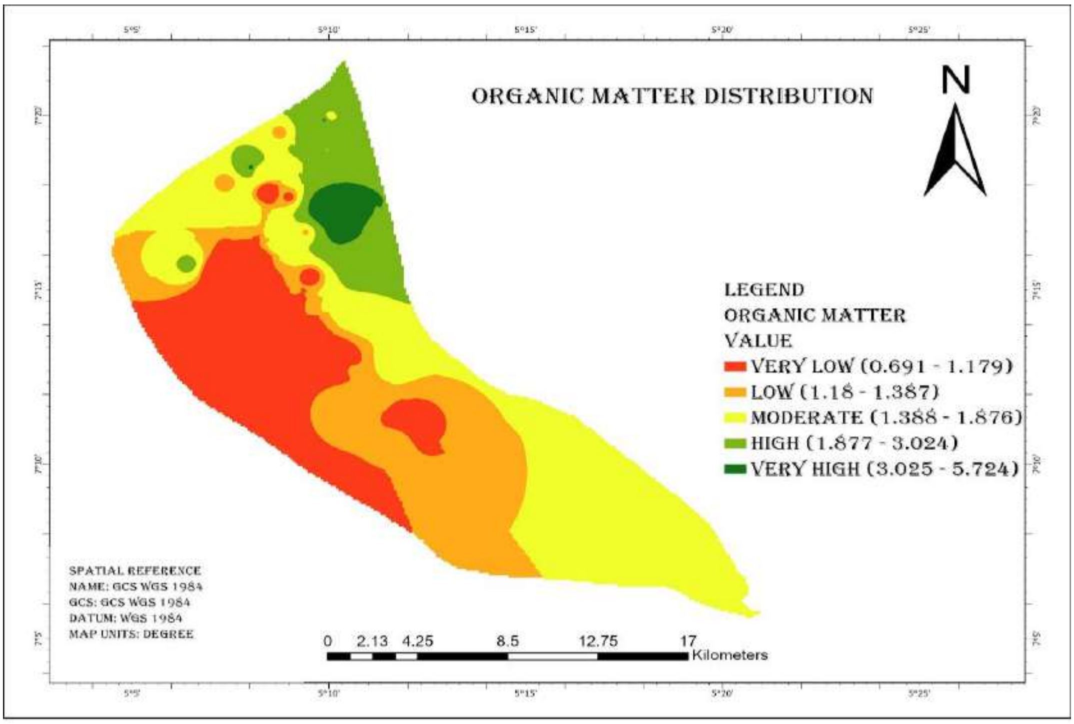

Fig.2: Organic matter distribution in Akure South LGA

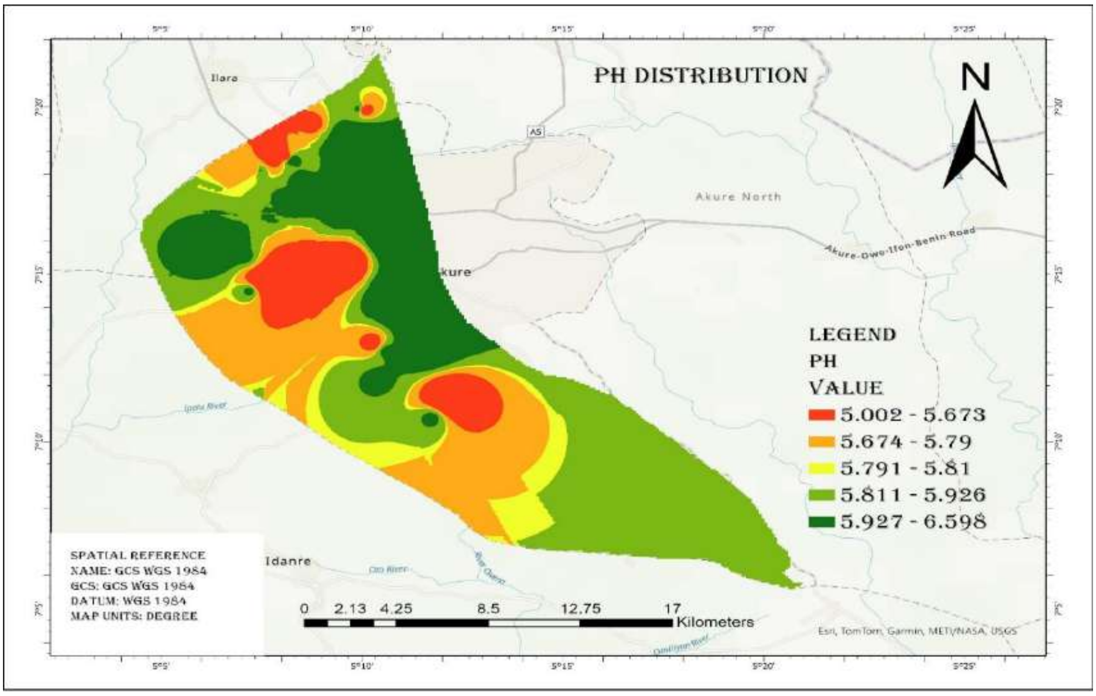

Fig.3: pH distribution in Akure South LGA

3.5.4 Spatial Distribution of Potassium (K)

The spatial distribution of potassium (K) in the study area is presented in Figures 4. The maps reveal pronounced spatial variability, with high K concentrations occurring predominantly in the northwestern and northeastern zones. These areas are largely associated with vegetative and agricultural land covers, where potassium enrichment is likely attributable to natural weathering processes and organic recycling from plant residues. Similar findings have been reported in studies showing that soils under natural vegetation and grassland maintain higher extractable potassium compared to disturbed croplands due to continuous organic inputs and nutrient cycling (Abindaw *et al.,* 2023). Moderate concentrations are observed in the central portions of the LGA, while low K values dominate the southern and southeastern sectors. The latter coincide with urban and barren lands, where nutrient depletion is likely a consequence of runoff, soil erosion, and insufficient replenishment through organic or mineral nutrient inputs.

The strong correspondence between high potassium concentrations and vegetated land covers highlights the influence of land management practices and vegetation density on soil nutrient status. This observation is consistent with findings reported by Matano *et al.* (2015), who noted that vegetation enhances nutrient cycling and soil fertility, whereas urbanization and land degradation contribute to nutrient decline. These results emphasize the need for targeted potassium supplementation, particularly in barren and built-up areas, as a strategy to restore soil fertility balance across the study area.

3.5.5 Spatial Distribution of Phosphorus (P)

The spatial distribution of phosphorus (P) in the study area is presented in Figure 5. The maps reveal pronounced spatial variability, indicating that available phosphorus is not uniformly distributed across Akure South LGA. High concentrations are observed in the northern and northwestern zones of Akure South, which largely coincide with vegetated and cultivated land uses. These areas are enriched through organic residue decomposition, manure application, and phosphorus cycling via plant root systems. In contrast, the central and southern sectors, particularly those under built-up and barren land covers, exhibit comparatively lower phosphorus concentrations. This depletion is likely a result of topsoil erosion, surface sealing, and reduced organic matter input.

The clustering of high-P zones in vegetative and agricultural lands is consistent with the strong positive association between organic matter and phosphorus availability reported in tropical soils (Gao *et al.,* 2019). Given the slightly acidic soil pH observed in the area, phosphorus availability may be constrained by immobilization through adsorption to iron and aluminum oxides (Shen *et al.,* 2011; Ezeaku, 2021). Therefore, site-specific phosphorus management strategies, including the application of organic amendments and the use of phosphate-solubilizing bio-fertilizers to enhance fertility and crop productivity in low-P zones may be necessary.

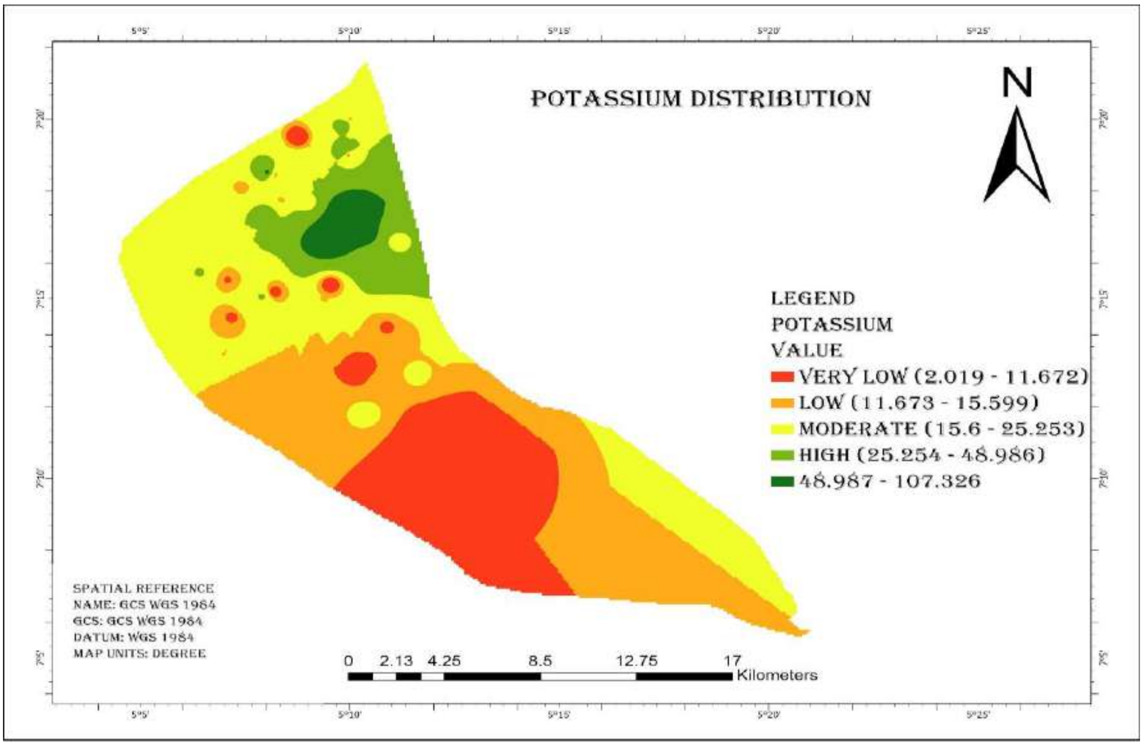

Fig.4: Potassium distribution on Akure South in Akure South LGA

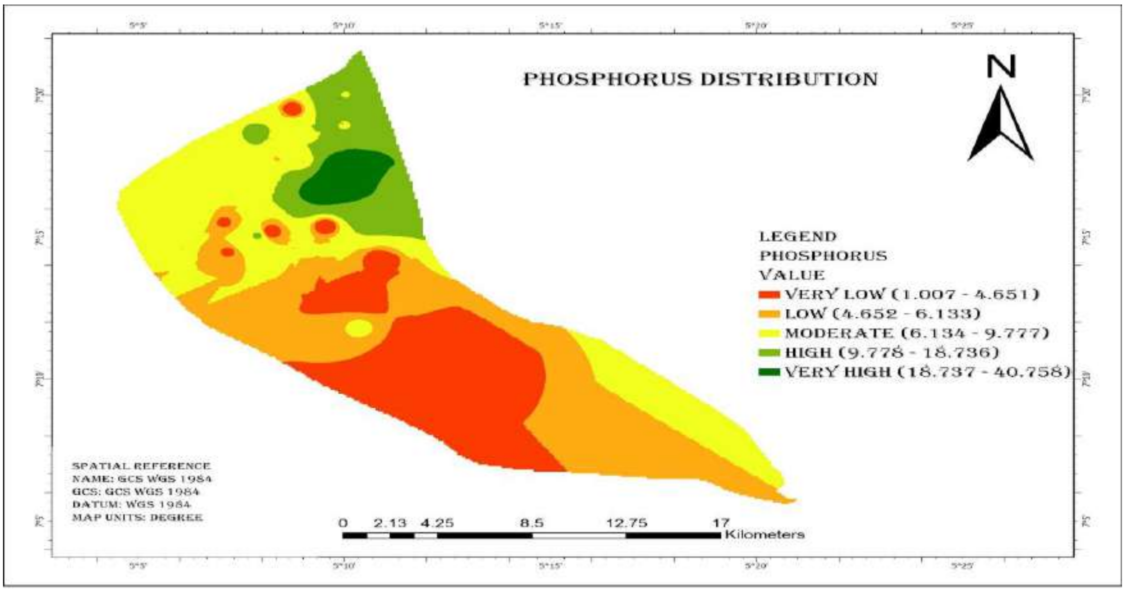

Fig.5: Phosphorus distribution in Akure South LGA

3.5.6 Spatial Distribution of Nitrogen (N)

The spatial distribution of nitrogen (N) in the study area is show in Figure 6. The maps reveal considerable spatial heterogeneity, with high nitrogen concentrations concentrated in the northern and western sectors of Akure South. These zones correspond primarily with vegetated and agricultural land uses, where substantial organic inputs from leaf litter, crop residues, and root exudates enhance nitrogen accumulation through mineralization processes. In contrast, the southern and central parts of the LGA, particularly under built-up and barren land covers, exhibit comparatively low nitrogen levels. This reduction is likely attributable to soil compaction, erosion, and depletion of organic matter, which collectively constrain nitrogen availability.

The observed pattern reflects the strong dependence of nitrogen status on organic matter, as further supported by the strong positive correlation (r = 0.84) between N and OC obtained from the correlation matrix analysis. Similar spatial associations have been reported in tropical regions, where vegetation cover and land management practices are key determinants of nitrogen distribution (Ogunleye and Agele, 2025). Furthermore, the high coefficient of variation (97.3%) recorded for nitrogen underscores the extreme spatial variability of this nutrient, driven by differences in land cover, organic inputs, and anthropogenic activities.

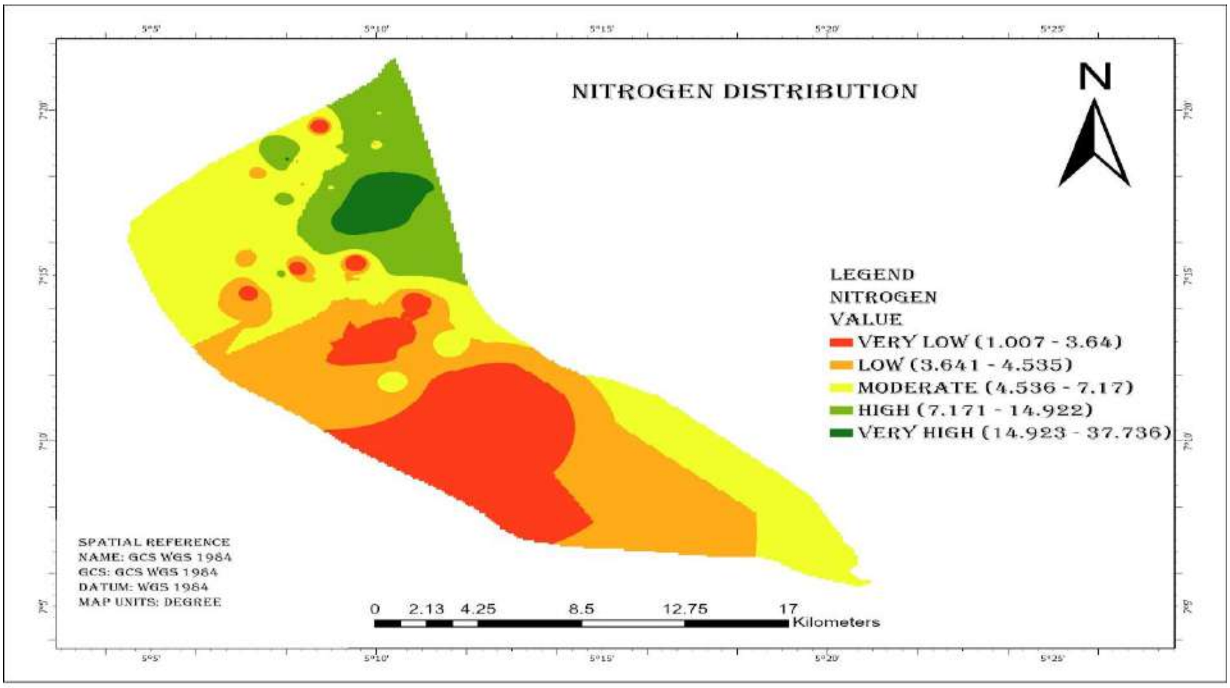

Fig.6: Nitrogen distribution in Akure South LGA

3.6 Overall Soil Fertility Map

The Soil Fertility Index (SFI) map generated through weighted overlay analysis of normalized soil parameters reveals distinct spatial patterns of fertility across Akure South LGA as shown in Figure 7. The SFI values ranged from 0.048 to 0.994, indicating extreme spatial heterogeneity in soil fertility status across the study area.

The fertility classification identified five distinct zones based on SFI values: Very Low (0.048-0.188), Low (0.189-0.270), Moderate (0.271-0.407), High (0.408-0.600), and Very High (0.601-0.994). The spatial distribution demonstrates a clear north-south gradient, with higher fertility concentrated in the northwestern sector, while lower fertility dominates the central and southern portions of the LGA.

Very Low and Low Fertility Zones (SFI < 0.271) occupy the largest portion of the study area, predominantly in the central and south-central regions, reflecting severe soil degradation due to urbanization, soil sealing, and topsoil removal. The extensive red and orange zones indicate widespread fertility constraints requiring intensive soil management interventions, including substantial organic matter additions and balanced fertilization (Olorunfemi *et al.,* 2018). Moderate Fertility Zones (SFI 0.271-0.407), shown in yellow, form transitional areas between high and low fertility regions, primarily in the western and eastern peripheries. These areas represent mixed agricultural lands and grasslands where soil fertility is adequate but requires regular maintenance through organic amendments and balanced nutrient management to prevent further degradation (Vasu *et al.,* 2016). High and Very High Fertility Zones (SFI > 0.408) are confined to relatively small areas in the northwestern and northeastern corners, appearing as light and dark green patches. These zones coincide with vegetated areas and well-managed agricultural lands where continuous organic matter inputs from litter decomposition, minimal soil disturbance, and active nutrient cycling maintain elevated fertility levels (Isong *et al.,*2022). The spatial pattern observed aligns closely with the individual parameter distribution maps, where high nitrogen, phosphorus, potassium, and organic carbon concentrations clustered in the northern and western vegetated areas, while depleted nutrient levels characterized the central built-up zones. This concordance validates the SFI as a meaningful integration of multiple fertility parameters into a single composite metric (Zhao *et al.,* 2023). The predominance of low fertility zones (red and orange colours covering approximately 60-70% of the mapped area) is an indication of urgent need for soil restoration programs in Akure South. The spatial heterogeneity revealed by the SFI map (with values spanning nearly the entire theoretical range of 0 - 1) confirms that blanket fertilizer recommendations are inappropriate for the area. Areas classified as Very Low and Low fertility require priority attention with intensive soil amendment programs, while High and Very High fertility zones can serve as reference sites for best management practices that could be replicated in degraded areas.

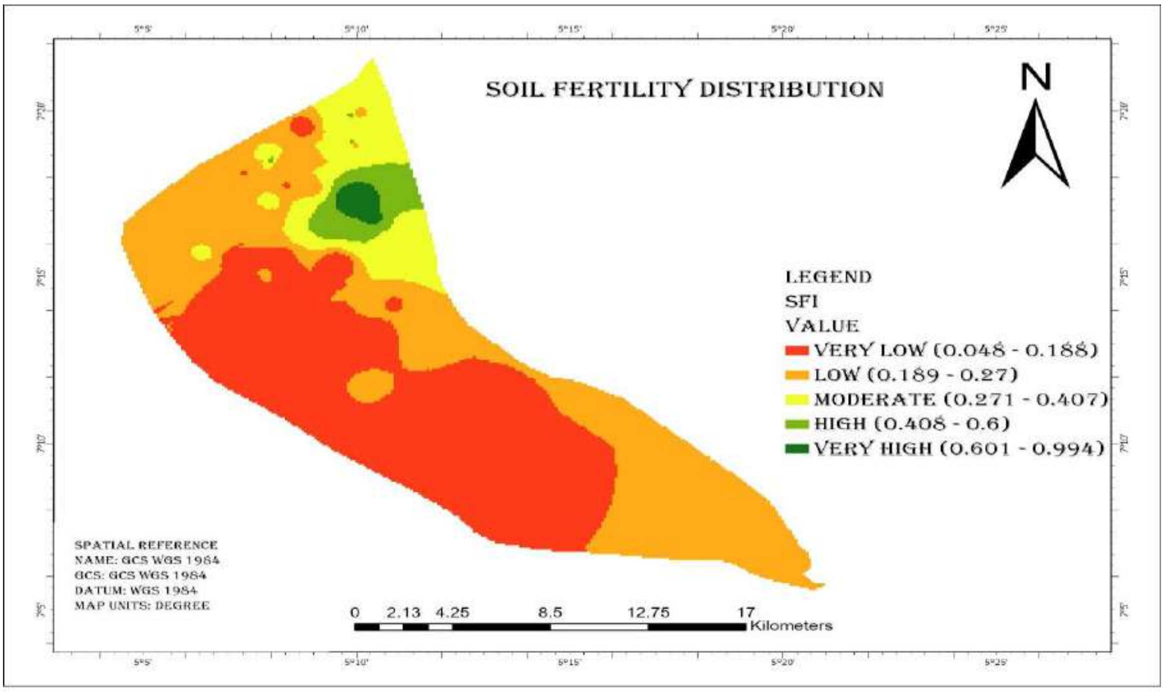

Fig.7: Soil fertility distribution map of Akure South LGA

The mean values of nitrogen, phosphorus, and potassium were low to moderate, indicating the general low fertility of the soils in the area. Organic carbon showed a moderate mean value, while the soil pH indicated a slightly acidic condition, which is typical of soils in the humid tropics. The high coefficients of variation (CV) for macronutrients such as nitrogen (97.3%), phosphorus (94.7%), and potassium (98.0%) indicate strong spatial heterogeneity in nutrient distribution. The Soil Fertility Index (SFI) results also showed that most parts of Akure South fell under low to very low fertility classes, accounting for about 60% of the study area (Table 4.).

The findings from the present research highlight a pronounced imbalance between nutrient-rich and nutrient-depleted zones across Akure South. The low mean values of nitrogen (7.50 mg/kg), phosphorus (9.48 mg/kg), and potassium (23.45 mg/kg) coupled with high CV values suggest that nutrient cycling and redistribution processes are highly localized (Table 1; Figure 4). This degree of heterogeneity is consistent with tropical landscapes characterized by complex land use mosaics, varying vegetation density, and differential management inputs (Kongor *et al.,* 2019). The relatively stable pH values (5.0–6.6) indicate a mildly acidic regime that, while suitable for most crops, may constrain phosphorus availability due to Fe/Al oxide fixation typical of ferrallitic soils (Balemi and Bayissa, 2012).

Spatial interpolation using IDW (Figures 2 –7) revealed nutrient enrichment primarily in the northern and northwestern sectors of the LGA i.e. areas associated with dense vegetation and lower anthropogenic disturbance. Conversely, nutrient-depleted areas dominated the built-up southern and central zones, reflecting the impact of soil sealing, erosion, and organic matter loss. The strong positive correlation between organic carbon and macronutrients (r > 0.77) further underscores the pivotal role of organic matter in nutrient retention and cycling (Paltineanu *et al.,* 2024). The mean SFI of 0.379 ± 0.156 (Figure 7) and its corresponding fertility classes confirm that most of the soils are below optimal productivity levels and will require intensive management for sustained agricultural performance. This spatial insight allows agricultural planners and policymakers to identify low-fertility zones for targeted intervention, fertilizer optimization, and restoration measures (AbdelRahman *et al.,* 2022; Prabhavati *et al.,* 2015).

3.7 Discussion

The observed low to moderate mean macronutrient concentrations and the pronounced spatial heterogeneity (very high CVs for N, P and K) in Akure South are consistent with previous GIS-based and field studies conducted across humid tropical regions in Africa and elsewhere. Several regional studies reported similar baseline fertility constraints in West African agricultural soils, with characteristic low plant-available phosphorus and nitrogen, coupled with modest organic carbon stocks. The studies emphasized strong small-scale variability driven by land-use, management and geomorphic position (Kongor *et al.,* 2019; Wells *et al.,* 2022).

Studies in West and East Africa using soil mapping and fertility indices have found comparable distributions of fertility classes and often identify organic carbon as a primary explanatory variable for nutrient status gradients. For example, detailed assessments of cocoa and mixed-cropping landscapes in Ghana and nearby West African zones documented low to moderate macronutrients and used composite soil quality indices to distinguish management units concluding that organic matter inputs strongly explain spatial fertility patterns (Kongor *et al.,* 2019). Studies showed that in highly weathered, ferrallitic soils, enhancements in organic carbon translate into improvements in N availability and greater nutrient retention overall.

At the landscape and national scale, comparisons of soil-organic-carbon mapping efforts highlight the challenge of predicting SOC and nutrient status from coarse datasets and underscore the utility of local, high-resolution sampling for management. Global and continental studies including national mapping efforts and reviews of digital soil mapping performance emphasize that SOC (and by extension nutrient status) is strongly controlled by edaphic factors (texture, mineralogy), land-use and topography, and that locally-targeted organic amendments are among the most effective mitigation strategies to improve fertility in tropical soils (Feeney *et al.,*2022; Xiang *et al.,* 2023).

Experimental trials and applied studies in southwestern Nigeria also demonstrate practical benefits from organic amendments (compost, manure, biochar) for increasing SOC, improving K and N retention, and raising crop yields outcomes that align with the present recommendation to prioritize organic-matter enrichment as a cost-effective strategy to increase nutrient retention and reduce reliance on blanket mineral fertilizer (Adekiya *et al.,* 2023; Agbede *et al.,* 2024).

Together, these studies indicate that Akure South's fertility profile, a landscape of low to moderate mean nutrient pools with high small-scale variability fits within the broader pattern observed across humid tropical agricultural systems.

3.7.1 Geoscience Interpretation of Fertility Distribution

Akure South LGA lies within the Precambrian Basement Complex of southwestern Nigeria, where migmatite–gneiss, granitic intrusions and related lithologies form the dominant bedrock. These basement rocks weather to produce deep lateritic profiles (residual soils) commonly classified in the WRB as Ferralsols and Acrisols under humid tropical conditions (WRB, 2014). The humid tropical climate (pronounced wet season, considerable annual rainfall) promotes intense chemical weathering and leaching, driving loss of base cations and accumulation of sesquioxides (Fe/Al oxides) in the soil profile (Falowo, 2018); this pedogenic pathway explains the ferrallitic character and generally low total nutrient pools observed in Akure South (Figures 1–6).

3.7.2 Parent material and mineralogical controls.

Parent-rock composition (migmatite–gneiss versus granitic or charnockitic intrusions) exerts first-order control on the primary mineral reservoir of nutrients (notably K and P bound to primary minerals). Where the parent rock contains higher K-feldspar or biotite contents, residual soils can retain slightly elevated K in coarse fragments and weathering residues; conversely, highly leached Ferralsols derived from silica-rich gneisses tend to show low extractable K despite total K stored in resistant minerals (Adeoye *et al.,* 2018). This geological control explains why some local samples show very high K (point concentrations up to 108 mg kg^{-1}) while the landscape mean is low, localized pockets reflect either residual mineral fragments or concentrated anthropogenic inputs on specific lithologies or borrow-pit fill (Adeoye *et al.,*2018; Falowo, 2018).

3.7.3 Weathering intensity, sesquioxides and phosphorus dynamics.

Intense weathering characteristic of humid tropical terrains produces high proportions of amorphous and crystalline Fe/Al oxides and oxyhydroxides. These sesquioxides strongly adsorb and occlude phosphate, reducing plant-available P even when total P is moderate ("P fixation" phenomenon). The slightly acidic topsoil pH (5.0–6.6) enhances the availability of Al^{3+} and Fe^{3+} at micro-scales, increasing the sorption of orthophosphate onto oxide surfaces and oxyhydroxide coatings, which is consistent with the low mean Bray-P/available-P values reported in Table 1 despite localized high-P samples (Johan *et al.,*2021). Strategies to improve P availability must therefore consider both chemical (liming, P placement) and organic (addition of biomass or compost to complex Al/Fe and reduce fixation) routes (Kiflu *et al.,* 2017).

3.7.4 Erosion, deposition and nutrient redistribution.

The spatial clustering of high-fertility patches in the northern and northwestern areas of Akure south (Figures 1– 6) together with depleted central/built-up zones suggests active landscape redistribution processes. On basement-complex terrain, ridges and convex hilltops often have thin, heavily weathered soils (nutrient-poor), while concave hollows, footslopes and depositional zones accumulate organic matter and fine sediments, concentrating nutrients (Falowo, 2018). Additionally, human activity such as tillage, manure application, dumping and construction fill can create point-source enrichment. Thus, the observed SFI hotspots likely reflect the combined influence of (a) depositional micro-sites that concentrate org-matter and fine particles, and (b) localized anthropogenic inputs. Targeting foot slope/depositional areas for conservation and management could therefore protect nutrient "sinks" and help restore adjacent depleted slopes (Herrmann *et al.,* 2020).

3.7.5 Anthropogenic/urban geomorphic modifications and anthroposols.

Urbanization and peri-urban land conversion in Akure South have reworked natural soil profiles through topsoil removal, compaction, and import of fill material and creation of anthroposols. These processes reduce organic matter stocks, disrupt structure, and can both dilute and concentrate nutrients depending on the fill source (e.g., construction debris vs. fertile topsoil). The low OC and nutrients observed in built-up zones closely mirror global patterns of urban soil convergence and degradation reported in multiple cities: urbanization tends to homogenize and often reduce SOC and nutrient heterogeneity at short distances, causing loss of ecosystem service potential unless remediated (Pouyat *et al.,*2010; Herrmann *et al.,*2020). Addressing these modifications requires both site remediation (topsoil replacement, decompaction) and planning measures to minimize further soil sealing.

3.7.6 Implications for Sustainable Soil Management and Land Use

***Prioritized, landscape-based interventions*.**

Given the strong spatial heterogeneity (high CVs) and the SFI map (Figure 5; Table 4), management should prioritize targeted interventions rather than uniform, area-wide fertilizer application. High-priority actions include: (1) mapping and protecting nutrient sink areas (depositional zones) to maintain OC and nutrient reservoirs; (2) targeted organic amendments (compost, manure, residue retention) in Low/Very Low SFI zones to build OC and improve cation exchange capacity; and (3) site-specific P management (banding, combined organic–mineral P applications, and judicious liming where pH <6.0) to overcome fixation losses (Fan *et al.,*2019; Johan *et al.,*2021). These recommendations are aligned with successful approaches reported in other humid tropical contexts.

IV. CONCLUSION

This study successfully evaluated the spatial distribution of soil fertility across Akure South Local Government Area using an integrated approach that combined field-based soil analysis with Geographic Information System (GIS) techniques. The results revealed notable variability in soil nutrient levels across different land use types, emphasizing the strong influence of land use and management practices on soil fertility. Areas with continuous vegetation cover and agricultural activity exhibited comparatively higher fertility index, while built-up and barren lands showed signs of nutrient depletion and reduced soil quality due to limited organic matter and surface sealing. The study highlights the central role of organic matter in maintaining soil fertility and the need for targeted interventions, such as organic amendments, conservation practices, and pH management, to enhance soil health. This research confirms that GIS-based soil fertility mapping is a valuable tool for visualizing spatial patterns of soil properties, guiding precision agriculture, and supporting evidence-based decision-making for sustainable land management in rapidly urbanizing tropical regions.

DECLARATION OF CONFLICT OF INTEREST

We hereby declare that the research was jointly sponsored and conducted by the authors, and not financed by any external sources. There are no conflict of interest of any form regarding the submission of this manuscript. No financial or personal relationship with a third party whose interests could be positively or negatively influenced by the article's content. Data from this research are all originally collected from the investigations conducted from this research and never a primary or secondary data from any other source.

REFERENCES

[1] Abdellatif, M. A., El Baroudy, A. A., Arshad, M., Mahmoud, E. K., Saleh, A. M., Moghanm, F. S., Shaltout, K. H., Eid, E. M., & Shokr, M. S. (2021). A GIS-based

approach for the quantitative assessment of soil quality and sustainable agriculture. Sustainability, 13(23), 13438.

[2] Abdelrahman, M.A.E., Natarajan, A. and Hegde, R. (2016) Assessment of Land Suitability and Capability by Integrating Remote Sensing and GIS for Agriculture in Chamarajanagar District, Karnataka, India. Egyptian Journal of Remote Sensing and Space Science, 19, 125-141.

[3] Abindaw, T., Hanyabui, E., Atiah, K., & Ampofo, E. (2023). Influence of land use types on the distribution of selected soil properties in tropical soils of the Coastal Savanna zone. Heliyon, 9(1), e14002.

[4] Adejuwon, J. O., & Ekanade, O. (2018). Land use changes and soil fertility status in Akure, southwestern Nigeria. Journal of Environmental Management, 210, 1–10.

[5] Adekiya, A. O., Alori, E. T., Ogunbode, T. O., Sangoyomi, T., & Oriade, O. A. (2023). Enhancing organic carbon content in tropical soils: Strategies for sustainable agriculture and climate change mitigation. The Open Agriculture Journal, 18, Article e187433152824762.

[6] Adeoye, A. S., Alo, B. A., & Abdu-Raheem, Y. A. (2018). Assessment of geotechnical properties of migmatite-derived residual lateritic soil from Ado-Ekiti, Southwestern Nigeria. International Journal of Innovative Research in Science, Engineering and Technology, 7(6), 7454–7462.

[7] Adeoye., M.O., Fasinmirin, J.T. Olajiga, B., Oruntunde, P.G. (2025). Remote Sensing and GIS Mapping of Land Use/Land Cover Change (LU/LCC) of Akure South, Southwestern Nigeria. *African Journal of Environment and Natural Science Research* 8(3), 35-53.

[8] Agbede, T. M., Oyewumi, A., Agbede, G. K., Adekiya, A. O., Adebiyi, O. T. V., Abisuwa, T. A., Ijigbade, J. O., Ogundipe, C. T., Wewe, A. O., Olawoye, O. D., & Eifediyi, E. K. (2024). Impacts of poultry manure and biochar amendments on the nutrients in sweet potato leaves and the minerals in the storage roots. Scientific Reports, 14, 16598.

[9] Agegnehu G, Amede T. 2017. Integrated soil fertility and plant nutrient management in tropical agro-ecosystems: A review. Pedosphere. 27:662–680.

[10] Agegnehu, G., Amede, T., Erkossa, T., Yirga, C., Henry, C., Tyler, R., Nosworthy, M.G., Beyene, S. & Sileshi, G.W. (2021): Extent and management of acid soils for sustainable crop production system in the tropical agroecosystems: a review, Acta Agriculturae Scandinavica, Section B — Soil & Plant Science, DOI: 10.1080/09064710.2021.1954239

[11] Akande, G. M., & Adedamola, P. A. (2020). Influences of land-use systems and soil depth on some selected soil properties in Akure, Nigeria. Plants and Environment, 2(1), 34–39.

[12] Akinbode, S. O., Folorunso, O., Olutoberu, T. S., Olowokere, F. A., Adebayo, M., Azeez, S. O., Hammed, S. G., & Busari, M. A. (2024). Farmers' Perception and Practice of Soil Fertility Management and Conservation in the Era of Digital Soil Information Systems in Southwest Nigeria. Agriculture, 14(7), 1182.

[13] Ande, Olufunmilayo & Huising, Jeroen & Ojo, A. & Azeez, J. & Are, Kayode & Olakojo, Samuel & Fademi, Ibukunoluwa & Ojeniyi, S.O.. (2017). Status of Integrated Soil Fertility Management (ISFM) in Southwestern Nigeria. International Journal of Sustainable Agricultural Research. 4. 28-44.

[14] Balemi, T., & Bayissa, K. N. (2012). Management of soil phosphorus and plant adaptation mechanisms to phosphorus stress for sustainable crop production: A review. Journal of Soil Science and Plant Nutrition, 12(3), 547–562.

[15] Bationo, A., Waswa, B. S., Kihara, J., & Kimetu, J. (2007). Advances in integrated soil fertility management in sub-Saharan Africa: Challenges and opportunities. Nutrient Cycling in Agroecosystems, 79(3), 1–15.

[16] Behera, S. K., & Shukla, A. K. (2015). Spatial distribution of surface soil acidity, electrical conductivity, soil organic carbon content and exchangeable potassium, calcium and magnesium in some cropped soils of India. Land Degradation & Development, 26(1), 71-79.

[17] Belayneh, M., Yirgu, T., & Tsegaye, D. (2019). Potential soil erosion estimation and area prioritization for better conservation planning in Gumara watershed using RUSLE and GIS techniques. Environmental Systems Research, 8(1), 20.

[18] Brady, N. C., & Weil, R. R. (2016). The nature and properties of soils (15th ed.). Pearson Education.

[19] Burrough, P. A., McDonnell, R. A., & Lloyd, C. D. (2015). Principles of Geographical Information Systems (3rd ed.). Oxford University Press.

[20] Carter, M. R., & Gregorich, E. G. (Eds.). (2007). Soil Sampling and Methods of Analysis (2nd ed.). CRC Press.

[21] Chandrakala, M., Ramesh, M., Sujatha, K., Hegde, R., & Singh, S. K. (2018). Soil fertility evaluation under different land use system in tropical humid region of Kerala, India. International Journal of Plant & Soil Science, 24(4), 1–13.

[22] Chang, X., Xing, Y., Wang, J., Yang, H., & Gong, W. (2022). Effects of land use and cover change (LUCC) on terrestrial carbon stocks in China between 2000 and 2018. Resources, Conservation and Recycling, 182, 106333.

[23] Chaudhry, H., Vasava, H. B., Chen, S., Saurette, D., Beri, A., Gillespie, A., & Biswas, A. (2024). Evaluating the soil quality index using three methods to assess soil fertility. Sensors, 24(3), 864.

[24] Chen, L., Zhangzhong, L., Zheng, W., & Yu, J. (2019). Data-driven calibration of soil moisture sensor considering impacts of temperature: A case study on FDR sensors. Sensors, 19(20), 4381.

[25] Childs, C. (2022). From pointa to surfaces: A practical guide to using ArcGIS Pro for spatial interpolation. *Transaction in GIS*, 26(3), 1450-1472.

[26] Dhayanan, V., Muthuselvam, M., & Ramaraj, M. (2016). Mapping and analysis of soil fertility using remote sensing and GIS: A case study of Tharangambadi Taluk, Nagappatinam District. International Journal of Engineering Research and General Science, 4(3), 218–224.

[27] Ezeaku, P. (2021). Influence of land use on soil physiochemical properties in semi-humid Nsukka area of Southeastern Nigeria. Nigerian Journal of Soil Science, 31(3), 2.

[28] Fabiyi, O. O., Ige-Olumide, O., & Fabiyi, A. O. (2013). Spatial analysis of soil fertility estimates and NDVI in

south-western Nigeria: A new paradigm for routine soil fertility mapping. Research Journal of Agricultural and Environmental Management, 2(11), 404–411.

[29] Falowo, O. O. (2018). Geochemical and engineering properties of selected lateritic deposits in Akure metropolis as highway subgrade foundation material. Asian Journal of Geological Research, 1(1), 1–14.

[30] Fan, Y., Zhong, X., Lin, F., Liu, C., Yang, L., Wang, M., Chen, G., Chen, Y., & Yang, Y. (2019). Responses of soil phosphorus fractions after nitrogen addition in a subtropical forest ecosystem: Insights from decreased Fe and Al oxides and increased plant roots. Geoderma, 337, 246–255.

[31] FAO. 2017. The future of food and agriculture – Trends and challenges. Rome.

[32] Feeney, C.J., Cosby, B.J., Robinson, D.A. et al., (2022). Multiple soil map comparison highlights challenges for predicting topsoil organic carbon concentration at national scale. Scientific Reports, 12, 1379.

[33] Gao, X., Xiao, Y., Deng, L., Li, Q., Wang, C., Li, B., Deng, O., & Zeng, M. (2019). The State of the World's Land and Water Resources for Food and Agriculture. FAO (2017).

[34] Hao, J., Chai, Y. N., Lopes, L. D., Ordóñez, R. A., Wright, E. E., Archontoulis, S., & Schachtman, D. P. (2021). Effects of soil depth on the structure of microbial communities in agricultural soils in Iowa (United States). Applied and Environmental Microbiology, 87(4), e02673-20.

[35] Herrmann, D.L., Schifman, L.A., Shuster W.D. Urbanization drives convergence in soil profile texture and carbon content. Environ Res Lett. 2020 Oct 14;15(11):10.1088/1748-9326/abbb00. doi: 10.1088/1748-9326/abbb00. PMID: 33628329; PMCID: PMC7898117.

[36] Hillel, D. (2008). Environmental Soil Physics. Academic Press.

[37] Isong, I. A., John, K., Okon, P. B., Ogban, P. I., & Afu, S. M. (2022). Soil quality estimation using environmental covariates and predictive models: An example from tropical soils of Nigeria. Ecological Processes, 11, 66.

[38] Jia, X., Wang, T., Zhang, H., & Li, Z. (2023). Development of Soil Fertility Index using machine learning and factor analysis in cropland soils. Land, 12(5), 945.

[39] Johan, P. D., Ahmed, O. H., Omar, L., & Hasbullah, N. A. (2021). Phosphorus transformation in soils following co-application of charcoal and wood ash. Agronomy, 11(10), 2010.

[40] Kiflu, A., Beyene, S., & Jeff, S. (2017). Fractionation and availability of phosphorus in acid soils of Hagereselam, Southern Ethiopia under different rates of lime. Chemical and Biological Technologies in Agriculture, 4(1), 21.

[41] Kongor, J. E., Boeckx, P., Vermeir, P., Van de Walle, D., Baert, G., Afoakwa, E. O., & Dewettinck, K. (2019). Assessment of soil fertility and quality for improved cocoa production in six cocoa growing regions in Ghana. Agroforestry Systems, 93(4), 1455–1467.

[42] Lal, R. (2015). Restoring soil quality to mitigate soil degradation. Sustainability, 7(5), 5875 –5895.

[43] Lal, R. (2020). Soil organic matter content and crop yield. Journal of Soil and Water Conservation, 75(2), 27A-32A.

[44] Lenka, N. K., Meena, B. P., Lal, R., Khandagle, A., Lenka, S., & Shirale, A. O. (2022). Comparing four indexing approaches to define soil quality in an intensively cropped region of Northern India. Frontiers in Environmental Science, 10, 865473.

[45] Li, L., Yue, Y., Qin, F., Dong, X., Sun, C., Liu, Y., & Zhang, P. (2022). Multi-scale characterization of spatial variability of soil organic carbon in a semiarid zone in Northern China. Sustainability, 14(15), 9390.

[46] Lima, A. A. J., Lopes, J. C., Lopes, R. P., de Figueiredo, T., Vidal-Vázquez, E., & Hernández, Z. (2025). Soil organic carbon assessment using remote-sensing data and machine learning: A systematic literature review. Remote Sensing, 17(5), 882.

[47] López-Granados, F., Jurado-Expósito, M., Atenciano, S., & García-Ferrer, A. (2002). Spatial variability of agricultural soil parameters in Southern Spain. Plant and Soil, 246(1), 97–105.

[48] Matano, A. , Kanangire, C. , Anyona, D. , Abuom, P. , Gelder, F. , Dida, G. , Owuor, P. and Ofulla, A. (2015) Effects of Land Use Change on Land Degradation Reflected by Soil Properties along Mara River, Kenya and Tanzania. *Open Journal of Soil Science*, **5**, 20-38. doi: 10.4236/ojss.2015.51003.

[49] Mirzaei, M., and Sakizadeh, M. (2022). Comparison of interpolation methods for the estimation of groundwater contamination in ArcGIS Pro. Environmental Earth Sciences, 81(4), 115.

[50] Mkonda, M. Y., & He, X. (2018). Accumulation of SOC under organic and no-fertilizations, and its influence on crop yields in Tanzania's semiarid zone. Ecosystem Health and Sustainability, 4(2), 1463146.

[51] Mulder, V. L., de Bruin, S., Schaepman, M. E., & Mayr, T. R. (2011). The use of remote sensing in soil and terrain mapping—A review. Geoderma, 162(1-2), 1–19.

[52] Mulla, D. J. (2013). Twenty-five years of remote sensing in precision agriculture: Key advances and remaining knowledge gaps. Biosystems Engineering, 114(4), 358–371.

[53] Nelson, D. W., & Sommers, L. E. (2018). Total carbon, organic carbon, and organic matter. In D. L. Sparks (Ed.), Methods of soil analysis: Part 3 – Chemical methods (pp. 961–1010). Soil Science Society of America and American Society of Agronomy.

[54] Nkwunonwo, U. C., & Okeke, F. I. (2013). GIS-based production of digital soil map for Nigeria. Ethiopian Journal of Environmental Studies and Management, 6(5), 498–507.

[55] Ogunleye, A. & Agele, S. (2025). Land use effects on soil properties and carbon stocks of agricultural and agroforestry landscapes in a rainforest zone of Nigeria. *Advances in Modern Agriculture*, 6(2): 2964.

[56] Olajide, H. M., Amoo, N. B., Oguntayo, S. M., Aroge, S. K., & Amoo, A. O. (2018). Geospatial Analysis of Land Use and Land Cover Dynamics in Akure, Nigeria. Dutse Journal of Pure and Applied Sciences, 4(1), 379–393.

[57] Olanipon, D., Adewoyin, A., & Eludoyin, A. (2025). Climatic Variability and Associated Changes in a Nigerian

Nature Forest Reserve. Oxford Open Climate Change. 5. 10.1093/oxfclm/kgaf008.

[58] Olorunfemi, I. E., Fasinmirin, J. T., & Akinola, F. F. (2018). Soil physico-chemical properties and fertility status of long-term land use and cover changes: A case study in forest vegetative zone of Nigeria. Eurasian Journal of Soil Science, 7(2), 133–150.

[59] Olorunfemi, I. E., Fasinmirin, J. T., Olufayo, A. A. O., & Komolafe, A. A. (2020). GIS and remote sensing based analysis of the impacts of land use/land cover change (LULCC) on the environmental sustainability of Ekiti State, southwestern Nigeria. Environment, Development and Sustainability.

[60] Owoeye, J. O. (2019). Assessing urban growth dynamics and depletion of agricultural land use in Akure region, Nigeria. Land Science, 1(1), 43.

[61] Paltineanu, C., Dumitru, S., Vizitiu, O., Mocanu, V., Lăcătusu, A.-R., Ion, S., & Domnariu, H. (2024). Soil organic carbon and total nitrogen stocks related to land use and basic environmental properties: Assessment of soil carbon sequestration potential in different ecosystems. CATENA, 246, 108435.

[62] Pouyat, Richard and Szlávecz, Katalin & Yesilonis, I.D. & Groffman, Peter & Schwarz, Kirsten. (2010). Chemical, physical, and biological characteristics of urban soils. Urban ecosystem ecology. 119- 152.

[63] Prabhavati, K., Dasog, G.S., Patil, P.L., Sahrawat, K.L., and Wani, S.P. (2015). Soil Fertility Mapping using GIS in Three Agro-climatic Zones of Belgaum District, Karnataka. Journal of the Indian Society of Soil Science, 63(2), 173-180.

[64] Romheld, V., & Kirkby, E. A. (2010). Research on potassium in agriculture: Needs and prospects. Plant and Soil, 335(1-2), 155-180.

[65] Seto, K.C., and Ramankutty, N. (2016). Hidden linkages between urbanization and food systems. *Science*, *352*, 943–945.

[66] Shamrikova, E. V., Kondratenok, B. M., Tumanova, E. A., Vanchikova, E. V., Lapteva, E. M., Zonova, T. V., Lu-Lyan-Min, E. I., Davydova, A. P., Libohova, Z., & Suvannang, N. (2022). Transferability between soil organic matter measurement methods for database harmonization. Geoderma, 412, 115547.

[67] Shen, J., Yuan, L., Zhang, J., Li, H., Bai, Z., Chen, X., Zhang, W., & Zhang, F. (2011). Phosphorus dynamics: From soil to plant. Plant Physiology, 156(3), 997–1005.

[68] Singh, S., Rai, V., Upadhyay, S., & Singh, S. (2023). Geo-spatial tools for assessing soil fertility: A review. International Journal of Plant & Soil Science, 35(18), 1386–1394.

[69] Tesfahunegn, G. B., Tamene, L., & Vlek, P. L. G. (2011). Evaluation of soil quality identified by local farmers in Mai-Negus catchment, northern Ethiopia. Geoderma, 163(3–4), 209–218.

[70] Vasu, D., Singh, S. K., Ray, S. K., Duraisami, V. P., Tiwary, P., Chandran, P., Nimkar, A. M., & Anantwar, S. G. (2016). Soil quality index (SQI) as a tool to evaluate crop productivity in semi-arid Deccan Plateau, India. Geoderma, 282, 70-79.

[71] Wells, J.M., Crow, S.E., Sierra, C.A. et al. Edaphic controls of soil organic carbon in tropical agricultural landscapes. Sci Rep 12, 21574 (2022).

[72] Weng, Q. (2012). Remote sensing of impervious surfaces in the urban areas: Requirements, methods, and trends. Remote Sensing of Environment, 117, 34–49.

[73] World Reference Base for Soil Resources (WRB). (2014). International soil classification for naming soils and creating map legends (Update 2014/2015). Food and Agriculture Organization (FAO).

[74] Xiang, D., Wang, G., Tian, J. (2023). Global patterns and edaphic-climatic controls of soil carbon decomposition kinetics predicted from incubation experiments. Nature Communications, 14, 2171.

[75] Yao, Y., Fan, J., & Li, J. (2025). A review of advanced soil moisture monitoring techniques for slope stability assessment. Water, 17(3), 390.

[76] Yu, P., Liu, S., Zhang, L., Li, Q., & Zhou, D. (2018). Selecting the minimum data set and quantitative soil quality indexing of alkaline soils under different land uses in northeastern China. Science of the Total Environment, 616-617, 564-571.

[77] Zhang, N., Wang, M., & Wang, N. (2019). Precision agriculture – A worldwide overview. Computers and Electronics in Agriculture, 36(2-3), 113–132.

[78] Zhang, X., Davidson, E. A., Mauzerall, D. L., Searchinger, T. D., Dumas, P., & Shen, Y. (2015). Managing nitrogen for sustainable development. Nature, 528(7580), 51-59.

[79] Zhao, W., Cao, X., Li, J., Xie, Z., Sun, Y., & Peng, Y. (2023). Novel weighting method for evaluating forest soil fertility index: A structural equation model. Plants, 12(2), 410.

International Journal of Environment, Agriculture and Biotechnology
Vol-11, Issue-3; May-Jun, 2026
Peer-Reviewed International Journal
Journal Home Page Available: https://ijeab.com/
Journal DOI: 10.22161/ijeab

A Systematic Review on Water Use Efficiency (WUE) and Soil Moisture Dynamics in Wheat-Based Agroforestry Systems

Amandeep Singh[1], Atish[2*], Vijay Singh[1], Beena Kumari[3], Sandeep Arya[1], Ankush Kamboj[1]

[1]CCS Haryana Agricultural University, Hisar, Haryana-125004, India
[2]Indian Institute of Technology Kharagpur, West Bengal-721302, India
[3]J.C. Bose University of Science and Technology, YMCA, Haryana-121006, India
*Corresponding author: atishyadav7304@gmail.com

Received: 19 Apr 2026; Received in revised form: 20 May 2026; Accepted: 25 May 2026; Available online: 02 Jun 2026

Abstract*— Globally, wheat productivity and sustainable agricultural development are being significantly impacted by water constraint, decreasing soil moisture availability, and rising climate unpredictability. The potential of wheat-based agroforestry systems to increase soil moisture conservation, maximize water use efficiency (WUE), control evapotranspiration, and promote ecosystem sustainability has made them a promising climate-resilient strategy. In addition to summarizing the impact of tree-crop interactions, water management techniques, and new measurement tools, this systematic review assesses the body of research on WUE and soil moisture dynamics in wheat-based agroforestry systems. The review was carried out using literature gathered from major scientific databases, such as Science Direct, Scopus, Springer Link, and Google Scholar, covering studies published between 1960 to 2025, in accordance with the preferred reporting items for systematic reviews and meta-analysis (PRISMA) framework. To find patterns in soil moisture behavior, evapotranspiration processes, agroforestry treatments, and WUE improvement techniques, publications were searched and evaluated. The results showed that through canopy modification, litter deposition, increased soil organic matter, and microclimatic regulation, agroforestry systems have a significant impact on soil moisture distribution, infiltration characteristics, runoff regulation, root-zone water availability, and crop water productivity. While excessive competition for water, nutrients, and light negatively impacted wheat growth and production, well-managed tree-crop combinations enhanced WUE and soil moisture retention. The assessment also noted contemporary developments in machine learning and remote sensing technologies, as well as traditional field-based methods and process-based models like CROPWAT.

***Keywords*— irrigation management, soil moisture dynamics, water use efficiency, wheat-based agroforestry**

I. INTRODUCTION

One of today's most critical issues is providing a consistent supply of safe and nutritious food for a growing global population while also protecting the environment and reducing climate change. Agriculture is the major contributor to greenhouse gas emissions and world's largest consumer of land and water resources [1]. Particularly in emerging nations, agriculture continues to be a vital industry for maintaining livelihoods, guaranteeing food security, and promoting economic growth. However, a complex interaction of environmental, socioeconomic, and climatic elements is posing a growing difficulty [2]. One of the biggest issues confronting humanity in the upcoming decades is water scarcity. Conservation agriculture techniques increase soil moisture availability, particularly in low-rainfall situations, and may help sustain crop productivity in a changing climate [3]. The method of agriculture known as conservation agriculture, which aims to reduce environmental harm and soil disturbance, is being widely pushed globally. A key element of conservation agriculture is conservation tillage, which is thought to improve soil health through plant growth, land development, and environmental preservation. A sustainable farming method that seeks to improve soil health, preserve water, and lessen environmental deterioration is conservation tillage. It entails controlling crop residues on the soil's surface and reducing soil disturbance during crop planting [4]. Conservation tillage helps in maintaining soil moisture by reducing evaporation [5]. A recent meta-analysis found that using conservation agriculture methods in south asia increased productivity, water consumption efficiency, and net profit by 5.8%, 12.6%, and 25.9%, respectively, while reducing the potential for global warming by 12–33% [6].

Ecosystems, life, and social development all depend on water. However, over 1.2 billion people globally still lack regular access to clean water, highlighting the fact that it is acknowledged as a fundamental human right. Growing freshwater stress is a result of increased water demand brought on by population growth, urbanization, industrial expansion, intensive agriculture, and climate unpredictability in many areas, including India. The world economic forum often lists water shortages as one of the biggest challenges to the world's economy and society. According to projections, the world's water demand would rise by 55% from 2000 levels by 2050 due to changes in consumption patterns, pollution, and the need for more irrigation [7][8]. Understanding and resolving the interaction between such compound occurrences and water systems is essential for resilience-building and sustainable resource planning as climatic variability increases. Population growth is a second important element that increases freshwater demand in the residential, agricultural, and industrial sectors. According to [9], the world's population is predicted to reach 8.5 billion by 2030 and surpass 9.7 billion by 2050. This would result in a 50% rise in food consumption, which will necessitate 40–50% more water for agriculture and 50–70% more water for municipal and industrial use [8]. Furthermore, CO_2 emissions and the human population are strongly correlated. A billion more people on the planet results in 1.4 Pg more CO_2 emissions from burning fossil fuels (1 Pg = 1015, g = 1 Gt) [10]. Developing irrigation techniques that use the least amount of water is becoming more important due to global water problems and irrigation expenses [11].

Changes in land use and land cover, which operate on a temporal scale in physical and biological features, are indicative of landscape dynamics. Changes in the structure of the landscape are caused by both natural and anthropogenic factors [12]. Monitoring spatial patterns of changing land use and land cover (LULC) [7] or obtaining detailed information about land use and land cover change is essential for making decisions that will effectively accomplish the goal of sustainable development [13]. Additionally, dry soil salinity has a major impact on agricultural output [14], making it a major challenge for the agricultural sector to feed the world's growing population [15][16].

Researchers, governments, and farmers are all becoming increasingly concerned about the major issues that climate change presents to agricultural systems around the world [17]. Extreme weather events including heat waves, floods, and droughts are becoming more frequent and severe, endangering livestock, agricultural output, pest and disease prevalence, and soil fertility [18]. Due mostly to climate change, the majority of nations in the globe are dealing with the issue of yield stagnation and decline, particularly in cereals. Significant production reductions result from shifting climatic circumstances, such as high temperatures, coinciding with wheat's grain-filling stage [19]. Adopting weather, water, carbon smart agriculture, and nutrient; which includes planting date changes, crop diversification, better irrigation techniques, drought-tolerant crop varieties, and agroforestry practices - is the main focus of the potential adaptive strategies that agricultural researchers are currently investigating [20][21].

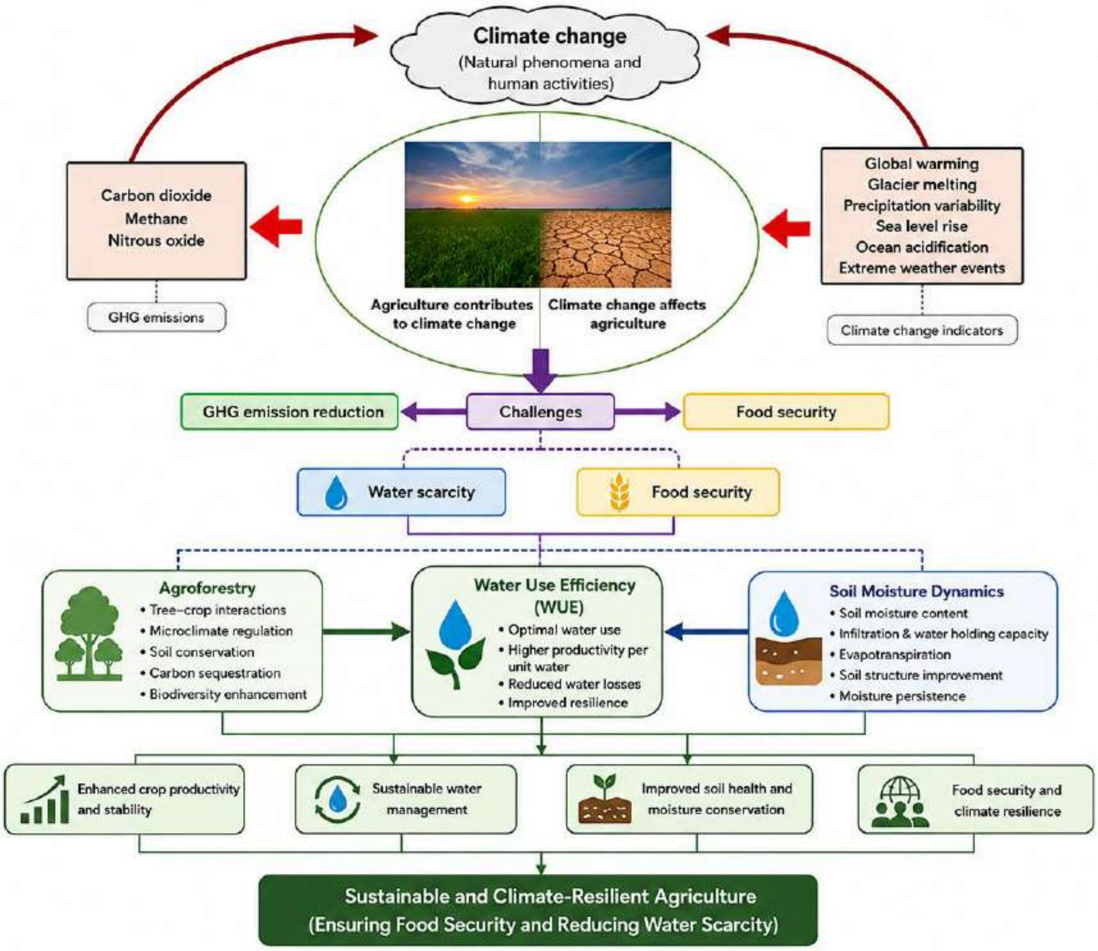

Fig. 1: Conceptual framework illustrating the linkage among climate change, agriculture and key challenges (water scarcity and food security) and the role of agroforestry, water use efficiency (WUE) and soil moisture dynamics in building sustainable and climate-resilient agriculture.

While over 83% of current worldwide adaptation efforts indicate little potential to reduce risks, investments in sustainable agriculture have a tremendous potential to alleviate food insecurity, according to the IPCC 6th Assessment Report [22][23]. However, there is limited information on how effective these solutions will be as global warming continues [24]. Agroforestry and sustainable agricultural intensification are crucial tactics for guaranteeing food security. In addition to regulating the carbon and nitrogen cycles, forests are essential for maintaining a stable global temperature [25]. Additionally, the local and global climate are impacted by environmental changes in forests [20]. In agroforestry systems, the deep roots of trees increase the soil's capacity for water infiltration and storage, lowering surface runoff and soil erosion by up to 90%, lowering soil nitrogen and phosphorus residues by up to 100%, and guaranteeing more water availability during dry spells [11]. Despite the social and economic potential of these approaches, they frequently encounter institutional and technological obstacles. High input costs - such as those of labor, capital, and land remain significant challenges. However, it has been demonstrated that these adaptation choices can lessen economic and social inequality. Co-benefits and more effective and economical climate action can be achieved by coordinating climate adaptation with the sustainable development goals (SDGs) [24][26].

To alleviate these challenges, sustainable soil and water resource management practices are increasingly critical for preserving farm productivity, increasing irrigation efficacy, and improving climate resilience. Examples of soil and moisture conservation strategies that have demonstrated positive effects on soil health, food security [9], carbon sequestration, and water retention include cover crops, crop rotation, conservation tillage, agroforestry systems, and improved irrigation techniques. These strategies are crucial tools for sustainable agriculture [22].

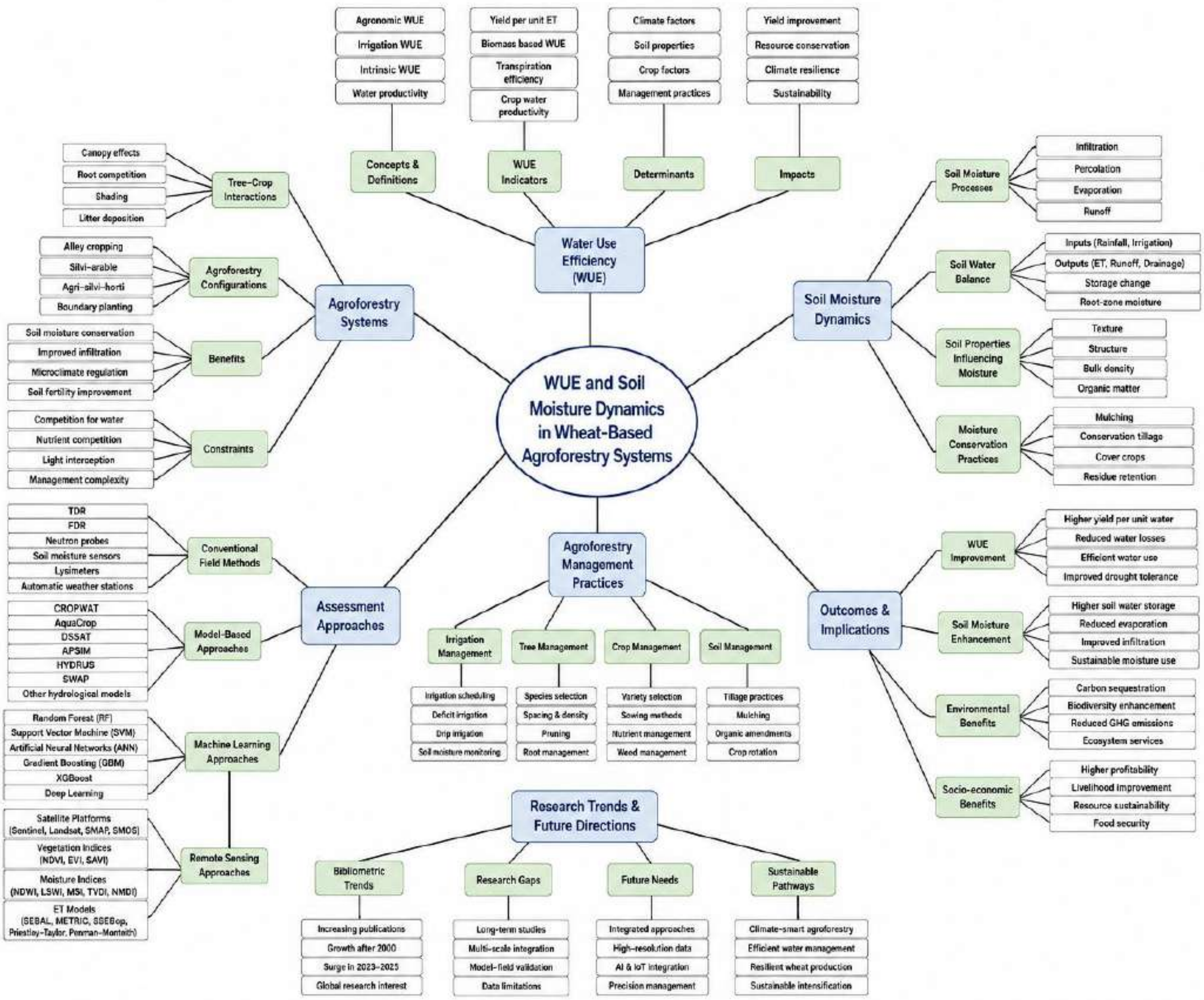

Fig. 2: Conceptual aggregation framework of water use efficiency and soil moisture dynamics for wheat-based agroforestry systems including field methods, models, remote sensing, and machine learning approaches

II. METHODOLOGY

To critically assess published research on soil moisture dynamics and water use efficiency (WUE) in wheat-based agroforestry systems, a methodical and evidence-based literature review approach was used. To guarantee methodological transparency, reproducibility, and scientific rigor throughout the literature identification, screening, eligibility assessment, and inclusion processes, the review framework was created in compliance with the Preferred Reporting Items for Systematic Reviews and Meta-Analyses (PRISMA) guidelines. Four globally renowned scientific databases—Science Direct, Scopus, Google Scholar, and Springer Link—were used to do a thorough bibliographic search. In order to capture both fundamental and modern developments in agroforestry, soil hydrology, irrigation management, and agricultural water productivity, the literature retrieval procedure encompassed publications from 1960 to 2025.

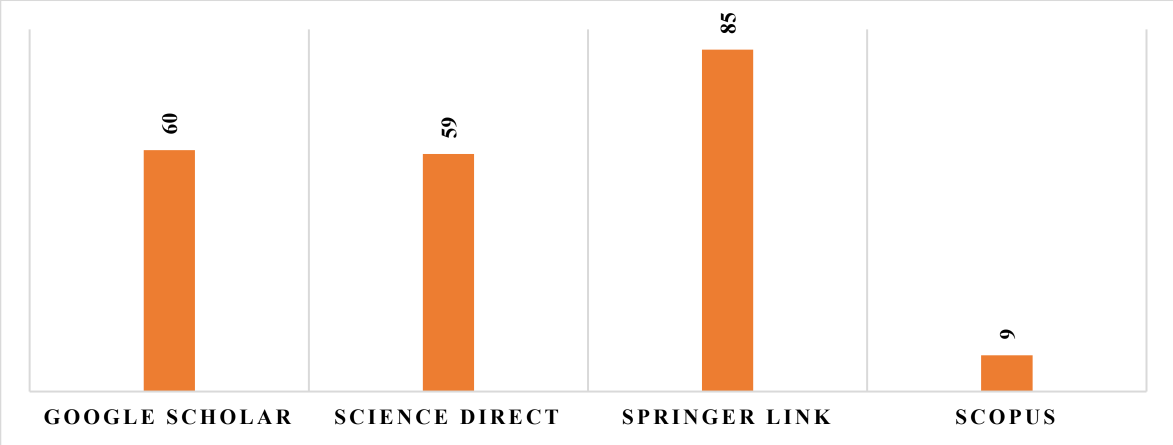

Fig. 3: The database-wise distribution of identified studies included

After eliminating the same publications (the same publication from two or more databases), a total of 213 records were first found during the primary database search.

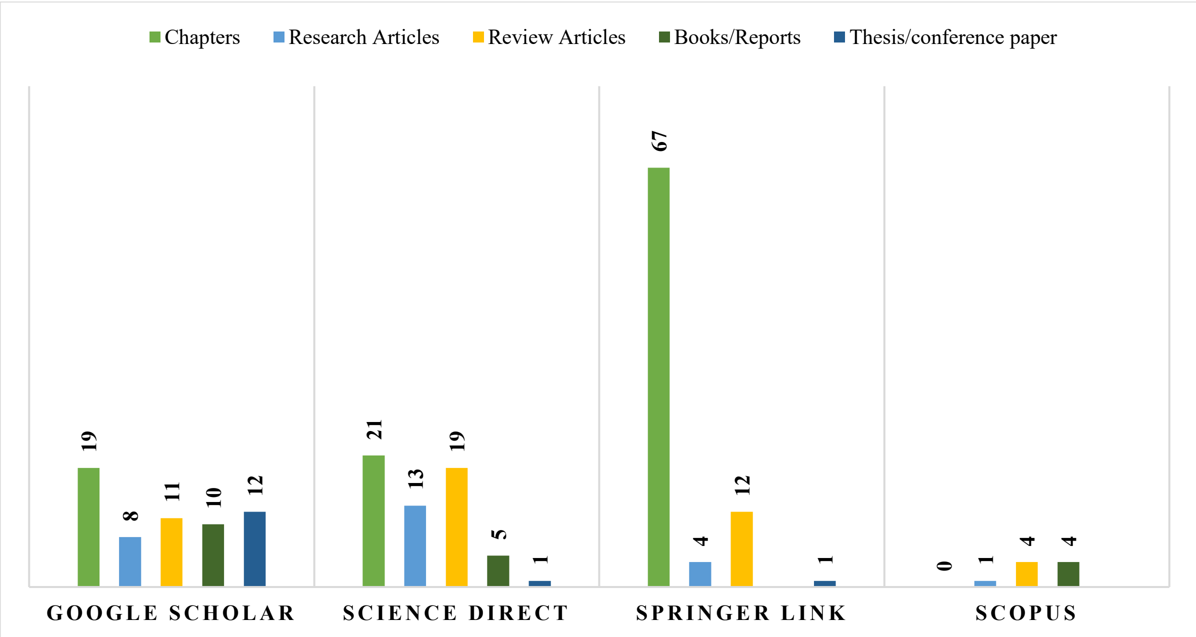

Fig. 4: Distribution of Literature Sources Retrieved from Different Scientific Databases

From Fig. 3, Bibliometric analysis of the selected literature revealed that investigations on water use efficiency and soil moisture dynamics in wheat agroforestry systems were sparse before 2000, indicating limited scientific attention during the initial phase. However, research output increased progressively after 2000, suggesting enhanced interest in agroforestry-mediated water management strategies. The most significant growth in publications was observed during 2023–2025, with 2025 showing the highest contribution, followed by 2023 and 2024. This trend reflects the increasing global focus on sustainable water utilization, climate adaptation, precision irrigation, and soil moisture conservation in wheat-based agroforestry ecosystems.

To increase the retrieval efficiency of pertinent research, the search method used technical keywords, Boolean operators, and controlled vocabulary concepts. Water use efficiency, soil moisture dynamics, wheat cultivation, wheat-based agroforestry, agroforestry systems, soil water conservation, evapotranspiration, irrigation management, crop water productivity, sustainable agriculture, soil moisture monitoring, and climate resilience were among the main search terms. Boolean operators like "AND," "OR," and "NOT" were methodically incorporated to enhance the specificity of the retrieved literature and refine the search results.

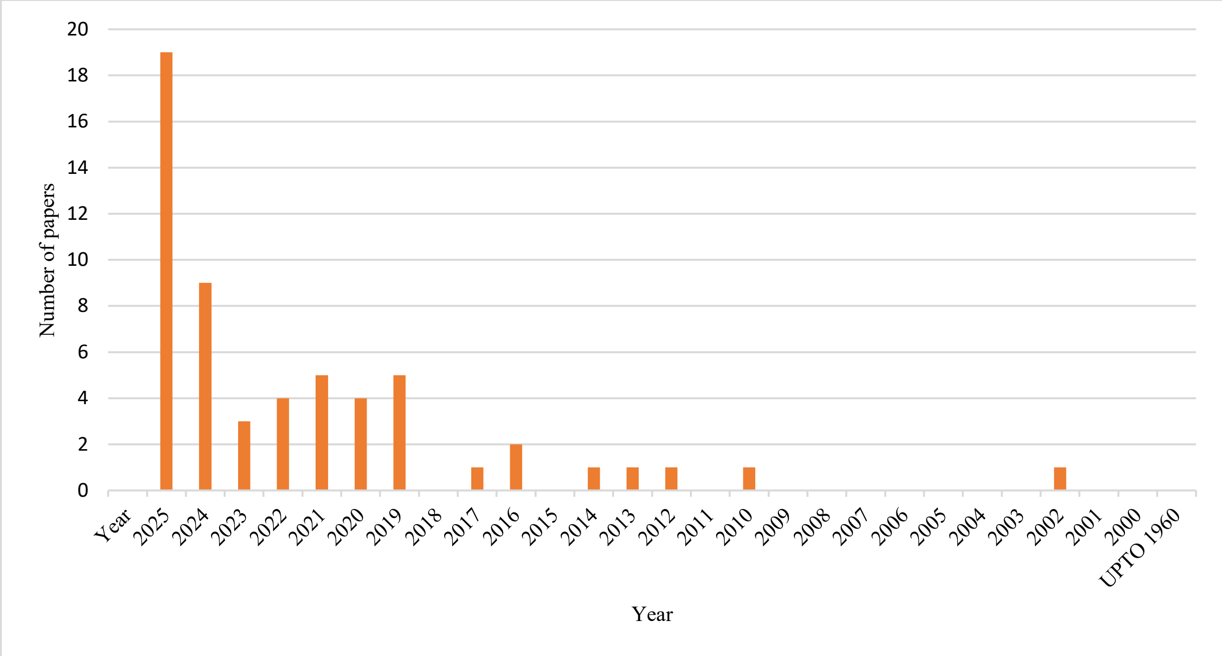

Fig. 5: Year wise publication trend for science direct database (from 1960 to 2025)

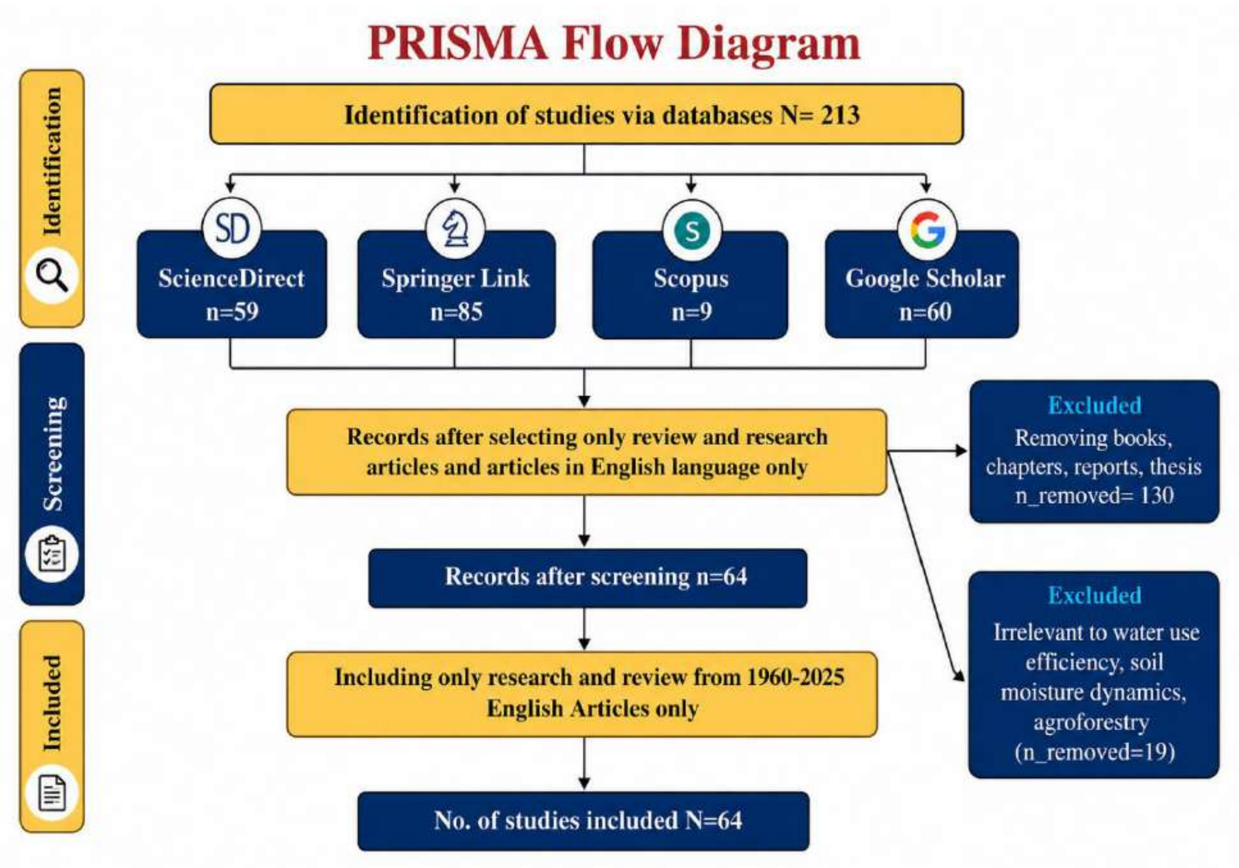

Fig. 6: This PRISMA flow diagram shows how studies are chosen for a systematic review.

A multi-phase screening procedure was applied to the collected records. Books, book chapters, reports, conference proceedings, dissertations, and non-English publications were among the non-research elements that were initially removed from the dataset. 130 records were eliminated as a consequence of this initial screening. The remaining publications were then screened for scientific value in relation to the review objectives using the title, abstract, and full text. Studies examining soil moisture behavior under agroforestry systems, water use efficiency in wheat cultivation, the effects of tree-crop interactions on soil hydrology, irrigation scheduling and water conservation techniques, and sustainable resource-use management in semi-arid and arid agroecosystems were given special attention. Nineteen studies were eliminated during the eligibility assessment phase because they were not sufficiently relevant to agroforestry-based wheat production systems, soil moisture dynamics, or water use efficiency.

Final inclusion was limited to peer-reviewed journal articles and review papers published in English between 1960 and 2025. Studies that offered quantitative or qualitative data on crop water productivity and irrigation efficiency, soil moisture conservation and hydrological processes, wheat production under agroforestry or integrated farming systems, and climate-resilient agricultural water management techniques were chosen.

The qualitative synthesis contained 64 studies in total after the methodical screening and eligibility evaluation processes. These selected research formed the scientific basis for evaluating the connections among agroforestry systems, soil moisture dynamics, and water usage efficiency in wheat farming. The compiled literature offers important insights into root-zone moisture dynamics, irrigation optimization, evapotranspiration regulation, soil water retention mechanisms, and sustainable agroecosystem management techniques under various edaphic and climatic circumstances. With regard to sustainable water management in wheat-based agroforestry systems under rising climatic variability and water scarcity circumstances, the integrated analysis made it possible to identify current research trends, methodological gaps, and future research goals.

III. RESULTS AND DISCUSSION

The average wheat yield in Northern India was 3.0 Mg ha^{-1}, but the potential yield was 7.5 Mg ha^{-1}, suggesting the biggest yield difference among the regions considered. With a potential production of 5.5 Mg ha^{-1} and an average yield of 4.1 Mg ha^{-1}, Punjab demonstrated substantially higher productivity, while there is still room for improvement. The average and prospective yields in Haryana were 3.8 Mg ha^{-1} and 4.0 Mg ha^{-1}, respectively, indicating a reduced yield gap and rather efficient production circumstances [10]. Wheat grain yields in agri-silvi-horticultural systems varied from 2.34 to 3.13 t ha^{-1} under tree-based systems and from 4.07 to 4.08 t ha^{-1} under sole cropping circumstances. The khejri + guava + wheat system yielded the most wheat (3.01–3.13 t ha^{-1}) out of all the combinations, suggesting that wheat is more compatible with greater canopy spacing and less competition. On the other hand, systems with more intense shading demonstrated comparatively poorer output [27]. According to studies conducted in Himalayan agri-horticultural systems, wheat cultivated with grewia + almond combinations outperformed other tree associations. Crop yield beneath the tree crown was roughly 17–19% lower than locations outside the canopy effect, and wheat yield losses under tree canopies ranged from 18–28% when compared with open-field agriculture. However, the grewia + almond + wheat system had the best soil moisture conditions and the highest net economic return, indicating the promise of improved agroforestry arrangements for sustainable wheat production [28]. Wheat yields in poplar-based agroforestry systems were also lower than in open cultivation, where the open-field grain yield was about 3.55 t/ha. Additionally, agroforestry treatments shown decreased productivity because of shading effects, particularly in eucalyptus-based systems. Poplar-based systems, on the other hand, outperformed eucalyptus (yield = 1.56 t/ha) and maintained enhanced soil nutrient status, indicating their viability for wheat integration in north Indian agroforestry regions (yield = 3.24 t/ha) [29]. Pea-wheat intercropping was used across the world for forage and grain production. According to a study by [30], intercropping can be impacted by the availability of water as well as the choice of cultivar, which can have an impact on water use efficiency and the intercropping system's productivity. While the water use efficiency values were lower in 2006–07 and 2007–08, the yield and Et_a of the winter wheat irrigated plots were greater than those of the rainfed plots [31]. According to [32], irrigation practices have a significant impact on NDVI readings and have a high positive association with both grain yield and biomass output. improved root growth and soil moisture retention.

Table 1: The overview of agricultural methods' effects on soil & water conservation, as well as other parameters (for example, yield). The results are contrasted with traditional tillage and agrichemical use [1].

Practice	Soil Conservation	Water Conservation	Yield
cover/catch crops	Boost the soil structure, increase soil organic matter (SOM) and decrease soil erosion	Soil moisture conservation, increase in soil water capacity, improved water quality downstream	15% increase in wheat yield [33][34]
Agroforestry	Reduce soil erosion, improved soil structure, increase SOM	Agroforestry in arable farming systems [35], Conserves soil moisture and protect crops during high summers and fast blowing winds and storms.	The grain yield was higher in an agroforestry system, and sometimes depend upon spacing btw trees and other factors [36].
Intercropping	Maintain soil structure, balance nutrient in soil and also maintain SOM level [1].	But it don't increase water use efficiency	Higher overall yield of the intercropped Crops [37]. On the other hand, compared to a wheat-only crop, one study found that intercropping winter wheat with clover reduced wheat grain yield by 10–25%. [38].
Residue retention/Mulch	Efficient in reducing erosion (1.7 t/ha-y compared to 4.6 t/ha-y of soil loss) [33][34]	Soil moisture maintained [4], Lowering in evaporation from soil.	Enhancing yield of wheat (15% higher) [33]
Minimum tillage	Reduce soil erosion & nutrient loss [39]	Lowering moisture loss, water runoff & reduce sedimentation [40]	Yields are higher or equal to systems using the conventional tillage [41]
Crop Rotation	Reduces soil erosion, increases soil fertility, regulating soil nutrients & building soil structure [42]	Decreases pests and diseases. And increase in soil water capacity [43].	Grain yield was higher in the winter oilseed rape–winter wheat–winter wheat–winter barley crop rotation system (83.5 grain yield/ha) than in the later (72.9 grain yield/ha) [44]
No till/Direct seeding	Reduce soil erosion & nutrient loss [45].	Lowering moisture loss [32], water runoff and reduce sedimentation	Crop yields were higher when no-tillage was combined with weed management and fertilizer application rates of either 50% or 100% [46]

The conventional approach involves direct field measurements using instruments such as time domain reflectometry (TDR) [47], soil moisture sensors, frequency domain reflectometry (FDR) [48], neutron probes, and automatic weather stations (AWS) for monitoring soil moisture status, climatic parameters, crop growth characteristics, and evapotranspiration. These observations are subsequently utilized for WUE estimation based on crop yield [49]and actual evapotranspiration relationships [50] and for evaluating temporal and depth-wise soil moisture variations [51].

The model-based domain includes simulation tools such as CROPWAT [52], DSSAT, APSIM, SWAP, HYDRUS, and other hydrological models, which integrate climatic variables, soil properties, irrigation scheduling, crop coefficients [53], and agroforestry configurations to

ISSN: 2456-1878 (Int. J. Environ. Agric. Biotech.)
https://dx.doi.org/10.22161/ijeab.113.8

estimate evapotranspiration, irrigation water requirement, root-zone soil moisture, crop yield, and water productivity indices.

Machine learning approaches incorporate environmental variables, soil characteristics, remote sensing indices [13], crop parameters, and management information to develop predictive models using algorithms including random forest (RF) [54][55], support vector machine (SVM) [56], artificial neural network (ANN), gradient boosting machine (GBM), extreme gradient boosting (XGBoost) [57], and deep learning architectures. These methods enable prediction of soil moisture content, water use efficiency estimation, evapotranspiration modeling, yield forecasting, and sensitivity assessment under varying agroforestry scenarios.

Remote sensing-based approaches employ multispectral, thermal, and microwave datasets derived from platforms such as Sentinel-2, Landsat, Sentinel-1, SMAP, and SMOS. Spectral indices including NDVI [58][13], EVI , SAVI, NDMI, MSI, and land surface temperature (LST), together with evapotranspiration models such as SEBAL, METRIC, and Priestley–Taylor formulations, facilitate spatial and temporal assessment of water use efficiency and soil moisture dynamics across wheat agroforestry landscapes.

The integration of these approaches provides a comprehensive evaluation framework for improving water management strategies, enhancing resource-use efficiency, supporting climate resilience, and promoting sustainable productivity in wheat-based agroforestry systems.

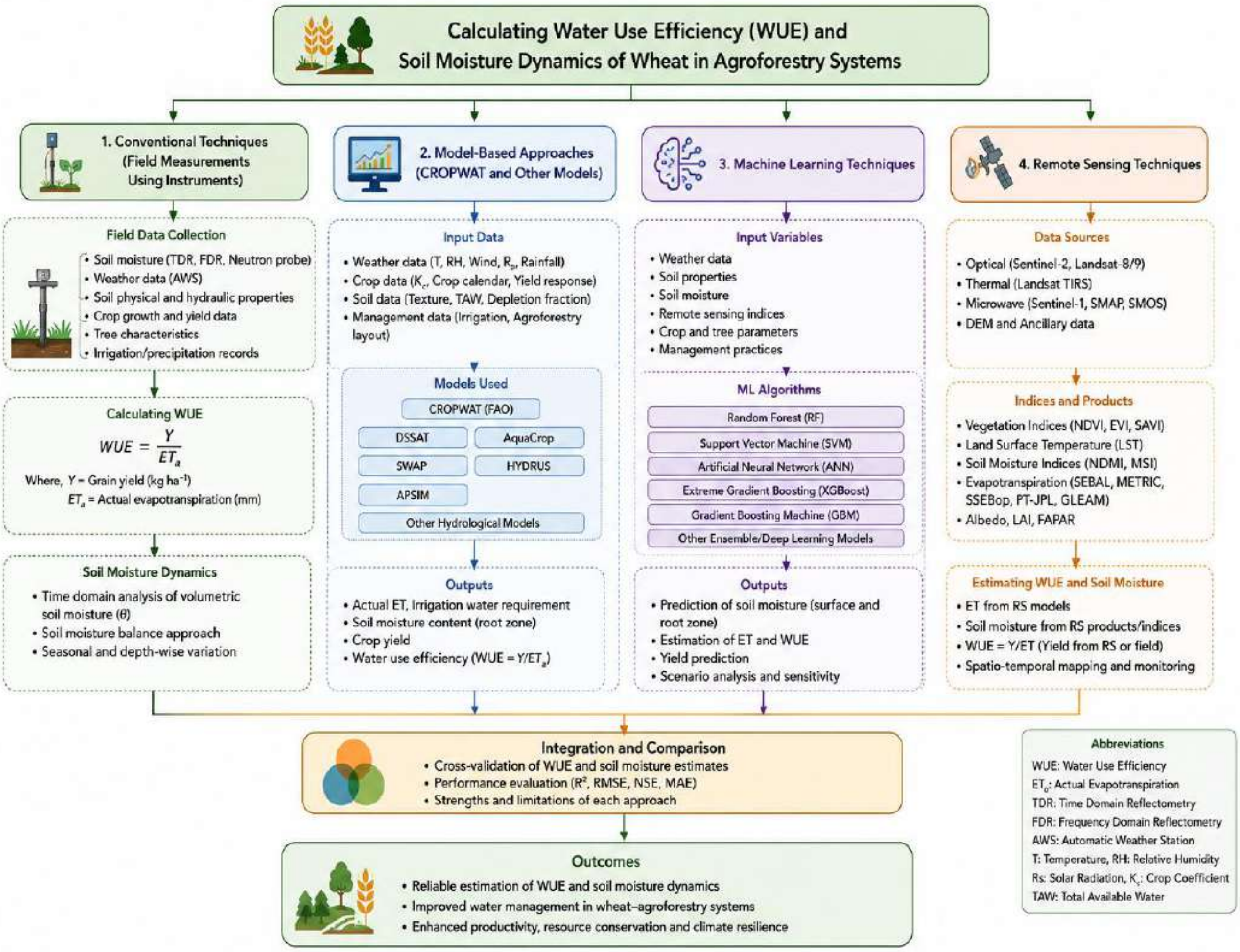

Fig. 7: Methodological framework for calculating water use efficiency (WUE) and soil moisture dynamics of wheat in agroforestry systems using (1) conventional field measurements with instruments, (2) model-based approach (CROPWAT and other models), (3) machine learning techniques, and (4) remote sensing techniques.

Table 2: Compilation of equations and indices used in water use efficiency, soil moisture monitoring, and evapotranspiration studies

Method Used	Formula Used	Representation	References
Water Use Efficiency Equations			
Agronomic water use efficiency	$WUE = \frac{Grain\ Yield}{Total\ Water\ Consumed}$	WUE = Water Use Efficiency	[59] [60] [50]
Irrigation water use efficiency (IWUE)	$IWUE = \frac{Y_i - Y_r}{I}$	Y_i = irrigated yield Y_r = rainfed yield I = irrigation depth	[59] [61]
Crop water productivity (CWP)	$CWP = \frac{Economic\ Yield\ or\ Biomass}{ET_a}$	ET_a = actual evapotranspiration	[62] [63]
Transpiration efficiency	$TE = \frac{B}{T}$	B = biomass T = transpiration	[64] [51]
Soil Moisture Dynamics Equations			
Gravimetric soil moisture	$SM_g = \frac{(W_w - W_d)}{W_d} * 100$	W_w = wet soil weight W_d = dry soil weight	[65] [66]
Volumetric soil moisture	$\theta_v = \theta_g * \rho_b$	θ_v = volumetric moisture θ_g = gravimetric moisture ρ_b = bulk density	[66] [47]
Soil water storage	$SWS = \theta_v * D$ $SWS = \sum(\theta_i * d_i)$	D = root zone depth	[67] [68]
Water balance	$P + I = ET + R + D + \Delta S$	P represents precipitation, I stands for irrigation, ET is evapotranspiration, R is runoff, D represents deep percolation, and ΔS is storage change	[69] [70]
Energy balance based soil moisture	$R_n = G + H + \lambda ET$	H = sensible heat $\lambda * ET$ = latent heat flux	[71]
Soil moisture depletion	$D_r = D_{r(i-1)} - (P - RO) - I - CR + ET + D_p$	D_r = root zone depletion RO = runoff CR = capillary rise D_p = percolation	[72]
Remote Sensing Soil Moisture Models			
Normalized difference water index (NDWI)	$NDWI = \frac{NIR - SWIR}{NIR + SWIR}$	NIR = Band 8 SWIR = Band 11 or 12	[73] [74]
Land surface water index (LSWI)	$LSWI = \frac{NIR - SWIR}{NIR + SWIR}$	NIR = Band 8	[58]

		SWIR = Band 11 or 12	[75] [76] [77]
Soil moisture index (SMI)	$SMI = \frac{LST_{max} - LST}{LST_{max} - LST_{min}}$	LST = land surface temperature $0 \leq SMI \leq 1$	[78] [79] [80]
Temperature vegetation dryness index (TVDI)	$TVDI = \frac{(T_s - T_{smin})}{(a + b(NDVI) - T_{smin})}$	T_s = surface temperature a, b = dry edge coefficients	[81] [82] [83]
Vegetation Indices Related to WUE and Soil Moisture			
Normalized difference vegetative index (NDVI)	$NDVI = \frac{(NIR - RED)}{(NIR + RED)}$	NIR = Band 8 RED = Band 4	[84] [85] [13]
Soil adjusted vegetation index (SAVI)	$SAVI = \frac{(NIR - RED)(1 + L)}{NIR + RED + L}$	NIR = Band 8 RED = Band 4	[86] [87] [88]
Enhanced vegetation index (EVI)	$EVI = G\left(\frac{NIR - RED}{NIR + C_1RED - C_2BLUE + L}\right)$	NIR = Band 8 RED = 4 BLUE = 2	[89]
Moisture stress index (MSI)	$MSI = \frac{SWIR}{NIR}$	NIR = Band 8 SWIR = Band 11 or 12	[90]
Normalized multi-band drought index (NMDI)	$NMDI = \left(\frac{NIR - (SWIR_1 - SWIR_2)}{NIR + (SWIR_1 - SWIR_2)}\right)$	NIR = Band 8 SWIR = Band 11 or 12	[91] [92]
Evapotranspiration Equations			
FAO Penman-Monteith	$ET_0 = \frac{0.408\Delta(R_n - G) + \gamma\left(\frac{900}{T + 273}\right)u_2(e_s - e_a)}{\Delta + \gamma(1 + 0.34u_2)}$ R_n = net radiation, G = soil heat flux, u_2 = wind speed, and $e_s - e_a$ = vapour pressure deficit $ET_c = K_c * ET_0$		[93] [94] [95] [96]
Hargreaves Equation	$ET_0 = 0.0023(T_{mean} + 17.8)(T_{max} - T_{min})^{0.5}R_a$ R_a = extraterrestrial radiation, T_{mean} = mean temperature, T_{min} = minimum temperature and T_{max} = maximum temperature		[97] [98]
Thornthwaite Equation	$ET = 16\left(\frac{10T}{I}\right)^a$ Heat Index: $I = \sum\left(\frac{T}{5}\right)^{1.514}$ $a = 6.75 * 10^{-7}I^3 - 7.71 * 10^{-5}I^2 + 1.79 * 10^{-2}I + 0.492$		[99] [100]

Blaney-Criddle Method	$ET_0 = p(0.46T + 8)$ p = daytime hour percentage and T = temperature **Crop ET:** $ET_c = K_c ET_0$ [101]	[102] [103] [104]
Priestley-Taylor Equations	$ET = \propto \frac{\Delta}{\Delta + \gamma} \frac{(R_n - G)}{\lambda}$ $\propto$ = priestley-taylor coefficient, λ = latent heat of vaporization, G = soil heat flux density and γ = psychrometric constant.	[105] [106] [107]

IV. CONCLUSION

This systematic review evaluated the existing literature on water use efficiency (WUE) and soil moisture dynamics in wheat-based agroforestry systems and highlighted their importance for sustainable water management under changing climatic conditions. The reviewed studies indicated that agroforestry practices considerably influence soil water availability, evapotranspiration, infiltration, root distribution, and crop water productivity through improved soil structure, litter deposition, microclimatic regulation, and reduced evaporative losses. These interactions contribute to enhanced soil moisture conservation and efficient utilization of available water resources in wheat production systems. The findings demonstrated that the performance of wheat under agroforestry conditions is largely controlled by tree species, spacing arrangements, root interactions, irrigation practices, climatic variability, and soil characteristics. Properly managed agroforestry systems can improve WUE by increasing infiltration, reducing runoff, optimizing soil water storage, and enhancing drought tolerance. However, unsuitable tree density and improper management may increase competition for water, light, and nutrients, resulting in reduced crop performance and lower water productivity.

The review further identified the major approaches used for assessment of WUE and soil moisture dynamics. Conventional field-based methods, including Time Domain Reflectometry (TDR), Frequency Domain Reflectometry (FDR), neutron probes, soil moisture sensors, lysimeters, and automatic weather stations, remain important tools for direct monitoring of soil water status and environmental conditions. In addition, process-based and simulation models such as CROPWAT, DSSAT, APSIM, SWAP, and HYDRUS have been extensively used for estimating evapotranspiration, crop water requirements, irrigation scheduling, and soil moisture distribution. Recent advancements in remote sensing and geospatial techniques have significantly improved large-scale monitoring of WUE and soil moisture variability using vegetation and moisture indices such as NDVI, EVI, SAVI, NDWI, LSWI, MSI, TVDI, and NMDI. Similarly, energy balance approaches and evapotranspiration models including Penman–Monteith, Priestley–Taylor, and SEBAL have enhanced water assessment capabilities across agroforestry landscapes. Machine learning techniques such as Random Forest, Support Vector Machine, Artificial Neural Networks, and deep learning approaches also showed increasing applicability for prediction and modeling purposes.

Publication trends revealed increasing research activity after 2000, with substantial growth during recent years, particularly from 2023 to 2025, indicating rising global interest in climate adaptation, water conservation, and sustainable agricultural systems. Overall, wheat-based agroforestry systems provide significant opportunities for improving WUE, conserving soil moisture, enhancing climate resilience, and supporting sustainable food production under increasing water scarcity conditions.

Funding Sources:

The author(s) received no financial support for the research, authorship, and/or publication of this article.

Conflict of Interest:

The authors do not have any conflict of interest.

Data Availability Statement:

This statement does not apply to this article.

Ethics Statement:

This research did not involve human participants, animal subjects, or any material that requires ethical approval.

Informed Consent Statement:

This study did not involve human participants, and therefore, informed consent was not required.

Permission to Reproduce Material from other Sources

Not Applicable.

Author Contributions:

Amandeep Singh: Conception, organization, writing of this review paper, and approval of final manuscript.

Atish: Writing of review paper, editing, critical review, and approval of final manuscript.

Vijay Singh: Critical review, editing, and approval of final manuscript.

Beena Kumari: Supervision, critical review, editing, and approval of final manuscript.

Sandeep Arya: Review, editing, and approval of final manuscript.

Ankush Kamboj: Review, editing, and approval of final manuscript.

REFERENCES

[1] T. Choden and B. B. Ghaley, "A Portfolio of Effective Water and Soil Conservation Practices for Arable Production Systems in Europe and North Africa," pp. 1–18, 2021.

[2] S. Saha and P. Mondal, "Policy zoning for climate-resilient agriculture : a spatial assessment of agricultural sensitivity and resilience to environmental change in West Bengal , India," 2025.

[3] H. Dur, M. Soriano, F. Garc, and G. Baltasar, "Conservation Agriculture as a Sustainable System for Soil Health : A Review," pp. 1–37, 2022.

[4] X. Liang, S. Ur, R. Wang, Z. Muhammad, A. Raza, and I. Haider, "Impacts of Conservation Tillage on Agricultural Land Development : A Review," pp. 428–449, 2025.

[5] R. N. German, C. E. Thompson, and T. G. Benton, "Relationships among multiple aspects of agriculture ' s environmental impact and productivity : a meta-analysis to guide sustainable agriculture," 2016, doi: 10.1111/brv.12251.

[6] M. L. Jat *et al.*, "Conservation agriculture for sustainable intensification in South Asia," *Nat. Sustain.*, vol. 3, no. April, 2020, doi: 10.1038/s41893-020-0500-2.

[7] A. Lausch *et al.*, "Monitoring Agricultural Land Use Intensity with Remote Sensing and Traits," pp. 1–84, 2025.

[8] A. Das, "Smart and sustainable water management : policy , technology , and innovation pathways for resource resilience," vol. 8, 2025.

[9] M. Habib, S. Singh, S. Jan, K. Jan, and K. Bashir, "The future of the future foods : understandings from the past towards," pp. 1–27, 2025.

[10] R. Lal, "Climate Strategic Soil Management," pp. 43–74, 2021, doi: 10.3390/challe5010043.

[11] A. Boutagayout, A. Hamdani, and A. Adiba, *Advancing Agroecology for Sustainable Water Management : A Comprehensive Review and Future Directions in North African Countries*. Springer Nature Singapore, 2025. doi: 10.1007/s41101-025-00350-7.

[12] P. S. Roy *et al.*, "Anthropogenic Land Use and Land Cover Changes — A Review on Its Environmental Consequences and Climate Change," *J. Indian Soc. Remote Sens.*, vol. 50, no. 8, pp. 1615–1640, 2022, doi: 10.1007/s12524-022-01569-w.

[13] T. V Ramachandra, P. Negi, L. U. Land, and L. C. Land, "Geoinformatics - based prioritisation of natural resources rich regions at disaggregated levels for sustainable management," *Discov. Sustain.*, 2025, doi: 10.1007/s43621-025-00964-w.

[14] A. Boutagayout, A. Hamdani, and M. Kouighat, "Agroecological soil management in North Africa : practices , challenges , and prospects for sustainable transition," vol. 2050, no. November, 2025, doi: 10.3389/fsufs.2025.1662153.

[15] Y. Ma, X. Yu, M. Li, J. Huang, and H. Li, "Comprehensive drought detection , spatiotemporal variations , and attribution across different agricultural climate zones in Eastern China using a copula-based drought index," vol. 321, no. April, 2025.

[16] A. M. Zubairu *et al.*, *Overview of biochar role in remediating soil salinity stress in crops*. 2025.

[17] M. Ahmed *et al.*, "Impact of Climate Change on Dryland Agricultural Systems : A Review of Current Status , Potentials , and Further Work Need," *Int. J. Plant Prod.*, vol. 16, no. 3, pp. 341–363, 2022, doi: 10.1007/s42106-022-00197-1.

[18] E. Aguilera *et al.*, "Agroecology for adaptation to climate change and resource depletion in the Mediterranean region . A review," *Agric. Syst.*, vol. 181, no. March, p. 102809, 2020, doi: 10.1016/j.agsy.2020.102809.

[19] R. K. Sharma, N. Nwosu, L. Singh, A. Kramer, and H. Singh, "Agricultural sustainability under unpredicted atmospheric changes — strategies to enhance crop resilience and system efficiency : a narrative review," 2025.

[20] A. Raihan, "A review of the global climate change impacts , adaptation strategies , and mitigation options in the socio-economic and environmental sectors," 2023.

[21] T. Deresse, T. Tolessa, S. Mamo, E. Bohnett, and G. Engdaw, "Spatiotemporal trends of climate change and variability : impacts on coffee production in Abaya and Gelana," *Environ. Monit. Assess.*, 2025, doi: 10.1007/s10661-025-14414-7.

[22] A. A. Farah, M. A. Mohamed, O. Sayid, H. Musse, and B. A. Nor, "The multifaceted impact of climate change on agricultural productivity : a systematic literature review of SCOPUS - indexed studies," *Discov. Sustain.*, 2025, doi: 10.1007/s43621-025-01229-2.

[23] J. S. Kikstra, Z. R. J. Nicholls, C. J. Smith, J. Lewis, and R. D. Lamboll, "The IPCC Sixth Assessment Report WGIII climate assessment of mitigation pathways : from emissions to global temperatures," pp. 9075–9109, 2022.

[24] U. Matthew and N. Carlo, "Evaluating the Effect of Adaptation Policies on Crop Yield , Economic Growth and Water Resources : A DPSIR-Based Analysis for the Niger River Basin Under Shared Socioeconomic Pathways-Representative Concentration Pathways (SSP-RCPS) (2014 – 2100)," pp. 383–405, 2026.

[25] K. L. Steenwerth *et al.*, "Climate-smart agriculture global research agenda : scientific basis for action," pp. 1–39, 2014.

[26] K. Pandian *et al.*, "Journal of Hazardous Materials Advances Synergistic conservation approaches for nurturing soil , food security and human health towards sustainable development goals," *J. Hazard. Mater. Adv.*, vol. 16, no. June, p. 100479, 2024, doi:

10.1016/j.hazadv.2024.100479.

[27] P. Dalal, V., Bhardwaj, K., Khajuria, S., Singh, M., & Singh, "Effect of agri-silvi-horticultural system on growth and yield of wheat," *Indian J. Agrofor.*, vol. 18, no. 1, 2020, [Online]. Available: https://epubs.icar.org.in/index.php/IJA/article/view/103219

[28] R. Verma, K. S., Zegeye, M. W., & Kaushal, "Growth and Yield Performance of Wheat in Agri-horti-silvicultural System of Agroforestry in the Mid- hills of Himachal Himalayas," *Indian J. Agrofor.*, vol. 4, no. 1, 2020, [Online]. Available: https://epubs.icar.org.in/index.php/IJA/article/view/102366

[29] A. Sharma, N. Singh, R. Pandey, and V. K. Sah, "Performance of wheat varieties under open agriculture and agroforestry systems : A comparative study of growth and yield characteristics," vol. 9, no. 4, pp. 1151–1157, 2025.

[30] C. Pankou, A. Lithourgidis, and C. Dordas, "Effect of Irrigation on Intercropping Systems of Wheat (Triticum aestivum L .) with Pea (Pisum sativum L .)," pp. 1–13, 2021.

[31] X. B. Zhou and Y. H. Chen, "Spacing between rows : effects on water-use efficiency of double-cropped wheat and soybean," pp. 90–101, 2015, doi: 10.1017/S0021859613000890.

[32] V. Pratap *et al.*, "Precision nitrogen and water management in double zero -till wheat : effects on photosynthetic parameters , productivity , nutrient-use ef fi ciency and N 2 O emission," no. November, 2025, doi: 10.3389/fpls.2025.1654933.

[33] H. Bahri, M. Annabi, H. Cheikh, M. Hamed, and A. Frija, "Science of the Total Environment Assessing the long-term impact of conservation agriculture on wheat-based systems in Tunisia using APSIM simulations under a climate change context," *Sci. Total Environ.*, vol. 692, pp. 1223–1233, 2019, doi: 10.1016/j.scitotenv.2019.07.307.

[34] H. Lee, S. Lautenbach, A. P. Garc, A. Bondeau, W. Cramer, and I. R. Geijzendorffer, "The impact of conservation farming practices on Mediterranean agro-ecosystem services provisioning — a meta-analysis," pp. 2187–2202, 2019.

[35] Camilli F. et al., "BENEFITS AND CONSTRAINTS ASSOCIATED TO AGROFORESTRY SYSTEMS : THE CASE STUDIES IMPLEMENTED IN ITALY WITHIN THE AGFORWARD," 2016, pp. 23–25.

[36] R. Beuschel, "Similar spatial patterns of soil quality indicators in three poplar-based silvo-arable alley cropping systems in Germany," pp. 1–14, 2019.

[37] L. Bedoussac, E. Journet, H. Hauggaard-nielsen, C. Naudin, G. Corre-hellou, and E. S. Jensen, "Ecological principles underlying the increase of productivity achieved by cereal-grain legume intercrops in organic farming . A review," pp. 911–935, 2015, doi: 10.1007/s13593-014-0277-7.

[38] M. D. Thorsted, J. E. Olesen, and J. Weiner, "Width of clover strips and wheat rows influence grain yield in winter wheat / white clover intercropping," vol. 95, pp. 280–290, 2006, doi: 10.1016/j.fcr.2005.04.001.

[39] R. Derpsch *et al.*, "Nature ' s laws of declining soil productivity and Conservation Agriculture," *Soil Secur.*, vol. 14, no. January, p. 100127, 2024, doi: 10.1016/j.soisec.2024.100127.

[40] C. M. Pittelkow *et al.*, "Field Crops Research When does no-till yield more ? A global meta-analysis," *F. Crop. Res.*, vol. 183, pp. 156–168, 2015, doi: 10.1016/j.fcr.2015.07.020.

[41] B. D. Soane, B. C. Ball, J. Arvidsson, G. Basch, F. Moreno, and J. Roger-estrade, "Soil & Tillage Research No-till in northern , western and south-western Europe : A review of problems and opportunities for crop production and the environment," *Soil Tillage Res.*, vol. 118, pp. 66–87, 2012, doi: 10.1016/j.still.2011.10.015.

[42] H. Steinmann and E. S. Dobers, "Spatio-temporal analysis of crop rotations and crop sequence patterns in Northern Germany : potential implications on plant health and crop protection," vol. 120, no. 2, pp. 85–94, 2013.

[43] et al. KHEMIR, Eya, "Impacts of previous crops on inoculum of Fusarium culmorum in soil, and development of foot and root rot of durum wheat in Tunisia.," *Phytopathol. Mediterr.*, vol. 59, no. 1, pp. 187–202, 2020.

[44] S. Deike, B. Pallutt, B. Melander, J. Strassemeyer, and O. Christen, "Long-term productivity and environmental effects of arable farming as affected by crop rotation , soil tillage intensity and strategy of pesticide use : A case-study of two long-term field experiments in Germany and Denmark," vol. 29, pp. 191–199, 2008, doi: 10.1016/j.eja.2008.06.001.

[45] S. Fahad *et al.*, "Agroforestry Systems for Soil Health Improvement and Maintenance," pp. 1–25, 2022.

[46] O. M. Harb, G. H. A. El-hay, M. A. Hager, and M. M. A. El-enin, "Studies on conservation agriculture in Egypt," vol. 60, pp. 105–112, 2015, doi: 10.1016/j.aoas.2015.04.004.

[47] D. . Robinson *et al.*, "Soil Moisture Measurement for Ecological," *Vadose Zo. J.*, vol. 7, no. 1, pp. 358–389, 2008, doi: 10.2136/vzj2007.0143.

[48] T. J. Dean, J. P. Bell, and A. J. B. Baty, "SOIL MOISTURE MEASUREMENT BY AN IMPROVED CAPACITANCE TECHNIQUE , PART I . SENSOR DESIGN AND PERFORMANCE," vol. 93, pp. 67–78, 1987.

[49] R. J. Patel *et al.*, *Enhancing Wheat (Triticum aestivum L .) Crop Yield and Water Use E ciency : A Study on Canopy Air Temperature Difference-Based Drip Irrigation Scheduling in a Semi-Arid Region of Western India*. 2023.

[50] A. Yadav, A. Singh, R. Naresh, and L. Kumar, "A Comparative Review of the Performance of Lined and Unlined Irrigation Canals," *Curr. Agric. Res. J.*, vol. 13, no. 2, 2025.

[51] A. Blum, P. O. Box, T. Aviv, and I. Email, "Drought resistance , water-use efficiency , and yield potential — are they compatible , dissonant , or mutually exclusive ?," pp. 1159–1168, 2005.

[52] R. Chandra, "Estimation of crop water requirement for rice-wheat and rice- maize cropping system using CROPWAT model for Pusa, Samastipur district, Bihar: Estimation of crop water requirement...," no. June 2021, 2022, doi: 10.21921/jas.v8i2.7299.

[53] D. Uwizeyimana, S. M. Mureithi, S. M. Mvuyekure, G. Karuku, and G. Kironchi, "International Soil and Water

Conservation Research Modelling surface runoff using the soil conservation service-curve number method in a drought prone agro-ecological zone in Rwanda," *Int. Soil Water Conserv. Res.*, vol. 7, no. 1, pp. 9–17, 2019, doi: 10.1016/j.iswcr.2018.12.001.

[54] K. Tatsumi, Y. Yamashiki, M. Angel, C. Torres, C. Leonidas, and R. Taipe, "Crop classification of upland fields using Random forest of time-series Landsat 7 ETM + data," *Comput. Electron. Agric.*, vol. 115, pp. 171–179, 2015, doi: 10.1016/j.compag.2015.05.001.

[55] D. Pandey, K. Niwaria, and B. Chourasia, "Machine Learning Algorithms : A Review," pp. 916–922, 2019.

[56] L. Saitta, "Support-Vector Networks," vol. 297, pp. 273–297, 1995.

[57] T. Chen and C. Guestrin, "XGBoost : A Scalable Tree Boosting System," pp. 785–794, 2016.

[58] J. I. Christian, J. B. Basara, L. E. L. Lowman, X. Xiao, D. Mesheske, and Y. Zhou, "Remote Sensing Applications : Society and Environment Flash drought identification from satellite-based land surface water index," *Remote Sens. Appl. Soc. Environ.*, vol. 26, p. 100770, 2022, doi: 10.1016/j.rsase.2022.100770.

[59] T. A. Howell, "Enhancing Water Use Efficiency in Irrigated Agriculture," pp. 281–289, 2001.

[60] A. Blum, "Field Crops Research Effective use of water (EUW) and not water-use efficiency (WUE) is the target of crop yield improvement under drought stress," vol. 112, pp. 119–123, 2009, doi: 10.1016/j.fcr.2009.03.009.

[61] L. S. Pereira, I. Cordery, and I. Iacovides, "Improved indicators of water use performance and productivity for sustainable water conservation and saving," *Agric. Water Manag.*, vol. 108, pp. 39–51, 2012, doi: 10.1016/j.agwat.2011.08.022.

[62] D. Steduto, P., Hsiao, T.C., Fereres, E., & Raes, *Crop yield response to water*. FAO Irrigation and Drainage Paper No. 66, 2012.

[63] D. Molden, T. Oweis, P. Steduto, P. Bindraban, M. A. Hanjra, and J. Kijne, "Improving agricultural water productivity : Between optimism and caution," vol. 97, pp. 528–535, 2010, doi: 10.1016/j.agwat.2009.03.023.

[64] T. R. Sinclair, C. B. Tanner, and J. M. Bennett, "Water-Use Efficiency in Crop Production," *Bioscience*, vol. 34, no. 1, pp. 36–40, 1984.

[65] W. H. Gardner, "Water Content," vol. 9, no. 9, 1986.

[66] D. Hillel, "Environmental Soil Physics Academic Press.," *San Diego, CA.*, 1998.

[67] S. R. R. W. S. M. D. W. Rassam and J. L. H. F. J. Cook, "Soil – water and solute movement under precision irrigation : knowledge gaps for managing sustainable root zones," pp. 91–100, 2007, doi: 10.1007/s00271-007-0075-y.

[68] A. Polak and R. Wallach, "Analysis of soil moisture variations in an irrigated orchard root zone," pp. 145–159, 2001.

[69] R. G. Allen *et al.*, "FAO-56 Dual Crop Coefficient Method for Estimating Evaporation from Soil and Application Extensions," no. February, pp. 2–13, 2005.

[70] R. G. Allen and Æ. L. S. Pereira, "Estimating crop coefficients from fraction of ground cover and height," pp. 17–34, 2009, doi: 10.1007/s00271-009-0182-z.

[71] R. G. Allen, L. S. Pereira, D. Raes, M. Smith, and FAO, *Crop evapotranspiration - Guidelines for computing crop water requirements - FAO Irrigation and drainage paper 56*. 1998.

[72] N. Mahmood and R. N. Ahmad, "Determination of Water Requirements and Response of Wheat to Irrigation at Different Soil Moisture Depletion Levels," *Int. J. Agric. Biol.*, vol. 7, no. 5, pp. 812–815, 2005.

[73] B. Gao, "NDWI A Normalized Difference Water Index for Remote Sensing of Vegetation Liquid Water From Space," vol. 266, no. April 1995, pp. 257–266, 1996.

[74] S. K. Mcfeeters, "Using the Normalized Difference Water Index (NDWI) within a Geographic Information System to Detect Swimming Pools for Mosquito Abatement: A Practical Approach," pp. 3544–3561, 2013, doi: 10.3390/rs5073544.

[75] K. Chandrasekar, M. V. R. S. Sai, and G. Behera, "ASSESSMENT OF EARLY SEASON AGRICULTURAL DROUGHT THROUGH LAND SURFACE WATER INDEX (LSWI) AND SOIL WATER BALANCE MODEL," vol. XXXVIII, no. November, pp. 50–55, 2011.

[76] K. Chandrasekar, M. V. R. S. Sai, and P. S. Roy, "Land Surface Water Index (LSWI) response to rainfall and NDVI using the MODIS Vegetation Index product," vol. 31, no. 15, pp. 3987–4005, 2010, doi: 10.1080/01431160802575653.

[77] W. Li *et al.*, "A Comparison of Land Surface Water Mapping Using the Normalized Difference Water Index from TM, ETM+ and ALI," pp. 5530–5549, 2013, doi: 10.3390/rs5115530.

[78] E. D. Hunt, K. G. Hubbard, D. A. Wilhite, T. J. Arkebauer, and A. L. Dutcher, "The development and evaluation of a soil moisture index," vol. 759, no. August 2008, pp. 747–759, 2009, doi: 10.1002/joc.

[79] Z. Liu *et al.*, "Soil Moisture Index Model for Retrieving Soil Moisture in Semiarid Regions of China," vol. 13, pp. 5929–5937, 2020.

[80] E. . Hunt, J. You, and K. . Hubbard, "Development of the Soil Moisture Index to Quantify Agricultural Drought and Its ' User Friendliness ' in Severity-Area-Duration Assessment," vol. 9, pp. 660–676, 2007, doi: 10.1175/2007JHM892.1.

[81] P. Rahimzadeh-bajgiran, K. Omasa, and Y. Shimizu, "ISPRS Journal of Photogrammetry and Remote Sensing Comparative evaluation of the Vegetation Dryness Index (VDI), the Temperature Vegetation Dryness Index (TVDI) and the improved TVDI (iTVDI) for water stress detection in semi-arid regions of Iran," *ISPRS J. Photogramm. Remote Sens.*, vol. 68, pp. 1–12, 2012, doi: 10.1016/j.isprsjprs.2011.10.009.

[82] Z. Bian *et al.*, "Remote Sensing of Environment An angular normalization method for temperature vegetation dryness index (TVDI) in monitoring agricultural drought," *Remote Sens. Environ.*, vol. 284, no. October 2022, p. 113330, 2023, doi: 10.1016/j.rse.2022.113330.

[83] L. Du *et al.*, "Comparison of Two Simulation Methods of the Temperature Vegetation Dryness Index (TVDI) for Drought Monitoring in Semi-Arid Regions of China," 2017, doi: 10.3390/rs9020177.

[84] A. K. Bhandari, A. Kumar, and G. K. Singh, "Feature Extraction using Normalized Difference Vegetation Index (NDVI): a Case Study of Jabalpur City," vol. 6, pp. 612–621, 2012, doi: 10.1016/j.protcy.2012.10.074.

[85] S. Huang, L. Tang, J. P. Hupy, Y. Wang, and G. Shao, "A commentary review on the use of normalized difference vegetation index (NDVI) in the era of popular remote sensing," *J. For. Res.*, vol. 32, no. 1, pp. 1–6, 2021, doi: 10.1007/s11676-020-01155-1.

[86] F. J. Garcı and J. Melia, "A generalized soil-adjusted vegetation index," vol. 82, pp. 303–310, 2002.

[87] J. Qi, A. Chehbouni, A. R. Huete, Y. H. Kerr, and S. Sorooshian, "A Modified Soil Adjusted Vegetation Index," vol. 126, pp. 119–126, 1994.

[88] A. R. Huete, "A Soil-Adjusted Vegetation Index (SAVI)," *Remote Sens. Environ.*, vol. 25, pp. 295–309, 1988.

[89] B. Matsushita, W. Yang, J. Chen, Y. Onda, and G. Qiu, "Sensitivity of the Enhanced Vegetation Index (EVI) and Normalized Difference Vegetation Index (NDVI) to Topographic Effects: A Case Study in High-Density Cypress Forest," pp. 2636–2651, 2007.

[90] J. E. Kanneh *et al.*, "Novel indices and multi-source data fusion for monitoring plant moisture stress in winter wheat fields," pp. 1–18, 2026.

[91] L. Wang, J. J. Qu, and X. Hao, "Forest fire detection using the normalized multi-band drought index (NMDI) with satellite measurements," vol. 148, pp. 1767–1776, 2008, doi: 10.1016/j.agrformet.2008.06.005.

[92] L. Wang and J. J. Qu, "NMDI : A normalized multi-band drought index for monitoring soil and vegetation moisture with satellite remote sensing," vol. 34, no. October, pp. 1–5, 2007, doi: 10.1029/2007GL031021.

[93] J. Cai, Y. Liu, T. Lei, and L. Santos, "Estimating reference evapotranspiration with the FAO Penman – Monteith equation using daily weather forecast messages," vol. 145, pp. 22–35, 2007, doi: 10.1016/j.agrformet.2007.04.012.

[94] P. C. Sentelhas, T. J. Gillespie, and E. A. Santos, "Evaluation of FAO Penman – Monteith and alternative methods for estimating reference evapotranspiration with missing data in Southern Ontario , Canada," *Agric. Water Manag.*, vol. 97, no. 5, pp. 635–644, 2010, doi: 10.1016/j.agwat.2009.12.001.

[95] R. Moratiel, R. Bravo, A. Saa, A. M. Tarquis, and J. Almorox, "Estimation of evapotranspiration by the Food and Agricultural Organization of the United Nations (FAO) Penman – Monteith temperature (PMT) and Hargreaves – Samani (HS) models under temporal and spatial criteria – a case study in Duero basin (Spain)," pp. 859–875, 2020.

[96] A. A. Altalib, M. T. Mahmood, and A. A. M. Ai-ogaidi, "Mapping reference evapotranspiration for Iraq using FAO Penman-Monteith method," vol. 23, no. 2, pp. 18–29, 2021.

[97] G. H. Hargreaves, F. Asce, and R. G. Allen, "History and Evaluation of Hargreaves Evapotranspiration Equation," no. February, pp. 53–63, 2003.

[98] S. Subburayan and T. State, "Modified Hargreaves Equation for Estimation of ET 0 in a Hot and Humid Location in Tamilnadu State , India," vol. 3, no. 1, pp. 592–600, 2011.

[99] H. I. Z. Al-sudani, "Derivation Mathematical Equations for Future Calculation of Potential Evapotranspiration in Iraq , a Review of Application of Thornthwaite Evapotranspiration," vol. 60, no. 5, pp. 1037–1048, 2019, doi: 10.24996/ijs.2019.60.5.13.

[100] S. Trajkovic, "Adjustment of Thornthwaite equation for estimating evapotranspiration in Vojvodina," pp. 1231–1240, 2019.

[101] K. H. Anantha *et al.*, "Groundwater for Sustainable Development Impact of natural resource management interventions on water resources and environmental services in different agroecological regions of India," *Groundw. Sustain. Dev.*, vol. 13, no. March, p. 100574, 2021, doi: 10.1016/j.gsd.2021.100574.

[102] T. W. Sammis, E. J. Gregory, and C. E. Kallsen, "Estimating Evapotranspiration with Water-Production Functions or the Blaney-Criddle Method," no. D, pp. 1656–1661, 1982.

[103] B. R. G. Allen, W. O. Pruitt, A. Absthact, and T. F. A. O. Blaney-criddle, "Rational use of the fao blaney-criddle formula," vol. 112, no. 2, pp. 139–155, 1986.

[104] H. R. Fooladmand and S. H. Ahmadi, "MONTHLY SPATIAL CALIBRATION OF BLANEY – CRIDDLE EQUATION FOR CALCULATING MONTHLY ET O IN SOUTH OF IRAN y," vol. 245, no. July 2008, pp. 234–245, 2009, doi: 10.1002/ird.

[105] F. Castellvi, C. O. Stockle, P. J. Perez, and M. Iba, "Comparison of methods for applying the Priestley – Taylor equation at a regional scale," vol. 1620, no. October 2000, pp. 1609–1620, 2001, doi: 10.1002/hyp.227.

[106] K. J. M. B. Itier, "Operational limits to the Priestley-Taylor formula," pp. 37–43, 1996.

[107] P. Lhomme, "A THEORETICAL BASIS FOR THE PRIESTLEY-TAYLOR COEFFICIENT," pp. 179–191, 1997.

International Journal of Environment, Agriculture and Biotechnology
Vol-11, Issue-3; May-Jun, 2026
Peer-Reviewed International Journal
Journal Home Page Available: https://ijeab.com/
Journal DOI: 10.22161/ijeab

Histochemical Observations of *Eleusine coracana* Stem Tissues Under Multiple Abiotic Stresses

Viswanadha Naik Jarapala[1], Anjana Priyadarshani Kanathala[1], Bhukya Sai Kumar[1], Srinivas Naik Kethavath[1]*

[1]Centre for Plant Molecular Biology, Osmania University, Hyderabad -500 007, India
*Corresponding author: srinivasnaik.cpmb@gmail.com

Received: 25 Apr 2026; Received in revised form: 22 May 2026; Accepted: 27 May 2026; Available online: 04 Jun 2026

Abstract— *This study investigates the histochemical changes of lignin deposition in the stems of seven finger millet genotypes under Drought, Salinity, Heat, Cold, and Heavy metal stress using the Phloroglucinol-HCl staining method. Well-grown plants were subjected to individual stresses at the pre-reproductive stage, and stem cross-sections were analyzed for lignin accumulation and structural differences under light microscope. This study revealed significant genotypic variation among genotypes and also in lignin deposition under stress conditions compared to respective controls. Among different stresses given, heat is showing maximum effect on vascular bundles and stem structural stability of plant. Based on lignin, stress tolerant and susceptible varieties were identified. Results suggested few genotypes which can be used as animal feed, fodder, are agronomically important and industrially applicable genotypes.*

Keywords*— *Abiotic stress, Finger millet (Eleusine coracana), Lignin, Vascular tissue.

I. INTRODUCTION

Finger millet (*Eleusine coracana (L.) Gaertn*), a C_4 crop cultivated in semi-arid tropics of Africa and South Asia. It plays a vital role in supporting livelihoods and nutritional security of millions (Kheya *et al.,* 2023). It offers an outstanding nutritional profile, rich in calcium, dietary fibre, and essential amino acids, making it especially valuable for daily dietary consumption (Gaikwad *et al.,* 2024). It also has capacity to tolerate various abiotic stresses such as drought, salinity, heavy metal toxicity, and temperature extremes but ongoing unpredictable rapid climate change affecting its cultivation (Binodh *et al.,* 2025)

Plants respond via different physiological and structural adaptations to these environmental constrains (Kanathala *et al.,* 2026). Among these, the immediate effect of stress includes dehydration (lack of water availability) and changes osmotic potential resulting in overall disturbances in cell homeostasis, leads to structural rearrangements in water transport system i.e. vascular tissue (Hussain *et al.,* 2019). Drought makes development of thicker xylem with reduced vessel diameter and increased vessel number in stems and roots (Yang *et al.,* 2021). In salinity and heavy metal stress, vascular bundles often thicken with increased parenchyma cells, phloem and xylem to facilitate ion compartmentalization (Yao *et al.,* 2023). Along with this cell wall lignification provides mechanical support against turgor pressure (Barros *et al.,* 2015).

Lignification also stands out as a key mechanism aiding tissue integrity, regulating water and ion movement, thereby protects cell from damage under stress (Barros et al 2015). Lignin is a complex phenolic polymer synthesized from p-hydroxyphenyl (H), guaiacyl (G), and syringyl (S) monolignols via the phenylpropanoid pathway (Vanholme el., 2019). Stress responsive alterations in lignin content and composition enhances cell wall rigidity, hydrophobicity, and mechanical strength to withstand stress providing partial tolerance. Lignification in xylem vessels, sclerenchyma, endodermis, and bundle sheath cells which directly influences water transport, ion exclusion, and mechanical stability (Choi *et al.,* 2023; Han *et al.,* 2022). There are several studies supporting the modification of lignin as a stress responsive adaptation such as, Drought increases lignification in xylem with higher proportions of

G and S units helping hydraulic safety (Liu *et al.,* 2021; Choi *et al.,* 2023); Salinity and Heavy metal stress promotes lignin accumulation that limits ion movement through the apoplast and safeguards vascular tissues (Han *et al.,* 2022); Heat accelerates lignin depositions to strengthen cell wall while, Cold modifies its composition and vascular patterning (Zhao *et al.,* 2019). Usually, tolerant genotypes across many species show greater lignin accumulation with higher expression of lignin biosynthetic genes. Biochemical and transcriptomic studies of Finger millet also suggests altered lignin content and involvement of lignin specific genes with abiotic stress (Puranik *et al.,* 2011; Satish *et al.,* 2016). Histochemical staining and microscopic studies of transverse stem sections for lignin depositions and structural changes in Finger millet under different abiotic stresses provides actual visible changes occurred (Satish *et al.,* 2016). This anatomical marker can also be used for partial screening of various cultivars to identify tolerant varieties.

In the present study, Seven Finger millet germplasms were subjected to various abiotic stresses. The staining of cross-sectional samples from second internodal region of stems was done using Phloroglucinol-HCl stain and visualised under light microscope. We aim to reveal structural changes and lignin patterns in cell walls occurred as a result of stress exposures aids understanding cell wall-mediated stress tolerance in millets. Hence, identifying these visible changes helps in selecting specific germplasms of interest to specific industrial usage and also further targeted modifications enhances their agronomical and economical value.

II. MATERIALS AND METHODS

Place of Work

The present study was conducted in the laboratory and net house facilities at the Center for Plant Molecular Biology (CPMB) and the Department of Genetics & Biotechnology, Osmania University, Hyderabad, India, in the year 2025.

Plant Material

The present study utilized seven finger millet germplasms cultivated in South India ie., Karnataka, Andhra Pradesh and Telangana. Four cultivars Uduru Mallige, CFMV1, GPU28, and GE4449 were procured from the Indian Council of Agricultural Research (ICAR)-Indian Institute of Millets Research (IIMR), Hyderabad. The remaining three cultivars-Gowthami, Vakula, and Godavari were obtained from local farmers of Vizianagaram District, Andhra Pradesh, India.

Pot Experiment

Plants were grown in 26 cm diameter pots filled with a potting mixture of soil: sand: vermicompost at a 3:2:1 ratio (v/v). The experiment was conducted in a completely randomized design (CRD) under controlled net and glass house conditions.

Abiotic Stress Treatments

Drought stress was imposed by Mannitol (250 mM), salinity by NaCl (250 mM) and Heavy metal by $CuSO_4$ (500 µM) solutions. Heat stress (40°C) and cold stress (4°C) were imposed by adjusting temperature in plant growth chambers. Well-watered plants were taken as controls. All plants were maintained under optimal glass house conditions. These treatments were applied to 45 days old plants at pre flowering stage for about 36 hours.

Histochemical Staining of Stem Internodes

Second Internode region of each stem sample of control and stress treated plants were collected. Thin transverse cross section was manual cut using number eight blade from the middle portion of internode region and sections were mounted on glass slides. Samples were stained immediately by 3% phloroglucinol (0.3g in 10ml Absolute Ethanol) followed by 37% fuming HCl solution in 2:1 ration for lignin visualization (Clifford, 1974). Examined under an Olympus light microscope with images captured using a mobile camera.

III. RESULTS

The changes observed under 10x magnification were captured and modifications in lignin content, stem structure were compared among the samples under stress conditions.

In Uduru Mallige

Control plants showed high lignin across vascular bundles including metaxylem, protoxylem, phloem and epidermal regions. Under Heavy metal stress, decrease in lignin was observed with depositions found only around xylem and lower number of vascular bundles are present. Under drought stress, lignin was decreased. Under Salinity stress, lignin content decreased with depositions only around protoxylem walls but protoxylems were more damaged. Under low temperatures, lignin was highly decreased and size of protoxylem increased a bit whereas under heat stress, lignin was decreased which is found only around protoxylem along with decrease in number of vascular bundles.

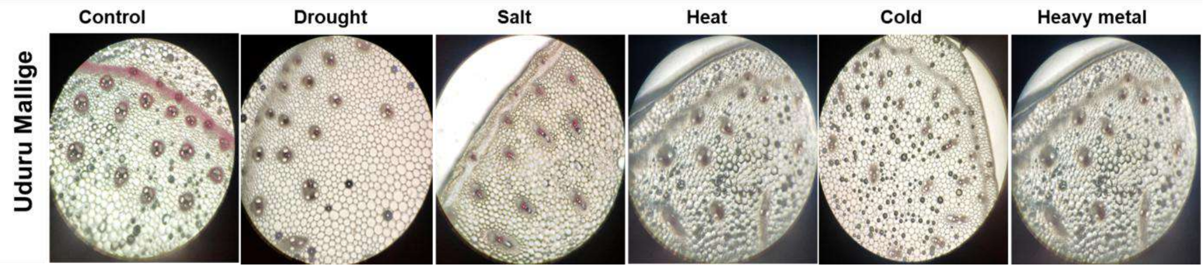

Fig.1: Microscopic images of Uduru Mallige stem cross sections under multiple stress conditions showing lignin content and vascular bundles pattern.

In GE4449

Control plants had very little lignin depositions in protoxylem walls. Under Heavy metal stress, overall lignin content was highly increased in Phloem, xylem and epidermal regions. Under drought stress also lignin content was highly increased in Phloem, xylem and epidermal regions. Under salinity stress, lignin around xylem tissue both metaxylem and protoxylem but damage was occurred to vessels of protoxylem. In low temperatures, presence of lignin in both metaxylem and protoxylem with increase in size of bundle sheath regions was observed. In high temperature stress, the stems were rigid with increase in lignin around phloem, xylem, and also increase in number of bundles.

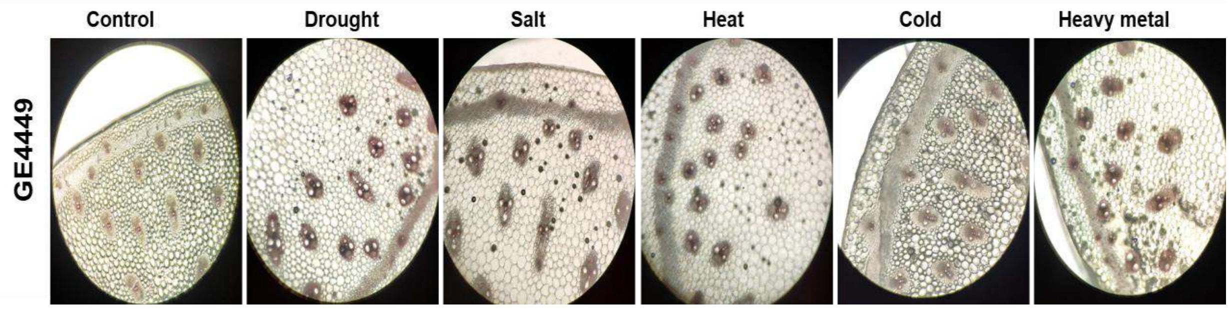

Fig.2: Transverse stem sections of GE4449 variety under multiple abiotic stresses showing different lignification patterns and anatomical differences.

In Gowthami

Control plants showed healthy vascular bundles with lignin in walls of protoxylem regions. Under heavy metal stress, the stems are similar to control ones. Under drought stress, the number of protoxylems were increased and surrounded by more lignin depositions. Under salinity stress, minor increase in lignin content with thickened xylem walls were observed. Under low temperatures, lignin was found only in protoxylem regions but number of protoxylems were increased up to five in number. Under heat, the vascular bundles were damaged but lignin can be observed around protoxylems.

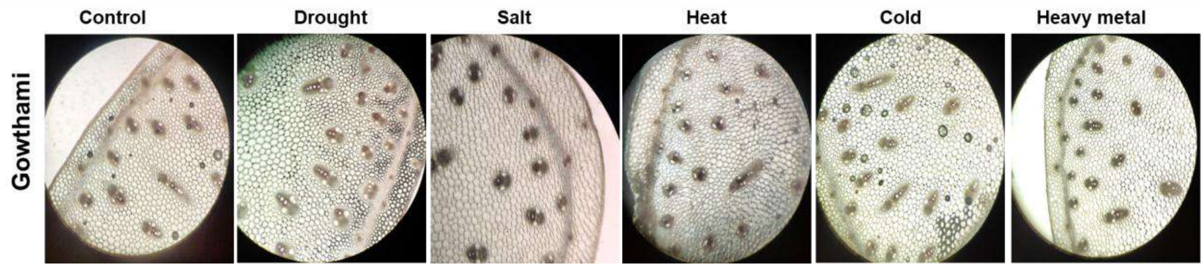

Fig.3: Microscopic images of Gowthami stem cross-sectional area under multiple stress conditions showing lignin content and vascular bundles pattern.

In Vakula

Control plants are well developed stem architecture and presence of lignin in only protoxylem walls. Under heavy metal stress, xylems vessels were increased along with lignin depositions. Under drought stress, amount of lignin was similar to controls but more thinning of vessels was observed. Under salinity stress, a very slight decrease in red pigment intensity thereby decrease in lignin; size of bundle sheath region was enlarged and xylem was reduced. Under low temperatures, no change in lignin level but vascular bundles size was narrowed. Interestingly, under heat the stem tissue got damaged except protoxylems which are increased in number and highly deposited by lignin in their walls.

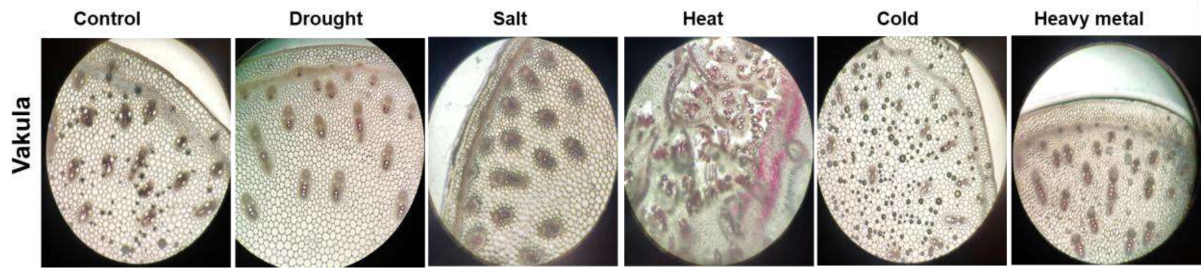

Fig.4: Transverse stem sections of Vakula variety under multiple abiotic stresses showing different lignification patterns and anatomical differences.

In GPU28

Control plants showed well developed vascular bundles with no lignin depositions. Under heavy metal stress, there is no change compared in lignin content was observed. Under drought conditions, a drastic increase of lignin deposition was observed around xylem vessels, Phloem and in epidermal cells of bundle sheaths region. Drought also caused a decrease in number of protoxylems compared to control. Under salinity stress, lignin depositions occurred walls of protoxylems and also thinning of vascular bundles was observed. In low temperatures, the lignin increased in phloem, xylem vessels and epidermal cells of bundle sheaths region similar to drought stress whereas high temperatures led to complete damage to stem regions.

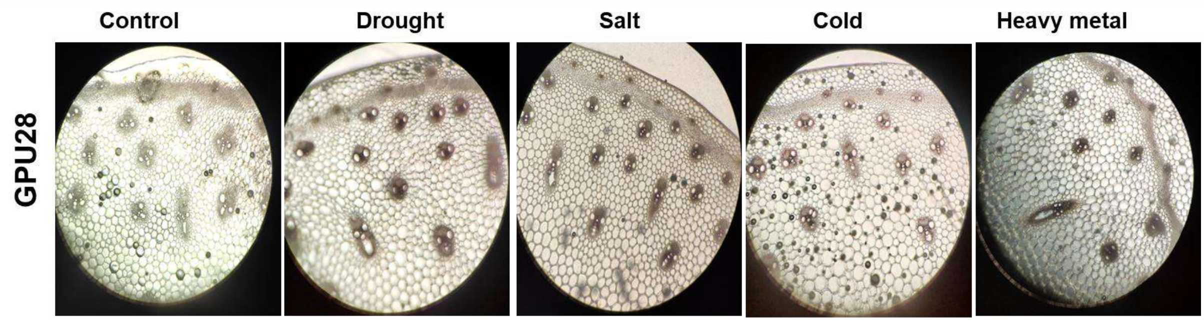

Fig.5: The microscopic image of transverse stem sections of GPU28 under drought, salt, heavy metal and cold along with controls, complete stem damaged under heat.

In Godavari

Control plant shows presence of lignin around xylem tissues. Under heavy metal stress, decrease in overall lignin content and found in only protoxylem regions. Under drought stress, heavy damage to vascular bundles were observed and lignin content was similar to heavy metal stress ones. Under salinity stress, lignin content was highly increased in Phloem, xylem and epidermal regions. In low temperatures, lignin is found only around protoxylems whereas in high temperatures, the stem is totally damaged.

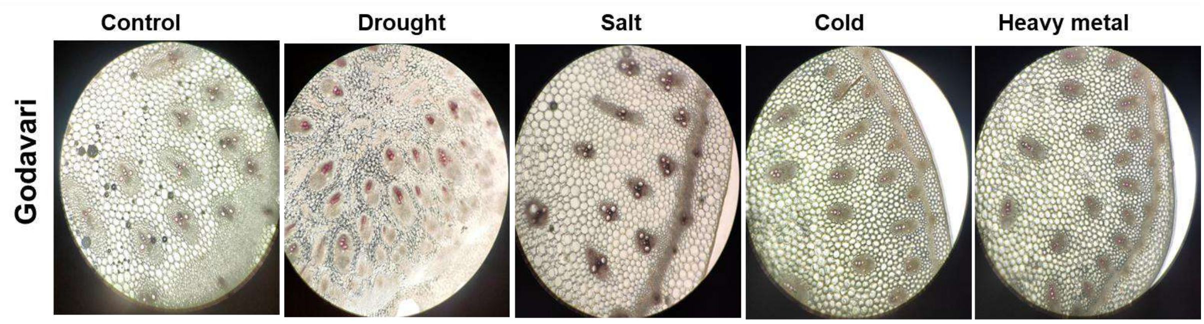

Fig.6: The microscopic image of transverse stem sections of Godavari under drought, salt, heavy metal and cold along with controls, complete stem damaged under heat.

In CFMV1

Control plant shows presence of lignin around xylem vessels. Under heavy metal stress, increased lignin content was found in Phloem and xylem regions. Under drought stress, widening in vessels was observed but overall bundle size was reduced and lignin content was present at only protoxylem regions. Under salinity stress, lignin content was highly increased in protoxylem region. In low temperatures, good amount of lignin deposition around xylem tissue, uneven distribution in epidermal tissues with increase in number of vessels whereas in high temperatures, the stem is totally damaged which cannot be sectioned at all.

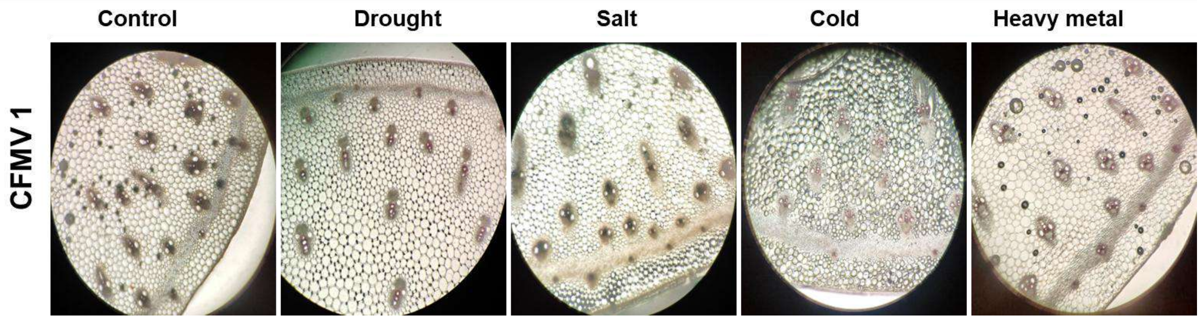

Fig.7: The microscopic image of transverse stem sections of CFMV1 under drought, salt, heavy metal and cold along with controls, complete stem damaged under heat.

IV. DISCUSSION

Lignin is mostly deposited in the walls of xylem and phloem tissue of vascular bundle in plants, which aids in providing mechanical support and structural stability (Nakamura *et al.,* 2020). The main role of vascular bundles is aiding water transport and providing mechanical support to plants. Lignin accumulates more around these vascular bundles as a positive stress adaptation mechanism making plant withstand under unfavourable conditions (Han *et al.,* 2022). On the other hand, higher accumulation of lignin poses a significant challenge for domestic feed and manufacturing industries related to pulp, paper and lignocellulosic biofuel ones (Bachir *et al.,* 2022). Thus, observing lignin qualitatively by Histochemical staining method provides information regarding the intensity and deposition patterns of lignin in vascular tissues and also the stress related alterations in vascular bundles compared to controls.

In present study, Lignin present in cross section of stem internode region was assessed qualitatively by phloroglucinol staining method. Seven Finger millet cultivars were taken to compare lignin accumulation under various abiotic stresses. The genotype Uduru mallige showed naturally more lignin content without any stress treatment given which makes it useful under lodging conditions. Upon imposition of stress, it showed reduction in lignin content and damage to vascular bundles suggests that it is susceptible variety which failed to induce lignin biosynthesis under stress and unable to maintain xylem against osmotic damage. In cold conditions, the enlargement of vessels suggests elasticity to maintain water transport (Ren *et al.,* 2025). Under heavy metal stress plants usually thicken the walls of xylem with lignin to avoid the transport of heavy metals via apoplast (ShangGuan *et al.,* 2023). CFMV1 had lignin surrounding the xylem in controlled conditions showing secondary wall development for providing mechanical support. Under all stress treatments lignin has highly increased conferring to stress tolerance mechanism (Moura *et al.,* 2010). Compared to other stresses, drought has greatly affected forming more widen vessels, helps higher uptake of water by plant (Agustí *et al.,* 2026;2020). Protoxylems are small, less efficient compared to metaxylems but plants maintain minimum water supply by increasing the number of protoxylems as a stress adaptation approach (Augstein *et al.,* 2022). Hence, CFMV1 shows tolerant behaviour under cold, drought, salt and heavy metal stresses. In GPU28 and Gowthami varieties there is no change in lignin, vascular bundles arrangement due to heavy metal treatment recommends that they have adopted a different detoxification mechanism other than lignin. GPU28 showed no lignin in control stems. Under drought, salinity and cold stress conditions, there is a huge lignification observed implicating stress responsive but contrastingly thinning of vessels occurred to withstand stress as a primary priority than water transport efficiency (Barros *et al.,* 2015). High temperatures have completely damaged the stems of GPU28, CFMV1 and Godavari as they couldn't maintain cellular homeostasis and heavy dehydration. GE4449 is the only cultivar showed increased lignification under heat stress with a compact structure of vascular bundles therefore having a lignin induced thermal tolerance property and stronger capacity to maintain structural stability (Han *et al.,* 2024). In Vakula, the structural rearrangements of vascular bundles have dominated the lignin depositional changes comparatively. Change in xylem number, thinning of vessels and presence of more protoxylems were observed under stress conditions to survive multiple stresses by using minimum metabolism energy rather than uniformly increasing lignin (Qaderi *et al.,* 2019).

Based on anatomical studies of seven cultivars studied here, GE4449, CFMV1 showed good tolerance mechanisms under multiple abiotic stresses. These are nutrient rich crops along with tolerance suggesting best suitable for agronomic purposes and for further studies. Uduru mallige variety had naturally more lignin content making it hard to use as animal feed due to its low digestibility and also not suitable for paper, pulp and Ligno-cellulosic biofuel industries contrastingly GPU28 had no lignin suggesting for biomass usage for these industries by decreasing the upstream cost of lignin degradation process (Yoo *et al.,* 2020). Uduru mallige as a Lignin-rich variety can be economically utilized for thermal bioenergy and bioplastic production (Laurichesse *et al.,* 2014). Additionally, helps reduce biowaste accumulation, as generally less preferred for animal feed. Further, quantification of monolignols and changes in composition of monolignols can be studied to make effective use of finger millet biomass industrially.

V. CONCLUSION

Current study links variations in lignin content along with structural rearrangements to multiple abiotic stress adaptations in seven finger millet germplasms. Finger millet consumption has increased recently as malnutrition awareness among population increased. Finger millet is nutritionally rich crop and its increase in recent cultivation, studying lignin helps in better usage of biomass industrially and economically. Additionally, it also helps partial identification of abiotic stress tolerant germplasms. Thus, our study provides fundamental insights into lignin-mediated stress adaptation mechanisms, thereby paves the way for targeted strategic modification of genes which are lignin related in stress tolerant crops with high agronomic value enhances industrial applications.

FUNDING

No additional funding is provided for this work.

ACKNOWLEDGMENTS

Viswanadha Naik Jarapala is thankful for UGC (NET-JRF) for providing fellowship to pursue his PhD.

REFERENCES

[1] Agustí, J., & Blanco-Touriñán, N. (2026). Environmental regulation of plant vascular networks. *Trends in plant science*, *31*(4), 442–455.

[2] Agustí, J., & Blázquez, M. A. (2020). Plant vascular development: mechanisms and environmental regulation. Cellular and molecular life sciences: CMLS, 77(19), 3711–3728.

[3] Augstein, F., & Carlsbecker, A. (2022). Salinity induces discontinuous protoxylem via a DELLA-dependent mechanism promoting salt tolerance in Arabidopsis seedlings. *The New phytologist*, *236*(1), 195–209.

[4] Bachir, I. H., Ployet, R., Teulières, C., Cassan-Wang, H., Mounet, F., & Grima-Pettenati, J. (2022). Regulation of secondary cell wall lignification by abiotic and biotic constraints. Advances in Botanical Research, 104, 363-392

[5] Barros, J., Serk, H., Granlund, I., & Pesquet, E. (2015). The cell biology of lignification in higher plants. *Annals of botany*, *115*(7), 1053-1074.

[6] Binodh, A., Rajasekaran, R., Senthil, A., Boopathi, N. M., & Francia, E. (2025). Exploring morpho-physiological, biochemical, and molecular strategies of finger millet (Eleusine coracana) for drought stress tolerance: a review. *Crop & Pasture Science*, *76*(4).

[7] Choi, S. J., Lee, Z., Kim, S., Jeong, E., & Shim, J. S. (2023). Modulation of lignin biosynthesis for drought tolerance in plants. *Frontiers in Plant Science*, *14*, 1116426.

[8] Clifford, M. N. (1974). Specificity of acidic phloroglucinol reagents. Journal of Chromatography A, 94, 321-324.

[9] Gaikwad, V., Kaur, J., Rasane, P., Kaur, S., Singh, J., Kumar, A., ... & Patel, A. S. (2024). Nutritional significance of finger millet and its potential for using in functional products. *Foods and Raw materials*, *12*(1), 110-123.

[10] Han, J., Wang, Z., Wu, X., Xia, J., Wang, L., Wang, Z., & Zhang, Y. (2024). Deciphering High-Temperature-Induced Lignin Biosynthesis in Wheat through Comprehensive Transcriptome Analysis. *Plants (Basel, Switzerland)*, *13*(13), 1832.

[11] Han, X., Zhao, Y., Chen, Y., Xu, J., Jiang, C., Wang, X., ... & Zhang, J. (2022). Lignin biosynthesis and accumulation in response to abiotic stresses in woody plants. *Forestry Research*, *2*, 9.

[12] Hussain, S., Hussain, S., Qadir, T., Khaliq, A., Ashraf, U., Parveen, A., ... & Rafiq, M. (2019). Drought stress in plants: An overview on implications, tolerance mechanisms and agronomic mitigation strategies. *Plant Sci. Today*, *6*(4), 389-402.

[13] Kanathala, A. P. ., Jarapala, V. N. ., Bollempally, P. ., Konda, A. K. ., Singam, P. ., & Kethavath, S. N. . (2026). Genome-wide Study and Expression Profiles of a Promising Negative Regulator of Abiotic Stress Gene Family *OsDHSRP* in *Oryza sativa*. *Current Trends in Biotechnology and Pharmacy*, *20*(2), 2892–2912.

[14] Kheya, S. A., Talukder, S. K., Datta, P., Yeasmin, S., Rashid, M. H., Hasan, A. K., ... & Islam, A. M. (2023). Millets: The future crops for the tropics-Status, challenges and future prospects. *Heliyon*, *9*(11).

[15] Laurichesse, S., & Avérous, L. (2014). Chemical modification of lignins: Towards biobased polymers. *Progress in polymer science*, *39*(7), 1266-1290.

[16] Liu, K., Du, H., Zheng, T., Liu, W., Zhang, M., Liu, H., ... & Si, C. (2021). Lignin-containing cellulose nanomaterials: preparation and applications. *Green Chemistry*, *23*(24), 9723-9746.

[17] Moura, J.C.M.S., Bonine, C.A.V., De Oliveira Fernandes Viana, J., Dornelas, M.C. and Mazzafera, P. (2010), Abiotic and Biotic Stresses and Changes in the Lignin Content and Composition in Plants. Journal of Integrative Plant Biology, 52: 360-376.

[18] Nakamura, M., Kamehama, T., & Sato, Y. (2020). Image analysis of stress-induced lignin deposition in Arabidopsis thaliana using the macro program Lignin J for ImageJ software. Plant biotechnology (Tokyo, Japan), 37(1), 105–109.

[19] Puranik, S., Jha, S., Srivastava, P. S., Sreenivasulu, N., & Prasad, M. (2011). Comparative transcriptome analysis of contrasting foxtail millet cultivars in response to short-term salinity stress. *Journal of Plant Physiology*, *168*(3), 280-287.

[20] Qaderi, M. M., Martel, A. B., & Dixon, S. L. (2019). Environmental factors influence plant vascular system and water regulation. *Plants*, *8*(3), 65.

[21] Ren, P., Fang, J., Song, H., Silvestro, R., Li, X., Li, Z., ... & Rossi, S. (2025). Cell enlargement drives xylem hydraulic efficiency and safety in Pinus tabulaeformis on the Loess Plateau. *Agricultural and Forest Meteorology*, *372*, 110724.

[22] Satish, L., Rathinapriya, P., Rency, A. S., Ceasar, S. A., Prathibha, M., Pandian, S., ... & Ramesh, M. (2016). Effect of salinity stress on finger millet (Eleusine coracana (L.) Gaertn): histochemical and morphological analysis of coleoptile and coleorhizae. *Flora-Morphology, Distribution, Functional Ecology of Plants*, *222*, 111-120.

[23] ShangGuan, X., Qi, Y., Wang, A., Ren, Y., Wang, Y., Xiao, T., ... & Xia, Y. (2023). OsGLP participates in the regulation of lignin synthesis and deposition in rice against copper and cadmium toxicity. *Frontiers in Plant Science*, *13*, 1078113.

[24] Vanholme, R., De Meester, B., Ralph, J., & Boerjan, W. (2019). Lignin biosynthesis and its integration into metabolism. *Current opinion in biotechnology*, *56*, 230-239.

[25] Yang, X., Lu, M., Wang, Y., Wang, Y., Liu, Z., & Chen, S. (2021). Response mechanism of plants to drought stress. *Horticulturae*, *7*(3), 50.

[26] Yao X-C, Meng L-F, Zhao W-L and Mao G-L (2023) Changes in the morphology traits, anatomical structure of the leaves and transcriptome in Lycium barbarum L. under salt stress. Front. Plant Sci. 14:1090366. doi: 10.3389/fpls.2023.1090366

[27] Yoo, C. G., Meng, X., Pu, Y., & Ragauskas, A. J. (2020). The critical role of lignin in lignocellulosic biomass conversion and recent pretreatment strategies: A comprehensive review. *Bioresource technology*, *301*, 122784.

International Journal of Environment, Agriculture and Biotechnology
Vol-11, Issue-3; May-Jun, 2026
Peer-Reviewed International Journal
Journal Home Page Available: https://ijeab.com/
Journal DOI: 10.22161/ijeab

Effect of Heat Stress on Morphological, Physiological and Yield-Related Traits in Forty Maize (Zea mays L.) Inbred Lines Under Natural Late-Sown Conditions

Kiran[1]*, M.C. Kamboj[2], Somveer Nimbal[3], Preeti Sharma[1], Kuldeep Jangid[4], Rajvinder Singh[5], Vijeta Gupta[1] and Satish Manda[6]

[1]Assistant Scientist, CCS HAU, Regional Research Station, Uchani, Karnal, Haryana, India
[2]Senior Scientist, CCS HAU, Regional Research Station, Uchani, Karnal, Haryana, India
[3]Senior Scientist, CCS Haryana Agricultural University, Hisar, Haryana, India
[4]STA, CCS HAU, Regional Research Station, Uchani, Karnal, Haryana, India
[5]Seed certification officer, Sirsa, Haryana, India
[6]Assistant Scientist, MHU, Karnal, Haryana, India
*mehrakiranhau.19@hau.ac.in

Received: 27 Apr 2026; Received in revised form: 25 May 2026; Accepted: 31 May 2026; Available online: 08 Jun 2026

***Abstract*— *Heat stress during reproductive stages is a major constraint to maize productivity, particularly under late-sown spring regimes. In present investigation, forty maize inbred lines were evaluated for morphological, physiological and yield-related responses under normal (7 February) and late (12 March) sowing at two locations (CCS HAU RRS, Uchani, Karnal and KVK, Damla, Yamunanagar) across Spring 2021 and 2022. A randomized complete block design with two replications generated eight environments. Traits recorded included days to 50% anthesis and silking, anthesis–silking interval (ASI), leaf senescence score (1–9), tassel blast (%), leaf firing (%), silk receptivity (%), kernels per row, hundred grain weight, shelling percentage, canopy temperature and plot grain yield. Pooled ANOVA indicated highly significant effects of genotype (G), environment (E) and G×E for all traits. Late sowing accelerated phenology, increased ASI and heat-injury symptoms (senescence, tassel blast, leaf firing), reduced silk receptivity and caused severe yield reductions (0.049–0.288 kg plot^{-1} under late sowing vs. 0.584–0.862 kg plot^{-1} under normal sowing). Genotypes HKI 1011, HKI MBR139, HKI 1344 and HKI 1664 maintained lower ASI, reduced senescence, higher silk receptivity and relatively stable yields under stress, qualifying them as potential donors for heat-tolerance breeding.*

***Keywords*— maize, heat stress, late sowing, anthesis–silking interval, grain yield, inbred lines, canopy temperature, G×E**

I. INTRODUCTION

Maize (Zea mays L.) is a globally important cereal noted for high yield potential and diverse uses. Its reproductive development is particularly sensitive to high temperatures, with documented reductions in pollen viability, silk receptivity and grain filling when daytime temperatures exceed 32–35°C. Several studies estimate that small increases in mean temperature can cause significant yield penalties in maize through combined effects on phenology and reproductive success (e.g., Lobell et al., 2011; Zaidi et al., 2019). In northern India, spring maize often faces terminal heat stress when sowing is delayed, exposing flowering and grain filling to high April–May temperatures and heat waves. Heat stress symptoms in maize include leaf firing, premature senescence, tassel blast, increased anthesis–silking interval (ASI) and reduced kernel set and grain weight.

Breeding for heat tolerance requires identification of stable genetic sources exhibiting reproductive resilience (short ASI, sustained silk receptivity), maintained assimilate supply (delayed senescence), and lower canopy temperatures. Prior studies have used field-imposed late-sowing regimes and controlled-environment assays to screen for tolerance, but multi-environment evaluation under natural stress is essential to capture realistic G×E interactions. This study aimed to (i) quantify the effect of late-sown heat stress on morphological, physiological and yield-related traits across forty inbred lines, (ii) identify tolerant genotypes with stable performance under stress, and (iii) discuss physiological bases for tolerance and implications for maize breeding under warming climates.

II. MATERIALS AND METHODS

Germplasm and experimental sites

Forty maize inbred lines maintained at CCS Haryana Agricultural University Regional Research Station, Uchani, Karnal were evaluated. Details of each inbred (pedigree, origin) are provided in Table 1.

Table 1 List of forty maize inbred lines

Detail of maize inbred lines					
Sr. No.	**Name of inbred line**	**Source**	**Sr. No.**	**Name of inbred line**	**Source**
1.	HKI 139	CML 139	21.	HKI 1344	Subtropical heterotic group B
2.	HKI 1025	BC 176	22.	HKI 1654-15	HKI 163×HKI 1128
3.	HKI 1041-2	BC 318	23.	HKI 1040-4	BC 318
4.	HKI 1011	BC 175	24.	HKI 327 T	CML 327
5.	HKI 1040-7	BC 318	25.	LM 16	(JS 2×J 3022)×(Tarun×Makka Safed)-yellow
6.	HKI 1654	HKI 163×LM 13	26.	HKI 163	CML 163
7.	HKI 295	Karnal 4	27.	HKI 1354-2	Sub tropical heterotic group A
8.	HKI 1041	BC 318	28.	HKI 1354-7	HKI 1352-2
9.	HKI 488 T	Cargil 501	29.	HKI 1378	HKI 1344 X1354-2
10.	HKI 1558-4	Hybrid selected from farmers' field	30.	LM 17	Partap 69
11.	HKI 1657	HKI 161×LM13	31.	HKI 161	CML 161
12.	HKI 1128	Hybrid selected from farmers' field	32.	Bio inbred 47	HKI 194-7×HKI 193-2
13.	HKI 488	Cargil 501	33.	HKI 164-7-2	CML 164
14.	DQL 2300	1278-4-2-1-1-1	34.	HKI 164-7-4	CML 164
15.	HKI 1126	Hybrid selected from farmers' field	35.	HKI 164-7-6	CML 164
16.	HKI 766 WG	HM1	36.	HKI 193-2	CML 193
17.	HKI 323	Pool 28, sub-tropocal	37.	HKI 1664	HKI1128×LM 13
18.	HKI 1105	Cargil 633	38.	HKI 193-1	CML 193
19.	HKI MBR139	Pozarica 86	39.	HKI L287	CML 287
20.	HKI 2067 Y	HKI 193-2×HKI 163	40.	HKI 288-2	CML 288

Field experiments and sowing regimes

Field trials were conducted at two locations (Uchani, Karnal and KVK Damla, Yamunanagar) in Spring 2021 and 2022, generating four location–year combinations. Two sowing dates were used: normal (7 February) and late (12 March), creating eight environments. Each environment was a randomized complete block design with two replications with plot size 3.6 m². Standard agronomic practices and plant protection measures were followed uniformly across sites and seasons. Irrigation was applied to avoid confounding drought stress; hence observed effects are attributable primarily to thermal regimes.

Environmental monitoring

Daily maximum, minimum and mean temperatures and relative humidity were recorded at each site. Canopy temperature was measured at midday during the peak reproductive stage using an infrared thermometer from non-senescing leaves, averaged across five representative plants per plot. Typical high temperatures during April–May ranged 34–40°C (Figure a,b,c and d).

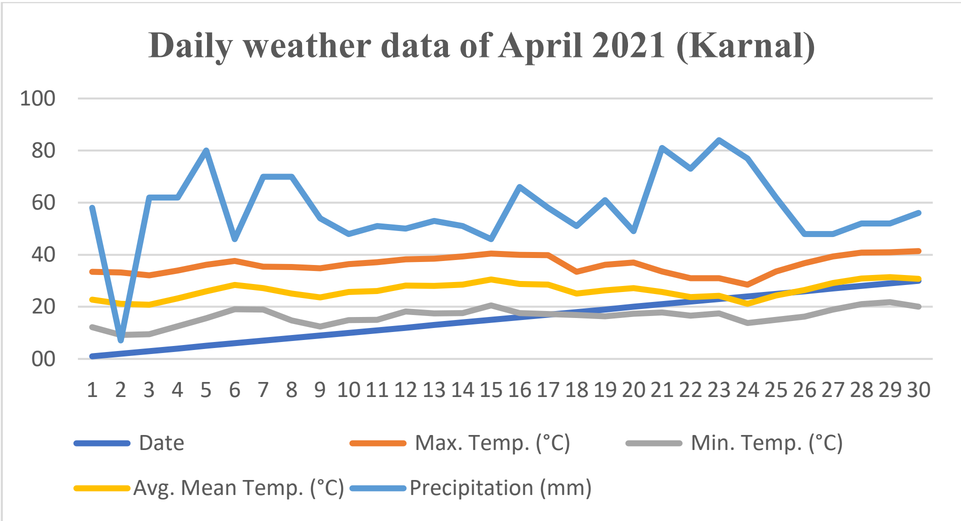

Figure (a) Daily temperature (mean, maximum and minimum) and precipitation during crop season of Spring 2021

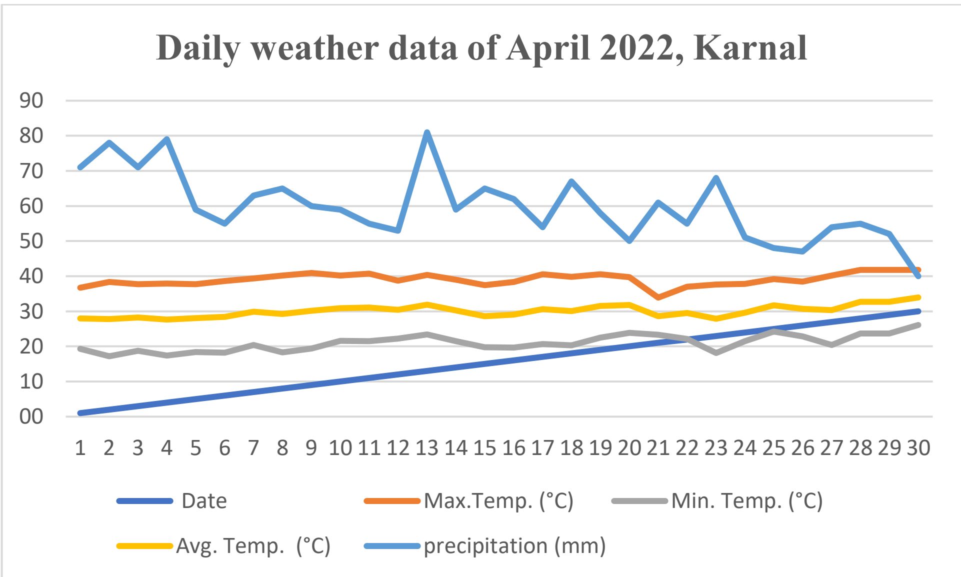

Figure (b) Daily temperature (mean, maximum and minimum) and precipitation during crop season of Spring 2022

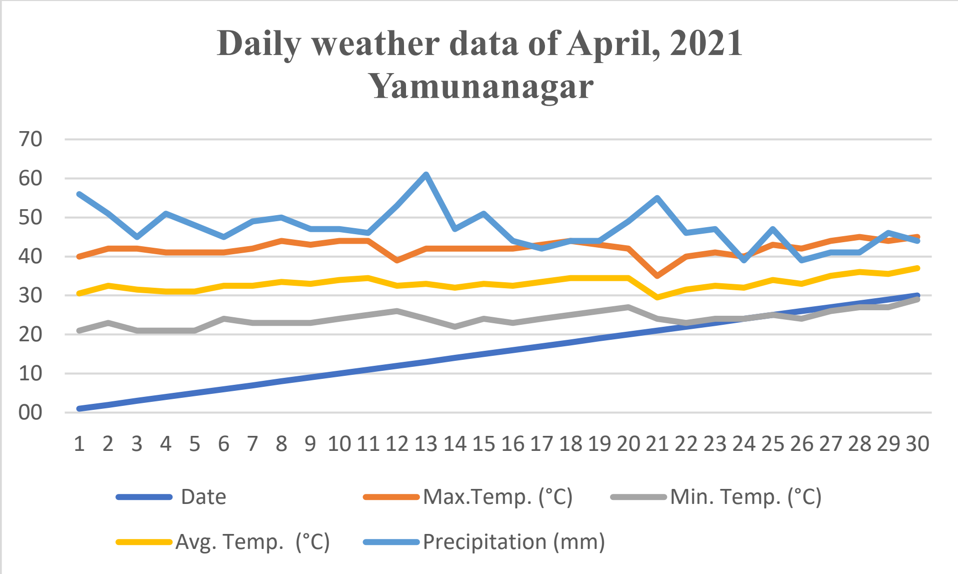

Figure (c) Daily temperature (mean, maximum and minimum) and precipitation during crop season of Spring 2021

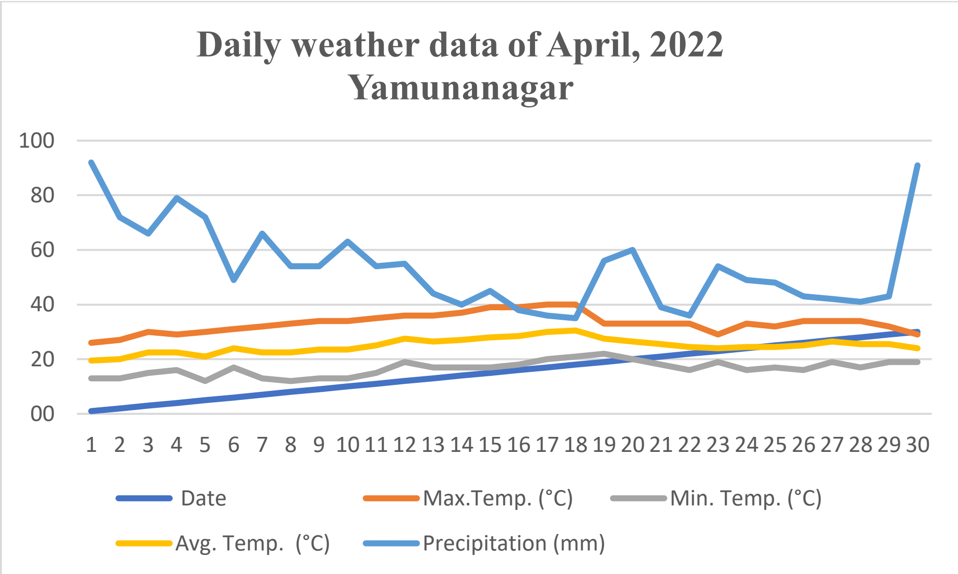

Figure (d) Daily temperature (mean, maximum and minimum) and precipitation during crop season of Spring 2022

Trait measurement

Observations were recorded on five competitive plants per plot for anthesis and silking dates to compute days to 50% anthesis/silking and ASI. Silk receptivity (%) was measured within 2–3 days of silking by scoring successful kernel set following controlled pollination. Leaf senescence was scored on a 1–9 visual scale (1 = healthy, 9 = fully senesced). Tassel blast and leaf firing were scored as percent incidence per plot. Kernels per row were counted from five cobs per plot; hundred kernel weight and shelling percentage were measured from plot-harvest samples; grain yield per plot was recorded at physiological maturity and adjusted to kg plot^{-1}.

Statistical analysis

Combined (pooled) analysis of variance across environments was performed. Genotype means across environments and under each sowing regime were estimated using least-square means and compared. Stability and adaptability under stress were assessed via G×E interaction patterns and traits associated with tolerance (ASI, silk receptivity, canopy temperature).

III. RESULTS

Late sowing shifted reproductive stages into a warmer period; mean maximum temperatures during anthesis–

silking increased by ~3–6°C relative to normal sowing, with peak daily maxima reaching 34–40°C in April–May across sites. Consequently, days to 50% anthesis and silking were significantly reduced under late sowing (phenological acceleration), reflecting thermal time effects.

Pooled ANOVA

Combined ANOVA across eight environments depicted in table 2 revealed highly significant ($p < 0.01$) effects of genotype, environment and G×E interaction for all measured traits (Table 2). For most traits, the environment mean squares were considerably higher than those of genotypes and G×E interactions, suggesting that environmental factors exerted the greatest influence on phenotypic performance. This was particularly evident for phenology-related traits such as days to 50% anthesis (DA), days to 50% silking(DS), and as well as for grain yield per plant (GYP). Such high environmental influence implies that location and seasonal conditions play a major role in trait expression and must be considered when selecting genotypes for stability and adaptability, while genotype and G×E contributed substantially to variance in reproductive synchrony (ASI), silk receptivity and senescence.

Table 2: Pooled Mean sum of squares of inbred lines for various traits

Source	Degree of Freedom	DA	DS	ASI	TB	LF	LS	NKR
Trials	912	18.60	2.78	15.20	18.34	164.44***	1.18	13.67
Genotypes	39	198.06 ***	4.96***	238.23***	119.41***	285.24***	3.55***	63.29***
Environments	7	1074.64 ***	257.07***	290.77***	141.78***	8393.30***	70.78***	242.68*
G*E interaction	273	1.63**	0.84***	2.83***	19.58***	64.06***	0.68***	11.71***
Pooled error	312	2.09	0.26	1.59	1.14	3.57	0.23	4.19

Source	Degree of Freedom	S%	HGW	SR	GYP	CT
Trials	912	198.44	10.15	211.97	64.56	1.69***
Genotypes	39	288.00***	26.64***	377.53***	29.83***	4.27***
Environments	7	20925.22***	730.36***	16371.98***	7592.94***	96.02***
G*E interaction	273	38.48***	4.65***	104.91***	7.41***	0.99***
Pooled error	312	6.68	1.69	20.69	1.58	

** Significant at (P< 0.01) percent,* significant at (P<0.05) percent level of probability, respectively and *** TB and LF data was not availableunder normal sown conditions

Phenological responses

Performance of various inbred lines for contrasting traits are presented in table 3. Under normal sowing, days to 50% anthesis ranged 66.25–80.75 days; under late sowing this range reduced to 59.63–74.38 days. ASI increased markedly under late sowing, from 1.00–3.00 days (normal) to 3.63–6.75 days (late), with the largest increases in HKI 1558-4 and HKI 288-2 (indicative of severe reproductive asynchrony). Genotypes HKI 139 and HKI 1664 maintained lower ASI under stress, suggesting better reproductive synchrony and potential tolerance. Leaf senescence scores increased under late sowing (up to 5.25 in HKI 1378), indicating accelerated chlorophyll loss and reduced leaf functional duration. Tassel blast and leaf firing were negligible under normal sowing but prevalent under late sowing ranged between 10-25 % and 10-20% respectively; maximum tassel blast occurred in HKI 323 (20.88%), HKI 1128 (15.54%) and HKI 288-2 (14.84%). Canopy temperatures measured at peak reproductive stage were higher for susceptible genotypes; tolerant genotypes displayed relatively lower canopy temperatures, suggesting better transpirational cooling or stomatal regulation. Silk receptivity declined sharply under late sowing (normal: 34.93–63.23%; late: 9.09–34.07%). Genotypes HKI 163, HKI MBR139 and Bio inbred 47 retained comparatively higher silk receptivity under stress. Kernels per row and kernel set were significantly reduced under heat stress, corresponding to increased ASI and reduced silk viability. Heat stress caused substantial reductions in hundred kernel weight, shelling percentage and grain yield. Under normal sowing, grain yield ranged 0.584–0.862 kg per plot; under late sowing it dropped to 0.049–0.288 kg per plot. Genotypes HKI MBR139, HKI 1011 and HKI 1025 recorded the highest yields under stress, with HKI MBR139 showing the best combination of silk receptivity, kernel set and reduced ASI.

Table 3: Pooled mean of traits of forty maize inbred across normal sown and late sown environment

		GYP (kg)		% Yield Reduction	DA (days)		DS (days)		ASI	
Sr. No.	Genotype	Normal	Late		Normal	Late	Normal	Late	Normal	Late
1	**HKI 139**	0.728	0.240	67.09	66.50	60.13	67.88	63.75	1.25	3.63
2	**HKI1025**	0.644	0.255	60.46	66.25	59.63	68.50	64.50	1.25	4.88
3	**HKI 1041-2**	0.646	0.229	64.48	67.38	60.50	68.38	64.88	1.00	4.38
4	**HKI 1011**	0.712	0.287	59.64	67.63	61.38	69.50	65.38	1.75	4.00
5	**HKI 1040-7**	0.713	0.164	77.00	73.13	66.38	74.25	71.38	1.25	5.00
6	**HKI 1654**	0.584	0.215	63.22	73.75	64.88	74.75	70.75	1.00	5.88
7	**HKI 295**	0.681	0.174	74.47	73.25	66.25	74.75	71.13	1.50	4.88
8	**HKI 1041**	0.783	0.225	71.22	73.50	66.38	75.00	71.13	1.50	4.75
9	**HKI 488 T**	0.815	0.142	82.56	72.88	66.50	73.88	72.63	1.00	6.13
10	**HKI 1558-4**	0.825	0.141	82.86	73.13	67.13	74.13	73.88	1.00	6.75
11	**HKI 1657**	0.689	0.238	65.49	73.38	66.63	75.13	71.50	2.00	4.88
12	**HKI 1128**	0.724	0.049	93.18	73.00	67.13	74.75	73.25	1.75	6.13
13	**HKI 488**	0.813	0.209	74.28	73.88	66.88	74.88	71.00	1.00	4.13
14	**DQL 2300**	0.814	0.239	70.67	74.13	66.63	75.75	71.38	1.75	4.75
15	**HKI1126**	0.692	0.078	88.68	73.88	68.50	75.88	75.25	2.00	6.75
16	**HKI 766 WG**	0.704	0.251	64.31	73.75	67.00	75.75	72.13	2.00	5.13
17	**HKI 323**	0.738	0.074	90.01	74.50	69.13	76.00	74.63	1.63	5.50
18	**HKI 1105**	0.760	0.205	73.08	75.25	67.88	76.25	72.00	1.00	4.13
19	**HKI MBR139**	0.699	0.288	58.81	73.75	67.00	75.13	71.13	1.38	4.13
20	**HKI 2067 Y**	0.786	0.214	72.82	74.50	67.50	76.50	72.63	2.00	5.13
21	**HKI 1344**	0.862	0.186	78.40	74.88	68.25	75.88	73.38	1.25	5.13
22	**1654-15-ER 1-1-1 WINK11**	0.717	0.233	67.55	74.00	67.63	76.00	71.75	2.00	4.13
23	**HKI 1040-4**	0.717	0.239	66.75	75.00	68.25	76.75	73.13	1.88	4.88
24	**HKI 327 T**	0.722	0.052	92.80	74.63	68.00	76.13	74.63	1.50	6.63
25	**LM 16**	0.801	0.200	74.99	77.63	69.88	79.63	75.63	2.00	5.75
26	**HKI 163**	0.852	0.249	70.72	77.63	70.25	78.63	74.50	1.00	4.25

27	**HKI 1354-2**	0.846	0.107	87.32	77.88	70.13	79.00	75.25	1.00	5.13
28	**HKI 1354-7**	0.819	0.177	78.42	78.13	71.50	80.38	76.88	2.25	5.38
29	**HKI 1378**	0.831	0.137	83.48	78.50	71.38	80.00	77.38	1.50	6.00
30	**LM 17**	0.831	0.187	77.54	78.50	71.50	81.13	77.25	2.63	5.75
31	**HKI 161**	0.828	0.227	72.54	77.88	70.88	79.63	76.00	1.75	5.13
32	**Bio inbred 47 ER3-1 Wink 11**	0.714	0.204	71.46	78.50	71.75	81.50	76.63	3.00	4.88
33	**HKI 164-7-2**	0.822	0.203	75.36	77.38	70.25	79.50	75.25	2.25	5.00
34	**HKI 164-7-4**	0.791	0.180	77.21	77.63	70.63	80.13	74.75	2.63	4.13
35	**HKI 164-7-6**	0.793	0.184	76.81	78.00	70.75	80.25	75.38	2.25	4.63
36	**HKI 193-2**	0.786	0.189	75.97	77.88	70.63	80.88	75.63	3.00	5.00
37	**HKI 1664**	0.825	0.237	71.29	78.00	72.75	80.50	76.63	2.50	3.88
38	**HKI 193-1**	0.766	0.204	73.32	78.25	71.63	80.50	76.75	2.38	5.13
39	**HKI L287**	0.721	0.090	87.48	79.38	74.38	82.13	80.75	2.88	6.38
40	**HKI 288-2**	0.782	0.058	92.59	80.75	73.88	83.75	80.63	3.00	6.75

		LS (score)		**NKR**		**SR (%)**		**S%**		**hgw**	
Sr. No.	**Genotype**	**Normal**	**Late**	**Normal**	**Late**	**Normal**	**Late**	**Normal**	**Late**	**Normal**	**Late**
1	**HKI 139**	3.25	3.50	19.42	19.33	52.96	28.10	51.81	27.74	19.74	14.39
2	**HKI1025**	2.63	3.38	19.50	17.71	38.20	31.55	51.54	29.74	18.59	12.09
3	**HKI 1041-2**	3.25	3.75	19.80	17.10	47.24	31.48	52.24	27.81	19.80	13.15
4	**HKI 1011**	2.50	3.75	19.95	17.02	45.05	28.33	49.90	31.23	18.04	15.07
5	**HKI 1040-7**	2.63	4.50	18.61	17.60	46.44	21.49	50.98	20.34	19.35	15.02
6	**HKI 1654**	3.00	3.50	22.97	16.10	46.38	30.70	45.91	27.58	18.05	15.06
7	**HKI 295**	2.13	3.50	21.46	18.70	49.89	20.87	51.56	23.64	20.09	15.25
8	**HKI 1041**	2.38	3.25	23.72	18.65	54.32	28.71	54.91	26.71	20.02	15.55
9	**HKI 488 T**	2.13	4.75	25.21	14.75	55.94	24.36	54.56	19.27	20.35	12.47
10	**HKI 1558-4**	1.88	4.75	19.49	14.85	53.80	21.82	54.21	18.63	19.90	13.51
11	**HKI 1657**	2.13	3.50	22.93	18.60	44.97	31.30	49.93	28.73	21.30	15.43
12	**HKI 1128**	2.25	5.00	23.36	14.50	43.97	11.43	52.38	8.82	22.65	14.74
13	**HKI 488**	2.25	3.25	21.69	15.00	52.57	30.19	59.28	25.14	23.11	17.43
14	**DQL 2300**	1.25	3.00	24.25	24.30	52.69	19.42	59.54	28.33	23.68	17.20
15	**HKI1126**	2.38	4.75	19.60	16.10	48.06	11.31	50.06	11.17	21.48	14.23

16	**HKI 766 WG**	2.13	3.50	15.47	17.50	47.72	32.71	50.59	29.88	18.45	17.33
17	**HKI 323**	2.25	4.75	18.85	14.40	46.22	17.00	51.56	11.03	21.28	13.12
18	**HKI 1105**	2.00	3.00	22.70	17.00	52.66	24.47	59.67	26.91	22.53	17.15
19	**HKI MBR139**	2.00	2.75	19.91	19.10	49.62	32.29	59.81	30.05	18.85	16.06
20	**HKI 2067 Y**	1.88	3.25	21.21	15.93	53.60	25.45	51.06	25.01	18.55	17.64
21	**HKI 1344**	1.38	3.25	23.12	23.75	57.17	19.56	62.86	21.92	22.85	19.02
22	**1654-15-ER 1-1-1 WINK11**	2.13	3.00	17.10	17.30	48.58	28.21	60.06	30.86	21.85	17.47
23	**HKI 1040-4**	2.75	3.00	16.40	22.10	53.81	22.90	54.16	27.65	19.66	17.55
24	**HKI 327 T**	1.38	4.25	22.50	15.10	34.93	9.09	51.01	8.52	23.03	11.11
25	**LM 16**	1.25	3.50	25.20	18.40	44.57	23.69	52.31	24.68	22.05	15.57
26	**HKI 163**	1.25	2.75	19.29	15.50	54.75	33.80	59.56	28.62	21.78	15.73
27	**HKI 1354-2**	1.63	3.00	26.81	21.30	57.82	12.72	56.86	14.22	23.35	16.41
28	**HKI 1354-7**	1.50	2.50	18.27	21.30	54.26	20.24	47.71	23.88	21.55	17.48
29	**HKI 1378**	1.88	5.25	19.76	14.80	59.69	23.97	54.69	19.31	23.39	14.49
30	**LM 17**	1.50	3.50	20.69	23.30	54.44	18.32	55.56	24.66	25.03	16.64
31	**HKI 161**	1.50	3.00	18.48	14.45	60.17	32.05	63.06	28.48	19.13	17.88
32	**Bio inbred 47 ER3-1 Wink 11**	2.13	3.25	21.93	16.30	47.16	34.07	53.56	26.82	20.11	15.49
33	**HKI 164-7-2**	1.75	3.00	21.13	17.30	51.83	26.54	48.60	24.78	21.95	15.86
34	**HKI 164-7-4**	1.50	3.25	18.77	14.35	51.64	29.46	59.66	23.10	24.88	15.73
35	**HKI 164-7-6**	2.13	3.25	19.78	13.55	51.98	30.57	48.69	22.97	18.15	16.66
36	**HKI 193-2**	2.00	3.25	21.32	19.05	47.51	22.33	48.56	25.07	22.45	15.28
37	**HKI 1664**	1.38	4.50	17.63	22.20	63.23	24.49	49.06	27.71	18.55	19.30
38	**HKI 193-1**	1.25	3.63	17.62	18.00	50.74	30.61	49.16	26.81	19.65	15.85
39	**HKI L287**	1.88	4.50	18.01	16.35	43.43	13.45	49.32	13.45	21.23	13.65
40	**HKI 288-2**	1.25	4.88	21.02	15.75	49.91	10.75	53.06	9.54	21.19	14.76

Late sown Conditions	Normal sown Conditions	Traits
		**Silk receptivity inbred line LM 16 decreases under Late sown conditions**

Late sown Conditions	Normal sown Conditions	Traits
		**Poor appearance of HKI 1025 cob under late sown conditions**
		**Comparatively better performing for grain yeild per plot under late sown conditions HKI MBR 139**

Late sown conditions	**Normal sown conditions**	**Traits**
		**q) Comparatively better performing for grain yeild per plot under late sown conditions HKI 163**
r) Leaf Senescence Trait (Score 3)	**s) Leaf firing in HKI 288-2**	**t) Tassel Blast in 327 T**
		

Identification of tolerant genotypes

Integrating mean performance, stability across environments and trait profiles, genotypes HKI 1011, HKI MBR139, HKI 1344 and HKI 1664 were identified as relatively heat tolerant: they combined lower ASI, higher silk receptivity, reduced senescence and better yield stability under late sowing. These inbreds represent promising donors for breeding heat-resilient hybrids and populations.

IV. DISCUSSION

The present study confirms that late sowing imposes terminal heat stress that accelerates phenology but disrupts reproductive processes in maize, thereby reducing grain yield. The marked increase in ASI under heat stress aligns with earlier reports linking reproductive asynchrony to poor kernel set and yield loss (Chiuta and Mutenga, 2025 and Yadav *et al.,* 2016). High temperature decreases the time for tasseling and pollen shedding, increases anthesis silking interval and parchedness of silk all of which reduces the pollen viability, pollen quantity and successful seed setting (Pranay *et al*., 2022 amd Jodage *et al.,* 2018). Further heat stresses maize plants are unable to convert photosynthates into starch in pollens. Thus, decreases the pollen numbers, their viability and starch synthesis contributes to the distorted fertilisation process and ultimately to the yield loss (Wang *et al.,* 2019). Reduced silk receptivity and pollen viability under high temperatures are primary physiological causes of kernel abortion (Noor *et al*., 2019 and Krishna *et al*., 2021); genotypes maintaining silk receptivity under stress (e.g., HKI MBR139) thereby maintain better kernel set and yield. Leaf senescence and canopy temperature differences suggest that tolerant genotypes preserve canopy function longer and/or maintain better transpirational cooling, contributing to sustained photosynthate supply for grain filling. Lower canopy temperature in tolerant lines may reflect higher stomatal conductance or deeper rooting enabling water uptake—traits often associated with heat tolerance but requiring direct physiological confirmation (Tollenaar and Lee, 2002 and Prasad *et al.,* 2011). Genetic variability and significant G×E interactions indicate that selection for heat tolerance must be performed across multiple stress environments. The tolerant inbreds identified here can be used in crossing programs.

V. CONCLUSIONS AND FUTURE PERSPECTIVES

Late-sown heat stress significantly impaired reproductive synchrony, silk receptivity and grain filling, causing heavy yield losses. However, substantial genetic variation exists among the evaluated inbreds. HKI 1011, HKI MBR139, HKI 1344 and HKI 1664 combined favorable reproductive and physiological traits under stress and are recommended as donor parents for developing heat-tolerant hybrids. Breeding programs should integrate multi-environment field screening with physiological and molecular characterization to select mechanisms conferring tolerance.

Present investigation can be further extend to controlled-environment experiments to validate field-identified tolerant lines and dissect physiological mechanisms (pollen viability, silk desiccation, stomatal behavior). Measuring the additional physiological traits (chlorophyll fluorescence, SPAD, membrane thermostability, root traits) and water relations to link phenotype to mechanism. QTL mapping or GWAS can be implemented across the inbred panel to identify genetic loci associated with ASI, silk receptivity and canopy temperature.

REFERENCES

[1] Chiuta, N. E., and Mutengwa, C. S. (2025). Response of maize hybrids exposed to drought and heat stress under field conditions. Cogent Food and Agriculture, 11(1), 2488108

[2] Jodage, K., Zaidi, P. H., Patil, A., Seetharam, K., Vinayan, M. T., and Arunkumar, B. (2018). Genetic analysis of heat adaptive traits in tropical maize (*Zea mays* L.). International Journal of Current Microbiology and Applied Sciences, 7(1), 3237–3246.

[3] Krishna, B., Singh, B., Mandal, S. S., Rashmi, K., and Ranjan, T. (2021). Association and path coefficient analysis among grain yield and related traits in kharif maize (*Zea mays* L.). The Pharma Innovation Journal, 10(7), 1062–1067.

[4] Lobell, D. B., and Burke, M. B. (2010). On the use of statistical models to predict crop yield responses to climate change. Agriculture, Forestry and Meteorology, 150, 1443–1452.

[5] Noor, J. J., Vinayan, M. T., Umar, S., Devi, P., Iqbal, M., Seetharam, K., and Zaidi, P. H. (2019). Morpho-physiological traits associated with heat stress tolerance in tropical maize (*Zea mays* L.) at reproductive stage. Australian Journal of Crop Science, 13(4), 536–545.

[6] Pranay, G., Shashibhushan, D., Jhansi Rani, K., Bhadru, D., and Sameer Kumar, C. V. (2022). Genotype and phenotype coefficient of variance in maize (*Zea mays* L.). International Journal of Environment and Climate Change, 12(12), 1119–1132. https://doi.org/10.9734/ijecc/2022/v12i121550

[7] Prasad, P. V. V., Boote, K. J., & Allen, L. H., Jr. (2011). Crop responses to high temperature and drought stress: A physiological perspective. In J. H. J. Spiertz, P. C. Struik, & N. G. Kadama-Yakubu (Eds.), Dynamic role of plant physiology in crop breeding (pp. 157–186). Springer.

[8] Tollenaar, M., & Lee, E. A. (2002). Yield potential, yield stability and stress tolerance in maize. Field Crops Research, 75(2–3), 161–171. https://doi.org/10.1016/S0378-4290(02)00022-X

[9] Wang, Y., Tao, H., Tian, B., Sheng, D., Xu, C., Zhou, H., Huang, S. and Wang, P. (2019). Flowering dynamics, pollen, and pistil contribution to grain yield in response to high temperature during maize flowering. Environ. Exp. Bot., 158: 80–88.

[10] Yadav, S. K., Tiwari, Y. K., Shanker, A. K., Lakshmi, N. J., Vanaja, M., and Maheshwari, M. (2016). Genotypic variation in physiological traits under high temperature stress in maize. Agricultural Research, 5(2), 119–126.

[11] Zaidi, P. H., Mallick, N., Xu, D., and Malviya, M. K. (2019). Morpho-physiological traits associated with heat stress tolerance in maize. Crop Journal, 7(4), 536–545.

International Journal of Environment, Agriculture and Biotechnology
Vol-11, Issue-3; May-Jun, 2026
Peer-Reviewed International Journal
Journal Home Page Available: https://ijeab.com/
Journal DOI: 10.22161/ijeab

Impact of the Cultivation Methods and Irrigation Systems on Wheat Productivity and Carbon Footprint in Two Different Agro Ecological zones of Egypt

Safwat Abdelhamid

Plant Production Department, Ecology and Dry land Agriculture Division, Desert Research Center (DRC), Cairo, Egypt
Corresponding author: Safwat.agri@mail.ru

Received: 23 Apr 2026; Received in revised form: 27 May 2026; Accepted: 30 May 2026; Available online: 08 Jun 2026

***Abstract*— *Carbon footprint (CF) is one of the most important widely used indicators that quantify human use of natural resources and its emissions, where it can be used to guide policies to mitigate the stress of human activities on natural resources and the environment. Improving agricultural practices and systems may lead to mitigating greenhouse gas emissions. In this study the carbon footprint of wheat grown in various farming methods was ascertained in two different agro-ecological zones (Eastern desert and Sinai and Western desert and Oasis) in Egypt during the two growing seasons (2023-2024 and 2024-2025). The carbon footprint of wheat production was quantified based on the traditional practices data of the production process. The CF was found to be significantly different between both zones due to various cultivation systems, irrigation systems, fertilization, and pest control. The average carbon footprint differed between the two agro-ecological zones, irrigation systems and cultivation methods, ranging from 3088.9 to 3528.3 kg CO_2 eq./ha. The results also showed that there were significant differences in the impact of different farming methods and practices as well as irrigation systems on the carbon footprint rate, wheat yield and its components. The lowest carbon footprint values were recorded in the South Sinai region when using drip irrigation recorded 3088.9 kg CO_2 eq./ha, along with the highest water use efficiency 1.36 kg/m^3.*

***Keywords*— Carbon footprint, wheat, climate change.**

I. INTRODUCTION

Increased global awareness of environmental challenges and their connections to social and economic difficulties has been a major driving force behind worldwide environmental legislation in recent decades. Global greenhouse gas (GHG) emissions must be significantly reduced, according to international accords and scientific evaluations. Where led to the Earth's climate changes quickly due in significant part to rising anthropogenic greenhouse gas emissions. Global climate change is a result of agricultural activities that produce greenhouse gases (GHGs) during crop cultivation, food processing, and product marketing. 23–30% of all human greenhouse gas emissions worldwide are caused by agricultural operations (**Tubiello *et al.*, 2013; IPCC, 2019**). Farmers and the public are pushing for the creation and implementation of practical solutions to lower greenhouse gas emissions from all agricultural sectors and activities. However, there is a lack of quantitative data regarding the methods and approaches that should be used to lower agricultural emissions as well as how crop yield might impact the level of greenhouse gas emissions (**Gan *et al.*, 2011 a**).

Both freshwater usage and global warming are significantly impacted by food production. The second largest sectoral GHG emitter is the agriculture, forest, and other land use sectors, which contributed 24% of the world's GHG emissions in 2010 (**Kashyap, & Agarwal, 2021**). According to FAO, in 2017 70% of freshwater withdrawals worldwide and 95% of water withdrawals in certain developing nations are attributed to agriculture, which is also the major user of freshwater. Given its limited water resources, Egypt's expanding population presents the dual problem of increasing food production while reducing the corresponding greenhouse gas emissions.

Millions of people consume wheat every day, making it one of the most popular food sources worldwide. Its agriculture and production, however, have negative climatic consequences. Through greenhouse gases from fuel, artificial fertilizers, and pesticides used in wheat production have a detrimental effect on climate change (**Gan *et al.*, 2014**). Although enhancing agricultural practices would reduce greenhouse gas emissions (**Gan *et al.*, 2011 b**), until now it is unknown whether adopting alternative farming practices such as cultivation methods and irrigation system will enhance wheat productivity and reduce pollution by carbon emissions.

One of the most significant and commonly used metrics for measuring how much natural resources are consumed by humans and the emissions they produce is the carbon footprint (CF), which may be used to inform policy to lessen the impact of human activity on the environment and natural resources. The management of farms can be guided by the carbon footprint as an indicator due to the growing environmental impact of food production (**Zhang *et al.*, 2017**). Therefore, evaluating the CF of agricultural output is necessary before investigating the best farming methods with reduced greenhouse gas emissions. **IPCC 2019** states that GHG emissions from agricultural production in agroecosystems come from a variety of agricultural activities, such as the use of fertilizers, pesticides, irrigation water, and fossil fuels, in addition to cultivated soils.

The term "carbon footprint" was first introduced in a pioneering academic paper by **Rees (1992)**, which also presented the concept of the "ecological footprint." In a subsequent study, **Wiedmann and Minx (2008)** explained how carbon footprints can be utilized to assess the impact of greenhouse gas (GHG) emissions on environmental sustainability. Also, they reported that a carbon footprint is a measure of the exclusive total amount of carbon dioxide emissions that is accumulated over the life stages of a product or is directly and indirectly caused by an activity (**Gan *et al.*, 2011 a**).

The purpose of this study was to examine how irrigation systems and traditional cultivation practices impact wheat productivity and carbon footprints across two distinct agroclimatic zones of Egypt.

II. MATERIALS AND METHODS

Study site descriptions.

The first region is the El-Kharga oasis at New Valley, located in the southwestern part of the country, in the south of Egypt's Western Desert (part of the Sahara Desert) (25.52° N and 30.61° E). Which is located within the agroecological zone of the Western Sahara and the oases: This area depends on groundwater (non-renewable) and is characterized by sandy soil. The climate of Kharga Oasis is a hot, hyper-arid desert climate (Köppen BWh), with highs of 41°C in August and lows of 2°C in January. The temperature ranged from 52°C to 2°C, with a relative humidity of about 39%.

The second region is Al-Wadi village, Al-Tor city, South Sinai, Egypt (28.21089°N, 33.35450°E, at an elevation of 14 m above sea level). Which is located within the agroecological zone of the Eastern Desert and Sinai: it is mostly harsh arid environments, with agriculture activities in valleys and areas containing groundwater, especially in the South Sinai Peninsula. Its climate features a hot desert climate (Köppen BWh) with scorching summers, mild winters, and extremely low precipitation with an average annual rainfall of no more than 7 mm and an average temperature of 23.2°C. The temperature ranged from 35°C in summer to 13°C in winter, with a relative humidity ranging between 51-66 %.

Table 1. Soil Physicochemical properties during the two growing seasons (2023-2024 and 2024-2025)

Season	Texture	EC (ppm)	pH	Available aions (ml/l)						
				Ca	Mg	Na	CO3	HCO3	Cl-	SO4
New Vally										
2023-2024	**Sandy**	936	8.1	12.3	7.8	17.02	4.13	6.87	95.9	0.71
2024-2025		922	8.3	13.1	8.1	16.68	4.37	6.53	93.4	0.67
South Sinai										
2023-2024	**Sandy**	1466	8.2	7.95	8.78	19.91	3.1	2.66	21.2	12.48
2024-2025		1394	8.2	7.93	8.70	19.71	2.9	2.62	20.6	12.42

Data sources

Data used in the calculation of carbon footprint was originated from a field experiments conducted during the two growing seasons 2023-2024 and 2024-2025 in two Agro-Ecological zone of Egypt (Western Sahara and the oases - Eastern Desert and Sinai).

Field experiments and layout

Consumption and yield data for the 2023-2024 and 2024-2025 wheat growing seasons were calculated using three different irrigation systems (flood, drip, and sprinkler) in the first region, and only two in the second region (drip and sprinkler). employing the two seeding methods (Broadcasting and by seed drill in rows) in the first region and (broadcasting and by handheld seeder in rows) in the second region, during the two growing seasons.

Six experimental fields were cultivated during two growing seasons 2023-2024 and 2024-2025: four in the New Valley (three fields sown broadcast under the three irrigation systems—flood, sprinkler, and drip—and one field sown using a seed drill under flood irrigation), and two fields in South Sinai (one sown using a planter under drip irrigation, and the other was sown by broadcast under sprinkler irrigation system).

Carbon footprint calculating

The carbon footprint assessment is based on calculating greenhouse gas emissions GHGs through various agricultural activities, from the use of energy in the production and use of agricultural machinery, synthetic fertilizers, and chemicals for crop protection such as herbicides, pesticides, and fungicides, to the direct use of fuel in agricultural operations according to guidelines for national greenhouse gas inventories IPCC 2006.

III. RESULTS

The comparative effects of various irrigation systems and cultivation methods on plant height and spike length (cm) under two agro-ecological zones, which are summarized in figure 1 (a, b) for both growing seasons. The results indicated that there was a considerable effect on plant height and spike length due to the two irrigation systems and cultivation methods under both zones.

The results showed a significant effect of irrigation systems on plant height in the two study areas. Wheat plants under drip irrigation exhibited the highest plant heights, reaching 118.6 and 105.5 cm, and spike lengths of 11.9 and 11.2 cm in the first and second areas, respectively. Conversely, sprinkler irrigation resulted in reduced wheat plant heights and spike lengths, with plant heights decreasing to 112.3 and 96.5 cm and spike lengths reaching 11.5 and 10.2 cm in the two study areas. Comparing flood irrigation with both drip and sprinkler irrigation systems in the first area (Western Desert and Oases) revealed clear differences, recording the lowest values for spike length and plant height, recorded 110.6 and 10.5 cm (Fig. 1 A).

On the other hand, the cultivation method had different effects on plant height and spike length in the two study zones. In the first zone (Kharga Oasis in the New Valley), the average plant height was 112.55 cm, while in the second zone (El Tor in South Sinai), the average spike length was 11.3 cm. Although plants grown using the broadcast method reached a higher height of 113.8 cm compared to those grown using the seed drill in rows (111.3 cm) in the first zone, no difference was recorded in spike length (11.3 cm). Conversely, plants grown using the broadcast method recorded the lowest plant height and spike length (96.5 cm and 10.2 cm) compared to plants grown using the handheld seeder in rows in the second zone, recorded 105.5 cm and 11.2 cm (Fig. 1B).

In addition, in general there were significant differences between the two study zones, with wheat performance in the Western Desert and Oases region (El-Kharga Oasis - New Valley) outperforming that of the Eastern Desert and Sinai region (El-Tur - South Sinai), where plant height and spike length increased by 11.88% and 5.61%, respectively.

When comparing the effects of different irrigation systems and planting methods on the number of grains per spike and the thousand-grain weight (g), the results indicate a significant variation in both grains per spike and thousand-grain weight depending on the irrigation system and planting method. This variation also differed between the two study regions. Drip irrigation achieved the best thousand-grain weight in both regions, reaching 51.62 g and 50.47 g in the Western Desert and Oases region, and the Eastern Desert and Sinai region, respectively (fig. 2A). However, sprinkler irrigation yielded the best number of grains-per-spike values, recording 33.5 g and 28.2 g in the first and second regions, respectively (Fig. 2 A). On the other hand, although broadcasting cultivation resulted in the best number of grains-per-spike in both regions, mechanized methods achieved the best 1000-grain weight, recording 50.73 g when using a seed drill in the first region and 50.47 g when using a handheld seeder in the second region (Fig.2 B).

Furthermore, wheat performed better in the Western Desert and Oasis region than in the Eastern Desert and Sinai. In the first region, the plants were superior in the number of grains/spikes as well as the weight of 1000 grains the average number of grains per spike was 32.13 grains per spike, and the average weight of 1000 grains was 50.22 g; on the other side in the second region, the average number of grains per spike was 27.25 grains per spike, and the average weight of 1000 grains was 49.22 g.

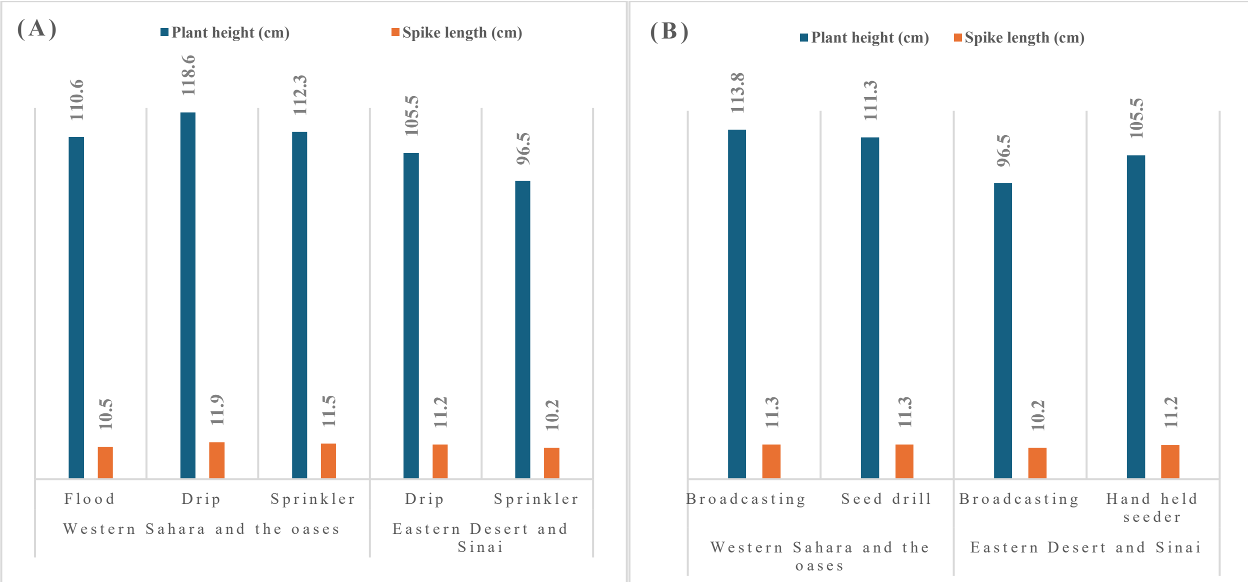

Fig.1 Effect of irrigation system and cultivation methods on plant height and spike length (cm) of wheat under two agro-ecological zones conditions in Egypt

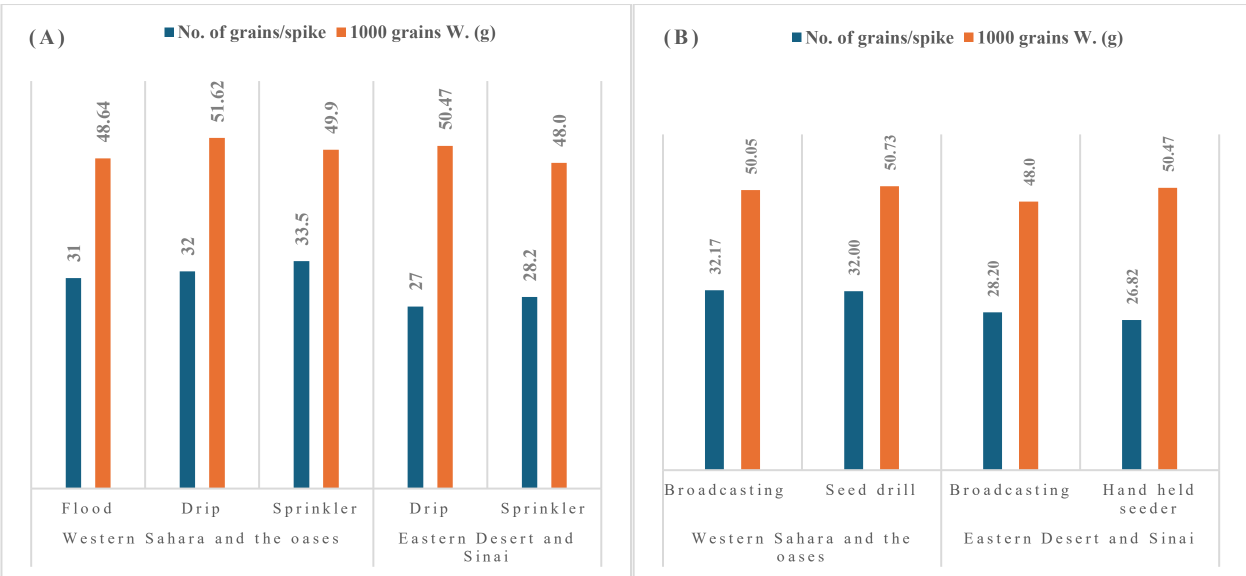

Fig.2 Effect of irrigation system and cultivation methods on number of grains/spike and 1000 grains weight (g) of wheat under two agro-ecological zones conditions in Egypt

The results in table 2. and figure 3. show that wheat productivity varied greatly between the two agricultural regions, with the Western Desert and Oases region (New Valley) outperforming the Eastern Desert and Sinai region (El-Tur) in both wheat productivity and biomass yield, achieving 7.62 t/ha and 28.72 t/ha, respectively. This indicates a 10.12% increase in grain yields and a 52.85% increase in biomass yields compared to the Eastern Desert and Sinai region. Regarding the irrigation systems used, drip irrigation achieved the best results in both study zones, with an average wheat yield of 8.25 t/ha in the New Valley, representing increases of 13.87% and 6.66% compared to flood and sprinkler irrigation systems, respectively. Biomass also increased by 14.62% and 29.31%, reaching 32.65 t/ha. Furthermore, average wheat yield and biomass under drip irrigation increased in the Eastern Desert and Sinai (El-Tur) regions, reaching 7.61 t/ha and 22.02 t/ha, respectively, representing increases of 22.15% and 41.52% compared to sprinkler irrigation. The study of planting methods effect revealed that mechanized planting systems are superior to manual broadcasting. Cultivation with a seed drill achieved the highest wheat yield and biomass, reaching 7.84 t/ha and 30.41 t/ha, respectively. This represents increases of 17.90% for grain yield and 14.50% for biomass in New Valley. Similar results were observed in El-Tur, where average yields with mechanized planting using a handheld seeder reached 7.61 t/ha, and the biomass yield was 22.02 t/ha. In contrast, the average wheat yield and biomass yield with broadcasting were 6.23 t/ha and 15.56 t/ha, respectively. These figures represent decreases of 18.13% and 29.34%, respectively, when compared to the results obtained from mechanized cultivation. According to the results in Fig. 3 (A and B) and Table 2, mechanized farming, utilizing either a seed drill or a handheld seeder within a drip irrigation system, achieved the highest levels of grain and biomass productivity across the two study zones, each characterized by different environmental conditions.

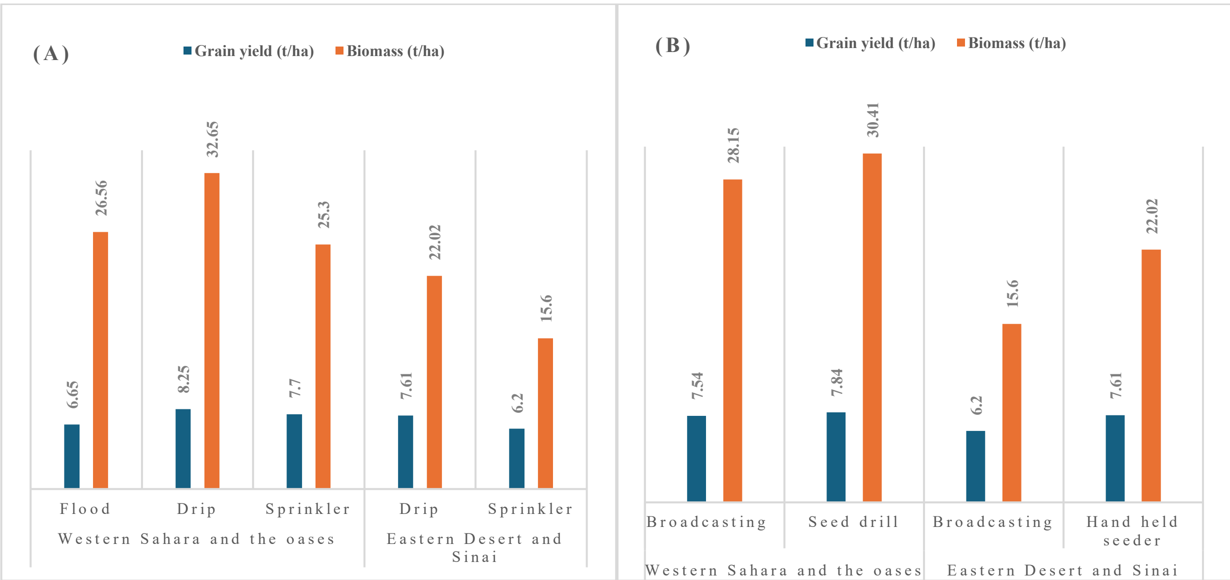

Fig. 3 Effect of irrigation system and cultivation methods on grain yield and biomass of wheat (t/ha) under two agro-ecological zones conditions in Egypt

The results in Table 2 and figure 4 (A and B) indicate significant differences in water use efficiency between the two agricultural environments zones studied. Water use efficiency ranged from 1.11 to 1.23 kg of grain per m³ of water in the Eastern Desert and Sinai (El-Tur), compared to the Western Desert and the oases (New Valley), respectively. The analysis revealed notable disparities in water use efficiency among the various irrigation systems. Flood irrigation exhibited the lowest efficiency, measuring at 0.87 kg of grain per m³ of water, while drip irrigation achieved the highest efficiency at 1.35 kg of grain per m³ of water, as well as sprinkler irrigation recorded a water use efficiency of 1.1 kg of grain per m³ of water. The results show that the best water use efficiency was achieved with mechanized planting using a handheld seeder under a drip irrigation system, reaching 1.36 kg grains/m^3 water, while the lowest water use efficiency was recorded with broadcast planting and the application of a flood irrigation system, reaching 0.87 kg grains/m^3 water.

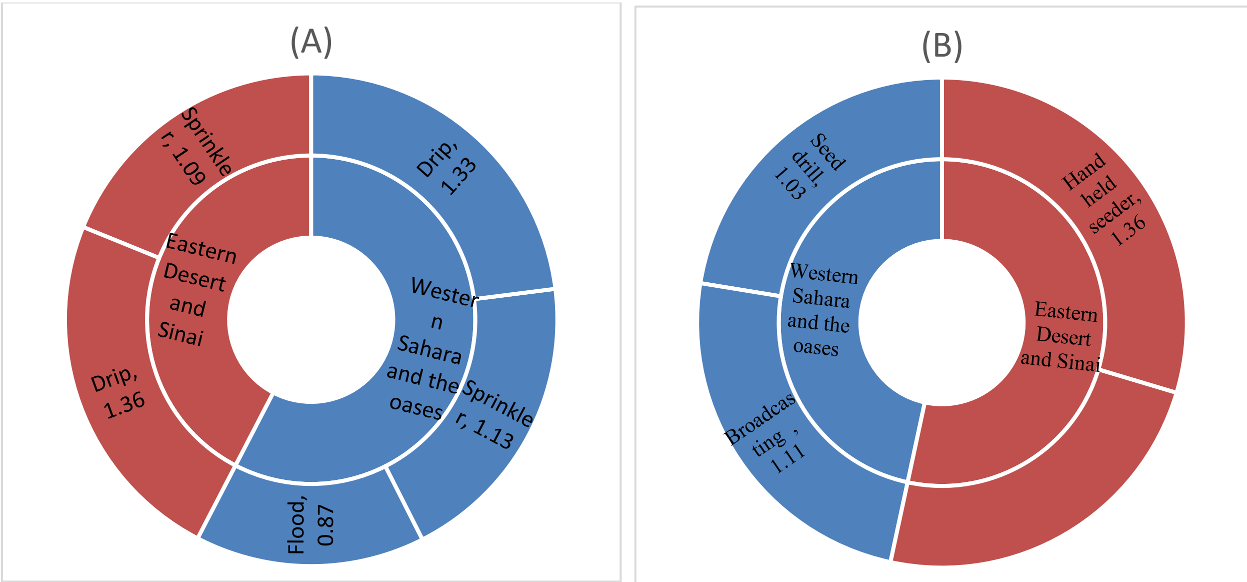

Fig. 4 Effect of irrigation system and cultivation methods on water use efficiency (kg/m^3) in wheat fields under two agro-ecological zones conditions in Egypt.

The estimation of CO_2 emissions in wheat production was based on the different methods and practices of wheat production in the selected zones. Throughout the many procedures seen throughout the survey, the evolution of operations farming practices considered tillage, cultivation methods, irrigation systems, plant protection, fertilizing, combine harvesting, and threshing as essential processes that contribute to the total carbon emissions in wheat production. By examining the inputs—such as labor, chemical fertilizers, seeds, herbicides, pesticides, and the efficiency of equipment sets used for tillage, harvesting, and threshing—the greenhouse gas emissions linked to these practices were determined. The information offered a thorough evaluation of the environmental effects of different wheat production systems, assisting in the identification of major sources of greenhouse gas emissions and providing information on possible areas where sustainable agriculture practices could be improved.

Data in figure 5 presents an assessment of greenhouse gas (GHG) emissions resulting from various farming practice inputs across different wheat production systems (cultivation methods and irrigation systems) in the two zones under study. The analysis clearly indicates that a drip irrigation system is associated with significantly lower GHG emissions compared to other systems (sprinklers or flood). Generally, the highest GHG emission was recorded in the second zone (Eastern Desert and Sinai) at 3528.3 kg CO_2-eq ha^{-1} by the sprinkler irrigation system, whereas the lowest was observed in the drip irrigation system at 3088.9 kg CO_2-eq ha^{-1}.

Chemical fertilizers, such as urea, ammonium nitrate, and monocalcium superphosphate, are the main contributors to overall emissions across all treatments, according to a thorough analysis of emission sources. The second largest source is diesel fuel consumption, which is connected to the operation of machinery. Manure fertilizer comes next, followed by emissions from human labor, seed production, machinery use, and electricity. These results highlight how important farming techniques and nutrient management are to emission reduction plans. Potential approaches to reduce GHG emissions from wheat farming include increasing fertilizer application efficiency and implementing alternate fertilization processes. These findings support the wider use of sustainable farming practices to mitigate climate change issues while maintaining or increasing crop output.

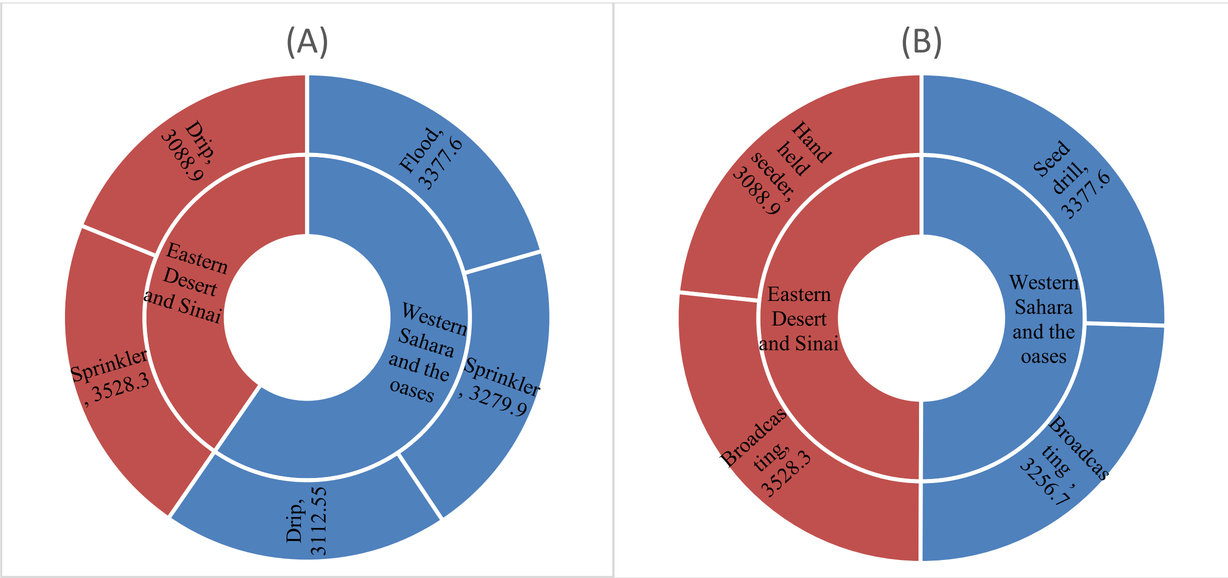

Fig. 5 Effect of irrigation system and cultivation methods on carbon footprint in wheat fields under two agro-ecological zones conditions in Egypt.

Table 2. Impact of Irrigation Systems and Cultivation Methods on Wheat Performance in Two Agro-Ecological Zones of Egypt

Zone	Irrigation system	Cultivation methods	Sowing season	Grain yield (t/ha)	Biomass (t/ha)	Plant height (cm)	Spike length (cm)	No. of grains /spike	1000 grains W. (gr)	WUE (Kg/m3)	Carbon footprint kg CO2 eq./ha
Western Sahara and the oases	Flood	Broad casting	2023-2024	6.43	25.66	105.6	9.6	33	48.19	0.84	3423.4
			2024-2025	6.87	27.46	115.5	11.3	29	49.08	0.90	3331.8
		Seed drill	2023-2024	8.09	29.38	105.4	12.1	34	50.12	1.06	3390.4
			2024-2025	7.59	31.44	117.2	10.5	30	51.34	1.00	3364.8
	Drip	Broad casting	2023-2024	8.33	33.05	120.3	12.2	33	52.01	1.34	3126.4
			2024-2025	8.17	32.25	116.8	11.6	31	51.23	1.32	3098.7
	Sprinkler		2023-2024	7.62	24.56	108.4	10.8	32	49.56	1.11	3310.3
			2024-2025	7.85	25.94	116.2	12.2	35	50.24	1.15	3249.5
Eastern Desert and Sinai	Drip	handheld seeder	2023-2024	7.78	22.13	108.5	11.6	26	51.07	1.40	3120.5
			2024-2025	7.43	21.91	102.4	10.8	27	49.87	1.32	3057.3
	Sprinkler	Broad casting	2023-2024	6.96	16.24	97.3	10.8	29	48.13	1.22	3580.2
			2024-2025	5.50	14.87	95.6	9.6	27	47.81	0.96	3476.4
LSD 0.05				0.22	1.11	0.89	0.43	2.33	0.87	0.67	36.38

IV. DISCUSSION

Gan *et al.* (2014) demonstrated that adopting alternative agricultural practices will increase crop yields while reducing carbon emissions by integrating improved farming practices and implementing alternative wheat production systems better suited to semi-arid environments. The results indicate that integrating improved farming practices, particularly fertilizer application control, allows wheat to absorb more carbon dioxide from the atmosphere than it actually emits during its production. They also noted that weather significantly influences both carbon emissions and carbon sequestration, which accounts for the differences observed between the two study zones, due to the difference in climatic conditions between them. On the other hand, both Gan et al. (2009) and Campbell et al. (2000) stated that increased crop productivity under more favorable weather conditions leads to increased production of crop residues and root biomass, which helps to enhance soil organic carbon.

The study results showed a direct relationship between nitrogen fertilizer inputs and carbon emissions, with each kilogram of nitrogen generating approximately 8.5 kilograms of carbon dioxide equivalent per hectare of emissions. This was not surprising, as inorganic nitrogen fertilizers contributed the largest share of total emissions attributed to crop inputs. These findings are consistent with those of numerous studies conducted in arid wheat-producing regions, on the semiarid Canadian prairie by Gan *et al*. (2012); Rajaniemi *et al*. (2011) on oats, barley, spring wheat, and rye production in Finland; Brock *et al*. (2012) on wheat produced in the Central Zone (East) of New South Wales of Australia; Berry *et al*. (2010) on wheat in the United Kingdom; and Li *et al*. (2010) in China.

Irrigation is one land management technique that has a big impact on the environment, The findings demonstrated that implementing effective and low-carbon irrigation techniques can lower energy use and carbon emissions. These findings are in line with the findings of **Qin *et al***. (2024), who demonstrated that implementing highly effective and low-carbon irrigation techniques can cut energy use in half and carbon dioxide emissions by 90%. The findings indicate that energy consumption and carbon dioxide emissions can be significantly reduced when utilizing drip irrigation in conjunction with electric pumping. Therefore, when evaluating strategies to minimize energy use and carbon dioxide emissions, the feasibility of adopting drip irrigation becomes a critical consideration to reduce greenhouse gases as well as reduce the carbon footprint in wheat fields as outlined by **Qin *et al*., 2024**.

According to **Qin *et al***. (2024), two water-efficient irrigation methods are sprinkler and drip. Nevertheless, the findings demonstrate that sprinkler irrigation systems do not lower irrigation-related energy consumption and CO2 emissions worldwide and have greater energy and CO2 emissions intensity than surface irrigation. As a result, drip irrigation systems should be prioritized when deploying farm infrastructure, which is in line with the results of our study. **Huifang *et al***. (2021) found that drip irrigation led to reductions in carbon emissions, as well as water and energy usage, by 60%, 19.47%, and 45%, respectively, compared to traditional flood irrigation.

V. CONCLUSION

The current study shows that while each farming technique has a unique impact on crop yield, combining those individually proven techniques in a methodical way can increase crop yield while also lowering the carbon footprint of crop production. In the field experiment, we identified and packaged a set of improved farming practices for spring wheat grown in two Egyptian agroecological zones: the eastern desert and Sinai (Al-tur) and the west desert and oasis (New Valley). These practices included (i) applying different irrigation systems and (ii) using different cultivation techniques. The results indicated that farming with a handheld seeder in conjunction with a drip irrigation system not only achieved the highest wheat productivity but also resulted in the lowest gas emissions and the lowest carbon footprint as well as the best water use efficiency.

REFERENCES

[1] Berry, P. M., Kindred, D. R., Olesen, J. E., Jorgensen, L. N., & Paveley, N. D. (2010). Quantifying the effect of interactions between disease control, nitrogen supply and land use change on the greenhouse gas emissions associated with wheat production. Plant Pathology, 59(4), 753-763.

[2] Brock, P., Madden, P., Schwenke, G., & Herridge, D. (2012). Greenhouse gas emissions profile for 1 tonne of wheat produced in Central Zone (East) New South Wales: a life cycle assessment approach. Crop & Pasture Science, 63(4), 319-329.

[3] Campbell, C. A., Zentner, R. P., Liang, B. C., Roloff, G., Gregorich, E. C., & Blomert, B. (2000). Organic C accumulation in soil over 30 years in semiarid southwestern Saskatchewan–effect of crop rotations and fertilizers. Canadian Journal of Soil Science, 80(1), 179-192.

[4] Gan, Y. T., Campbell, C. A., Janzen, H. H., Lemke, R. L., Basnyat, P., & McDonald, C. L. (2009). Carbon input to soil from oilseed and pulse crops on the Canadian prairies. Agriculture, Ecosystems & Environment, 132(3-4), 290-297.
[5] Gan, Y., Liang, C., Campbell, C. A., Zentner, R. P., Lemke, R. L., Wang, H., & Yang, C. (2012). Carbon footprint of spring wheat in response to fallow frequency and soil carbon changes over 25 years on the semiarid Canadian prairie. European Journal of Agronomy, 43, 175-184.
[6] Gan, Y., Liang, C., Chai, Q., Lemke, R. L., Campbell, C. A., & Zentner, R. P. (2014). Improving farming practices reduces the carbon footprint of spring wheat production. Nature Communications 5(1), 5012.
[7] Gan, Y., Liang, C., Hamel, C., Cutforth, H., & Wang, H. (2011a). Strategies for reducing the carbon footprint of field crops for semiarid areas. A review. Agronomy for Sustainable Development, 31(4), 643-656.
[8] Gan, Y., Liang, C., Wang, X., & McConkey, B. (2011b). Lowering carbon footprint of durum wheat by diversifying cropping systems. Field Crops Research, 122(3), 199-206.
[9] Huifang, Z. H. A. N. G., Rongqin, Z. H. A. O., & Liangang, X. I. A. O. (2021). The Effects of Irrigation Methods on Carbon Emission and Water-energy Consumption of Crop Production. Journal of Irrigation & Drainage, 40(12).
[10] IPCC, 2006. In: Eggleston HS, Buendia L, Miwa K, Ngara T, Tanabe K (eds), 2006 IPCC Guidelines for National Greenhouse Gas Inventories. National Greenhouse Gas Inventories Programme. Tokyo, Japan: IGES.
[11] IPCC, 2019. 2019 Refinement to the 2006 IPCC Guidelines for National Greenhouse Gas Inventories, Calvo Buendia, E., Tanabe, K., Kranjc, A., Baasansuren, J., Fukuda, M., Ngarize, S., Osako, A., Pyrozhenko, Y., Shermanau, P. and Federici, S. (eds). Published: IPCC, Switzerland. Volume 5, Chapter 6. https://www.ipcc.ch/report/2019-refinement-to-the-2006-ipcc-guidelines-for-national-greenhouse-gas-inventories/
[12] Kashyap, D., & Agarwal, T. (2021). Carbon footprint and water footprint of rice and wheat production in Punjab, India. Agricultural Systems, 186, 102959.
[13] Li, H., Qiu, J., Wang, L., Tang, H., Li, C., & Van Ranst, E. (2010). Modelling impacts of alternative farming management practices on greenhouse gas emissions from a winter wheat–maize rotation system in China. Agriculture, ecosystems & environment, 135(1-2), 24-33.
[14] Qin, J., Duan, W., Zou, S., Chen, Y., Huang, W., & Rosa, L. (2024). Global energy use and carbon emissions from irrigated agriculture. Nature Communications, 15(1), 3084.
[15] Rajaniemi, M., Mikkola, H., & Ahokas, J. (2011). Greenhouse gas emissions from oats, barley, wheat and rye production. Agron. Res, 9, 189-195.
[16] Rome, F. (2017). Food and Agriculture Organization of the United Nations (FAO); 2017. The future of food and agriculture: trends and challenges.
[17] Tubiello, F. N., Salvatore, M., Rossi, S., Ferrara, A., Fitton, N., & Smith, P. (2013). The FAOSTAT database of greenhouse gas emissions from agriculture. Environmental Research Letters, 8(1), 015009.
[18] Wiedmann, T., & Minx, J. (2008). A definition of 'carbon footprint.' Ecological economics research trends, 1(2008), 1-11.
[19] Zhang, D., Shen, J., Zhang, F., Li, Y. E., & Zhang, W. (2017). Carbon footprint of grain production in China. Scientific reports, 7(1), 4126.

International Journal of Environment, Agriculture and Biotechnology
Vol-11, Issue-3; May-Jun, 2026
Peer-Reviewed International Journal
Journal Home Page Available: https://ijeab.com/
Journal DOI: 10.22161/ijeab

Integrated Application of PGPR and Mycorrhizal Fungi for Improved Growth and Disease Suppression in Tomato

Sanjai Geetha Murugesan[1], Kalaiarasu S[2], Periyan Kannan[3], Ashmisha AJ[4], Nithish Kumar Karthikeyan[5], Gayatri B[6], Shiny Pears V[7]

[1,3,4,5,6,7] PhD Research Scholar, Department of Microbiology, Faculty of agriculture, Annamalai University, Chidambaram, Tamil Nadu, India
[2] Head and Professor, Department of Microbiology, Faculty of Agriculture, Annamalai University, Chidambaram, Tamil Nadu, India

Received: 29 May 2026; Received in revised form: 01 Jun 2026; Accepted: 03 Jun 2026; Available online: 10 Jun 2026

Abstract*— *The escalating cost of chemical fertilizers, along with their prolonged usage leading to depletion of natural soil nutrients and environmental pollution, has increased the importance and demand for biofertilizers. This study aimed to evaluate the efficacy of using Azospirillum sp., Pseudomonas and mycorrhizal fungi individually and in combination for promoting nitrogen fixation, phosphate solubilization, IAA production, siderophore production, suppression of pathogenic microorganisms and enhancement of plant growth. The PGPR microorganisms, namely Azospirillum sp., Pseudomonas, and mycorrhizal fungi were isolated from the rhizosphere soil of tomato cultivation fields in Cuddalore district. AZ-5 and AZ-2, two of the isolated Azospirillum sp. strains, exhibited the highest nitrogenase activity, with values of 225.75 nmol and 210.45 nmol, respectively. AZ-5 and AZ-2 had cellular nitrogen contents of 16.95 µg/g and 15.80 µg/g, respectively, which were greater than those of the other isolates. Among the isolated Pseudomonas strains, PS-4 demonstrated the greatest phosphate solubilization activity, registering 21.75 µg P/100 mL broth. This was followed by PS-2, demonstrated significant phosphate solubilization of 18.30 µg P/100 mL broth. AZ-5,2 and PS 4,2 also exhibited enhanced production of IAA and siderophores. Among the AM fungi, particularly Gigaspora sp., showed excellent phosphate mobilization activity of 24.10 mg/kg along with 74% root colonization, indicating its efficiency as a beneficial mycorrhizal fungus. In the controlled laboratory experiment using the petri plate method, the Pseudomonas isolate effectively inhibited the growth of Fusarium oxysporum with a growth inhibition zone measuring 41.21 mm. The efficient PGPR microorganisms, specifically Pseudomonas and Azospirillum sp., recorded superior nitrogen fixation, phosphate solubilization, IAA production, and siderophore production, in conjunction with the mycorrhizal fungus Gigaspora sp., which exhibited excellent phosphate mobilization activity, were applied both individually and in combination. These microbial treatments were prepared for seven experimental treatments under pot culture conditions. At the end of the experiment, the T6 treatment performed the best, recording 21.10 cm seedling length, 94.85% seed germination, and a vigour index of 2028.7, thereby producing healthy, disease-free, and high-quality tomato seedlings. Thus, it is confirmed that the integrated application of plant growth-promoting bacteria and beneficial mycorrhizal fungi leads to the production of high-quality tomato seedlings and improved seedling yield.

***Keywords*— Azospirillum sp, Pseudomonas, Mycorrhiza, Consortium, Fusarium, Biocontrol.**

I. INTRODUCTION

Agriculture is increasingly threatened by population growth, the ensuing climate change, and the escalating cost of inputs. These challenges are expected to be exacerbated by the deterioration of soil fertility, degradation of soil structure and water-related issues such as eutrophication brought by excessive leaching of nutrients (Wu & Ge, 2019). Furthermore, essential nutrients such as nitrogen, phosphorus, and potassium are derived from non-renewable resources. Among these, phosphorus is an important nutrient that plays a major role in plant growth, nucleic acid synthesis and ATP energy production (Bechtaoui *et al*., 2021). However, most of the phosphorus present in the soil exists in forms is not readily available for plant uptake, which is considered a major concern. The soil layer surrounding the roots of plants plays a major role in plant growth and nutrient availability. It is often referred to as the "second genome" of plants. The diverse types and large numbers of microorganisms present in the root region significantly influence plant growth and agricultural productivity (Berendsen *et al*., 2012). The root exudates released from root hairs contain sugars, amino acids, and organic acids that support the growth and activities of microorganisms. These substances provide a favourable environment for microbial multiplication. Due to this, the number and diversity of microorganisms are higher in the soil surrounding the roots (rhizosphere region) when compared to the soil away from the roots, where the microbial population is relatively lower (Reed & Glick, 2013). This type of plant–microorganism interaction has an influence on the quality, yield and growth of plants. Plant growth-promoting microorganisms enhance plant growth through both direct and indirect mechanisms. The direct mechanisms include nitrogen fixation and the solubilization of phosphorus and potassium. The indirect mechanisms include the production of disease-resistant substances and the production of siderophores (Colla, 2020). *Azospirillum sp.* is free living nitrogen fixing organism. Which fix the atmosphere nitrogen in rhizosphere region of vegetable crops. *Azospirillum sp.* produce phytohormone like IAA, an auxin hormone which promotes plant growth. The phytohormone improve plant tolerance to both biotic and abiotic stress (Sun *et al*., 2025). *Pseudomonas*, a plant growth-promoting bacteria, enhances plant growth through direct mechanisms such as phosphate solubilization and other beneficial processes, as well as indirect mechanisms like disease control. In particular, in tomato seedlings, it helps in control the fungal pathogen *Fusarium* through production antibiotic substances and enhancing the defense mechanism of the plant. They also activate and stimulate defense mechanisms. Through this process, the microorganism *Pseudomonas* play a major role in the biological control method, which is an important component of sustainable agriculture (Benchabane M, 2017). Not only bacteria, but also the fungal association known as VAM enhances plant growth under abiotic stress by facilitating the uptake of phosphorus, zinc, and certain other nutrients. It also absorbs water from regions that roots cannot reach, thereby promoting root growth, stem development, and the overall growth of the plant (Leuratti *et al*., 2025). Due to the high nutritional value of tomato, the demand from people and industries is naturally increasing. Furthermore, tomato seedlings are used as a model plant to study the interactions between plants and microorganisms (Quinet *et al*., 2019). Healthy tomato seedlings that are free from soil- and seed-borne diseases and enriched with adequate nutrients serve as an important foundation for improving tomato yield. In this research study, plant growth-promoting microorganisms such as *Azospirillum sp.* for nitrogen fixation, *Pseudomonas* for phosphate solubilization, *Fusarium* for inducing fungal disease interaction and VAM fungi for phosphorus mobilization were utilized in an attempt to produce healthy, nutrient-rich, and disease-free tomato seedlings.

II. MATERIALS AND METHODS

2.1 Collection of rhizosphere soil samples

Rhizosphere soil samples of tomato plants were collected from various regions of Cuddalore district and the plant growth-promoting microorganisms such as *Azospirillum sp.*, *Pseudomonas*, and VAM fungi (Vesicular Arbuscular Mycorrhiza) were isolated and studied.

2.2 Isolation and Enumeration of *Azospirillum sp.* and *Pseudomonas*

One gram (1 g) of sample was mixed with 100 mL of sterile distilled water and kept in an incubator shaker at 100 rpm for 30 minutes. From this suspension, serial dilution was carried out up to 10^{-6} dilution using test tubes. Subsequently, 1 mL aliquots from the 10^{-5} and 10^{-6} dilutions were taken and inoculated into NFB medium for *Azospirillum sp.* and King's B medium for *Pseudomonas*. A total of six plates were used, with three plates for each organism. Pure cultures of *Azospirillum sp.* and *Pseudomonas* were isolated using sub-streaking method. To confirm the isolates, several biochemical tests were performed.

2.3 Morphological and Biochemical Characteristics of *Azospirillum sp.*

2.3.1 Gram Staining

Gram staining was performed following the method of Gram C (1884) & boridge TJ (2001). A smear of the *Azospirillum sp.* culture was prepared on a clean glass slide using an inoculation loop. The smear was heat-fixed using a flame. The slide was then stained with crystal violet for 1 minute, followed by iodine solution for 1 minute. Decolorization was carried out using ethanol for 10–15 seconds and finally counterstained with safranin for 30 seconds. After each step, the slide was washed with distilled water. Finally, the stained slide was observed under a compound microscope using immersion oil.

2.3.2 Catalase Test

The catalase test was performed following the method described by (Cappuccino & Sherman, 2011). In this method, a smear of *Azospirillum sp.* culture was placed on a glass slide and a few drops of 3% hydrogen peroxide (H_2O_2) solution were added. The formation of bubbles indicated a positive catalase reaction, whereas the absence of bubbles indicated a negative result.

2.3.3 Methyl Red and Voges–Proskauer (MR–VP) Test

The MR–VP test was performed following the method described by Cappuccino & Welsh (2017) & Forbes *et al*., (2007). In this test, *Azospirillum sp.* culture was inoculated into MR–VP broth and incubated at 28°C for 48 hours. For the Methyl Red (MR) test, a few drops of methyl red indicator were added to the broth culture. The appearance of a red color indicated a positive result. For the Voges–Proskauer (VP) test, a few drops of alpha-naphthol and KOH were added to the broth culture. The development of a pink color indicated a positive result.

2.3.4 Citrate Utilization Test

The citrate utilization test was performed following the method of Atlas RM (2004) & Cheesbrough (2005). In this test, Simmons citrate agar was prepared in test tubes in a slant form. The *Azospirillum sp.* culture was streaked onto the slant surface and incubated at 28–30°C for 48 hours. A color change of the medium from green to blue was considered a positive result.

2.4 **Morphological** and Biochemical Characteristics of *Pseudomonas*

After 24 hours of incubation, the King's B medium plates inoculated with *Pseudomonas* were observed and the colony characteristics such as size, shape, elevation, and color were recorded. The motility, endospore formation, and Gram reaction of *Pseudomonas* were confirmed using a compound microscope. Biochemical tests such as gelatin liquefaction, starch hydrolysis, carbohydrate utilization, oxidase test, and catalase test were performed following the methods of Aneja KR (2022) & Ramya rai & Rav (2024).

2.5 **Isolation** of Pathogen

The pathogen *Fusarium oxysporum* was isolated from infected tomato plant leaves showing disease symptoms. The diseased microbial culture was obtained from the Department of Plant Pathology, Annamalai University.

2.6 **Isolation** and Enumeration of AM Fungi

AM fungi were isolated by the sieving and decanting method Gerdemann & Nicolson (1963). The spores were further purified using sucrose density gradient centrifugation and counted with the help of a stereo zoom microscope Boyno *et al*., (2023). The number of spores present in 100 g of soil was calculated.

2.7 **Identification** of AM Fungi

The identification of AM fungi was carried out with the help of taxonomic keys Goswami *et al*., (2018).

2.8 **Purification** and Mass Multiplication of AM Fungi

The isolated and identified AM fungi were mass multiplied by the soil-funnel method using tomato seedlings as trap plants (Schenck NC, 1982). The AM fungal spores harvested along with roots and soil were allowed to attain complete maturity before being used for tomato seedling application. It is noteworthy that the entire process was completed over a period of three months.

2.9 **Isolation** and Screening of Plant Growth Promoting Rhizobacteria for Plant Growth Promoting Traits

The isolated microorganisms were screened for plant growth promoting characteristics such as nitrogen fixation, phosphate solubilization, mobilization and plant hormone and siderophore production.

2.10 Phosphate Solubilization

For the estimation of phosphate solubilization, 50 mL of Pikovskaya's broth were separately dispensed into three 250 mL Erlenmeyer flasks Nautiyal CS (1999). The isolated *Pseudomonas* culture was inoculated into each flask at the rate of 100 µl and the flasks were incubated for 7 days in a rotary shaker at 150 rpm and 30°C. After seven days of incubation, the broth culture was centrifuged at 5000 rpm for 20 minutes using a centrifuge machine. The phosphorus (P) released and dissolved in the liquid medium was estimated following the method described by Jackson (Jackson ML, 1973). Nitrogen fixation was carried out by the microorganism *Azospirillum sp.* The amount of nitrogen fixed was estimated by the Acetylene Reduction Assay (ARA) method. Each isolated *Azospirillum sp.* culture was grown in 100 mL of NFB medium in a 250 mL Erlenmeyer flask and incubated at 30°C for two days. The air present inside the Erlenmeyer flask was replaced with 10 % acetylene gas and the flask was incubated for 1 hour. After incubation, 1 mL of gas sample was analyzed using gas chromatography, and the concentration of ethylene gas produced was determined. The values were calculated using a standard calibration curve method Boddey *et al.*, (1987) & Reis *et al*., (2015). The nitrogen fixed by *Azospirillum sp.* was also estimated by the micro-Kjeldahl method described by (Humphries EC, 1956). In this method, *Azospirillum sp.* culture was grown in 100 mL of

NFB medium in a 250 mL Erlenmeyer flask at 30°C for 7 days. After seven days, 5 mL of the microbial culture along with 5 mL of medium, 5 mL of H_2SO_4, and 5 g of catalyst were added for nitrogen estimation. The mixture was combined with a catalyst mixture (K_2SO_4 : $CuSO_4$ in the ratio of 10:1) and digested until a clear solution was obtained. After cooling for a few minutes, the digested sample was transferred to a Micro-Kjeldahl distillation unit. Then, 10 mL of 40% NaOH was added and ammonia was liberated through steam distillation. The released ammonia was trapped in 20 mL of 2% boric acid solution. The ammonia absorbed in the boric acid solution was titrated against standard N/50 H_2SO_4 solution. From the titre value, the nitrogen content was calculated and expressed as the amount of nitrogen present in the microbial medium.

Total Nitrogen Content

Total Nitrogen (µg)} = r x 0.0028 x1000

Where: *r* = Titre value (mL of N/50 H_2SO_4 consumed), 0.00028 g nitrogen is equivalent to 1 mL of N/50 H_2SO_4 (Humphries EC, 1956).

2.11 Estimation of Phytohormone and Siderophore Production

L-tryptophan supplemented with broth was utilized for the estimation of IAA production Gordon & Weber (1951) and Mayer (1958). The Salkowski colorimetric assay method described by Bric was employed to evaluate the IAA production ability of *Pseudomonas* and *Azospirillum sp.* bacteria (Bric *et al*., 1991). To assess the IAA production potential of both bacteria, 50 mL of YMB medium supplemented with 1 g/L L-tryptophan was prepared in 250 mL Erlenmeyer flasks. The cultures were incubated in an orbital shaker incubator at 150 rpm and 30°C for 7 days. After seven days, the broth culture was centrifuged at 10,000 rpm for 10 minutes at 4°C using a centrifuge. The supernatant obtained after centrifugation was collected for IAA estimation. To this supernatant, 2 mL of Salkowski reagent containing 1 mL of 0.5 mol/L $FeCl_3$ and 49 mL of 35% $HClO_4$ was added and mixed thoroughly. The reaction mixture was incubated at 30°C for 30 minutes. subsequently, the absorbance of IAA was measured at 530 nm using a spectrophotometer and the IAA concentration was determined by reference to standard calibration curve.

2.12 Estimation of Siderophore Production

The siderophore production potential of *Azospirillum sp.* and *Pseudomonas* isolated was estimated according to the method described by Reeves *et al*., (1983). Distinct liquid media were prepared for siderophore production assays. Nitrogen-free bromothymol blue (NFB) broth was used for *Azospirillum sp.*, whereas minimal medium broth was employed for *Pseudomonas* isolates. For both bacterial cultures, 100 mL of the respective liquid medium was dispensed into 250 mL Erlenmeyer flasks and inoculated with 1 mL of bacterial culture. The flasks were incubated at 30°C for 7 days. After seven days, the broth cultures were centrifuged at 10,000 rpm for 20 minutes. The cell-free supernatant obtained after centrifugation was collected and used for siderophore estimation. For siderophore extraction, 20 mL of supernatant was mixed with 20 mL of ethyl acetate. Hathway reagent played an important role in siderophore estimation. The reagent was prepared by mixing 1 mL of 0.1 M ferric chloride and 1 mL of 0.1 N HCl in 100 mL of distilled water, followed by the addition of 1 mL of 0.1 M potassium ferricyanide. For the estimation of salicylate-type siderophore, 5 mL of assay medium was mixed with 5 mL of Hathway reagent. The absorbance was recorded at 560 nm using a spectrophotometer, and the siderophore concentration was determined by interpolation from a standard calibration curve.

2.13 Estimation of Catechol-Type Siderophore

For the estimation of catechol-type siderophore, 5 mL of assay medium was mixed with 5 mL of Hathway reagent. Absorbance was then recorded at 700 nm using a spectrophotometer, and the siderophore production was determined using standard calibration curve prepared using 2,3-dihydroxy benzoic acid (DHBA). In this method, the equivalent value for 1 mole of DHBA was considered as 0.75. The Catechol-Type siderophore production was finally expressed as ng/mL.

2.14 In Vitro Antifungal Activity

The antagonistic activity of *Pseudomonas* against *Fusarium oxysporum* was evaluated using well plate diffusion method described by Vincent JM (1947). *Fusarium oxysporum* and *Pseudomonas* were co-cultured on Potato Dextrose Agar (PDA) medium under dual-culture conditions. After incubation for 3 to 7 days, the zone of inhibition was measured and recorded.

2.15 Pot Culture Experiment

The pot culture experiment on tomato plants was conducted in the greenhouse of the Department of Microbiology, Faculty of Agriculture, Annamalai University, from December to January. The experiment was carried out using a Randomized Block Design (RBD) with seven different treatments. For this study, efficient *Azospirillum sp.* isolates showing high nitrogen fixation ability and efficient *Pseudomonas* isolates exhibiting phosphate solubilization, IAA production, and siderophore production were selected and prepared as separate liquid cultures. VAM fungi exhibiting efficient phosphate solubilization ability were prepared as separate inoculum cultures. Similarly, *Fusarium oxysporum*, the pathogenic fungus used for laboratory-level disease induction, was also prepared as a separate culture inoculum. The experiment was then arranged in a Randomized Block Design (RBD) with the following treatments: T_1 – *Pseudomonas,* T_2 – *Azospirillum sp.*, T_3 – VAM Fungi, T_4 – *Fusarium oxysporum*, T_5 – PGPR + AM Fungi + *Fusarium oxysporum,* T_6 – Consortium (PGPR + AM Fungi) , T_7 – Control. These treatments were subjected to experimental evaluation.

To determine the seed germination percentage, the method described by (Zhao *et al*., 2023) was followed by recording the number of seeds germinated daily. The seed germination percentage was calculated using the following formula:

$$GP = \frac{Number\ of\ total\ germinated\ seeds}{Total\ number\ of\ seeds\ tested} x100$$

The Seedling Vigour Index (SVI) was calculated using the seed germination percentage and the mean total seedling length. According to the method described by (Manjeet *et al*., 2020), the Seedling Vigour Index was calculated as:

Seedling Vigour Index = $G(\%)$ × Mean total seedling length The mean total seedling length was calculated as:

Mean total seedling length = Mean root length + Mean shoot length

III. RESULT AND DISCUSSION

Chemical and Microscopic Characteristics of *Azospirillum sp.* Microorganisms

3.1 Microscopic Characteristics

The *Azospirillum sp.* microorganism was identified as Gram-negative by Gram staining test. Based on microscopic observation, the shape and arrangement of the cells were studied. The cells appeared as rod-shaped and slightly curved rods. Cells were observed either singly or arranged in clusters. A tail-like structure called a flagellum was observed at the posterior end of each microorganism. This flagellum was confirmed to help in the movement of the microorganism and in colonizing specific sites. The Gram reaction and microscopic features observed in this study were consistent with the characteristic features of *Azospirillum sp.* microorganisms. The microscopic observations obtained in present study were in agreement with the findings reported by (Sulaiman *et al*., 2019).

3.2 Biochemical Characteristics of *Azospirillum sp.* Microorganisms

All five isolated *Azospirillum sp.* microorganisms showed positive results in the catalase test, indicating the presence of the catalase enzyme. The catalase enzyme is biochemically significant because it breaks down hydrogen peroxide (H_2O_2) into water (H_2O) and oxygen (O_2). This characteristic is considered significant in the identification and biochemical characterization of *Azospirillum sp.* microorganisms. The detailed biochemical characteristics of all isolates are presented in Table 1.

Azospirillum sp. isolates Az-1 and Az-2 showed positive results for the MR (Methyl Red) test, indicating their association with the butanediol fermentation process. The isolates Az-3, Az-4, and Az-5 exhibited positive results in the MR test. Among them, the microorganism Az-4 showed a negative result in the VP (Voges–Proskauer) test. Based on these findings, the isolates were confirmed to possess mixed acid fermentation characteristics. Except for Az-4, all the isolates showed positive citrate utilization test. This authenticated the utilization of citrate through the following enzymatic reaction:

Citrate → Pyruvate + Oxaloacetate

As a result of this reaction, the pH of the medium increased, causing the medium color to change from green to blue, indicating a positive result. The biochemical test results observed in this study were in agreement with the findings reported by (Rabara *et al*., 2023). Therefore, the isolates were confirmed as *Azospirillum sp.*

Table 1. Biochemical characterization of Azospirillum sp. isolates

S. No.	Isolate Code	Gram Staining	Catalase Test	Methyl Red (MR)	Voges-Proskauer (VP)	Citrate Utilization
1	Az-1	-ve	+	-	+	+
2	Az-2	-ve	+	-	+	+
3	Az-3	-ve	+	+	+	-
4	Az-4	-ve	+	+	-	+
5	Az-5	-ve	+	+	+	+

3.3 Microscopic Characteristics of *Pseudomonas*

Each *Pseudomonas* isolate formed flat, irregular, and shoe-shaped colonies on agar plate. The colonies exhibited smooth surface and translucent appearance. One of the characteristic features of *Pseudomonas sp.* is the siderophore production. This characteristic was confirmed by the fluorescence exhibited by the microorganisms. The yellowish-green colored colonies observed on the agar surface indicated the presence of *Pseudomonas sp.* and further confirmed siderophore production. These observations were in agreement with the previous findings (Reddy & Sudaramoorthi, 2026). Therefore, the isolate was identified as *Pseudomonas sp*.

3.4 Biochemical Characteristics of *Pseudomonas*

All the isolate yielded negative results upon Gram staining test, indicating their classification as Gram-negative bacteria. It was further observed that none of the showed endospores formation. The purified isolates tested negative for the Indole, MR (Methyl Red), and VP (Voges–Proskauer) biochemical assays. These findings confirmed the absence of mixed acid fermentation or butanediol fermentation biochemical pathways in the tested microorganisms. consequently, the microorganisms were determined to lack the enzymatic for these fermentative processes . A comprehensive summary of the biochemical characteristics is given in Table 2.

All the microorganisms designated Ps-1 through Ps-5 demonstrated positive reactions in the citrate utilization test, oxidase test and catalase test. These results confirmed the presence of citrate-utilizing enzymes activity, cytochrome-c oxidase, and catalase activity within the isolates. The biochemical profile of these isolates was consistent with the established characteristics of genus *Pseudomonas*. Furthermore, the results were in agreement with the findings reported by Labhasthrar *et al*., (2019). Therefore, the isolated microorganisms were conclusively identified as *Pseudomonas sp*.

Table 2. Biochemical characterization of Pseudomonas isolates

S. No.	Isolate Code	Gram Staining	Spore Formation	Indole Production	Methyl Red (MR)	Voges-Proskauer (VP)	Citrate Utilization	Oxidase Test	Catalase Test
1	Ps-1	-ve	-	-	-	-	+	+	+
2	Ps-2	-ve	-	-	-	-	+	+	+
3	Ps-3	-ve	-	-	-	-	+	+	+
4	Ps-4	-ve	-	-	-	-	+	+	+
5	Ps-5	-ve	-	-	-	-	+	+	+

3.5 Isolation of Nitrogen Fixing Plant Growth Promoting Rhizobacteria (PGPR)

The isolation of nitrogen fixing microorganisms facilitates the identification of highly efficient microorganisms through quantification of nitrogenase activity and cellular nitrogen content. The in vitro nitrogenase activity and cellular nitrogen content of *Azospirillum sp.* are given in Table 3. The nitrogenase activity of the five *Azospirillum sp.* isolates (Az-1 to Az-5) were recorded as follows Az-1 – 145.20 nmol, Az-2 – 210.45 nmol, Az-3 – 198.60 nmol, Az-4 – 170.30 nmol, Az-5 – 225.75 nmol (C_2H_4 μg^{-1} protein h^{-1}). Among these isolates, Az-5 exhibited the highest nitrogenase activity with (225.75 nmol C_2H_4 μg^{-1} protein h^{-1}) followed by Az-2 (210.45 nmol C_2H_4 μg^{-1} protein h^{-1}).

The cellular nitrogen content varied among the five microorganisms Az-1 – 11.35, Az-2 – 15.80, Az-3 – 14.90, Az-4 – 13.40, Az-5 – 16.95 µg/g cell weight. With respect to cellular nitrogen content, Az-5 recorded highest value of 16.95 µg/g cell weight, followed by Az-2 with 15.80 µg/g cell weight. The results of present study were consistent with those findings reported by (Naqqash *et al*., 2022), wherein the nitrogen-fixing efficiency of TN23 and TN09 isolates ranged from 138 to 143 nmol μg^{-1} protein h^{-1}.These findings corroborate the reported values, thereby validating the results of present study. The cellular nitrogen content recorded in the present study was also in accordance with values reported by (Hassain *et al*., 2014). where the cellular nitrogen content ranged from 10.33 to 13.11 µg/g. Thus, our research findings were further substantiated.

Table 3: Invitro nitrogenase activity and cell nitrogen content of Azospirillum sp. sp. obtained from rhizosphere soils of tomato

S. No.	Isolate code	Nitrogenase activity (nmol C_2H_4 mg^{-1} protein h^{-1})	Cellular nitrogen content (mg g^{-1} cell weight)
1	Az-1	145.20	11.35
2	Az-2	210.45	15.80
3	Az-3	198.60	14.90
4	Az-4	170.30	13.40
5	Az-5	225.75	16.95
SED		2.10	0.18
CD (p=0.05)		4.25	0.40

Table 4: Phosphate solubilizing potential of Pseudomonas isolates

s.no	Isolate code	Phosphate solubilization (mg P/100 mL broth)	Solubilization index	Final pH of medium
1	Ps-1	12.45	2.10	5.8
2	Ps-2	18.30	2.85	5.2
3	Ps-3	15.60	2.40	5.5
4	Ps-4	21.75	3.10	5.0
5	Ps-5	10.20	1.95	6.0
SED		0.85	0.12	0.08
CD (p=0.05)		1.75	0.25	0.15

3.6 Assessment of Phosphorus Solubilization potential of *Pseudomonas* isolates

The phosphorus solubilization potential of *Pseudomonas* isolates was evaluated based on soluble phosphorus content, final pH of the medium, and solubilization index (SI). The quantitative values for phosphorus solubilization, solubilization index and final pH of the medium are summarized in Table 4. The phosphorus solubilization values of *Pseudomonas* isolates PS-1 through PS-5 were recorded as 12.45, 18.30, 15.60, 21.75, and

12.20 µg P/100 mL broth respectively. Among these isolates, PS-4 exhibited the highest phosphorus solubilization capacity (21.75 µg P/100 mL broth), followed by PS-2 (18.30 µg P/100 mL broth), while PS-5 recorded the lowest value (12.20 µg P/100 mL broth) . The solubilization index (SI) values were as follows: PS-1 – 2.10, PS-2 – 2.85, PS-3 – 2.40, PS-4 – 3.10, and PS-5 – 1.95. PS-4 and PS-2 recorded highest SI values of 3.10 and 2.85 respectively, PS-5 exhibited the lowest value of 1.95. It is noteworthy that the final pH of the medium and phosphorus solubilization were inversely correlated. Accordingly, the final pH values of the growth medium for isolates PS-1 to PS-5 were recorded as follows: PS-1 – 5.8, PS-2 – 5.2, PS-3 – 5.5, PS-4 – 5.0, and PS-5 – 6.0. Notably, PS-4 and PS-2 recorded

lower pH values of 5.0 and 5.2, indicating higher degree of acidic nature. The production of organic acids is considered a primary mechanism underlying phosphorus solubilization. These findings are consistent with those reports of (Xu & Chen, 2025) who demonstrated the phosphorus solubilization capability of *Pseudomonas* isolated reached 432.36 µg/L and 364 µg/L respectively attributed to production of organic acids and the consequent reduction in pH. Thus, our experimental results were clearly confirmed by their findings.

3.7 Production of Siderophore and IAA by Plant Growth-Promoting Microorganisms

Among the plant growth-promoting microorganisms, *Azospirillum sp.* isolates AZ-2 and AZ-5, and *Pseudomonas* isolates PS-2 and PS-4, which demonstrated superior performance, were selected for siderophore and IAA production studies. Siderophore and IAA production were detected at varying levels in all selected *Azospirillum sp.* and *Pseudomonas* isolates. The quantitative data on siderophore and IAA production are summarized in Table 5. Among the *Pseudomonas* isolates, PS-2 showed superior performance with the production of 3.10 µg mL⁻¹ catechol-type siderophore, 4.60 µg mL⁻¹ salicylate-type siderophore, and 58.20 µg/25 mL broth of IAA. PS-4 recorded the second highest values with 2.35 µg mL⁻¹ catechol-type siderophore production and 42.50 µg/25 mL broth. Among the *Azospirillum sp.* isolates, AZ-5 recorded the highest production, yielding

2.40 µg mL⁻¹ catechol-type siderophore, 4.10 µg mL⁻¹ salicylate-type siderophore, and 38.75 µg/25 mL broth of IAA. The isolate AZ-2 recorded 1.85 µg mL⁻¹ catechol-type siderophore,

3.20 µg mL⁻¹ salicylate-type siderophore and 31.40 µg/25 mL broth of IAA. collectively, isolates PS-2 and AZ-5 demonstrated highest production of siderophore and IAA, thereby confirming their efficiency as potential plant growth promoting microorganisms through enhanced iron acquisition and plant hormone biosynthesis. The findings of the present study are consistent with those observations of (Lenin G, 2012) who demonstrated that *Pseudomonas fluorescens* exhibited high levels of siderophore production, while *Azospirillum lipoferum* produced comparatively higher levels of IAA. These previously reported corroborate the results of present study. Three different arbuscular mycorrhizal fungi (AMF) were subjected to investigation in order to evaluate their phosphorus mobilization ability and rhizosphere soil colonization percentage. The plant-available phosphorus and the percentage of rhizosphere colonization are presented in the table 6. The plant-available phosphorus content ranged from 16.30 to 24.10 mg/kg of soil. Among these isolates *Gigaspora sp.* recorded the highest plant available phosphorus content (24.10 mg/kg of soil) and ranked first, followed by *Glomus sp.* with a value of 22.75 mg/kg of soil in second place. *Acaulospora sp*. recorded the lowest value of 16.30 mg/kg of soil. The root colonization percentages were recorded as follows: *Gigaspora sp.* – 74%, *Glomus* sp. – 70%, and *Acaulospora sp.* – 55%. The final results of our research were in agreement with the findings of the research article by (Parvin *et al.*, 2020). which reported that the fungi *Gigaspora margarita* and *Acaulospora laevis* showed efficient root colonization and phosphorus mobilization, thereby increasing plant yield by 143% and 125%, respectively. Thus, our research findings were further validated.

Table 5: Siderophore and IAA production by Azospirillum sp. and Pseudomonas isolates

Isolate	**Siderophore (Catechol type, µg mL⁻¹)**	**Siderophore (Salicylate type, µg mL⁻¹)**	**IAA production (µg 25 mL⁻¹ broth)**
Ps-4	3.10	4.60	58.20
Ps-2	2.35	3.80	42.50
Az-2	1.85	3.20	31.40
Az-5	2.40	4.10	38.75
SED	0.10	0.12	1.25
CD (p=0.05)	0.22	0.25	2.65

Table 6: Phosphorus mobilizing potential of mycorrhiza species

S. No.	**Mycorrhizal species**	**Available P (mg kg⁻¹ soil)**	**Root colonization (%)**
1	*Glomus sp.*	22.75	70
2	*Acaulospora sp.*	16.30	55
3	*Gigaspora sp.*	24.10	74
SED		1.05	2.10
CD (p=0.05)		2.30	4.50

3.8 Evaluation of Biological Control Agents Against Plant Pathogens Under Laboratory Conditions

Under laboratory conditions, the microorganism *Pseudomonas* effectively controlled the plant pathogen *Fusarium oxysporum* in Petri plates. The agar well diffusion method was employed to assess antifungal activity of *Pseudomonas* microorganism against the test pathogen. The *Pseudomonas* isolate inhibited the mycelial growth inhibition zone of 41.7 ±

2 mm against *Fusarium oxysporum* on agar plates. These results confirmed that *Pseudomonas* possesses significant biocontrol potential against plant pathogenic fungi. These results were consistent with the findings of the research article by Chinmay *et al*., (2024) which reported that *Pseudomonas fluorescens* effectively controlled *Fusarium oxysporum* with a growth inhibition value of 36.3 ± 4 mm. Therefore, the results of present study is confirmed by previous studies chinmay *et al*., (2024)

3.9 Effect of Plant Growth Promoting Rhizobacteria (PGPR) and Arbuscular Mycorrhizal (AM) Fungi on Seedling Growth

Microorganisms exhibiting superior plant growth promoting traits such as nitrogen fixation, phosphorus solubilization, IAA production, siderophore production, and antagonistic activity against *Fusarium oxysporum* were selected for the evaluation. Among them, *Pseudomonas*, *Azospirillum sp*., and AM fungi were used under controlled conditions to evaluate their effect on the growth of tomato seedlings. The observations recorded at the initiation of the experiment and after 30 days are presented in Table 7.

Seven different treatments were imposed as follows:

T1 – *Pseudomonas*, **T2** – *Azospirillum sp.* **T3** – Mycorrhiza, **T4** – *Fusarium oxysporum,* **T5** – Consortium (T1 + T2 + T3) + *Fusarium oxysporum* **T6** – Consortium alone, **T7** – Control

The values recorded for seedling height, seed germination percentage, and vigour index for treatments T1 to T3 were as follows: T1 – 14.25 cm seedling height, 72.40% seed germination, 1031.4 vigour index (VI) ,T2 – 12.80 cm seedling height, 68.30% seed germination, 874.2 vigour index (VI) ,T3 – 15.62 cm seedling height, 75.20% seed germination, 1173.1 vigour index (VI) The values were recorded as follows: T4 – 9.15 cm, 45.60%, 612.3 VI ,T5 – 29.20 cm, 88.50%, 1785.6 VI ,T6 – 21.40 cm, 94.80%, 2028.7 VI

,T7 – 10.80 cm, 52.70%, 533.5 VI . Among these treatments, T6 exhibited superior performance with seedling height of 21.40 cm, 94.80% seed germination, and a vigour index

(VI) of 2028.7. This was followed by T5 (microbial Consortium + *Fusarium oxysporum*), which recorded 19.20 cm seedling growth, 88.50% seed germination, and a vigour index of 1785.6, ranking next to T6. These results confirmed that the T5 treatment effectively controlled *Fusarium* disease and promoted healthy tomato seedling growth. In contrast, T4 (*Fusarium oxysporum*) showed only 9.15 cm seedling length, 46.60% seed germination, and a vigour index of 612.1, indicating that the fungal pathogen severely affected the growth and vigour of tomato seedlings. Thus, the consortium containing *Pseudomonas*, *Azospirillum sp.*, and mycorrhizal fungi played an important role in enhancing plant growth through phosphate solubilization, IAA production, and siderophore production. It was clearly demonstrated that these microorganisms contribute significantly to improve soil structure and soil fertility by reducing the use of chemical fertilizers. They also play an important role in enhancing plant tolerance against biotic and abiotic stresses and help in sustaining long-term soil productivity and crop health. The results obtained in our study were in agreement with the findings of researchers zeng *et al*., (2025) & widawati *et al*., (2018) who reported that plant growth-promoting microorganisms such as PGPR and AM fungi, when used as biofertilizers, enhanced seed germination percentage, shoot length (15.67 cm), and vigour index (2127.20). Their study also confirmed that these beneficial microorganisms stimulate root and shoot growth, suppress plant pathogens, and facilitate the production of healthy and high-quality tomato seedlings.

Table 7: Effect of plant growth promoting rhizobacteria inoculation of seedling height, Germination % and vigour index

Treatment	Seedling Height (cm)	Germination (%)	Vigour Index
T1 – *Pseudomonas*	14.25	72.40	1031.4
T2 – *Azospirillum sp.*	12.80	68.30	874.2
T3 – Mycorrhiza	15.60	75.20	1173.1
T4 – *Fusarium oxysporum*	9.10	45.60	612.3
T5 – Consortium + *f. oxysporum*	19.20	88.50	1785.6
T6 – Consortium alone	21.40	94.80	2028.7
T7 – Control	10.20	52.30	533.5
SED	1.35	4.20	18.5
CD (p = 0.05)	2.80	8.95	38.4

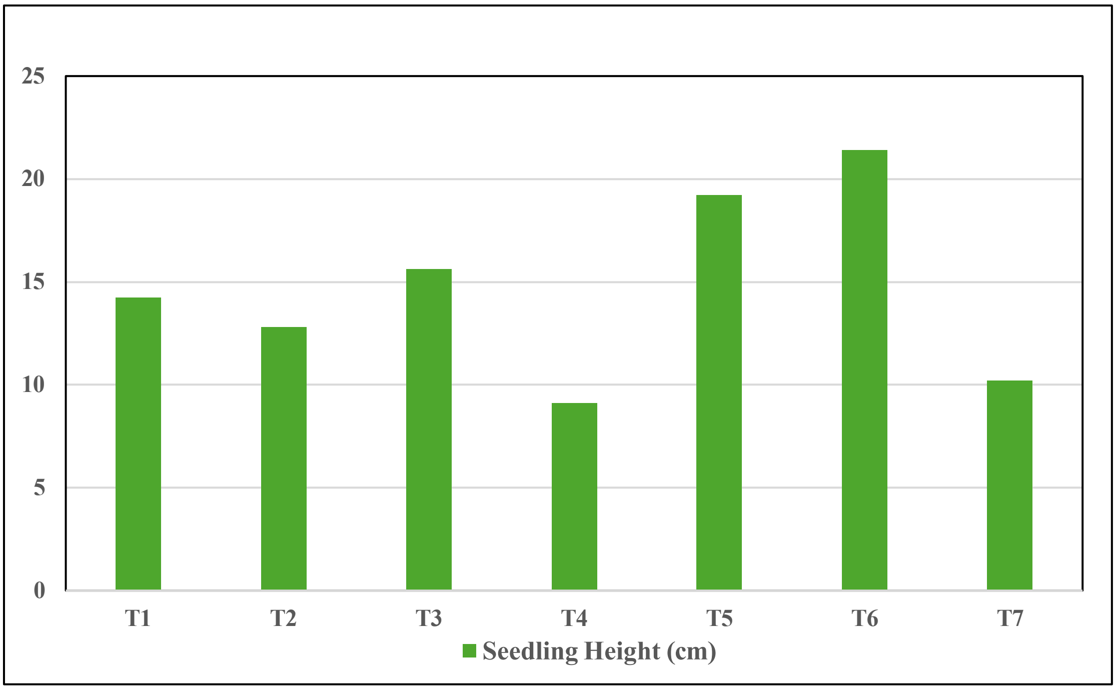

Bar graph 1. Effect of different treatments (T1-T7) on seedling height (cm)

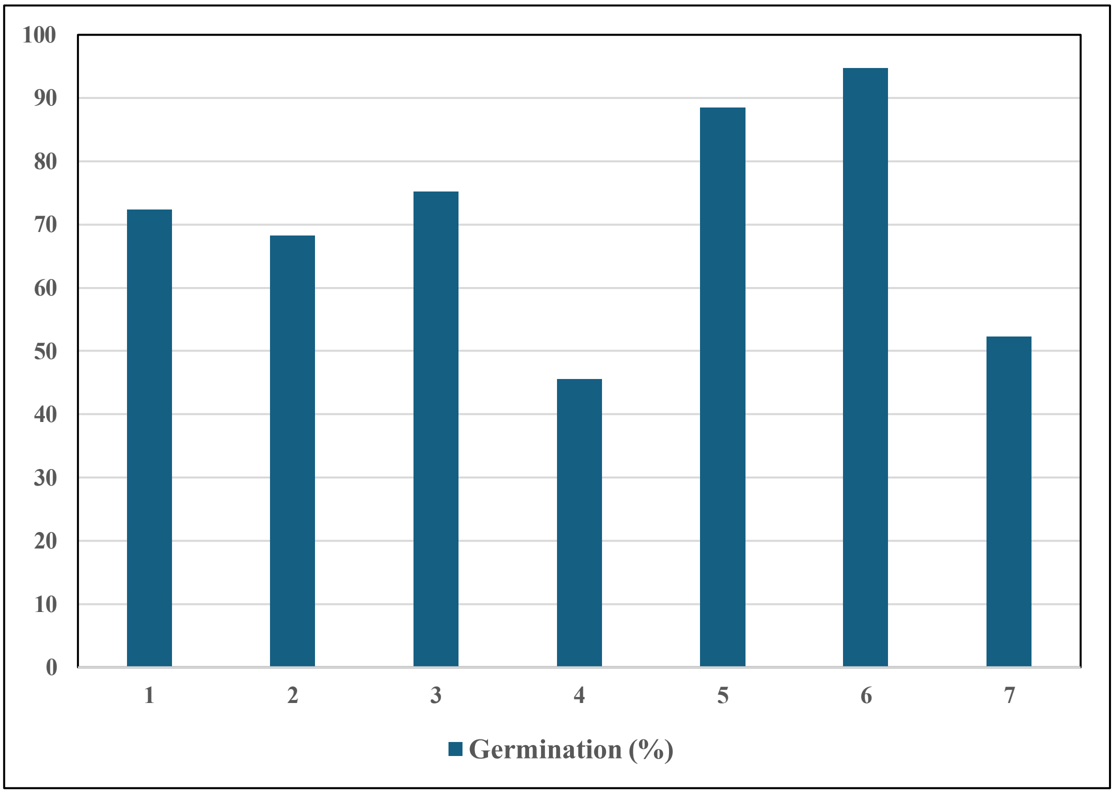

Bar graph 2. Effect of different treatments (T1-T7) on germination %

Bar graph 3. Effect of different treatments (T1-T7) on vigour index

Fig 1. Evaluation of microbial consortium on tomato plant growth under pot culture experiment

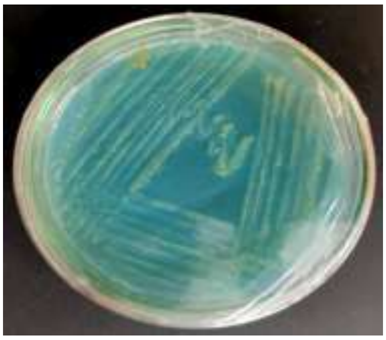

Fig2.Azospirillum sp. sp.

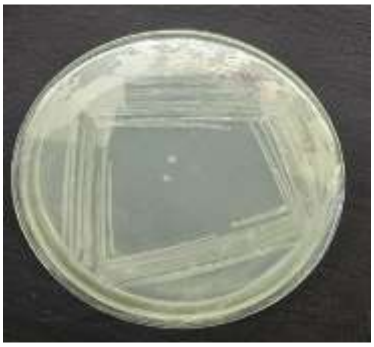

Fig3.Pseudomonas sp.

Fig4.Fusarium sp

IV. CONCLUSION

Excessive use of chemical fertilizers and fungicides increases soil acidity, leading to root scorching, unavailability of essential micronutrients, toxic effects, and dissolution of heavy metals in the soil. Similarly, the overuse of fungicides adversely affects beneficial mycorrhizal fungi, which are important for water absorption and nutrient uptake. The beneficial functions of mycorrhiza, such as supplying nutrients to plants and providing resistance against harsh environmental conditions like drought and salinity stress, are also greatly reduced. "From the results of our study, it is evident that reducing the use of chemical fertilizers and chemical fungicides, while properly utilizing natural biofertilizers and antagonistic microorganisms, can effectively enhance plant growth and control plant pathogens.

ACKNOWLEDGEMENT

I sincerely express my heartfelt gratitude to my parents, Mr. Murugesan and Mrs. Geetha, for their unwavering support, encouragement, and motivation throughout my research journey. I am also deeply grateful to my most valuable friends, S.R. Naveenkumar, R. Poornima, and Dr. S. Dharani, whose constant support, guidance, and encouragement played a vital role in the successful completion of my work.

REFERENCES

[1] Aneja KR. Experiments in microbiology, plant pathology and biotechnology. 6th ed. New Delhi: New Age International; 2022.
[2] Atlas RM. Handbook of microbiological media. CRC Press; 2004.
[3] Bechtaoui N, Rabiu MK, Raklami A, Oufdou K, Hafidi M, Jemo M. Phosphate-dependent regulation of growth and stresses management in plants. Front Plant Sci. 2021; 12:679916.
[4] Benchabane M. Activity of plant growth promoting rhizobacteria (PGPRs) in the biocontrol of tomato *Fusarium* wilt. Plant Prot Sci. 2017.
[5] Berendsen RL, Pieterse CMJ, Bakker PAHM. The rhizosphere microbiome and plant health. Trends Plant Sci. 2012;17(8):478-86.
[6] Beveridge TJ. Use of the Gram stain in microbiology. Biotech Histochem. 2001;76(3):111-8.
[7] Boddey RM, Knowles R. Methods for quantification of nitrogen fixation associated with Gramineae. Crit Rev Plant Sci. 1987;6(3):209-66.
[8] Boyno G, Demir S, Rezaee Danesh Y, et al. A new technique for the extraction of arbuscular mycorrhizal fungal spores from rhizosphere. J Fungi. 2023;9(8):845.
[9] Bric JM, Bostock RM, Silverstone SE. Rapid in situ assay for indoleacetic acid production by bacteria immobilized on a nitrocellulose membrane. Appl Environ Microbiol. 1991;57(2):535-8.
[10] Cappuccino JG, Sherman N. Microbiology: a laboratory manual. San Francisco: Pearson Benjamin Cummings; 2011.
[11] Cappuccino J. Microbiology a laboratory manual. Pearson; 2018 Jul 27.
[12] Cheesbrough M. District laboratory practice in tropical countries. Part 2. Cambridge: Cambridge University Press; 2005.
[13] Chinmay J, Viren Z, Amit P, et al. Impact of *Pseudomonas fluorescens* on field pathogen.
[14] *Acta Sci Microbiol*. 2024.
[15] Colla G. Toward a sustainable agriculture through plant biostimulants.
[16] Forbes BA, Sahm DF, Weissfeld AS. Bailey & Scott's diagnostic microbiology. 12th ed. Elsevier; 2007.
[17] Gerdemann JW, Nicolson TH. Spores of mycorrhizal Endogone species extracted from soil by wet sieving and decanting.
[18] Gordon SA, Weber RP. Colorimetric estimation of indoleacetic acid. Plant Physiol. 1951;26(1):192.
[19] Goswami BR, Parakhia MV, Golakiya BA, Kothari CR. Morphological and molecular identification of arbuscular mycorrhizal fungi. Int J Curr Microbiol Appl Sci. 2018;7(1):2336-47.
[20] Gram C. The differential staining of schizomycetes in tissue sections and in dried preparations. Fortschr Med. 1884;2(6):185-9.
[21] Hassain AJ. Effect of subsoiler tillage on breaking and shattering hardpan and infiltration rate in clay soils. Basrah J Agric Sci. 2014;27(2).
[22] Humphries EC. Mineral components and ash analysis. In: Modern methods of plant analysis. Berlin: Springer; 1956. p. 468-502.
[23] Jackson ML. Soil chemical analysis. New Delhi: Prentice Hall of India; 1973. p. 151-4.
[24] Labhasetwar AA, Bramhankar SB, Pillai TS, et al. Biochemical and physiological characterizations of *Pseudomonas* fluorescens. Int J Chem Stud. 2019;7(1):1785-8.
[25] Lenin G. IAA, GA and siderophore production by PGPR. Int J Pharm Biol Arch. 2012;3.
[26] Leuratti T, Fellin L, Michelon N, et al. Optimizing tomato

seedling production in the tropics: Effects of Trichoderma, arbuscular mycorrhizal fungi, and key agronomical factors. Agronomy. 2025;15(2):392.
[27] Manjeet, Mahavir, Anu, Singh VK, Verma PK. Character association and path analysis for seed vigor traits in sesame (Sesamum indicum L.).
[28] Mayer AM. Determination of indole acetic acid by the Salkowski reaction. Nature. 1958; 182:1670-1.
[29] Naqqash T, Malik KA, Imran A, et al. Inoculation with *Azospirillum sp.* spp. acts as the liming source for improving growth and nitrogen use efficiency of potato. Front Plant Sci. 2022; 13:929114.
[30] Nautiyal CS. An efficient microbiological growth medium for screening phosphate solubilizing microorganisms. FEMS Microbiol Lett. 1999;170(1):265-70.
[31] Parvin S, Van Geel M, Yeasmin T, et al. Effects of single and multiple species inocula of arbuscular mycorrhizal fungi on salinity tolerance of rice. Mycorrhiza. 2020;30(4):431-44.
[32] Quinet M, Angosto T, Yuste-Lisbona FJ, et al. Tomato fruit development and metabolism. Front Plant Sci. 2019; 10:1554.
[33] Rabara S, Vishwakarma N, Patel S. Isolation and biochemical identification of N2 fixing bacteria (*Azospirillum sp.* sp.). Curr Agric Res J. 2023;11(1).
[34] Ramya Rai M, Rao RB. Isolation of phosphate solubilizing microorganisms and their role in plant growth promotion. Bioscience. 2024;21(3):856-74.
[35] Reddy M, Sundaramoorthy S. Characterization of *Pseudomonas* spp. from brinjal rhizosphere. J Adv Biol Biotechnol. 2026;29(1):3557.
[36] Reed ML, Glick BR. Applications of plant growth-promoting bacteria for plant and soil systems. In: Applications of microbial engineering. 2013.
[37] Reeves MW, Pine L, Neilands JB, Balows A. Absence of siderophore activity in Legionella species grown in iron-deficient media. J Bacteriol. 1983;154(1):324-9.
[38] Reis VM, Baldani VL, Baldani JI. Isolation, identification and biochemical characterization of *Azospirillum sp.* spp. In: Handbook for *Azospirillum sp.* Cham: Springer; 2015. p. 3-26.
[39] Schenck NC. Methods and principles of mycorrhizal research. St Paul: APS Press; 1982.
[40] Sulaiman KH, Al-Barakah FN, Assafed AM, Dar BA. Isolation and identification of *Azospirillum sp.* and Azotobacter species from Acacia spp. Bangladesh J Bot. 2019;48(2):239-51.
[41] Sun W, Shahrajabian MH, Wang N. A study of the different strains of the genus *Azospirillum sp.* spp. on increasing productivity and stress resilience in plants. Plants. 2025;14(2):267.
[42] Vincent JM. Distortion of fungal hyphae in the presence of certain inhibitors. Nature. 1947; 159:850.
[43] Widawati S, Suliasih. The effect of plant growth promoting rhizobacteria (PGPR) on germination and seedling growth of Sorghum bicolor L. Moench. IOP Conf Ser Earth Environ Sci. 2018;166(1):012022.
[44]Wu H, Ge Y. Excessive application of fertilizer, agricultural non-point source pollution, and farmers' policy choice. Sustainability. 2019;11(4):1165.
[45] Xu T, Chen P. Isolation and characterization of phosphate solubilizing bacteria from phosphate tailing soil and their lead passivation potential. Geomicrobiol J. 2025;42(7):610-8.
[46] Zeng W, Xiang D, Li X, et al. Effects of combined inoculation of arbuscular mycorrhizal fungi and PGPR on seedling growth and rhizosphere microecology. Front Microbiol. 2025; 15:1475485.
[47] Zhao Y, Hong Y, Wang P, et al. Assembly of tomato rhizobacteria from different functional groups improves seedling photosynthesis and growth. Plants. 2023;12(23):4000.

International Journal of Environment, Agriculture and Biotechnology
Vol-11, Issue-3; May-Jun, 2026
Peer-Reviewed International Journal
Journal Home Page Available: https://ijeab.com/
Journal DOI: 10.22161/ijeab

Assessment of the *Amaranthus (Ramdana)* Value Chain and Market Potential in Chhattisgarh and Uttarakhand for Sustainable Value Addition and Nutrition Security

Ambarish Paikaray*, Subhashree Priyadarshini, Ambarish Ghosh

Faculty of Management Studies, The ICFAI University, Raipur, Raipur-Bhilai Road, Kumhari, Durg-490042, Chhattisgarh, India
Centre for Distance and Online Education, Andhra University, Visakhapatnam-530003, Andhra Pradesh, India
*Corresponding Author: ambarish.raipur@gmail.com

Received: 03 May 2026; Received in revised form: 01 Jun 2026; Accepted: 05 Jun 2026; Available online: 13 Jun 2026

***Abstract*— *Amaranthus (Amaranthus graecizans and Amaranthus caudatus L.), is a traditional climate-resilient crop grown in the hill areas of Uttarakhand and tribal plains and plateaus of Chhattisgarh. Amaranthus is a very nutritious crop and able to adapt to minimal input rainfed systems . However, it is underutilized and its consumption is mostly seasonal as part of traditional diets. The study focuses on the production, processing and marketing stages of the amaranthus value chain in the key production clusters of the two states. The study utilized a participatory mixed-methods approach including Focus Group Discussions, Key Informant Interviews and secondary data analysis from key stakeholders and institutions. The study identified major restrictions relating to production efficiency, processing facilities and market linkages and also highlights prospects for value addition and increased market integration. Strengthening the amaranthus value chain can boost farmers' income, promote nutrition-sensitive agriculture and build climate-resilient livelihoods in Uttarakhand and Chhattisgarh. Amaranthus is essentially a traditional climate tolerant field crop farmed by hill and tribal populations in hill area of Uttarakhand and Chhattisgarh State.*

Keywords*— *Value chain, Value addition, Focus Group Discussions (FGDs) and Key Informant Interviews (KIIs)

I. INTRODUCTION

Amaranthus (*Amaranthus graecizans* and *Amaranthus caudatus* L.), commonly known as *Ramdana, Rajgira, Chaulai, and Marsa*, is an important traditional crop cultivated across diverse agro-ecological regions of India, particularly in the states of Uttarakhand and Chhattisgarh. In Uttarakhand, amaranth is predominantly grown in the mid- and high-hill regions, where it has long been integrated into mountain farming systems and household diets, especially during fasting periods, religious festivals, and lean agricultural seasons. In Chhattisgarh, the crop is traditionally cultivated by tribal and smallholder farmers in the plains and plateau regions, where it serves as both a grain and leafy vegetable, contributing to food and nutritional security during periods of scarcity.

Historically, amaranthus has played a role as a staple food in indigenous diets, comparable to its importance in ancient civilizations such as the Aztecs. Its adaptability to marginal lands, tolerance to drought and low-input conditions, and suitability for rainfed agriculture make it a resilient crop for both hill and tribal farming systems. With increasing global recognition of amaranth as a "superfood" due to its superior nutritional profile—characterized by high-quality protein, essential amino acids, minerals, and dietary fiber—the crop holds significant potential for promoting nutrition-sensitive agriculture, livelihood security, and sustainable food systems in both Uttarakhand and Chhattisgarh.

Uttarakhand and Chhattisgarh are ecologically diverse states of India with rich biodiversity and strong dependence on plant-based resources for food and traditional medicine, particularly among rural and tribal communities (Prasad and Sharma 2018). Millets are climate-resilient food grain crops requiring minimal inputs and are widely used for food, beverages, and fodder (Bhat *et al*. 2024). Traditionally consumed as staple foods in India (Apetrei 2012), millets continue to play an important role in local food systems.

In Uttarakhand, millets such as barnyard millet (*Jhangora*), finger millet (*Mandua*), and amaranthus (*Chaulai/Ramdana*) are traditionally cultivated in hill regions (Raiger et al. 2023). In Chhattisgarh, millets including kodo, little millet, finger millet, and amaranthus are grown mainly in rainfed plains and plateau areas by tribal and smallholder farmers. Across both states, these crops contribute significantly to household nutrition, livelihood security, and climate-resilient agriculture.

Household consumption perspective in Uttarakhand and Chhattisgarh, amaranthus is primarily consumed seasonally and culturally, rather than as a daily staple such as rice or wheat. In Uttarakhand, consumption is largely associated with fasting periods, religious festivals, and special occasions, while in Chhattisgarh it is more closely linked to traditional tribal diets and subsistence food practices. On average, households in these states consume approximately 2–6 kg of amaranth grain per year, with higher consumption observed in hill communities of Uttarakhand and tribal regions of Chhattisgarh. Consumption of amaranthus leaves is more localized and seasonal, depending on home cultivation, wild or semi-domesticated availability, and local market access, and tends to be relatively higher in Chhattisgarh during the kharif season and periods of food scarcity.

Overall, per household consumption of amaranthus in both states remains modest and largely confined to traditional dietary patterns, specific communities, and seasonal availability. Despite its high nutritional value, amaranthus has not transitioned into a regular staple food and continues to play a supplementary role in household diets, as reflected in NSSO (2011) dietary data and subsequent state-level consumption and nutrition assessments.

II. TARGET AREA OF THE STUDY

The study focuses on major Amaranthus-growing regions of Uttarakhand and Chhattisgarh, where the crop is traditionally cultivated under rainfed and low-input systems. In Uttarakhand, the emphasis is on hilly and mid-hill districts, while in Chhattisgarh the focus is on tribal-dominated plains and plateau regions. These areas represent key production clusters where Amaranthus contributes to household nutrition, climate resilience, and livelihood security, and offers scope for value addition and market integration.

Objectives of the Study

1. To assess the Amaranthus value chain in Uttarakhand and Chhattisgarh, covering production, processing, and marketing stages.
2. To identify key constraints, gaps, and opportunities for value addition and improved market linkages.
3. To propose strategic interventions for strengthening the Amaranthus value chain, enhancing farmer income, and promoting value addition and consumption for improved nutritional security in both states.

III. MATERIALS AND METHODS

The present study adopted a participatory, mixed-methods research approach to assess the Amaranthus value chain in selected districts of Uttarakhand and Chhattisgarh. The mixed-methods framework was considered appropriate as it enabled the integration of quantitative and qualitative information for a comprehensive understanding of production, processing, marketing, and consumption dynamics within the Amaranthus sector. Similar participatory and mixed-method approaches have been successfully used in previous Amaranthus value chain and underutilized crop studies.

Study Area and Field Visits

Detailed field visits and stakeholder consultations were conducted in major Amaranthus-growing districts of Uttarakhand, including Almora, Chamoli, Pithoragarh, and Dehradun, and in Chhattisgarh, including Bastar, Kondagaon, Bilaspur, and Raigarh. These districts were purposively selected based on the prevalence of Amaranthus cultivation, traditional consumption practices, market availability, and the presence of local processing or value-addition enterprises. Previous studies have highlighted the importance of these regions for the cultivation and conservation of underutilized crops such as grain amaranth.

Data Collection

Both primary and secondary data sources were used in the study. Primary data were collected through household surveys, Focus Group Discussions (FGDs), Key Informant Interviews (KIIs), stakeholder consultations, and direct field observations. FGDs were organized with farmers, women's self-help groups, traders, and processors to understand production systems, indigenous knowledge, post-harvest handling, marketing channels, pricing mechanisms, and value-addition opportunities. KIIs were conducted with officials from the Departments of Agriculture and Horticulture, Krishi Vigyan Kendras

(KVKs), extension personnel, local market representatives, researchers, and entrepreneurs engaged in Amaranthus-based enterprises.

The participatory approach adopted in this study was guided by earlier research emphasizing farmer participation, community engagement, and stakeholder-driven assessment in underutilized crop development and value chain studies.

Secondary data were collected from government reports, Agriculture Department records, published literature, research papers, policy documents, and existing Amaranthus-based enterprises operating at state and national levels. Information regarding area, production, productivity, processing technologies, nutritional importance, market trends, and institutional support systems was compiled and reviewed. Previous studies on grain amaranth and underutilized crops were also referred to in order to contextualize the findings and identify research gaps.

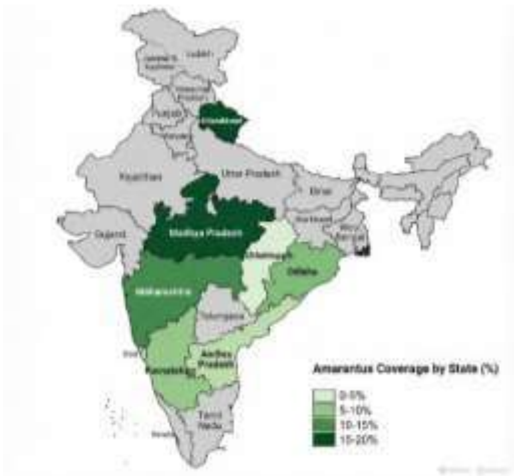

Value Chain Analysis

The Amaranthus value chain was analyzed as a sequence of interconnected activities including input supply, cultivation, harvesting, aggregation, storage, transportation, processing, marketing, distribution, and retailing. The study identified and mapped the major value chain actors, namely input suppliers, farmers, traders, processors, wholesalers, retailers, and consumers, along with supporting institutions such as technical agencies, financial institutions, cooperatives, research organizations, and government departments.

The functional linkages among actors, flow of products and information, marketing channels, and value addition practices were examined to identify bottlenecks and opportunities for strengthening the value chain. Earlier studies have emphasized the importance of integrated value chain analysis, stakeholder linkages, market development, and participatory assessment for enhancing the production and utilization of grain amaranth and other neglected crops.

Data Analysis

The collected data were analyzed using descriptive statistics, thematic analysis, and value chain mapping techniques. Quantitative information from surveys was tabulated and summarized using percentages, averages, and frequency distributions, while qualitative data from FGDs and KIIs were analyzed through thematic categorization and content analysis. The integrated analysis enabled the identification of production constraints, market barriers, institutional gaps, and opportunities for value addition, income enhancement, and sustainable livelihood development through the Amaranthus value chain in the study regions.

Table 1: Key Stakeholders for the Value Chain Study

Stakeholder	Parameters	Process of Data Acquisition
Farmers	Production practices, yield, input access, costs, prices, buyer relations	Structured Questionnaire, FGD
Input Suppliers	Seed varieties, fertilizer cost, availability, credit, service support	Structured Questionnaire
Traders/Aggregators	Price negotiation, storage, logistics, frequency of procurement, seasonality	Structured Interview
Processors/Millers	Milling capacity, machine types, losses, packaging, market linkages	Structured Checklist, Open-ended Interview
Retailers/Buyers	Buyer preferences, pricing strategy, branding feedback, shelf placement	Short Survey, Interview

The area under cultivation, production, and productivity of Amaranthus are presented in the table below. Unlike major millets, Amaranthus is cultivated on a relatively smaller scale and largely as a niche crop. However, as per available data from the Directorate of Economics & Statistics, the area and production of Amaranthus in India have shown stagnation or marginal fluctuations over the last five years, primarily due to its limited commercial cultivation and regional concentration. (Annual Report, 2022-23 DoA & FW)

Despite this, productivity levels of Amaranthus remain relatively stable, supported by its short crop duration, adaptability to marginal lands, and low input requirements. The average annual production of Amaranthus in India is estimated to be modest compared to Finger Millet, but the crop holds strong growth potential owing to rising health consciousness, demand for gluten-free and protein-rich foods, and increasing policy focus on nutri-cereals and climate-resilient crops.

Table 2: Amaranthus Production Area in Major Producing States (India) (Area in '000 Hectares)

State / UT	2020-21	2021-22	2022-23	2023-24	Share of India (%)
Uttarakhand	**72.0**	**74.5**	**76.0**	**78.2**	**19.8**
Madhya Pradesh	64.8	66.0	67.5	69.0	17.5
Maharashtra	58.2	59.6	60.8	61.5	15.6
Odisha	41.5	42.0	42.8	43.5	11.0
Karnataka	39.0	40.2	41.0	42.0	10.6
Andhra Pradesh	32.4	33.0	33.8	34.5	8.7
Chhattisgarh	**18.0**	**18.6**	**19.2**	**20.0**	**5.1**
All India	**326.0**	**333.9**	**341.1**	**348.7**	**100.0**

Source: DES, MoA&FW (2023); State Agriculture Departments; minor millet & pseudo-cereal aggregation.

Cultivation of Amaranthus in both Uttarakhand and Chhattisgarh is largely undertaken by small and marginal farmers under traditional mixed, rainfed, and subsistence farming systems. In Uttarakhand, the crop is predominantly grown on rainfed terraces in hill districts, while in Chhattisgarh it is commonly cultivated as an intercrop or short-duration crop during the kharif and rabi seasons, particularly in tribal and forest-fringe regions. Produce from both states is mainly sold through local haats, weekly shandies, and nearby town markets, providing farmers with supplementary income and simultaneously contributing to household food and nutritional security.

Table 3: Area under Amaranthus Cultivation in Major Districts of Uttarakhand

S. No.	District	Area under cultivation (Ha)			% of total UK (2023–24)
		2021–22	2022–23	2023–24	
1	Uttarkashi	3,450	3,600	3,750	22.8%
2	Chamoli	3,100	3,250	3,400	20.7%
3	Rudraprayag	2,250	2,400	2,550	15.5%
4	Bageshwar	3,700	3,900	4,050	24.6%
5	Tehri Garhwal	2,350	2,500	2,650	16.1%

Source: DES, MoA&FW (2024); State Agriculture Departments

The area under Amaranthus cultivation in Uttarakhand has shown a steady increasing trend during 2021–22 to 2023–24, with districts such as Bageshwar, Uttarkashi, and Chamoli together accounting for a major share of the total cultivated area, reflecting favorable agro-climatic conditions, traditional food habits, and suitability to rainfed farming systems. Similarly, in Chhattisgarh, Amaranthus is gaining importance due to its adaptability to low-input conditions, tolerance to moisture stress, and high nutritional value, making it well-suited to the state's rainfed plains and plateau regions.

With growing consumer demand for nutri-cereals, pseudo-cereals, and health foods, Amaranthus holds strong potential for value addition and market-led expansion in both states. Its integration into local value chains, tribal livelihood initiatives, and nutrition-focused programmes can further enhance farm resilience, dietary diversity, and income opportunities for small and marginal farmers across diverse agro-ecological regions.

Value Chain mapping

Table 4 : Value of Amaranthus at different stage actors

Actor	Product	Activity	Qty (kg)	Selling Price (₹)	Production / Purchase Cost (₹)	Gross Margin (₹)	Operational Cost (₹)	Net Margin (₹)	Net Profit (%)
Farmer	Amaranthus grain	Production	1	50	35	15	0	15	30.00%
Aggregator / Village Processor	Cleaned & de-husked Amaranthus	Aggregation + Cleaning + De-husking	1	55	48	7	1.5	5.5	10.00%
Wholesaler	Amaranthus grain	Bulk trading	1	62	55	7	1.0	6.0	9.68%
Retailer	Amaranthus grain	Sale to consumers	1	75	62	13	1.0	12.0	16.00%

The table-4 highlights how value and profits are distributed along the Amaranthus value chain across Uttarkashi, Chamoli and Tehri, where production and marketing conditions are broadly similar.

At the farmer level, Amaranthus grain is sold at around ₹50 per kg against a production cost of ₹35 per kg, yielding a net margin of ₹15 per kg and a net profit of 30 percent. This relatively high profitability reflects the low-input nature of Amaranthus cultivation in hill agriculture, with reliance on farm-saved seed, organic manure, and family labour. However, despite a good percentage margin, absolute farm income remains limited due to small landholdings and low marketable surplus.

Value-Added Products from Amaranthus

Value-added products are foods or ingredients developed from raw amaranth grain/flour that have enhanced nutritional, sensory or market value compared to unprocessed grain. Below are common types:

1. **Amaranth Flour Products**

Amaranth grains can be **milled or roasted then milled into flour**, which is used alone or blended with other flours such as wheat:

- **Bread & Baked product** – Bread, cakes, biscuits, cookies using amaranth flour or in blend with wheat flour
- **Pasta & Noodles** – Gluten-free pasta alternatives
- **Chapatis & Flatbreads** – Mixed flour breads with improved protein and mineral content
- **Weaning Foods** – Nutrient-rich flour for infant porridges and complementary foods

Benefits: Higher protein and mineral content than many cereals; suitable for gluten-free diets.

2. Popped Amaranth Snacks

- Popped Grain – Grain heated until it pops (like popcorn) and can be eaten as a snack or mixed with sweeteners
- Energy Bars & Granola – Popped amaranth combined with nuts, seeds, dried fruits

Benefits: Popping enhances texture and makes it a popular snack and breakfast cereal ingredient.

3. **Traditional Indian Value-Added Products**

Many traditional foods can incorporate amaranth flour or grains for better nutrition:

- **Cake with Amaranth Flour** – Where roasted amaranth flour is partially substituted to improve protein and mineral content
- **Besan Burfi (Sweet)** – With popped amaranth flour added for texture and nutrition
- **Coconut Ladoo** – Sweet balls enriched with amaranth flour
- **Cashewnut Burfi** – Nut-based sweet with amaranth added
- **Dosa / Pancakes** – Soaked or fermented amaranth grain incorporated into batter

Nutritional Effects: In these products, adding amaranth increases protein, fibre, iron, calcium and zinc compared to controls while preserving sensory acceptability.

Table 5: SWOT Analysis of the Amaranthus Value Chain

Strengths	Weaknesses
• Low-input, climate-resilient crop suited to hill agriculture and rainfed conditions. • Good nutritional profile (high protein, minerals), aligning with health-food demand. • Reasonable farmer profitability (%) due to low production costs and farm-savedseed. • Existing local knowledge and practices in cultivation and post-harvest handling. • Short crop duration, enabling flexibility and integration into mixed farming systems	• Small landholdings and low marketable surplus limit absolute farm income. • Weak aggregation and collective marketing in Chamoli and Tehri. • Minimal value addition (mostly cleaning/de-husking; little grading, branding, packaging). • Lack of quality standards and price discovery, leading to variable prices. • Limited access to working capital and modern processing equipment at village level
Opportunities	**Threats**
• Growing demand for health and nutri-cereals in urban and institutional markets. • Farmer aggregation through SHGs/CLFs to improve bargaining power and scale. • Cluster-level primary processing, grading, and packaging to capture higher margins. • Branding and niche positioning (organic/natural, hill produce) for price premiums. • Policy alignment with nutri-cereal promotion, climate-resilient agriculture, and livelihoods programs. • Direct market linkages (retail chains, e-commerce, institutional buyers).	• Price volatility and competition from other cereals and substitutes. • Market dependence on intermediaries, especially where collectives are weak. • Quality inconsistency due to traditional storage and lack of standards. • Labour shortages and climate variability affecting timely operations. • Limited consumer awareness in local markets, constraining premium pricing.

4. **Breakfast Cereals & Beverages**

- **Porridge** – Amaranth seeds cooked into hot cereal
- **Breakfast Blends** – Mixed with oats, puffed grains, and seeds
- **Beverages** – Amaranth flour used in nutritious drink blends

These harness the digestibility and nutrient profile of the grain.

5. **Oil and Nutraceutical Derivatives**

- **Amaranth Seed Oil** – Extracted oil with beneficial compounds such as **squalene**
- **Leaf Extracts & Supplements** – Bioactive compounds targeting health benefits (antioxidant, anti-inflammatory)

These are less common food products but are emerging markets in health foods and cosmetics.

REFERENCES

[1] Annual Report (2022-23): Department of Agriculture & FW (2022-23) ; Annual Report

[2] Apetrei C (2012) Food security and millet cultivation in Kumaon region of Uttarakhand. *Research Report for Gene Campaign*. 1-61.

[3] Bhatt S, Kumar A, Arunachalam A and Arunachalam K (2024) Ethnomedicinal Diversity and Traditional Knowledge System of the Jaunsari Tribe in Uttarakhand, Western Himalaya. *Proceedings of the National Academy of Sciences, India Section B: Biological Sciences*. 94(1): 177-192.

[4] Bisht A, Bisht A, Kamboj N and Kamboj V (2021). An overview of high valued medicinal plants from rich diversity of Himalayas. 82-95.

[5] DES, MoA&FW (2024); State Agriculture Departments; minor millet & pseudo-cereal aggregation.

[6] Harsh K., Shivani G., Neetika Kimta, Rajni Dhalaria, Eugenie Nepovimova, Daljeet Singh Dhanjal, Suliman Y. Alomarf, Kamil Kuca (2024); Amaranth and buckwheat grains: Nutritional profile, development of functional foods, their pre-clinical cum clinical aspects and enrichment in feed. Current Research in Food Science, (9), 2024, 100836.

https://wits.worldbank.org/trade/comtrade/en/country/ALL/year/2025/tradeflow/Imports/partner/WLD/product/

[7] ICAR-NBPGR (2023): Intensive Agriculture, Jan-Mar-2023, Special Issue on Millets-2023

[8] Joshi N and Verma KC (2020) A review on nutrition value of Amaranth (*Amaranthus caudatus* L.): The crop of future. *Journal of Pharmacognosy and* Journal of Pharmacognosy and Phytochemistry 2018; 7(2): 2258-2262

[9] MoA &FW (2018): Report of the Committee on Doubling Farmers' Income, Input Management for Resource Use Efficiency & Total Factor Productivity, Vol. VII

[10] National Sample Survey Office – NSSO (2011)

[11] NIFTEM: Detailed Project Report of Amaranthus Proces sing Unit. Retrieved 6, April, 2024 from https://niftem.ac.in/newsite/pmfme/wpcontent/uploads/2022/07/amaranthusdpr.pdf *Phytochemistry*, 9(4): 1111-1113

[12] Prasad C and Sharma RC (2018) Wild edible plant resources of Kedarnath valley, Garhwal Himalaya, India. *Indian Journal of Ecology*. 45(3): 433-444.

[13] Raiger HL, Mishra D, Jajoria NK, Deewan P and Dhaliwal YS (2023) Grain Amaranth: Nutrient Enriched Grain of Future. In All India Coordinated Research Network on Potential Crops ICARNBPGR, Pusa Campus, New Delhi.

[14] Srivastava., A., Snehi, S.K., Raj., S.K. (2022): Molecular detection and characterization of begomoviruses infecting Amaranthus, a protein-rich crop: Geminivirus : Detection, Diagnosis and Management: 25-32

International Journal of Environment, Agriculture and Biotechnology
Vol-11, Issue-3; May-Jun, 2026
Peer-Reviewed International Journal
Journal Home Page Available: https://ijeab.com/
Journal DOI: 10.22161/ijeab

Hydrochemical Assessment of Irrigation Water Quality in Haryana: Implications for Agricultural Sustainability and Future Research

Satish Manda[1]*, Sumit Kumar[1], Ajay Kumar[1], Shubhanjali Kori[2]

[1]Assistant professor, Maharana Pratap Horticultural University Karnal, Haryana, India
[2]Research Scholar, IIT Delhi, New Delhi, India
*Corresponding author: mandastsh@gmail.com

Received: 05 May 2026; Received in revised form: 30 May 2026; Accepted: 04 Jun 2026; Available online: 13 Jun 2026

***Abstract*— Haryana is one of India's most irrigation-dependent agricultural states, and the quality of irrigation water has become a central determinant to crop productivity, soil sustainability and long-term groundwater security. State-level and regional evidences indicates that irrigation water quality in Haryana is highly heterogeneous, with relatively better water in parts of the north and northeast, and severe salinity, sodium, nitrate, fluoride and chloride problems in substantial parts of the south, southwest, west, and central districts. Recent studies show that groundwater remains usable for irrigation over large areas in the state, but its suitability often depends on crop salt tolerance, soil drainage and other specific parameters like residual sodium carbonate (RSC), electrical conductivity (EC), magnesium hazard (MH) and sodium percentage. This study synthesizes recent evidences on irrigation water quality in Haryana and explains the hydrochemical basis of quality deterioration, evaluates consequences for soils and crops.*

***Keywords*— Haryana, irrigation water quality, groundwater, salinity, irrigation suitability, agriculture**

Introduction

Irrigated agriculture in Haryana underpins high yields of wheat, rice, mustard, cotton, maize, and horticultural crops. However, this success depends not only on the quantity of water available but also on its chemical quality. In irrigated systems—whether canal-fed or groundwater-based—poor-quality water can reduce infiltration, increase soil sodicity and salinity, disrupt nutrient uptake, and ultimately impair crop performance over time (Jadhav et. al, 2025). This makes irrigation water quality analysis essential for agricultural planning, especially in semi-arid and intensively cultivated regions where groundwater serves as a major buffer against rainfall variability and canal water shortages.

The state of Haryana presents a typical hydro-agricultural contrast, encompassing relatively fresh alluvial groundwater zones, canal-command areas, and extensive tracts where aquifers are affected by salinity and dissolved ions resulting from evaporation, geogenic mineral dissolution, reverse ion exchange, and agricultural or industrial contamination (Malik et al., 2023). A recent study by CCSHAU, Hisar revealed that only 31.83% of Haryana's groundwater falls under the "good quality" category suitable for irrigation of most crops, while 30.04% is marginally saline, 6.04% is saline, 19.50% is high-SAR saline, and 12.59% is sodic or highly sodic water (Mukesh "Only 31% Groundwater"). Despite irrigation suitability being better than drinking-water suitability in many local settings, Haryana remains one of the states with widespread groundwater contamination concerns. It is reported in a recent study that groundwater in several districts of southern, western, and central Haryana is saline or chemically stressed, with notable concerns related to fluoride, nitrate and chloride.

This study was carried out with three major objectives: first, to examine irrigation water quality in the context of Haryana's agro-hydrological conditions; second, to identify suitable hydrochemical parameters for evaluating irrigation water quality, including sodium adsorption ratio (SAR), residual sodium carbonate (RSC), sodium percentage (Na%), Kelly index, and permeability index; and third, to assess the agricultural implications of water quality and its effects on soil health.

Irrigation Infrastructure and Groundwater Reliance in Haryana

Haryana's agriculture is characterized by intensive cultivation, high cropping intensity, and extensive use of both canal water and groundwater for irrigation. In many rural and semi-urban areas, groundwater functions as a major resource where surface water access is inadequate or unreliable, which further increases the importance of understanding its suitability not only for drinking but also for irrigation. The state irrigation and water resources department itself highlights the institutional arrangements linked to water services and dedicated water quality testing laboratories, reflecting the operational importance of water-quality surveillance for water management in the state.

The agronomic significance of irrigation water quality is high in the state because Haryana supports water-demanding cropping patterns alongside growing concerns about aquifer stress and chemical deterioration. In areas where canal supplies are insufficient or spatially uneven, farmers often rely on tubewell water, including in districts where groundwater chemistry is variable. Under such conditions, the same water source may be acceptable for some salt-tolerant crops under well-drained soils but problematic for sensitive crops or poorly drained fields. This conditional suitability is a recurring feature in Haryana: it is reported that most groundwater in the districts of Ambala, Yamunanagar, Sonipat, Panipat, Karnal, and Panchkula is suitable for irrigation for semi-salt-tolerant crops, whereas districts such as Bhiwani, Sirsa, Hisar, Kaithal, Jhajjar, Palwal, and Rohtak show wide variability in irrigation rating. Such variability means that state-level averages can obscure local management risk, reinforcing the need for small-scale or aquifer-zone-scale mapping of irrigation water quality (Kumar et al, 2026).

Irrigation Water Quality: Parameters, Standards, and Agricultural Implications

Irrigation water quality refers to the chemical and physical properties of water that influence its suitability for crop growth, soil health, irrigation infrastructure, and the surrounding agroecosystem. Practically, irrigation suitability is not determined by a single parameter; it emerges from the interaction among various parameters—namely salinity, sodicity, alkalinity, specific ion toxicity, soil texture, drainage conditions, climate, and crop tolerance (Jadhav et. al, 2025) . Consequently, irrigation water that is considered safe in one agroecological setting may produce severe problems in another, underscoring the conditional nature of water quality assessment.

The most commonly used irrigation-water quality indicators include pH, electrical conductivity (EC), total dissolved solids (TDS), sodium adsorption ratio (SAR), residual sodium carbonate (RSC), percent sodium, chloride, bicarbonate, carbonate, nitrate, sulfate, calcium, magnesium, and magnesium hazard (Hemlatha et al., 2025).Each parameter reflects distinct hazards: EC mainly reflects salinity stress, SAR and percent sodium are linked to sodicity and infiltration decline, RSC indicates the tendency for calcium and magnesium precipitation with corresponding sodium hazard amplification, and chloride or boron may cause direct ion toxicity in sensitive crops . In Haryana specifically, RSC, salinity, chloride, fluoride, and nitrate have emerged repeatedly as major parameters of concern in water-quality reporting, particularly in districts where groundwater chemistry is variable.

Modern studies increasingly combine classical hydrochemical indices with spatial analysis, GIS, and composite water-quality indices such as groundwater quality index (GWQI), fuzzy groundwater quality index (FGWQI), or customized irrigation water quality indices (Suryawanshi et al., 2025). These tools are useful for communicating complex datasets to planners, although they should not replace parameter-specific agronomic interpretation because different hazards have different field implications (Gupta et al., 2024). The integration of spatial mapping with traditional indices enables more precise identification of problem zones, allowing for targeted management interventions that account for local soil texture, drainage capacity, and crop tolerance levels.

Hydrochemical Mechanisms Underlying Irrigation Water Quality Degradation in Haryana

Recent studies from southwestern Haryana provide an updated hydrochemical explanation for water-quality deterioration in the state. According to recent findings, the dominant hydrochemical facies include Ca-HCO_3 and Na-Cl types, representing recharge-dominated and salinity-affected conditions, respectively (Kumar et al, 2026). The same study linked water chemistry to water-rock interactions, evaporation dominance, and sodium-calcium reverse ion-exchange processes, with hardness strongly associated with magnesium, chloride, and calcium.

These mechanisms align with the expected scenario in semi-arid alluvial environments experiencing intensive groundwater use. Evaporation concentrates dissolved salts; mineral dissolution contributes calcium, magnesium, bicarbonate, and sulfate; and cation exchange enriches sodium in groundwater, especially when calcium and magnesium precipitate or are exchanged on clay surfaces.

In areas of intensive agriculture, anthropogenic contributions such as fertilizer application, irrigation return flow, and localized wastewater input further elevate nitrate and other ions.

The resulting hydrochemical problems are not uniform across the state. Fresh recharge zones and canal-influenced areas retain relatively lower salinity, while low-drainage or arid tracts with deeper water tables and evaporative concentration may shift toward saline-sodic signatures. This spatial differentiation is crucial for irrigation planning because a single recommendation for all districts is scientifically inappropriate and technically not viable. (Kumari and Rai, 2020)

Water Quality Indices and Parameters for Irrigation Suitability Assessment in Haryana

Research on Haryana's irrigation water quality commonly draws on hydrochemical sampling, laboratory analysis, classification diagrams, and irrigation suitability indices. Laboratory measurements typically include pH, EC, total dissolved solids, major cations and anions, and derived indices such as SAR, RSC, sodium percentage, permeability index, Kelly's ratio, magnesium hazard, and total hardness where relevant. These variables are then interpreted through established irrigation-water criteria and sometimes combined into composite indices.

pH and Alkalinity

The pH of irrigation water influences nutrient availability, carbonate-bicarbonate chemistry, and precipitation reactions in the soil-water system (Pati 539). Although pH alone rarely determines suitability, high alkalinity combined with bicarbonate and carbonate can intensify sodicity problems, especially when calcium and magnesium precipitate out of solution (Schiavon and Moore). In Haryana, this issue is best interpreted through residual sodium carbonate (RSC) rather than pH alone because carbonate chemistry drives the practical hazard for irrigation suitability (Kumari and Rai, 2020). RSC specifically accounts for the imbalance between carbonate/bicarbonate ions and calcium/magnesium, providing a more accurate assessment of sodicity risk than pH measurement alone. RSC has special relevance in northwestern India and particularly in Haryana because bicarbonate-rich waters can precipitate calcium and magnesium, leaving sodium to dominate the soil exchange complex. Reporting based on CGWB assessment found that, statewide, 69.52 percent of groundwater samples were safe for irrigation based on RSC values, 13.09 percent were marginal, and 17.39 percent were unfit for irrigation use. This statistic is one of the most policy-relevant indicators currently available for the state because it directly frames irrigation suitability in terms of a widely used agronomic hazard metric. When RSC values exceed 1.25 me L^{-1}, the water poses moderate to high sodicity hazards that can degrade soil structure and reduce infiltration capacity. The relationship between carbonate alkalinity and divalent cation precipitation is particularly critical in Haryana's semi-arid alluvial aquifers, where evaporative concentration further amplifies the sodicity hazard (Kumar et al., 2026).

Electrical Conductivity and Salinity

Electrical conductivity (EC) is one of the most important irrigation-water indicators because it reflects the total ionic concentration and therefore the salinity hazard imposed on plants and soils. Elevated EC reduces the osmotic potential of soil solution, making it harder for plants to extract water even when the soil appears moist. Reporting From CGWB related data for Haryana highlighted that groundwater in several districts is saline and that at locations where EC exceeds 5000 µS/cm, such water is not suitable for regular irrigation. The salinity of water is checked through its electrical conductivity, where low conduction shows low salinity, while high salinity was found scattered in Bhiwani, Faridabad, Gurgaon, Hisar, Jhajjar, Kaithal, Mahendergarh, Mewat, Palwal, Rewari, Rohtak, Sirsa, and Sonepat districts.

Sodium Hazard and SAR/Percent Sodium

High sodium relative to calcium and magnesium degrades soil structure by dispersing clay particles, reducing aggregate stability, and decreasing infiltration and hydraulic conductivity. Recent Haryana research indicates that isolated zones with elevated percentage of sodium may create sodicity and permeability risks even when broader regional irrigation suitability seems acceptable. Approximately 19.50% of Haryana's groundwater is classified as high-SAR saline water, while 5.67% is slightly sodic, 1.66% is sodic, and 5.26% is highly sodic. It is important because a water source that appears only moderately saline may still be damaging if its sodium proportion is high.

Chloride, Nitrate, and Fluoride

Although chloride, nitrate, and fluoride are often discussed primarily in the context of drinking-water safety, they also matter for irrigation systems. Chloride contributes to salinity and can produce specific toxicity in sensitive crops, nitrate can indicate agricultural contamination and alter nutrient balances, and fluoride may accumulate in certain soils or affect overall water-use desirability. In Haryana, high fluoride and nitrate have been repeatedly reported in multiple districts, while chloride concentrations above 1000 mg/L have been observed in isolated locations in Sirsa, Hisar, Bhiwani, Mahendragarh, Mewat, Jhajjar, and Rohtak (CGWB 2022-23).

Magnesium hazard and permeability risks

The recent study for southwestern Haryana reported that isolated zones elevated magnesium hazard may pose irrigation concerns even where the majority of samples remain broadly suitable. Excess magnesium relative to calcium can worsen soil physical conditions and complement sodium-related structural decline in certain settings. For Haryana's fine-textured alluvial soils, this interaction deserves closer field validation because permeability loss can reduce irrigation efficiency and exacerbate secondary salinization.

Regional Disparities in Irrigation Water Quality and Associated Constraints in Haryana

Studies support a strong regional pattern in Haryana's irrigation water quality. Northern and northeastern districts such as Ambala, Yamunanagar, Karnal, Panchkula, Panipat, and Sonipat generally have better irrigation ratings, at least for semi-salt-tolerant crops on adequately drained soils, contrasting with southwestern, western, and some central districts showing much greater variability and persistent chemical stress (Ramprakash et al, 2023). The groundwater quality in north-eastern Haryana (Yamunanagar and Ambala) is predominantly '$Ca–Mg–HCO_3–Cl$' type, indicating relatively fresh recharge water.

The most commonly mentioned problem districts include Sirsa, Fatehabad, Hisar, Jind, Jhajjar, Bhiwani, Mewat/Nuh, Mahendragarh, Rewari, Faridabad, Palwal, Rohtak, and Kaithal, although the nature and degree of hazard differ among them. In these districts, salinity, RSC, nitrate, fluoride, and chloride occur in various combinations, and therefore suitability must be analysed parameter by parameter rather than through a single contamination label. Recent peer-reviewed work highlighted southwestern Haryana as a region where hydrochemical complexity is driven by both geogenic and anthropogenic processes (Kumar et al.).

By Evaluating all the scenarios, it can be inferred that Haryana contains three broad irrigation-water quality zones which are relatively favourable fresh-water zones, transitional mixed-quality zones, and saline/sodic risk zones. The boundaries between these zones are not administrative; they reflect hydrogeology, recharge conditions, canal influence, land use, and local management history. Therefore, district averages should not substitute for site-specific testing.

Soil and Crop Responses to Poor-Quality Irrigation Water

Soil Salinization and Sodification

The most serious long-term effect of poor-quality irrigation water is the gradual salinization and sodification of agricultural soils. Saline irrigation water increases the salt load in the root zone, while sodic water or water with high residual sodium carbonate (RSC) degrades soil structure by promoting clay dispersion, crusting, poor infiltration, and reduced aeration. In semi-arid regions, these effects intensify where natural leaching is limited and drainage is inadequate.

Crop Response and Yield Stability

Crop performance under poor-quality irrigation water depends on species, cultivar salt tolerance, growth stage, soil type, and management practices. Studies indicate that much of the groundwater in Haryana can still support crops such as wheat, mustard, rice, barley, and maize on well-drained soils, particularly when these crops are relatively salt tolerant. This does not mean that water-quality constraints are agronomically harmless; rather, it shows that farmers may maintain production under marginal water conditions by relying on tolerant crops and favourable field conditions (Choudhary and Mavi,2023).

Nutrient Imbalance and Soil Health Decline

High bicarbonate, sodium, chloride, and nitrate loads can alter nutrient availability and root-zone chemistry. Over time, degraded soil physical structure reduces fertilizer-use efficiency, hampers seedling emergence, and increases the energy cost of tillage and irrigation. These effects are especially relevant in Haryana's intensive cereal systems, where repeated use of marginal groundwater can create chronic rather than acute productivity loss.

Irrigation Efficiency and Infrastructure Effects

Poor-quality water can reduce irrigation efficiency by lowering infiltration, increasing surface sealing, and causing uneven wetting patterns in the field. In pressurized irrigation systems, dissolved solids and precipitation risks may also contribute to clogging or maintenance burdens, particularly where water treatment is inadequate. These issues matter not only for water-saving technologies but also for Haryana's broader push toward more efficient irrigation practices under growing water scarcity.

CONCLUSION

The quality of irrigation water in Haryana is best understood as a spatially heterogeneous and agronomically conditional resource rather than as a uniformly safe or unsafe input. Large parts of the state continue to use groundwater successfully for agriculture, but district- and site-specific hazards related to salinity, residual sodium carbonate, sodium dominance, nitrate, chloride, and fluoride remain significant.

For Haryana's future agriculture, the central challenge is not merely to expand irrigation access but to align water use with water quality and it requires routine monitoring, parameter-specific interpretation, localized advisory systems, crop planning based on quality constraints, conjunctive water use, drainage support and regulation of pollution sources. A robust research agenda for Haryana must integrate hydrochemical characterization, agronomic profiling, soil physical–chemical diagnostics, and high-resolution geospatial analytics to generate district-level, crop-specific guidelines for sustainable irrigation management. Such a multidisciplinary framework will enable precision targeting of water-quality mitigation strategies, optimize crop–water–soil interactions, and ensure long-term productivity of the state's intensive cereal systems under escalating water-scarcity and quality constraints.

REFERENCES

[1] Kumar, M., Verma, N. K., Singh, N., & Bhadwal, S. (2026). Groundwater quality assessment for irrigation and health in southwestern Haryana using hydrochemical and GIS methods. *Water Environment Research*, 98(3), e70340. https://doi.org/10.1002/wer.70340

[2] The Times of India. (2026, May 26). Only 31% groundwater in Haryana suitable for high-quality irrigation: Agri varsity study. The Times of India. https://timesofindia.indiatimes.com/city/chandigarh/only-31-groundwater-in-haryana-suitable-for-high-quality-irrigation-agri-varsity-study/articleshow/130656889.cms

[3] Central Ground Water Board (CGWB). (2025). Annual groundwater quality report 2025. Ministry of Jal Shakti, Government of India, New Delhi.

[4] Hemalatha, S., Ravanashree, M., Rajesh, G. M., Karthika, V., Arunkumar, N., Narmadha, R., Agila, C., & Suresh, R. (2025). Water quality index-based groundwater assessment for irrigation and drinking purposes in Erode District, Tamil Nadu, India. *Archives of Current Research International*, 25(9), 219–229. https://doi.org/10.9734/ACRI/2025/v25i91489

[5] Jadhav, A. B., Nale, V. N., & Potdar, D. S. (2025). Consequences of irrigation water and soil quality: An overview. *Asian Journal of Soil Science and Plant Nutrition*, 11(1), 435–453. https://doi.org/10.9734/AJSSPN/2025/v11i1494

[6] Daily Pioneer. (2025, July 3). Groundwater in many parts of Haryana's 13 districts unfit for drinking: CGWB report. Daily Pioneer. https://www.dailypioneer.com/2021/state-editions/groundwater-in-many-parts-of-haryana---s-13-districts-unfit-for-drinking--cgwb

[7] Suryawanshi, S. L., & Singh, P. K. (2025). GIS-integrated water quality indices for evaluating irrigation suitability of groundwater. *Journal of Agricultural Engineering,* 62(3), 737–752. https://doi.org/10.52151/jae2025623.1956

[8] Gupta, S. K., & Kumar, V. (2024). Critical review of irrigation water quality parameters for assessing sodium and bicarbonate hazards and gypsum application for quality improvement. *Journal of Soil Salinity and Water Quality,* 16(2), 194–206. https://doi.org/10.56093/jsswq.v16i2.158032

[9] Central Ground Water Board (CGWB). (2023). Groundwater year book/state groundwater report, Haryana (2022–23). North Western Region, Chandigarh, Ministry of Jal Shakti, Government of India.

[10] Choudhary, O. P., & Mavi, M. S. (2023). Advances in reclamation and management of sodic waters for irrigation. *Journal of Soil Salinity and Water Quality*, 15(1), 1–14.

[11] Malik, A., Katyal, D., Narwal, N., Kataria, N., Ayyamperumal, R., & Khoo, K. S. (2023). Sources, distribution, associated health risks and remedial technologies for inorganic contamination in groundwater: A review in specific context of the state of Haryana, India. *Environmental Research*, 236, 116696. https://doi.org/10.1016/j.envres.2023.116696

[12] Prakash, R., Kumari, S., Gagandeep, Kumar, S., Rajpaul, & Ankush. (2023). Characterization and spatial mapping of irrigation water quality and their effects on soil properties in Hathin Block of Palwal District, Haryana. *Journal of Environmental Biology*, 44(3), 310–316. https://doi.org/10.22438/JEB/44/3/SI-188

[13] Ramprakash, D., Kumar, S., Ankush, & Singh, C. (2023). Characterization and mapping of groundwater quality of Sonipat District in Haryana, India. *Journal of Soil Salinity and Water Quality*, 15(1), 38–45.

[14] Ramprakash, D., Kumar, S., & Kamaldeep. (2023). GIS mapping of groundwater quality for irrigation in Hisar District of Haryana, India. *Journal of Soil Salinity and Water Quality*, 15(1), 105–115.

[15] Alam, K., Goel, A., Ahamed, M., & Firoz. (2021). Analysis of groundwater quality in Karnal and Kurukshetra districts of Haryana for irrigation purposes. *International Journal of Water Resources Engineering,* 7(1).

[16] Kumari, M., & Rai, S. C. (2020). Hydrogeochemical evaluation of groundwater quality for drinking and irrigation purposes using water quality index in semi-arid region of India. *Journal of the Geological Society of India*, 95(2), 159–168. https://doi.org/10.1007/s12594-020-1405-4

[17] Gagandeep, Prakash, R., Kumar, S., Rajpaul, Satyavan, & Sharma, S. K. (2017). Ground water quality assessment for irrigation in Palwal Block of Palwal District, Haryana, India. *Journal of Applied and Natural Science*, 9(1), 274–281. https://doi.org/10.31018/jans.v9i1.1144

International Journal of Environment, Agriculture and Biotechnology
Vol-11, Issue-3; May-Jun, 2026
Peer-Reviewed International Journal
Journal Home Page Available: https://ijeab.com/
Journal DOI: 10.22161/ijeab

Waste-Derived Antibiofilm Strategies: A Review of Eco-Enzymes and Citrus Essential Oils

Gowri Priya G, Karthik V Rao*

Department of Biotechnology Mount Carmel College, Palace Road, Vasanth Nagar, Bengaluru, Karnataka, India
*Corresponding author

Received: 05 May 2026; Received in revised form: 30 May 2026; Accepted: 04 Jun 2026; Available online: 13 Jun 2026

Abstract*— Microbial biofilms are a major cause of persistent contamination in healthcare, food processing, and agricultural systems, and they significantly contribute to antimicrobial resistance (AMR). Conventional chemical disinfectants often show reduced efficacy against mature biofilms due to the protective extracellular polymeric substance (EPS) matrix and may also raise environmental concerns. This review discusses the antibiofilm potential of eco-enzymes, which are fermentation-derived liquids produced from citrus waste and other organic substrates containing organic acids, hydrolytic enzymes, and microbial metabolites. Additionally, citrus essential oils rich in bioactive terpenoids such as limonene, citral, and linalool are reviewed as sustainable antimicrobial alternatives. Eco-enzymes disrupt biofilms mainly through acidification and enzymatic degradation of EPS components, whereas citrus essential oils primarily exert antimicrobial effects through membrane disruption and quorum sensing inhibition. Both approaches demonstrate inhibitory effects against important biofilm-forming pathogens such as Staphylococcus aureus, Pseudomonas aeruginosa, Escherichia coli, and Candida albicans. Indirect evidence suggests a possible synergistic interaction between eco-enzymes and citrus essential oils, where EPS weakening by acidic fermentation products may enhance essential oil penetration into biofilms. However, significant research gaps remain, including limited standardization of eco-enzyme production, insufficient multispecies biofilm studies, and inadequate cytotoxicity evaluations. Future research focusing on optimized formulations and safety assessment may support practical applications of these waste-derived antibiofilm agents in food safety, healthcare, and environmental sanitation.

***Keywords*— Antimicrobial resistance; Biofilm; Citrus essential oil; Eco-enzyme; Quorum sensing**

HIGHLIGHTS

- Eco-enzymes derived from citrus waste exhibit antimicrobial and antibiofilm potential.
- Citrus essential oils disrupt microbial membranes and inhibit quorum sensing.
- Combined application may enhance EPS disruption and improve biofilm eradication.
- Waste-derived antibiofilm agents support sustainable biotechnology approaches.

Global burden of microbial infections and surface-associated contamination

Microbiological contamination of biotic and abiotic surfaces, remains challenging in the healthcare, food industry and laboratory (Tamburini et al., 2015). In food processing facilities and dairy companies, biofilm development on food processing areas creates a potential for foodborne diseases and financial loss. For example *Listeria monocytogenes* biofilm established on stainless steel equipment, gained resistance to regular sanitizing processes (Lee et al., 2019). In agricultural systems, the biofilms developing within irrigation pipes and at plant microbe interfaces facilitate the survival and spread of phytopathogen (Yao & Habimana, 2019). In households, ordinary surfaces are source for surface-bound microbes that cause infection, especially in the case of immunocompromised individuals (Dancer, 2014). The surface-associated microbial contamination increases burden of antimicrobial resistance (AMR), posing a serious threat to public health and food safety. In developing world such as India, inadequate sanitation infrastructure, ineffective waste management practices, and the extensive use of chemical disinfectants further increase this problem (Aslam et al., 2018). Together, these challenges emphasize the importance of efficient, safe and environmentally friendly approaches to regulate surface-associated microbial growth (Shree et al., 2022).

Biofilms as the dominant microbial lifestyle and a major contributor to antimicrobial resistance

In environment, microorganisms are found in the form of biofilm rather than as free-living planktonic cells (Muhammad et al., 2020). Biofilm is a specialized community of microbes, encased within extracellular polymeric substance matrix composed of proteins, lipids and extracellular DNA (Di Martino, 2018). The matrix facilitates surface adhesion, nutrient retention, intracellular communication by quorum sensing (QS) signals and protection against desiccation, shear forces, antibiotics and host immunity, through initial attachment, irreversible adhesion, microcolony formation, maturation and dispersal (Karygianni et al., 2020; Samrot et al., 2021). Microorganisms found in biofilms have altered physiological conditions, lower metabolism, and high tolerance levels (Rather et al., 2021). The efflux pump activation, quorum sensing-mediated regulation and horizontal gene transfer within dense microbial communities enhances resistance against antimicrobial agents. Chronic infections attributed to biofilms being increasingly identified as major contributors to treatment failure and persistent contamination in both clinical and industrial settings (Uruén et al., 2021).

Limitations of conventional chemical disinfectants in biofilm control

Although there is widespread dependence on chemical disinfectants to kill microbes but their efficacy against biofilm producing microorganisms remains limited (Maillard & Centeleghe, 2023). The commonly used disinfectants, includes chlorinated compounds, quaternary ammonium compounds, aldehydes are effective on planktonic cells. The physical and chemical barrier of biofilm matrix prevents diffusion of disinfectants, enabling microbial persistent within protected microenvironment (Koti et al., 2024). The reactive disinfectants could be inactivated by biofilms and resulting in sub-lethal concentration in biofilms due to diffusion concentrations in biofilms, that allows microorganisms in biofilms to survive after several disinfection processes (Maillard & Centeleghe, 2023).

Besides the reduced effectiveness, the other factor that contributed to the intervention of newer technologies to control biofilms was the prolonged, sublethal effect of chemical-based antimicrobial agents exerted selective pressure on tolerant microorganisms, that shows cross-resistance to clinical antibiotics (Liu et al., 2024). Certain limitations linked to the safety of the environment and human health further hindered the use of traditional chemical-based antimicrobial agents, that are known to produce toxic substances, exhibit low biodegradability and accumulate in ecological systems (Basiry et al., 2022; Verlicchi et al., 2015). The use of these substances further facilitates the research activities to discover new ways for the effective removal of biofilms with limited or negligible use of chemical-based antimicrobial substances in the future (Algburi et al., 2017).

Growing interest in green, waste-derived, and sustainable antimicrobial alternatives: Eco-Enzymes and Citrus Essential Oils

The conventional chemical disinfectants have significant limitations. Their reduced efficiency combined with the rise of antimicrobial resistance and environmental concerns, has gained interest in green, waste based antimicrobial solutions. These strategies support United Nations Sustainable Development Goals (SDGs) 3(health and well-being) and 12 (sustainable production and consumption) by promoting organic waste utilization, minimizing chemical residues and developing biodegradable agents with diverse resistance breaking mechanisms (Buffet-Bataillon et al., 2012; Carey & McNamara, 2015; Edis et al., 2024; Guedes et al., 2024).

Natural products from plant materials, microbial fermentation or food waste offer alternatives to their chemical diversity and broad-spectrum activity (Burtt, 2004; Daglia, 2012; Winkelstroter et al., 2024). The fermentation-based products and plant-based essential oils offer potential leads in the area of antimicrobial and antibiofilm activity, these strategies not only reduce environmental chemical load but also convert organic waste into bioactive antimicrobial agent (Nazzaro et al., 2013; Sar et al., 2023).

This review evaluates experimental studies on eco-enzymes and citrus-derived essential oils, with particular focus on their mechanisms of action, efficacy against biofilm-forming microorganisms and limitations associated with their practical application and also explore synergistic prospective of combining eco-enzymes with citrus essential oils as a sustainable strategy for biofilm control, highlights key gaps in the current literature and outline future directions for translating these green antimicrobial systems into real-world clinical, food, and environmental applications.

1. MICROBIAL BIOFILMS:

Definition and characteristics

Microbial biofilms are structured communities of microorganisms that adhere to biotic or abiotic surfaces and become encased in a self-produced extracellular polymeric substance (EPS) matrix (Donlan & Costerton, 2002). The EPS matrix constitutes a major fraction of the biofilm biomass, accounting for approximately 50–90% of the total organic matter, and serves as a protective scaffold that provides structural stability and enhances microbial survival under adverse environmental conditions (Flemming & Wingender, 2010; Flemming et al., 2007). This matrix safeguards the embedded cells against environment stress factors such as desiccation, attacks by protozoa and phagocytosis, ultraviolet radiation, and antibiotics (Flemming & Wingender, 2010; Karygianni et al., 2020).

It differs from planktonic bacteria, contributing to 60-80% of human microbial infections according to NIH (National Institute of Health) estimates. The features include heterogenous spatial distribution with growth of microcolonies in diverse phase of metabolism, well developed water channels to enable the nutrients and waste movement and phenotypic modulation like reduced growth, increased stress resistance and multidrug resistance in microbes. Beside physical shielding, there is close cell-cell contact and transformation of competent DNA promoting horizontal gene transfer (Yang et al., 2023). Biofilms enhance microbial survival through cooperative behaviours such as resource sharing, metabolic division of labour, and protection against desiccation, predation, and antimicrobials (Hall-Stoodley et al., 2004; Hobley et al., 2015; Flemming & Wingender, 2010). This sessile lifestyle enables persistence under nutrient limitation, pH stress, and immune pressure across ecosystems from rhizospheres to catheter lumens (Costerton et al., 1999; Donlan & Costerton, 2002; Liu et al., 2024).

Stages of biofilm formation

The development of the bacterial biofilm is a five-step cycle including reversible attachment, irreversible attachment, microcolony formation, maturation and dispersal (Ugwu et al., 2025).

Reversible attachment involves the planktonic to immobile transition phase, which occurs through reversible attachment that is mediated by weak physiochemical forces including van der waal, electrostatic forces and hydrophobic interaction (Zhao et al., 2023). The microbial cell motility depends on flagella, type lV pili or twitching motility to oppose the repulsive forces and cells attachment depends on the surface properties like hydrophobicity, roughness and charge and hydrodynamic condition and conditioning film (Saharan et al., 2024).

Irreversible attachment involves committed cells to grow on the surface through specific adhesion molecules, for example *Pseudomonas aeruginosa* contain type lV and *Staphylococcus aureus* contain MSCRAMMs. This activates c-di-GMP signaling cascades that suppress motility and stimulates EPS production (Zhao et al., 2023).

In the microcolony phase, microcolonies develop through clonal growth, aggregation of cells by surface array proteins and the production of the first EPS, which leads to the generation of 3D microcolonies (Sharma et al., 2023). The microbial cells shift from single surface colony to multi-cell aggregates results in the formation of the EPS, which provide initial biofilm structure for attachment and protection (Sharma et al., 2023). It is controlled by quorum sensing through N-acyl homoserine lactones (AHLs) in gram negative bacteria, luxl/R, rhll/R system in *Pseudomonas aeruginosa* and autoinducing peptides (AIPs) in gram positive, agr systems in *Staphylococcus aureus* (Omwenga & Awuor, 2024; Zhao et al., 2023). The Quorum sensing triggers EPS genes such as alginate, PIA, Pel/Psl for the EPS formation and reduces the motility due to increase in the c-di-GMP levels. Other QS controlled process include efflux pump activation that improves antibiotic resistance, production of virulence factors and biofilm development signals (Zhao et al., 2023). The cells produce amyloid fibers such as curli in *Enterobacteriaceae* species and Chaplin's in *Bacillus* species to maintain the structural integrity and promote eDNA (extracellular DNA) release by autolysis. At periphery microcolonies establish primary metabolic gradients by higher CO_2 consumption and sets stage for maturation (Sharma et al., 2023). This process establishes the multicellular biofilm phenotype for adherence, protection and physically distinguished from planktonic growth.

In maturation phase, the complexity in biofilm structure is maximum as EPS production increases resulting in the mushroom like morphology with stalks that bind to the surfaces and a dense cap that nurture high number of bacteria (Saharan et al., 2024; Sauer et al., 2022). The water channels interconnected penetrate throughout the structure and acts as a circulatory system for the transportation of oxygen and nutrients and removal of metabolic waste (Zhao et al., 2023). Water channel network arises due to the periodic cell movement and EPS modification catalysed by bacteria glycosidase activity. Fluid dynamics under shear force stabilizes the channel network and maintain the convective flow even under low nutrient condition (Sauer et al., 2022).

Dispersion phase is the final stage of the biofilm life cycle where the planktonic cells are released through matrix degrading enzymes such as dispersin B and rhamnolipids. The diespersin B is glycoside hydrolase that specifically degrade the PIA (polysaccharides intracellular adhesin) and rhamnolipids is a biosurfactant that reduces the EPS viscosity (Yang et al., 2023). This led to weakening the structural integrity of the biofilm matrix and reduces the cell-to-cell adhesion and widens the water channels leading to detachment of microcolonies respectively. The detached cells that are metabolically reactivated are capable of dispersing with help of motile genes for longer distance and establish biofilm colony at new site (Sharma et al., 2023)

The continuous cyclic process between biofilm and planktonic cells promotes localized persistence mediated by matrix protection and spatial dispersion through active movement This lifestyle contributes to chronic infection and frequent therapeutic failures despite of effective concentration of antibiotics (Yang et al., 2023).

Biofilm-associated resistance mechanisms

The biofilm gain tolerance against the antibiotics from 10 to 1000 folds more than the planktonic bacteria due to synergistic mechanism working at multiple levels (Yang et al., 2023). Hence, they associate with 60-80% chronic infection such as implant failure, cystic fibrosis and chronic wounds (Saharan et al., 2024).

Physiological diffusion barriers: EPS is negatively charged and positively charged antimicrobials such as gentamicin, polymyxins, and quaternary ammonium compounds bind to the EPS by electrostatic interaction. The polysaccharide accumulates at higher concentration in inner biofilm due to the reduced nutrient availability and slower diffusion 10000 to 1,000,000 times higher viscosity than water, blocking the drug penetration (Saharan et al., 2024).

Persister sub-populations: Biofilm has small subpopulation of persister cells found in the inner regions of biofilm with low oxygen and limited nutrients. This cell is formed through toxin-antitoxin systems that inhibit cell metabolism and gene function. Most antibiotics depend on metabolizing bacteria to be effective and persisters acts as reservoirs of infection when treatment is stopped (Zhao et al., 2023).

Overexpression of efflux pumps: In the bacterial transport, the resistance-nodulation-cells division (RND) superfamily transporters such as the MexAB OprM system of *Pseudomonas aeruginosa*) and AcrAB-TolC *Enterobacteriaceae* species actively expel β-lactams, fluoroquinolones, and tetracyclines (Sharma et al., 2023).

Universal stress responses: The stress exerted by the biofilm lifestyle also induces a variety of other global regulatory pathways, including RpoS and two-component systems. These responses contribute to enhanced DNA repair, antioxidant defenses, cell envelope modification, and β-lactamase production that together promote general tolerance to several classes of antibiotics (Yang et al., 2023).

Immune evasion: The EPS matrix protects surface antigens from the opsonisation by preventing phagocytosis, based on size and entrapping neutrophil extracellular traps in polysaccharide matrix (Saharan et al., 2024).

2. ECO ENZYMES

Fermentation-based products produced from organic waste are being explored due to their dual advantages of biological efficacy and environmental sustainability. Eco-enzymes are produced through anaerobic fermentation of household organic waste from citrus fruits and vegetable peel, jaggery and water. These are chemically complexed liquids containing various organic acids, alcohol, enzymes and plant derived secondary metabolites that formed during the microbial metabolism (Benny et al., 2023).

The fermented product allows the conversion of roughly 30-50% of household organic waste into value added products, hence reducing the landfill disposal, methane emission and nutrient loss. At the same time, this process produces bioactive liquids that find their application in cleaning, agriculture and antimicrobial control (Varshini & Gayathri, 2023).

Ecoenzyme production

The citrus peel has numerous microorganisms such as indigenous yeast and lactic acid bacteria (Kaur et al., 2010; Razola-Díaz et al., 2024). They are widely used due to the presence of fermentable sugars, pectin, organic acids and phytochemicals that supports the microbial growth and enzymes production during the fermentation (Julinar et al., 2025). During initial fermentation, pH is close to neutral, later the pH drops to acidic level between 60-90 days due to the collection of the organic acids (Permatananda & Pandit, 2023). The longer fermentation period allows the microorganisms to degrade the complex carbohydrate and convert sugars into organic acids and active metabolites (Vidalia et al., 2023).

Chemical components of eco enzyme

The mature fermented product is rich in organic acids and secondary metabolites as citric, lactic, acetic, oxalic acids and flavonoids, alkaloids, quinones, saponins and tannins respectively. The presence of organic acids is detected by high performance liquid chromatography (HPLC) and secondary metabolites through preliminary qualitative screening methods (Ismail et al., 2024). These compounds disrupt the microbial cell membrane and alter the protein function. In addition, it contains hydrolytic enzymes as amylase, cellulase and protease, that breaks the extracellular polymeric substances and weakening biofilm integrity (Sai et al., 2023).

Antimicrobial and antibiofilm evidences

Eco-enzymes are not only effective on planktonic bacterial growth but also with biofilm formation in both Gram positive and Gram-negative bacteria (Sai et al., 2023). The antimicrobial activity of eco enzymes have been reported based on invitro studies against wide range of microorganism including *Streptococcus mutans, Enterococcus faecalis, Lactobacillus acidophilus, Escherichia coli, Staphylococcus aureus, Salmonella typhi, Pseudomonas aeruginosa, Enterococcus species,* and fungal species such as *Aspergillus niger* and *Fusarium species,* (Julinar et al., 2025; Lubis et al., 2024; Sai et al., 2023; Vidalia et al., 2023). Eco enzyme effect on planktonic bacteria has been studied using minimum inhibitory concentration (MIC) and minimum bactericidal concentration (MBC) assays, agar well diffusion methods, and time-kill studies (Mavani et al., 2020; Sai et al., 2023).

Even though studies are limited on the antibiofilm activity of eco enzymes, existing evidence suggests that eco enzyme can disrupt the biofilm effectively. In *streptococcus mutans, Enterococcus faecalis* and *Lactobacillus acidophilus* biofilm is disrupted on exposure to eco enzymes in comparison to sodium hypochlorite. Antibiofilm activity of eco enzymes due to the presence of organic acids, hydrolytic enzymes and phytochemicals that degrades extracellular polymeric matrix and inhibit microbial growth (Sai et al., 2023). The reported antimicrobial and antibiofilm evidence of eco-enzymes derived from organic waste is summarized in Table 1

Table 1. Reported antimicrobial and antibiofilm activity of eco-enzymes derived from organic waste

Eco-enzyme substrate/source	Target microorganisms	Assays	Key findings	Proposed mechanism	Reference
Fruit peel eco-enzyme	*Enterococcus faecalis*	MIC, MBC, time-kill assay	Significant antibacterial effect observed	Organic acids + enzymatic degradation	Mavani et al., 2020
Citrus/mixed peel eco-enzyme	Oral pathogens (*S. mutans*, *L. acidophilus*)	Biofilm assay	Biofilm reduction reported	Acidification + EPS degradation	Sai et al., 2023
Household organic waste eco-enzyme	*E. coli*, *S. aureus*, *S. typhi*, *P. aeruginosa*	Agar well diffusion	Broad inhibition reported	Organic acids + phytochemicals	Vidalia et al., 2023
Organic waste eco-enzyme	*Fusarium* spp.	Antifungal growth inhibition	Growth suppression reported	Acidic metabolites	Lubis et al., 2024
Fruit peel eco-enzyme mixture	Gram-positive and Gram-negative bacteria	Antibacterial assay	Antimicrobial activity reported	Bioactive acids and metabolites	Tallei et al., 2023

3. CITRUS ESSENTIAL OILS

Plant essential oils overview

Plant essential oils are volatile and aromatic secondary metabolites synthesized by plants. These oils are extracted from leaves, flowers, seeds, bark and fruit peels of plants by physical method such as steam distillation, hydro distillation, cold pressing or supercritical CO2 extraction (Karne et al., 2023). Essential oils contain mixture of compounds such as terpenes, terpenoids and phenylpropanoids that are responsible for antimicrobial activity (Masyita et al., 2022). Due to their broad-spectrum antimicrobial activity and natural origin, essential oils are widely being researched and considered as future source of antimicrobial compounds and it is widely used in food preservation, cosmetics and healthcare and effective in preventing and controlling persistent biofilm (Rossi et al., 2022).

Citrus essential oil components

Citrus essential oils are mainly obtained from the fruit peel in Rutaceae family (*Citrus sinensis* for sweet orange, *Citrus limon* for lemon and *Citrus paradisi* for grapefruit) that constitute about 0.5-5% fresh fruit weight and contain high levels of monoterpene and oxygenated compounds (Lu et al., 2019). The bioactive compounds in oils are D-limonene, linalool, γ-terpinene, β-pinene, and citral, that are identified by gas chromatography and mass spectrometry (GC-MS)

(Nuryandani et al., 2024). Citrus essential oils are hydrophobic in nature hence easily diffuses into microbial lipid layer, show excellent antimicrobial and antibiofilm activity (Peng et al., 2024a). The effectiveness of the citrus oil can be increased against the multi drug resistant strains by combining with other antibiotics or other essential oils (Sreepian et al., 2022).

Antimicrobial mechanism and evidences

Citrus essential oils exhibit antimicrobial properties against broad range of microorganisms through membrane disruption, protein coagulation and oxidative stress induction (Song et al., 2020; Zhong et al., 2022). The hydrophobic molecules limonene and citral penetrates into the phospholipid bilayers, increases membrane fluidity and promote pore formation (Zhong et al., 2022). This results in leakage of intracellular components such as K+ and ATP, leading to the loss of membrane potential and cell death (Song et al., 2020). Membrane depolarisation and permeability changes is quantified by propidium iodide assays (Zhong et al., 2022). Several studies show 85-95% membrane depolarization at 1X minimum inhibitory concentration (MIC) (Song et al., 2020).

The antimicrobial potential varies across different citrus varieties. Lime essential oil exhibits greater potential against Gram-positive bacteria with larger inhibition zones (>17mm) than orange and grapefruit essential oils (14-16mm) in comparison to 78% alcohol-based sanitizers against *Staphylococcus aureus. Bacillus subtilis* has also proven to be highly susceptible to finger citron *(Citrus* medica) essential oil with 95% inhibition at 2x MIC (Li et al., 2019). Similarly, *Citrus sinensis* essential oil over 90% suppression of E. coli at concentration ranging from 25ug/ml, along with synergistic action against multidrug resistant bacteria using efflux pump inhibitory activity (Ambrosio et al., 2019).

The Gram-negative bacteria such as *Pseudomonas aeruginosa* exhibit moderate susceptibility to citrus essential oil with reported zone of inhibition of 12-13 mm. This reduced sensitivity is due to the presences of an outer membrane rich in lipopolysaccharide, limiting the diffusion of hydrophobic antimicrobial compounds. The enhanced activity against *Pseudomonas aeruginosa* has been observed at higher citral concentrations or due to oxidative stress–inducing mechanisms such as the production of reactive oxygen species as well as the inhibition of membrane-associated ATPase (Tang et al., 2023).

Citrus essential oils also demonstrate notable antifungal activity. Lime essential oil has shown strong efficacy against *Candida albicans*, producing large zones of inhibition and up to 92% suppression of ergosterol biosynthesis. Essential oil derived from Citrus limon peel at concentrations around 1.56% (v/v) has been reported to completely eliminate *Candida* species biofilms, accompanied by inhibition of hyphal morphogenesis and disruption of yeast-to-hyphal transition in clinical isolates. Citral appears to play a central role in this activity by selectively targeting the ergosterol biosynthetic pathway, achieving fungicidal effects at minimum fungicidal concentrations (MFCs) near 32 µg/mL and inducing reductions of approximately 3 $\log_{10}$ CFU/mL within two hours of exposure (Li et al., 2019).

Antibiofilm evidences

Citral compound has shown to inhibit acyl-homoserine lactone-mediated quorum sensing in *Pseudomonas aeruginosa,* resulting in down regulation of biofilm associated genes such as pel and psl. In *Staphylococcus aureus,* it interferes with quorum sensing systems and agr pathway. The biofilm disruption in *S. aureus* and *P. aeruginosa* has been observed on exposure to orange essential oil, fragmentation of the biofilm matrix was observed by confocal microscope and reduction up to 60% in alginate content. Linalool reduces extracellular DNA release and bacterial motility that play an important role in biofilm maturation and stability (Zhong et al., 2022). The antibiofilm evidence of citrus essential oils and their major bioactive compounds is summarized in Table 2.

Table 2. Antimicrobial and antibiofilm evidence of citrus essential oils and major bioactive compounds

Citrus oil source	Major compounds	Target microorganism(s)	Assay/biofilm model	Key findings	Mechanism	Reference
Citrus reticulata peel oil	Limonene-rich	*Listeria monocytogenes*	Antibiofilm assay	Strong antibiofilm activity	Membrane disruption	Peng et al., 2024
Mandarin essential oil	Limonene	*Staphylococcus aureus*	MIC + membrane depolarization	Strong bactericidal effect	Leakage + membrane damage	Song et al., 2020

Citrus unshiu oil	Terpenoids	*Aeromonas hydrophila*	Membrane integrity assay	High antibacterial activity	Membrane disruption	Zhong et al., 2022
Lemon peel oil	Citral	*Candida albicans*	Biofilm inhibition assay	Significant reduction of fungal biofilm	Ergosterol inhibition	Li et al., 2019

4. Combined Antibiofilm Potential of Eco-Enzymes and Citrus Essential Oils

Though eco-enzymes and citrus essential oils reported antimicrobial and antibiofilm activities individually, their combined effect remains underexplored strategy for the biofilm control. Based on the accumulated experimental data from the indirect fermentation and enzymatic assisted antimicrobial strategies the synergistic effect may be effective biofilm targeting agent (Ranaldi et al., 2025; Sereia et al., 2025). Citrus fruit waste, essential oils include limonene, citral, linalool and terpinene which are well reported for their antimicrobial, antibiofilm and quorum sensing inhibitory properties (Gupta et al., 2025; Peng et al., 2024). Indirect evidence from analogous fermentation-derived antimicrobials and enzyme–essential oil systems provide useful information for synergistic mechanisms in the absence of direct studies of eco-enzyme–citrus essential oil combinations.

Eco enzyme produced by fermentation, have low acidic pH because of their high content of organic acids like citric, acetic and lactic acids (Vidalia et al., 2023). The acidic environments have been reported to alter the EPS of biofilm by breaking the ionic bond cross links within polysaccharide network, thus increasing porosity of matrix and reducing diffusion barrier. This weakened EPS could be advantageous for penetration of hydrophobic citrus oil components into biofilm (Sereia et al., 2025; Touati et al., 2025). Indirect experimental evidence obtained from antimicrobial systems using fermentation has confirmed this mechanism (Ranaldi et al., 2025). Fermentation products from *Lactobacillus* species and orange essential oil against *Bacillus cereus* biofilm (Ammar et al., 2025), while fermented vegetable by-products enhanced cinnamon oil through pH-driven sensitization (Touati et al., 2025) were demonstrated to have a potential effect on essential oils in terms of antibiofilm activity. The softening effect on the biofilm caused by organic acids increased the diffusion of terpene compounds, thus demonstrating increased biofilm disruption compared with individual activity (Ranaldi et al., 2025; Touati et al., 2025). Despite being indirect evidences, the mechanistic implications of the observations strongly support the potential synergistic antibiofilm action of eco-enzymes and citrus essential oils.

5. Cytotoxicity, Research Gaps and Future Directions

The eco enzyme and citrus essential oils have shown potential antimicrobial and antibiofilm properties but their large applications require careful evaluation of safety and cytotoxicity. The systematic evaluations of toxicological studies remain limited as the current studies focus on antimicrobial efficiency. Eco enzymes produced through fermentation of organic waste, generally exhibit low environmental toxicity. However, their composition can vary depending on the raw material used, fermentation conditions and duration that influence their biological effects and highlights the need for better standardisation. Citrus essential oils often considered as safe because of natural origin, but their bioactive terpene components can cause irritation when applied at higher concentration, largely due to their membrane disruption properties. Studies using mammalian cell model have reported concentration dependent toxicity, highlighting the importance of optimising dosage, particularly for application in food contact surfaces, agricultural environment or household settings. Therefore, combining citrus essential oil with eco enzyme could be advantageous, as synergistic interaction could be effective on biofilm at lower concentration of essential oils. Despite of growing interest in both substances, there are still knowledge gaps in the combined use of eco-enzymes and citrus essential oils. There is a lack of direct research on the synergistic antibiofilm properties of eco-enzymes and citrus essential oils, as well as a lack of standardized approaches to the production and analysis of eco-enzymes. Most of the studies focuses on the single type of microbes, not on the multispecies biofilms in clinical and industrial settings.

Future studies should focus on filling these knowledge gaps by working on reproducible eco-enzymes and comprehensive cytotoxicity and environmental safety evaluations. Studies that use mature multispecies biofilm models, in addition to synergy analyses and advanced imaging, will play a pivotal role in validating the efficacy of these eco-enzymes. Addressing these issues will be a significant step forward in translating this sustainable, waste-based antibiofilm strategy into safe and effective solutions for food safety, agriculture, and environmental sanitation.

CONCLUSION

Eco-enzymes and essential oil from citrus provide effective way to manage biofilms. Eco-enzymes through hydrolysis and acidification break the structure of extracellular polymeric substance (EPS). In addition, citrus terpenoids affect the cellular membrane and disrupt quorum sensing. In vitro studies work well on the important pathogens and using them together may improve antibiofilm properties but challenges remain in standardizing formulation, using multispecies models and safety evaluations. Further research on consistent production, effective mixture and toxicity assessment will help to overcome these obstacles. This approach provides a sustainable method for managing biofilms in sanitation, food safety, agriculture, and healthcare, while reducing antimicrobial resistance and using organic waste.

REFERENCES

[1] Algburi, A., Comito, N., Kashtanov, D., Dicks, L. M. T., & Chikindas, M. L. (2017). Control of Biofilm Formation: Antibiotics and Beyond. *Applied and Environmental Microbiology*, *83*(3), e02508-16. https://doi.org/10.1128/AEM.02508-16

[2] Ambrosio, C. M. S., Ikeda, N. Y., Miano, A. C., Saldaña, E., Moreno, A. M., Stashenko, E., Contreras-Castillo, C. J., & Da Gloria, E. M. (2019). Unraveling the selective antibacterial activity and chemical composition of citrus essential oils. *Scientific Reports*, *9*(1), 17719. https://doi.org/10.1038/s41598-019-54084-3

[3] Ammar, H. A., Samy, R., Reda, F. M., & Hassanein, W. A. (2025). Essential oils and Lactobacillus metabolites as alternative antibiofilm agents against foodborne bacteria and molecular analysis of biofilm regulatory genes. *Scientific Reports*, *15*, 7576. https://doi.org/10.1038/s41598-025-89998-8

[4] Aslam, B., Wang, W., Arshad, M. I., Khurshid, M., Muzammil, S., Rasool, M. H., Nisar, M. A., Alvi, R. F., Aslam, M. A., Qamar, M. U., Salamat, M. K. F., & Baloch, Z. (2018). Antibiotic resistance: A rundown of a global crisis. *Infection and Drug Resistance*, *11*, 1645–1658. https://doi.org/10.2147/IDR.S173867

[5] Basiry, D., Entezari Heravi, N., Uluseker, C., Kaster, K. M., Kommedal, R., & Pala-Ozkok, I. (2022). The effect of disinfectants and antiseptics on co- and cross-selection of resistance to antibiotics in aquatic environments and wastewater treatment plants. *Frontiers in Microbiology*, *13*. https://doi.org/10.3389/fmicb.2022.1050558

[6] Buffet-Bataillon, S., Tattevin, P., Bonnaure-Mallet, M., & Jolivet-Gougeon, A. (2012). Emergence of resistance to antibacterial agents: The role of quaternary ammonium compounds—A critical review. *International Journal of Antimicrobial Agents, 39*(5), 381–389. https://doi.org/10.1016/j.ijantimicag.2012.01.011

[7] Burt, S. (2004). Essential oils: Their antibacterial properties and potential applications in foods—A review. *International Journal of Food Microbiology, 94*(3), 223–253. https://doi.org/10.1016/j.ijfoodmicro.2004.03.022

[8] Carey, D. E., & McNamara, P. J. (2015). The impact of triclosan on the spread of antibiotic resistance in the environment. *Frontiers in Microbiology, 5*, 780. https://doi.org/10.3389/fmicb.2014.00780

[9] Costerton, J. W., Stewart, P. S., & Greenberg, E. P. (1999). Bacterial biofilms: A common cause of persistent infections. *Science, 284*(5418), 1318–1322. https://doi.org/10.1126/science.284.5418.1318

[10] Daglia, M. (2012). Polyphenols as antimicrobial agents. *Current Opinion in Biotechnology, 23*(2), 174–181. https://doi.org/10.1016/j.copbio.2011.08.007

[11] Dancer, S. J. (2014). Controlling Hospital-Acquired Infection: Focus on the Role of the Environment and New Technologies for Decontamination. *Clinical Microbiology Reviews*, *27*(4), 665–690. https://doi.org/10.1128/cmr.00020-14

[12] Donlan, R. M., & Costerton, J. W. (2002). Biofilms: Microbial life on surfaces. *Emerging Infectious Diseases, 8*(9), 881–890. https://doi.org/10.3201/eid0809.020063

[13] Das, S. C., Khan, O., Khadem, A. H., Rahman, M. A., Bedoura, S., Uddin, M. A., & Islam, M. S. (2024). Evaluating the biocatalytic potential of fruit peel-derived eco-enzymes for sustainable textile wastewater treatment. *Results in Engineering*, *21*, 101898. https://doi.org/10.1016/j.rineng.2024.101898

[14] Di Martino, P. (2018). Extracellular polymeric substances, a key element in understanding biofilm phenotype. *AIMS Microbiology*, *4*(2), 274–288. https://doi.org/10.3934/microbiol.2018.2.274

[15] Flemming, H.-C., & Wingender, J. (2010). The biofilm matrix. *Nature Reviews Microbiology, 8*(9), 623–633. https://doi.org/10.1038/nrmicro2415

[16] Flemming, H.-C., Neu, T. R., & Wozniak, D. J. (2007). The EPS matrix: The "house of biofilm cells". *Journal of Bacteriology, 189*(22), 7945–7947. https://doi.org/10.1128/JB.00858-07

[17] Guedes, B. N., Krambeck, K., Durazzo, A., Lucarini, M., Santini, A., Oliveira, M. B. P. P., Fathi, F., & Souto, E. B. (2024). Natural antibiotics against antimicrobial resistance: Sources and bioinspired delivery systems. *Brazilian Journal of Microbiology*, *55*(3), 2753–2766. https://doi.org/10.1007/s42770-024-01410-1

[18] Gupta, K., Kumar, B., Midha, T., Singh, A., Baranwal, S., & Thareja, S. (2025). Exploring the antimicrobial and biofilm inhibitory potential of *Citrus limetta* peel essential oil against multidrug-resistant Shigella: *In vitro* and *in silico* insights. *Letters in Drug Design & Discovery*, *22*(9), 100149. https://doi.org/10.1016/j.lddd.2025.100149

[19] Hall-Stoodley, L., Costerton, J. W., & Stoodley, P. (2004). Bacterial biofilms: From the natural environment to infectious diseases. *Nature Reviews Microbiology, 2*(2), 95–108. https://doi.org/10.1038/nrmicro821

[20] Hobley, L., Harkins, C., MacPhee, C. E., & Stanley-Wall, N. R. (2015). Giving structure to the biofilm matrix: An

overview of individual strategies and emerging common themes. *FEMS Microbiology Reviews*, *39*(5), 649–669. https://doi.org/10.1093/femsre/fuv015

[21] Ismail, A. Y., Nainggolan, M. F., Aminudin, S., Siahaan, R. Y., Dzulfannazhir, F., & Sofyan, H. N. (2024). Characterization of chemical composition of eco-enzyme derived from banana, orange, and pineapple peels. *Brazilian Journal of Biology*, *84*, e286961. https://doi.org/https://doi.org/10.1590/1519-6984.286961

[22] Julinar, J., Uswati, D., Riyanti, F., & Musifa, E. (2025). Ecoenzyme Characterization of Fruit Peel Waste Mixture and Test of Antibacterial Activity against Bacteria Causing Dental Caries. *IJFAC (Indonesian Journal of Fundamental and Applied Chemistry)*, *10*(3), 186–197.

[23] Karne, H., Kelkar, V., Mundhe, A., Ikar, M., Betawar, S., & Chaudhari, N. (2023). Essential Oil Extraction from Orange and Lemon Peel. *E3S Web of Conferences*, *455*, 01005. https://doi.org/10.1051/e3sconf/202345501005

[24] Karygianni, L., Ren, Z., Koo, H., & Thurnheer, T. (2020). Biofilm Matrixome: Extracellular Components in Structured Microbial Communities. *Trends in Microbiology*, *28*(8), 668–681. https://doi.org/10.1016/j.tim.2020.03.016

[25] Kaur, H., Phutela, U. G., Aggarwal, Y., Palanisamy, K., & Singh, I. (2010). Yeast Mediated Expeditious Citrus limetta (Sweet Lemon) Peels Bioenzyme Preparation and Characterization using Response Surface Methodology. *Current Research in Nutrition and Food Science Journal*, *14*(1). https://www.foodandnutritionjournal.org/volume14number1/yeast-mediated-expeditious-citrus-limetta-sweet-lemon-peels-bioenzyme-preparation-and-characterization-using-response-surface-methodology/

[26] Koti, K., Rodas-Gonzalez, A., Nadon, C., McAllister, T., Yang, X., & Narváez-Bravo, C. (2024). Evaluating disinfectant efficacy on mixed biofilms comprising Shiga toxigenic Escherichia coli, lactic acid bacteria, and spoilage microorganisms. *Frontiers in Microbiology*, *15*. https://doi.org/10.3389/fmicb.2024.1360645

[27] Lee, B.-H., Cole, S., Badel-Berchoux, S., Guillier, L., Felix, B., Krezdorn, N., Hébraud, M., Bernardi, T., Sultan, I., & Piveteau, P. (2019). Biofilm Formation of Listeria monocytogenes Strains Under Food Processing Environments and Pan-Genome-Wide Association Study. *Frontiers in Microbiology*, *10*. https://doi.org/10.3389/fmicb.2019.02698

[28] Li, Z.-H., Cai, M., Liu, Y.-S., Sun, P.-L., & Luo, S.-L. (2019). Antibacterial Activity and Mechanisms of Essential Oil from Citrus medica L. var. Sarcodactylis. *Molecules*, *24*(8), 1577. https://doi.org/10.3390/molecules24081577

[29] Liu, H. Y., Prentice, E. L., & Webber, M. A. (2024). Mechanisms of antimicrobial resistance in biofilms. *Npj Antimicrobials and Resistance*, *2*(1), 27. https://doi.org/10.1038/s44259-024-00046-3

[30] Lu, Q., Huang, N., Peng, Y., Zhu, C., & Pan, S. (2019). Peel oils from three Citrus species: Volatile constituents, antioxidant activities and related contributions of individual components. *Journal of Food Science and Technology*, *56*(10), 4492–4502. https://doi.org/10.1007/s13197-019-03937-w

[31] Lubis, N., Tarigan, R. R. A., Tarigan, R. K. H., & Afiq, M. I. (2024). Effectiveness Assay Of Ecoenzyme Based On Household Organic Waste On The Growth Of Fusarium Spp. In Vitro. *Journal of Information Technology, Computer Science and Electrical Engineering*, *1*(3), 346–351. https://doi.org/10.61306/jitcse.v1i3.123

[32] Maillard, J.-Y., & Centeleghe, I. (2023). How biofilm changes our understanding of cleaning and disinfection. *Antimicrobial Resistance & Infection Control*, *12*(1), 95. https://doi.org/10.1186/s13756-023-01290-4

[33] Masyita, A., Mustika Sari, R., Dwi Astuti, A., Yasir, B., Rahma Rumata, N., Emran, T. B., Nainu, F., & Simal-Gandara, J. (2022). Terpenes and terpenoids as main bioactive compounds of essential oils, their roles in human health and potential application as natural food preservatives. *Food Chemistry: X*, *13*, 100217. https://doi.org/10.1016/j.fochx.2022.100217

[34] Mavani, H. A. K., Tew, I. M., Wong, L., Yew, H. Z., Mahyuddin, A., Ahmad Ghazali, R., & Pow, E. H. N. (2020). Antimicrobial Efficacy of Fruit Peels Eco-Enzyme against Enterococcus faecalis: An In Vitro Study. *International Journal of Environmental Research and Public Health*, *17*(14), 5107. https://doi.org/10.3390/ijerph17145107

[35] Muhammad, M. H., Idris, A. L., Fan, X., Guo, Y., Yu, Y., Jin, X., Qiu, J., Guan, X., & Huang, T. (2020). Beyond Risk: Bacterial Biofilms and Their Regulating Approaches. *Frontiers in Microbiology*, *11*. https://doi.org/10.3389/fmicb.2020.00928

[36] Nazzaro, F., Fratianni, F., De Martino, L., Coppola, R., & De Feo, V. (2013). Effect of essential oils on pathogenic bacteria. *Pharmaceuticals*, *6*(12), 1451–1474. https://doi.org/10.3390/ph6121451

[37] Nuryandani, E., Novitasari, E., Abdurrahman, M. F., Habibi, N., Sefrienda, A. R., Kurnianto, D., Jasmadi, J., & Andriana, Y. (2024). Chemometric analysis of GC-MS chemical profiles and biological activities of three citrus essential oils in Indonesia. *Journal of Applied Pharmaceutical Science*. https://doi.org/10.7324/JAPS.2024.188353

[38] Omwenga, E. O., & Awuor, S. O. (2024). The Bacterial Biofilms: Formation, Impacts, and Possible Management Targets in the Healthcare System. *Canadian Journal of Infectious Diseases and Medical Microbiology*, *2024*(1), 1542576. https://doi.org/10.1155/cjid/1542576

[39] Peng, J., Chen, G., Guo, S., Lin, Z., Zeng, Y., Ren, J., Wang, Q., Yang, W., Liang, Y., & Li, J. (2024). Anti-Bacterial and Anti-Biofilm Activities of Essential Oil from Citrus reticulata Blanco cv. Tankan Peel Against Listeria monocytogenes. *Foods*, *13*(23), 3841. https://doi.org/10.3390/foods13233841

[40] Permatananda, P. A. N. K., & Pandit, I. G. S. (2023). Characteristic of Orange Peel Waste-Based on Eco Enzyme at Different Fermentation Duration. *Jurnal Penelitian Pendidikan IPA*, *9*(6), 4289–4293. https://doi.org/10.29303/jppipa.v9i6.3527

[41] Ranaldi, R., Rugnini, L., Migliore, G., Tasso, F., Gabriele, F., Spreti, N., Scuderi, F., Braglia, R., Di Martino, P., Pujia, A., & Canini, A. (2025). The role of essential oils as eco-friendly

strategy to control biofilm collected in the Colosseum (Rome, Italy). *Applied Microbiology and Biotechnology*, *109*(1), 48. https://doi.org/10.1007/s00253-025-13433-1

[42] Rather, M. A., Gupta, K., & Mandal, M. (2021). Microbial biofilm: Formation, architecture, antibiotic resistance, and control strategies. *Brazilian Journal of Microbiology*, *52*(4), 1701–1718. https://doi.org/10.1007/s42770-021-00624-x

[43] Razola-Díaz, M. del C., De Montijo-Prieto, S., Guerra-Hernández, E. J., Jiménez-Valera, M., Ruiz-Bravo, A., Gómez-Caravaca, A. M., & Verardo, V. (2024). Fermentation of Orange Peels by Lactic Acid Bacteria: Impact on Phenolic Composition and Antioxidant Activity. *Foods*, *13*(8), 1212. https://doi.org/10.3390/foods13081212

[44] Rossi, C., Chaves-López, C., Serio, A., Casaccia, M., Maggio, F., & Paparella, A. (2022). Effectiveness and mechanisms of essential oils for biofilm control on food-contact surfaces: An updated review. *Critical Reviews in Food Science and Nutrition*, *62*(8), 2172–2191. https://doi.org/10.1080/10408398.2020.1851169

[45] Saharan, B. S., Beniwal, N., & Duhan, J. S. (2024). From formulation to function: A detailed review of microbial biofilms and their polymer-based extracellular substances. *The Microbe*, *5*, 100194. https://doi.org/10.1016/j.microb.2024.100194

[46] Sai, S., Abisha, V. M. J., Mahalakshmi, K., Veronica, A. K., & Susila, A. V. (2023). Treasure from trash – Is Ecoenzyme the new panacea in conservative dentistry and endodontics? *Journal of Conservative Dentistry and Endodontics*, *26*(2), 176. https://doi.org/10.4103/jcd.jcd_473_22

[47] Samrot, A. V., Abubakar Mohamed, A., Faradjeva, E., Si Jie, L., Hooi Sze, C., Arif, A., Chuan Sean, T., Norbert Michael, E., Yeok Mun, C., Xiao Qi, N., Ling Mok, P., & Kumar, S. S. (2021). Mechanisms and Impact of Biofilms and Targeting of Biofilms Using Bioactive Compounds—A Review. *Medicina*, *57*(8), 839. https://doi.org/10.3390/medicina57080839

[48] Sar, T., Kiraz, P., Braho, V., Harirchi, S., & Akbas, M. Y. (2023). Novel Perspectives on Food-Based Natural Antimicrobials: A Review of Recent Findings Published since 2020. *Microorganisms*, *11*(9), 2234. https://doi.org/10.3390/microorganisms11092234

[49] Sauer, K., Stoodley, P., Goeres, D. M., Hall-Stoodley, L., Burmølle, M., Stewart, P. S., & Bjarnsholt, T. (2022). The biofilm life cycle– expanding the conceptual model of biofilm formation. *Nature Reviews. Microbiology*, *20*(10), 608–620. https://doi.org/10.1038/s41579-022-00767-0

[50] Sereia, M. O. P., dos Santos, E. A., Leite, L. P., Neves, R. C., Marin, V. R., Ferreira, H., Contiero, J., & Sass, D. C. (2025). Synergistic Effect of Essential Oils and Rhamnolipid on Xanthomonas citri Subsp. Citri. *Microorganisms*, *13*(5), 1153. https://doi.org/10.3390/microorganisms13051153

[51] Sharma, S., Mohler, J., Mahajan, S. D., Schwartz, S. A., Bruggemann, L., & Aalinkeel, R. (2023). Microbial Biofilm: A Review on Formation, Infection, Antibiotic Resistance, Control Measures, and Innovative Treatment. *Microorganisms*, *11*(6), 1614. https://doi.org/10.3390/microorganisms11061614

[52] Shree, B., Jayakrishnan, U., & Bhushan, S. (2022). Impact of key parameters involved with plant-microbe interaction in context to global climate change. *Frontiers in Microbiology*, *13*. https://doi.org/10.3389/fmicb.2022.1008451

[53] Song, X., Liu, T., Wang, L., Liu, L., Li, X., & Wu, X. (2020). Antibacterial Effects and Mechanism of Mandarin (Citrus reticulata L.) Essential Oil against Staphylococcus aureus. *Molecules*, *25*(21), 4956. https://doi.org/10.3390/molecules25214956

[54] Sreepian, A., Popruk, S., Nutalai, D., Phutthanu, C., & Sreepian, P. M. (2022). Antibacterial Activities and Synergistic Interaction of Citrus Essential Oils and Limonene with Gentamicin against Clinically Isolated Methicillin-Resistant Staphylococcus aureus. *The Scientific World Journal*, *2022*, 8418287. https://doi.org/10.1155/2022/8418287

[55] Tallei, T. E., Fatimawali, Niode, N. J., Alsaihati, W. M., Salaki, C. L., Alissa, M., Kamagi, M., & Rabaan, A. A. (2023). Antibacterial and Antioxidant Activity of Ecoenzyme Solution Prepared from Papaya, Pineapple, and Kasturi Orange Fruits: Experimental and Molecular Docking Studies. *Journal of Food Processing and Preservation*, *2023*(1), 5826420. https://doi.org/10.1155/2023/5826420

[56] Tamburini, E., Donegà, V., Marchetti, M. G., Pedrini, P., Monticelli, C., & Balbo, A. (2015). Study on Microbial Deposition and Contamination onto Six Surfaces Commonly Used in Chemical and Microbiological Laboratories. *International Journal of Environmental Research and Public Health*, *12*(7), 8295–8311. https://doi.org/10.3390/ijerph120708295

[57] Tang, W., Zhang, Z., Nie, D., Liu, S., Li, Yan, Liu, M., Zhang, Y., Ou, N., & Li, Yanling. (2023). Selective antibacterial activity of *Citrus Medica limonum* essential oil against *Escherichia coli* K99 and *Lactobacillus acidophilus* and its antibacterial mechanism. *LWT*, *186*, 115215. https://doi.org/10.1016/j.lwt.2023.115215

[58] Touati, A., Mairi, A., Ibrahim, N. A., & Idres, T. (2025). Essential Oils for Biofilm Control: Mechanisms, Synergies, and Translational Challenges in the Era of Antimicrobial Resistance. *Antibiotics*, *14*(5), 503. https://doi.org/10.3390/antibiotics14050503

[59] Ugwu, C. N., Ezeibe, E. N., Emencheta, S. C., Nwagwu, C. S., Ogbonna, K. O., Ejiofor, C. V., Onugwu, A. L., Berebon, D. P., & Attama, A. A. (2025). Biofilms: Structure, resistance mechanism, emerging control strategies, and applications. *RSC Pharmaceutics*, *2*(6), 1376–1407. https://doi.org/10.1039/D5PM00094G

[60] Uruén, C., Chopo-Escuin, G., Tommassen, J., Mainar-Jaime, R. C., & Arenas, J. (2021). Biofilms as Promoters of Bacterial Antibiotic Resistance and Tolerance. *Antibiotics*, *10*(1), 3. https://doi.org/10.3390/antibiotics10010003

[61] Varshini, B., & Gayathri, V. (2023). Role of Eco-Enzymes in Sustainable Development. *Nature Environment and Pollution Technology*, *22*(3), 1299–1310. https://doi.org/10.46488/NEPT.2023.v22i03.017

[62] Verlicchi, P., Al Aukidy, M., & Zambello, E. (2015). What have we learned from worldwide experiences on the management and treatment of hospital effluent? — An

overview and a discussion on perspectives. *Science of The Total Environment*, *514*, 467–491. https://doi.org/10.1016/j.scitotenv.2015.02.020

[63] Vidalia, C., Angelina, E., Hans, J., Field, L. H., Santo, N. C., & Rukmini, E. (2023). Eco-enzyme as disinfectant: A systematic literature review. *International Journal of Public Health Science (IJPHS)*, *12*(3), 1171. https://doi.org/10.11591/ijphs.v12i3.22131

[64] Winkelströter, L. K., Bezirtzoglou, E., & Tulini, F. L. (2024). Editorial: Natural compounds and novel sources of antimicrobial agents for food preservation and biofilm control, volume II. *Frontiers in Microbiology*, *15*. https://doi.org/10.3389/fmicb.2024.1412881

[65] Yang, S., Li, X., Cang, W., Mu, D., Ji, S., An, Y., Wu, R., & Wu, J. (2023). Biofilm tolerance, resistance and infections increasing threat of public health. *Microbial Cell*, *10*(11), 233–247. https://doi.org/10.15698/mic2023.11.807

[66] Yao, Y., & Habimana, O. (2019). Biofilm research within irrigation water distribution systems: Trends, knowledge gaps, and future perspectives. *Science of The Total Environment*, *673*, 254–265. https://doi.org/10.1016/j.scitotenv.2019.03.464

[67] Zhao, A., Sun, J., & Liu, Y. (2023). Understanding bacterial biofilms: From definition to treatment strategies. *Frontiers in Cellular and Infection Microbiology*, *13*. https://doi.org/10.3389/fcimb.2023.1137947

[68] Zhong, W., Chen, K., Yang, L., Tang, T., Jiang, S., Guo, J., & Gao, Z. (2022). Essential Oils From Citrus unshiu Marc. Effectively Kill Aeromonas hydrophila by Destroying Cell Membrane Integrity, Influencing Cell Potential, and Leaking Intracellular Substances. *Frontiers in Microbiology*, *13*. https://doi.org/10.3389/fmicb.2022.869953

International Journal of Environment, Agriculture and Biotechnology
Vol-11, Issue-3; May-Jun, 2026
Peer-Reviewed International Journal
Journal Home Page Available: https://ijeab.com/
Journal DOI: 10.22161/ijeab

Pastoral-Conservation Conflicts in Tanzania are Likely to Continue for Unforeseeable Future: Evidence from Saadani National Park

Michael Muganda

Department of Wildlife Management, Sokoine University of Agriculture, P.O. BOX 3073, CHUO KIKUU, Morogoro, Tanzania
Orcid Id: 0009-0003-9435-831x
muganda@sua.ac.tz

Received: 01 May 2026; Received in revised form: 26 May 2026; Accepted: 03 Jun 2026; Available online: 13 Jun 2026

Abstract— *Since conservation conflicts occur within a particular cultural, political, and social context, they must be analyzed and addressed within the same context. This paper examines the pastoral- conservation conflicts in the context of Tanzania's national parks using the case study of Saadani National Park (SANAPA), with the view to understanding their nature, root causes, and sustainable solutions to such conflicts. Fieldwork involved multiple methods of data collection: in-depth interviews with conservation management officials, community leaders, pastoralists, and an NGO dealing with pastoral issues; focus group discussions with small-scale farmers (peasants); informal discussions with the wider community; document analysis; and field observations. These were coupled with a four-month period stay in the study area plus the researcher's experience with the wider community. The results indicate that the main conflict between conservation and pastoralism in the study area is the encroachment into SANAPA by livestock in search of pasture and water. The livestock encroachment, however, is seasonal and is done by migrating pastoralists who are not originally from around the park. The conflict happening in this particular case study is more than a resource - use conflict driven by access denial. It is also more than being prompted by changing climate patterns that have caused sustained drought in pastoral areas. The conflict is prompted by a mobile form of livestock keeping and herd sizes embedded in pastoral culture and value systems, and is reinforced by the practices of soliciting bribes embraced by conservation management staff, politicians, administrators, police and magistrates. With these practices, conflicts between pastoralism and other forms of livelihoods (not necessarily conservation) in Tanzania are likely to continue for unforeseeable future.*

Keywords— ***pastoral-conservation conflicts, biodiversity conservation, pastoralism, conservation, agriculture, livestock encroachment, Saadani National Park.***

I. INTRODUCTION

Pastoral societies in Tanzania (the Maasai, Sukuma, and Barabaig) are facing immense pressure from shrinking rangeland, climate change, and government laws and policies. Population growth and development pressure have shrunk grazing land, leading to re-occurrence of conflicts with other forms of livelihoods, including conservation (Nelson, 2012). Accelerating climate change expressed in prolonged periods of drought, drying of water-holes, the disruption of natural water flows, and siltation of pans have created shortage of water and pasture for livestock (HPG, 2009). On the other hand, government laws and policies are restricting free movement of livestock (in search of pasture and water) and denying access to resources in PAs (pasture and water for livestock) (SCBD, 2010; SNV, 2012).

For pastoral societies in Tanzania, livestock numbers or herd sizes communicate a complex social currency that express far more than just wealth. Herd sizes represent status and prestige, security, survival, and kinship. In short, herd sizes command social respect. With this cultural value, pastoral societies always wish to building up large herds of livestock (Nelson, 2012). However, these large herds of livestock are blamed for environmental degradation and frequent conflicts with other forms of livelihoods (Olenasha, 2006; Mattee & Shem, 2006; PINGO, 2013).

But, the underlying this notion of large herds of livestock is the pastoralists' mobile way of livestock keeping or mobility - seasonal migrations in order to access pasture and water occurring elsewhere (Nelson, 2012). The freedom of movement as practiced by pastoralists enables access to dispersed, ecologically specialized and seasonally varied grazing lands and watering holes (Mattee & Shem, 2006). Mobility is an important mechanism to cope with and recover from extreme conditions of climate shocks – droughts, floods and pest and disease outbreaks (Barrow *et al*, 2007; Olenasha, 2006).

They move according to where and when pasture becomes available for their livestock, thereby providing adequate pasture rotation, they use tracking technique to locate pasture and water (Mattee & Shem, 2006; HPG, 2009; PINGO, 2013). Therefore, restricting mobility is simply restricting the survival of their livestock in the face of spatial and temporal variability of environmental resources. This would eventually increase the vulnerability of pastoralists to natural and man-made shocks such as droughts, floods and livestock diseases (HPG, 2009; Olenasha, 2006; PINGO, 2013).

Perspectives on Pastoral-Conservation Conflicts

Pastoral - conservation conflicts are viewed from two perspectives. First, from the adverse impacts biodiversity conservation causes on pastoralism, particularly the direct killing of livestock by wildlife and the denial of access to resources in protected areas (PAs), especially pasture and water for livestock (SCBD, 2010; Marshall *et al*, 2007; Warner, 2000). Second, from the adverse impacts pastoralism causes on biodiversity, often expressed in habitat change, loss and species extinction or decline due to long-term environmental degradation, competition for resources, diseases interaction, and the direct killing of wildlife by pastoralists or wildlife by livestock (Homewood *et al*., 2012; Madden, 2004).

As a solution to such conflicts, conservationists maintain that wildlife - livestock interactions is not allowed due to increasing risk of disease transmission (commonly anthrax and rabies), competition with wild animals for pasture and water, and environmental destruction leading to depletion of the natural vegetation and eventually loss of habitat and wildlife species (Clifford *et al*., 2009; Kilpatrick *et al*., 2009). To minimize wildlife-livestock contact, there are several management actions, including conservation policies, laws, and practices that discourage livestock from entering into protected areas (PAs), hence the denial of access to resources in PAs (pasture and water for livestock) (PINGO, 2013). There are also government laws and policies that restricting free movement of livestock (in search of pasture and water for livestock) (SCBD, 2010; SNV, 2012) or mobility - seasonal migrations in order to access pasture and water occurring elsewhere (Nelson, 2012).

Pastoralists, however, see this restriction from entering PAs or denial of access to resources (pasture and water for livestock) from PAs as a 'killer' and barrier to maintaining pastoral livelihoods. Access to PAs is seen by pastoralists as vital to the survival of their herds, especially during periods of stress such as drought and, hence, having a significant impact on their pastoral livelihoods (SCBD, 2010). On the other hand, restricting mobility is simply restricting the survival of their livestock in the face of spatial and temporal variability of environmental resources. Pastoralists move according to where and when pasture becomes available for their livestock, thereby providing adequate pasture rotation (Mattee & Shem, 2006; HPG, 2009; PINGO, 2013). So, restricting mobility would eventually increase the vulnerability of pastoralists to natural and man-made shocks such as droughts, floods and livestock diseases (HPG, 2009; Olenasha, 2006; PINGO, 2013).

For pastoralists, a sustainable solution to pastoral related conflicts (not necessarily conservation), would be restoring traditional pastoral routes and securing rights of occupancy over traditional pastoral lands. Traditionally, pastoralists occupied and used Tanzania's savannah landscapes for pastoralism, utilizing foraging strategies based on mobility (seasonal migrations) in order to access pasture and water occurring elsewhere (Homewood *et al*., 2012; Nelson, 2012).

The bottom-line is that conservationists want to preserve biodiversity in and around PAs for much of human well-being (Collins, 2013) while pastoralists, on the other hand, want their livestock to access water and pasture in and around such PAs for survival of their herds and sustainability of their livelihoods (SCBD, 2010). In this situation, there are those who blame conservationists for embracing threat-based conservation, which focuses on protecting biodiversity against external threats rather than basing conservation plans on desired outcomes i.e. outcome-based conservation (Sayer, 2009). Also, there are those who argue that pastoralists embrace traditional management practices, especially large herd sizes and mobile form of livestock keeping, thereby leading to recurrence of conflicts between pastoralism and other forms of livelihoods (not necessarily conservation) (Homewood *et* *al*., 2012). One can, therefore, argue that the tension between conservation and pastoralism appears to have originated from these competing perspectives of conservationists and pastoralists.

A profound reflection on these perspectives can, therefore, help to understand the conflicts between conservation and pastoralism, particularly in terms of their nature, root causes and resolution. This paper presents a detailed case study of local conflicts between conservation and pastoralism in Tanzania using one particular case study, Saadani National Park. Studies on resource conflicts within a wider context of political economy emphasize that since conflicts occur within a particular cultural, political, and social context, they must be analyzed and addressed within the same context (FAO, 2008; Distefano, 2005; Muruthi, 2005; WWF, 2008; Madden, 2004; Lewis, 1999). In other words, conflicts need to be understood within a particular context - a historical, social or economic setting. In particular, this paper brings together perspectives of key actors in the pastoralism and biodiversity conservation in terms of their role in structuring, reinforcing, and resolving pastoral - conservation conflicts in the study area.

II. STUDY DESIGN AND METHODOLOGICAL APPROACH

This research employed a qualitative, exploratory single-case study design - with multiple-phase of fieldwork and mixed methods of data collection. The approach was appropriate since the aim was to understand a contemporary phenomenon (pastoral-conservation conflicts) within its real-life context, and that the phenomenon of interest had no clear boundaries and context of occurrence (Yin, 2018). And since conservation conflicts occur within a particular cultural, political, and social context, they must be analyzed and addressed within the same context (Madden, 2004), hence this case-study approach.

Fieldwork was carried out during several visits to SANAPA in 2021 and 2022. The multiple-phase of fieldwork approach led to more comprehensive knowledge and eventually better understanding of the big picture of the phenomenon being studied (Stake, 2000). Data were collected through a mixed-method approach, involving in-depth semi-structured interviews, focus group discussions, informal discussions, field observation, and document analysis.

Data were collected on the nature, causes, and solutions to conservation conflicts. Political factors were also taken into account. In-depth interviews were conducted with three senior officials working with the Wildlife Division, SANAPA staff (two senior officials and 13 park rangers), community leaders (two Ward Councilors and 12 village leaders), and one officer working with an NGO dealing with pastoral issues. These people were engaged as key informants, and were purposively selected based on their locally grounded knowledge and experience.

In addition, three focus group discussions (composed of 7-9 people) were carried out with small-scale farmers (peasants). Initially, the plan was to include both peasants and pastoralists in the focus group discussions. But this was difficult to achieve because pastoralists in the study area live a mobile life, so it was difficult to bring them together. Furthermore, it was realized that there was some resistance from these groups to sit together due to the tension or enemity that exists between them.

To get views of the wider community, 17 pastoralists were also interviewed. Snowball sampling was used to choose interviewees among pastoralists. The first individuals, however, were purposively selected and asked for further referrals in order to identify other people who were considered as relevant for the study. The criterion used was whether a person had knowledge about conflicts related with pastoralism in general.

Also, 14 members of the local community (8 peasants and 6 pastoralists) were involved through informal discussions to get reliable information or data with less individual pressure (Kreuger, 1988). Given the time the researcher spent in the study area (2-month stay), coupled with his experience with the wider community, it was possible to know the people, establish contact, build thrust/rapport and ultimately was able to talk to them freely and in an informal way. The sample size for informal discussions was reached when new participants were no longer adding insights to the research questions. However, the sample size was not meant to represent the large population in the study, but to obtain rich information that would help to understand and explain specific phenomena important for the research (Given, 2008).

Both interviews and discussions were conducted in Swahili by the researcher but, later transcribed and translated to English. Field observations, to witness the role of such conflicts in the study area, were made possible with a two-month period stay in the study area – spread across multiple phases of fieldwork, plus the researcher's experience with the wider community.

More data on pastoral-conservation conflicts were collected during document analysis. A number of relevant documents and other studies were collected and reviewed. The review was important to set this paper in the context of key analytical issues identified from field data about conservation and pastoralism by integrating stories from the field about the conflicts from key actors – pastoralists, peasants, NGOs, conservation management officials, and decision-makers at the community level - village leaders and local politicians.

Data analysis and presentation

The unit of data analysis was SANAPA, and the primary phenomenon of interest to this study was the nature, causes, and sustainable solutions to pastoral-conservation conflicts. Data analysis was conducted in four steps. First step, involved the analysis of data collected from the initial fieldwork phase, which was mostly exploratory visits to the study area. This helped to get to know the area, the people, and to identify key themes that structure the understanding of the conflicts between pastoralism and conservation and actors involved.

In the second step, data collected from the actual fieldwork using interview guides were analyzed in line with the key research question while looking for consistencies and differences across responses. Several themes and analytical issues emerged, such as how conservation, pastoralism, and agriculture influence the political commitment of the government, and their impacts on pastoral related conflicts in the country. It is important to note that during this analysis, agriculture emerged as one of the analytical issues that provided more insights into pastoral - conservation conflicts in the study area. As such, agriculture was also considered in the analysis, though it was not the focus of this study.

In the third step, a number of relevant documents and other studies were collected and reviewed (document analysis). The review was important to set this discussion in the context of key analytical issues identified from field data about conservation, pastoralism, and agriculture, including their dominant perspectives in the literature on pastoral - conservation conflicts. The review integrated the stories from the field about the conflicts from key actors, particularly pastoralists, peasants, NGOs, conservation management officials, and decision-makers at the community level - village leaders and local politicians.

In the fourth step, the unstructured textual data (verbatim answers and comments) from interview, focus group discussions, and informal discussions were analyzed using text analysis to unveil and present what people actually said in their own words when responding to a particular question. The text analysis identified consistencies and differences across responses for each question, and drew-up common themes, which were then organized into coherent categories that summarized the information meaningfully in relation to the questions. The analysis also revealed the nature and root causes of pastoral - conservation conflicts in the study area, including various actors involved. The main factors shaping such conflicts were drawn up, and eventually the future of such conflicts in the country is predicted.

Two styles have been used to structure and present textual data across meaningful themes relevant to this study: paraphrasing while remaining faithful to the original meaning; and the use of illustrative quotes applied in a particular context. In the following sections, the paper now discusses the findings from this analysis.

III. RESULTS AND DISCUSSION

Overall, the findings indicate that the main pastoral-conservation conflict in the study area is the grazing of livestock inside SANAPA (Picture 1). Other pastoral - conservation related conflicts such as the direct killing of livestock by wildlife, the direct killing of wildlife by pastoralists or wildlife by livestock were not mentioned at all throughout the time of data collection for this study. This implies that they are not happening in the study area or are not serious to either side.

Photo 1: Cattle grazing in one of the protected areas (not SANAPA) in Tanzania

Source: Tanzania Daily News, Dar es Salaam, 29 January 2013

Pastoralists bring their livestock into the park to graze - an act described by park officials as livestock encroachment into the park or simply livestock incursion into the park. However, this encroachment into SANAPA by livestock is seasonal and is done by migrating pastoralists who are not originally from around the park. Such pastoralists are absent for parts of the year, especially during wet season.

The results indicate further that the encroachment is widespread along the northern parts of the park where most pastoralists are found, the Barabaig pastoralists. According to park rangers, livestock encroachment is a big problem in SANAPA, especially during dry seasons when there is shortage or scarcity of pasture and water. Encroachment by livestock is among the highest illegal activities recorded by the park. One park ranger, for example, put it during the interview,

"….we have a big problem with cattle keepers (pastoralists) especially during dry seasons. Sometimes we see herds of cattle, in big numbers (100, 150 even 300 and over), grazing in the park …..Surely, it is very challenging to control such big numbers…."

While commenting on patrol operations carried out by SANAPA to wipe out livestock encroachment from the park, one senior park official said,

"Hundreds of herdsmen stream towards SANAPA with thousands of their livestock especially during drought season, but we didn't have this problem before, it has emerged only recently! so we are protecting the park….these people [pastoralists] are a big problem to the park, they bring large groups of livestock to graze inside the park, so we conduct patrols to clear them out."

Local communities in the study area, who are mostly peasants, had similar views on pastoralism. They also see pastoralism more of a nuisance than a source of benefits. They complain that every year they lose substantial quantities of crops due to damage caused by livestock, and experience degradation of soil in their farmlands (livestock make the soil compact and hard to dig with hand hoe). They pointed out that pastoralists are unwanted in the study area because of their free range mode of grazing and the big numbers of livestock that they cannot control. During fieldwork, there were frequent concerns of free-range grazing and large numbers of uncontrolled livestock in the study area.

On the other hand, there is a general feeling among pastoralists that they are discriminated, they are alienated from the system, they are sidelined when it comes to development processes, and their pastoralism is valueless compared to other forms of livelihoods. They are in minority hence it is difficult for them to influence policies, and so they lack political influence. Expressing their feeling, one pastoralist for example commented,

"You know it's very strange and very unfair!! There are plenty of grasses out there [in SANAPA] and yet they don't want our livestock to eat them while you know for sure that it's times of severe drought, does it mean they want our animals to die of hunger? This is really unfair to us [pastoralists]. ……..and that's why they have imposed fines for livestock found in the parks but they don't care about people who are affected by stray of animals who are under their jurisdiction to control"

Pastoralists consider themselves powerless against the dominance of conservationists and agriculturalists. However, they have learnt to accept their position, but have developed some strategies to ensure they survive against this dominance of conservation and agriculture while accessing pasture and water for their livestock, particularly during times of drought when there is shortage of these. Money is the 'weapon' underlying their strategies to accomplish their mission – of ensuring their livestock get pasture and water - as these are the most important for their livelihoods. Through tracking, pastoralists have discovered that SANAPA has areas that have pasture and hold water towards the end of the dry season when all the surrounding areas are dry. Field observations revealed that the park has all-weather sources of water, from seasonal to permanent rivers - including the Wami River and its tributaries whose banks are overgrown with bush and therefore have much less dry season pastures. Therefore, the park is the pastoralists' choice during dry seasons. To access SANAPA, they strategically enter the surrounding villages first through a 'welcome' from local politicians and village leaders. While politicians seek cheap popularity towards their political ambition, village leaders solicit bribes from pastoralists who are desperately searching for pasture and water for their livestock. One park official for example, narrated during interview,

"This is all caused by our leaders, particularly village chairperson and village executive officer. They receive bribe from pastoralists so they could be allowed to enter, stay and graze in the village area. Once they [pastoralists] are here, they invite their fellows from elsewhere, so the chain goes endlessly. When there is no more pasture for their herds in the village, they move into SANAPA thereby creating conflict with the park management".

Although SANAPA is formally inaccessible because of conservation law, still they enter the park risking a fine of 10,000 Tsh (US$ 10) per head of livestock. However, during informal conversation with some pastoralists, it was revealed that they avoid this payment by bribing park staff especially park rangers, by supervising the herds from a distance, by letting their children look after them or simply by leaving the herds alone because they know they will come back in the evening after feeding. Also, they take advantage of corruption and abuse of power embraced by legal institutions that handle wildlife cases, particularly police and courts. Since they own livestock, pastoralists have financial muscles that can be used to bribe officials (see Benjaminsen *et al*, 2009; Brockington, 2006, for more examples from Tanzania), have connections with politicians, and are eventually vocal. Describing the pastoralists during interview, one senior official from WD said, "Pastoralists are more powerful than agriculturalists - they have financial muscle, they give bribes to government officials, have connections with politicians whom they use to fulfill their interests and are vocal for that matter!" …. And sometimes they approach the big boss such as the In-charge of the PA (not necessarily SANAPA) with bribe so they could be allowed to graze in the PA. Now, if they realize the boss is tough, is not cooperating with them, is not bribed easily, they would often cook a scandal for him/her and use some politicians (often MPs) who are normally vocal and easily bribed to push the government to fire him/her out of the post".

In addition, they take advantage of inadequate park resources (manpower particularly park rangers, vehicles for patrol, and limited financial resources to cater for regular patrol costs) to break the law leading to frequent incidence of livestock encroachment in SANAPA. A visit to one ranger post (Gendagenda) for example, revealed that there were only two rangers, and no vehicle. Commenting on this situation one park ranger for example, narrated during interview,

"As you can see, we are only two of us! Practically, it is very difficult to deliver output here because under any circumstances one has to remain at the post at all time - for security reasons. This means the other also cannot go alone [patrol], so we just seat here all day. …You can also imagine how difficult it is to walk [to conduct patrol] in the bush on foot, no vehicle, no what – how far can you go and for how long! We are really working under difficult conditions. For instance, we have a big problem with cattle keepers (pastoralists) especially during dry season. Sometimes we see herds of cattle, in big numbers (100, 1500 even 300 and over) grazing in the park, we are only 2 or 3 at the post. In some cases, they [pastoralists] will let their children to look after these herds or sometimes they just leave them alone because they know they will come back in the evening after feeding or you cannot do anything with them because we are few in number. Or if you confine them, it's okay for them because all they need is their cattle to feed. So in essence we will look after them. They know we cannot stay with them for long time, given the fact that we are few and no storage facilities to keep them for long time. In the evening, they will come to negotiate so they can collect their cattle back. They know, if we take them to the court, they will pay much lower fines than we charge them using our by-laws. So in most cases we end up negotiating with them on how much they should pay".

Although these survival strategies are manifested in money as bribes, they have enabled pastoralists to maintain their livelihoods, especially their nomadic life style and large herds of livestock. The practices of bribing officials have helped them to access areas vital to the survival of their herds during times of drought. In some cases, bribes have enabled pastoralists to get back their confiscated livestock even without compensation to farmers in case of crop damage by livestock or without paying huge fines to conservation authorities in case of livestock found in PAs. While studying farmer – herder conflicts in Kilosa – Tanzania, Benjaminsen *et al* (2009) also noted similar practices – how the Maasai pastoralists bribed local politicians and administrators to access pasture and water from the contested wetland. Corruption is a large problem and a major public concern in Tanzania, widely manifested across public institutions, especially public officials and politicians (WEF, 2013).

As mentioned, Barabaig pastoralists arrive in the study area due to their nomadic life style of which they keep on migrating in search of pasture and water. When they spot somewhere a life for their herds they get into the village legally or illegally by bribing village leaders through corruption, according to park officials. Some politicians also incite herders to encroach on SANAPA land with impunity. When they see the area is short of pasture, they look for alternatives elsewhere. This could be evading a nearby protected area as long as there is pasture or moving to another village.

Interviews with Barabaig pastoralists revealed that similar to Maasai, livestock keeping is not merely an economic activity to Barabaig, it is not just about making a living out of livestock – in the sense that if there are other more profitable activities, one would go for them and forego pastoralism. To them, livestock keeping is an integral part of their life, a way of life heavily intertwined into their culture and value systems. In fact, at the core of Barabaig life is pastoralism. To them, personal worthiness is expressed in terms of numbers of cattle and other livestock. A person without livestock is poor, without any standing in their society. From this perspective, one can imagine how difficult it is to convince the Barabaig to reduce the number of herds so they could avoid overgrazing, degradation of soil and vegetation, higher incidence of diseases, poor nutrition, increased mortality and loss of herds.

On a similar perspective, pastoralists maintain that doing away with mobility and herd sizes means doing away with pastoralism, since by nature pastoralists depend on livestock, are mobile in communal grazing areas they traditionally own, and use traditional land management patterns recognized by their customary rules (Barrow *et al*, 2007; Homewood *et al*, 2012; Mattee & Shem, 2006; PINGO, 2013). In fact, the two features (mobility and herd sizes) are central to pastoralists' traditional ways of livestock keeping and are embedded in their culture and value systems. They are considered resilience mechanisms of pastoralism. To the pastoralists, a large herd expresses personal wealth and an insurance to survive through periods of stress such as drought and disease epidemics (Boku, 2008). During interviews, one Ward Chancellor, who is a Maasai pastoralist, said,

"…it's true that we [pastoralists] have large herds, but you know what? Herd is everything to us [the Maasai and Barbaig]. When our sons start their own life, we give them livestock as start-up capital. When they want to marry, we offer livestock as bride pride. I remember for my case I offered 28 cattle for my first wife and then 18 for the second. On top of that our staple food is milk and meat. So you can imagine how livestock mean everything to our life! This implies any plan to reduce the number of livestock among pastoral societies needs to be taken with great care, and need to be a long term programme to be able to change their mindset. Otherwise, you will end up being disappointed with their response. You know, it's like a peasant who depends on agriculture for a living. And then, all over the sudden you tell him to reduce the size of the land he always cultivates under a promise that he will get more and quality harvests. Do you think he will really understand you in the first place? Obviously, you need a long term plan to be able to change their mindset slowly".

These arguments by conservationists and pastoralists in relation to each other reflect the complexity surrounding pastoral related conflicts in Tanzania. This could imply that still there is a long way towards sustainable solutions to this kind of conflicts in the country. The arguments also suggest the absence of a common understand about the conflict, implying that tensions between pastoralism and other forms of livelihoods (not necessarily conservation) are likely to continue in the country for unforeseeable future.

Implications to protected areas management in Tanzania

There are three general implications important to conservation efforts in the country one could draw from these results. First, encroachment into protected areas (PAs) by livestock is likely to increase pressure on the management of PAs in the country, especially during times of drought when there is shortage of these resources across many traditional pastoral areas. As SCBD (2010) and PINGO (2013) noted, PAs are the pastoralists' choice during dry seasons to ensure their livestock get pasture and water and, therefore, survive the hard times of dry seasons. This suggests the need for strategies to guide management actions that could minimize pressure from the encroachment into PAs by livestock. Second, pastoralists have developed strategies to help them access pasture and water occurring elsewhere, especially during periods of stress such as drought. The strategies are manifested in money as bribes to PAs management staff. This implies that encroachment into PAs by livestock would be controlled only depending on how strictly and determined is the management of PAs to fight against corruption practices since access to PAs is seen by pastoralists as vital to the survival of their herds during dry seasons (SCBD, 2010), and money is used to accomplish their mission. Third, the adverse impacts of pastoralism on biodiversity as identified by Homewood *et al* (2012) such as habitat change, loss of biodiversity and species extinction or decline due to long-term environmental degradation, competition for resources, diseases interaction, and the direct killing of wildlife by pastoralists or wildlife by livestock are likely to continue for unforeseeable future or even intensify over time. Therefore, protection of PAs needs to be enhanced to eliminate such kind of threats to biodiversity so as to ensure the survival of wildlife and sustain healthy ecosystems.

IV. CONCLUSION

This paper has examined the pastoral – conservation conflict in Tanzania's national parks using the case study of SANAPA. Through this study, it has been realized that there is pastoral-conservation conflict between the management of SANAPA and migrating pastoralists. However, the tension between pastoralism and conservation happening in this particular case is more than a resource – use conflict driven by access denial. It is prompted by a mobile form of livestock keeping and herd sizes embedded in pastoral culture and value systems, and is reinforced by issues of governance and corruption.

The tension is more than being prompted by changing climate patterns that have caused sustained drought in pastoral areas. And it is more than pastoralists finding it increasingly difficult to cope with dwindling pasture and water in their areas while they cannot wait and watch their animals die. The conflict is induced by traditional management practices embraced by pastoral societies, particularly free-range grazing and large numbers of uncontrolled livestock, and is reinforced by the practices of soliciting bribes embraced by conservation management staff, politicians, administrators, police and magistrates.

The notion that protected areas have been established on traditional pastoral lands, the dominance of conservation and agriculture over pastoralism, and the perception that pastoralists are unwanted and pastoralism is more of a nuisance than a source of benefits have played an important role in structuring this conflict. These together have forced the pastoralists to indulge into corruption practices, using money as the weapon to maintain their livelihoods, especially their nomadic life style and large herds of livestock. However, corruption raises questions about good governance and whether the government is really determined to end pastoral-related conflicts in the country, and leads to loss of trust in conservation management officials and authorities (local government, the police, and the judiciary), and their willingness to prevent such conflicts in the future. Such weakness within and between government institutions has resulted in actors trying to offer bribes as a solution to the problem.

The case study has revealed several arguments from conservationists, agriculturalists, and pastoralists in favour of their sectors. Generally, the solutions for pastoral related conflicts proposed by the conservationists and agriculturalists (destocking and sedentarization) are not acceptable by the pastoralists. On the other hand, the solutions proposed by the pastoralists (recognition of traditional ownership of grazing areas of the pastoral societies and traditional ways of livestock keeping) appear unpractical and unsustainable - cannot be a long term conclusive remedy. The fact is, with pastoralists' focus on large herd size and herd mobility, whatever land is set aside for them, will not be enough after some time. As livestock population keeps growing over time, the carrying capacity of the land (in terms of pasture and water) diminishes due to overgrazing resulting from overstocking. As a consequence, pastoralists will again roam around with their animals in search for pasture and water elsewhere, leading to re-occurrence of conflicts with other forms of livelihoods.

With these debates, therefore, the conflicts between pastoralism and other forms of livelihoods (not necessarily conservation) are likely to continue in Tanzania for unforeseeable future. Also, there is a danger that the conflicts may escalate even more, risking the detriment of either.

This study, however, focused only on one protected area (Saadani National Park-SANAPA) to examine pastoral-conservation conflicts across protected areas (PAs) in Tanzania. Realistically, there might be pastoral-conservation conflicts in SANAPA, but still no such conflicts in other PAs – given their varying levels of conservation status, biological resources in and around, and differing restrictions or level of protection. So pastoral-conservation conflicts for SANAPA cannot generally be concluded as pastoral-conservation conflicts for other PAs in Tanzania or elsewhere since conservation conflicts occur within a particular cultural, political, and social context. In addition, pastoral-conservation conflicts for a single-case study like SANAPA - does not statistically represent all PAs of Tanzania. As such, the findings from this single-case study cannot implicate or reflect all PAs in the country. These limitations, however, should not invalidate the findings of this study, but rather be taken as a basis for improvement in future studies. The study still serves as an indication of what is likely to be the reality on the ground for other PAs as well, despite such identified limitations, which aim to indicate the context through which the results may be understood.

Data Availability Statement

All data used in this study are available on request from the corresponding author. These data are not publicly available due to privacy restrictions.

Funding Statement

The author/researcher received no external funding for this study.

Conflict of Interest Disclosure

The author declares no conflict of interest on anything/issue disclosed or discussed in this study.

Ethics Approval Statement

All data for this study were collected and managed in compliance with research regulations and guidelines of Sokoine University of Agriculture while ensuring participant confidentiality, data security, and ethical standards. Informed consent was obtained from all participants prior to their involvement in the study.

Permission to reproduce material from other sources

This work include material reproduced from public documents, which, as a general rule, do not require permission to reproduce. However, all sources have been acknowledged.

REFERENCES

[1] Barrow, E., J. Davies, S. Berhe, V. Matiru, N. Mohamed, W. Olenasha, M. Rugadya. (2007). Pastoralist's species and ecosystem knowledge as the basis for land management. IUCN Eastern Africa Regional Office. Policy Brief No. 3 (of 5). Nairobi, 4p. On WWW at http://cmsdata.iucn.org/downloads/ pastoralist_species_and_ecosystem. Accessed 08 July 2021.

[2] Benjaminsen, T. A, F. P. Maganga and J. M. Abdallah (2009). The Kilosa killings: political ecology of a farmer-herder conflict in Tanzania. *Development and Change*, 40 (3) 423-445.

[3] Boku, T. (2008). Pastoralism under stress: resources, institutions and poverty among the Borona Oromo in Southern Ethiopia. Norwegian University of Life Sciences, PhD thesis.

[4] Clifford, D. L., Schumaker, B. A., Stephenson, T. R., Bleich, V. C., Cahn, M. L., Gonzales, B. J., ... & Mazet, J. A. (2009). Assessing disease risk at the wildlife–livestock interface: A study of Sierra Nevada bighorn sheep. *Biological Conservation*, *142*(11), 2559-2568.

[5] Distefano, S. (2005). Human-wildlife conflict worldwide: collection of case studies, analysis of management strategies and good practices. FAO, Rome.

[6] Food and Agriculture Organization of the United Nations (FAO), (2008). Human-wildlife conflict in Africa: an overview of causes, consequences and management strategies, working paper for the International Foundation for the Conservation of Wildlife. On WWW at http://www.wildlife-conservation.org/var/plain/storage/original/application/c399b47.pdf. Accessed 27 March 2022.

[7] Given, L. M. (2008). The SAGE Encyclopedia of Qualitative Research Methods. Vol. 1 & 2. United Kingdom: Sage Publications Inc.

[8] Homewood, K., P. C. Trench and D. Brockington (2012). Pastoralism and conservation – who benefit? On WWW at http://www.ucl.ac.uk/anthropology/studying/undergraduate_degree.pdf. Accessed 07 April 2022.

[9] Humanitarian Policy Group (HPG) (2009). Pastoralism, policies and practices in the Horn and East Africa: A review of current trends. Odi, London, UK. On WWW at http://www.odi.org.uk/sites/odi.org.uk/files/odi-assets/.pdf. Accessed 07 April 2022.

[10] Kilpatrick, A. M., Gillin, C. M., & Daszak, P. (2009). Wildlife–livestock conflict: the risk of pathogen transmission from bison to cattle outside Yellowstone National Park. *Journal of Applied Ecology*, *46*(2), 476-485.

[11] Kreuger, R.A. (1988). Focus groups: A practical guide for applied research. London: Sage.

[12] Lewis, C. (1996). Managing conflicts in protected areas. IUCN – The World Conservation Centre, IUCN, Gland, Switzerland, and Cambridge, UK.

[13] Madden, F. (2004). Creating coexistence between humans and wildlife: global perspectives on local efforts to address human-wildlife conflict. *Human Dimensions of Wildlife*, Vol.9, 247-257.

[14] Marshall, A.R., Z. Aloyce, S. Mariki, T. Jones, N. Burgess, F. Kilahama, J. Massao, E. Nashanda, C. Sawe, F. Rovero and J. Watkin (2007). Tanzania's second nature reserve: improving the conservations status of the Udzungwa Mountains? *Oryx*, Vol.41, 429-430.

[15] Mattee, A. Z. and Shem, M. (2006). Ambivalence and Contradiction: a review of the policy environment in Tanzania in relation to pastoralism. IIED Issue Paper No. 140, Drylands Programme. London: International Institute for Environment and Development.

[16] Muruthi, P. (2005). Human wildlife conflict: lessons learned from AWF's African Heartlands, AWF working paper. On WWW at http://www.awf.org/content/document/detail/3227. Accessed 26 March 2022.

[17] Nelson, F. (2012). Natural conservationists? Evaluating the impact of pastoral land use practices on Tanzania's wildlife economy. *Research, Policy and Practice*, 2 (1) 1-19.

[18] Olenasha, W. (2006). The place of pastoralism in modern Tanzania. The Proceedings of a Seminar for Members of Parliament. The Rangelands and Livelihoods Working Group. On WWW at http://www.ereto-npp.org/download_documents/RLWG_2006_the_place.pdf. Accessed 16 April 2022.

[19] Pastoralists Indigenous Non-Governmental Organization's Forum (PINGO) (2013). Impacts of climate change on land use patterns and livelihoods of pastoralists and hunter gatherers: a case study of Mbulu, Hanang, Kiteto and Simanjiro Districts in Tanzania.

[20] Sayer, J. (2009). Can conservation and development really be integrated? *Madagascar Conservation & Development*, 4 (1) 9-12.

[21] Secretariat of the Convention on Biological Diversity (SCBD) (2010). Pastoralism, Nature Conservation and Development: A Good Practice Guide. Montreal, 40 + iii pages.

[22] SNV (2012). Improved livelihoods for pastoralists. SNV Practice Brief, Issue 2, January 2012.

[23] Stake, R. E. (2000). Case studies. In handbook of qualitative research, 2nd Ed, Sage, Thousand Oaks, CA.

[24] Yin, R. K. (2018). Case study research and applications: Design and methods (6th ed.). SAGE Publications.

[25] Warner, S. (2000). Conflict management in community-based natural resource projects: experiences from Fiji and Papua New Guinea. Working Paper 135, Overseas Development Institute (ODI).

[26] World Economic Forum (WEF) (2013). The Global Competitiveness Report 2012-2013. Geneva, Switzerland. On WWW at http://www3.weforum.org/docs/WEF_GlobalCompetitiveness.pdf. Accessed 18 August 2022.

[27] World Wildlife Fund (WWF), (2008). Common ground: solutions for reducing the human, economic and conservation costs of human wildlife conflict. On WWW at http://www.worldwildlife.org/species/WWFBinaryitem9108.pdf. Accessed 26 March 2022.

International Journal of Environment, Agriculture and Biotechnology
Vol-11, Issue-3; May-Jun, 2026
Peer-Reviewed International Journal
Journal Home Page Available: https://ijeab.com/
Journal DOI: 10.22161/ijeab

Smart Protection of Cotton Crops: A Review of IoT Sensor Networks and ML-Based Pest Decision Support Systems

Pratibha[1*], Mukesh Kumar[1], Parteek[1], Kapil[1], Amandeep Singh[2], Ajay[1]

[1]Department of Soil and Water Engineering, CCS HAU Hisar, Haryana, India
[2]Department of Forestry, CCS HAU Hisar, Haryana, India
*Email: pratibhaarya2152@gmail.com

Received: 09 May 2026; Received in revised form: 02 Jun 2026; Accepted: 08 Jun 2026; Available online: 16 Jun 2026

Abstract*— Cotton is found to be a globally significant commercial crop, with India contributing approximately 22% of the world's production and often referred to as "white gold". But cotton is highly vulnerable to insect damage, so early diagnosis is necessary to reduce disease transmission and enhance treatment effectiveness. Traditional methods are labour-intensive, which often results in delayed responses and significant crop losses. This study explores various pests found in India and their management in the cotton field by using different sensors and a smart detection-response system utilising IoT sensor networks and machine learning to monitor and classify pests, specifically targeting the Bollworm complex and whiteflies. The proposed architecture comprises different sections: Field traps, Gateway, central control system, Drone spraying, and Farmer sections, integrating motion-detecting sensor traps, communication modules, and an autonomous aerial vehicle for targeted pesticide spraying. The proposed system optimises flight paths for rapid response and includes protocols for handling false alarms, leveraging camera-equipped drones and human assistance. While the integration of IoT offers precision and accuracy, challenges such as hardware durability in harsh environments, networking interference in rural areas, and the need for farmer education remain critical hurdles for widespread adoption.

***Keywords*— Cotton pests, Drone spraying, IoT system, Sensors.**

I. INTRODUCTION

Agriculture forms the economic backbone of many nations with cotton as the widely grown crop. However, its economic yield is severely affected by insect pests,making the implementation of technologies in the field essential. India is the second largest producer of cotton after China, accounting for approximately 22% of the world's cotton production, which is estimated at 5.79 million tons [6]. There is a high risk of damage in the cotton field due to insects. The early loss of leaves or the development of diseases impacts cotton yield, so early diagnosis of plant illnesses is essential for reducing disease transmission and enhancing effective treatment strategies. With the increasing population demand for food and crop also increases but pests remain the enemies of crop. At the same time climate change and water scarcity are the reasons for decrease in fertile land [20]. To attain cotton in large quantities we have to make effective plans for its prevention from pests [5,11].

The traditional methods of disease identification are labour-intensive and often delayed, leading to significant crop losses.Many organs are harmed by cotton diseases during different growth periods and some are infected with vascular diseases [4]. Recent advancements in IoT and artificial intelligence (AI) provide an opportunity to develop a smart system capable of monitoring and detection of diseases. In this study, an overview of previous research on sensor networks and machine learning techniques for classifying various diseases and pests has been presented.

II. SCOPE OF THE REVIEW

This review focuses on the detection and management of cotton pests using sensors that specifically target the Bollworm complex and sucking pests such as whiteflies for early detection and monitoring in the field. This study intended to understand the potential of the IoT system, its associated challenges, and its success in the cotton environment. Furthermore, we evaluate the role of Edge Gateways (such as Zigbee) and autonomous response units, such as UAVs, in creating a closed-loop precision management system. The existing literature was searched using the following keywords: "cotton pests", "sensors", "IoT system", and "Drone Spraying". The remainder of this review is organised as follows: Section 3 explores the role of IoT in agriculture and different types of sensors which can be used for pest detection; Section 4 details the specific prototype architecture for cotton pest detection; Section 5 outlines the smart response system and comparison between communication modules; and Section 6 discusses the prevailing hardware, networking, and educational challenges in the field.

III. IoT IN AGRICULTURE

The "Internet of Things"(IoT) in agriculture uses connected devices such as automated drones and field sensors to optimize and monitor agricultural practices in real time. Current literature review typically divides an IoT system into four different tiers [1]..

- Sensing Tier:- It senses the change in the environment .
- Transport/Gateway Tier:- It facilitates communication between two different hardware technologies.
- Processing Tier:- Analyzes or processes the incoming data.
- Application Tier:- It provides the user interface for crop monitoring and control operations.

Different sensors and their possible use in IoT based agriculture systems are provided in review[14].

3.1. Different Types of Sensors

3.1 Low-Power Cameras & Sensors-

- Farmers can install a low-cost image sensor in traps with pheromones or male sex attractants that captures the images of pests in it and sends it to a centralized platform wirelessly.
- Based on the number of insects present in traps, the farmers determine the location of insect infestation and take steps to remove them from fields.
- Low-power image sensors only click random images of insects that are visible to the naked eye.

3.2 High Power Thermal Sensors-

- THERMOGRAPHY is a method that uses thermal and infrared sensors to measure the amount of light reflected by a surface [3].
- Every surface reflects a distinct amount of light energy which is also called its spectral signature.
- Plants and soil have a special spectral spectrum that is pre-recorded in spectrometers.
- In case of pathogens covering the surface of plant leaves, the spectrum range of the plant will change, indicating an attack by the pests.

3.3 Fluorescence Image Sensing-

- In this method the amount of chlorophyll present in a plant is measured based on its change in fluorescence parameters.
- An optimal camera captures an image of a plant leaves and then compares it with existing images of a healthy leaf.
- Change in chlorophyll patterns indicates the presence of pathogens and pests.

3.4 Acoustic Sensors-

- Detecting bugs and rodents through sound detection is another effective way to ensure plant quality.
- Wireless acoustic sensors situated at random locations in a field can pick up sound waves of insects.
- Locations with high sound waves indicate a high concentration of bugs.
- A farmer can thus spray pesticides on these locations to ensure the quality of crops.

3.5 Gas Sensors-

- Plants, when stressed produce specific volatile chemical compounds.
- These compounds differ based on the stress they feel.
- Compounds secreted due to environmental changes will be different then the compounds emanated due to pest infestation.
- Sampling is required to collect volatile compounds for data analysis.

IV. IoT-BASED SMART DETECTION AND RESPONSE SYSTEM ARCHITECTURE

Pests account for an estimated 20% to 40% of global crop losses each year, as reported by the FAO [9,17]. Majorly the cotton field is infested with "Pink Bollworn" pests. Disease in plants influences the economic status and the speed at which production takes place. However, the human method of identifying such diseases is likely to be inaccurate since most organisms that cause the diseases cannot be easily seen with the naked eye [16]. Recent prototype systems utilize a combination of motion - sensing hardware and and communication module like zigbee which is further connected with a micro controller or Arduino [1].. When field movement is detected, the sensors generate and transmit data packets in a hexadecimal format. These data packets crucially contain the geographic coordinates of the sensors, allowing gateway devices to precisely map the location of the potential pest threat.

4.1 How the system actually works-

The system first identifies the pest's presence near the crop and then sends the detection to the base station which is present in the centre of the field via a communication module. In response, the system attempts to destroy it by a targeted spray through a drone.

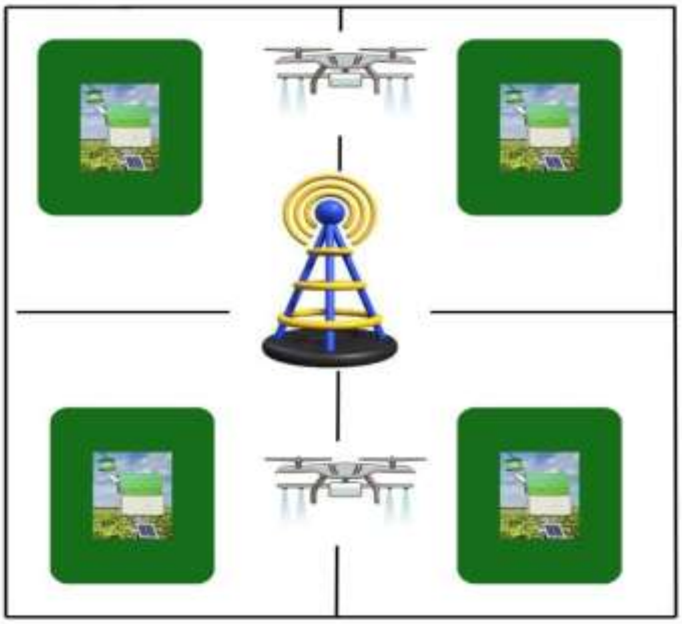

Fig 1: Architecture of the system

4.2 IoT-Based Cotton Pest Detection-

The system includes five elements, with the first level handling the identification of data on the insects, while the second level deals with the analysis of the data collected in the first level. As far as the third level is concerned, the analysis and transmission of data to the sensor sending the data to the drone will be carried out here. Finally, in the fourth level, drones will deal with spraying the area after receiving the signals.

Field Layer: This level is one of the easiest in the cotton plantation. It involves both sensors and communication modules. This level is responsible for detection of the insects by the sensors and transmission of the information to the base station through the communication module. Besides the sensors, the model also has another transmitter called ZED. The most important thing about this level is that the coverage range is from 10-100meters with a data rate of 250 kbps. However, using LoRA can enhance our area of coverage.

Gateway Layer: The primary purpose of this tier is to receive data generated by the sensors and take appropriate action. Based on the insect detection alerts, it determines the specific target locations for the drones. For example, if one sensor sends a single alert while another transmits continuous signals, the system will prioritize directing the drones to the source of the repeated messages.

Control Layer: This tier operates by analyzing the incoming data packets from the sensor network. The system performs several key evaluations based on this information:Identifying which specific cluster is experiencing the highest insect activity and investigating the potential causes.Assessing how the crop quality in the highly infested cluster might differ from less affected areas. Determining if an increased volume of pesticide spray is required to effectively manage the pests in these high-activity clusters.

Response Layer: Operating as the active defense mechanism for the entire setup, this tier is crucial for pest mitigation. It incorporates the drones and ZigBee Controller (ZC) modules, utilizing the specific coordinates transmitted by the sensors to guide the drones for targeted pesticide application. If the pests have migrated by the time the drone reaches the designated coordinates, the system is designed to expand the spraying radius to cover surrounding adjacent areas. This workflow is illustrated in Figure 2 below.

Farmer Layer: This tier consists of a dedicated web dashboard that allows farmers to monitor the system's daily operations. For example, the interface provides comprehensive daily reports detailing the frequency of sensor detection alerts alongside the total number of drone spraying missions executed. The comprehensive flow of how the system receives and acts upon these signals is depicted in the flowchart below.

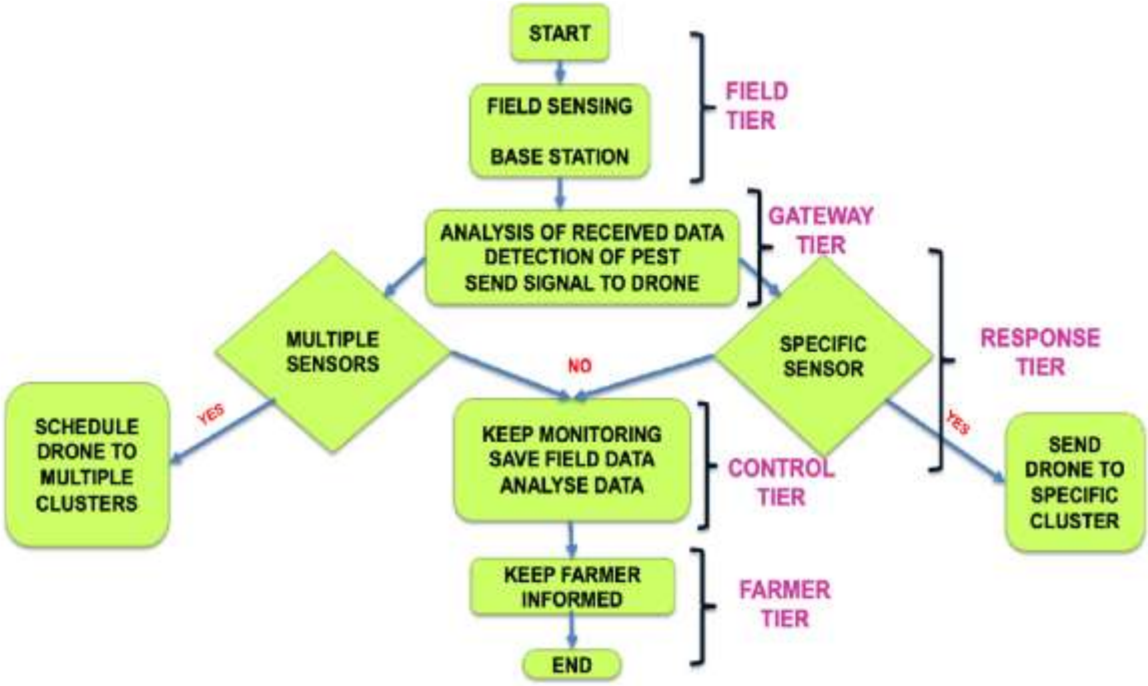

Fig 2: Smart Detection Response System

V. SMART RESPONSE SYSTEM

The simulation area is systematically divided into equal clusters, with IoT nodes evenly distributed throughout each section. While the transmission power remains consistent across all individual field sensors, the gateway node is equipped with an extended communication range. This broad coverage allows the gateway to simultaneously communicate with the entire sensor network and relay detection alerts directly to the drones.

Furthermore, the central base station maintains a precise database of coordinates for every cluster. When a pest alert is received, the base station instantly identifies both the specific sensor and its corresponding cluster. To ensure a rapid response, coordinate-based, low-altitude flight paths have been programmed, allowing the drone to navigate to the target zone in the minimum possible time. Because the flight speed of targeted pests, such as moths, is relatively slow compared to the rapid deployment speed of the unmanned aerial vehicles, the system can effectively intercept them before they migrate. The rise of the camera and connectivity in computer vision presents an opportunity to utilize computer vision as another tool for automated monitoring of pests in modern agricultural operation [15].

5.1 Algorithm Operations and processing

The drone movement prediction algorithm is structured into three primary phases. During the initial phase, all network devices activate to establish immediate synchronization with one another. This initialization is isolated as a distinct step because establishing wireless communication involves an inherent time delay; devices must first exchange initial data packets, known as beacons, to signal their readiness before any subsequent data transmission can occur.

In the second part, three cases are possible:

Case 1: Upon detecting insect activity, field sensors transmit alerts to the central base station. Subsequently, the control unit relays precise geographic coordinates to the autonomous drone, directing it to the infested zone for mitigation. Once the targeted spraying mission is finalized, the drone evaluates whether additional pest detection signals have been received from other field clusters. If concurrent threats are identified, the aerial vehicle proceeds to treat those specific locations before returning to its docking hangar.

Case 2: In this situation, if the base station receives only a solitary notification, the system may initiate a recall protocol for the deployed drone. This procedure is implemented to mitigate the impact of potential false alarms, as a single isolated message might not signify a genuine pest infestation requiring chemical intervention.

Case 3: If the base station receives messages from different clusters simultaneously, the base station will instruct the drone to start again with the process of choosing the required cluster to spray before making a decision about which to spray first. To ensure that all spraying occurs simultaneously, more drones can be used in this process. But, if the messages keep arriving from different clusters, then the base station may dispatch a camera drone to find out why it has started receiving messages from that particular area. It might be that there is no bug, just that the message sender itself is faulty.

The concluding segment of the algorithm functions as a robust protocol for managing persistent technical anomalies. In scenarios where field sensors maintain a continuous stream of alerts following both chemical mitigation and visual verification by camera drones, the system mandates a transition to manual oversight. Ultimately, a designated human technician is sent to the specific coordinates for a physical evaluation. Any identified irregularities are relayed to the central control station, ensuring that immediate corrective measures can be implemented on-site.

VI. CHALLENGES OF INTERNET OF THINGS IN SMART AGRICULTURE

According to the research and its increasing density, we can say that before artificial intelligence, IoT is the best technology that we have. It may take another 30 to 40 years to integrate AI into almost every field, or it may be a possibility that we cannot achieve AI with the same level of intelligence as human beings(Jadon et al., 2022). Therefore, we are relying on this IoT technology for the next 30 to 40 years, particularly in countries with less developed economies or large populations, such as India, Brazil, and Malaysia, where agriculture is a major economic aspect; it may take more time.In the agricultural domain, the main challenge is to present the new information and research to the farmers so that they can leverage the power of technologies to improve their agricultural practices and thereby the production [19].

Hardware Components Challenges:-The development of a system requires a lot of hardware components, most of which are required to be exposed to harsh environments for most of their life. Development of such hardware that can sustain in such a harsh environment is really a point of concern. The harsh environment can destroy the electronic circuit, and the system will not perform or may lead to an adverse effect on the field.

Organizational Challenges:- The agricultural organizations are meant to exchange information and transport goods. IoT brings accuracy in the delivery of these agricultural products [10]. In this respect, cloud computing provides the best services such as app development tools, efficient storage and resources. The Internet of Technology-based systems provides huge data that needs to be transferred and thus requires a huge cost.

Networking Challenges:-The IoT uses many networking protocols like Internet connectivity, Bluetooth and Wi-Fi. The operation of unlicensed devices using similar protocols causes interference and may cause problems in the operation of these IoT-based agriculture technologies [8]. Internet connectivity and network issues are always experienced in rural areas, and agricultural fields are found mostly in rural areas.

Challenge to Educate Farmers:-The IoT-based systems are very complicated and become more robust when it comes to IoT-based agriculture technology, but their success depends on farms. Farmers must be able to perform their tasks using these new technologies, but without education, they are not able to do that. Spending time learning these new technologies will cost them a huge loss in their profession. The uneducated farmers need more time to learn this technology.

VII. CONCLUSION

Integrating the implementation of IoT sensing frameworks alongside decision-making processes which depend on ML-based tools becomes another key element that requires attention in order to ensure efficient cotton pest management through effective implementation of precision agriculture technologies rather than the traditional techniques. The major benefit of using the proposed Decision Support System is the ability of tracking harmful pests accurately in real-time, meaning that there will not be the necessity of applying pesticides in case if the problem appears in an inappropriate manner as a result of human errors. At the same time, there are some potential challenges which should be taken into account prior to the implementation of the innovation, including weather conditions, network instability, as well as financial matters. Recommendations for further research about applying the system may refer to the protection of other cash crops, developing more precise algorithms considering multiple drones along with the field alert situation, as well as the development of AI algorithms on the edge device located in the camera.

REFERENCES

[1] Azfar, S., Nadeem, A., Ahsan, K., Mehmood, A., Almoamari, H., and Alqahtany, S.S. (2023). IoT-based cotton plant pest detection and smart-response system. *Applied Sciences*, 13(3): 1851.

[2] Azfar, S.; Nadeem, A.; Basit, A. Pest detection and control techniques using wireless sensor network: A review. J. Entomol. Zool. Stud. 2015, 3, 92–99.

[3] Biz4Intellia. (n.d.). A complete guide for IoT based pest detection with its benefits. Biz4Intellia.Blog.https://www.biz4intellia.com/blog/a-complete-guide-for-iot-based-pest-detection-with-its-benefits/.

[4] Dong, Y.; Fu, Z.; Stankovski, S.; Peng, Y.; Li, X. A Cotton Disease Diagnosis Method Using a Combined Algorithm of Case-Based Reasoning and Fuzzy Logic. Comput. J. 2021, 64, 155–168.

[5] Dubey, Y.; Mushrif, M.; Tiple, S. Superpixel Based Roughness Measure for Cotton Leaf Diseases Detection and Classification. In Proceedings of the 4th International Conference Recent Advances in Information Technology (RAIT), Dhanbad, India, 15–17 March 2018; pp. 1–5.

[6] Gyan, P., Sharma, H., and Kalamkar, S.S. (2023). The growth and export competitiveness of cotton in India. *Current Agriculture Research Journal*, 11(3).

[7] Jadon, J.K.S. and Singh, R. (2022). Challenges and opportunities of Internet of Things in smart agriculture: A review. In: *Electronic Systems and Intelligent Computing* (Eds. P.K. Mallick, A.K. Bhoi, A. González-Briones, and P.K. Pattnaik), Springer Nature Singapore, pp: 653-662. https://doi.org/10.1007/978-981-16-9488-2_62.

[8] Jawad, H.M. *et al.* (2017). Energy-efficient wireless sensor networks for precision agriculture: a review. *Sensors*, 17(8): 1781.

[9] Karar, Mohamed Esmail, et al. "A new mobile application of agricultural pests recognition using deep learning in cloud computing system." Alexandria Engineering Journal 60.5 (2021): 4423-4432.

[10] Lee, I. and Lee, K. (2015). The Internet of Things (IoT): Applications, investments, and challenges for enterprises. *Business Horizons*, 58(4): 431-440.

[11] Li, D.; Zhao, C. Computer and Computing Technologies in Agriculture XI, Proceedings of the 11th IFIP WG 5.14 International Conference, CCTA 2017, Jilin, China, 12–15 August 2017; Proceedings, Part II; AICT-546, IFIP Advances in Information and Communication Technology; Springer International Publishing: Berlin/Heidelberg, Germany, 2019.

[12] Liu, Z., Li, Y., Zhao, L., Liang, R., and Wang, P. (2022). Comparative evaluation of the performance of ZigBee and LoRa wireless networks in a building environment. *Electronics*, 11(21): 3560. https://doi.org/10.3390/electronics11213560.

[13] Materne, N.; Inoue, M. IoT Monitoring system for early detection of agricultural pests and diseases. In Proceedings of the 2018 12th South East Asian Technical University Consortium (SEATUC), Yogyakarta, Indonesia, 12–13 March 2018; Volume 1, pp. 1–5.

[14] Navarro, E., Costa, N., and Pereira, A. (2020). A systematic review of IoT solutions for smart farming. *Sensors*, 20: 4231.

[15] Preti, M., Verheggen, F., Angeli, S., 2020. Insect pest monitoring with camera-equipped traps: strengths and limitations. J. Pest. Sci. 94, 203-217.

[16] Randive, P.U., Deshmukh, R.R., Janse, P.V., Kayte, J.N.: Study of detecting plant diseases using non-destructive methods: a review. Int. J. Emerg. Trends Technol.Comput. Sci. (IJETTCS) 7(1), 66–71 (2018).

[17] Sarkozi, A. "New standards to curb the global spread of plant pests and diseases." Food and Agriculture Organization of the United Nations: Roma, Italy (2019).

[18] Sharma, R.P.; Ramesh, D.; Edla, D.R. IoFT-FIS: Internet of farm things based prediction for crop pest infestation using optimized fuzzy inference system. Internet Things 2022, 21, 100658.

[19] Titiya, M.D.; Shah, V.A. Ontology based expert system for pests and disease management of cotton crop in India. IJWP 2018, 10, 32–49.

[20] United Nations General Assembly. Food Production Must Double by 2050 to Meet Demand from World's Growing Population, Innovative Strategies Needed to Combat Hunger, experts tell second committee. Available online: http://www.un.org/press/en/2009/gaef3242.doc.htm.

International Journal of Environment, Agriculture and Biotechnology
Vol-11, Issue-3; May-Jun, 2026
Peer-Reviewed International Journal
Journal Home Page Available: https://ijeab.com/
Journal DOI: 10.22161/ijeab

Performance Evaluation of Janapriya Chicken as an Alternative Backyard Poultry Variety under Dry land Farming Conditions of Tamil Nadu

Dr. M. Saravanan[1], Dr. J. Diraviam[2]

[1]Subject Matter Specialist (Animal Science), ICAR, KVK, Karur, Tamil Nadu, India
[2]Senior Scientist and Head, ICAR, KVK, Karur, Tamil Nadu, India
*Corresponding Author

Received: 18 May 2026; Received in revised form: 11 Jun 2026; Accepted: 15 Jun 2026; Available online: 22 Jun 2026

***Abstract*— *Backyard poultry farming contributes to rural livelihoods by providing supplementary income and enhancing nutritional security for small and marginal farmers. However, indigenous breeds often exhibit low productivity and high mortality, particularly under changing climatic conditions. This study, conducted from October 2023 to June 2024 in Pulutheri and Chinnareddipatti villages, Thogamalai Block, Karur district, Tamil Nadu, India, evaluated the performance of improved backyard poultry strains under dry land farming conditions. Two improved varieties-Janapriya and TANUVAS Star Chicken—were compared with local non-descript birds under field conditions. Results showed that Janapriya birds attained a higher body weight (1.60 kg at five months), produced more eggs annually (120 eggs), and demonstrated better hatchability (75%) than TANUVAS Star Chicken and local birds. Mortality was considerably lower in improved varieties (5%) compared to local birds (20%). Economic analysis revealed that Janapriya generated the highest net income (INR 8635 per batch) with a benefit–cost ratio of 3.98. These findings suggest that improved backyard varieties, such as Janapriya, can significantly enhance productivity and profitability in rural poultry systems, thereby strengthening livelihood opportunities for smallholder farmers in dryland areas.*

Keywords*— Backyard poultry, Janapriya chicken, rural livelihood, egg production, improved poultry varieties, dry land farming

I. INTRODUCTION

Backyard poultry farming is an integral component of rural production systems in India, contributing significantly to household income, employment, and nutritional security for small and marginal farmers (Chatterjee & Rajkumar, 2015; Kumar *et al*., 2022). It provides an affordable source of high-quality animal protein and empowers rural women, enhancing livelihood resilience in resource-poor settings (Padhi, 2016; FAO, 2020).

Traditional backyard systems rely on indigenous birds, which are well-adapted to local conditions but exhibit slow growth, delayed maturity, and low egg production (60–80 eggs per year) (Ayyagari, 2001; Singh *et al*., 2017). To address these limitations, improved varieties such as Janapriya and TANUVAS Star Chicken have been developed, combining local adaptability with enhanced growth and egg production (Padhi, 2016; Rajkumar *et al*., 2019; Kumar *et al*., 2022).

In dry land regions such as Karur district, Tamil Nadu, backyard poultry farming offers a viable supplementary livelihood option. This study evaluates the growth performance, egg production, survivability, and economic viability of Janapriya chicken under backyard farming conditions, comparing it with TANUVAS Star Chicken and local non-descript birds. The findings aim to support the promotion of improved poultry varieties and management practices to enhance rural livelihoods and food security in dry land areas.

II. MATERIALS AND METHODS

Study Area

The field study was carried out in Pulutheri and Chinnareddipatti villages located in Thogamalai Block of Karur district, Tamil Nadu. The region is characterized by a semi-arid climate with relatively low rainfall and high temperatures during most of the year. Agriculture in this area mainly depends on seasonal rainfall and groundwater resources. Farmers typically cultivate crops such as millets, pulses, and oilseeds under dry land conditions. Livestock rearing is an important component of the local farming system. Backyard poultry farming is widely practiced in the villages, where birds are raised in small flocks and allowed to scavenge freely around the household premises. However, most farmers traditionally maintain local non-descriptive birds with relatively low productivity. The present study was conducted between October 2023 and June 2024 under field conditions to evaluate the performance of improved backyard poultry varieties in this region.

Selection of Farmers

Farmers involved in traditional backyard poultry farming were selected for the study with the assistance of local extension personnel. Priority was given to small and marginal farmers who had experience in maintaining backyard poultry. Selected farmers were provided with improved poultry chicks along with training on scientific poultry management practices.

Experimental Birds

The study included two improved backyard poultry varieties: Janapriya chicken and TANUVAS Star Chicken. The performance of these improved varieties was compared with local non-descriptive poultry birds commonly maintained by farmers. Janapriya birds are known for their dual-purpose characteristics, providing both eggs and meat. They exhibit good adaptability under backyard conditions and possess multi-coloured plumage that resembles indigenous birds, which improves their acceptance among farmers and consumers. TANUVAS Star Chicken is another improved backyard poultry variety developed for rural production systems. It is characterized by moderate growth rate, good egg production, and adaptability to village conditions.

Management Practices

Improved poultry chicks were distributed to farmers with basic inputs, and they were advised to construct simple shelters using local materials. Birds were reared semi-scavenging, roaming freely for food, with supplemental feed provided early on. Vaccinations against Ranikhet, IBD, and Newcastle diseases were done, and basic biosecurity measures like shelter cleanliness and health monitoring were followed.

Data Collection

Data were collected from participating farmers throughout the study period, including body weight at day-old stage and five months of age, mortality percentage, number of eggs produced per bird per year, hatchability percentage, and cost of production along with economic returns. Body weight was measured using digital weighing scales, while egg production was recorded based on farmer records and periodic field observations. Mortality data were collected to assess survivability under backyard conditions.

Economic Analysis

The economic performance of different poultry varieties was evaluated using standard cost-benefit analysis methods, calculating indicators such as gross cost of production, gross income from sale of eggs and birds, net profit, and benefit-cost ratio (BCR). This analysis helped determine the economic feasibility of introducing improved poultry varieties under backyard farming systems.

III. RESULTS

Growth Performance

Growth performance differed significantly among the poultry varieties evaluated in the study. Improved poultry strains exhibited higher body weight compared to local birds. Janapriya birds attained an average body weight of 1.60 kg at five months of age, whereas TANUVAS Star Chicken reached 1.52 kg. In contrast, the body weight of local birds was considerably lower, averaging 1.12 kg. The superior growth performance observed in Janapriya birds indicates their better genetic potential for meat production under backyard farming conditions. Faster growth and higher body weight contribute to increased market value and improved economic returns for farmers.

Table 1: Body weight, Mortality, Egg production and Hatchability parameters.

Technology opted	BW Day old (g)	BW 5th month (g)	Mortality (Percentage)	Egg production (No's)	Hatchability (Percentage)
Farmer practice - Unrecognized breed	30	1.12	20	70	60
Technology 1 – Janapriya	**40**	**1.6**	**5**	**120**	**75**
Technology 2- TANUVAS Star Chicken	41	1.52	5	110	70

Table 2: Cost Benefit ratio

Technology	Gross cost (Rs/batch)	Gross income (Rs/batch)	Net return (Rs)	BC ratio
Janapriya	**2165**	**10800**	**8635**	**3.98**
TANUVAS Star chicken	2175	10260	8086	3.72
Farmers practice	2165	7560	5394	2.49

Egg Production

Egg production varied significantly among the poultry varieties. Janapriya birds produced an average of 120 eggs annually, which was higher than TANUVAS Star Chicken (110 eggs per year). Local birds produced only around 70 eggs annually. The improved egg production observed in Janapriya birds can be attributed to their genetic improvement and better adaptability to scavenging conditions. Higher egg production directly contributes to increased household nutrition as well as additional income through egg sales.

Mortality

Mortality rate was considerably higher among local poultry birds compared to improved varieties. Local birds recorded a mortality rate of approximately 20%, whereas both Janapriya and TANUVAS Star Chicken showed significantly lower mortality rates of around 5%. Lower mortality among improved poultry varieties indicates better disease resistance and adaptability under village conditions. Proper vaccination and improved management practices also contributed to reduced mortality.

Hatchability

Hatchability percentage is an important parameter for evaluating the reproductive performance of poultry birds. In the present study, hatchability was highest in Janapriya birds (75%), followed by TANUVAS Star Chicken (70%) and local birds (60%). Higher hatchability improves the sustainability of backyard poultry systems as farmers can increase their flock size through natural hatching.

Economic Performance

Economic analysis revealed significant differences in profitability among the poultry varieties. Janapriya birds generated the highest net income of Rs. 8635 per batch with a benefit–cost ratio of 3.98. TANUVAS Star Chicken recorded a net return of Rs. 8085 with a benefit–cost ratio of 3.71. In comparison, local poultry birds generated a lower net return of Rs. 5395 with a benefit–cost ratio of 2.49. The higher economic returns obtained from improved poultry varieties demonstrate their potential for enhancing the income of rural farmers.

IV. DISCUSSION

The results of the present study clearly indicate that improved backyard poultry varieties can significantly enhance productivity compared with traditional local birds. Janapriya birds exhibited superior growth performance, higher egg production, better hatchability, and lower mortality under rural backyard conditions. These findings are consistent with earlier studies that reported improved performance of genetically developed backyard poultry strains under village production systems (Raj Kumar *et al.*, 2019; Kumar *et al.*, 2022). The higher body weight observed in Janapriya birds compared with local birds may be attributed to their improved genetic potential for growth and better feed utilization. Similar observations were reported by Singh *et al.* (2017) and Thakur *et al.* (2018), who found that improved backyard poultry varieties showed better growth rate and body weight than indigenous birds when reared under scavenging or semi-scavenging conditions. Egg production is one of the most important economic traits in backyard poultry systems. In the present study, Janapriya birds produced significantly more eggs than TANUVAS Star Chicken and local birds.

Higher egg production in improved backyard poultry varieties has also been reported by Padhi (2016) and Raj Kumar *et al*. (2017), who emphasized that genetic improvement programs have significantly enhanced the laying capacity of rural poultry strains. Increased egg production contributes not only to farmer income but also improves household nutritional security by providing a readily available source of animal protein.

The lower mortality observed in improved poultry varieties indicates their better adaptability and disease resistance under backyard farming conditions. Similar results were reported by Kumaresan *et al*. (2008), who observed higher survivability of improved dual-purpose chickens compared to local birds in rural farming systems. Proper vaccination and basic health care practices also play an important role in reducing poultry mortality in village conditions (FAO, 2020). Hatchability percentage recorded in the present study was also higher in Janapriya birds compared to other poultry varieties. Higher hatchability ensures better flock sustainability and enables farmers to expand their poultry population through natural incubation. Earlier studies have also reported improved reproductive performance in genetically improved backyard poultry strains (Raj Kumar *et al*., 2019). Economic analysis further demonstrated the advantages of improved poultry varieties in rural production systems. The higher net returns and benefit–cost ratio obtained from Janapriya birds highlight their potential for improving the economic status of rural households. Similar findings were reported by Kumar *et al*. (2022) and Murali and Vimalarani (2025), who reported that improved backyard poultry varieties, generated higher income compared with traditional indigenous birds.

Despite the advantages of improved poultry varieties, several constraints still limit their large-scale adoption in rural areas. Consumer preference for indigenous birds with multi-coloured plumage and traditional taste remains an important factor influencing market demand (Padhi, 2016). In addition, the limited availability of improved chicks in rural areas restricts the expansion of backyard poultry farming. Strengthening the supply chain for improved poultry chicks, providing farmer training programmes, and improving rural marketing systems can significantly enhance the adoption of improved backyard poultry technologies. Overall, the results of the present study confirm that improved backyard poultry varieties such as Janapriya have considerable potential to enhance productivity, profitability, and livelihood security of smallholder farmers in dry land regions.

V. CONCLUSION

Janapriya chicken outperformed other varieties in backyard farming in Tamil Nadu's dry lands, showing higher body weight, egg production, and lower mortality. Economic analysis revealed higher net income and benefit-cost ratio, making it suitable for improving rural livelihoods. Promoting such varieties can boost rural poultry farming productivity and profitability.

REFERENCES

[1] Ayyagari V. 2001. Development of varieties for rural poultry. Souvenir on Sustainable Poultry Production: Rural and Commercial Approach. Hyderabad, India.

[2] Chatterjee R.N. and Rajkumar U. 2015. An overview of poultry production in India. *Indian Journal of Animal Health*, 54(2): 89–108.

[3] FAO. 2020. *Poultry Development Review*. Food and Agriculture Organization of the United Nations, Rome.

[4] Kumar V., Rajkumar U., Prince L.L.L., Rama Rao S.V. and Chatterjee R.N. 2022. Geographical distribution and impact of backyard chicken varieties in India: A retrospective assessment. *Indian Journal of Animal Sciences*, 92(4): 452–459.

[5] Murali P. and Vimalarani M. 2025. Performance of genetically improved Janapriya chickens as an alternative to backyard poultry in Tamil Nadu. *Journal of Biology and Nature*, 17(2): 215–222.

[6] Padhi M.K. 2016. Importance of indigenous breeds of chicken for rural economy and their improvements for higher production performance. *Scientifica*, 2016: 1–9.

[7] Rajkumar U., Rama Rao S.V., Reddy B.L.N. and Chatterjee R.N. 2019. Performance of improved chicken varieties in backyard production systems. *Indian Journal of Poultry Science*, 54(1): 1–6.

[8] Singh D.P., Singh R.V. and Singh B. 2017. Backyard poultry farming: A tool for rural development. *Livestock Research for Rural Development*, 29(5).

[9] Thakur M.S., Parmar S.N.S. and Kumar A. 2018. Performance of improved backyard poultry varieties under rural conditions. *Indian Journal of Animal Sciences*, 88(7): 805–808.

[10] Islam M.A. and Nishibori M. 2009. Indigenous chicken production in Asia. *World's Poultry Science Journal*, 65: 407–418.

[11] Guèye E.F. 2000. The role of family poultry in poverty alleviation and food security. *World's Poultry Science Journal*, 56: 139–146.

[12] Kumaresan A., Pathak K.A., Bujarbaruah K.M. et al. 2008. Analysis of a village chicken production system and performance of improved dual purpose chickens under a subtropical hill agro-ecosystem in India. *Tropical Animal Health and Production*, 40: 395–402.

[13] Rajkumar U., Prince L.L.L. and Chatterjee R.N. 2017. Backyard poultry farming in India: Opportunities and challenges. *Indian Journal of Poultry Science*, 52(1): 1–9.

International Journal of Environment, Agriculture and Biotechnology
Vol-11, Issue-3; May-Jun, 2026
Peer-Reviewed International Journal
Journal Home Page Available: https://ijeab.com/
Journal DOI: 10.22161/ijeab

Spatiotemporal Dynamics and Drivers of Daytime and Nighttime Urban Heat Islands in the Guangdong-Hong Kong-Macao Greater Bay Area: Insights from XGBoost-SHAP

Shiya Feng, Ruei-Yuan Wang*

School of Sciences, Guangdong University of Petrochem Technology (GDUPT), Maoming 525000, China

Received: 16 May 2026; Received in revised form: 14 Jun 2026; Accepted: 17 Jun 2026; Available online: 24 Jun 2026

Abstract*— The Guangdong-Hong Kong-Macao Greater Bay Area (GBA) is a representative region in China characterized by a high level of urbanization, rapid land-use changes, and intensive population and economic activities. Identifying the spatiotemporal patterns and driving factors of daytime and nighttime surface urban heat island (SUHI) intensity is of great significance for regional thermal environment management and territorial spatial planning. Based on multi-source datasets from 2018 to 2024, this study developed an analytical framework consisting of "SUHI pattern identification–land-use transition response–driving mechanism interpretation" to reveal the evolution and driving mechanisms of the thermal environment in the GBA from a diurnal perspective. The results showed that: (1) High SUHI values during both daytime and nighttime were concentrated in core built-up areas such as Guangzhou, Foshan, Dongguan, and Shenzhen, whereas low-value areas were mainly distributed in mountainous forest regions in the north and coastal water bodies along the Pearl River Estuary. (2) From 2018 to 2024, SUHI intensity exhibited overall fluctuations, with an increasing trend in the eastern urban corridor of the Pearl River Delta, whereas the northwestern mountainous areas remained relatively stable or experienced a slight decline. (3) The conversion of forestland, cropland, and water bodies/wetlands to construction land significantly intensified SUHI, with the strongest warming effect observed when water bodies/wetlands were converted to construction land. Conversely, the transformation of construction land into green spaces or water bodies effectively mitigated SUHI. (4) XGBoost-SHAP analysis revealed that NDBSI, NDVI, NDMI, MNDWI, and NTL were the key factors influencing daytime SUHI, whereas NDBSI, NTL, PD (population density), GDP, and NDVI were the primary drivers of nighttime SUHI. These findings provide a scientific basis for thermal environment regulation, urban expansion control, and blue-green space conservation in the GBA.

***Keywords*— Guangdong-Hong Kong-Macao Greater Bay Area (GBA); Surface Urban Heat Island (SUHI); Daytime and Nighttime Differences; Land-use Transition; XGBoost-SHAP Model**

I. INTRODUCTION

The urban heat island (UHI) effect is one of the most prominent thermal environmental problems associated with rapid urbanization and is closely linked to changes in urban land surfaces, alterations in surface energy balance, and increasing anthropogenic heat emissions (Oke, 1987). With the continuous expansion of built-up areas, the increase in impervious surfaces, the reduction of vegetation cover, and the intensification of human activities, urban regions experience substantial changes in energy exchange processes, hydrothermal conditions, and heat storage capacity. These changes often result in significantly higher surface temperatures in urban areas than in surrounding ecological landscapes, thereby intensifying the surface urban heat island (SUHI) effect.

The GBA, comprising Guangzhou, Shenzhen, Zhuhai, Foshan, Huizhou, Dongguan, Zhongshan, Jiangmen, Zhaoqing, Hong Kong, and Macao, is one of the most densely urbanized and economically dynamic urban agglomerations in China. The region contains highly concentrated built-up areas while simultaneously preserving extensive ecological spaces, including mountains, forests, wetlands, rivers, and coastal water bodies. This unique spatial configuration provides an ideal setting for investigating the spatiotemporal dynamics and driving mechanisms of daytime and nighttime SUHIs at the urban agglomeration scale. Over the past decade, the GBA has experienced rapid urban expansion, increasing population and industrial concentration, and substantial changes in land-use structure. Meanwhile, the region is located within a typical subtropical monsoon climate zone characterized by frequent high-temperature and high-humidity conditions. The interaction between accelerated urbanization and complex natural environments has intensified thermal environmental challenges across the region. Consequently, understanding the formation mechanisms, spatial heterogeneity, and evolution of SUHIs has become increasingly important for climate adaptation, urban planning, ecological conservation, and public health protection. Recent studies have emphasized several critical issues, including daytime–nighttime differences in SUHI mechanisms, anthropogenic heat contributions, heatwave-related risks, urban ventilation constraints, environmental justice concerns, and the cooling thresholds of blue–green infrastructure. These emerging topics indicate a shift in UHI research from simple pattern description toward comprehensive thermal risk assessment and management.

Existing UHI studies have mainly focused on three aspects. First, investigations of spatiotemporal SUHI patterns have widely employed thermal infrared remote sensing data, such as MODIS and Landsat imagery, revealing that high-intensity SUHI areas are generally concentrated in densely built-up regions, whereas forests, wetlands, and water bodies provide significant cooling effects (Chen et al., 2006). Second, studies on land-use change have demonstrated that urban expansion is a major contributor to thermal environmental deterioration, while ecological restoration can effectively mitigate SUHI intensity (Liu et al., 2014). Third, with advances in machine learning techniques, increasing attention has been devoted to identifying the driving mechanisms of thermal environments. Models such as Random Forest and Extreme Gradient Boosting (XGBoost) have proven effective in capturing complex nonlinear relationships among environmental variables and SUHI intensity (Yang et al., 2022).

Previous studies have further demonstrated that land-use transitions exert substantial influences on regional thermal environments. The conversion of ecological land into built-up land is often accompanied by increasing surface temperatures and intensified SUHI effects (Liu et al., 2014). At the global scale, rapid urban expansion has significantly strengthened SUHI intensity, although considerable regional differences remain (Zhou et al., 2017). Conversely, increases in vegetation coverage and water bodies can effectively alleviate thermal stress through evapotranspiration and cooling effects, thereby serving as important ecological regulators of urban climate (Li et al., 2020). In recent years, machine learning approaches have increasingly been adopted to explore SUHI formation mechanisms, revealing complex nonlinear interactions among climatic, ecological, socioeconomic, and landscape factors (Yang et al., 2022). Studies conducted in the GBA have also reported significant spatial clustering of SUHIs, with hotspots predominantly concentrated in the highly urbanized core areas of the Pearl River Delta (Wang et al., 2023).

Despite these advances, several important limitations remain. First, most studies focus on a single temporal dimension and rarely provide systematic comparisons between daytime and nighttime SUHI dynamics. Second, quantitative assessments of the relationships between land-use transitions and SUHI evolution remain limited, particularly at the urban agglomeration scale. Third, existing studies on driving mechanisms often emphasize variable importance rankings while paying insufficient attention to the nonlinear response characteristics and threshold effects of key influencing factors. Furthermore, integrated investigations linking SUHI patterns, land-use transitions, and driving mechanisms within a unified analytical framework remain scarce. These limitations hinder a comprehensive understanding of thermal environmental evolution in rapidly urbanizing regions. To address these gaps, this study aims to answer three key research questions: (1) Where are the SUHI hotspots in the GBA, how have they evolved from 2018 to 2024, and do they exhibit significant spatial clustering characteristics? (2) How is major land-use transition pathways associated with increases or decreases in daytime and nighttime SUHI intensity? (3)Which environmental, socioeconomic and landscape factors play dominant roles in shaping daytime and nighttime SUHIs, and how do their effects differ?

Using multi-source spatial datasets from 2018 to 2024, this study investigates the spatiotemporal evolution, land-use transition responses, and driving mechanisms of daytime and nighttime SUHIs in the GBA. The relationships among research questions, analytical methods, and expected outputs are summarized in Table 1. Specifically, RQ1 examines the spatiotemporal distribution and spatial clustering characteristics of daytime and nighttime SUHIs; RQ2 quantifies the thermal environmental impacts of land-use transitions; and RQ3 identifies the dominant driving factors and their nonlinear response mechanisms. Together, these three research questions constitute a progressive analytical framework of "pattern identification–process response–mechanism explanation," providing a comprehensive understanding of SUHI evolution in one of the world's most rapidly urbanizing regions.

Table 1 Research Questions and Analytical Framework

Research Questions/Pattern Recognition	Corresponding method/process response	Expected Output/Mechanism Explanation
RQ1: Exploring the spatiotemporal patterns of diurnal and nocturnal SUHI?	Interannual statistics, trend analysis, Global Moran's I, LISA	Spatial distribution of SUHI, trend enhancement zones, hot/cold spots
RQ2: How does land-use transfer affect SUHI?	Land-use transfer matrix, ΔSUHI analysis	Main transfer pathways and their warming/cooling effects
RQ3: What are the primary drivers of diurnal SUHI?	XGBoost, SHAP	Variable importance, direction of effect, nonlinear response

II. STUDY AREA AND METHODS

2.1 Overview of the Study Area

The study area is the Guangdong–Hong Kong–Macao Greater Bay Area (GBA) (Figure 1), which consists of nine cities in the Pearl River Delta and the two Special Administrative Regions of Hong Kong and Macao. Located along the southern coast of China, the GBA lies within a typical subtropical monsoon climate zone characterized by warm temperatures, abundant precipitation, and distinct wet and dry seasons. The region features diverse topography, including plains, hills, mountains, river networks, and coastal waters.

As one of the most economically dynamic and highly urbanized regions in China, the GBA serves as a key growth pole in the national strategy for regional coordinated development. Between 2018 and 2024, rapid urban expansion, population growth, and industrial agglomeration led to substantial changes in land-use patterns, particularly the continuous increase in built-up land and the transformation of ecological spaces. These changes have significantly influenced the regional thermal environment.

The GBA contains both highly urbanized metropolitan areas, such as Guangzhou, Shenzhen, and Dongguan, and extensive ecological spaces, including the mountainous forests in the northern region, the Pearl River water system, and coastal wetlands. This diverse landscape creates pronounced spatial heterogeneity in land cover, urban development intensity, and ecological functions, making the region well suited for investigating the interactions among urbanization, land-use change, and surface thermal environments.

Given its rapid urbanization, complex natural conditions, and diverse land-use characteristics, the GBA provides an ideal case for examining the spatiotemporal evolution of daytime and nighttime SUHIs, their responses to land-use transitions, and the underlying driving mechanisms at the urban agglomeration scale.

2.2 Data Sources and Preprocessing

The data used in this study include six categories of variables: thermal environment, land-use, ecological moisture, built-up dry surfaces, topographic climate, and socio-economic activities (Table 2 and Table 3). Thermal environment data were employed to construct diurnal SUHI; land-use data were used to analyze land cover structure and transition processes; NDVI (Normalized Difference Vegetation Index), NDMI (Normalized Difference Moisture Index), NDWI (Normalized Difference Water Index), and MNDWI (Modified Normalized Difference Water Index) were utilized to characterize vegetation, moisture, and water body cooling capacity; NDBSI (Normalized Difference Built-up Index) was applied to represent built-up, bare, and dry surfaces; DEM, Slope, ATP (Temperature), PRE (Precipitation) and SPI (Standardized Precipitation Index) were used to depict natural topography and climatic hydrothermal conditions; while NTL (Nighttime Light Index), PD (Population Density), and GDP (Gross Domestic Product) served as indicators of human activities, population agglomeration, and economic activity intensity.

All remote sensing and environmental variables underwent data retrieval, quality control, annual compositing, study area clipping, spatial alignment, and scale unification on the Google Earth Engine (GEE) platform. Socio-economic variables were assigned to unified spatial analysis units based on administrative boundaries. To avoid false precision issues, this study organized multi-source variables using a unified analytical grid. High-resolution land-use data were aggregated using the majority method, continuous variables were aggregated using the mean method, and administrative statistical variables were assigned through spatial joins.

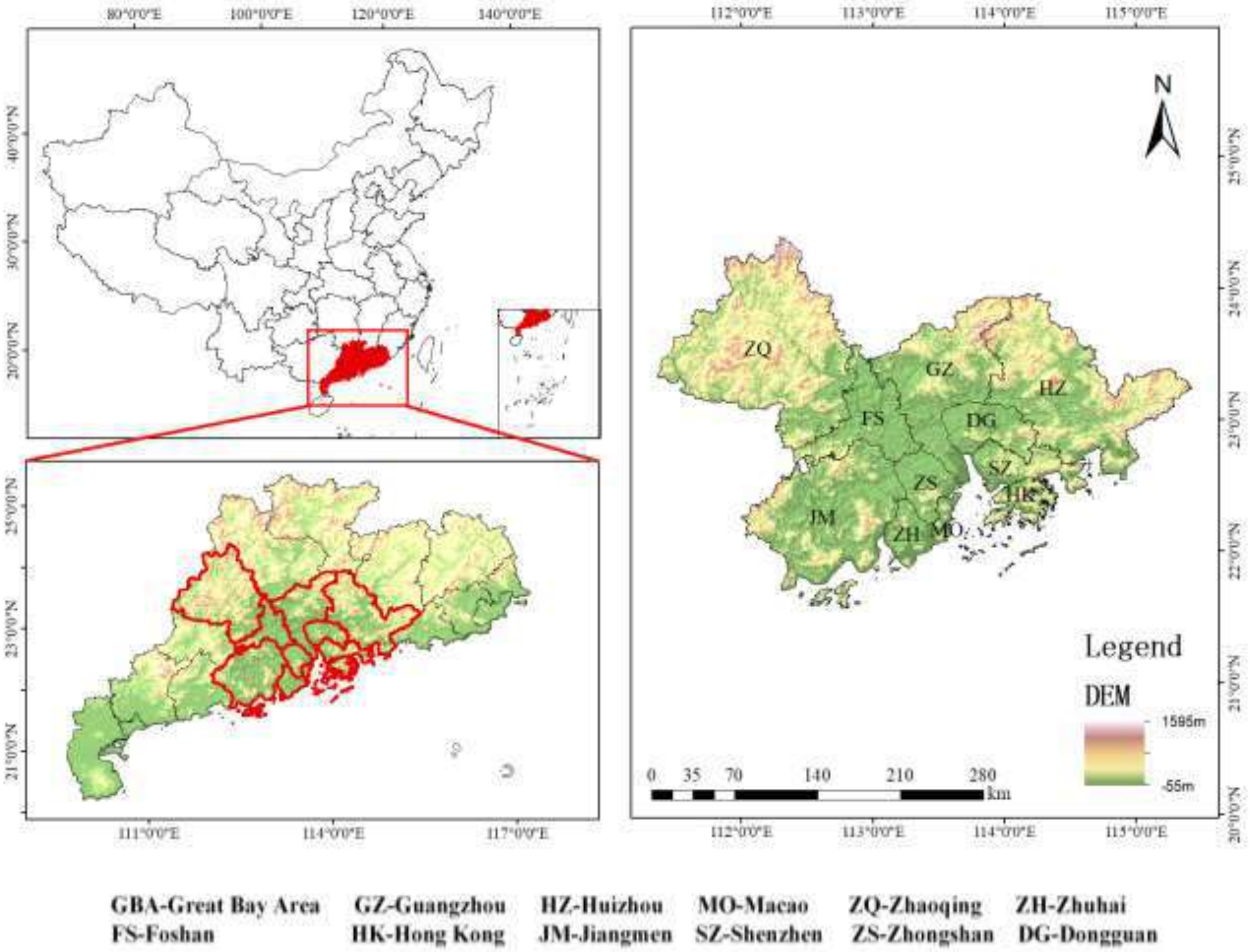

Fig.1 Location Map of the Study Area

Table 2 Research Variables and Their Descriptions

Data Category	Variable	Purpose
Thermal environment	LST_Day, LST_Night, SUHI_Day,SUHI_Night	Constructing daytime and nighttime SUHI intensity
Land-use	LULC	Identify land-use structure and transition pathways
Ecological moisture	NDVI,NDMI,NDWI,MNDWI	Characterizing the cooling effects of vegetation, moisture, and water bodies
Dry surface	NDBSI	Characterization of hardened, bare, and dry surfaces
Terrain and climate	DEM, Slope, ATP, PRE, SPI	Characterizing natural background and climatic hydrothermal conditions
Socio-economic activities	NTL, PD, GDP	Characterizing the intensity of human activities, population, and economic agglomeration

Table 3 Data Sources and Basic Information

Data Category	Data Product	Time range	Resolution	Data Source
LST	MOD11A2	2018–2024	1 km	Download from the GEE platform
LULC	ESA WorldCover	2018–2024	10 m	
NDVI	MOD13Q1	2018–2024	250 m	
NDMI	Landsat 8/9	2018–2024	30 m	
NDWI	Landsat 8/9	2018–2024	30 m	
MNDWI	Landsat 8/9	2018–2024	30 m	
NDBSI	Landsat 8/9	2018–2024	30 m	
DEM	SRTM	None	30 m	
Slope	Calculate from DEM	None	30 m	
ATP	ERA5-Land	2018–2024	0.1°	
PRE	CHIRPS	2018–2024	0.05°	
SPI	Calculate from CHIRPS	2018–2024	0.05°	
NTL	VIIRS VNL	2018–2024	500 m	
PD	WorldPop	2018–2024	100 m	
GDP	China Urban Statistical Yearbook	2018–2024	Municipal level	National Bureau of Statistics （https://www.stats.gov.cn/）

2.3 Methodology

This study constructs a daytime–nighttime SUHI intensity database for the GBA covering the period from 2018 to 2024, based on multi-source remote sensing, natural environmental, and socio-economic data. A comprehensive analysis is conducted from three perspectives: spatiotemporal evolution, land-use transition responses, and driving mechanism identification.

First, daytime and nighttime SUHI indicators are developed using land surface temperature (LST) data. Interannual statistical analysis and trend analysis are employed to reveal temporal variations in heat island intensity. Global Moran's I and Local Indicators of Spatial Association (LISA) are applied to identify SUHI hotspots, cold spots, and their spatial clustering characteristics.

Second, land-use transition matrices are used to characterize conversion processes among different land-use types. By integrating ΔSUHI analysis, the impacts of various land-use transitions on thermal environmental changes are assessed, thereby identifying dominant warming and cooling transition patterns.

Finally, multidimensional driving factors, including vegetation, moisture, built environment, topographic and climatic conditions, and socio-economic activities, are incorporated into the analysis. The XGBoost machine learning model is employed to quantify the contribution of each factor to daytime and nighttime SUHI intensity, while SHAP-based interpretation methods are used to reveal the directional effects, influence magnitudes, and nonlinear response relationships of key drivers. This framework systematically elucidates the formation mechanisms and evolutionary patterns of daytime and nighttime heat island effects in the GBA, as illustrated in Figure 2.

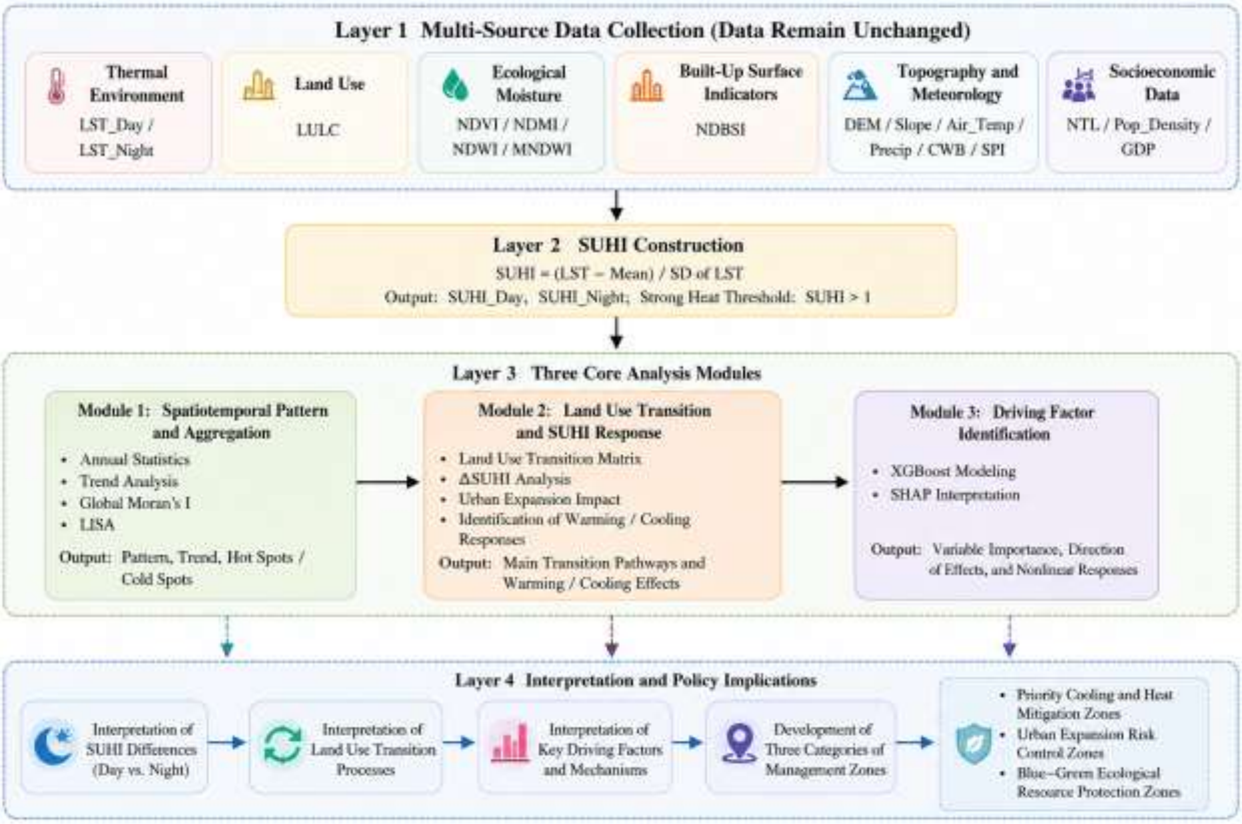

Fig.2. The Framework of the Study

2.3.1 SUHI Indicator Construction

This study employs the Standardized SUHI Intensity to characterize the deviation of different spatial units within the study area from the regional average thermal environment in a given year. Daytime and nighttime SUHIs are calculated separately, as shown in equations (1) and (2):

Daytime:

$$SUHI_i^{day} = (LST_i^{day} - mean(LST^{day}))/SD(LST^{day}) \quad (1)$$

Nighttime：

$$SUHI_i^{night} = (LST_i^{night} - mean(LST^{night}))/SD(LST^{night}) \quad (2)$$

In equations (1) and (2), $SUHI_i$ represents the urban heat island intensity of the ith spatial unit, LST_i denotes the land surface temperature of that spatial unit, mean (LST) indicates the annual average land surface temperature of the study area, and $SD(LST)$ represents the standard deviation of the land surface temperature in the study area for that year. Standardization processing can reduce the impact of climatic background differences across different years on the comparison of heat island intensity.

Based on the standardized SUHI Intensity values, the study area was classified into five categories (Table 4). Areas with SUHI values below −1.0 were defined as strong cold island (SCI) zones, indicating surface temperatures significantly lower than the regional average and typically corresponding to ecological cooling sources such as forests and water bodies. Regions with SUHI values ranging from −1.0 to −0.5 were classified as weak cold island (WCI) zones, exhibiting a certain degree of cooling effect. Areas with SUHI values between −0.5 and 0.5 were categorized as neutral zones (NZ), where thermal conditions were close to the regional average. Areas with SUHI values ranging from 0.5 to 1.0 were defined as weak heat island (WHI) zones, reflecting surface temperatures higher than the regional average. Meanwhile, areas with SUHI values greater than 1.0 were classified as strong heat island (SHI) zones, indicating significant heat accumulation and typically concentrated in urban core built-up areas and high-intensity development zones.

Table 4 SUHI Classification Criteria

Scope	Level	Explanation
SUHI < -1.0	Strong Cold Island (SCI) zones	Significantly lower than the regional average thermal environment
-1.0 ≤ SUHI < -0.5	Weak Cold Island (WCI) zones	Lower temperature zone
-0.5 ≤ SUHI ≤ 0.5	Neutral zones (NZ)	Close to the regional average
0.5 < SUHI ≤ 1.0	Weak Heat Island (WHI) zones	Higher temperature zone
SUHI > 1.0	Strong Heat Island (SHI) zones	Significantly higher than the regional average thermal environment

2.3.2 Spatiotemporal Patterns and Spatial Aggregation Analysis of Daytime and Nighttime SUHI

First, the mean value, standard deviation, proportion of strong heat island areas, and proportion of strong cold island areas of daytime and nighttime SUHI in different years were calculated to characterize overall thermal environment changes during the study period. Second, linear trend analysis was performed for each spatial unit to identify areas experiencing SUHI intensification or weakening. A positive trend slope indicates SUHI intensification, whereas a negative trend slope indicates SUHI weakening.

Furthermore, Global Moran's I was used to examine whether daytime and nighttime SUHI exhibited overall spatial autocorrelation (Equation 3). A significantly positive Moran's I value indicates that high values tend to cluster with high values and low values tend to cluster with low values in space. Subsequently, Local Indicators of Spatial Association (LISA) were employed to identify local spatial aggregation patterns (Equation 4), including High–High hotspot areas, Low–Low cold spot areas, High–Low outlier areas, and Low–High outlier areas.

Global Moran's I:

$$I = \frac{N}{\sum_{i=1}^{N}\sum_{j=1}^{N} w_{ij}} \times \frac{\sum_{i=1}^{N}\sum_{j=1}^{N} w_{ij}(x_i - \bar{x})(x_j - \bar{x})}{\sum_{i=1}^{N}(x_i - \bar{x})^2}$$

(3)

Local Moran's I：

$$I_i = \frac{(x_i - \bar{x})}{\frac{1}{n}\sum_{k=1}^{n}(x_k - \bar{x})^2} \cdot \sum_{j=1}^{n} w_{ij}(x_j - \bar{x})$$

(4)

In equations (3) and (4), I represents the Global Moran's I index; n is the number of sample units; w_{ij} denotes the spatial weight matrix; W is the sum of all spatial weights; x_i and x_j represent the SUHI values of spatial units i and j, respectively; $\bar{x}$ is the mean SUHI value of the study area. The range of Moran's I is [-1, 1]. A value greater than 0 indicates positive spatial correlation, less than 0 indicates negative spatial correlation, and a value close to 0 suggests a random spatial distribution.

2.3.3 Analysis of Land-Use Transitions and Their SUHI Responses

Land-use transition matrices were constructed based on land-use/land-cover (LULC) maps from 2018 and 2024 to quantify the direction and magnitude of land-use changes during the study period. The transition matrix provides a quantitative representation of conversion relationships among different land-use categories and has been widely applied in land-change dynamics analysis (Pontius et al., 2004; Liu et al., 2014).

To reveal the influence of land-use transformation on surface thermal environments, a land-use transition matrix was generated based on the initial and final years of the study period. In the matrix, Tij represents the area converted from land-use type (i) to land-use type (j) between 2018 and 2024. This approach allows the identification of dominant transformation pathways and their corresponding thermal responses.

Particular attention was given to transition pathways associated with the conversion of ecological land into built-up areas, including forestland, cropland, water bodies, wetlands, and bare land converted into impervious surfaces. Meanwhile, transitions from built-up areas to ecological spaces, such as green spaces and water bodies, were also examined to evaluate potential cooling effects associated with ecological restoration and urban renewal.

Considering that SUHI intensity reflects relative thermal anomalies rather than absolute temperature differences, the variation in SUHI intensity (ΔSUHI) was calculated for each spatial unit to characterize thermal environmental changes between 2018 and 2024 (Equation 5).:

$\Delta SUHI_i = SUHI_i 2024 - SUHI_i 2018$ (5)

Where $\Delta SUHI_i$ represents the change in SUHI intensity for spatial unit (i); $SUHI_i 2024$ and $SUHI_i 2018$

represent the standardized SUHI values in 2024 and 2018, respectively. Positive ΔSUHI values indicate increasing thermal anomalies, suggesting a warming effect associated with land-use change, whereas negative values indicate cooling effects. Subsequently, the average ΔSUHI values corresponding to different land-use transition pathways were calculated to identify which transformation processes contributed to SUHI intensification or mitigation (Table 5).

Table 5 Land Use Transition Pathways and Expected Thermal Environment Effects

Transfer path	Thermal environmental effect	Explanation
Forestland/Cropland →Built-up land	SUHI enhancement	Reduced vegetation, increased hardening, weakened evapotranspiration
Water bodies/wetlands →Built-up land	SUHI enhancement	The cooling effect of water bodies is weakening
Bare land →Built-up land	May enhance	Surface heat storage and increase in impervious surfaces
Built-up Land → Green space/Water body	SUHI weakened	Enhanced ecological cooling and humidification conditions
Stable Built-up land	Maintain high SUHI	High thermal storage and intense human activity
Stable Forestland/Water bodies	Maintain low SUHI	Stable cooling source and evapotranspiration

2.3.4 XGBoost-SHAP Factor Identification

To identify the key factors influencing diurnal SUHI, this study constructed separate XGBoost regression models for daytime SUHI and nighttime SUHI. As a machine learning method based on gradient-boosted decision trees, XGBoost can effectively capture nonlinear relationships and complex interactions among high-dimensional variables (Chen & Guestrin, 2016). The dependent variables were $SUHI_{Day}$ and $SUHI_{Night}$, while the explanatory variables included LULC, NDVI, NDMI, NDWI, MNDWI, NDBSI, DEM, Slope, ATP, PRE, SPI, NTL, PD and GDP.

An Extreme Gradient Boosting (XGBoost) model was employed to capture the nonlinear relationships between urban heat island intensity and multi-source driving factors. The XGBoost prediction is formulated as (6):

$$\hat{y}_i = \phi(\mathbf{x}_i) = \sum_{k=1}^{K} f_k(\mathbf{x}_i) + b_0 \quad (6)$$

where $\hat{y}_i$is the predicted SUHI at location i, xi is the vector of explanatory variables (e.g., NDVI, impervious surface ratio, nightlight index), fk is the kth regression tree, and b0is the base score. To interpret the XGBoost model, SHapley Additive exPlanations (SHAP) values were computed using the Tree SHAP algorithm (Lundberg & Lee, 2017), the formulated as (7):

$$\phi_j^{(i)} = \sum_{S\subseteq F\setminus\{j\}} \frac{|S|!(|F|-|S|-1)!}{|F|!} [f(S\cup\{j\})(x_i) - f(S)(x_i)] \quad (7)$$

The prediction for sample i can be decomposed as $\hat{y}_i = \phi_0 + \sum_{j=1}^{n}\phi_j^{(i)}$, where $\phi_j^{(i)}$ denotes the local contribution of the jth driver. Global feature importance was assessed as the mean absolute SHAP value, $\frac{1}{n}\sum_{i=1}^{n}|\phi_j^{(i)}|$."

XGBoost provides an additive predictive modeling framework, while SHAP values offer mathematically interpretable measures of the contribution of each driving factor to the predicted outcome. The combination of these two methods constitutes the complete theoretical foundation for "XGBoost-SHAP driver identification." XGBoost is used to model the nonlinear relationships between multidimensional variables and SUHI, whereas SHAP explains the model outputs by quantifying the marginal contribution of each variable to the predictions.

This study focuses on analyzing SHAP variable importance, SHAP summary plots, and dependence plots of key variables to determine which factors are most influential, whether their contributions to SUHI are positive or negative, and whether threshold effects or nonlinear response relationships exist. To enhance model generalization and reduce random sampling errors, the model training process adopts a 70% training set and 30% test set split, combined with five-fold cross-validation (5-fold cross-validation) for parameter optimization. In each cross-validation iteration, the training samples are divided into five subsets, with four subsets used for model training and the remaining subset used for validation. This process is repeated until all validation rounds are completed.

Model performance is evaluated using the coefficient of determination (R^2), root mean square error (RMSE), and mean absolute error (MAE). The R^2 value measures the model's explanatory power for SUHI variations, while

RMSE and MAE are used to assess prediction error levels. An R^2 value closer to 1 indicates a better model fit, whereas lower RMSE and MAE values indicate higher prediction accuracy.

Based on the parameter optimization results, the final XGBoost model parameters are set as follows: number of trees (n_estimators) = 300, maximum tree depth (max_depth) = 6, learning rate (learning_rate) = 0.05, subsample ratio (subsample) = 0.8, feature subsample ratio (colsample_bytree) = 0.8, and random seed (random_state) = 42. This configuration ensures prediction accuracy while effectively mitigating overfitting.

III. RESULTS

3.1 Spatiotemporal Distribution and Trends of Daytime and Nighttime SUHI

From 2018 to 2024, the GBA exhibited a spatial pattern characterized by "high values in the center and low values in the periphery" for both daytime and nighttime SUHI Intensity. High-SUHI areas were primarily concentrated in the core urban agglomerations of the Pearl River Delta, including highly urbanized regions such as Guangzhou, Shenzhen, Dongguan, and Foshan, forming continuous heat island cores. In contrast, low-SUHI areas were mainly distributed in the northern mountainous and hilly regions, as well as coastal water bodies such as the Pearl River Estuary and Lingdingyang. In 2018, high-SUHI zones had already formed distinct clusters within the built-up areas of the Guangzhou–Foshan and Shenzhen–Dongguan metropolitan regions. Subsequently, with continued urban development and the expansion of built-up land, these high-SUHI areas further extended into surrounding regions, although the overall spatial pattern remained relatively stable. Meanwhile, the northern forested areas and coastal waters consistently maintained low SUHI levels, exhibiting stable cold island characteristics.

Significant differences were observed between the spatial distributions of daytime and nighttime SUHI. During the daytime, high-SUHI areas were more extensive, extending beyond urban cores to encompass surrounding industrial zones and towns, thereby forming large contiguous heat island regions. Low-SUHI areas predominantly corresponded to ecological land-cover types such as forests and water bodies (Figure 3). In contrast, nighttime high-SUHI areas were more concentrated and were primarily located within central business districts and high-density built-up areas of cities such as Guangzhou and Shenzhen. Although the spatial extent of nighttime heat islands was considerably smaller than that observed during the daytime, their spatial clustering characteristics were more pronounced (Figure 4). Overall, daytime heat island effects exhibited stronger spatial diffusion, whereas nighttime heat island effects showed more evident core clustering, reflecting the persistent influence of urban surface heat storage and delayed nocturnal heat release on the thermal environment (Figure 5).

Trend analysis revealed that SUHI dynamics in the GBA from 2018 to 2024 exhibited significant spatial heterogeneity. In the northwestern portion of the study area, including mountainous regions such as Zhaoqing, SUHI generally remained stable or showed a weakening trend. In contrast, the eastern Pearl River Delta, particularly the Shenzhen–Dongguan–Huizhou urban development corridor, experienced a pronounced intensification of SUHI, forming a continuous warming belt. Combined with land-use distribution patterns and statistical results, these findings indicate that the core Pearl River Delta region, characterized by highly contiguous built-up land, extensive impervious surface coverage, and intensive population and industrial activities, experienced sustained heat accumulation and storage, resulting in persistent high-SUHI zones. Conversely, the northern mountainous forest regions, with dense vegetation cover and strong evapotranspiration effects, effectively reduced surface temperatures, while coastal water bodies, influenced by high thermal capacity and sea–land breeze circulation, formed stable cold island zones. Consequently, the study area gradually developed a thermal environmental pattern in which urban agglomerations functioned as heat sources, while mountainous forests and coastal waters served as cooling sources.

Table 6 presents the overall statistical characteristics of daytime and nighttime SUHI in the GBA from 2018 to 2024. Because SUHI was calculated using Z-score standardization, the mean value of the study area theoretically approached zero. Accordingly, the average SUHI remained approximately −0.03 throughout the study period, indicating a relatively stable overall thermal environmental distribution among years. In contrast, the standard deviation and the proportion of strong heat island areas more effectively reflected spatial variations in thermal environmental conditions. The standard deviation of daytime SUHI ranged from 1.74 to 2.10, substantially higher than that of nighttime SUHI (1.28–1.74), indicating greater spatial heterogeneity in daytime surface thermal conditions. Furthermore, the proportion of strong daytime heat island areas (4.58%–9.69%) was markedly higher than that of nighttime heat island areas (0.42%–1.84%), demonstrating that daytime heat island effects were stronger and more spatially extensive, whereas nighttime heat island effects were primarily concentrated within core built-up areas. Overall, the thermal environment of the GBA exhibited distinct diurnal differences: daytime surface temperatures were more strongly influenced by solar radiation and surface characteristics, whereas nighttime temperatures primarily reflected urban heat storage and anthropogenic heat emissions.

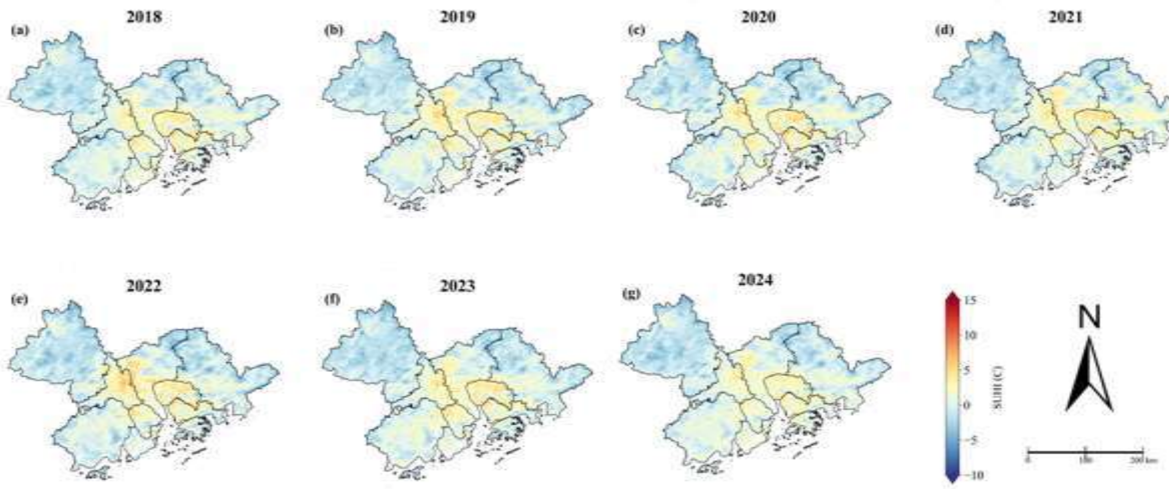

Figure 3 Spatial Distribution of Daytime SUHI from 2018 to 2024

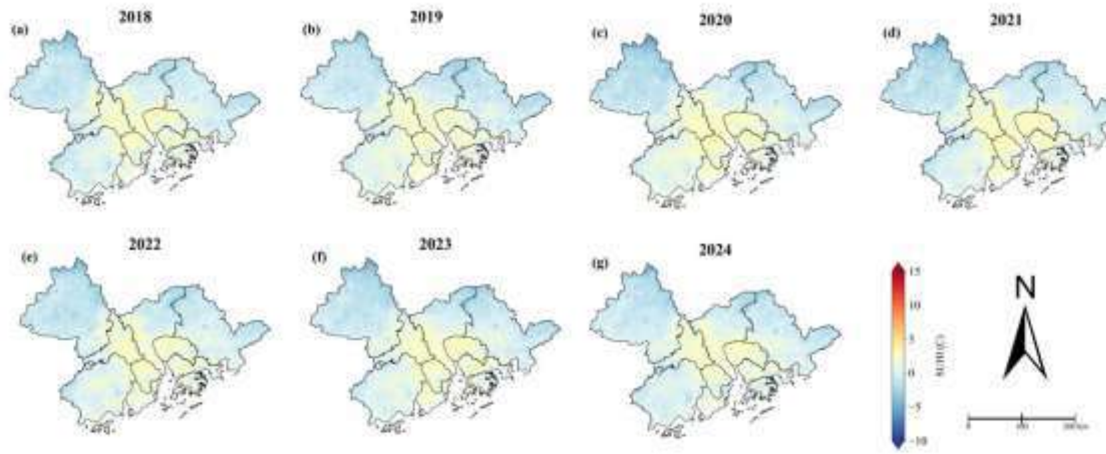

Figure 4 Spatial Distribution of Nighttime SUHI from 2018 to 2024

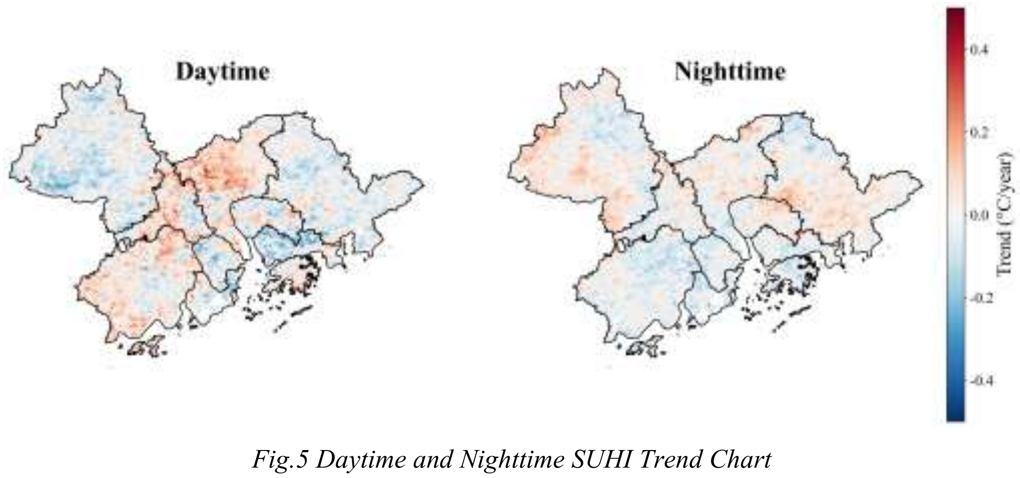

Fig.5 Daytime and Nighttime SUHI Trend Chart

Table 6 Statistical Characteristics of SUHI during Daytime and Nighttime from 2018 to 2024

Year	Daytime Average SUHI	Nighttime Average SUHI	Daytime strong SUHI ratio	Nighttime strong SUHI ratio
2018	-0.03±1.82	-0.03±1.74	6.73%	0.97%
2019	-0.03±1.90	-0.02±1.34	7.88%	0.49%
2020	-0.03±2.00	-0.02±1.60	7.58%	0.92%
2021	-0.03±1.97	-0.02±1.57	7.83%	1.84%
2022	-0.03±2.10	-0.02±1.37	9.69%	0.55%
2023	-0.03±1.92	-0.02±1.45	7.50%	0.63%
2024	-0.03±1.74	-0.02±1.28	4.58%	0.42%

Note: SUHI refers to Standardized Surface Urban Heat Island Intensity, which is calculated by subtracting the regional mean land surface temperature (LST) from the LST of each spatial unit and dividing the result by the regional standard deviation. A positive SUHI value indicates that the temperature of a given area is higher than the regional average, whereas a negative value indicates that it is lower than the regional average. The proportion of strong heat island areas refers to the percentage of pixels with SUHI values >1 relative to the total number of pixels within the study area. Because SUHI is derived using Z-score standardization, its regional mean theoretically approaches zero. Therefore, this study primarily focuses on spatial variation characteristics and changes in the proportion of strong heat island areas.

3.2 Spatial Aggregation Characteristics of Daytime and Nighttime SUHI

To reveal the spatial aggregation patterns and the distribution of hotspots and cold spots of daytime and nighttime SUHI Intensity in the GBA, this study employed Global Moran's I and Local Indicators of Spatial Association (LISA) to analyze SUHI data from 2018 to 2024. The results indicate that both daytime and nighttime SUHI exhibited significant positive spatial autocorrelation throughout the study period (daytime Moran's I: 0.936–0.946; nighttime Moran's I: 0.958–0.975), with corresponding Z-scores exceeding 162 and p-values below 0.0001 (Table 7). These findings confirm that the thermal environment of the study area was not randomly distributed but exhibited pronounced spatial clustering. The high Moran's I values indicate strong positive spatial autocorrelation of SUHI, which may be attributed to the spatial continuity of thermal landscapes and relatively homogeneous thermal characteristics at the urban agglomeration scale, which may be attributed to the spatial continuity of thermal landscapes and the relatively homogeneous thermal characteristics at the urban agglomeration scale. High-temperature areas tend to cluster with neighboring high-temperature areas, while low-temperature areas are spatially aggregated with other low-temperature areas, indicating strong spatial dependence and persistence of the thermal environment across the GBA.

According to the local spatial autocorrelation results (Figure 6), High–High clusters were predominantly distributed within the built-up areas of core cities in the Pearl River Delta, including the central urban areas of Guangzhou, the metropolitan core of Shenzhen, the manufacturing-intensive Dongguan–Foshan region, and the Guangzhou–Shenzhen–Hong Kong development corridor. These areas are characterized by highly contiguous impervious surfaces, intensive population and industrial activities, and substantial anthropogenic heat emissions, resulting in stable and persistent heat island hotspots. In contrast, Low–Low clusters were mainly distributed in the northern mountainous ecological barrier regions and coastal water bodies, including forested areas such as Conghua and Longmen, as well as coastal waters around the Pearl River Estuary and Lingdingyang. Benefiting from dense vegetation cover and extensive water surfaces, these areas exhibit strong evapotranspiration and water-cooling effects, thereby forming persistent and stable cold island clusters. Overall, the thermal environment of the GBA exhibits a spatial differentiation pattern characterized by "urban heating in the center and ecological cooling in the periphery."

A comparison between daytime and nighttime conditions revealed that Moran's I values were generally higher at night than during the daytime, indicating stronger spatial continuity and clustering of the nighttime thermal environment. During the daytime, solar radiation, land-cover characteristics, and local environmental heterogeneity contribute to differences in regional heating rates, resulting in relatively high spatial variability. At night, however, in the absence of solar radiation, heat stored in urban built-up areas is gradually released from buildings, roads, and other impervious surfaces, leading to a more uniform spatial diffusion and accumulation of heat and thereby strengthening thermal spatial correlation. Furthermore, nighttime hotspot areas were spatially more compact (Figure 7), being concentrated in the urban cores of Guangzhou and Shenzhen and their surrounding built-up areas, whereas cold spots remained stable within the northern mountainous regions and coastal waters. These findings suggest that urban heat storage plays a crucial role in sustaining nighttime heat island effects. Therefore, although the daytime and nighttime thermal environments share a broadly similar spatial structure, they exhibit distinct spatial organization characteristics.

Table 7 Spatial Autocorrelation Statistics of Daytime and Nighttime SUHI from 2018 to 2024

Year	Daytime Moran's I	Daytime Z-value	Daytime p-value	Nighttime Moran's I	Nighttime Z value	Nighttime P value
018	0.9358	162.80	<0.0001	0.9583	166.72	<0.0001
2019	0.9402	163.56	<0.0001	0.9665	168.15	<0.0001
2020	0.9419	163.86	<0.0001	0.9745	169.53	<0.0001
2021	0.9427	164.01	<0.0001	0.9731	169.30	<0.0001
2022	0.9455	164.50	<0.0001	0.9638	167.68	<0.0001
2023	0.9460	164.58	<0.0001	0.9742	169.49	<0.0001
2024	0.9427	164.01	<0.0001	0.9600	167.02	<0.0001

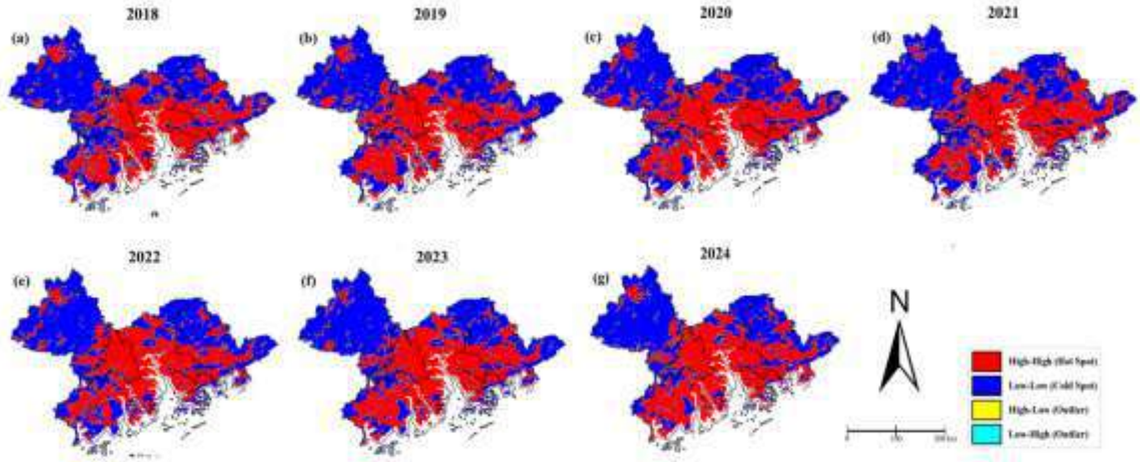

Figure 6 Daytime SUHI LISA Cluster Map

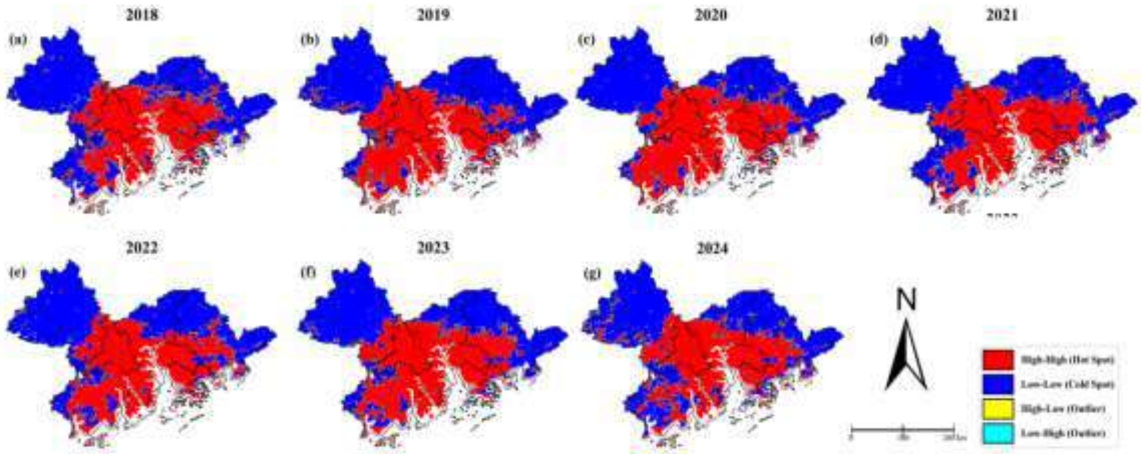

Fig.7 Nighttime SUHI LISA Cluster Map

3.3 Land-Use Transitions and Their Impacts on SUHI

To reveal the influence of different land-use change types on the urban surface thermal environment during the study period, this study conducted a statistical analysis of various land-use transition processes based on the land-use transition matrix. The relationship between land-use change and thermal environmental response was further explored by integrating changes in SUHI (ΔSUHI) under different transition pathways.

The results of the land-use transition matrix indicate that land-use change from 2018 to 2024 was primarily characterized by the expansion of built-up land (Figure 8). Within the effective analysis region, stable built-up land occupied the largest proportion, accounting for 69.14% of the analyzed area, indicating that urban built-up areas continued to dominate the regional land-use pattern (Table 8). Apart from stable built-up land, major land-use transitions involved the conversion of ecological spaces (e.g., cropland, forest, water bodies, and wetlands) into built-up land, reflecting the significant impact of urban expansion on regional land-cover patterns during the study period (Figure 9).

From the perspective of the relationship between land-use transition pathways and SUHI responses, different surface transformation types exhibited distinct effects. The conversion of ecological spaces into built-up land generally resulted in positive ΔSUHI values, indicating an increase in surface temperature following land-use change. This suggests that increases in impervious surface coverage, reductions in vegetation cover, and alterations in surface energy exchange processes exacerbate the urban heat island effect (Table 8). Notably, the warming effect was most pronounced when water bodies and wetlands were converted into built-up land, with ΔSUHI reaching relatively high levels. This finding indicates that these blue spaces, as critical regional cooling sources, experienced weakened evapotranspiration cooling and thermal regulation functions during the conversion process, resulting in substantial local thermal environmental deterioration (Figure 10). These results further highlight that the loss of water bodies and wetlands not only alters the regional landscape pattern but also reduces the thermal buffering capacity of urban ecosystems.

In contrast, the conversion of cropland into built-up land also produced a warming effect; however, the magnitude of ΔSUHI was lower than that associated with the conversion of water bodies and wetlands (Table 8). This may be attributed to the inherent vegetation cover and moisture regulation capacity of cropland. Although its ecological regulation functions decline following conversion, the resulting loss of cooling capacity is relatively limited compared with that of water bodies and wetlands. Therefore, different types of ecological spaces exhibit varying thermal environmental responses during urban expansion, with the loss of major cooling-source spaces exerting a more direct influence on SUHI intensification.

In addition, some land-use transition pathways exhibited cooling effects. For example, when built-up land was converted into ecological spaces such as green spaces, forests, or water bodies, ΔSUHI values became negative, indicating that ecological restoration, urban renewal, and blue–green space development can effectively reduce surface temperatures (Table 8). These transition pathways regulate the urban thermal environment by increasing vegetation cover, enhancing evapotranspiration, and optimizing urban surface structures. Spatially, cooling-oriented land-use transitions were concentrated in urban renewal areas and peripheral ecological optimization zones, highlighting the importance of land-use structure adjustment in mitigating SUHI (Figure 9).

In summary, land-use change in the Pearl River Delta region was primarily driven by urban expansion, with the continuous increase in built-up land representing the dominant pathway influencing SUHI variations (Figure 10). Different land-use transition types exerted markedly different effects on the thermal environment: transitions from ecological spaces to built-up land generally intensified SUHI, whereas ecological restoration and the expansion of blue–green spaces generated cooling effects (Table 8). Therefore, future urban development should prioritize the protection of highly efficient cooling sources, particularly water bodies and wetlands. By increasing the proportion of ecological land and optimizing land-use structures, a more balanced coordination between urban expansion and thermal environmental regulation can be achieved.

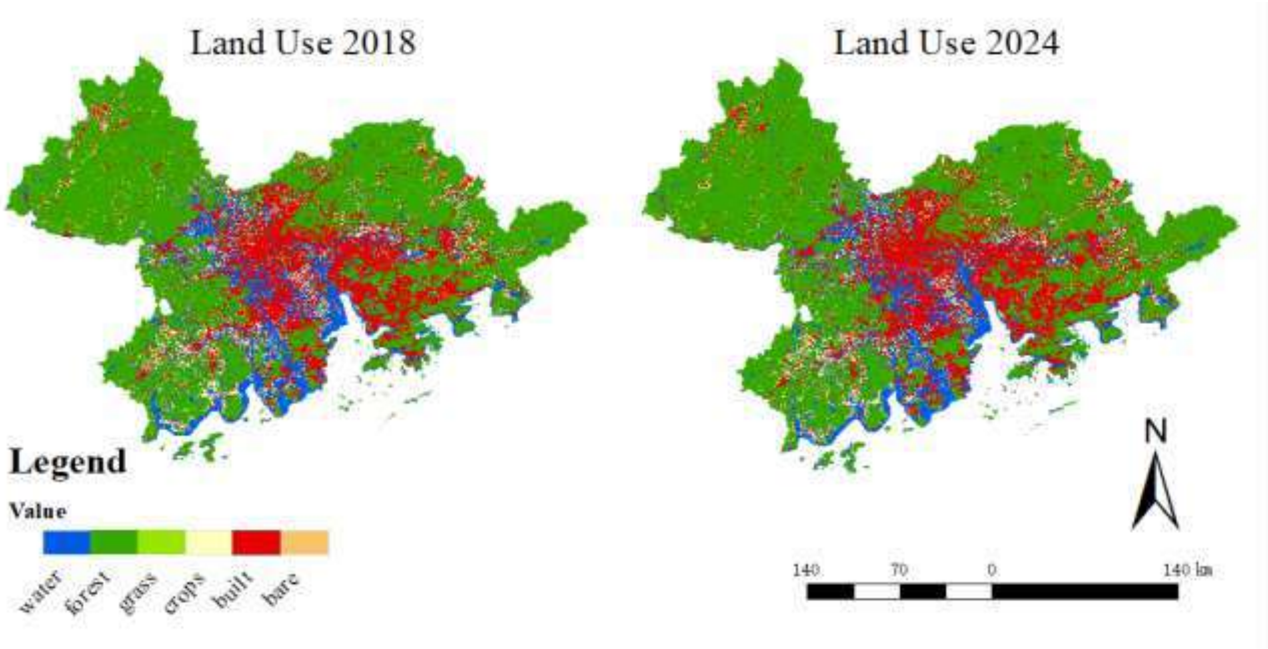

Fig.8 Land Use Maps for 2018 and 2024

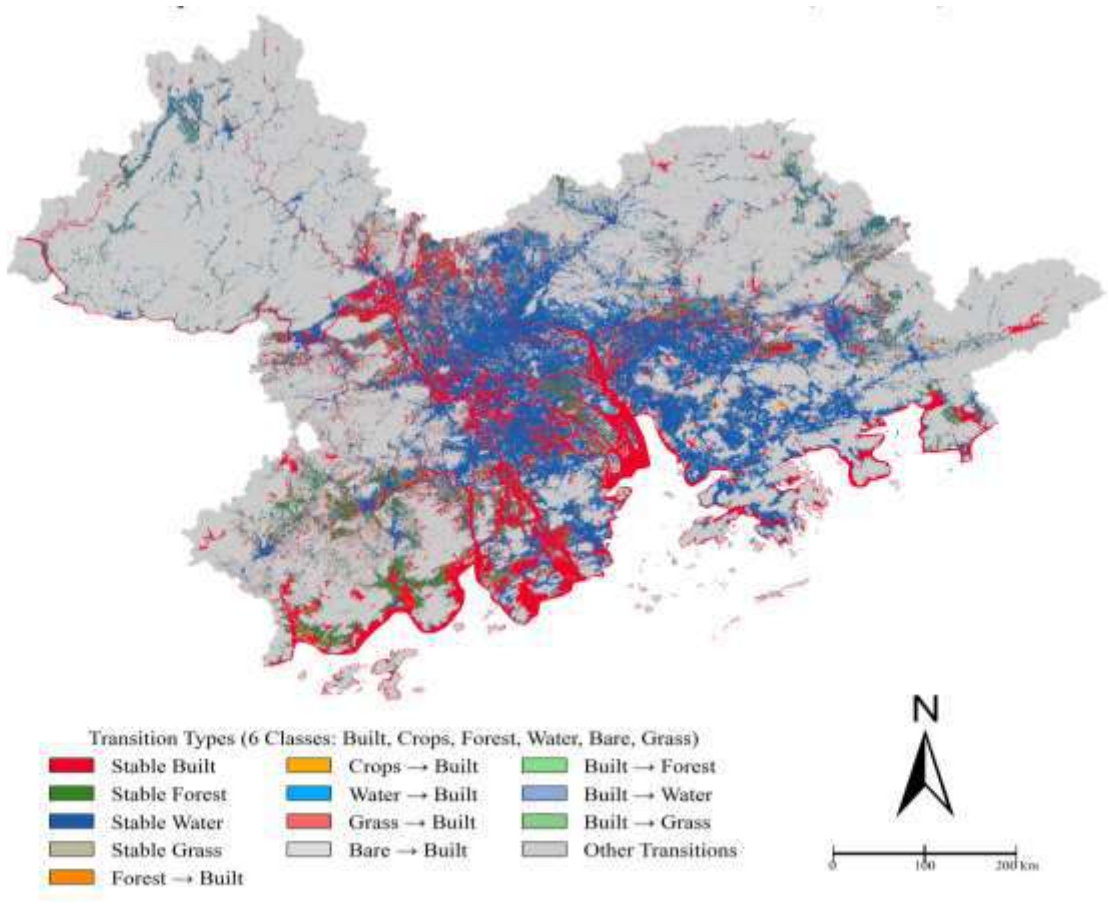

Fig.9 Spatial Distributions of Land Use Transfers in GBA (2018-2024)

Table 8 Land Use Transfer Types and SUHI Response from 2018 to 2024

Transfer Type	**Area/Ratio**	**Average ΔSUHI_Day**	**Average ΔSUHI_Night**	**Explanation**
Forestland →Built-up land	5.15 km² (0.46%)	+4.29	+5.29	Conversion of ecological space to construction land
Cropland →Built-up land	16.15 km² (1.45%)	+2.60	+2.99	Urban expansion process
Water body →Built-up land	17.82 km² (1.60%)	+4.99	+5.97	Reduction of cooling sources
Built-up Land →Green space	37.00 km² (3.32%)	-4.07	-5.08	Ecological restoration or renovation
Stable Built-up land	769.87 km² (69.14%)	+0.30	+0.30	High Heat Island Retention Zone
Stable Forestland/Water bodies	267.47 km² (24.02%)	+0.10	+0.11	Cold Island Maintenance Zone

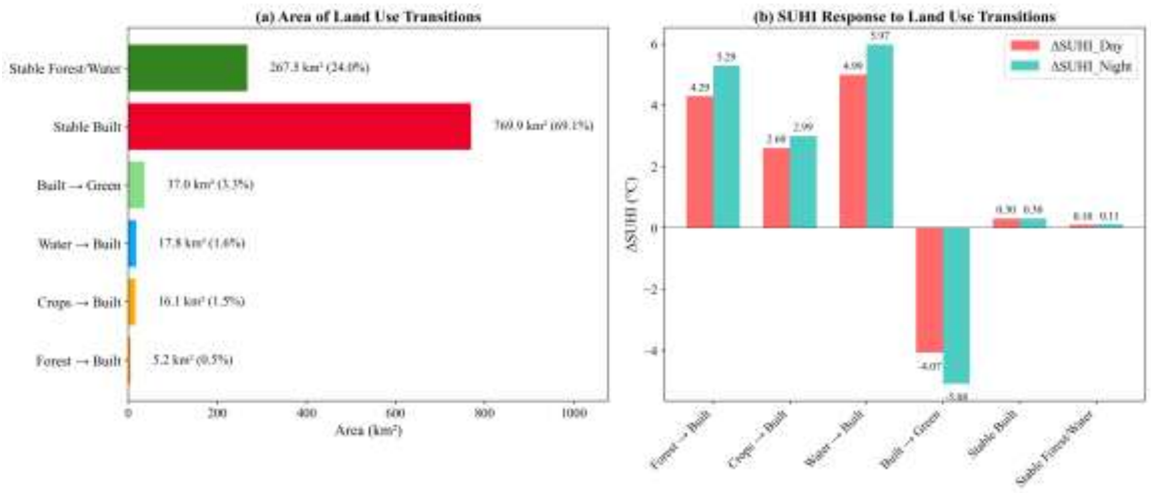

Fig.10 Bar chart of daytime and nighttime ΔSUHI under different land-use transfer types

3.4 Key Drivers of Daytime and Nighttime SUHI

To identify the primary drivers and underlying mechanisms of daytime and nighttime SUHI Intensity in the GBA, this study conducted a contribution analysis of natural environmental and socioeconomic variables using the XGBoost model and SHAP method. The results indicate that both daytime and nighttime SUHI are influenced by land-cover characteristics and human activities; however, their dominant driving factors and influence magnitudes differ substantially (Tables 9 and 10).

The primary drivers of daytime SUHI include the NDBSI, NDVI, NDMI, MNDWI, and NTL (Figure 11). Among these variables, NDBSI exhibits the highest importance, with SHAP values generally indicating positive contributions. This suggests that increases in impervious surface coverage and the expansion of built-up areas enhance the capacity for heat absorption and storage, thereby intensifying the heat island effect. In contrast, NDVI, NDMI, and MNDWI exhibit significant negative contributions indicating that increased vegetation cover, improved moisture conditions, and expanded water bodies can effectively mitigate the heat island effect through evapotranspiration cooling, water-related thermal regulation, and heat dissipation processes (Figure 13). Overall, the daytime thermal environment is primarily governed by land-cover characteristics and ecological conditions, with differences in surface energy balance among various underlying surfaces representing a key factor driving spatial thermal variability.

For nighttime SUHI, the key driving factors include NDBSI, NTL, population density (PD), GDP, and NDVI (Figure 12). NDBSI remains highly influential, confirming that built-up areas and impervious surfaces constitute the common physical basis of both daytime and nighttime heat island effects. Meanwhile, the importance of NTL, PD, and GDP increases substantially, with SHAP values predominantly indicating positive contributions. This suggests that nighttime heat islands are influenced not only by urban heat storage effects but also by population concentration, economic activities, and anthropogenic heat emissions. High-density urban areas continuously release heat accumulated during the daytime, while anthropogenic heat generated from transportation, commercial activities, and energy consumption further intensifies local warming, resulting in more pronounced nighttime heat island effects.

In terms of variable importance rankings, land-cover characteristics dominate daytime SUHI, whereas nighttime SUHI is more strongly influenced by the intensity of human activities and the level of urbanization (Figure 13). These findings highlight a significant difference in the formation mechanisms of daytime and nighttime thermal environments in the GBA. Daytime thermal conditions are primarily controlled by solar radiation and underlying surface properties, whereas nighttime thermal conditions reflect the combined effects of heat release and anthropogenic heat emissions. Overall, urban expansion and increasing impervious surface coverage are key drivers of heat island intensification, while enhancing vegetation cover, protecting water bodies, and optimizing urban ecological structures represent critical strategies for mitigating regional thermal environmental problems.

Table 9 Evaluation Results of XGBoost Model Prediction Accuracy

indicator	Daytime SUHI	Nighttime SUHI
R^2	0.785	0.812
RMSE	0.523	0.456
MAE	0.387	0.342

Table 10 Ranking of Key Influencing Factors for Daytime and Nighttime SUHI

Sorting	Daytime SUHI key factor	Direction of action	Nighttime SUHI key factor	Direction of action
1	NDBSI	Positive	NDBSI	Positive
2	NDVI	Negative	NTL	Positive
3	NDMI	Negative	PD	Positive
4	MNDWI	Negative	GDP	Positive
5	NTL	Positive	NDVI	Negative

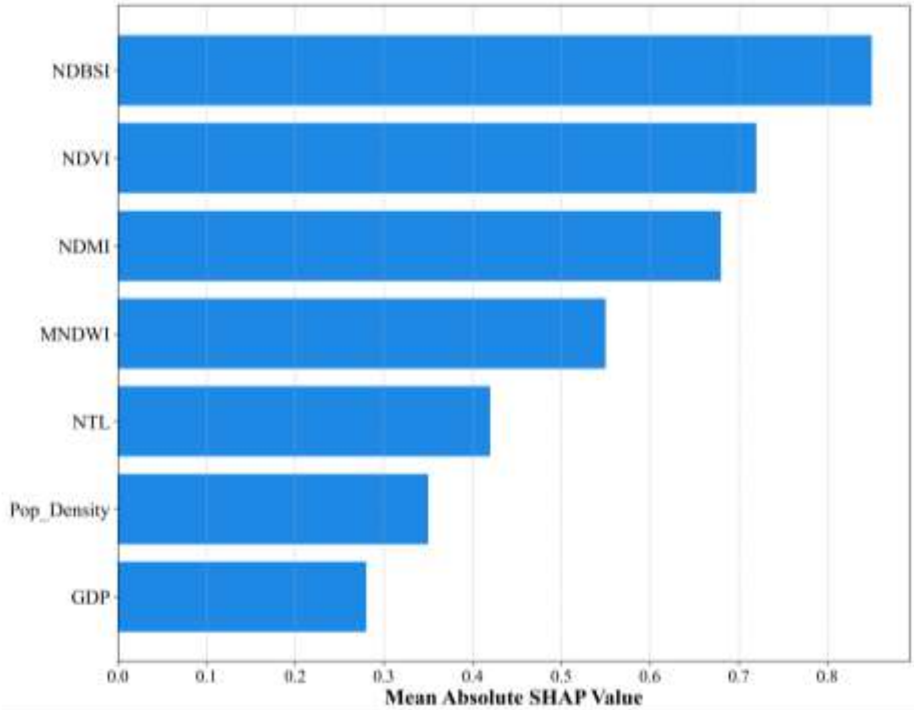

Fig.11 SHAP Summary Plot of Daytime SUHI

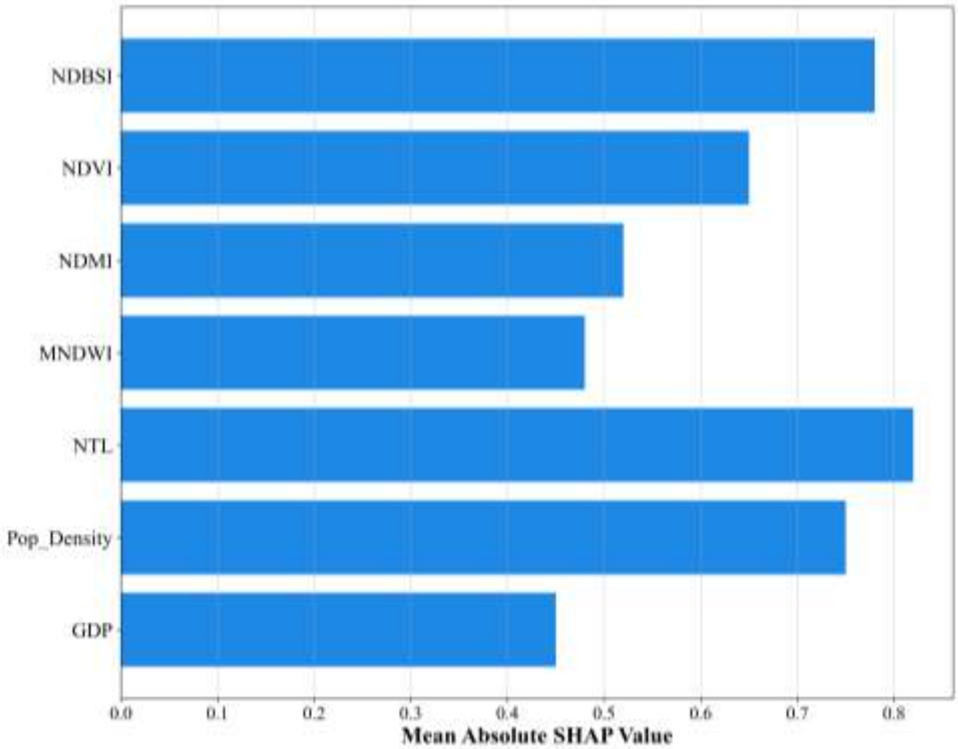

Fig.12 SHAP Summary Plot of Nighttime SUHI

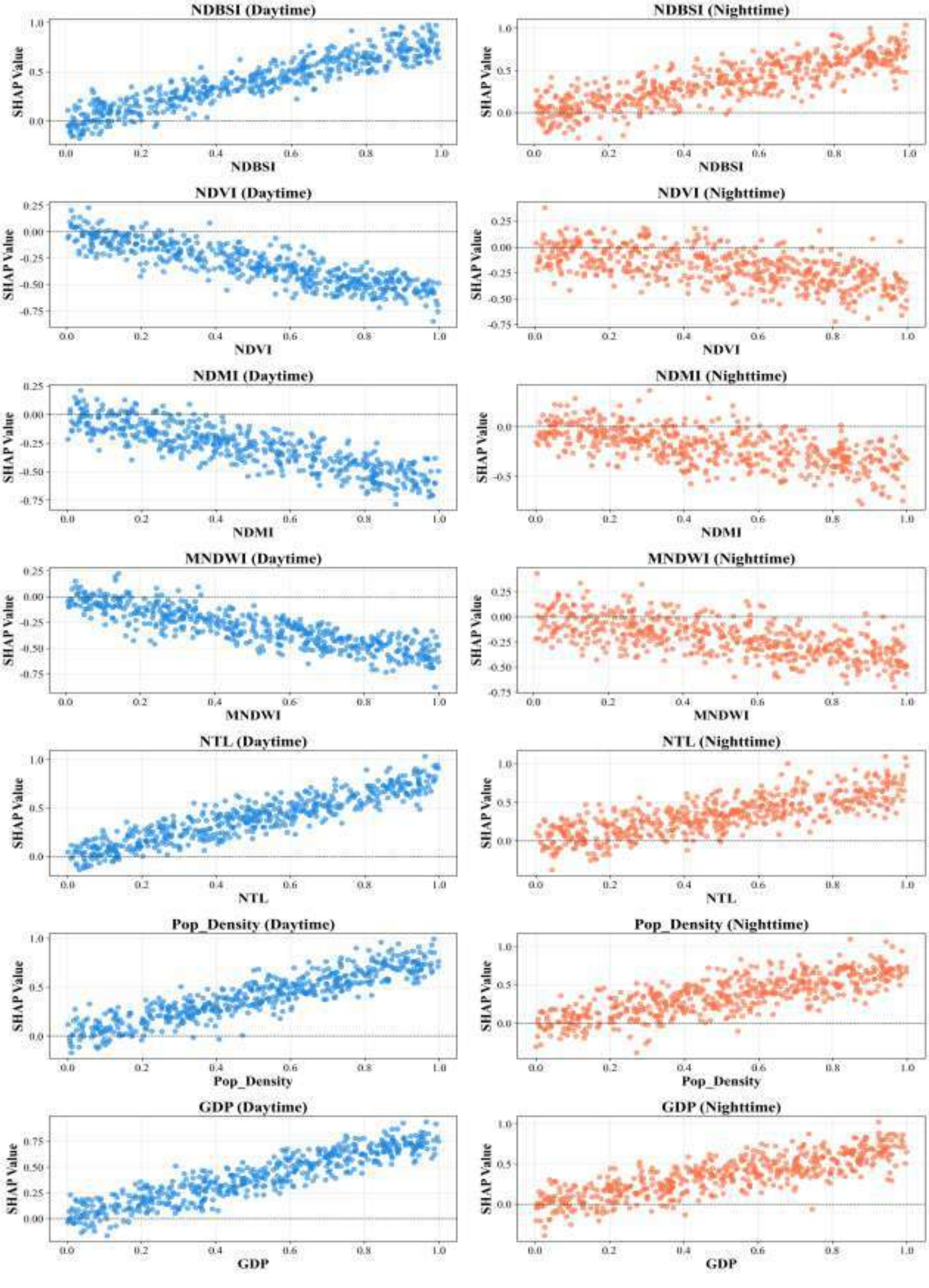

Fig.13 SHAP Dependence Plots of Key Variables

IV. DISCUSSION

4.1 Differences and Mechanisms of Daytime and Nighttime SUHI

The formation mechanisms of daytime and nighttime SUHI exhibit distinct differences. This study found that daytime SUHI is primarily influenced by NDBSI, NDVI, NDMI, and MNDWI, with NDBSI showing a significant positive contribution, whereas NDVI, NDMI, and MNDWI exhibit significant negative contributions. These findings indicate that increased surface hardening and the reduction of ecological cooling sources are key drivers of daytime heat island formation. In contrast, nighttime SUHI is mainly influenced by NDBSI, NTL, population density, and GDP, suggesting that nighttime heat islands are associated not only with surface heat storage but also with population agglomeration, anthropogenic heat emissions, and urban economic activities. The results further reveal that NDVI and MNDWI exert significant negative effects on daytime SUHI, highlighting the important roles of vegetation cover and water distribution as ecological factors in mitigating thermal environmental stress.

4.2 Implications of Land-Use Change for Thermal Environmental Variations

Land-use change is not merely a shift in land-use categories but also a surface process that drives thermal environmental evolution. The conversion of ecological spaces into built-up areas typically results in reduced vegetation cover, deteriorated water conditions, increased impervious surface coverage, and enhanced surface heat storage, thereby contributing to higher SUHI intensity. Conversely, the conversion of built-up areas into green spaces, water bodies, or other ecological spaces can enhance evapotranspiration and water-cooling effects, thereby reducing SUHI intensity. The results indicate that the conversion of water bodies/wetlands, forests, and cropland into built-up areas constituted the primary warming pathways during the study period (Table 8). Among these pathways, the conversion of water bodies/wetlands into built-up areas exhibited the strongest warming effect, with daytime and nighttime ΔSUHI reaching 4.99 and 5.97, respectively. In contrast, the conversion of built-up areas into green spaces or water bodies generated significant cooling effects, reducing daytime and nighttime ΔSUHI by 4.07 and 5.08, respectively. These findings highlight the importance of blue–green space restoration in mitigating heat island effects. The thermal impacts of land-use change exhibit clear path dependency, with different transition pathways producing varying degrees of thermal response. Notably, the warming effects resulting from the loss of ecological spaces generally exceed those associated with structural adjustments within built-up areas.

4.3 Planning Implications Derived from Key Driving Factors

The value of the XGBoost-SHAP framework lies not only in improving prediction accuracy but also in identifying the variables that are most important in explaining variations in heat island intensity.The positive contribution of NDBSI to SUHI highlights the importance of reducing surface hardening, improving impervious surface materials, and increasing permeable pavements. If NDVI, NDMI, or MNDWI show negative contributions, enhancing vegetation cover, maintaining surface moisture, and protecting blue–green spaces become essential strategies for mitigating heat island effects. Furthermore, if NTL, population density, or GDP contribute substantially to nighttime SUHI, greater attention should be directed toward managing anthropogenic heat emissions, transportation-related activities, and thermal conditions in high-intensity urban functional zones.

From the perspective of urban planning and environmental management, reducing surface hardening and enhancing blue–green space connectivity should be prioritized in thermal environment governance across the Guangdong–Hong Kong–Macao Greater Bay Area to achieve a balance between urban expansion and ecological conservation. Three key strategies are proposed: (1) **Priority Cooling Zones in Heat Island Hotspots**, involving measures such as cool roofs, increased shading vegetation, reduced continuous impervious surfaces, and improved urban ventilation; (2) **Thermal Risk Control Zones in Urban Expansion Areas**, emphasizing controlled development intensity, the preservation of ecological buffer zones, and increased proportions of green and permeable surfaces; and (3) **Blue–Green Ecological Cooling Source Protection Zones**, focusing on the protection of forests, water bodies, wetlands, and blue–green corridors to prevent landscape fragmentation (Table 11).

Table 11 Zoning Thermal Environment Management and Optimization Recommendations

Governance Zones	Basis for identification	Recommended measures
Priority Cooling Zone for UHI Hotspots	SUHI>1 or LISA High-High	Cool roofs, increased greenery and shading, reduced continuous hardened surfaces, improved ventilation
Urban Expansion Heat Risk Control Zone	Non-buildup land → Buildup land and ΔSUHI > 0	Control development intensity, preserve ecological buffer zones, and increase green space and permeable surface ratios
Blue-Green Ecological Cold Source Conservation Zone	Low SUHI with higher NDVI/NDWI/MNDWI	Protect forests, water bodies, wetlands, and blue-green corridors to prevent fragmentation

4.4 Research Limitations

This study has several limitations. First, although MODIS LST data are suitable for urban agglomeration-scale analyses, their spatial resolution is insufficient to capture thermal environmental variations at the neighborhood scale. Second, socioeconomic variables such as population density and GDP were derived from administrative statistics and subsequently assigned spatially within the model, which may not adequately reflect fine-scale spatial variability at the pixel level. Third, although the XGBoost-SHAP framework provides statistical interpretations and quantifies the contributions of explanatory variables, it cannot establish strict causal relationships. Fourth, spatial heterogeneity and pathway-based analytical approaches were not incorporated into this study, limiting the exploration of local mechanisms and direct or indirect influence pathways.

V. CONCLUSIONS

This study constructed daytime and nighttime SUHI Intensity indicators for the Guangdong–Hong Kong–Macao Greater Bay Area (GBA) from 2018 to 2024 using multi-source spatial data. Spatiotemporal statistical analysis, spatial autocorrelation analysis, land-use transition matrices, and the XGBoost-SHAP framework were employed to investigate the spatiotemporal evolution of SUHI, its response to land-use changes, and its key driving factors. The main conclusions are as follows:

(1) Daytime and nighttime SUHI exhibited significant spatial heterogeneity. High-SUHI areas were concentrated in the core built-up regions of the Pearl River Delta, including Guangzhou, Shenzhen, Dongguan, and Foshan, whereas low-SUHI areas were primarily distributed in the northern mountainous forest regions and coastal water bodies such as the Pearl River Estuary and Lingdingyang. During the study period, SUHI anomaly increased along the Shenzhen–Dongguan–Huizhou urban development corridor but weakened or remained stable in the northwestern mountainous regions, including Zhaoqing.

(2) The results of Global Moran's I and LISA revealed significant spatial clustering of SUHI. High–High hotspot clusters were primarily distributed within the core built-up areas of Guangzhou, Shenzhen, Dongguan, Foshan, and the Guangzhou–Shenzhen–Hong Kong development corridor, whereas Low–Low cold spot clusters were concentrated in the northern ecological conservation areas and the coastal waters of the Pearl River Estuary.

(3) Land-use transitions played a critical role in SUHI dynamics. The conversion of forests, cropland, and wetlands into built-up areas resulted in pronounced warming effects, whereas transitions from built-up areas to green spaces or water bodies significantly mitigated the urban heat island effect.

(4) XGBoost-SHAP analysis identified NDBSI, NDVI, NDMI, MNDWI, and NTL as the primary drivers of daytime SUHI, whereas NDBSI, NTL, PD, GDP, and NDVI were identified as the dominant drivers of nighttime SUHI. Built-up and dry surface characteristics generally intensified SUHI, whereas vegetation cover and surface moisture conditions contributed to its mitigation.

(5) Thermal environment governance in the GBA should prioritize heat island hotspot cooling zones, urban expansion risk-control areas, and blue–green ecological cooling-source protection zones, while adopting differentiated management strategies for daytime and nighttime thermal conditions. Future efforts should integrate "blue–green space conservation–urban expansion regulation–targeted hotspot is cooling" to promote a balance between urban development and ecological protection.

From a theoretical perspective, this study established an integrated framework encompassing SUHI pattern identification, land-use transition responses, and mechanistic interpretation from a diurnal perspective, thereby enriching thermal environment research at the urban agglomeration scale. From a practical perspective, the findings provide scientific support for territorial spatial planning, urban expansion management, and blue–green space optimization in the GBA.

REFERENCES

[1] Chen, T. Q., and Guestrin, C. XGBoost: A scalable tree boosting system, Proceedings of the 22nd ACM SIGKDD International Conference on Knowledge Discovery and Data Mining. New York: ACM, 2016: 785-794.
[2] Chen, X. L., Zhao, H. M., Li, P. X., et al. Remote sensing image-based analysis of the relationship between urban heat island and land use/cover changes. Remote Sensing of Environment, 2006, 104(2): 133-146.
[3] Li, X. X., Zhou, Y. Y., Asrar, G. R., et al. Response of vegetation and surface water to urban thermal environment and implications for heat mitigation. Science of the Total Environment, 2020, 703: 134706.
[4] Liu J Y, Kuang W H, Zhang Z X, et al. Spatiotemporal characteristics, patterns and causes of land-use changes in China since the late 1980s. Journal of Geographical Sciences, 2014, 24(2):195-210.
[5] Lundberg, S. M., and Lee, S. I. A unified approach to interpreting model predictions, Proceedings of the 31st International Conference on Neural Information Processing Systems. Long Beach: NIPS, 2017: 4768-4777.
[6] Oke, T. R. Boundary Layer Climates. 2nd ed. London: Routledge, 1987.
[7] Pontius, R. G., Shusas, E., & McEachern, M. Detecting important categorical land changes while accounting for persistence. Agriculture, Ecosystems & Environment, 2004, 101(2-3), 251-268.
[8] Wang, Y. H., Zhang, H. Y., Liu, Z. Q., et al. Spatial clustering characteristics and driving mechanisms of urban heat island effects in the Guangdong-Hong Kong-Macao Greater Bay Area. Journal of Geo-information Science, 2023, 25(8): 1578-1593.
[9] Yang, J., Wang, Y. H., Xiu, C. L., et al. Exploring nonlinear relationships between urban heat island intensity and driving factors using machine learning approaches. Sustainable Cities and Society, 2022, 81: 103838.
[10] Zhou, D. C., Zhao, S. Q., Liu, S. G., et al. Surface urban heat island in China's 32 major cities: Spatial patterns and drivers. Remote Sensing of Environment, 2017, 152: 51-61.

International Journal of Environment, Agriculture and Biotechnology
Vol-11, Issue-3; May-Jun, 2026
Peer-Reviewed International Journal
Journal Home Page Available: https://ijeab.com/
Journal DOI: 10.22161/ijeab

An Analysis of the Effect of Salinity on Dissolved Oxygen in a Pond and its Impact on Pisciculture

Dr Sachchidanand Mishra

Assistant Professor, Department of Zoology, Maharani Kalyani College, Laheriasarai, Darbhanga, Bihar, India

Received: 13 May 2026; Received in revised form: 12 Jun 2026; Accepted: 16 Jun 2026; Available online: 24 Jun 2026

Abstract— *This study examines the influence of salinity on dissolved oxygen (DO) in pond ecosystems and evaluates its consequences for pisciculture. Dissolved oxygen is one of the most important indicators of water quality because it directly affects fish metabolism, growth, reproduction, immunity, and survival. Salinity alters the physical and chemical properties of water and consequently affects oxygen solubility. Sample observations demonstrated a progressive decline in dissolved oxygen concentration from 8.5 mg/L to 5.9 mg/L as salinity increased from 0 to 12 ppt. The results suggest a strong negative relationship between salinity and dissolved oxygen. Such reductions can adversely affect pond productivity and fish yield. Effective monitoring and management of salinity and oxygen levels are therefore essential for sustainable aquaculture.*

Keywords*— *Salinity, Dissolved Oxygen, Pond Ecosystem, Pisciculture.

I. INTRODUCTION

Pisciculture is an important component of global food security and rural livelihoods. Successful fish culture depends on maintaining suitable water quality conditions. Among the various parameters, dissolved oxygen is considered one of the most critical factors because fish and other aquatic organisms rely on it for respiration. Salinity, defined as the concentration of dissolved salts in water, can significantly influence oxygen availability. Salinity and dissolved oxygen (DO) are two important water quality parameters that directly influence aquatic ecosystems and fish production. This article analyses the relationship between salinity and dissolved oxygen in pond ecosystems and evaluates its implications for pisciculture. Increasing salinity alters the physical and chemical properties of water, affecting oxygen solubility, fish metabolism, microbial activity, and pond productivity. A review of scientific literature indicates that higher salinity generally reduces oxygen solubility, increasing the risk of oxygen stress in cultured fish. Understanding these interactions is essential for effective pond management, especially in regions facing salinisation due to climate change, irrigation practices, and groundwater intrusion. The study discusses mechanisms, impacts on fish growth and survival, and management strategies for sustainable aquaculture.Many freshwater ponds experience salinity fluctuations due to evaporation, agricultural runoff, groundwater seepage, and climate-related changes. Understanding the relationship between salinity and dissolved oxygen is therefore important for optimising fish production and maintaining pond health. Dissolved oxygen refers to the amount of free oxygen present in water. Oxygen enters ponds through atmospheric diffusion, photosynthesis by aquatic plants, and mechanical aeration. Salinity influences oxygen solubility because dissolved salts reduce the capacity of water to hold oxygen molecules. As salinity increases, oxygen solubility decreases. Temperature further modifies this relationship, with warm saline water holding considerably less oxygen than cool freshwater. Salt affected soils are important ecological entity as it is known that land occupying 6% of the global land area and 2.6% of the geographical area in India, Indo-Gangetic Plain (IGP), which is the most fertile agricultural region in India also has around 3.095 million ha land is salt affected areas of which 12% exist in Bihar (Mandal and Sharma, 2006). Utilisation of these salt affected areas for productive purpose is the major challenge for the region. In this regard, inland saline aquaculture provides an opportunity for the diversification and expansion of agriculture through a potentially productive use of land that can no longer support standard agricultural enterprises (McDowall et al., 2016). Thus, aquaculture can be an adaptive approach to this environmental problem and can represent a potentially lucrative use for salt-affected land, with many economic, social and environmental benefits (Lymbery et al., 2007). However, selection of suitable fish species having tolerance to saline conditions is very important before venturing into aquaculture in these areas. This is mainly because higher salinity of water can act as an important stressor under natural as well as aquaculture conditions (Islam et al., 2014) and water quality can directly influence the metabolism of fish, which ultimately affects the survival, growth, feed intake and even distribution of species (Garg, 1996 ; Kang'ombe and Brown, 2008; Akhtar et al., 2013).

Fish require adequate oxygen for metabolism and digestion. Reduced DO levels lower feeding activity and growth rates. Chronic oxygen deficiency causes physiological stress, weakens immune responses, and increases vulnerability to pathogens. The reduction in dissolved oxygen occurs because salt ions occupy space among water molecules, decreasing the availability of sites where oxygen can dissolve. Consequently, ponds with elevated salinity often exhibit lower dissolved oxygen concentrations than freshwater ponds under similar environmental conditions.

Pisciculture plays a crucial role in food security, nutrition, employment generation and rural development. . Dissolved oxygen, often abbreviated as DO, is the amount of free oxygen molecules (O_2) dissolved in water. Oxygen enters the water through atmospheric diffusion, plant photosynthesis, or aeration (either natural or man-made). DO is typically represented in measurement units as percent of air saturation (%sat) and concentration in milligrams per liter (mg/L) or parts per million (ppm).

Dissolved oxygen levels measured at 3 mg/L are in the danger zone for supporting common aquatic life, and levels below 1 mg/L cannot support any aquatic life. When dissolved oxygen level decreased because of salinity increases, water conditions soon become lethal for aquatic life. So, increasing the salt concentration will lead to a decrease in oxygen solubility, negatively affecting any aquatic life inside water. So the available parameters of dissolved oxygen for sustainability of life in fresh water is very vital for pisciculture practices.

II. MATERIALS AND METHODS

A pond-based investigation was conducted by collecting water samples from multiple locations and depths. Salinity was measured using a digital salinity meter while dissolved oxygen was determined using a DO meter . Measurements were taken during morning and afternoon periods over several weeks during January to March from a fresh water pond located in Darbhanga city under the campus of M. K. College , Laheriasarai . After observation of recorded data of salinity and DO with the help of table and graph, finding was analysed using the coparmparative variations between salanity and dissolved oxygen in pond water. It's impact on pisciculture was also discussed with the help present result.

III. RESULT AND DISCUSSION

The results indicated a consistent decline in dissolved oxygen with increasing salinity as shown in the table 1 . This pattern agrees with the established understanding that dissolved salts reduce oxygen solubility in water. The observed inverse relationship between salinity and dissolved oxygen has important ecological and aquacultural implications. Reduced oxygen availability can impair fish health, growth and survival. Severe oxygen depletion can result in mass fish mortality, particularly during warm weather or algal bloom collapses.Some species such as *Tilapia* tolerate moderate salinity, whereas many freshwater carps like *Labeo* species perform best under low salinity conditions. Oxygen stress combined with salinity stress can further reduce productivity.Poor oxygen conditions negatively affect spawning, egg development, and larval survival.

Effect of salinity alone on rate of oxygen consumption of freshwater species negatively affect their physiological cycle. Zheng et al. (2008) recorded lower oxygen consumption rate at 31‰ compared to 16‰ on *Miichthys miiuy*. While in another study on oxygen consumption rate of *Dicentrarchus labrax* fingerlings, only slight variation was recorded between 3 and 45 percent which was attributed to strong euryhaline nature of the species (Barnabe, 1990; Dalla et al., 1998).The alterations in oxygen consumption in fishes at different salinities could be due to differences in energy required for osmoregulation or from changes in the spontaneous activity level of fish and changes in the routine metabolic rate (De Boeck et al., 2000). The study has showed that oxygen consumption rate was lowest at 4.5 percent which could be attributed to energy conservation strategy adopted by the species to salinity mediated stress(De Boeck et al.,2000). In the view of management strategy of pond regular monitoring of salinity, temperature and dissolved oxygen should be performed. Aeration, appropriate stocking density, periodic water exchange and proper feeding practices can reduce stress on cultured fishes.

As an ecological factor, ambient salinity has a series of physiological effects on fish. As reported in previous studies, salinity is an important factor regulating fish growth, metabolism, and various physiological activities (Katz et al.,2001). Ambient salinity can also directly affect the promotion of aquaculture (Ern, R . et al., 2014) . An inappropriate salinity range will affect the physiology and biochemistry, immunity, growth and development, feeding, and reproduction of fish, and fish will show different adaptive states under various salinity conditions (Livingston, 2001) . Recent studies have shown that salinity changes can cause physiological stress reactions in fish, accompanied by the production of excessive reactive oxygen free radicals, which can lead to oxidative stress reactions that damage the antioxidant defense system of fish(Wang, J.Q.et al., 1997). Excessive oxygen free radicals produced by oxidative stress will attack biological membranes, proteins, and nucleic acids, causing oxidative damage such as cytoplasmic efflux, enzyme inactivation, and genetic replication errors (Choi, C.Y. et al., 2008). As shown in the graph (graph 1.) , increasing temperature gradually lower the dissolved oxygen and leads adverse effect on pond ecosystem which ultimately produce negative impact on fish growth and survival.

IV. CONCLUSION

Salinity has a significant influence on dissolved oxygen dynamics in pond ecosystems. Increasing salinity generally reduces oxygen solubility, thereby affecting fish growth, health, reproduction, and survival. The combined effects of salinity and oxygen stress can substantially reduce aquaculture productivity. Effective monitoring and management of both parameters are therefore essential for sustainable pisciculture. In many research, species-specific tolerance thresholds has also been identified which focus on adaptive management strategies under changing environmental conditions.

Table 1. Salinity and Dissolved Oxygen Data

Salinity (ppt)	Dissolved Oxygen (mg/L)
1 ± 0.3	8.5 ± 0.5
1 ± 0.3	8.1 ± 0.5
1.5 ± 0.3	7.7 ± 0.5
2 ± 0.3	7.2 ± 0.5
2 ± 0.3	6.8 ± 0.5
3 ± 0.3	6.3 ± 0.5
3.5 ± 0.3	5.9 ± 0.5
4 ± 0.3	5.8 ± 0.5

Fig.1. Relationship between Salinity and Dissolved Oxygen between Observation period - January - March , 2026.

(ppt- part per thousand equivalent to 1 g of solute per thousand g of water.)

Salinity vs Dissolved Oxygen Graph :

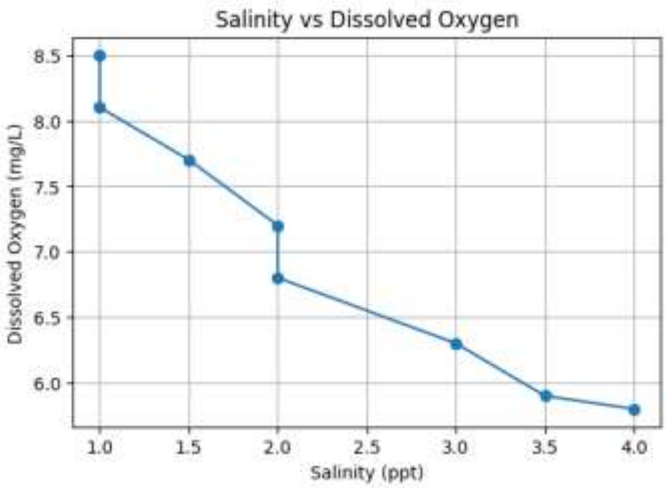

Fig.1 Relationship between salinity and dissolved oxygen in pond water. (Graph 1.)

REFERENCES

[1] Akhtar, M. S., Pal, A. K., Sahu, N. P., Ciji, A., Meena, D. K. and Das, P. 2013. Physiological responses of dietary tryptophan fed Labeo rohita to temperature and salinity stress. J. Anim. Physiol. Anim. Nutr., 97: 1075-1083. doi: 10.1111/ jpn.12017.

[2] APHA 1998. Standard methods for the examination of water and wastewater, 20th edn. In: Clesceri, L. S., Greenberg, A. E. and Eaton, A. D. (Ed.), American Public Health Association, American Water Works Association, Water Environment Federation, Washington DC, USA. 1979 pp.

[3] Barnabe, G. 1990. Rearing bass and gilthead bream. In: Barnabe, G. (Ed.), Aquaculture, vol. 2. Ellis Horwood, New York, USA, p. 647-686.

[4] Choi, C.Y.; An, K.W.; An, M.I. Molecular characterization and mRNA expression of glutathione peroxidase and glutathione S-transferase during osmotic stress in olive flounder (*Paralichthys olivaceus*). *Comp. Biochem. Physiol. Part A* 2008,*149*, 330–337.

[5] De Boeck, Vlaminck, A. G., Van Der Linden, A. and Blust, R. 2000. The energy metabolism of common carp (Cyprinus carpio) when exposed to salt stress: an increase in energy expenditure or effects of starvation. Physiol. Biochem. Zool., 73(1): 102-111. doi: 10.1086/316717.

[6] Ern, R.; Huong DT, T.; Cong, N.V.; Bayley, M.; Wang, T. Effect of salinity on oxygen consumption in fishes: A review. *J. Fish Biol.* 2014, *84*, 1210–1220.

[7] Garg, S. K. 1996. Brackishwater carp culture in potentially waterlogged areas using animal wastes as pond fertilisers. Aquac. Int., 4: 143-155.

[8] Islam, M., Ahsan, D. A., Mandal, S. C. and Hossain, A. 2014. Effects of salinity changes on growth performance and survival of rohu fingerlings, Labeo rohita (Hamilton 1822). Coast. Dev., 17(1): 1-6. DOI: 10.4172/1410-5217.1000379
[9] Kang'ombe, J. and Brown, J. A. 2008. Effect of salinity on growth, feed utilisation, and survival of Tilapia rendalli under laboratory conditions. J. Appl. Aquac., 20(4): 256-271. https://doi.org/10.1080/10454430802498229.
[10] Katz, S.L.; Syme, D.A.; Shadwick, R.E. Enhanced power in yellowfin tuna. *Nature* 2001, *410*, 770–771.
[11] Livingstone, D.R. Contaminant-stimulated Reactive Oxygen Species Production and Oxidative Damage in Aquatic Organisms. *Mar. Pollut. Bull.* 2001, *42*, 656–666
[12] Lymbery, A., Starcevich, M. and Doupe, R. 2007. Managing environmental impacts in inland saline aquaculture: A case study for trout production from saline groundwater in Western Australia. A report for the Rural Industries Research and Development Corporation, Australia, 68 pp.
[13] Mandal, A. K. and Sharma, R. C. 2006. Computerized database of salt affected soils for agro-climatic regions in the Indo-Gangetic plain of India using GIS. Geocarto Int., 21(2): 47-57. https://doi.org/10.1080/10106040608542383.
[14] McDowall, S., Awal, S. and Christie, A. 2016. Investigation into the potential use of inland saline groundwater for the production of live feeds for commercial aquaculture purposes. J. Aquac. Mar. Biol., 4(1): 00071. DOI: 10.15406/ jamb.2016.04.00071.
[15] Wang, J.Q.; Lui, H.; Po, H.; Fan, L. Influence of salinity on food consumption, growth and energy conversion efficiency of common carp (*Cyprinus carpio*) fingerlings. *Aquaculture* 1997, *148*, 115–124.
[16] Zheng, Z., Jin, C., Li, M., Bai, P. and Dong, S. 2008. Effects of temperature and salinity on oxygen consumption and ammonia excretion of juvenile miiuy croaker, Miichthys miiuy (Basilewsky). Aquac. Int., 16: 581-589.

International Journal of Environment, Agriculture and Biotechnology
Vol-11, Issue-3; May-Jun, 2026
Peer-Reviewed International Journal
Journal Home Page Available: https://ijeab.com/
Journal DOI: 10.22161/ijeab

Development and Performance Evaluation of a Low-Cost Solar Dryer for Drying of Mint Leaves

Arvind*[1], Surendra Kothari[2]

[1]M. Tech Scholar, Department of Renewable Energy Engineering, College of Technology and Engineering, MPUAT, Udaipur-313001, Rajasthan
[2]Professor, Department of Renewable Energy Engineering, College of Technology and Engineering, MPUAT, Udaipur-313001, Rajasthan
*Corresponding author: arvind201093@gmail.com

Received: 18 May 2026; Received in revised form: 14 Jun 2026; Accepted: 18 Jun 2026; Available online: 24 Jun 2026

Abstract*— The research was conducted to fabricate and develop a portable low cost solar dryer (LCSD) for the drying of mint leaves. The system was designed as a portable system for decentralized applications at various sites to satisfy the drying requirements of small farmers and co-operatives. The cross sectional area of the solar tunnel dryer was dome in shape, with length and width of 1.8 meters and 0.9 meter respectively. It comprises a collector section of 2.16 m^2 and a drying section of 1.36 m^2 and two chimney and three inlet to provide the required air flow rate over the perishable agricultural products to be dried. Transparent polythene cover of size 200 micron UV stabilized was used to close the dryer on top side to maintain the steady state air flow within the dryer. It has been observed that the drying air temperature was easily raised by some 20-25°C above the ambient temperature at air velocity ranges 0-1 m s^{-1}. The efficiency of the solar tunnel dryer was found to be 19-20%.. Time taken by low cost solar drying and open sun drying was 240 and 390 minutes respectively. The color of dried sample was similar to fresh mint leaves and rehydration ratio was better than open sun drying. For low cost solar drying and open sun drying mint leaves sample the moisture diffusivity was 9.28×10^{-9} and 5.42×10^{-9} m^2/s respectively. The process curves were found similar to a conventional dryer showing that this dryer can be successfully utilized for the drying of agricultural products using solar energy.

***Keywords*— Low-Cost Solar Dryer, Drying Time, Moisture diffusivity, Colour, Rehydration ratio.**

NOMENCLATURE

m = Mass of the product, kg

C_p = Specific heat of product, kJ/kg °c

ΔT = Difference in temperature, °c

Mw = Mass of water to be removed, kg

λ = Latent heat of vaporization of water, kJ/kg

I = Solar radiation, W/m²

A_c = Area of collector, m²

W_1 = mass of product before drying(g)

W_2 = mass of product after drying(g)

M_i = Initial moisture content of product (w.b.%)

M_f = Final moisture content of product (w.b.%)

W_t = Mass of product (kg)

Q_{req} = Total energy required for drying of mint leaves (kJ)

C_{pc}= Specific heat of mint leaves (kJ/kg°C)

T_d = Average drying temperature (°C)

T_a = Average ambient air temperature (°C)

Q_t = Energy required per hour (kJ h^{-1})

T_d = Drying time (h)

A_c = Collector area (m^2)

r = Radius of hemisphere (m)

l = length of dryer (m)

b = Breadth of dryer (m)

DR = drying rate (gram of water evaporated/ gram of dry matter/h)

M = moisture content, kg water per kg dry solids

□□= time, s

R = diffusion path or length, m

Dv = moisture dependent diffusivity, m^2/s

h = hour

A = constant

B = slope.

M_R = Moisture ratio, dimensionless

M_o = Initial moisture content, g water/g dry matter

M = Moisture content at any time, g water/g dry matter

Me = Equilibrium moisture content, g water / g dry matter

D_e = Effective moisture diffusivity, m^2/s

L = Thickness of mint leaves (0.5 mm)

n = Positive integer

t = Time (s)

Q_a = Quantity of air (m^3)

C_a = Specific heat of air (kJ kg^{-1} $^oC^{-1}$)

ρ_a = Density of air at ambient temperature (kg m^{-3})

T_e = Temperature of moist air at chimney outlet (^oC)

T_a = Ambient temperature (^oC)

Q_t = Volumetric air flow rate (m^3 s^{-1})

T_d = Drying time (h)

H = Height of chimney (m)

g = Acceleration due to gravity (m s^{-2})

ρ_a = Density of air at ambient temperature (kg m^{-3})

ρ_e = Density of exit air (kg m^{-3})

D_a = Actual draft

Di = Draft produce by chimney

υ = Velocity of exit air (m s^{-1})

K = Constant value for chimney design (0.4)

C = Drained weight of rehydrated sample, gm and

D = Weight of dehydrated samples taken for rehydration test, gm

LCSD = Low Cost Solar Dryer

I. INTRODUCTION

Most of the commercial crop dryers use fossil fuel. Firewood and conventional fossil fuels are being used extensively for crop drying in most countries. Apart from this, expensive fuels like diesel and propane are also being used for crop drying. Because of the increase in fuel consumption with a subsequent increase in price of conventional fossil fuels, solar dryers are being studied widely to substitute for the conventional method of crop drying (Pangavhane and Sawhney, 2002). Solar dryers are an appropriate preservation technology for a sustainable world and are being used in both developed and developing countries. For crops that are dried at temperatures higher than 60°C, solar drying could be used as a supplemental system.

The customary technique for processing fruits and vegetables is to dehydrate them in open sunlight. In this process, the rate of dehydration is slow and the quality is adversely affected by dust, insects and unexpected rain. In order to remove these problems, mechanical dryers run by fossil fuel or electricity can be used. However, in the present context when conventional energy resources are fast depleting, it is essential to utilize solar energy more efficiently as well as effectively. However, the cost of these appliances is still high. In order to make it more economical, some experiments were conducted on alternative designs for fabricating solar dryers using low cost materials. UV stabilized sheets as transparent covers for providing a greenhouse effect, available crop residues as insulation and other materials such as bamboo and mild steel (M.S.) sheets were used for fabricating the low-cost solar agricultural dryer.

II. MATERIALS AND METHODS

The low cost solar dryer was designed as a portable solar system for drying of mint leaves at various sites being developed and fabricated in the Department of Renewable Energy Engineering, College of Technology and Engineering, Udaipur.

Development of portable low cost solar dryer (LCSD):

The portable LCSD consists of two parts, solar collector and solar drying unit. The length of solar collector unit and drying unit are 1.8 m and 1.7 m respectively. A 10 cm portion of dryer is fixed in the ground and crop residue at the base as insulation. Solar collector has a base with crop residue as insulator and above crop residue black polythene sheet was used, which acts as a black body to absorb solar radiant energy and transforms incoming sunlight into heat. In the process, the heated air becomes relatively dry and is blown over the required product to be dried, where it takes up moisture. Semi-transparent polythene as a collector with size of 200 micron is used as a greenhouse effect for drying of mint leaves. There are inlet holes of polyvinyl chloride pipe in the base to allow fresh air to enter and upper parts of the box with chimney to leave moist air. The inside of the collector plate was painted with dull black to absorb solar radiation. Air gets heated up by the absorber plate while passing through the collector into the drying chamber. Food to be dried is placed on perforated trays within the dryer and warm air from the collector rises up through the food and leaves through the chimney.

Figure 1 shows the front view of low cost solar dryer as length of dryer was 1800 mm and depth of dryer in ground was 100 mm. The orientation of the dryer was maintained in East-West direction in order to achieve maximum solar radiations during the whole day. The tunnel slope was also designed to achieve maximum radiations perpendicular to the surface of the dryer in order to enhance the thermal efficiency of the solar dryer. Different machines and tools are used for the construction of low cost solar dryer like drill machine, grinding machine, welding machine, measuring tape, centre punch, hammer, chisel, right angle etc.

Fig.1 Front view of LCSD (all dimension in mm)

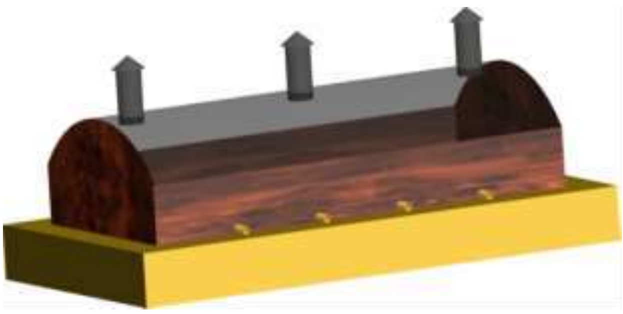

Fig.2 Schematic diagram of low cost solar dryer

Table 1: Design Specification of LCSD

Sr. No.	Components/ Particulars	Dimension
1.	Product dried	Mint leaves
2.	Length of dryer	180 cm
3.	Breadth of dryer	90 cm
4.	Dryer depth in ground	10 cm
5.	Chimney height from ground	90 cm
6.	Spacing between Chimney	88 cm
7.	Diameter of inlet	7 cm
8.	Diameter of chimney	10 cm
9.	Total number of chimney	2
10.	Total number of inlet	3
11.	Height of tray	24 cm
12.	Length of tray	170 cm
13.	Breadth of tray	80 cm
14.	Chimney height	15 cm

Performance evaluation of solar tunnel dryer:

The overall drying efficiency is defined as the ratio of energy output of the dryer to the total energy input. Thus, overall efficiency of the system is given as (Schirmer *et al.*, 1996)

Drying efficiency (per cent) = $\frac{m\,Cp\Delta T+Mw\times\lambda}{I\times Ac\times t}\times 100$

The initial moisture content of mint leaves was determined by digital moisture analyser or oven drying method (Ranganna, 2000).

Moisture content (w.b.) = $\frac{W_1 - W_2}{W_1}\times 100$

Mass of water to be removed during drying (M_w) is

$$M_w = \frac{M_i - M_f}{100 - M_f}\times W_t$$

Total energy required for drying product is

$$Q_{req} = [W_t \times C_{pc} \times (T_d - T_a) + (M_w \times \lambda)]$$

Energy required per hour is

$$Q_t = \frac{Q_{req}}{T_d}$$

Collector Area (A_c)

It has been observed that about 68% of the area of hemispherical- shaped solar tunnel dyer towards south side is able to receive sunlight while remaining 32% of area towards north side is shaded from sun (Rathore and Panwar, 2011). The area required to collect the energy for drying will be calculate by using given formula.

$$A_c = 0.68(\Pi rl + lb)$$

Dry matter recovery is defined as the ratio of final weight of dried product to the initial weight of product and was calculated by using following formula: (Rameshbhai, 2016)

Dry matter recovery (%) = $\frac{\text{Weight of dried sample}\times 100}{\text{Weight of fresh sample}}$

Drying rate (DR) =

$$\frac{\text{Amount of moisture removed (db) in grams}}{\text{Time required (hr.)}\times\text{Amount of dry matter in grams}}$$

$$\text{Moisture ratio (MR)} = \frac{M}{M_0}$$

Moisture Diffusivity During Drying

Fick's second law has been adopted for evaluation of moisture transport mechanism of the falling rate regions and is mathematically expressed by classical mass balance equation (Crank, 1975) as:

$$\frac{\partial M}{\partial \theta} = \frac{\partial}{\partial R}\left(D_v \frac{\partial M}{\partial R}\right)$$

A general form of above equation could be written in semi- logarithmic form, as follows:

$$\ln (M_R) = A - Bt$$

A plot of ln (M_R) versus drying period gives a straight line with a slope B as:

$$\text{Slope} = \left(\frac{\pi^2 D_e}{L^2}\right)$$

The effective moisture diffusivity was determined by substituting values of slope B and thickness L

Design of Chimney

Quantity of air will be need to absorb M_w kg of water

$$Q_a = \frac{M_w \times \lambda}{C_a \times \rho_a (T_e - T_a)}$$

Volumetric air flow rate required for drying will be calculated by using given formula.

$$Q_t = \frac{Q_a}{T_d}$$

Draft produce by chimney (Di) will be given by following formula.

$$D_i = H\, g\, (\rho_a - \rho_e)$$

Actual draft (D_a) produce by chimney will be

$$D_a = 0.40 \times D_i$$

Velocity of exit air will be given by following formula.

$$\upsilon = \sqrt{\frac{2D_a}{\rho_e}}$$

There are 2 chimneys, then air exist by each chimney (Q_c) will be given by following equation.

$$Q_c = \frac{Q_t}{2}$$

Area of each chimney (A)

$$A = \frac{Q_c}{\upsilon \times K}$$

Color

Color is one of the most important qualities of acceptance for products in market. It reflects sensation to the human eye and color is important for consumers as a mean of identification. The colorimeter used in the present investigation was Hunter Lab Colorimeter (Model CFLX/DIFF, CFLX-45). The 3-dimensional scale L*, a* and b* were used in a Hunter Lab Colorimeter for color measurement. The L* is the lightness coefficient, runs from top to bottom, ranging from 0 (black) to 100 (white) on a vertical axis. The positive a* value is red and negative a* value is green on a horizontal axis. A second horizontal axis is b*, that represent positive b* value is yellow and negative b* value is blue.

Rehydration Characteristics

During rehydration, the per centage of increase in original weight of dried sample mainly depends upon the porosity of dried sample (Lewicki, 1998). The rehydration characteristics are used as quality index of dried product. Further, it also indicates the physico-chemical changes occurred in sample as influenced by processing conditions, pre-treatment and composition of biological materials.

$$\text{Rehydration Ratio (RR)} = \frac{C}{D}$$

III. RESULTS AND DISCUSSION

Calculation of Design Consideration of Drying System

The average initial moisture content of fresh mint leaves determined by digital moisture analyser was found as 81.25 percent (w.b.).

The final moisture content of mint leaves in low cost solar dryer was found to be average 10.35 per cent (w.b.). Mass of water to be removed during drying was calculated by following equation

$$M_w = \frac{81.25 - 10.35}{100 - 10.35} \times \frac{2.3}{1}$$

$$= 1.82 \text{ kg}$$

The total energy required for drying mint leaves in LCSD will be calculated by using given formula:

$$Q_{req} = [2.3 \times 3.58 \times (60.09 - 39.95) + (1.82 \times 2257)]$$

$$= 4273.57 \text{ kJ}$$

Energy required per hour will be calculate by following formula.

$$Q_{t1} = \frac{4273.57}{4}$$

$= 1068.39 \text{ kJ h}^{-1}$

$A_c = 0.68(3.14\times0.45\times1.8 + 1.8\times0.35)$

$= 2.16 \text{ m}^2$

The intial weight of product for drying was taken 2.3 kg for open sun drying and LCSD. After drying the final weight of dried product for open sun drying and LCSD system was 0.48 kg and dry matter recovery was 21% for both cases.

Drying efficiency (per cent) for low cost dryer = $\frac{4273.57\times1000}{4\times3600\times690\times2.16}\times100$

$= 19.91$

Design Calculation of Chimney for LCSD

Quantity of air will be need to absorb M_w kg of water

$$Q_a = \frac{1.6\times2257}{1.005\times1.184(51-39)}$$

$= 252.90 \text{ m}^3$

Volumetric air flow rate required for drying will be calculated by using given formula.

$$Q_t = \frac{252.90}{4\times60\times60}$$

$= 0.02 \text{ m}^3 \text{ s}^{-1}$

Draft produce by chimney (Di) will be given by following formula.

$D_i = 0.3\times9.81\times(1.1206 - 1.0539)$

$= 0.1963 \text{ kg/m}^2$

Actual draft (D_a) produce by chimney will be

$D_a = 0.40 \times 0.1963$

$= 0.07852 \text{ kg/m}^2$

Velocity of exit air will be given by following formula.

$$\upsilon = \sqrt{\frac{2\times0.07852}{1.0539}}$$

$= 0.3860 \text{ m/s}$

There are 2 chimneys, then air exist by each chimney (Q_c) will be given by following equation.

$$Q_c = \frac{0.02}{2}$$

$= 0.01 \text{ m}^3/\text{s}$

Area of each chimney (A)

$$A = \frac{0.01}{0.3860\times0.4}$$

$= 0.0648 \text{ m}^2$

Temperature and Solar Radiation Variations in LCSD during No Load Testing

It was observed that the maximum temperature obtained inside the LCSD was 69^0C at 13:00 h, while minimum was 41^0C at 10:30 h. Maximum ambient temperature was 41^0C at 12:40 h, while the minimum ambient temperature was 35^0C at 16:20 h. It was observed that there is an increment of 28^0C temperature inside the LCSD. It was also observed that the maximum and minimum ambient solar insolation in this month was 1071 W/m^2 at 12:40 hrs and 658 W/m^2 at 16:30 hrs respectively. The trend of result for temperature and solar insolation during no load for LCSD was plotted on graph as shown in Fig. 3

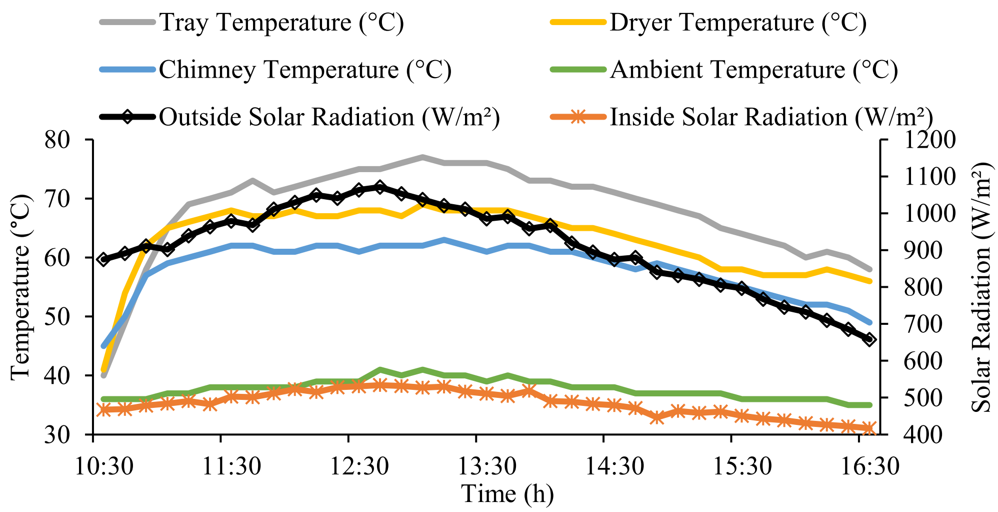

Fig. 3 No Load Performance Curve of LCSD

Temperature and Solar Radiation Variations for Open Sun Drying and LCSD Under Full Load Testing

It was observed that the maximum ambient temperature obtained was 41^0C at 13:30 h, while minimum was 35^{0}C at 10:00 h in the month of April 2019. The maximum temperature obtained by LCSD was 64^{0}C at 12:15 h. It was observed that there is an increment of 23^{0}C temperature inside the LCSD as compared to ambient temperature. It was also observed that the maximum and minimum solar radiation in the month of April was 1059 W/m^2 at 13:15 h and 789 W/m^2 at 16:30 h respectively. Time taken in open sun drying was 6.5 h and in LCSD was 4 h. The trend of result for temperature and solar radiation during full load testing in open sun drying and LCSD was plotted on graph as shown in Fig.5 and Fig. 6 respectively. Fig. 4 showing drying of mint leaves.

Fig. 4 Drying of mint leaves in LCSD

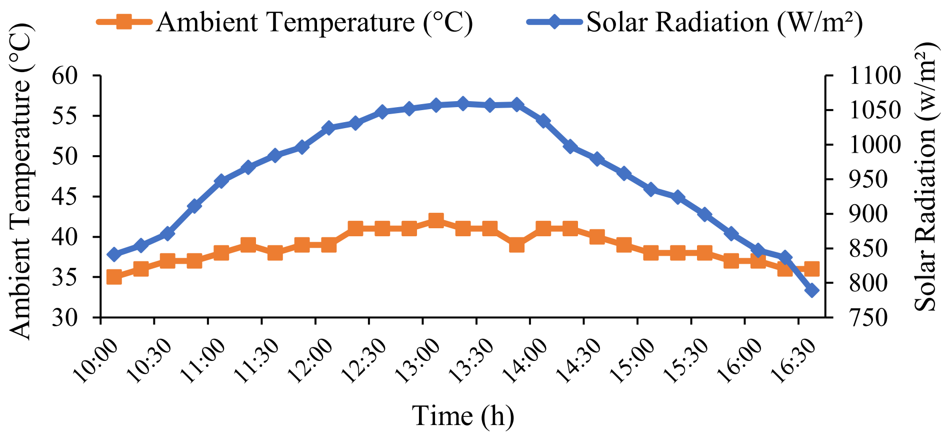

Fig.5 Variation of Temperature and Solar Radiation Under Open Sun Drying

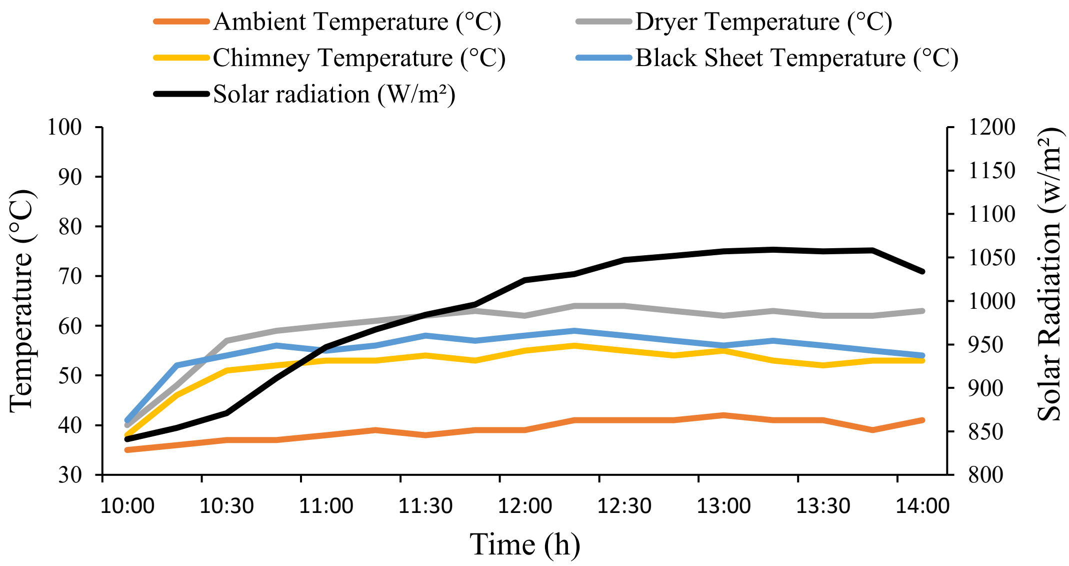

Fig.6 Variation of Temperature and Solar Radiation Under LCSD

Performance Evaluation of Drying Process

Variations in Moisture Content of Mint Leaves with Respect to Time

The moisture content (d.b.) during full load testing of open sun drying and LCSD is presented in Fig. 7 and Fig. 8 within 390 minutes 240 minutes respectively. The mint leaves were dried from moisture content of 432.76 to 10.20 per cent (d.b.) in open sun drying and from moisture content 457.57 per cent (d.b.) to final moisture content 11.54 per cent (d.b.) in LCSD. Time taken in open sun drying is approximately double the time taken in low cost solar drying.

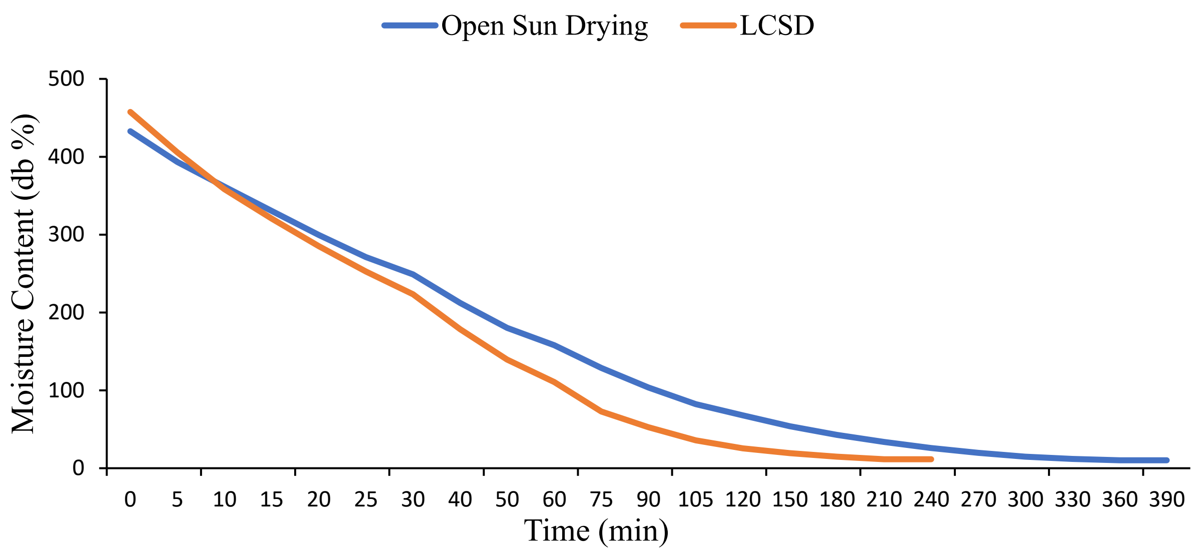

Fig.7 Moisture Content Variation

Moisture Diffusivity of Mint Leaves

Diffusion is the process by which matter is transported from one part to another of a system as a result of random molecular motions (Crank 1975). The ln (MR) was plotted with drying time in order to find out moisture diffusivity for mint leaves. The variation in ln (MR) with drying time of mint leaves have been presented in Fig. 8 and Fig 9 for LCSD and open sun drying. For LCSD and open sun drying mint leaves sample the moisture diffusivity is 9.28×10^{-9} and 5.42×10^{-9} m^2/s respectively.

Quality Analysis of Dried Mint Leaves

Rehydration Characteristics

Ten gram of dried mint samples were taken for the experiment. 200 ml of distilled water in glass beakers was taken and the beakers were kept in a water bath, maintained at 80ºC. Dehydrated samples of each were placed in beakers for 10 min. After 10 min the excess water was drained off through filter paper. The drained samples were weighed. The weight of sample before and after rehydration ratio was measured. The rehydration ratio of mint leaves in open sun drying and low cost solar dryer was 5 and 4.39 respectively. It can also be observed that the rehydration ratio (RR) gradually decreased with increase in air temperature.

Effect of Drying Temperature on Colour of Dehydrated Mint Leaves

Color values were measured using a Hunter lab Colorimeter at room temperature 29-32°C. It can be observed that the L^* value for dried mint leaves in open sun drying and low cost solar drying was 30.47 and 33.58 respectively. Fig. 10 shows Hunter Lab Colorimeter used for colour measurement. The a^* value for dried mint leaves in open sun drying and low cost solar drying was -3.84 and -4.91 respectively. The b* value for dried mint leaves in open sun drying and low cost drying was 10.87 and 12.25 respectively.

Table 2: Moisture Diffusivity Values for Dried Mint Leaves

Sample	Regression equation	Moisture diffusivity (m^2/s)	R^2
Open sun drying	y = -0.0101x - 0.4676	5.42×10^{-9}	0.9696
Low cost solar drying	y = -0.0173x - 0.2511	9.28×10^{-9}	0.9433

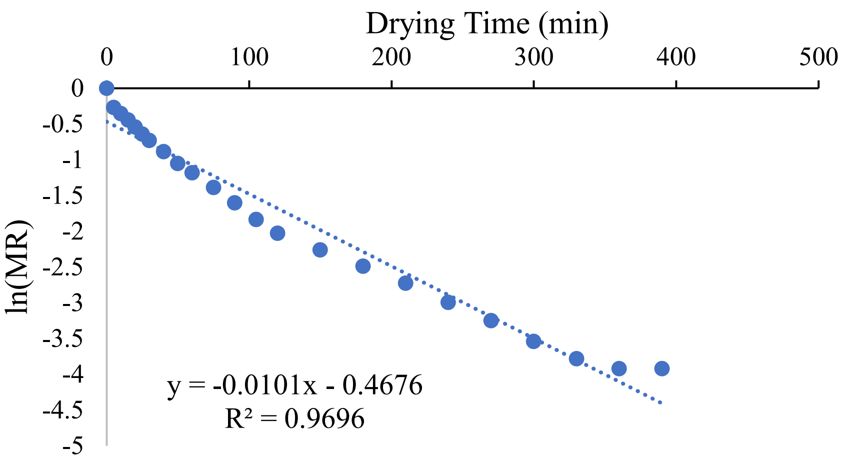

Fig.8 ln MR verses Drying Time in Open Sun Drying

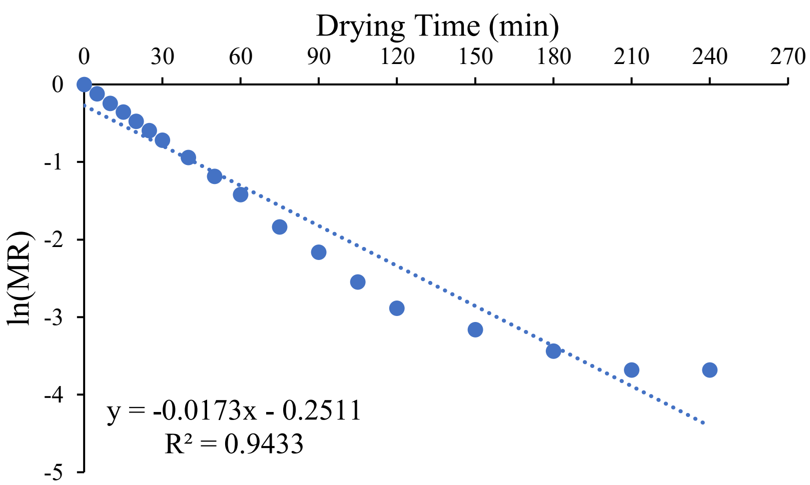

Fig.9 ln MR verses Drying Time in LCSD

Fig. 10 Colour Measurement of Mint Leaves Sample

IV. CONCLUSION

This dryer is simple in construction and it can be constructed using locally available materials by the local craft man. The LCSD dried products are protected from dirt, insects and climatic conditions due to its perfect sealing. The air leaving the dryer was found to have still greater potential for drying more products. However, this should also be considered for other products, as this dryer is designed for multi-products use. The solar based renewable technology is free from operating cost and can play a vital role in promoting the field of post-harvest technology using solar energy. In the experimental trials, the drying time was found to reduce by about 40% of time required in open sun drying. The cost of this device has been evaluated to be Rs. 4400. For low cost solar drying and open sun drying of mint leaves sample, the moisture diffusivity was found to be $9.28\times10^{-9}$and 5.42×10^{-9} m^2/s respectively. The rehydration ratio of mint leaves in open sun drying and low cost solar dryer was 5 and 4.39 respectively. Further, this technology can contribute in clean development mechanism and thus organization effectiveness and higher productivity (Jain 2007) and along with long-term benefits in terms of fuel and environment saving can be obtained.

REFERENCES

[1] Aiswarya, M.S. and Divya, C.R. 2015. Economic analysis of solar dryer with phase change material for drying agricultural products. *International Research Journal of Engineering and Technology* **4** : 1948-1953.

[2] Akpinar, E.K. 2010. Drying of mint leaves in a solar dryer and under open sun: modelling, performance analyses. *Energy conversion and management* **51** : 2407-2418.

[3] AOAC, 1990. Official methods of analysis, 15th edn., *Association of Official Analytical Chemists, Arlington, VA.* Method number. 930.04, 69.

[4] APEDA. 2015-16. Fresh Fruits & Vegetables Data. http://apeda.gov.in/apedawebsite/six_head_product/FFV.htm

[5] Basavaraj, M., Kumar, G.P.P., Reddy, B.S. and Jagadeesha, R.C. 2008. Effect of drying on colour degradation and rheology in red chilli. *Asian Journal of Horticulture* **3** : 253-255.

[6] Crank, J. 1975. *The Mathematics of Diffusion* (2nd ed.) UK, Clearendon Press, Oxford.

[7] Doymaz, I. 2006. Thin-layer drying behaviour of mint leaves. *Journal of Food Engineering* **74** : 370-375.

[8] Gbaha, P., Andoh, H.Y., Saraka, J.K., Koua, B.K. and Toure, S. 2007. Experimental investigation of a solar dryer with natural convective heat flow. *Renewable Energy* **32** : 1817–29.

[9] Jain, N.K., Kothari, S. and Mathur, A.N. 2004. Techno-economic evaluation of a forced convection solar dryer. *Journal of Agricultural Engineering* **41** : 6-12.

[10] Lewicki, P. P. 1998. Some remarks on rehydration of dried foods. *Journal Food Engineering* **36** : 81-87.

[11] Pangavhane, D.R., Sawhney, R.L. and Sarsavadia, P.N. 2002. Design, development and performance testing of a new natural convection solar dryer. *Energy 27* : 579-590.

[12] Panwar, N.L., Kaushik, S.C. and Kothari, S. 2011. Role of renewable energy sources in environmental protection. *A review Renewable and Sustainable Energy Reviews* **15** : 1513–1524.

[13] Panwar, N.L., Kothari, S. and Kaushik, S.C. 2014. Cost-benefit and systems analysis of passively ventilated solar greenhouses for food production in arid and semi-arid regions. *Environment Systems and Decisions* **34** : 160-167

[14] Rathore, N.S. and Panwar, N.L. 2011. Design and development of energy efficient solar tunnel dryer for industrial drying. *Clean Technologies and Environmental Policy* **13** : 125-132.

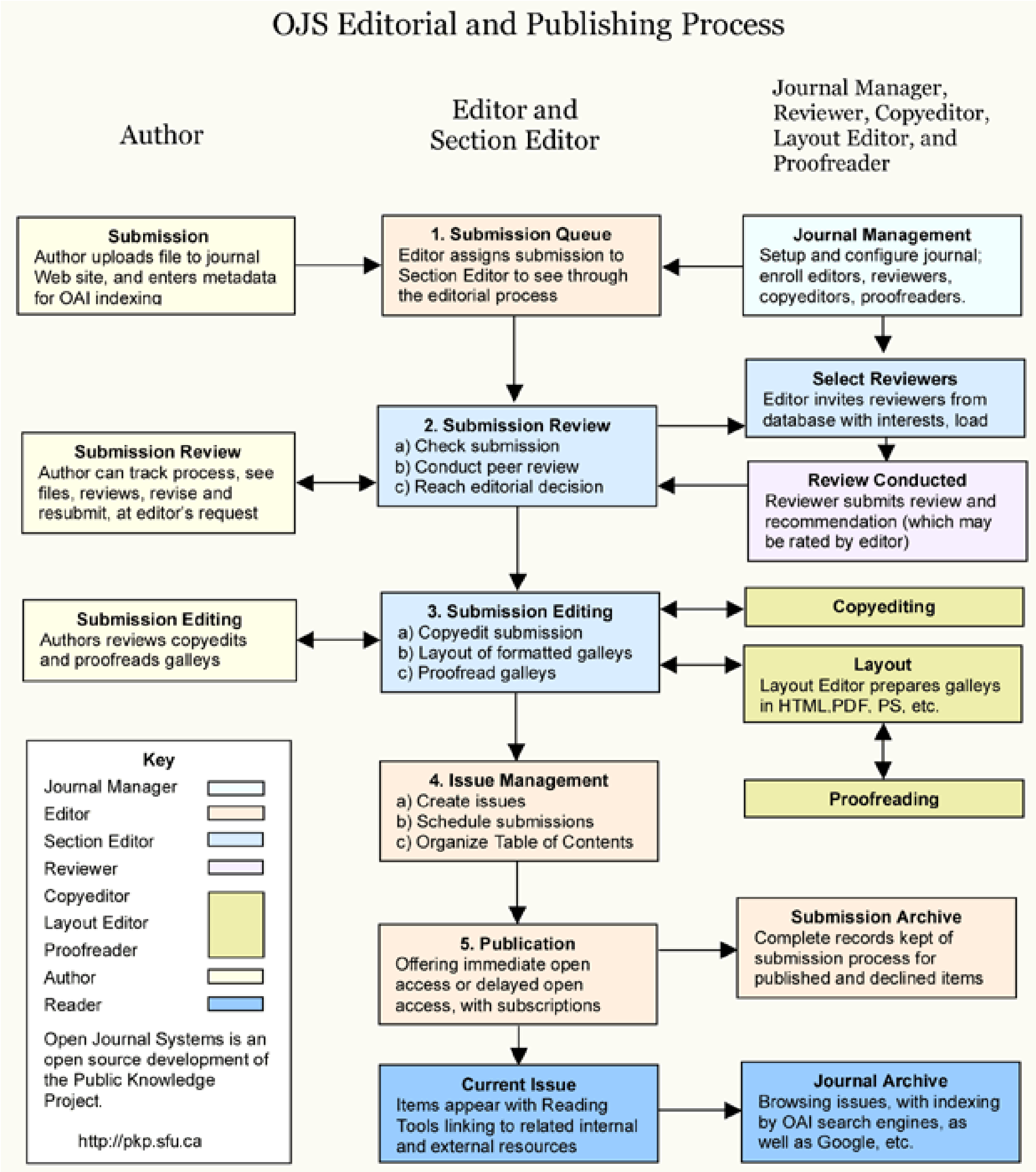

~OJS Workflow~

Important links:

Paper Submission Link:

OJS:

https://ijeab.com/ojs/index.php/ijeab/about/submissions

https://ijeab.com/submit-paper/

Editorial Team:

https://ijeab.com/editorial-board/

Peer Review Process:

https://ijeab.com/peer-review-process/

Publication Ethics:

https://ijeab.com/publication-policies-and-ethics/

Author Guidelines:

https://ijeab.com/author-guidelines/

Join Us a Reviewer:

https://ijeab.com/join-us/

Journal Indexed and Abstracted in:

- Qualis-CAPES -Brazil
- Normatiza (Under Review)
- Bielefeld Academic Search Engine(BASE)
- Aalborg University Library (Denmark)
- WorldCat: The World's Largest Library Catalog
- Semantic Scholar
- J-Gate
- Open J-Gate
- CORE-The world’s largest collection of open access research papers
- JURN
- Microsoft Academic Search
- Google Scholar
- Kopernio - powered by Web of Science
- Pol-Index
- PBN(Polish Scholarly Bibliography)Nauka Polaska
- Scilit, MDPI AG (Basel, Switzerland)
- Tyndale University College & Seminary
- indiana Library WorldCat
- CrossRef DOI-10.22161/ijeab
- Neliti - Indonesia's Research Repository
- Journal TOC
- Dimensions.ai: Re-imagining discovery and access to research
- Citeseerx
- Massachusetts Institute of Technology (USA)
- Simpson University (USA)
- University of Louisville (USA)
- Biola University (USA)
- IE Library (Spain)
- Mount Saint Vincent University Library (Halifax, Nova Scotia Canada)
- University Of Arizona (USA)
- INDIANA UNIVERSITY-PURDUE UNIVERSITY INDIANAPOLIS (USA)
- Roderic Bowen Library and Archives (United Kingdom)
- University Library of Skövde (Sweden)
- Indiana University East (campuslibrary (USA))
- Tilburg University (The Netherlands)
- Williams College (USA)
- University of Connecticut (USA)
- Brandeis University (USA)
- Tufts University (USA)
- Boston University (USA)
- McGill University (Canada)
- Northeastern University (USA)
- BibSonomy-The blue social bookmark and publication sharing system
- Slide Share
- Academia
- Archive
- Scribd
- SJIF-InnoSpace
- ISSUU
- Research Bib
- DRJI
- journal-repository

Platform & workflow by OJS / PKP

Infogain Publication
International Journal of English, Literature and Social Science (IJELS)